Imperial College London
Imperial College Business School

Large-scale Optimization under Uncertainty: Applications to Logistics and Healthcare

Shubhechyya Ghosal

Submitted in part fulfilment of the requirements for the degree of
Doctor of Philosophy of Imperial College and
the Diploma of Imperial College, August 2021

Declaration

I, Shubhechyya Ghosal, declare that the research presented in this thesis is my own work, except where acknowledged. No part of this thesis has been submitted before for any degree or examination at this or any other university.

Abstract

Many decision making problems in real life are affected by uncertainty. The area of optimization under uncertainty has been studied widely and deeply for over sixty years, and it continues to be an active area of research. The overall aim of this thesis is to contribute to the literature by developing *(i)* theoretical models that reflect problem settings closer to real life than previously considered in literature, as well as *(ii)* solution techniques that are scalable. The thesis focuses on two particular applications to this end, the vehicle routing problem and the problem of patient scheduling in a healthcare system.

The first part of this thesis studies the vehicle routing problem, which asks for a cost-optimal delivery of goods to geographically dispersed customers. The probability distribution governing the customer demands is assumed to be unknown throughout this study. This assumption positions the study into the domain of distributionally robust optimization that has a well developed literature, but had so far not been extensively studied in the context of the capacitated vehicle routing problem. The study develops theoretical frameworks that allow for a tractable solution of such problems in the context of rise-averse optimization. The overall aim is to create a model that can be used by practitioners to solve problems specific to their requirements with minimal adaptations.

The second part of this thesis focuses on the problem of scheduling elective patients within the available resources of a healthcare system so as to minimize overall years of lives lost. This problem has been well studied for a long time. The large scale of a healthcare system coupled with the inherent uncertainty affecting the evolution of a patient make this a particularly difficult problem. The aim of this study is to develop a scalable optimization model that allows for an efficient solution while at the same time enabling a flexible modelling of each patient in the system. This is achieved through a fluid approximation of the weakly-coupled counting dynamic program that arises out of modeling each patient in the healthcare system as a dynamic program with states, actions, transition probabilities and rewards reflecting the condition, treatment options and evolution of a given patient. A case-study for the National Health Service in England highlights the usefulness of the prioritization scheme obtained as a result of applying the methodology developed in this study.

Acknowledgements

I am extremely grateful to my supervisor, Prof. Wolfram Wiesemann, for his constant support, guidance and encouragement through the last few years that made the outcome of this thesis possible. I am truly indebted to him for the many learning opportunities that I have received and the research experience that I have gained over the course of my PhD.

I am thankful to my group members, Stefano Moret and Esma Koca, for being wonderful co-authors, and becoming my friends and confidantes. I will truly cherish the time that I spent working with them during my PhD. I also appreciate the advice that I have received from the post-doctoral researchers that have been part of this group during my time here: Clint Ho, Man-Chung Yue, Zhi Chen and Huikang Liu. I have also had the privilege of co-authoring with Clint and Huikang, and learning from them. I have benefited greatly from the wisdom of Hormoz Ramian, who has been a source of encouragement and advice.

I am grateful for the support and motivation that I received outside of my academic circle. My keen appreciation goes to Aarti, Ekta, Akhil, Venkat, Priya and all the others that I should have mentioned, for their valuable friendship. I am indebted to Allen for his support and patience throughout.

Last but not the least, none of this would have been possible without the unconditional love and support of my parents. Their unwavering faith in me has given me courage through all the times when I have not believed in myself. I count my blessings everyday to have them as my parents, and I dedicate this thesis to them.

To my parents.

Contents

List of Tables

List of Figures

Chapter 1

Introduction

1.1 Motivation

Large-scale organizations, across different industries, face problems affecting their day-to-day operations wherein they are required to make decisions in the face of incomplete or partially available information about the future. The numerous scenarios that could unfold in the future coupled with the large scale of the operations make these problems difficult to model. Moreover, these organizations are usually time bound to make these decisions. This necessitates that the developed models can be solved within a short time span to a desirable accuracy. Typically, organizations make simplifying assumptions to create suitable models to solve these problems effectively and efficiently. However, this simplification comes at the cost of the solution quality which ultimately may lead to suboptimal decisions for the organization. Eventually over time, this would translate to higher costs or lower profits for these organizations.

According to a recent Forbes article [Edw20], 85% of Fortune 500 companies, across different industries such as aviation, energy, telecommunications, logistics, finance and healthcare, use mathematical optimization in their operations. Aviation companies are required to decide the prices of their tickets months before they know the customer demand or the future costs of their operations (say, driven by uncertain fuel costs). They need to offer competitive pricing while maintaining or improving their profit margins. Within healthcare, hospitals are faced with the problem of improving surgery schedules while managing capacity for emergency procedures. This requires improvement in resource planning before the the demand for emergency procedures or staff availability become known. Moreover, healthcare providers are required to decide on a course of treatment for patients, without having full information about how the patient's condition will evolve given a particular treatment. E-commerce companies have to decide how to show appropriate assortment of products to new visitors to their websites so as to increase customer engagement and improve revenues. This is challenging due to the unknown preferences of the potential customers. Logistics companies are required to provide customers with estimated delivery times before they have complete information of the total demand that they will be needed to meet on that day. Suboptimal decisions result in higher costs or lower customer satisfaction for these companies. The integration of renewable energy sources, such as wind and solar, into energy production facilities have led to the problem of production planning under uncertainty for energy companies due to the weather dependent nature of the energy sources. These examples barely scratch the surface of the large-scale decision making problems under uncertainty that are faced by various industries.

The aim of this thesis is two-fold: *(i)* to contribute to the literature on decision making under uncertainty by creating theoretical frameworks that model large-scale decision making problems closer to real life than previous formulations considered in literature, and *(ii)* developing scalable solution techniques that can be easily adapted by practitioners. This thesis particularly focuses on two application domains: logistics and healthcare operations.

1.2 Background Information

The previous section has emphasized the importance of large-scale decision making problems under uncertainty. decision making problems can be modeled as optimization problems. Optimization problems under uncertainty have been studied by the Operations Research community since the 1950s, and has seen rapid growth in both theory and solution algorithms. The ever increasing complexity in operations has perpetuated the challenges that need to be addressed, and optimization under uncertainty has remained an active area of research. The general formulation for an optimization problem under uncertainty is

$$\min_{\boldsymbol{x}\in\mathcal{X}(\boldsymbol{x},\tilde{\boldsymbol{\xi}})} f(\boldsymbol{x},\tilde{\boldsymbol{\xi}})$$

where $\boldsymbol{x}$ is the vector of decision variables, $\mathcal{X}(\boldsymbol{x},\tilde{\boldsymbol{\xi}})$ is the feasibility set which may or may not depend on the uncertain parameter $\tilde{\boldsymbol{\xi}}$ and $f(\boldsymbol{x},\tilde{\boldsymbol{\xi}})$ is the objective function.

This section presents a brief overview of the methodologies developed to address optimization problems under uncertainty, and also highlight the merits and demerits of each method.

1.2.1 Stochastic Programming

In stochastic programming, the uncertain parameter is either assumed to be governed by a particular probability distribution on the basis of judgment, or is estimated from historical data wherein each observation is assigned an equal probability of occurrence (empirical distribution). The most generic formulation of stochastic programming is

$$\min_{\boldsymbol{x}\in\mathcal{X}(\boldsymbol{x},\tilde{\boldsymbol{\xi}})} \mathbb{E}_{\tilde{\boldsymbol{\xi}}}\{f(\boldsymbol{x},\tilde{\boldsymbol{\xi}})\}$$

where $\mathbb{E}_{\tilde{\boldsymbol{\xi}}}(\cdot)$ is the expectation operator. The above model falls under the purview of single-stage stochastic programming wherein a decision is made before the uncertainty parameters are realized. As such, single-stage stochastic programming is suitable for long-term strategic planning decisions.

However, organizations often face decision making problems affecting their day-to-day operations that call for a more flexible modeling approach. The multi-stage stochastic programming model formulates the problem so that decisions are made in stages as the uncertainty gradually unfolds in the future and more information becomes available. A first-stage decision is made before the random variables are realized, followed by recourse decisions that vary by the outcome of the random variables. The generic formulation for the T-stage stochastic programming problem is

$$\min_{\boldsymbol{x}_1,\boldsymbol{x}_2(\cdot),\ldots,\boldsymbol{x}_T(\cdot)} \mathbb{E}_{\tilde{\boldsymbol{\xi}}}[\{f_1(\boldsymbol{x}_1) + f_2(\boldsymbol{x}_2(\tilde{\boldsymbol{\xi}}_{[2]}),\tilde{\boldsymbol{\xi}}_2) + \ldots + f_T(\boldsymbol{x}_T(\tilde{\boldsymbol{\xi}}_{[T]}),\tilde{\boldsymbol{\xi}}_T)\}]$$
$$\text{s.t. } \boldsymbol{x}_1 \in \mathcal{X}_1,\ \boldsymbol{x}_t(\tilde{\boldsymbol{\xi}}_{[t]}) \in \mathcal{X}_t(\boldsymbol{x}_{t-1}(\tilde{\boldsymbol{\xi}}_{[t-1]}),\tilde{\boldsymbol{\xi}}_t),\ t = 2,\ldots,T.$$

Here $\tilde{\boldsymbol{\xi}}_1,\ldots,\tilde{\boldsymbol{x}}_T$ is a random data process, and $\boldsymbol{x}_t(\tilde{\boldsymbol{\xi}}_{[t]}$ represents the decision at time t as a function of the data process up to time t. Notice that the first-stage decision is deterministic.

Although, conceptually simple, stochastic programming requires modeling the underlying probability distribution which is rarely known with certainty. Moreover, stochastic programming models for real-world applications can quickly grow in size and become too complex for use. [BL11] and [WZ05] provide an overview of the theory and applications of stochastic programming.

1.2.2 Chance-constrained Programming

Chance-constrained programming (also called probabilistic programming) was first introduced by [CC59]. This approach aims to ensure that the optimal decision respects the feasibility of the model with a minimum pre-specified probability. The general representation for this model is as follows

$$\begin{aligned} &\text{minimize} && f(\boldsymbol{x},\tilde{\boldsymbol{\xi}}) \\ &\text{subject to} && \mathbb{P}(h_i(\boldsymbol{x},\tilde{\boldsymbol{\xi}}) \leqslant 0) \geqslant p \ \ \forall i = 1,\ldots,m \\ &&& \boldsymbol{x} \in \mathcal{X}(\boldsymbol{x},\tilde{\boldsymbol{\xi}}) \end{aligned}$$

where $p \in [0,1]$ is the minimum prefixed probability of ensuring the feasibility of the model constraints. This model allows for the constraints to be violated in a small number of scenarios, instead of being satisfied in all scenarios. This differs from the multi-stage stochastic programming approach wherein the recourse decisions are penalized for violating the feasibility of the multi-stage problem.

In the above model the probabilistic constraint applies to each constraint *individually*; the probabilistic constraint may also apply to all the constraints *jointly*:

$$\mathbb{P}(h_i(\boldsymbol{x}, \tilde{\boldsymbol{\xi}}) \leqslant 0 \ \ \forall i = 1, \ldots, m) \geqslant p$$

The individual chance constraints model is easier to solve that joint chance constraints. While the chance-constrained programming is suitable when the focus is on ensuring the reliability of a system under uncertainty, modeling the underlying probability distribution of the process as well as the complexity of evaluating the chance constraints pose limitations to this approach. [KJ21] provide a detailed review of this approach.

1.2.3 Robust Optimization

This modeling paradigm differs from the above approaches in that it does not take a probabilistic approach to modeling uncertainty. Instead, it models the uncertain parameters to belong to an *uncertainty set*. The objective is to generate decisions that are optimal with respect to the worst-case outcome of the uncertain parameters in the uncertainty set. The generic formulation for this model is

$$\begin{aligned} \text{minimize} \quad & f(\boldsymbol{x}, \boldsymbol{\xi}) \\ \text{subject to} \quad & \boldsymbol{x} \in \mathcal{X}(\boldsymbol{x}, \boldsymbol{\xi}) \\ & \boldsymbol{\xi} \in \mathcal{U} \end{aligned}$$

where $\mathcal{U}$ is the uncertainty set to which $\tilde{\boldsymbol{\xi}}$ belongs. The design of the uncertainty set is crucial to the success of the robust optimization solution, else the model may lead to overly conservative solutions. Some commonly studied uncertainty sets in literature include the polyhedral uncertainty set, 1-norm uncertainty sets, ∞-norm uncertainty sets, and elliptical uncertainty sets.

Although, robust optimization relaxes the requirement for the underlying distribution governing the uncertain parameters, the tractability of the solution approach as well as the conservativeness of the solution is dictated by the design of the uncertainty set. This limits the modeling flexibility of this approach. [BBC11b] provides a review of the theory and applications of robust optimization.

1.2.4 Distributionally Robust Optimization

While stochastic programming and chance-constrained programming require knowledge of the underlying probability distribution governing the uncertain parameters, robust optimization disregards all distributional knowledge about the uncertain parameters. Distributionally robust optimization bridges this gap by relaxing the requirement of knowing the exact probability distribution governing the uncertain parameters, however it requires the design of an *ambiguity set* to which the governing probability distribution must belong. Like robust optimization, the distributionally robust optimization approach optimizes in view of the realization of the worst-case distribution in the ambiguity set. The generic formulation for the distributionally robust optimization model is given by

$$\min_{\boldsymbol{x} \in \mathcal{X}(\boldsymbol{x}, \tilde{\boldsymbol{\xi}})} \max_{\mathbb{P}_{\tilde{\boldsymbol{\xi}}} \in \mathcal{P}} \mathbb{E}_{\mathbb{P}_{\tilde{\boldsymbol{\xi}}}} f(\boldsymbol{x}, \tilde{\boldsymbol{\xi}})$$

where $\mathbb{P}_{\tilde{\boldsymbol{\xi}}}$ is a plausible distribution governing the uncertain parameter $\tilde{\boldsymbol{\xi}}$ belonging to the ambiguity set $\mathcal{P}$. The ambiguity set may be characterized by support information of the uncertain parameters; estimates of mean or other dispersion measures from data; or as a function of a probability metric defined over a reference distribution estimated from data.

By design, the distributionally robust optimization offers more flexibility than the other modelling approaches described previously. Later on in this thesis, we consider specific ambiguity sets and show that the gain in modeling flexibility does not necessarily come at the cost of solution tractability. However, the ambiguity set requires careful attention to their design as poorly chosen ambiguity sets could lead to overly conservative solutions. [PM19] provides a review of distributionally robust optimization.

1.2.5 Dynamic Programs

Dynamic programming evolved in the 1950's as an alternative modeling approach to sequential decision making under uncertainty. Deviating from all the other approaches described so far, the multistage process is encoded by states, actions, rewards and transition probabilities. As opposed to solving a single optimization problem, dynamic programming aims to find an optimal policy that is a parametric description of optimal solutions to a family of optimization problems parameterized by the initial state of the dynamic system.

The generic form of the model is described as

$$V_t(S_t) = \min_{a \in \mathcal{A}} \left(C(S_t, a) + \gamma \sum_{s' \in \mathcal{S}} p(s'|S_t, a) V_{t+1}(s') \right)$$

where S_t is the state at time t, a is the action in set $\mathcal{A}$, $C(S_t, a)$ is the cost associated with the system being in state S_t and taking action a, $p(s'|s, a)$ is the probability of the system transitioning to state s' at time $t+1$ given that it was in state s at time t and action a was applied to the system at time t. Finally, $V_t(s)$ represents the value associated with being in state s at time t. The aim is to find a policy $\pi(\boldsymbol{s})$ that minimizes the value function. At each state of the system s, the policy $\pi(\boldsymbol{s})$ prescribes the action a that must be applied to the system.

Even though dynamic programming offers great modeling flexibility, it suffers from the curse of dimensionality as the problem size grows exponentially in the number of states and actions. Many papers in literature aim to address this issue; [Pow16] provides a review of these methods.

1.3 Research Objectives and Contributions

The overarching aim of this thesis is to contribute to the literature of decision making under uncertainty by: *(i)* creating more flexible models that allow modeling the problem under study closer to real life than previously done in literature, and *(ii)* create solution tractable and scalable solution algorithms for the models developed in *(i)*. The first part of the thesis studies the single-stage decision making problem under uncertainty, while the second part focuses on the multi-stage decision making problem under uncertainty.

As discussed in Section 1.2, distributionally robust optimization bridges the stochastic optimization and robust optimization paradigms. We study distributionally robust optimization in conjunction with risk measures to model the decision-maker's attitude towards uncertainty. We use this approach specifically to study the problem of the stochastic vehicle routing problem under demand uncertainty. In literature, stochastic optimization and robust optimization have been applied to solve this problem with varying degrees of success [OAW18, OAW17, SO08, GWF13b], which led to the question of how successfully could the distributionally robust optimization approach be applied to this problem.

The second part of the thesis studies a large-scale multi-stage decision making problem. As mentioned in Section 1.2, the modeling flexibililty of the dynamic programming approach is offset by the curse of dimensionality. This thesis aims to contribute to the dynamic programming literature by developing a close approximation model that scales more gracefully in problem dimensions, that allows for easier solution of large-scale dynamic programming problems. This approach was borne out of the need to solve the problem of optimally scheduling patients in NHS England during the COVID-19 pandemic.

1.3.1 Stochastic Vehicle Routing Problem

A fundamental problem in logistics concerns finding the optimal routes for a set of vehicles for the delivery of goods from a depot to a set of geographically dispersed customers. The objective may be to find the set of routes that take the shortest distance or minimize the cost of travel. The vehicle routing problem (VRP) has been studied since the 1950s [DR59], and it has found wide-spread applications in waste collection, dial-a-ride services, courier delivery and the routing of snow plow trucks, school buses as well as maintenance engineers.

We consider a complete and directed graph $G = (V, A)$ with nodes $V = \{0, \ldots, n\}$ and arcs $A = \{(i, j) \in V \times V \; : \; i \neq j\}$. The node $0 \in V$ represents the unique depot, and the nodes

$V_C = \{1, \dots, n\} \subset V$ denote the customers. The depot is equipped with m vehicles, which we index through the set $K = \{1, \dots, m\}$. Each vehicle incurs transportation costs of $c(i, j) \in \mathbb{R}_+$ if it traverses the arc $(i, j) \in A$. Throughout the thesis, we allow for asymmetric transportation costs. As is standard in the literature, our models simplify if the transportation costs satisfy $c(i, j) = c(j, i)$ for all $(i, j) \in A$; see, *e.g.*, [STV14].

The feasible routes of our problem must form an m-partition of the customer set, wherein each route is visited by a single vehicle; no two routes overlap at any customer node; the union of all routes must recover our customer set; and the routes should start and end at the depot node. We refer to the collection of m feasible routes as a route set. Additionally, each feasible route must satisfy some 'technological' constraints. In this chapter, we keep the notation informal in order to give a broad description of the study area. We make the notation more rigorous in the next chapters. We denote a route by $\boldsymbol{R}$ where $\boldsymbol{R}$ is an ordered list of customer nodes visited by a vehicle. We seek to find a collection of routes, called a route set, that forms an m-partition of the customer set along with satisfying the 'technological' constraints.

There are various variants of VRP, but the two variants that have received the most attention in the vehicle routing community are

(i) **Capacitated vehicle routing problem (CVRP).** The vehicles that have to deliver or pick up items from different locations before returning to the depot, have a maximum carrying capacity.

(ii) **Vehicle routing problem with time windows (VRPTW).** The vehicles have to visit the specific locations where they are to deliver or pick up goods within a specified time window.

The classical problem considers all parameters to be *deterministic*. In the case of CVRP, this would mean that the customer demands are known precisely before the delivery routes are planned, or that travel times are known exactly before the routes are planned for VRPTW.

In deterministic CVRP, each customer $i \in V_C$ has a known demand $q_i \in \mathbb{R}_+$ and the m vehicles are homogeneous with capacity Q. Moreover, for a route to be technologically feasible the sum of demand served by any single vehicle $\sum_{i \in \boldsymbol{R}} q_i$ must not exceed Q. The shorthand notation $\boldsymbol{R} \in \mathcal{R}(\boldsymbol{q})$ expresses the capactity constraint for the k-th vehicle, that is, $\sum_{i \in \mathbb{R}} q_i \leqslant Q$.

However, for VRPTW the travel times are highly uncertain depending on traffic conditions on any given day, and the customer requirements for pick up may become known only when the vehicle reaches the customer in the case of CVRP. These examples illustrate that deterministic vehicle routing problems are rarely useful in practice.

The *robust CVRP* seeks for a route set that satisfies the vehicle capacities for all anticipated demand realizations within an uncertainty set $\mathcal{Q}$. Thus, the formulation of the robust CVRP replaces the deterministic capacity constraints $\sum_{i \in \boldsymbol{R}} q_i \leqslant Q$ with the robust capacity constraints $\boldsymbol{R} \in \bigcap_{\boldsymbol{q} \in \mathcal{Q}} \mathcal{R}(\boldsymbol{q})$. The robust CVRP reduces to a deterministic CVRP if $\mathcal{Q} = \{\boldsymbol{q}\}$.

The *chance constrained CVRP* models the customer demands as a random vector $\widetilde{\boldsymbol{q}}$ governed by a known probability distribution $\mathbb{Q}$. The objective is to find a route set that satisfies all vehicle capacities with high probability. Thus, we replace the capacity constraints $\boldsymbol{R} \in \mathcal{R}(\boldsymbol{q})$ of the deterministic CVRP with the probabilistic capacity constraints $\mathbb{Q}\left[\boldsymbol{R} \in \mathcal{R}(\widetilde{\boldsymbol{q}})\right] \geqslant 1 - \epsilon$, where $\epsilon \in (0, 1)$ represents a prescribed tolerance for capacity violations. Note that the chance constrained VRP reduces to a deterministic CVRP if $\mathbb{P} = \delta_{\boldsymbol{q}}$, where $\delta_{\boldsymbol{q}}$ denotes the Dirac distribution that places unit mass on the demand realization $\widetilde{\boldsymbol{q}} = \boldsymbol{q}$.

The vehicle routing problem under uncertainty has become a major area of research, and draws large investments from logistics behemoths such as Amazon. The stochastic optimization community has contributed significantly to this area. However, most of the literature assumes that the uncertain parameters are independent and belong to a known probability distribution. We show in Chapter 2 the limitations of these assumptions in practice. There have been efforts made to solve the chance constrained VRP, but the scalability of the solution algorithms has remained limited. Chapter 2 of this thesis aims to alleviate the above problems and create more scalable algorithms using distributionally robust optimization to solve the chance constrained CVRP. To the best of our knowledge, this is the first attempt to address the gap in literature identified above.

In Chapter 2, the probability distribution governing the uncertain customer demands are modeled to belong to an ambiguity set. The chance constrained CVRP requires the feasibility of a route with a probability of at least $1 - \epsilon$ where $0 < \epsilon < 1$ denotes the risk tolerance of the route planner. We show that when the ambiguity set satisfies a subadditivity condition the distributionally robust CVRP can be solved using algorithms that scale favorably and can be implemented using off-the-shelf commercial solvers. Additionally, this subadditivity condition is satisfied by a wide range of ambiguity sets called the *moment ambiguity sets*. For a large class of moment ambiguity sets, we show that the distributionally robust chance constrained CVRP can be solved without much undue overhead over their deterministic counterparts.

In Chapter 2, the distributionally robust chance-constrained CVRP is shown to be equivalent to the distributionally robust CVRP under value-at-risk, which is popularly used risk measure in areas such as finance and energy management. Moreover, Chapter 2 focused exclusively on solving the distributionally robust CVRP under the moment ambiguity set. This led to the question of efficiently solving the distributionally robust CVRP under combinations of various ambiguity sets and risk measures. Additionally, could the same solution framework be applied to other variants of distributionally robust VRP apart from CVRP. While there have been attempts made to study the ditributionally robust VRP under some specific risk measures/ indices and ambiguity sets, there has been no attempt made so far towards a general study of the distributionally robust VRP under different risk measures and ambiguity sets. Chapter 3 aims to address these gaps in literature.

Chapter 3 considers an abstract definition of the vehicle routing problem, and derives necessary and sufficient conditions that a VRP instance must satisfy in order to be solvable by the 2VF formulation, which is the most commonly used mathematical model for VRP. These models can be solved efficiently using algorithms similar to ones developed in Chapter 2 and enjoying similar scalable properties. The generic consideration of the VRP allows us to solve the distributionally robust CVRP under different combinations of risk measures or disutility functions combined with complete or partial characterizations of the probability distribution governing the uncertain customer demands.

1.3.2 Healthcare Optimization

While Chapter 2 and Chapter 3 are concerned with solving the single-stage optimization problem under uncertainty, in the last chapter of the thesis we focus on the multi-stage optimization problem under uncertainty. Dynamic programming offers a rich formulation to model a multi-stage decision making problem under uncertainty. However, the solution algorithms scale poorly due to the curse of dimensionality. Chapter 4 aims to alleviate this shortcoming and derive a fluid approximation that lends itself to be solved via a linear program that scales favorably in the problem dimensions.

The first wave of COVID-19 in England challenged the healthcare system, and gave rise to a variety of decision-making problems under uncertainty. Healthcare operations management has been a major research area since the 1970s. Problems in this area are difficult because: (i) they require modeling of complex systems, (ii) they are affected by uncertainty, and (iii) they have multiple competing objectives such as reducing mortality while keeping costs low. However, there were not enough papers in this field to deal with the unprecedented surge in hospital care demand as was seen during COVID-19. Moreover, most papers focused on individual hospitals, rather than the entire healthcare system of a country that came under crumbling pressure during COVID-19 waves.

Motivated by the above gaps in literature, Chapter 4 aims to answer the problem of optimal scheduling of patients when the total demand for hospital care in a healthcare system far exceeds its capacity. We develop and apply the dynamic programming formulation as described earlier to the large-scale setting of NHS England.

Each patient is modeled as a dynamic program wherein the states encode the patient's health and treatment condition, the actions denote the available treatment options, the transition probabilities characterize the stochastic evolution of a patient's health, and finally the rewards are indicative of the contribution to the overall objectives of the health system. Moreover, each dynamic program is linked to the others via the common healthcare resources that they share. We characterize this problem using the concept of weakly coupled dynamic programs and obtain near optimal solutions using the fluid approximation that we mentioned earlier.

The optimization-based prioritization scheme schedules patients into general & acute as well as critical care to minimize the overall years of life lost (YLL)[1], hospital costs or a combination of both objectives. We consider the healthcare system at the national-level scale (rather than an individual hospital) in order to inform strategic public health policy-making. To the best of our knowledge, this is the largest application of the weakly coupled dynamic programming approach to a real life problem.

1.4 Structure of Thesis

This thesis aims to develop theoretical models and solution methods to address the challenges identified in the previous section in the field of vehicle routing and scheduling of elective patients in a healthcare system.

Apart from conclusions in Chapter 5, the thesis is divided into three chapters. The first two chapters investigate the vehicle routing problem, while the third chapter deals with the problem of scheduling elective patients in a healthcare system. In the remaining of this section, each of these chapters is summarized.

In Chapter 2, contrary to the classical CVRP, which assumes that the customer demands are deterministic, we model the demands as a random vector whose distribution is only known to belong to an ambiguity set. We require the delivery schedule to be feasible with a probability of at least $1 - \epsilon$, where ϵ characterizes the risk tolerance of the decision maker. We show that the emerging distributionally robust CVRP can be solved efficiently with standard branch-and-cut algorithms whenever the ambiguity set satisfies a subadditivity condition. We then show that this subadditivity condition holds for a large class of moment ambiguity sets. We derive efficient cut generation schemes for ambiguity sets that specify the support as well as (bounds

[1]YLL quantifies the years of life lost due to premature deaths, accounting for the age at which deaths occur.

on) the first and second moments of the customer demands. The contents of this chapter are published in

1. S. Ghosal and W. Wiesemann. *The Distributionally Robust Chance Constrained Vehicle Routing Problem.* Operations Research 68(3):716-732, 2020.

In Chapter 3, we propose a generic model for the single-stage CVRP under demand uncertainty. By combining risk measures or disutility functions with complete or partial characterizations of the probability distribution governing the demands, our formulation bridges the popular but often independently studied paradigms of stochastic programming, robust and distributionally robust optimization. We characterize when an uncertainty-affected CVRP is (not) amenable to a solution via a branch-and-cut scheme, and we elucidate how this solvability relates to the interplay between the employed decision criterion and the available description of the uncertainty. Our framework offers a unified treatment of several CVRP variants from the recent literature, such as formulations that optimize the requirements violation or the essential riskiness indices, while at the same time it allows us to study new problem variants, such as formulations that optimize the distributionally robust expected disutility over Wasserstein or ϕ-divergence ambiguity sets. All of our formulations can be solved by the same branch-and-cut algorithm with only minimal adaptations, which makes them attractive for practical implementations. The contents of this chapter will form the following paper:

2. S. Ghosal, C.P. Ho and W. Wiesemann. *A Unifying Framework for the Capacitated Vehicle Routing Problem under Risk and Ambiguity.* Submitted to Operations Research.

In Chapter 4, we propose a nation-wide prioritization scheme that models each individual patient as a dynamic program whose states encode the patient's health and treatment condition, whose actions describe the available treatment options, whose transition probabilities characterize the stochastic evolution of the patient's health and whose rewards encode the contribution to the overall objectives of the health system. The individual patients' dynamic programs are coupled through constraints on the available resources, such as hospital beds, doctors and nurses. We show that near-optimal solutions to the emerging weakly coupled counting dynamic program can be found through a fluid approximation that gives rise to a linear program whose size grows gracefully in the problem dimensions. We present a case study for the National Health Service in England to show the usefulness of our approach in saving lives and reducing costs. The contents of this chapter are split to form the following two publications:

3. J.C. D'Aeth, S. Ghosal, F. Grimm, et al. *Optimal National Prioritization Policies for Hospital Care during the SARS-CoV-2 Pandemic.* Nature Computational Science, doi: `https://doi.org/10.1038/s43588-021-00111-1`.

4. J.C. D'Aeth, S. Ghosal, F. Grimm, et al. *Optimal Hospital Care Scheduling During the SARS-CoV-2 Pandemic.* Available on Optimization Online `http://www.optimization-online.org/DB_HTML/2021/02/8261.html`. (Under minor revision at Management Science.)

Chapter 2

The Distributionally Robust Chance Constrained Vehicle Routing Problem

2.1 Introduction

In this chapter, we study single-stage decision making problems under uncertainty. Specifically, we focus on developing models and solution algorithms for the vehicle routing problem under uncertainty.

In Chapter 1, we motivated the importance of studying vehicle routing problems under uncertainty. In this chapter we review the various methods that have been applied to solve the vehicle routing problem under uncertainty. We discuss the limitations of stochastic programming, chance-constrained programming and robust optimization approaches to this problem. In an attempt to alleviate the identified challenges, we study the distributionally robust chance constrained CVRP, which assumes that the customer demands follow a probability distribution that is only partially known, and it imposes chance constraints on the vehicles' capacities for all distributions that are deemed plausible in view of the available information. There have been limited efforts to extensively study this problem through the lens of distributionally robust chance constraints in literature so far. We argue that this formulation can offer an attractive trade-off between the properties of the classical chance constrained CVRP and the robust

CVRP, introduced in Chapter 1. By replacing a single probability distribution with a set of plausible distributions, the distributionally robust chance constrained CVRP relieves the decision maker of estimating the entire joint demand distribution for all customers, and it replaces computationally intractable operations on probability distributions with efficiently solvable optimization problems. Likewise, since the distributionally robust chance constrained CVRP does not abandon probability distributions altogether, it can determine delivery schedules that are less conservative than those of the robust CVRP.

We aim to contribute to a deeper understanding of both the structural properties and the solution of the distributionally robust chance constrained CVRP. We show that the rounded capacity inequalities (RCIs), a popular class of cutting planes for the deterministic CVRP, can be adapted to the distributionally robust chance constrained CVRP whenever the underlying ambiguity set satisfies a subadditivity property. While several classes of popular ambiguity sets, such as ϕ-divergence [HH13, JG18] and Wasserstein [EK18, ZG18] ambiguity sets, violate this subadditivity property, the condition holds for a wide class of moment ambiguity sets [EOO03, DY10]. Motivated by this insight, we study marginal moment ambiguity sets, which characterize each customer demand individually, and generic moment ambiguity sets, which also describe the interactions between different customer demands. We find that the distributionally robust chance constrained CVRP over a marginal moment ambiguity set reduces to a deterministic CVRP with altered customer demands. The same problem over a generic moment ambiguity set, on the other hand, does not have an equivalent reformulation as a deterministic CVRP in general. We present RCI separation procedures for two classes of generic moment ambiguity sets. Our numerical experiments indicate that contrary to the deterministic CVRP, which appears to be best solved with branch-and-cut-and-price schemes, branch-and-cut algorithms may be competitive for the distributionally robust chance constrained CVRP.

More succinctly, the contributions of this chapter are summarized as follows.

1. We show that whether or not the distributionally robust chance constrained CVRP can be solved with a standard branch-and-cut scheme depends on the presence or absence of a subadditivity property in the employed ambiguity set. We prove that this subadditivity

property is present in a wide class of moment ambiguity sets.

2. We show that for marginal moment ambiguity sets, the distributionally robust chance constrained CVRP reduces to a deterministic CVRP with altered customer demands. We derive these demands for various classes of marginal moment ambiguity sets, and we describe the associated worst-case demand distributions in closed form.

3. We develop cut separation schemes for different classes of generic moment ambiguity sets, and we show that the associated worst-case distributions can be determined *a posteriori* through the solution of tractable optimization problems.

The intimate connection between the applicability of branch-and-cut schemes and the subadditivity of ambiguity sets appears to have implications well beyond the CVRP, and we believe that this relationship deserves further study in the wider context of distributionally robust optimization.

The remainder of this chapter is organized as follows. Section 2.2 covers literature review, and Section 2.3 introduces and motivates the distributionally robust chance constrained CVRP. Section 2.4 shows that the problem can be solved with branch-and-cut schemes whenever the ambiguity set satisfies a subadditivity condition, and that this subadditivity condition holds for a wide class of moment ambiguity sets. Section 2.5 studies the properties of marginal and generic moment ambiguity sets in 2.5.1 and 2.5.1 respectively. We present our numerical results in Section 2.6, and we offer concluding remarks in Section 2.7. The source code of the proposed branch-and-cut algorithm is available online at `http://wp.doc.ic.ac.uk/wwiesema/sourcecodes/`.

Notation. We denote scalars and vectors by regular and bold lowercase letters, whereas bold uppercase letters are reserved for matrices. The vectors $\mathbf{e}$ and $\mathbf{0}$ refer to the vectors of all ones and all zeros, respectively, while $\mathbf{e}_i$ is the i-th basis vector. For a set $A \subseteq \{1, \ldots, n\}$, the vector $\mathbf{1}_A \in \{0,1\}^n$ satisfies $(\mathbf{1}_A)_i = 1$ if and only if $i \in A$. We define the conjugate of a real-valued function $f : \mathbb{R}^n \mapsto \mathbb{R}$ by $f^\star(\boldsymbol{y}) = \sup\{\boldsymbol{y}^\top \boldsymbol{x} - f(\boldsymbol{x}) \, : \, \boldsymbol{x} \in \mathbb{R}^n\}$.

2.2 Literature Review

The classical CVRP assumes that the customer demands are known precisely. This assumption is frequently violated in pickup problems such as residential waste collection, where the amount of waste to be collected is only known when the vehicle has arrived at an individual household. The customer demands are also often uncertain in delivery problems. Internet retailers, online groceries and delivery companies tend to use simplified models to estimate the vehicle space consumed by each customer order (which can itself consist of multiple heterogeneous products). The cumulative space consumed by all customer orders assigned to a vehicle thus becomes an uncertain quantity which depends on the shapes of the involved products, the employed stacking configuration, operational loading constraints as well as the packing skills of the staff involved.

The CVRP with uncertain customer demands is typically solved as a two-stage stochastic program or as a chance constrained program [GLS96, CLSV06, TV14]. In the two-stage version, a tentative delivery schedule is selected here-and-now, that is, before the uncertain customer demands are known, and the routes can be modified through a recourse decision once the customer demands have been observed (*e.g.*, penalty payments for unsatisfied demands, [SG83], detours to the depot, [DT86] and [BSL96], or preventative restocking, [YMB00]). The chance constrained CVRP, which we focus on in this chapter, does not allow for any modification of the selected vehicles routes. Instead, it requires the vehicle routes to be feasible with a high, pre-specified probability. While being more restrictive than the two-stage model, the chance constrained CVRP can lead to simpler optimization problems, and it may be favored due to its planning stability.

Although the chance constrained CVRP reduces to a deterministic CVRP in special cases, *e.g*, when the demands are independent and identically distributed [GY79, DLL93], the problem is typically solved with tailored branch-and-cut methods [LLM92]. The vast majority of exact solution methods for the chance constrained CVRP assume that the customer demands are independent. A notable exception is [DFL18], who develop a branch-and-cut-and-price scheme for the chance constrained CVRP under the assumption that the customer demands follow either a joint normal distribution or a given discrete distribution.

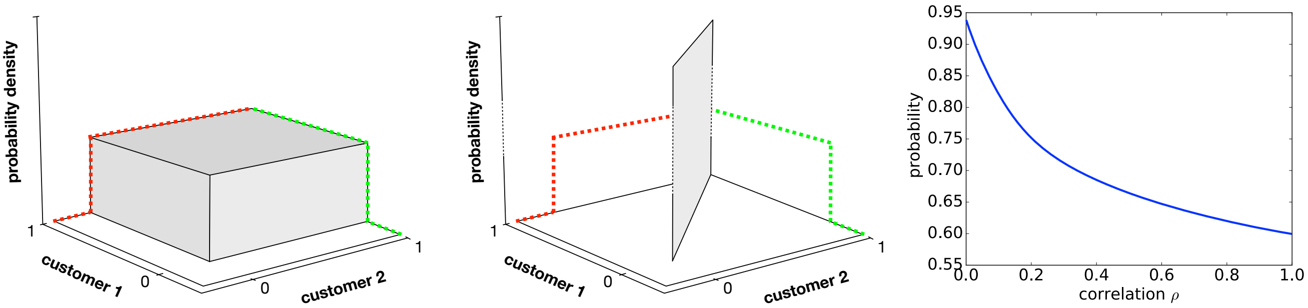

Figure 2.1: Chance constrained CVRP instance with uniformly distributed marginal customer demands (dotted lines) that are combined through a Gaussian copula. The left and middle graphs illustrate projections of the probability density functions corresponding to the correlations $\rho = 0$ and $\rho = 1$ onto two customers, respectively, and the right graph presents the probabilities of satisfying the vehicle's capacity for all 20 customers.

Although modeling the customer demands as a random vector that is governed by a known distribution is intuitively appealing, the practicability of the chance constrained CVRP is challenged in three ways: *(i)* most of the solution schemes for chance constrained CVRPs require the customer demands to be independent; *(ii)* merely establishing the (in-)feasibility of a fixed route plan can already be challenging from a computational perspective; and *(iii)* estimating the customer demand distribution from historical records may require unrealistically large amounts of data. In the following, we discuss each of these challenges in turn.

Example 2.1 (Independence) *Consider a chance constrained CVRP instance where a single vehicle of capacity $Q = 12$ serves the customers $V_C = \{1, \ldots, 20\}$. The marginal distribution of each customer's demand is a uniform distribution over the interval $[0, 1]$. We model the dependence between the customer demands via a Gaussian copula. The left and the middle graph in Figure 2.1 visualize the joint demand distribution for two customers when their demands are independent (correlation $\rho = 0$) and perfectly dependent (correlation $\rho = 1$), respectively. The right graph in Figure 2.1 visualizes the probability $\mathbb{Q}\big[\sum_{i \in V_C} \widetilde{q}_i \leqslant Q\big]$ of satisfying the capacity restriction of the vehicle for varying levels of demand dependence. While 20 customers with independently distributed demands can be served with a high probability of approximately 0.95, this probability decreases to 0.6 for perfectly correlated (comonotone) demands. We thus conclude that it is crucial to model demand dependencies that may be present in the problem instance.*

For a branch-and-cut-and-price algorithm for the chance constrained CVRP that does not require independent customer demands, we refer to [DFL18].

Example 2.2 (Complexity) *Consider a chance constrained CVRP instance where the customer demands are uniformly distributed over a hyperrectangle* $[\underline{\boldsymbol{q}}, \overline{\boldsymbol{q}}]$ *with* $\underline{\boldsymbol{q}}, \overline{\boldsymbol{q}} \in \mathbb{R}^n_+$. *In this case, evaluating the probability* $\mathbb{Q}\big[\sum_{i \in \boldsymbol{R}} \tilde{q}_i \leqslant Q\big]$ *of satisfying the capacity of a vehicle is tantamount to calculating the volume of the knapsack polytope, which is known to be #P-hard [DS06, HKW16]. This is problematic for exact solution schemes, which typically rely on the repeated evaluation of the feasibility of candidate routes to determine an optimal route set.*

We note that if the customer demands follow a multivariate normal distribution, then the cumulative demand along a candidate route is also normally distributed. In this case, the satisfaction of the corresponding vehicle's capacity reduces to evaluating the inverse cumulative distribution function of a standard normal distribution, which can be done efficiently. Moreover, by invoking a central limit theorem, a similar argument can be made for non-normally distributed customer demands as long as *(i)* the customer demands are (sufficiently) independent and *(ii)* each vehicle serves sufficiently many customers (with 30 being a common quote in the literature).

Example 2.3 (Estimation) *Consider a chance constrained CVRP instance where three vehicles of capacity* $Q = 10$ *serve the customer set* $V_C = \{1, \ldots, 8\}$. *The expected customer demands are* $\boldsymbol{\mu} = (3, 5, 2, 5, 1, 6, 1, 1)^\top$, *and each customer demand* $\tilde{q}_i$ *follows an independent uniform distribution supported on* $[(2/3)\mu_i, (4/3)\mu_i]$. *The left part of Figure 2.2 shows the route set which is feasible at the tolerance* $\epsilon = 0.05$ *since the vehicles' capacities are satisfied with probability* 0.97, 0.98 *and* 0.97, *respectively. (For ease of illustration, we have duplicated the depot in the figure.) In practice, the true distribution* $\mathbb{Q}$ *of the customer demands is typically unknown. In this case, the literature often suggests to replace the unknown true distribution* $\mathbb{Q}$ *with the empirical distribution* $\mathbb{Q}^\nu = \frac{1}{\nu} \sum_\ell \delta_{\boldsymbol{q}^\ell}$, *where* $\boldsymbol{q}^1, \ldots, \boldsymbol{q}^\nu$ *denote historical observations of the customer demands under the distribution* $\mathbb{Q}$; *this approach is often referred to as 'sample average approximation' in the stochastic programming literature [SDR14]. The right part of Figure 2.2*

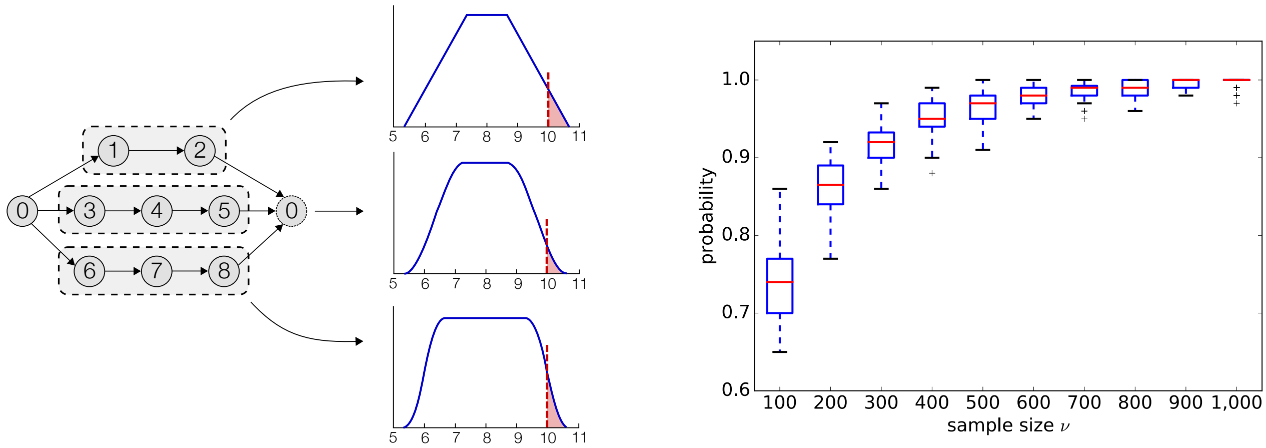

Figure 2.2: Chance constrained CVRP instance with independent and uniformly distributed customer demands. The three graphs in the middle visualize the true probability density functions of the cumulative customer demands, which correspond to generalized Irwin-Hall distributions, for the three routes on the left. The graph on the right shows the likelihood of the route set on the left being feasible if we replace the true distribution with an empirical distribution $\mathbb{Q}^\nu$ of varying sample size ν. The box-and-whisker plots report the ranges and the quartiles of 1,000 statistically independent sets of samples.

*shows the likelihood of the same route set being feasible (*i.e.*, satisfying the capacity constraints* $\mathbb{Q}^\nu\big[\tilde{q}_1 + \tilde{q}_2 \leqslant 10\big] \geqslant 0.95$, $\mathbb{Q}^\nu\big[\tilde{q}_3 + \tilde{q}_4 + \tilde{q}_5 \leqslant 10\big] \geqslant 0.95$ *and* $\mathbb{Q}^\nu\big[\tilde{q}_6 + \tilde{q}_7 + \tilde{q}_8 \leqslant 10\big] \geqslant 0.95$*) if we replace the unknown true distribution* $\mathbb{Q}$ *with the empirical distribution* $\mathbb{Q}^\nu$ *resulting from different sample sizes* ν*. We observe that despite the small number of customers and vehicles,* $\nu \geqslant 800$ *samples are required for the route set to be feasible under the chance constraints corresponding to the empirical distribution* $\mathbb{Q}^\nu$ *with a confidence of* 0.99.

The aforementioned shortcomings of the chance constrained CVRP can to some degree be addressed by the robust CVRP, which abandons probability distributions and instead requires the vehicle routes to be feasible for all customer demands within a pre-specified uncertainty set (*e.g.*, a box, polyhedron or ellipsoid). The robust CVRP is amenable to solution schemes that appear to scale better than those for the chance constrained CVRP. However, the solutions obtained from the robust CVRP can be overly conservative since all demand scenarios within the uncertainty set are treated as equally likely, and the routes are selected solely in view of the worst demand scenario from the uncertainty set. Furthermore, the shape of the uncertainty set is often selected *ad hoc*, and it remains unclear how this set should be calibrated to historical demand data that may be available in practice. Branch-and-cut schemes for the exact solution of the robust CVRP have been proposed by [SO08] and [GWF13b].

While distributionally robust chance constraints have been considered for other problem classes (see, *e.g.*, the reviews by [BTN01], [Nem12] and [HRKW15]) and other classes of distributionally robust models have been proposed for variants of the vehicle routing problem (see, *e.g.*, [CD13], [AJ16], [JQS16], [CBM18], [FBJ18] and [ZBST18]), the only treatment of the distributionally robust chance constrained CVRP appears to be in the electronic companion of [GWF13b] and in Section 4 of [DFL18]. [GWF13b] approximate a particular class of distributionally robust chance constrained CVRPs by a robust CVRP and solve instances with up to 23 customers using a standard branch-and-bound scheme, which limits the scalability of their solution algorithms. [DFL18] adapt their branch-and-cut-and-price scheme for the classical chance constrained CVRP to a distributionally robust chance constrained CVRP where the uncertain customer demands are characterized by their means and covariances. Under this assumption, the probability of satisfying a vehicle's capacity can be derived by replacing the unknown demand distribution with a normal distribution of the same mean and covariances if the risk tolerance ϵ is adjusted accordingly. Thus, the approach proposed in [DFL18] applies only to a very special set of distributionally robust chance constrained CVRP. In this chapter, we aim to address both the gaps in literature identified above, by developing a framework that applies to a more general class of distributionally robust chance constrained CVRP, and build solution algorithms that scale better than the previous approaches.

For a review of the vast literature on the CVRP, we refer the reader to [CLSV06], [GRW08], [Lap09] and [TV14].

2.3 Problem Formulation

We consider a complete and directed graph $G = (V, A)$ with nodes $V = \{0, \ldots, n\}$ and arcs $A = \{(i, j) \in V \times V : i \neq j\}$. The node $0 \in V$ represents the unique depot, and the nodes $V_C = \{1, \ldots, n\} \subset V$ denote the customers. The depot is equipped with m homogeneous vehicles of capacity $Q \in \mathbb{R}_+$, which we index through the set $K = \{1, \ldots, m\}$. Each vehicle incurs transportation costs of $c(i,j) \in \mathbb{R}_+$ if it traverses the arc $(i,j) \in A$. Throughout the chapter, we allow for asymmetric transportation costs. As is standard in the literature, our models simplify if the transportation costs satisfy $c(i,j) = c(j,i)$ for all $(i,j) \in A$; see, *e.g.*, [STV14].

We denote by $\mathfrak{P}(V_C, m)$ the set of all (ordered) partitions of the customer set V_C into m mutually disjoint and collectively exhaustive (ordered) routes $\boldsymbol{R}_1, \ldots, \boldsymbol{R}_m$:

$$\mathfrak{P}(V_C, m) = \left\{ (\boldsymbol{R}_1, \ldots, \boldsymbol{R}_m) \,:\, \boldsymbol{R}_k \neq \emptyset \;\; \forall k, \;\; \boldsymbol{R}_k \cap \boldsymbol{R}_l = \emptyset \;\; \forall k \neq l, \;\; \bigcup_k \boldsymbol{R}_k = V_C \right\}$$

In this definition, each route $\boldsymbol{R}_k = (R_{k,1}, \ldots, R_{k,n_k})$ is an ordered list, where $R_{k,l} \in V_C$ is the l-th customer and n_k the total number of customers visited by vehicle $k \in K$. With a slight abuse of notation, we apply set operations to routes whenever the interpretation is clear. We also refer to the collection of routes $\boldsymbol{R}_1, \ldots, \boldsymbol{R}_m$ as the route set $\mathbf{R}$.

The *distributionally robust chance constrained CVRP* is defined as:

$$\begin{aligned} &\text{minimize} && c(\mathbf{R}) \\ &\text{subject to} && \mathbb{P}\left[\boldsymbol{R}_k \in \mathcal{R}(\widetilde{\boldsymbol{q}})\right] \geqslant 1 - \epsilon \qquad \forall \mathbb{P} \in \mathcal{P}, \; \forall k \in K \\ &&& \mathbf{R} \in \mathfrak{P}(V_C, m) \end{aligned} \tag{RVRP($\mathcal{P}$)}$$

In this problem, the ambiguity set $\mathcal{P}$ contains all distributions that are deemed plausible for governing the random demand vector $\widetilde{\boldsymbol{q}}$. In particular, if the unknown true distribution $\mathbb{Q}$ is contained in $\mathcal{P}$, then any feasible solution to RVRP($\mathcal{P}$) is guaranteed to satisfy each vehicle's capacity constraint with a probability of at least $1 - \epsilon$ under $\mathbb{Q}$, that is, the corresponding route set is feasible in the chance constrained CVRP with the unknown true distribution $\mathbb{Q}$. Note that RVRP($\mathcal{P}$) reduces to a deterministic CVRP if $\mathcal{P} = \{\delta_{\boldsymbol{q}}\}$, to a robust CVRP if $\mathcal{P} = \{\delta_{\boldsymbol{q}} \,:\, \boldsymbol{q} \in \mathcal{Q}\}$ and to a chance constrained CVRP if $\mathcal{P} = \{\mathbb{Q}\}$. In the remainder of the chapter, we use the terms 'distributionally robust chance constrained CVRP', 'distributionally robust CVRP' and 'RVRP($\mathcal{P}$)' interchangeably.

As we will see in the following, the distributionally robust CVRP simultaneously addresses all three of the challenges mentioned for chance constrained CVRP in Chapter 1: *(i)* it caters for dependent customer demands through ambiguity sets that contain both independent and dependent demand distributions; *(ii)* for large classes of ambiguity sets, the (in-)feasibility of a fixed route set can be established in polynomial time; and *(iii)* since an ambiguity set only characterizes certain properties of the unknown true distribution $\mathbb{Q}$, its estimation requires less data and can often be done using historical records.

At this stage it is worth pointing out the potential *shortcomings* of the distributionally robust CVRP. Firstly, the tractability of RVRP($\mathcal{P}$) crucially depends on the shape of the ambiguity set $\mathcal{P}$. As we will see in the remainder of the chapter, some intuitively appealing ambiguity sets lead to tractable reformulations, whereas others do not. Secondly, since the ambiguity set $\mathcal{P}$ only characterizes certain properties of the unknown true distribution $\mathbb{Q}$, it may contain other distributions that are unlikely to govern the customer demands $\widetilde{\boldsymbol{q}}$ but that still need to be considered in the vehicles' capacity constraints in RVRP($\mathcal{P}$). Finally, and closely related, the worst-case distribution $\inf_{\mathbb{P} \in \mathcal{P}} \mathbb{P}\big[\boldsymbol{R}_k \in \mathcal{R}(\widetilde{\boldsymbol{q}})\big]$ minimizing the probability of the k-th vehicle's capacity constraint being satisfied is typically a pathological distribution that is unlikely to be encountered in practice. In fact, we will see that for the classes of ambiguity sets considered in this chapter, one can construct worst-case distributions that are supported on two demand realisations only. The aforementioned shortcomings are intrinsic to the distributionally robust optimization methodology and are not specific to the distributionally robust CVRP. We emphasize that despite these weaknesses, distributionally robust optimization has been successfully applied in many diverse application areas, ranging from finance [GI03] and energy systems [ZJ18] to communication networks [LSM14] and healthcare [MQZ$^+$15]. We therefore believe that the distributionally robust CVRP serves as a complement to the existing modeling paradigms for the CVRP under uncertainty, such as the robust CVRP and the chance constrained CVRP. In particular, the most appropriate formulation for a specific application may depend on a variety of factors, such as runtime and scalability requirements, the acceptable degree of conservatism and the availability of historical records, and it ultimately needs to be decided upon by the domain expert.

Remark 2.4 (Joint Chance Constrained CVRP) *Following the conventions of the vehicle routing literature, we consider* individual *chance constraints. Instead, one could consider a* joint *chance constraint, where the individual capacity requirements* $\mathbb{P}[\boldsymbol{R}_k \in \mathcal{R}(\widetilde{\boldsymbol{q}})] \geqslant 1-\epsilon$, $k \in K$, *are replaced with a single joint capacity requirement* $\mathbb{P}[\boldsymbol{R}_k \in \mathcal{R}(\widetilde{\boldsymbol{q}}) \;\; \forall k \in K] \geqslant 1-\epsilon$. *The individual chance constraints provide a guarantee for each individual route (and hence, for every customer along that route), whereas the joint chance constraint offers a guarantee for the entire route plan. Since joint chance constrained optimization problems are typically much more challenging from a computational perspective (see,* e.g., *[HRKW17] and [XA18]), we will focus on the individually chance constrained CVRP throughout this chapter.*

The distributionally robust CVRP enforces chance constraints for each route $\boldsymbol{R}_k$ with respect to all probability distributions $\mathbb{P} \in \mathcal{P}$, of which there could be uncountably many. It is therefore not *a priori* clear how RVRP($\mathcal{P}$) can be solved numerically. In the following, we show that under certain conditions, RVRP($\mathcal{P}$) is equivalent to a two-index vehicle flow (2VF) formulation of the form

$$
\begin{array}{lll}
\text{minimize} & \displaystyle\sum_{(i,j)\in A} c(i,j)\, x_{ij} & \\
\text{subject to} & \displaystyle\sum_{\substack{j\in V:\\(i,j)\in A}} x_{ij} = \sum_{\substack{j\in V:\\(j,i)\in A}} x_{ji} = \delta_i & \forall i \in V \\
& \displaystyle\sum_{i\in V\setminus S}\sum_{j\in S} x_{ij} \geqslant d_{\mathcal{P}}(S) & \forall S \subseteq V_C,\ S \neq \emptyset \\
& x_{ij} \in \{0,1\} & \forall (i,j) \in A,
\end{array}
\qquad (2\text{VF}(\mathcal{P}))
$$

where $\delta_i = 1$ for $i \in V_C$ and $\delta_0 = m$, and the demand estimator $d_{\mathcal{P}} : 2^{V_C} \mapsto \mathbb{R}_+$ maps subsets of the customer set V_C to the non-negative real line. In this formulation, we have $x_{ij} = 1$ if and only if one of the m vehicles traverses the arc $(i,j) \in A$. The objective function minimizes the overall transportation costs across all vehicles. The first constraint set ensures that each customer is visited by exactly one vehicle, and that m vehicles leave and return to the depot. The second constraint set is commonly referred to as rounded capacity inequalities (RCIs), and they ensure that the vehicles' capacity constraints are met and that every route contains the depot node.

For a fixed set S of customers, the left-hand side of the associated RCI represents an upper bound on the number of vehicles entering S (since some vehicles may enter S several times). Thus, the demand estimator $d_{\mathcal{P}}(S)$ on the right-hand side of the RCI has to provide a (sufficiently tight) lower bound on the number of vehicles required to serve the customers in S. Since there are exponentially many RCIs, they are typically introduced iteratively as part of a branch-and-cut scheme. 2VF($\mathcal{P}$) is one of the most well-studied formulations for the CVRP, and a large number of branch-and-cut schemes have been designed for its solution (see, *e.g.*, [LLE04] and [STV14]). Thus, if we can show that RVRP($\mathcal{P}$) is equivalent to 2VF($\mathcal{P}$) for some demand estimator $d_{\mathcal{P}}$, then we can solve RVRP($\mathcal{P}$) as long as we can evaluate $d_{\mathcal{P}}$ quickly.

For the deterministic CVRP, a popular choice for the demand estimator is $\left\lceil \frac{1}{Q} \sum_{i \in S} q_i \right\rceil$, which represents the minimum number of vehicles required to serve S if the deliveries could be split continuously across vehicles, rounded up to the next integer number. It has been shown that this lower bound is sufficiently tight to ensure that the capacity constraint of each vehicle is met by any feasible solution to the corresponding 2VF formulation [LND85]. Moreover, this demand estimator eliminates short cycles that do not contain the depot node as long as the customer demands satisfy $\boldsymbol{q} > \mathbf{0}$ component-wise. Although tighter RCIs could in principle be obtained through the solution of bin packing problems, the increased strength of the cuts typically does not justify the additional computational effort required to evaluate the demand estimator.

To quantify the number of vehicles required to serve a customer set S in the distributionally robust CVRP, we define the value-at-risk of a random variable $\tilde{X}$ governed by the distribution $\mathbb{Q}$ as

$$\mathbb{Q}\text{-VaR}_{1-\epsilon}\big[\tilde{X}\big] = \inf\left\{x \in \mathbb{R} \,:\, \mathbb{Q}\big[\tilde{X} \leqslant x\big] \geqslant 1 - \epsilon\right\},$$

which denotes the $(1-\epsilon)$-quantile of $\tilde{X}$. Indeed, we have that

$$\mathbb{Q}\big[\tilde{X} \leqslant \tau\big] \geqslant 1 - \epsilon \quad \Longleftrightarrow \quad \mathbb{Q}\text{-VaR}_{1-\epsilon}\big[\tilde{X}\big] \leqslant \tau,$$

which in the case of the CVRP translates to

$$\mathbb{Q}\left[\boldsymbol{R}_k \in \mathcal{R}(\tilde{\boldsymbol{q}})\right] \geqslant 1-\epsilon \quad \Longleftrightarrow \quad \mathbb{Q}\Big[\sum_{i \in \boldsymbol{R}_k} \tilde{q}_i \leqslant Q\Big] \geqslant 1-\epsilon \quad \Longleftrightarrow \quad \mathbb{Q}\text{-VaR}_{1-\epsilon}\Big[\sum_{i \in \boldsymbol{R}_k} \tilde{q}_i\Big] \leqslant Q.$$

Instead of considering a single probability distribution $\mathbb{Q}$, however, RVRP($\mathcal{P}$) enforces chance constraints for *all* probability distributions $\mathbb{P} \in \mathcal{P}$. A similar reasoning as before shows that

$$\mathbb{P}\big[\tilde{X} \leqslant \tau\big] \geqslant 1-\epsilon \;\; \forall \mathbb{P} \in \mathcal{P} \quad \Longleftrightarrow \quad \mathbb{P}\text{-VaR}_{1-\epsilon}\big[\tilde{X}\big] \leqslant \tau \;\; \forall \mathbb{P} \in \mathcal{P} \quad \Longleftrightarrow \quad \sup_{\mathbb{P} \in \mathcal{P}} \mathbb{P}\text{-VaR}_{1-\epsilon}\big[\tilde{X}\big] \leqslant \tau,$$

or, in the context of our distributionally robust CVRP,

$$\begin{aligned} \mathbb{P}\left[\boldsymbol{R}_k \in \mathcal{R}(\tilde{\boldsymbol{q}})\right] \geqslant 1-\epsilon \;\; \forall \mathbb{P} \in \mathcal{P} \quad &\Longleftrightarrow \quad \mathbb{P}\Big[\sum_{i \in \boldsymbol{R}_k} \tilde{q}_i \leqslant Q\Big] \geqslant 1-\epsilon \;\; \forall \mathbb{P} \in \mathcal{P} \\ &\Longleftrightarrow \quad \sup_{\mathbb{P} \in \mathcal{P}} \mathbb{P}\text{-VaR}_{1-\epsilon}\Big[\sum_{i \in \boldsymbol{R}_k} \tilde{q}_i\Big] \leqslant Q. \end{aligned} \tag{2.1}$$

In view of the above equivalences and inspired by the RCIs for the deterministic CVRP, we are led to the following demand estimator for the distributionally robust CVRP:

$$d_{\mathcal{P}}(S) = \max\left\{\left\lceil \frac{1}{Q} \sup_{\mathbb{P} \in \mathcal{P}} \mathbb{P}\text{-VaR}_{1-\epsilon}\Big[\sum_{i \in S} \tilde{q}_i\Big]\right\rceil, 1\right\} \qquad \forall S \neq \emptyset, \tag{2.2}$$

as well as $d_{\mathcal{P}}(\emptyset) = 0$. In this expression, the supremum corresponds to the worst-case $(1-\epsilon)$-quantile of the cumulative customer demands in S (also called $(1-\epsilon)$-worst-case value-at-risk), and the division of this term by Q is supposed to provide a lower bound on the number of vehicles required to serve the customers in S. We take the maximum between this quantity (rounded up to the next integer) and 1 to ensure the elimination of short cycles. Indeed, contrary to the cumulative customer demands in the deterministic CVRP, the worst-case $(1-\epsilon)$-quantile could be zero even if no individual customer demand is deterministically zero. Similar to the deterministic RCIs, our demand estimator could in principle be tightened through the solution of a distributionally robust chance constrained bin packing problem. As in the deterministic case, however, this would usually not be attractive from a computational perspective.

2.3.1 Branch-and-Cut Algorithm

Notice that the problem 2VF($\mathcal{P}$) introduced above is an integer linear programming problem (ILP). More specifically it is a binary integer linear program.

Relaxing the ILP to an LP by removing the requirement that the decision variables need to be integral lead to solutions that may not only be suboptimal, but may also be infeasible. However, this method can provide a bound on the objective value of an ILP. Integer linear programming is an active area of research and we have many exact solution algorithms that perform well.

The branch-and-bound algorithm involves dividing the problem into subproblems (branching), and using LP-relaxation of the ILP of the subproblem to avoid enumerating the entire solution space (bounding). The bounding step is essential as branching alone would imply that the tree of all possible subproblems would grow exponentially in the number of decision variables of the model. However, the potentially large space implies that the branch-and-bound method is typically slow for large problems. This is alleviated by the branch-and-cut algorithm that introduces cuts into the branch-and-bound algorithm, that helps in reducing the search space.

The branch-and-cut algorithm requires that the model has valid inequalities that can be used as cutting planes. The added cutting planes remove fractional solutions without removing integral solutions, and thus reduce the search space for the branch-and-bound algorithm. For a problem of the form 2VF($\mathcal{P}$), the exponentially many constraints means that finding valid cuts can be extremely slow. However, the benign structure of 2VF($\mathcal{P}$) lends itself to branch-and-cut algorithm wherein the RCIs can be used as the cutting planes. The branch-and-cut algorithm begins by solving a relaxation of 2VF($\mathcal{P}$) where the RCIs are disregarded. In subsequent iterations, the RCIs are introduced iteratively as cutting planes to weed out infeasible and non-integral solutions.

There are many off-the-shelf commercial solvers that implement the branch-and-cut algorithm. In this chapter, the branch-and-cut algorihtm is implemented with the separation of RCI cuts according to the Tabu Search procedure proposed by [ABB+98]

2.4 Theoretical Contributions

One could expect RVRP($\mathcal{P}$) and 2VF($\mathcal{P}$) to be equivalent under any ambiguity set $\mathcal{P}$ as long as the demand estimator $d_{\mathcal{P}}$ is chosen as in (2.2). Unfortunately, this is *not* the case.

Example 2.5 *Consider a distributionally robust CVRP instance with* $n = 2$ *customers and* $m = 2$ *vehicles of capacity* $Q = 1$*. We define the ambiguity set for the customer demands as*

$$\mathcal{P} = \left\{ \mathbb{P} \in \mathcal{P}_0(\mathbb{R}^2) \; : \; \begin{bmatrix} \mathbb{P}(\tilde{q}_1 = 1) = 0.925, & \mathbb{P}(\tilde{q}_1 = 2) = 0.075 \\ \mathbb{P}(\tilde{q}_2 = 1) = 0.925, & \mathbb{P}(\tilde{q}_2 = 2) = 0.075 \end{bmatrix} \right\},$$

that is, each customer has a demand of 1 *(*2*) with probability* 0.925 *(*0.075*). Note that the ambiguity set does* not *specify that the customer demands are independent.*

For $\epsilon = 0.1$*, the route set* $\mathbf{R} = (\boldsymbol{R}_1, \boldsymbol{R}_2)$ *with* $\boldsymbol{R}_1 = (1)$ *and* $\boldsymbol{R}_2 = (2)$ *is feasible in RVRP(*$\mathcal{P}$*) since* $\mathbb{P}\big[\tilde{q}_i \leqslant 1\big] = 0.925 \geqslant 1 - \epsilon = 0.9$ *for* $i = 1, 2$ *and all* $\mathbb{P} \in \mathcal{P}$*. However, this route set* $\mathbf{R}$ *is infeasible in 2VF(*$\mathcal{P}$*) since it violates the RCI constraint for* $S = \{1, 2\}$*. Indeed, we have that*

$$\begin{aligned} d_{\mathcal{P}}(\{1,2\}) \;&=\; \max\left\{ \left\lceil \frac{1}{Q} \sup_{\mathbb{P} \in \mathcal{P}} \; \mathbb{P}\text{-VaR}_{1-\epsilon}\left[\tilde{q}_1 + \tilde{q}_2\right] \right\rceil, 1 \right\} \\ &\geqslant\; \mathbb{P}^\star\text{-VaR}_{1-\epsilon}\left[\tilde{q}_1 + \tilde{q}_2\right] \;=\; 3 \end{aligned}$$

since the probability distribution $\mathbb{P}^\star$ *with the dependence structure*

$$\tilde{q}_1 = \begin{cases} 2 & \textit{if } \tilde{u} \in [0, 0.075], \\ 1 & \textit{otherwise}, \end{cases} \qquad \tilde{q}_2 = \begin{cases} 2 & \textit{if } \tilde{u} \in [0.1, 0.175], \\ 1 & \textit{otherwise}, \end{cases}$$

where $\tilde{u}$ *is a uniformly distributed random variable supported on* $[0, 1]$*, is contained in* $\mathcal{P}$ *(see Figure 2.3). We thus conclude that RVRP(*$\mathcal{P}$*) and 2VF(*$\mathcal{P}$*) are* not *equivalent for this instance.*

Intuitively, the equivalence between RVRP($\mathcal{P}$) and 2VF($\mathcal{P}$) fails to hold in Example 2.5 due to the combination of two differences between the formulations. Firstly, RVRP($\mathcal{P}$) ignores the amount by which a capacity restriction is violated, whereas this amount is considered

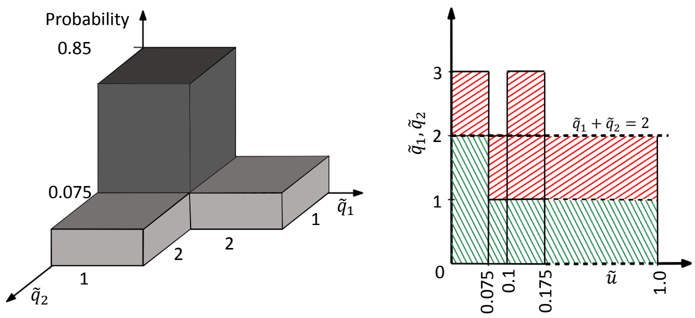

Figure 2.3: Probability distribution $\mathbb{P}^\star$ which illustrates that RVRP($\mathcal{P}$) and 2VF($\mathcal{P}$) are not equivalent. The left graph shows the probability distribution itself, whereas the right graph visualises the customer demands $\tilde{q}_1$ and $\tilde{q}_2$ as a function of the underlying random variable $\tilde{u}$ used in the construction of $\mathbb{P}^\star$.

in the demand estimator (2.2) of 2VF($\mathcal{P}$). In particular, whenever the cumulative demands within a single vehicle exceed that vehicle's capacity in Example 2.5, then the cumulative demands are so large that they could not be served by both vehicles in 2VF($\mathcal{P}$) either, even if the demands could be split continuously. Secondly, since the vehicles' capacity restrictions in Example 2.5 are violated in non-overlapping scenarios, the probability of exceeding *some* vehicle's capacity is equal to the sum of probabilities of exceeding each individual vehicle's capacity. More generally, RVRP($\mathcal{P}$) only considers the probabilities of violating each individual vehicle's capacity, whereas the demand estimator (2.2) of 2VF($\mathcal{P}$) considers the joint violation probability (under the assumption that customer demands can be split continuously).

The aforementioned differences between RVRP($\mathcal{P}$) and 2VF($\mathcal{P}$) relate to the fact that the RCIs are agnostic to the assignment of customers to vehicles, and as such they consider the interplay between demands allocated to different vehicles even though such dependencies should be ignored. To avoid this problem, the demand estimator $d_\mathcal{P}$ should not assign 'excessively large' numbers of vehicles $d_\mathcal{P}(S)$ to large customer subsets S. It turns out that this intuition can be formalized.

(**S**) **Subadditivity.** For all customer subsets $S, T \subseteq V_C$, we have $d_\mathcal{P}(S \cup T) \leqslant d_\mathcal{P}(S) + d_\mathcal{P}(T)$.

Indeed, the demand estimator in Example 2.5 violates the subadditivity condition (**S**).

Example 2.6 *For the distributionally robust CVRP instance from Example 2.5, we have*

$$\sup_{\mathbb{P}\in\mathcal{P}} \mathbb{P}\text{-VaR}_{0.9}(\tilde{q}_1) \;=\; \sup_{\mathbb{P}\in\mathcal{P}} \mathbb{P}\text{-VaR}_{0.9}(\tilde{q}_2) \;=\; 1,$$

but at the same time we have

$$\begin{aligned}\sup_{\mathbb{P}\in\mathcal{P}} \mathbb{P}\text{-VaR}_{0.9}(\tilde{q}_1+\tilde{q}_2) \;&\geqslant\; \mathbb{P}^\star\text{-VaR}_{0.9}(\tilde{q}_1+\tilde{q}_2) \;=\; 3\\ &>\; \sup_{\mathbb{P}\in\mathcal{P}} \mathbb{P}\text{-VaR}_{0.9}(\tilde{q}_1) \;+\; \sup_{\mathbb{P}\in\mathcal{P}} \mathbb{P}\text{-VaR}_{0.9}(\tilde{q}_2) \;=\; 2.\end{aligned}$$

*In other words, the demand estimator $d_{\mathcal{P}}$ violates the subadditivity condition (**S**) since*

$$d_{\mathcal{P}}(\{1\}\cup\{2\}) \;\nleqslant\; d_{\mathcal{P}}(\{1\}) \;+\; d_{\mathcal{P}}(\{2\}).$$

We now show that the condition (**S**) is sufficient for RVRP($\mathcal{P}$) and 2VF($\mathcal{P}$) to be equivalent.

Theorem 2.7 *Assume that $\widetilde{\boldsymbol{q}} \geqslant \mathbf{0}$ $\mathbb{P}$-a.s. for all $\mathbb{P}\in\mathcal{P}$ and that $d_{\mathcal{P}}$ satisfies the subadditivity condition (**S**). Then the problems* RVRP($\mathcal{P}$) *and* 2VF($\mathcal{P}$) *are equivalent in the following sense:*

(i) Any route set $\mathbf{R}$ *that is feasible in* RVRP($\mathcal{P}$) *induces a unique solution $\boldsymbol{x}$ that is feasible in* 2VF($\mathcal{P}$) *via*

$$x_{ij} = 1 \iff \exists k\in K,\ \exists l\in\{0,\dots,n_k\} \,:\, (i,j) = (R_{k,l}, R_{k,l+1}), \tag{2.3}$$

and $\boldsymbol{x}$ and $\mathbf{R}$ *attain the same transportation costs.*

(ii) Any solution $\boldsymbol{x}$ that is feasible in 2VF($\mathcal{P}$) *induces a route set* $\mathbf{R}$ *that is feasible in* RVRP($\mathcal{P}$) *via* (2.3)*, and this route set is unique up to a reordering of the individual routes $\boldsymbol{R}_1,\dots,\boldsymbol{R}_m$. Moreover, $\boldsymbol{x}$ and* $\mathbf{R}$ *attain the same transportation costs.*

Proof of Theorem 2.7. For the first statement, assume that the route set $\mathbf{R}$ is feasible in RVRP($\mathcal{P}$). We need to show that $\boldsymbol{x}$ defined through (2.3) satisfies the constraints of 2VF($\mathcal{P}$)

and attains the same transportation costs. One readily verifies that $\boldsymbol{x}$ satisfies the binarity and the degree constraints of 2VF($\mathcal{P}$). In view of the RCI constraints, we note that for any $S \subseteq V_C$, $S \neq \emptyset$, we have

$$\begin{aligned} d_{\mathcal{P}}(S) &= d_{\mathcal{P}}\Big(\bigcup_{k \in K} [\boldsymbol{R}_k \cap S]\Big) \leqslant \sum_{\substack{k \in K: \\ \boldsymbol{R}_k \cap S \neq \emptyset}} d_{\mathcal{P}}(\boldsymbol{R}_k \cap S) \leqslant \sum_{\substack{k \in K: \\ \boldsymbol{R}_k \cap S \neq \emptyset}} d_{\mathcal{P}}(\boldsymbol{R}_k) \\ &= |k \in K \, : \, \boldsymbol{R}_k \cap S \neq \emptyset| \leqslant \sum_{i \in V \setminus S} \sum_{j \in S} x_{ij}(\boldsymbol{R}), \end{aligned}$$

where the first identity follows from the fact that $\mathbf{R} \in \mathfrak{P}(V_C, m)$ and thus $\bigcup_k \boldsymbol{R}_k = V_C$, the first inequality holds because $d_{\mathcal{P}}$ is subadditive, and the second inequality is due to the fact that $\boldsymbol{R}_k \cap S \subseteq \boldsymbol{R}_k$ and $\tilde{\boldsymbol{q}} \geqslant \mathbf{0}$ $\mathbb{P}$-a.s. for all $\mathbb{P} \in \mathcal{P}$, which in turn implies that $d_{\mathcal{P}}(S) \leqslant d_{\mathcal{P}}(T)$ for all $S \subseteq T \subseteq V_C$. The second equality holds since $\mathbb{P}\left[\boldsymbol{R}_k \in \mathcal{R}(\tilde{\boldsymbol{q}})\right] \geqslant 1 - \epsilon$ for all $\mathbb{P} \in \mathcal{P}$ implies that $\sup_{\mathbb{P} \in \mathcal{P}} \mathbb{P}\text{-VaR}_{1-\epsilon}\big[\sum_{i \in \boldsymbol{R}_k} \tilde{q}_i\big] \leqslant Q$ and hence $d_{\mathcal{P}}(\boldsymbol{R}_k) = 1$. In view of the last inequality, let $j_k \in \boldsymbol{R}_k \cap S$ be the first customer on the route $\boldsymbol{R}_k$ that is contained in S, where $k \in K$ satisfies $\boldsymbol{R}_k \cap S \neq \emptyset$. By the feasibility of $\mathbf{R}$ and the definition of j_k, we have $\sum_{i \in V \setminus S} x_{ij_k}(\boldsymbol{R}) = 1$. The inequality now follows from the fact that there are $|k \in K \, : \, \boldsymbol{R}_k \cap S \neq \emptyset|$ different customer nodes j_k with this property.[1] We thus conclude that $\boldsymbol{x}$ also satisfies the RCI constraints of 2VF($\mathcal{P}$). Moreover, equation (2.3) implies that the transportation costs of $\boldsymbol{x}$ and $\mathbf{R}$ coincide.

For the second statement, we fix a feasible solution $\boldsymbol{x} \in$ 2VF($\mathcal{P}$) and construct a route set $\mathbf{R}$ satisfying (2.3) as follows. Since $\sum_{j \in V_C} x_{0j} = m$, there are $j_1, \ldots, j_m \in V_C$, $j_1 < \ldots < j_m$, such that $x_{0,j_1} = \ldots = x_{0,j_m} = 1$. For each route $\boldsymbol{R}_k$, $k \in K$, we set $R_{k,1} \leftarrow j_k$ and $n_k \leftarrow 1$. Since $\sum_{j \in V} x_{R_{k,n_k},j} = 1$, we either have $x_{R_{k,n_k},j} = 1$ for some $j \in V_C$ or $x_{R_{k,n_k},0} = 1$. In the former case, we extend route k by the customer $R_{k,n_k+1} \leftarrow j$, we set $n_k \leftarrow n_k + 1$ and we continue the procedure with customer j. In the latter case, we have completed the route $\boldsymbol{R}_k$. By construction, the resulting route set $\mathbf{R}$ satisfies (2.3). We now show that $\mathbf{R}$ is feasible in RVRP($\mathcal{P}$).

To see that $\mathbf{R} \in \mathfrak{P}(V_C, m)$, we first observe that $\boldsymbol{R}_k \neq \emptyset$ due to the existence of the customers

[1]Note that the same vehicle may enter and leave the customer set S several times, which implies that we cannot strengthen the inequality to an equality in general.

$j_1, \dots, j_m$. Moreover, the degree constraints in 2VF($\mathcal{P}$) ensure that $\boldsymbol{R}_k \cap \boldsymbol{R}_l = \emptyset$ for all $k \neq l$. It remains to be shown that $\bigcup_k \boldsymbol{R}_k = V_C$. Imagine, to the contrary, that there is a customer $j \in V_C$ such that $j \notin \bigcup_k \boldsymbol{R}_k$. By construction of the above algorithm, j must lie on a short cycle $S \subset V_C$ that is not connected to the depot node 0. Since $d_{\mathcal{P}}(S) \geqslant 1$ but $\sum_{i \in V \setminus S} \sum_{j \in S} x_{ij} = 0$, the RCI constraint corresponding to the customer set S is violated. We thus conclude that $\boldsymbol{x}$ cannot be feasible in 2VF($\mathcal{P}$), which is a contradiction.

We now show that $\mathbb{P}\left[\boldsymbol{R}_k \in \mathcal{R}(\widetilde{\boldsymbol{q}})\right] \geqslant 1 - \epsilon$ for all $\mathbb{P} \in \mathcal{P}$ and $k \in K$. By construction of the route set $\mathbf{R}$ and the feasibility of $\boldsymbol{x}$ in 2VF($\mathcal{P}$), we have $\sum_{i \in V \setminus \boldsymbol{R}_k} \sum_{j \in \boldsymbol{R}_k} x_{ij} = 1 \geqslant d_{\mathcal{P}}(\boldsymbol{R}_k)$ for all $k \in K$, and the definition of $d_{\mathcal{P}}$ then implies that $\sup_{\mathbb{P} \in \mathcal{P}} \mathbb{P}\text{-VaR}_{1-\epsilon}\big[\sum_{i \in \boldsymbol{R}_k} \tilde{q}_i\big] \leqslant Q$ and thus $\mathbb{P}\left[\boldsymbol{R}_k \in \mathcal{R}(\widetilde{\boldsymbol{q}})\right] \geqslant 1 - \epsilon$ for all $\mathbb{P} \in \mathcal{P}$.

Finally, imagine that two route sets $\mathbf{R}$ and $\mathbf{R}'$ satisfy (2.3), and that there is no reordering of the routes in $\mathbf{R}'$ that yields $\mathbf{R}$. Then there must be a customer pair $(i, j) \in V_C \times V_C$ such that (i, j) is visited by the same vehicle in immediate succession in $\mathbf{R}$ but not in $\mathbf{R}'$. This, however, violates the assumption that both $\mathbf{R}$ and $\mathbf{R}'$ satisfy (2.3), as x_{ij} would have to be both 0 and 1 in that case. We thus conclude that the route set $\mathbf{R}$ satisfying (2.3) is indeed unique up to a reordering of the individual routes $\boldsymbol{R}_1, \dots, \boldsymbol{R}_m$. ∎

According to the theorem, any ambiguity set $\mathcal{P}$ whose demand estimator $d_{\mathcal{P}}$ satisfies the subadditivity condition (**S**) allows us to use a branch-and-cut algorithm to solve 2VF($\mathcal{P}$) *in lieu* of RVRP($\mathcal{P}$). Example 2.5 has shown that the subadditivity condition may be violated if the ambiguity set $\mathcal{P}$ specifies the marginal distribution of each customer's demand. The example immediately implies that hypothesis test ambiguity sets [BGK18], which converge to ambiguity sets that exactly specify the marginal distribution of each customer's demand as the available data increases, also give rise to demand estimators that violate the subadditivity condition. Moreover, data-driven ambiguity sets, such as ϕ-divergence ambiguity sets [BTdHdW$^+$13], Wasserstein ambiguity sets [EK18] and hypothesis test ambiguity sets [BGK18], converge to singleton ambiguity sets as the available data increases, and the resulting demand estimators also violate the subadditivity condition since the involved worst-case values-at-risk converge to values-at-risk which are known to violate subadditivity.

In this chapter, we study moment ambiguity sets of the form

$$\mathcal{P} = \{\mathbb{P} \in \mathcal{P}_0(\mathbb{R}^n) \,:\, \mathbb{P}(\widetilde{\boldsymbol{q}} \in \mathcal{Q}) = 1, \;\; \mathbb{E}_{\mathbb{P}}[\widetilde{\boldsymbol{q}}] = \boldsymbol{\mu}, \;\; \mathbb{E}_{\mathbb{P}}[\boldsymbol{\varphi}(\widetilde{\boldsymbol{q}})] \leqslant \boldsymbol{\sigma}\} \,. \tag{2.4}$$

The moment ambiguity set (2.4) specifies that the uncertain customer demands $\widetilde{\boldsymbol{q}}$ are supported on a rectangular set $\mathcal{Q} = [\underline{\boldsymbol{q}}, \overline{\boldsymbol{q}}]$ with $\underline{\boldsymbol{q}} \geqslant \mathbf{0}$. It also stipulates that the expected customer demands $\mathbb{E}_{\mathbb{P}}[\widetilde{\boldsymbol{q}}]$ are known to be $\boldsymbol{\mu}$, and that the upper bounds σ_i on the demand variations $\mathbb{E}_{\mathbb{P}}[\varphi_i(\widetilde{\boldsymbol{q}})]$, $i = 1, \ldots, p$, of the customer demands are known. The demand variations are characterized by a dispersion measure $\boldsymbol{\varphi} : \mathbb{R}^n \mapsto \mathbb{R}^p$ which measures how 'stretched out' the joint probability distribution of the customer demands is. Possible choices of dispersion measures include the mean absolute deviations, $\varphi_i(\boldsymbol{q}) = |q_i - \mu_i|$, the variances $\varphi_i(\boldsymbol{q}) = (q_i - \mu_i)^2$, higher order moments $\varphi_i(\boldsymbol{q}) = |q_i - \mu_i|^q$, $q \geqslant 3$, or Huber loss functions of the customer demands $\widetilde{\boldsymbol{q}}$. We will explore different dispersion measures in Sections 2.5.1 and 2.5.2. Throughout this chapter, we make the standard regularity assumptions that $\boldsymbol{\mu} \in \operatorname{int} \mathcal{Q}$, that is, the expected demands are contained in the interior of the support $\mathcal{Q}$, that the dispersion measure $\boldsymbol{\varphi}$ is closed and component-wise convex, and that $\boldsymbol{\varphi}(\boldsymbol{\mu}) < \boldsymbol{\sigma}$. These assumptions will allow us to invoke strong convex duality, which is required for our results to hold. Moment ambiguity sets are amongst the most popular ambiguity sets studied in the distributionally robust optimization literature, see, *e.g.*, [EOO03], [DY10], [ZKR13] and [WKS14].

We now show that in contrast to ambiguity sets constructed by marginal histograms, hypothesis tests or deviation measures such as the Wasserstein distance and ϕ-divergences, moment ambiguity sets lead to demand estimators $d_{\mathcal{P}}$ that satisfy the desired subadditivity property.

Theorem 2.8 *The demand estimator $d_{\mathcal{P}}$ for moment ambiguity sets of the form* (2.4) *is subadditive.*

Please see the appendix of this chapter for the proof of Theorem 2.8.

In addition to satisfying the subadditivity condition (**S**), the distributions that minimize the probability of satisfying a vehicle's capacity requirement have a particularly simple structure if we restrict ourselves to moment ambiguity sets of the form (2.4).

Proposition 2.9 *Consider an instance of the moment ambiguity set* (2.4). *Then for any customer subset $S \subseteq V_C$, there is a sequence of two-point distributions $\mathbb{P}^t = p_1^t \cdot \delta_{\boldsymbol{q}_1^t} + p_2^t \cdot \delta_{\boldsymbol{q}_2^t} \in \mathcal{P}$, $p_1^t, p_2^t \in \mathbb{R}_+$ and $\boldsymbol{q}_1^t, \boldsymbol{q}_2^t \in \mathcal{Q}$, such that $\mathbb{P}^t\text{-VaR}_{1-\epsilon}\big[\sum_{i \in S} \tilde{q}_i\big] \longrightarrow \sup_{\mathbb{P} \in \mathcal{P}} \mathbb{P}\text{-VaR}_{1-\epsilon}\big[\sum_{i \in S} \tilde{q}_i\big]$ as $t \longrightarrow \infty$.*

Proof of Proposition 2.9. The proof of Theorem 2.8 implies that for every $\tau \geqslant \sup_{\mathbb{P} \in \mathcal{P}} \mathbb{P}\text{-VaR}_{1-\epsilon}\big[\boldsymbol{\lambda}^\top \tilde{\boldsymbol{q}}\big]$, the optimal value of the optimization problem

$$
\begin{array}{ll}
\text{maximize} & \alpha + \boldsymbol{\mu}^\top \boldsymbol{\beta} - \boldsymbol{\sigma}^\top \boldsymbol{\gamma} \\
\text{subject to} & \underline{\boldsymbol{q}}^\top \underline{\boldsymbol{\nu}}_1 - \overline{\boldsymbol{q}}^\top \overline{\boldsymbol{\nu}}_1 - \displaystyle\sum_{i=1}^{p} \gamma_i \varphi_i^\star(\boldsymbol{\phi}_{1i}/\gamma_i) \geqslant \alpha - 1 \\
& \underline{\boldsymbol{q}}^\top \underline{\boldsymbol{\nu}}_0 - \overline{\boldsymbol{q}}^\top \overline{\boldsymbol{\nu}}_0 + \tau\eta - \displaystyle\sum_{i=1}^{p} \gamma_i \varphi_i^\star(\boldsymbol{\phi}_{0i}/\gamma_i) \geqslant \alpha \\
& \displaystyle\sum_{i=1}^{p} \boldsymbol{\phi}_{1i} = \underline{\boldsymbol{\nu}}_1 - \overline{\boldsymbol{\nu}}_1, \quad \sum_{i=1}^{p} \boldsymbol{\phi}_{0i} = \boldsymbol{\beta} + \underline{\boldsymbol{\nu}}_0 - \overline{\boldsymbol{\nu}}_0 + \eta \boldsymbol{\lambda} \\
& \alpha \in \mathbb{R}, \quad \boldsymbol{\beta} \in \mathbb{R}^n, \quad \boldsymbol{\gamma} \in \mathbb{R}^p_+, \quad \underline{\boldsymbol{\nu}}_1, \overline{\boldsymbol{\nu}}_1, \underline{\boldsymbol{\nu}}_0, \overline{\boldsymbol{\nu}}_0 \in \mathbb{R}^n_+ \\
& \eta \in \mathbb{R}_+, \quad \boldsymbol{\phi}_{1i}, \boldsymbol{\phi}_{0i} \in \mathbb{R}^n, \; i = 1, \ldots, p
\end{array}
\tag{2.5}
$$

is greater than or equal to $1-\epsilon$. We claim that for $\tau = \tau^\star$, where $\tau^\star = \sup_{\mathbb{P} \in \mathcal{P}} \mathbb{P}\text{-VaR}_{1-\epsilon}\big[\boldsymbol{\lambda}^\top \tilde{\boldsymbol{q}}\big]$, the optimal value of problem (2.5) is in fact *equal to* $1-\epsilon$. Indeed, assume to the contrary that for $\tau = \tau^\star$, the optimal solution $(\alpha^\star, \boldsymbol{\beta}^\star, \boldsymbol{\gamma}^\star, \underline{\boldsymbol{\nu}}_i^\star, \overline{\boldsymbol{\nu}}_i^\star, \eta^\star, \boldsymbol{\phi}_{ij}^\star)$ to problem (2.5) satisfied $\alpha^\star + \boldsymbol{\mu}^\top \boldsymbol{\beta}^\star - \boldsymbol{\sigma}^\top \boldsymbol{\gamma}^\star > 1-\epsilon$. In that case, we could replace $\alpha^\star$ with $\hat{\alpha} < \alpha^\star$ such that $(\hat{\alpha}, \boldsymbol{\beta}^\star, \boldsymbol{\gamma}^\star, \underline{\boldsymbol{\nu}}_i^\star, \overline{\boldsymbol{\nu}}_i^\star, \eta^\star, \boldsymbol{\phi}_{ij}^\star)$ remains feasible for $\hat{\tau} < \tau^\star$ and still satisfies $\hat{\alpha} + \boldsymbol{\mu}^\top \boldsymbol{\beta}^\star - \boldsymbol{\sigma}^\top \boldsymbol{\gamma}^\star \geqslant 1 - \epsilon$. This, however, would contradict the definition of $\tau^\star$ as the smallest value of τ for which there is $(\alpha, \boldsymbol{\beta}, \boldsymbol{\gamma}, \underline{\boldsymbol{\nu}}_i, \overline{\boldsymbol{\nu}}_i, \eta, \boldsymbol{\phi}_{ij})$ feasible in problem (2.5) with an objective value greater than or equal to $1-\epsilon$. We thus conclude that the optimal value of the problem (2.5) for $\tau = \tau^\star$ is *exactly* $1-\epsilon$. Strong convex duality, which holds since problem (2.5) admits a Slater point, then implies that the optimal value of the dual problem,

$$\begin{array}{lll} \text{minimize} & \xi_1 & \\ \text{subject to} & \xi_0 + \xi_1 = 1, \ \ \boldsymbol{\zeta}_0 + \boldsymbol{\zeta}_1 = \boldsymbol{\mu} & \\ & \xi_i \underline{\boldsymbol{q}} \leqslant \boldsymbol{\zeta}_i \leqslant \xi_i \overline{\boldsymbol{q}} & \forall i \in \{0,1\} \\ & \boldsymbol{\lambda}^\top \boldsymbol{\zeta}_0 \geqslant \xi_0 \tau^\star & \\ & \xi_0 \cdot \boldsymbol{\varphi}(\boldsymbol{\zeta}_0/\xi_0) + \xi_1 \cdot \boldsymbol{\varphi}(\boldsymbol{\zeta}_1/\xi_1) \leqslant \boldsymbol{\sigma} & \\ & \xi_i \in \mathbb{R}_+, \ \ \boldsymbol{\zeta}_i \in \mathbb{R}^n, \ i = 0, 1, & \end{array} \tag{2.6}$$

is also equal to $1 - \epsilon$. Let $(\xi_i^\star, \boldsymbol{\zeta}_i^\star)$ be an optimal solution to this problem.

We claim that the sequence of two-point distribution $\mathbb{P}^t$ defined by

$$\mathbb{P}^t = (\xi_1^\star - 1/t) \cdot \delta_{\frac{\boldsymbol{\zeta}_1^\star}{\xi_1^\star}} + (\xi_0^\star + 1/t) \cdot \delta_{\frac{\boldsymbol{\zeta}_0^\star}{\xi_0^\star} + \frac{1}{t(\xi_0^\star + 1/t)}\left(\frac{\boldsymbol{\zeta}_1^\star}{\xi_1^\star} - \frac{\boldsymbol{\zeta}_0^\star}{\xi_0^\star}\right)}, \quad t = 1, 2, \ldots,$$

satisfies *(i)* $\mathbb{P}^t \in \mathcal{P}$ for sufficiently large t as well as *(ii)* $\mathbb{P}^t\text{-VaR}_{1-\epsilon}\big[\boldsymbol{\lambda}^\top \tilde{\boldsymbol{q}}\big] \longrightarrow \tau^\star$ as $t \longrightarrow \infty$.

In view of statement *(i)*, we note that $\mathbb{P}^t$ is a probability distribution for t sufficiently large since $(\xi_0^\star, \xi_1^\star) = (\epsilon, 1 - \epsilon)$ due to the first constraint set in (2.6). Also, $\mathbb{P}^t$ is supported on $\mathcal{Q}$ for sufficiently large t since $\boldsymbol{\zeta}_i^\star / \xi_i^\star \in [\underline{\boldsymbol{q}}, \overline{\boldsymbol{q}}]$, $i = 0, 1$, due to the second constraint in (2.6) and for t sufficiently large, $\frac{\boldsymbol{\zeta}_0^\star}{\xi_0^\star} + \frac{1}{t(\xi_0^\star + 1/t)}\left(\frac{\boldsymbol{\zeta}_1^\star}{\xi_1^\star} - \frac{\boldsymbol{\zeta}_0^\star}{\xi_0^\star}\right)$ is a convex combination of $\boldsymbol{\zeta}_0^\star / \xi_0^\star$ and $\boldsymbol{\zeta}_1^\star / \xi_1^\star$. Likewise, we have

$$\mathbb{E}_{\mathbb{P}^t}\big[\tilde{\boldsymbol{q}}\big] \ = \ (\xi_1^\star - 1/t) \cdot \frac{\boldsymbol{\zeta}_1^\star}{\xi_1^\star} + (\xi_0^\star + 1/t) \cdot \frac{\boldsymbol{\zeta}_0^\star}{\xi_0^\star} + \frac{1}{t}\left(\frac{\boldsymbol{\zeta}_1^\star}{\xi_1^\star} - \frac{\boldsymbol{\zeta}_0^\star}{\xi_0^\star}\right) \ = \ \boldsymbol{\mu}$$

due to the first constraint set in (2.6) as well as, for t sufficiently large,

$$\begin{aligned} \mathbb{E}_{\mathbb{P}^t}\big[\boldsymbol{\varphi}(\tilde{\boldsymbol{q}})\big] \ &= \ (\xi_1^\star - 1/t) \cdot \boldsymbol{\varphi}\left(\frac{\boldsymbol{\zeta}_1^\star}{\xi_1^\star}\right) + (\xi_0^\star + 1/t) \cdot \boldsymbol{\varphi}\left(\frac{\boldsymbol{\zeta}_0^\star}{\xi_0^\star} + \frac{1}{t(\xi_0^\star + 1/t)}\left[\frac{\boldsymbol{\zeta}_1^\star}{\xi_1^\star} - \frac{\boldsymbol{\zeta}_0^\star}{\xi_0^\star}\right]\right) \\ &\leqslant \ (\xi_1^\star - 1/t) \cdot \boldsymbol{\varphi}\left(\frac{\boldsymbol{\zeta}_1^\star}{\xi_1^\star}\right) + \frac{1}{t} \cdot \boldsymbol{\varphi}\left(\frac{\boldsymbol{\zeta}_1^\star}{\xi_1^\star}\right) + \xi_0^\star \cdot \boldsymbol{\varphi}\left(\frac{\boldsymbol{\zeta}_0^\star}{\xi_0^\star}\right) \ \leqslant \ \boldsymbol{\sigma}, \end{aligned}$$

where the inequalities follow from the convexity of $\boldsymbol{\varphi}$ and the fourth constraint in (2.6), respectively.

To show statement *(ii)*, we note that $\mathbb{P}^t$ places a probability mass of $\xi_0^\star + 1/t = \epsilon + 1/t$ on the scenario $\frac{\zeta_0^\star}{\xi_0^\star} + \frac{1}{t(\xi_0^\star + 1/t)} \left(\frac{\zeta_1^\star}{\xi_1^\star} - \frac{\zeta_0^\star}{\xi_0^\star} \right)$, which satisfies

$$\boldsymbol{\lambda}^\top \left[\frac{\boldsymbol{\zeta}_0^\star}{\xi_0^\star} + \frac{1}{t(\xi_0^\star + 1/t)} \left(\frac{\boldsymbol{\zeta}_1^\star}{\xi_1^\star} - \frac{\boldsymbol{\zeta}_0^\star}{\xi_0^\star} \right) \right] \;\geqslant\; \tau^\star \;+\; \frac{1}{t(\xi_0^\star + 1/t)} \boldsymbol{\lambda}^\top \left(\frac{\boldsymbol{\zeta}_1^\star}{\xi_1^\star} - \frac{\boldsymbol{\zeta}_0^\star}{\xi_0^\star} \right) \;\underset{t \longrightarrow \infty}{\longrightarrow}\; \tau^\star.$$

Here, the inequality follows from the fact that $\boldsymbol{\lambda}^\top \boldsymbol{\zeta}_0^\star / \xi_0^\star \geqslant \tau^\star$ due to the third constraint in (2.6). The convergence of the middle expression to $\tau^\star$ holds since $\boldsymbol{\lambda}^\top \left(\boldsymbol{\zeta}_1^\star / \xi_1^\star - \boldsymbol{\zeta}_0^\star / \xi_0^\star \right)$ is finite while $t(\xi_0^\star + 1/t) \longrightarrow \infty$ as $\xi_0^\star = \epsilon > 0$. We have thus established that $\mathbb{P}^t\text{-VaR}_{1-\epsilon}\big[\boldsymbol{\lambda}^\top \tilde{\boldsymbol{q}}\big] \longrightarrow \tau'$ with $\tau' \geqslant \tau^\star$ as $t \longrightarrow \infty$. Since $\mathbb{P}^t \in \mathcal{P}$ for sufficiently large t, on the other hand, the definition of $\tau^\star$ implies that $\tau' \leqslant \tau^\star$ as well, which concludes the proof. ∎

Proposition 2.9 shows that for moment ambiguity sets of the form (2.4), the worst-case value-at-risk $\sup_{\mathbb{P} \in \mathcal{P}} \mathbb{P}\text{-VaR}_{1-\epsilon}\big[\sum_{i \in S} \tilde{q}_i \big]$ is asymptotically attained by a series of probability distributions that place all probability mass on two demand scenarios. We emphasize that the two-point nature of the worst-case distribution does *not* depend on the number of moment constraints contained in the ambiguity set (2.4). In that sense, Proposition 2.9 strengthens the findings of the Richter-Rogosinski theorem [SDR14, Theorem 7.37], which applies to more general risk measures, to the special case of the worst-case value-at-risk.

Proposition 2.9 confirms our intuition that the distributionally robust CVRP constitutes a compromise between the deterministic CVRP, which optimizes in view of a single expected (or most likely) demand scenario, and the robust CVRP, which optimizes in view of the worst demand scenario contained in an uncertainty set. At the same time, the distributionally robust CVRP also offers a trade-off between the classical chance constrained CVRP, which is often challenging to solve as it optimizes in view of a distribution that may place positive probability mass on many demand scenarios, and the robust CVRP, which optimizes in view of a single worst-case scenario.

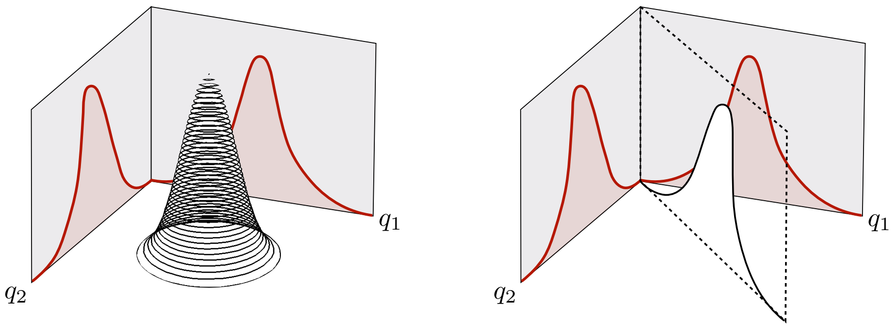

Figure 2.4: Examples of probability distributions contained in a marginalized ambiguity set. Since the conditions in the ambiguity set (2.7) only restrict the shapes of the marginal distributions, the ambiguity set contains distributions of varying dependence structure, ranging from independent (left graph) to perfectly correlated (right graph) ones.

2.5 Efficient Reformulations for Demand Estimators

In this section, we consider some commonly used moment ambiguity sets and derive reformulations to efficiently evaluate $d_{\mathcal{P}}$ over these ambiguity sets.

2.5.1 Marginalized Moment Ambiguity Set

In this section we study marginalized moment ambiguity sets of the form

$$\mathcal{P} = \{\mathbb{P} \in \mathcal{P}_0(\mathbb{R}^n) \,:\, \mathbb{P}(\tilde{\boldsymbol{q}} \in \mathcal{Q}) = 1, \;\; \mathbb{E}_{\mathbb{P}}[\tilde{\boldsymbol{q}}] = \boldsymbol{\mu}, \;\; \mathbb{E}_{\mathbb{P}}[\boldsymbol{\varphi}_i(\tilde{q}_i)] \leqslant \boldsymbol{\sigma}_i \;\; \forall i \in V_C\}\,, \tag{2.7}$$

where $\mathcal{Q} = [\underline{\boldsymbol{q}}, \overline{\boldsymbol{q}}]$ with $\underline{\boldsymbol{q}} \geqslant \mathbf{0}$, $\boldsymbol{\mu} \in \operatorname{int} \mathcal{Q}$, and $\boldsymbol{\varphi}_i : \mathbb{R} \mapsto \mathbb{R}^{p_i}$ is closed as well as component-wise convex and satisfies $\boldsymbol{\varphi}_i(\mu_i) < \boldsymbol{\sigma}_i$ with $\boldsymbol{\sigma}_i \in \mathbb{R}^{p_i}$, $i \in V_C$. In contrast to the generic moment ambiguity set (2.4), a marginalized moment ambiguity set only specifies the variability of individual customer demands and does not characterize the interactions between different customer demands. Nevertheless, Figure 2.4 shows that the customer demands may still exhibit dependencies under the probability distributions contained in a marginalized moment ambiguity set.

Marginalized moment ambiguity sets of the form (2.7) constitute a subclass of the generic moment ambiguity sets (2.4), and thus the demand estimator $d_{\mathcal{P}}$ over the ambiguity set (2.7) is subadditive due to Theorem 2.8. In fact, a much stronger additivity property holds for the ambiguity set (2.7).

Theorem 2.10 *Every marginalized moment ambiguity set of the form* (2.7) *satisfies*

$$\sup_{\mathbb{P}\in\mathcal{P}} \mathbb{P}\text{-VaR}_{1-\epsilon}\Big[\sum_{i\in S}\tilde{q}_i\Big] \;=\; \sum_{i\in S}\sup_{\mathbb{P}\in\mathcal{P}} \mathbb{P}\text{-VaR}_{1-\epsilon}\big[\tilde{q}_i\big] \qquad \forall S\subseteq V_C,\, S\neq\emptyset.$$

Proof of Theorem 2.10. Since the assumptions of Theorem 2.8 are satisfied, we conclude that

$$\sup_{\mathbb{P}\in\mathcal{P}} \mathbb{P}\text{-VaR}_{1-\epsilon}\Big[\sum_{i\in S}\tilde{q}_i\Big] \;\leqslant\; \sum_{i\in S}\sup_{\mathbb{P}\in\mathcal{P}} \mathbb{P}\text{-VaR}_{1-\epsilon}\big[\tilde{q}_i\big] \qquad \forall S\subseteq V_C,\, S\neq\emptyset.$$

To show the reverse inequality, we note that for any $\kappa > 0$, we have

$$\begin{aligned}\sum_{i\in S}\sup_{\mathbb{P}\in\mathcal{P}} \mathbb{P}\text{-VaR}_{1-\epsilon}\big[\tilde{q}_i\big] \;&\leqslant\; \sum_{i\in S}\big(\mathbb{P}_i^\star\text{-VaR}_{1-\epsilon}\big[\tilde{q}_i\big]+\kappa\big)\\ &=\; \sum_{i\in S}\big(\mathbb{P}^\star\text{-VaR}_{1-\epsilon}\big[\tilde{q}_i\big]+\kappa\big) \;=\; \mathbb{P}^\star\text{-VaR}_{1-\epsilon}\Big[\sum_{i\in S}\tilde{q}_i\Big]+|S|\kappa.\end{aligned} \tag{2.8}$$

Here, $\mathbb{P}_i^\star \in \mathcal{P}$ is a distribution that satisfies $\mathbb{P}_i^\star\text{-VaR}_{1-\epsilon}\big[\tilde{q}_i\big] \geqslant \sup_{\mathbb{P}\in\mathcal{P}} \mathbb{P}\text{-VaR}_{1-\epsilon}\big[\tilde{q}_i\big] - \kappa$, which implies the first inequality. In the second row, we define the probability measure $\mathbb{P}^\star$ via

$$\mathbb{P}^\star\big(\tilde{\boldsymbol{q}}\leqslant\boldsymbol{q}\big) \;=\; \min_{i\in S}\, \mathbb{P}_i^\star\big(\tilde{q}_i\leqslant q_i\big) \qquad \forall\boldsymbol{q}\in\mathbb{R}^n.$$

By construction, $\mathbb{P}^\star$ has the same marginal distributions as $\mathbb{P}_i^\star$, $i\in V_C$, that is, $\mathbb{P}^\star\big(\tilde{q}_i\in A\big) = \mathbb{P}_i^\star\big(\tilde{q}_i\in A\big)$ for all $i\in V_C$ and for every measurable set A [DDG$^+$02, Theorem 2]. From the definition of the marginalized moment ambiguity sets, we thus conclude that $\mathbb{P}^\star\in\mathcal{P}$. Since $\mathbb{P}^\star$ is comonotonic [DDG$^+$02, Definition 4 and Theorem 2], the last equality in (2.8) follows from the comonotone additivity of the value-at-risk [Pfl00, Proposition 3]. As κ was chosen arbitrarily in (2.8) and since $\mathbb{P}^\star\in\mathcal{P}$, we thus conclude that

$$\sum_{i\in S}\sup_{\mathbb{P}\in\mathcal{P}} \mathbb{P}\text{-VaR}_{1-\epsilon}\big[\tilde{q}_i\big] \;\leqslant\; \sup_{\mathbb{P}\in\mathcal{P}} \mathbb{P}\text{-VaR}_{1-\epsilon}\Big[\sum_{i\in S}\tilde{q}_i\Big]$$

as desired. This completes the proof. ∎

Theorem 2.10 shows that the worst-case value-at-risk for a marginalized moment ambiguity set is additive. Nevertheless, the following example illustrates that for individual probability distributions within a marginalized moment ambiguity set of the form (2.7), the corresponding values-at-risk typically *fail* to be additive.

Example 2.11 *Consider the following marginalized moment ambiguity set for two customers:*

$$\mathcal{P} = \left\{\mathbb{P} \in \mathcal{P}_0(\mathbb{R}^2) \,:\, \mathbb{P}(\tilde{\boldsymbol{q}} \in [2,7] \times [5,15]) = 1,\ \ \mathbb{E}_{\mathbb{P}}[\tilde{\boldsymbol{q}}] = (3.2,\, 7.8)^\top,\ \ \mathbb{E}_{\mathbb{P}}[|\tilde{q}_i - \mu_i|] \leqslant 1.5,\, i = 1,2\right\}$$

Here, $|\cdot|$ *denotes the absolute value operator. We have* $\mathbb{P}_1 \in \mathcal{P}$ *for the distribution* $\mathbb{P}_1 = \mathbb{P}_{11} \times \mathbb{P}_{12}$ *under which the two customer demands are independent and governed by the marginal distributions* $\mathbb{P}_{11} = 0.8 \cdot \delta_3 + 0.2 \cdot \delta_4 \in \mathcal{P}_0(\mathbb{R})$ *and* $\mathbb{P}_{12} = 0.8 \cdot \delta_7 + 0.2 \cdot \delta_{11} \in \mathcal{P}_0(\mathbb{R})$*. One readily verifies that*

$$14 \;=\; \mathbb{P}_1\text{-VaR}_{0.9}\left[\tilde{q}_1 + \tilde{q}_2\right] \;<\; \mathbb{P}_1\text{-VaR}_{0.9}\left[\tilde{q}_1\right] + \mathbb{P}_1\text{-VaR}_{0.9}\left[\tilde{q}_2\right] \;=\; 4 + 11,$$

that is, the 0.9*-value-at-risk is* subadditive *under* $\mathbb{P}_1$*. Likewise, we have* $\mathbb{P}_2 \in \mathcal{P}$ *for the distribution* $\mathbb{P}_2 = \mathbb{P}_{21} \times \mathbb{P}_{22}$ *with the marginals* $\mathbb{P}_{21} = 0.6 \cdot \delta_2 + 0.4 \cdot \delta_5 \in \mathcal{P}_0(\mathbb{R})$ *and* $\mathbb{P}_{22} = 0.9 \cdot \delta_7 + 0.1 \cdot \delta_{15} \in \mathcal{P}_0(\mathbb{R})$*. The distribution* $\mathbb{P}_2$ *satisfies*

$$12 \;=\; \mathbb{P}_2\text{-VaR}_{0.9}\left[\tilde{q}_1 + \tilde{q}_2\right] \;=\; \mathbb{P}_2\text{-VaR}_{0.9}\left[\tilde{q}_1\right] + \mathbb{P}_2\text{-VaR}_{0.9}\left[\tilde{q}_2\right] \;=\; 5 + 7,$$

that is, the value-at-risk is additive *under* $\mathbb{P}_2$*. Finally, we have* $\mathbb{P}_3 \in \mathcal{P}$ *for* $\mathbb{P}_3 = \mathbb{P}_{31} \times \mathbb{P}_{32}$ *with the marginals* $\mathbb{P}_{31} = 0.9 \cdot \delta_3 + 0.1 \cdot \delta_5 \in \mathcal{P}_0(\mathbb{R})$ *and* $\mathbb{P}_{32} = 0.9 \cdot \delta_7 + 0.1 \cdot \delta_{15} \in \mathcal{P}_0(\mathbb{R})$*. One verifies that*

$$12 \;=\; \mathbb{P}_3\text{-VaR}_{0.9}\left[\tilde{q}_1 + \tilde{q}_2\right] \;>\; \mathbb{P}_3\text{-VaR}_{0.9}\left[\tilde{q}_1\right] + \mathbb{P}_3\text{-VaR}_{0.9}\left[\tilde{q}_2\right] \;=\; 3 + 7,$$

that is, the value-at-risk is superadditive *under* $\mathbb{P}_3$*.*

An immediate consequence of Theorem 2.10 is the following.

Corollary 2.12 *The distributionally robust CVRP over a marginalized moment ambiguity set* (2.7) *is equivalent to the deterministic CVRP with customer demands* $q_i = \sup_{\mathbb{P}\in\mathcal{P}} \mathbb{P}\text{-VaR}_{1-\epsilon}\big[\tilde{q}_i\big]$, $i \in V_C$.

Proof of Corollary 2.12. Since the ambiguity set $\mathcal{P}$ is subadditive, Theorem 2.7 implies that RVRP($\mathcal{P}$) is equivalent to 2VF($\mathcal{P}$). Moreover, Theorem 2.10 allows us to interpret 2VF($\mathcal{P}$) as the two-index vehicle flow formulation of a deterministic CVRP with customer demands $q_i = \sup_{\mathbb{P}\in\mathcal{P}} \mathbb{P}\text{-VaR}_{1-\epsilon}\big[\tilde{q}_i\big]$, $i \in V_C$. The statement now follows from the well-known equivalence of the two-index vehicle flow formulation and the deterministic CVRP. ■If only marginal moment information is available, then Corollary 2.12 implies that a distributionally robust CVRP can be solved with existing solution schemes for deterministic CVRPs, such as branch-and-cut [LLE04, STV14] or branch-and-cut-and-price [FLL$^+$06, PPPU17] algorithms. In other words, we can 'robustify' a deterministic CVRP instance without modifying the employed solution scheme by replacing the deterministic demands q_i with the (deterministic) worst-case value-at-risks $\sup_{\mathbb{P}\in\mathcal{P}} \mathbb{P}\text{-VaR}_{1-\epsilon}\big[\tilde{q}_i\big]$ for all customers $i \in V_C$.

While very attractive from a computational perspective, Corollary 2.12 also points at several weaknesses of the marginalized moment ambiguity sets. Firstly, marginalized moment ambiguity sets fail to capture any potentially known dependencies between customer demands. As a result, under the worst-case distribution all customer demands will attain their worst values jointly with probability ϵ. This contradicts the common wisdom that extreme demands are not typically attained simultaneously across all customers. Secondly, when using marginalized moment ambiguity sets we are unable to obtain a structurally different feasible region than for a suitably modified deterministic problem instance. As we will see in Section 2.5.2, this is in stark contrast to generic moment ambiguity sets that may not correspond to any deterministic problem instance. Finally, under the marginalized moment ambiguity sets the worst-case demand distribution does not depend on the selected route set, as we would usually expect to be the case under the distributionally robust optimization framework. In other words, under the marginalized moment ambiguity sets the decision maker cannot benefit from knowing the true probability distribution, as long as this distribution could be any of the distributions within the ambiguity set.

If we remove the expectation and the dispersion constraint in the marginalized moment ambiguity set (2.7), then the distributionally robust CVRP reduces to a deterministic CVRP with component-wise worst-case customer demands $\boldsymbol{q} = \overline{\boldsymbol{q}}$. If we remove the support and the dispersion constraint, on the other hand, then the distributionally robust CVRP becomes infeasible since the distribution $\kappa \cdot \delta_{\boldsymbol{q}_1} + (1-\kappa) \cdot \delta_{\boldsymbol{q}_2}$ with $\kappa \in (\epsilon, 1)$, $\boldsymbol{q}_1 = 2Q \cdot \mathbf{e}$ and $\boldsymbol{q}_2 = (\boldsymbol{\mu} - 2\kappa Q \cdot \mathbf{e})/(1-\kappa)$ is contained in the ambiguity set and places probability mass $\kappa > \epsilon$ on the demand scenario $2Q \cdot \mathbf{e}$, resulting in a worst-case value-at-risk of $\sup_{\mathbb{P} \in \mathcal{P}} \mathbb{P}\text{-VaR}_{1-\epsilon}\big[\sum_{i \in S} \tilde{q}_i\big] = 2Q|S|$. In the next three subsections, we develop closed-form solutions for the worst-case value-at-risk under support and expectation constraints combined with first-order, variance and semi-variance dispersion measures.

2.5.1.1 First-Order Ambiguity Sets

We begin with first-order marginalized moment ambiguity sets of the form

$$\mathcal{P} = \left\{ \mathbb{P} \in \mathcal{P}_0(\mathbb{R}^n) \;:\; \mathbb{P}\left(\tilde{\boldsymbol{q}} \in \mathcal{Q}\right) = 1, \;\; \mathbb{E}_{\mathbb{P}}\left[\tilde{\boldsymbol{q}}\right] = \boldsymbol{\mu}, \;\; \mathbb{E}_{\mathbb{P}}\left[|\tilde{\boldsymbol{q}} - \boldsymbol{\mu}|\right] \leqslant \boldsymbol{\sigma} \right\}, \tag{2.9}$$

where the absolute value operator $|\cdot|$ is applied component-wise. As before, we assume that $\mathcal{Q} = [\underline{\boldsymbol{q}}, \overline{\boldsymbol{q}}]$ with $\underline{\boldsymbol{q}} \geqslant \mathbf{0}$ and $\boldsymbol{\mu} \in \operatorname{int} \mathcal{Q}$, and we additionally stipulate that $\boldsymbol{\sigma} > \mathbf{0}$. Note that (2.9) is a special case of the marginalized moment ambiguity set (2.7) where $\varphi_i(q_i) = |q_i - \mu_i|$, $i \in V_C$. The dispersion constraint imposes an upper bound of σ_i on the mean absolute deviation $\mathbb{E}_{\mathbb{P}}\left[|\tilde{q}_i - \mu_i|\right]$ of customer i's demand, $i \in V_C$.

Similar to the standard deviation, the mean absolute deviation measures the dispersion of a random variable around its expected value. Compared to the standard deviation, however, the mean absolute deviation is less affected by outliers and deviations from the standard modeling assumptions (such as normality). Due to these properties, the mean absolute deviation is preferred in the robust statistics literature, see, *e.g.*, [CB02].

We now show that the worst-case value-at-risk of a customer's demand $\tilde{q}_i$ under the marginalized first-order moment ambiguity set (2.9) admits a closed-form solution.

Proposition 2.13 *Every marginalized first-order ambiguity set of the form* (2.9) *satisfies*

$$\sup_{\mathbb{P}\in\mathcal{P}} \mathbb{P}\text{-VaR}_{1-\epsilon}\big[\tilde{q}_i\big] \;=\; \mu_i + \min\left\{\overline{q}_i - \mu_i,\; \frac{1-\epsilon}{\epsilon}(\mu_i - \underline{q}_i),\; \frac{1}{2\epsilon}\sigma_i\right\} \qquad \forall i \in V_C. \tag{2.10}$$

Proof of Proposition 2.13. We apply Theorem 2.21 to conclude that the worst-case value-at-risk $\sup_{\mathbb{P}\in\mathcal{P}} \mathbb{P}\text{-VaR}_{1-\epsilon}\big[\tilde{q}_i\big]$ is equal to the optimal objective value of the following problem.

$$\begin{array}{ll} \text{minimize} & \mu_i + \min\left\{ \big(\overline{q}_i - \mu_i\big),\; \dfrac{1-\epsilon}{\epsilon}\big(\mu_i - \underline{q}_i\big) \right\} \cdot [1-2\gamma]_+ + \dfrac{1}{\epsilon}\nu\gamma \\ \text{subject to} & \gamma \in \mathbb{R}_+. \end{array}$$

The first and second terms in the objective function are constant and non-decreasing in γ, respectively, for $\gamma \geqslant 1/2$. Without loss of generality, we can therefore assume that $\gamma \leqslant 1/2$ at optimality. We thus obtain a linearized version of the problem as follows.

$$\begin{array}{ll} \text{minimize} & \mu_i + \min\left\{ \big(\overline{q}_i - \mu_i\big),\; \dfrac{1-\epsilon}{\epsilon}\big(\mu_i - \underline{q}_i\big) \right\} \cdot [1-2\gamma] + \dfrac{1}{\epsilon}\nu\gamma \\ \text{subject to} & \gamma \in [0,\; 1/2] \end{array}$$

Since the objective function is linear in γ, the problem is optimized by either $\gamma = 0$ or $\gamma = 1/2$. The result now follows from a case distinction. ∎

Proposition 2.13 confirms our intuition that the worst-case value-at-risk of the demand of customer $i \in V_C$ increases with the range $\overline{q}_i - \underline{q}_i$, the safety threshold $1-\epsilon$ as well as the upper bound on the mean absolute deviation σ_i. In particular, if customer i's demand is unbounded, then the worst-case value-at-risk simplifies to $\mu_i + \frac{1}{2\epsilon}\sigma_i$, and if the dispersion bound in (2.9) is disregarded, then the worst-case value-at-risk becomes $\min\big\{\overline{q}_i,\; \frac{1}{\epsilon}\mu_i - \frac{1-\epsilon}{\epsilon}\underline{q}_i\big\}$.

It is tempting to conclude from Proposition 2.13 that the worst-case value-at-risk (2.10) is attained by the Dirac distribution that places all probability mass on the single demand realisation $\boldsymbol{\mu} + \min\big\{\overline{\boldsymbol{q}} - \boldsymbol{\mu},\; \frac{1-\epsilon}{\epsilon}(\boldsymbol{\mu} - \underline{\boldsymbol{q}}),\; \frac{1}{2\epsilon}\boldsymbol{\sigma}\big\}$, where the minimum is applied component-wise.

This distribution, however, is *not* contained in the ambiguity set as it violates the expected value constraint in (2.9). Nevertheless, one can construct sequences of two-point distributions that are contained in the ambiguity set and that attain the worst-case value-at-risk (2.10) asymptotically.

Proposition 2.14 *A sequence of distributions $\mathbb{P}_i^t \in \mathcal{P}$, $t = 1, 2, \ldots$, that attain the worst-case value-at-risk* $\sup_{\mathbb{P}\in\mathcal{P}} \mathbb{P}\text{-VaR}_{1-\epsilon}\big[\tilde{q}_i\big]$ *in Proposition 2.13 asymptotically as $t \longrightarrow \infty$ can be defined as follows:*

(i) *If* (2.10) *is minimized by $\overline{q}_i - \mu_i$, then $\mathbb{P}_i^t = (1 - \epsilon - 1/t) \cdot \delta_{\boldsymbol{q}_1} + (\epsilon + 1/t) \cdot \delta_{\boldsymbol{q}_2}$ with $\boldsymbol{q}_1 = \boldsymbol{\mu} - \frac{\epsilon}{1-\epsilon}(\overline{q}_i - \mu_i)\mathbf{e}_i$ and $\boldsymbol{q}_2 = \boldsymbol{\mu} + \frac{1-\epsilon-1/t}{\epsilon+1/t}\frac{\epsilon}{1-\epsilon}(\overline{q}_i - \mu_i)\mathbf{e}_i$.*

(ii) *If* (2.10) *is minimized by $\frac{1-\epsilon}{\epsilon}(\mu_i - \underline{q}_i)$, then $\mathbb{P}_i^t = (1 - \epsilon - 1/t) \cdot \delta_{\boldsymbol{q}_1} + (\epsilon + 1/t) \cdot \delta_{\boldsymbol{q}_2}$ with $\boldsymbol{q}_1 = \boldsymbol{\mu} - (\mu_i - \underline{q}_i)\mathbf{e}_i$ and $\boldsymbol{q}_2 = \boldsymbol{\mu} + \frac{1-\epsilon-1/t}{\epsilon+1/t}(\mu_i - \underline{q}_i)\mathbf{e}_i$.*

(iii) *If* (2.10) *is minimized by $\frac{1}{2\epsilon}\sigma_i$, then $\mathbb{P}_i^t = (1-\epsilon-1/t)\cdot\delta_{\boldsymbol{q}_1} + (\epsilon+1/t)\cdot\delta_{\boldsymbol{q}_2}$ with $\boldsymbol{q}_1 = \boldsymbol{\mu} - \frac{\sigma_i}{2(1-\epsilon)}\mathbf{e}_i$ and $\boldsymbol{q}_2 = \boldsymbol{\mu} + \frac{1-\epsilon-1/t}{\epsilon+1/t}\frac{\sigma_i}{2(1-\epsilon)}\mathbf{e}_i$.*

Proof of Proposition 2.14. We have to show for each of the three cases that $\mathbb{P}_i^t \in \mathcal{P}$, that is, that *(a)* $\mathbb{P}_i^t$ is supported on $\mathcal{Q}$, *(b)* $\mathbb{E}_{\mathbb{P}_i^t}\big[\tilde{\boldsymbol{q}}\big] = \boldsymbol{\mu}$ and *(c)* $\mathbb{E}_{\mathbb{P}_i^t}\big[|\tilde{\boldsymbol{q}} - \boldsymbol{\mu}|\big] \leqslant \boldsymbol{\sigma}$ hold. The claim of the proposition then follows since in each of the three cases, the distribution places a probability mass of $\epsilon + 1/t$ on $\boldsymbol{q}_2$, and q_{2i} converges to $\sup_{\mathbb{P}\in\mathcal{P}} \mathbb{P}\text{-VaR}_{1-\epsilon}\big[\tilde{q}_i\big]$ as $t \longrightarrow \infty$. The proof that $\mathbb{P}_i^t \in \mathcal{P}$ follows along similar lines as the proof of Proposition 2.9 and is thus omitted for the sake of brevity. ∎

Proposition 2.14 presents a sequence of worst-case distributions $\mathbb{P}_i^t$ for the demand $\tilde{q}_i$ of each *individual* customer $i \in V_C$. Using similar arguments as in the proof of Theorem 2.10, we can construct a sequence of worst-case distributions $\mathbb{P}^t$ for the demand of *all* customers $i \in V_C$ via the Fréchet-Hoeffding upper bound copula

$$\mathbb{P}^t(\tilde{\boldsymbol{q}} \leqslant \boldsymbol{q}) = \min_{i\in V_C} \mathbb{P}_i^t(\tilde{q}_i \leqslant q_i).$$

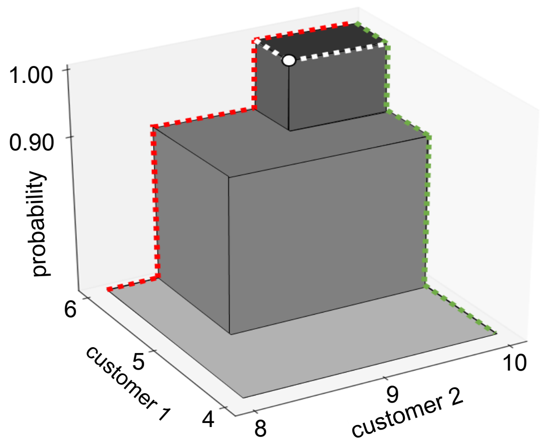

Figure 2.5: Fréchet-Hoeffding upper bound copula $\mathbb{P}^\star$ for a distributionally robust CVRP instance with two customers and a marginalized first-order ambiguity set (2.9) with support $\mathcal{Q} = [4,6] \times [8,10]$, mean $\boldsymbol{\mu}^\top = (4.5, 9)$, mean absolute deviation bounds $\boldsymbol{\sigma}^\top = (0.1, 0.15)$ and risk threshold $\epsilon = 0.1$. The marginal distributions are highlighted via dotted green and red lines, and the worst-case value-at-risk $\sup_{\mathbb{P} \in \mathcal{P}} \mathbb{P}\text{-VaR}_{1-\epsilon}\big[\tilde{q}_1 + \tilde{q}_2\big]$ (the worst-case demand realization) is indicated by a white (dark gray) circle.

For the ambiguity set (2.9), this sequence of worst-case distributions $\mathbb{P}^t$ has a simple description: it satisfies $\mathbb{P}^t \longrightarrow (1-\epsilon) \cdot \delta_{\boldsymbol{q}_1} + \epsilon \cdot \delta_{\boldsymbol{q}_2}$ for the two-point distribution characterized by

$$(q_{1i}, q_{2i}) = \begin{cases} \left(\frac{1}{1-\epsilon}\mu_i - \frac{\epsilon}{1-\epsilon}\overline{q}_i,\ \overline{q}_i\right) & \text{if (2.10) is minimized by } \overline{q}_i - \mu_i, \\ \left(\underline{q}_i,\ \frac{1}{\epsilon}\mu_i - \frac{1-\epsilon}{\epsilon}\underline{q}_i\right) & \text{if (2.10) is minimized by } \frac{1-\epsilon}{\epsilon}(\mu_i - \underline{q}_i), \\ \left(\mu_i - \frac{\sigma_i}{2(1-\epsilon)},\ \mu_i + \frac{\sigma_i}{2\epsilon}\right) & \text{if (2.10) is minimized by } \frac{1}{2\epsilon}\sigma_i \end{cases} \qquad \forall i \in V_C.$$

This joint worst-case distribution is illustrated in Figure 2.5 for an example with two customers.

Example 2.15 *Proposition 2.13 shows that the* 0.9*-worst-case values-at-risk for the two customer demands* $\tilde{q}_1$ *and* $\tilde{q}_2$ *from Example 2.11 are* 5 *and* 15*, respectively. Moreover, Proposition 2.14 implies that each individual worst-case value-at-risk is attained asymptotically by a sequence of distributions that converges to the asymptotic distribution* $0.9 \cdot \delta_{\boldsymbol{q}_1} + 0.1 \cdot \delta_{\boldsymbol{q}_2}$ *with* $\boldsymbol{q}_1 = (3, 7)^\top$ *and* $\boldsymbol{q}_2 = (5, 15)^\top$*. Finally, since each element of the sequence is a two-point distribution that places a probability mass greater than* 0.1 *on each scenario, the value-at-risk is indeed additive for each member of the sequence. Note, however, that although the worst-case values-at-risk of* $\tilde{q}_1 + \tilde{q}_2$ *converge to* 20 *for the distributions in the sequence, the worst-case* *value-at-risk under the asymptotic distribution is* 10.

2.5.1.2 Variance Ambiguity Sets

We next consider marginalized variance ambiguity sets of the form

$$\mathcal{P} = \left\{ \mathbb{P} \in \mathcal{P}_0(\mathbb{R}^n) \,:\, \mathbb{P}\left[\tilde{\boldsymbol{q}} \in \mathcal{Q}\right] = 1, \;\; \mathbb{E}_{\mathbb{P}}\left[\tilde{\boldsymbol{q}}\right] = \boldsymbol{\mu}, \;\; \mathbb{E}_{\mathbb{P}}\left[(\tilde{q}_i - \mu_i)^2\right] \leqslant \sigma_i \;\; \forall i \in V_C \right\}, \tag{2.11}$$

where $\mathcal{Q} = [\underline{\boldsymbol{q}}, \overline{\boldsymbol{q}}]$ with $\underline{\boldsymbol{q}} \geqslant \mathbf{0}$ and $\boldsymbol{\mu} \in \operatorname{int} \mathcal{Q}$ as well as $\boldsymbol{\sigma} > \mathbf{0}$.

Similar to the mean absolute deviation, the worst-case value-at-risk of a customer's demand $\tilde{q}_i$ under the marginalized variance ambiguity set (2.11) admits a closed-form solution.

Proposition 2.16 *Every marginalized variance ambiguity set of the form* (2.11) *satisfies*

$$\sup_{\mathbb{P} \in \mathcal{P}} \mathbb{P}\text{-VaR}_{1-\epsilon}\big[\tilde{q}_i\big] \;=\; \mu_i + \min\left\{ \overline{q}_i - \mu_i, \; \frac{1-\epsilon}{\epsilon}(\mu_i - \underline{q}_i), \; \sqrt{\frac{1-\epsilon}{\epsilon}}\sigma_i \right\} \qquad \forall i \in V_C. \tag{2.12}$$

Proof of Proposition 2.16. We apply Theorem 2.26 to conclude that the worst-case value-at-risk $\sup_{\mathbb{P} \in \mathcal{P}} \mathbb{P}\text{-VaR}_{1-\epsilon}\big[\tilde{q}_i\big]$ is equal to the optimal objective value of the problem

$$\begin{array}{ll} \text{maximize} & \mu_i + q_i \\ \text{subject to} & \boldsymbol{q}^\top \boldsymbol{\Sigma}^{-1} \boldsymbol{q} \leqslant \dfrac{1-\epsilon}{\epsilon} \\ & \boldsymbol{q} \in \left[\boldsymbol{q}^\ell, \, \boldsymbol{q}^{\mathrm{u}}\right], \end{array} \tag{2.13}$$

where $\boldsymbol{q}^\ell = \max\left\{-\frac{1-\epsilon}{\epsilon}(\overline{\boldsymbol{q}} - \boldsymbol{\mu}), \, \underline{\boldsymbol{q}} - \boldsymbol{\mu}\right\}$, $\boldsymbol{q}^{\mathrm{u}} = \min\left\{\frac{1-\epsilon}{\epsilon}(\boldsymbol{\mu} - \underline{\boldsymbol{q}}), \, \overline{\boldsymbol{q}} - \boldsymbol{\mu}\right\}$ and the covariance matrix satisfies $\boldsymbol{\Sigma} = \operatorname{diag}(\sigma_1, \sigma_2, \ldots, \sigma_n)$. If $\boldsymbol{q}$ is feasible for the above problem, then so is $\boldsymbol{q}'$ with $q'_i = q_i$ and $q'_j = 0$ for all $j \neq i$. Indeed, we have $\boldsymbol{q}^\ell \leqslant \mathbf{0}$ since $-\frac{1-\epsilon}{\epsilon}(\overline{\boldsymbol{q}} - \boldsymbol{\mu}) \leqslant \mathbf{0}$ and $\underline{\boldsymbol{q}} - \boldsymbol{\mu} \leqslant \mathbf{0}$, as well as $\boldsymbol{q}^{\mathrm{u}} \geqslant \mathbf{0}$ since $\frac{1-\epsilon}{\epsilon}(\boldsymbol{\mu} - \underline{\boldsymbol{q}}) \geqslant \mathbf{0}$ and $\overline{\boldsymbol{q}} - \boldsymbol{\mu} \geqslant \mathbf{0}$. Moreover, we have $\boldsymbol{q}^\top \boldsymbol{\Sigma}^{-1} \boldsymbol{q} = \sum_{j=1}^{n} q_j^2/\sigma_j \geqslant q_i^2/\sigma_i = \boldsymbol{q}'^\top \boldsymbol{\Sigma}^{-1} \boldsymbol{q}'$. Since $\boldsymbol{q}$ and $\boldsymbol{q}'$ attain the same objective value in (2.13), we thus conclude that problem (2.13) attains the same optimal value as the univariate optimization problem

$$\begin{array}{ll} \text{maximize} & \mu_i + q_i \\ \text{subject to} & q_i^2/\sigma_i \leqslant \dfrac{1-\epsilon}{\epsilon} \\ & q_i \in \left[q_i^\ell,\, q_i^{\mathrm{u}}\right]. \end{array} \tag{2.14}$$

At optimality we have $q_i^2/\sigma_i = \frac{1-\epsilon}{\epsilon}$ or $q_i = q_i^{\mathrm{u}}$. The result now follows from a case distinction. ∎

The worst-case value-at-risk in Proposition 2.16 differs from the one in Proposition 2.13 only in the last term of the minimum operator, which corresponds to the variance bound in (2.11). Similar to the previous subsection, the expression (2.12) can be used to derive the worst-case value-at-risk if the support constraints or the variance constraint in (2.11) is disregarded.

Proposition 2.17 *A sequence of distributions $\mathbb{P}_i^t \in \mathcal{P}$, $t = 1, 2, \ldots$, that attain the worst-case value-at-risk $\sup_{\mathbb{P}\in\mathcal{P}} \mathbb{P}\text{-VaR}_{1-\epsilon}\left[\tilde{q}_i\right]$ in Proposition 2.16 asymptotically as $t \longrightarrow \infty$ can be defined as follows:*

(i) *If (2.12) is minimized by $\overline{q}_i - \mu_i$, then $\mathbb{P}_i^t = (1-\epsilon-1/t)\cdot\delta_{\boldsymbol{q}_1} + (\epsilon+1/t)\cdot\delta_{\boldsymbol{q}_2}$ with $\boldsymbol{q}_1 = \boldsymbol{\mu} - \frac{\epsilon}{1-\epsilon}(\overline{q}_i - \mu_i)\mathbf{e}_i$ and $\boldsymbol{q}_2 = \boldsymbol{\mu} + \frac{1-\epsilon-1/t}{\epsilon+1/t}\frac{\epsilon}{1-\epsilon}(\overline{q}_i - \mu_i)\mathbf{e}_i$.*

(ii) *If (2.12) is minimized by $\frac{1-\epsilon}{\epsilon}(\mu_i - \underline{q}_i)$, then $\mathbb{P}_i^t = (1-\epsilon-1/t)\cdot\delta_{\boldsymbol{q}_1} + (\epsilon+1/t)\cdot\delta_{\boldsymbol{q}_2}$ with $\boldsymbol{q}_1 = \boldsymbol{\mu} - (\mu_i - \underline{q}_i)\mathbf{e}_i$ and $\boldsymbol{q}_2 = \boldsymbol{\mu} + \frac{1-\epsilon-1/t}{\epsilon+1/t}(\mu_i - \underline{q}_i)\mathbf{e}_i$.*

(iii) *If (2.12) is minimized by $\sqrt{\frac{1-\epsilon}{\epsilon}\sigma_i}$, then $\mathbb{P}_i^t = (1-\epsilon-1/t)\cdot\delta_{\boldsymbol{q}_1} + (\epsilon+1/t)\cdot\delta_{\boldsymbol{q}_2}$ with $\boldsymbol{q}_1 = \boldsymbol{\mu} - \sqrt{\frac{\epsilon}{1-\epsilon}\sigma_i}\mathbf{e}_i$ and $\boldsymbol{q}_2 = \boldsymbol{\mu} + \frac{1-\epsilon-1/t}{\epsilon+1/t}\sqrt{\frac{\epsilon}{1-\epsilon}\sigma_i}\mathbf{e}_i$.*

Proof of Proposition 2.17. This proposition can be proved in the same way as Proposition 2.14. ∎

2.5.1.3 Semi-Variance Ambiguity Sets

We finally consider marginalized semi-variance ambiguity sets of the form

$$\mathcal{P} = \left\{ \mathbb{P} \in \mathcal{P}_0(\mathbb{R}^n) \ : \ \left[\begin{array}{l} \mathbb{P}\left[\tilde{\boldsymbol{q}} \in \mathcal{Q}\right] = 1, \ \ \mathbb{E}_{\mathbb{P}}\left[\tilde{\boldsymbol{q}}\right] = \boldsymbol{\mu}, \\ \mathbb{E}_{\mathbb{P}}\left[[\tilde{q}_i - \mu_i]_+^2\right] \leqslant \sigma_i^+, \ \ \mathbb{E}_{\mathbb{P}}\left[[\mu_i - \tilde{q}_i]_+^2\right] \leqslant \sigma_i^- \ \ \forall i \in V_C \end{array} \right] \right\}, \tag{2.15}$$

where $\mathcal{Q} = [\underline{\boldsymbol{q}}, \overline{\boldsymbol{q}}]$ with $\underline{\boldsymbol{q}} \geqslant \mathbf{0}$ and $\boldsymbol{\mu} \in \operatorname{int} \mathcal{Q}$ as well as $\boldsymbol{\sigma}^+, \boldsymbol{\sigma}^- > \mathbf{0}$.

As in the preceding two subsections, the worst-case value-at-risk of a customer's demand $\tilde{q}_i$ under the marginalized semi-variance ambiguity set (2.15) admits a closed-form solution.

Proposition 2.18 *Every marginalized semi-variance ambiguity set of the form* (2.15) *satisfies*

$$\sup_{\mathbb{P} \in \mathcal{P}} \ \mathbb{P}\text{-VaR}_{1-\epsilon}\big[\tilde{q}_i\big] \ = \ \mu_i + \min\left\{ \overline{q}_i - \mu_i, \frac{1-\epsilon}{\epsilon}(\mu_i - \underline{q}_i), \sqrt{\frac{\sigma_i^+}{\epsilon}}, \frac{\sqrt{(1-\epsilon)\sigma_i^-}}{\epsilon} \right\} \qquad \forall i \in V_C. \tag{2.16}$$

Please see the appendix of this chapter for the proof of Proposition 2.18.

The worst-case value-at-risk in Proposition 2.18 differs from the previous ones in the last two terms of the minimum operator, which correspond to the semi-variance bounds in (2.15). Again, the expression (2.16) can be used to derive the worst-case value-at-risk if the support constraints or either or both of the two semi-variance constraint in (2.15) are disregarded.

Proposition 2.19 *A sequence of distributions $\mathbb{P}_i^t \in \mathcal{P}$, $t = 1, 2, \ldots$, that attain the worst-case value-at-risk $\sup_{\mathbb{P} \in \mathcal{P}} \mathbb{P}\text{-VaR}_{1-\epsilon}\big[\tilde{q}_i\big]$ in Proposition 2.18 asymptotically as $t \longrightarrow \infty$ can be defined as follows:*

(i) *If* (2.16) *is minimized by $\overline{q}_i - \mu_i$, then $\mathbb{P}_i^t = (1 - \epsilon - 1/t) \cdot \delta_{\boldsymbol{q}_1} + (\epsilon + 1/t) \cdot \delta_{\boldsymbol{q}_2}$ with $\boldsymbol{q}_1 = \boldsymbol{\mu} - \frac{\epsilon}{1-\epsilon}(\overline{q}_i - \mu_i)\mathbf{e}_i$ and $\boldsymbol{q}_2 = \boldsymbol{\mu} + \frac{1-\epsilon-1/t}{\epsilon+1/t}\frac{\epsilon}{1-\epsilon}(\overline{q}_i - \mu_i)\mathbf{e}_i$.*

(ii) *If* (2.16) *is minimized by $\frac{1-\epsilon}{\epsilon}(\mu_i - \underline{q}_i)$, then $\mathbb{P}_i^t = (1 - \epsilon - 1/t) \cdot \delta_{\boldsymbol{q}_1} + (\epsilon + 1/t) \cdot \delta_{\boldsymbol{q}_2}$ with $\boldsymbol{q}_1 = \boldsymbol{\mu} - (\mu_i - \underline{q}_i)\mathbf{e}_i$ and $\boldsymbol{q}_2 = \boldsymbol{\mu} + \frac{1-\epsilon-1/t}{\epsilon+1/t}(\mu_i - \underline{q}_i)\mathbf{e}_i$.*

(iii) *If* (2.16) *is minimized by* $\sqrt{\frac{\sigma_i^+}{\epsilon}}$, *then* $\mathbb{P}_i^t = (1-\epsilon-1/t)\cdot\delta_{\boldsymbol{q}_1} + (\epsilon+1/t)\cdot\delta_{\boldsymbol{q}_2}$ *with* $\boldsymbol{q}_1 = \boldsymbol{\mu} - \frac{\epsilon}{1-\epsilon}\sqrt{\frac{\sigma_i^+}{\epsilon}}\mathbf{e}_i$ *and* $\boldsymbol{q}_2 = \boldsymbol{\mu} + \frac{1-\epsilon-1/t}{\epsilon+1/t}\frac{\epsilon}{1-\epsilon}\sqrt{\frac{\sigma_i^+}{\epsilon}}\mathbf{e}_i$.

(iv) *If* (2.16) *is minimized by* $\frac{\sqrt{(1-\epsilon)\sigma_i^-}}{\epsilon}$, *then* $\mathbb{P}_i^t = (1-\epsilon-1/t)\cdot\delta_{\boldsymbol{q}_1} + (\epsilon+1/t)\cdot\delta_{\boldsymbol{q}_2}$ *with* $\boldsymbol{q}_1 = \boldsymbol{\mu} - \sqrt{\frac{\sigma_i^-}{1-\epsilon}}\mathbf{e}_i$ *and* $\boldsymbol{q}_2 = \boldsymbol{\mu} + \frac{1-\epsilon-1/t}{\epsilon+1/t}\sqrt{\frac{\sigma_i^-}{1-\epsilon}}\mathbf{e}_i$.

Proof of Proposition 2.19. This proposition can be proved in the same way as Proposition 2.14. ■

2.5.2 Generic Moment Ambiguity Sets

We now study generic moment ambiguity sets of the form (2.4), where the dispersion measure $\boldsymbol{\varphi}$ characterizes the joint variability of multiple demands. In particular, we consider ambiguity sets that stipulate bounds on the mean absolute deviations (Section 2.5.2.1) and the covariances (Section 2.5.2.2).

2.5.2.1 First-Order Ambiguity Sets

We begin with first-order generic moment ambiguity sets of the form

$$\mathcal{P} = \left\{\mathbb{P} \in \mathcal{P}_0(\mathbb{R}^n) \,:\, \mathbb{P}\left[\tilde{\boldsymbol{q}} \in \mathcal{Q}\right] = 1,\;\; \mathbb{E}_{\mathbb{P}}\left[\tilde{\boldsymbol{q}}\right] = \boldsymbol{\mu},\;\; \mathbb{E}_{\mathbb{P}}\left[\mathbf{1}_{S_i}^\top|\tilde{\boldsymbol{q}} - \boldsymbol{\mu}|\right] \leqslant \nu_i \;\; \forall i = 1,\ldots,p\right\}, \quad (2.17)$$

where $\mathcal{Q} = [\underline{\boldsymbol{q}}, \overline{\boldsymbol{q}}]$ with $\underline{\boldsymbol{q}} \geqslant \mathbf{0}$, $\boldsymbol{\mu} \in \operatorname{int}\mathcal{Q}$ and $\boldsymbol{\nu} > \mathbf{0}$. As in Section 2.5.1.1, the absolute value operator $|\cdot|$ is applied component-wise. Note that (2.17) is a special case of the generic moment ambiguity set (2.4) where $\varphi_i(\boldsymbol{q}) = \sum_{j\in S_i} |\tilde{q}_j - \mu_j|$, $i = 1,\ldots,p$. In particular, the demand estimator $d_{\mathcal{P}}$ over the ambiguity set (2.17) is subadditive due to Theorem 2.8.

As we pointed out in Section 2.5.1.1, the mean absolute deviation in (2.17) is a popular dispersion measure in robust statistics. It is reminiscent of the standard deviation in classical statistics, but it is less affected by outliers and deviations from the classical model assumptions (*e.g.*, normality), which makes it more robust if the distribution is estimated from historical data. It can be shown that the sample mean absolute deviation outperforms the standard deviation in terms of asymptotic relative efficiency if the sample distribution has fat tails or if it is contaminated with another distribution [CB02]. For the use of the mean absolute deviation in (distributionally) robust optimization, see [BB12], [WKS14] and [PBTdM18].

The first-order generic moment ambiguity set (2.17) generalizes the first-order marginalized moment ambiguity set (2.9). The possibility to impose upper bounds on the mean absolute deviations of sums of customer demands allows to reduce the ambiguity whenever customer demands are not perfectly correlated. While one could in principle impose upper dispersion bounds on the cumulative demands of any customer subset $S_i \subseteq V_C$, this approach would require large amounts of data to estimate the corresponding dispersion bounds ν_i, and it would be computationally demanding to determine the associated RCI cuts. Instead, one may impose upper dispersion bounds on some 'canonical' customer subsets that are dictated by the application area, for example, all customers within a specific municipality, county or state. For a given set of demand observations, the dispersion bounds ν_i for different subsets $S_i \subseteq V_C$ can be derived analytically using asymptotic arguments [PGH01, Seg14] or empirically via bootstrapping [Che07].

Contrary to the marginalized ambiguity sets studied in Section 2.5.1, distributionally robust CVRPs with ambiguity sets of the form (2.17) typically *cannot* be reformulated as deterministic CVRPs.

Theorem 2.20 *For some instances of the distributionally robust CVRP with ambiguity set* (2.17) *there is no deterministic CVRP instance with the same set of feasible route sets.*

Proof of Theorem 2.20. To prove the statement, we consider a distributionally robust CVRP instance with $n = 4$ customers, $m = 2$ vehicles of capacity $Q = 10$, a risk threshold $\epsilon = 0.1$ and a first-order generic moment ambiguity set of the form (2.17) with support $\mathcal{Q} = [1, 10]^4$, expected demands $\boldsymbol{\mu} = 4.6\mathbf{e}$ and the following dispersion constraints:

$$\mathbb{E}_{\mathbb{P}}\left[|\tilde{q}_1 - \mu_1| + |\tilde{q}_3 - \mu_3|\right] \leqslant 0.1, \quad \mathbb{E}_{\mathbb{P}}\left[|\tilde{q}_2 - \mu_2| + |\tilde{q}_4 - \mu_4|\right] \leqslant 0.1$$

Evaluating the worst-case values-at-risk of all customer subsets shows that the subsets $\{1\}$, $\{2\}$, $\{3\}$, $\{4\}$, $\{1,3\}$ and $\{2,4\}$ can all be served by a single vehicle, $\{1,2\}$, $\{1,4\}$, $\{2,3\}$, $\{3,4\}$, $\{1,2,3\}$, $\{1,2,4\}$, $\{1,3,4\}$ and $\{2,3,4\}$ require two vehicles, and the set of all customers also requires two vehicles. This implies that the set of feasible route sets consists of the permutations of $\{\{1,3\},\{2,4\}\}$. We claim that there is no deterministic CVRP instance that has this set of feasible route sets.

Assume to the contrary that there is a demand vector $\boldsymbol{q}$ such that the associated deterministic CVRP instance has the aforementioned set of feasible route sets. In this case, we have $q_1 + q_2 > 10$ since $\{1,2\}$ cannot be served by a single vehicle. Since the four customers together require two vehicles, we also have $10 < q_1 + q_2 + q_3 + q_4 \leqslant 20$. We thus conclude that $q_3 + q_4 \leqslant 10$. This is not possible, however, since the route $\{3,4\}$ cannot be served by a single vehicle. ∎

Intuitively speaking, the non-existence of a deterministic reformulation is owed to the fact that the deterministic CVRP cannot capture dependencies between customer demands. The proof of Theorem 2.20 constructs a distributionally robust CVRP instance with four customers where the demands of the customers 1 and 3 (as well as 2 and 4) cannot vary much jointly, whereas the demands of the customers 1 and 2 (as well as 3 and 4) can vary much jointly. As a result, the customer subsets $\{1,3\}$ and $\{2,4\}$ can each be served by a single vehicle in the distributionally robust CVRP instance. In the deterministic CVRP, on the other hand, the potential presence of joint variability of customer demands implies that at least some of the demands have to be sufficiently high, which in turn excludes the possibility to serve all customers by two vehicles.

Although we are unable to evaluate the worst-case value-at-risk $\sup_{\mathbb{P}\in\mathcal{P}} \mathbb{P}\text{-VaR}_{1-\epsilon}\left[\sum_{i\in S} \tilde{q}_i\right]$ in closed form for the ambiguity set (2.17), the quantity can be computed in polynomial time.

Theorem 2.21 *The worst-case value-at-risk* $\sup_{\mathbb{P}\in\mathcal{P}} \mathbb{P}\text{-VaR}_{1-\epsilon}\big[\sum_{i\in S}\tilde{q}_i\big]$ *over the generic first-order ambiguity set* (2.17) *is equal to the optimal objective value of the following optimization problem.*

$$\begin{aligned} &\text{minimize} && \mathbf{1}_S{}^\top \boldsymbol{\mu} + \min\left\{ (\overline{\boldsymbol{q}} - \boldsymbol{\mu}),\ \frac{1-\epsilon}{\epsilon}(\boldsymbol{\mu} - \underline{\boldsymbol{q}}) \right\}^\top \left[\mathbf{1}_S - 2\sum_{i=1}^{p} \gamma_i \mathbf{1}_{S_i} \right]_+ + \frac{1}{\epsilon}\boldsymbol{\nu}^\top \boldsymbol{\gamma} \\ &\text{subject to} && \boldsymbol{\gamma} \in \mathbb{R}^p_+ \end{aligned} \tag{2.18}$$

Please see the appendix of this chapter for the proof of Theorem 2.21.

Problem (2.18) minimizes a non-smooth convex function over the non-negative orthant. It can be reformulated as a linear program and solved with a 'practical' complexity of $\mathcal{O}([|S| + p]^3)$, see [BV04, §11]. Faster solution times can be obtained through warm-starting.

We can derive a sequence of distributions that attain the worst-case value-at-risk asymptotically.

Proposition 2.22 *A sequence of distributions* $\mathbb{P}^t \in \mathcal{P}$, $t = 1, 2, \ldots$, *that attain the worst-case value-at-risk* $\sup_{\mathbb{P}\in\mathcal{P}} \mathbb{P}\text{-VaR}_{1-\epsilon}\big[\sum_{i\in S}\tilde{q}_i\big]$ *in Theorem 2.21 asymptotically as* $t \longrightarrow \infty$ *can be defined as* $\mathbb{P}^t = (\xi_1 - 1/t)\cdot\delta_{\boldsymbol{q}_1} + (\xi_2 + 1/t)\cdot\delta_{\boldsymbol{q}_2}$, *where* $\boldsymbol{q}_1 = \frac{\boldsymbol{\zeta}_1}{\xi_1}$ *and* $\boldsymbol{q}_2 = \frac{\boldsymbol{\zeta}_2}{\xi_2} - \frac{1}{t}\left(\frac{\boldsymbol{\zeta}_2}{\xi_2} - \frac{\boldsymbol{\zeta}_1}{\xi_1}\right)$, *and* $(\xi_i, \boldsymbol{\zeta}_i)$ *is an optimal solution to the linear program*

$$\begin{aligned} &\text{minimize} && \xi_1 \\ &\text{subject to} && \xi_1 + \xi_2 = 1, \qquad \boldsymbol{\zeta}_1 + \boldsymbol{\zeta}_2 = \boldsymbol{\mu} \\ &&& \underline{\boldsymbol{q}}\xi_i \leqslant \boldsymbol{\zeta}_i \leqslant \overline{\boldsymbol{q}}\xi_i, \quad -\boldsymbol{\rho}_i \leqslant \boldsymbol{\zeta}_i - \boldsymbol{\mu}\xi_i \leqslant \boldsymbol{\rho}_i \\ &&& \xi_2\tau \leqslant \mathbf{1}_S^\top \boldsymbol{\zeta}_2, \qquad \mathbf{S}(\boldsymbol{\rho}_1 + \boldsymbol{\rho}_2) \leqslant \boldsymbol{\nu} \\ &&& \xi_i \in \mathbb{R}_+,\ \boldsymbol{\zeta}_i \in \mathbb{R}^n,\ \boldsymbol{\rho}_i \in \mathbb{R}^n_+,\ i = 1, 2, \end{aligned}$$

where $\mathbf{S}$ *is a* $p \times n$ *matrix with rows* $\mathbf{1}_{S_i}^\top$, $i = 1, \ldots, p$.

Proof of Proposition 2.22. The proof follows along similar lines as the proof of Proposition 2.9. ∎

Although problem (2.18) can be solved in polynomial time, its solution may still be prohibitively expensive for large CVRP instances, where many RCIs have to be separated during the execution of a branch-and-cut scheme. It is therefore instructive to study special cases of the first-order generic moment ambiguity set (2.17) that allow for a faster computation of the worst-case value-at-risk (2.18).

Corollary 2.23 *If the ambiguity set* (2.17) *satisfies* $S_i \cap S_j = \emptyset$, $1 \leqslant i < j < p$, $\bigcup_{i=1}^{p-1} S_i = V_C$ *and* $S_p = V_C$, *then the worst-case value-at-risk* $\sup_{\mathbb{P} \in \mathcal{P}} \mathbb{P}\text{-VaR}_{1-\epsilon}\big[\sum_{i \in S} \tilde{q}_i\big]$ *evaluates to*

$$\mathbf{1}_S{}^\top \boldsymbol{\mu} + \min\left\{\frac{\nu_p}{2\epsilon},\ \sum_{i=1}^{p-1} \min\left\{\mathbf{1}_{S \cap S_i}{}^\top \hat{\boldsymbol{q}},\ \frac{\nu_i}{2\epsilon}\right\}\right\}, \tag{2.19}$$

where $\hat{\boldsymbol{q}} = \min\left\{\left(\overline{\boldsymbol{q}} - \boldsymbol{\mu}\right),\ \frac{1-\epsilon}{\epsilon}\left(\boldsymbol{\mu} - \underline{\boldsymbol{q}}\right)\right\}$.

Proof of Corollary 2.23. Under the assumption that $\bigcup_{i=1}^{p-1} S_i = V_C$, problem (2.18) can be written as

$$\begin{array}{ll} \text{minimize} & \mathbf{1}_S{}^\top \boldsymbol{\mu} + \displaystyle\sum_{i=1}^{p-1} \sum_{j \in S \cap S_i} \hat{q}_j \Big[1 - 2(\gamma_i + \gamma_p)\Big]_+ + \frac{1}{\epsilon} \boldsymbol{\nu}^\top \boldsymbol{\gamma} \\ \text{subject to} & \boldsymbol{\gamma} \in [\mathbf{0}, \mathbf{e}/2]. \end{array}$$

For a fixed value of γ_p, an optimal choice of γ_i, $i = 1, \ldots, p-1$, is $\gamma_i = 0$ if $\mathbf{1}_{S \cap S_i}{}^\top \hat{\boldsymbol{q}} \leqslant \nu_i/(2\epsilon)$ and $\gamma_i = \frac{1}{2} - \gamma_p$ otherwise. The problem thus simplifies to the one-dimensional problem

$$\begin{array}{ll} \text{minimize} & \mathbf{1}_S{}^\top \boldsymbol{\mu} + \displaystyle\sum_{i=1}^{p-1} \min\left\{(1 - 2\gamma_p)\mathbf{1}_{S \cap S_i}{}^\top \hat{\boldsymbol{q}},\ \frac{\nu_i}{\epsilon}\left[\frac{1}{2} - \gamma_p\right]\right\} + \frac{\nu_p}{\epsilon}\gamma_p \\ \text{subject to} & \gamma_p \in [0, 1/2]. \end{array}$$

Since the objective function is concave, its minimum is attained at $\gamma_p^\star \in \{0, 1/2\}$. ∎

The assumption that $\bigcup_{i=1}^{p-1} S_i = V_C$ comes without loss of generality as we can always add an auxiliary customer set S_i with a sufficiently large dispersion bound ν_i. The ambiguity set in

Corollary 2.23 is a generalization of the first-order marginalized ambiguity set (2.9) that allows to impose upper dispersion bounds on the cumulative demand of arbitrary non-overlapping customer subsets as well as on the sum of all customer demands. The expression (2.19) can be evaluated in time $\mathcal{O}(|S|)$. Moreover, if a customer subset $S' \subseteq V_C$ differs from a customer subset $S \subseteq V_C$ through the inclusion or removal of a single customer, then the expression (2.19) associated with S' can be computed from the expression (2.19) associated with S in time $\mathcal{O}(p)$.

An important special case of Corollary 2.23 arises when $p = n + 1$ and $S_i = \{i\}$, $i = 1, \ldots, p$.

Corollary 2.24 *If the ambiguity set* (2.17) *satisfies* $p = n + 1$, $S_i = \{i\}$, $i = 1, \ldots, n$, *and* $S_{n+1} = V_C$, *then the worst-case value-at-risk* $\sup_{\mathbb{P} \in \mathcal{P}} \mathbb{P}\text{-VaR}_{1-\epsilon}\big[\sum_{i \in S} \tilde{q}_i\big]$ *has the closed-form expression*

$$\mathbf{1}_S{}^\top \boldsymbol{\mu} + \min\left\{ \frac{\nu_{n+1}}{2\epsilon},\ \sum_{i \in S} \min\left\{ \hat{q}_i,\ \frac{\nu_i}{2\epsilon} \right\} \right\}, \tag{2.20}$$

where $\hat{\boldsymbol{q}} = \min\left\{ (\overline{\boldsymbol{q}} - \boldsymbol{\mu}),\ \frac{1-\epsilon}{\epsilon}(\boldsymbol{\mu} - \underline{\boldsymbol{q}}) \right\}$.

Proof of Corollary 2.24. The statement immediately follows from Corollary 2.23 if we use the definitions of the sets S_i in (2.19) and reorder the summation terms. ∎

Compared to the first-order marginalized ambiguity set (2.9), the ambiguity set in Corollary 2.24 additionally imposes an upper bound on the sum of mean absolute deviations of all customer demands. The expression (2.20) can be evaluated in time $\mathcal{O}(|S|)$. Moreover, if a customer subset $S' \subseteq V_C$ differs from a customer subset $S \subseteq V_C$ through the inclusion or removal of a single customer, then the expression (2.20) associated with S' can be computed from the expression (2.20) associated with S in constant time $\mathcal{O}(1)$. If no support is present in Corollary 2.24, then the worst-case value-at-risk (2.20) reduces to $\mathbf{1}_S{}^\top \boldsymbol{\mu} + \min\{\nu_{n+1},\ \sum_{i \in S} \nu_i\}/(2\epsilon)$, which is reminiscent of a budget uncertainty set in classical robust optimization [BS04].

2.5.2.2 Covariance Ambiguity Sets

We now consider second-order generic ambiguity sets (or *covariance ambiguity sets*) of the form

$$\mathcal{P} = \left\{ \mathbb{P} \in \mathcal{P}_0(\mathbb{R}^n) \, : \, \mathbb{P}\left[\tilde{\boldsymbol{q}} \in \mathcal{Q}\right] = 1, \;\; \mathbb{E}_{\mathbb{P}}\left[\tilde{\boldsymbol{q}}\right] = \boldsymbol{\mu}, \;\; \mathbb{E}_{\mathbb{P}}\left[(\tilde{\boldsymbol{q}} - \boldsymbol{\mu})(\tilde{\boldsymbol{q}} - \boldsymbol{\mu})^\top\right] \preceq \boldsymbol{\Sigma} \right\}, \tag{2.21}$$

where $\mathcal{Q} = [\underline{\boldsymbol{q}}, \overline{\boldsymbol{q}}]$ with $\underline{\boldsymbol{q}} \geqslant \mathbf{0}$, $\boldsymbol{\mu} \in \operatorname{int} \mathcal{Q}$ and $\boldsymbol{\Sigma} \succ \mathbf{0}$. Note that (2.21) is a special case of the generic moment ambiguity set (2.4) where $\varphi(\boldsymbol{q}) = \max_{\boldsymbol{z} \in \mathbb{R}^n \setminus \{\mathbf{0}\}} \left\{ \boldsymbol{z}^\top \left[(\boldsymbol{q} - \boldsymbol{\mu})(\boldsymbol{q} - \boldsymbol{\mu})^\top - \boldsymbol{\Sigma} \right] \boldsymbol{z} \right\}$ and $\sigma = 0$, and thus the demand estimator $d_{\mathcal{P}}$ over the ambiguity set (2.21) is subadditive due to Theorem 2.8.

The covariance ambiguity set (2.21) generalizes the marginalized variance ambiguity set (2.11). Similar to the mean absolute deviations on sums of customer demands in the previous subsection, the possibility to impose upper bounds on the covariances between pairs of customer demands allows to reduce the ambiguity whenever customer demands are not perfectly correlated. For a given set of demand observations, the upper covariance bound $\boldsymbol{\Sigma}$ can be derived analytically using McDiarmid's inequality [DY10] or empirically via bootstrapping [Che07].

As in the previous section, distributionally robust CVRPs with ambiguity sets of the form (2.21) typically *cannot* be reformulated as deterministic CVRPs.

Theorem 2.25 *For some instances of the distributionally robust CVRP with ambiguity set* (2.21) *there is no deterministic CVRP instance with the same set of feasible route sets.*

Proof of Theorem 2.25. To prove the statement, we consider the same distributionally robust CVRP instance as in the proof of Theorem 2.20, with the exception that the expected demands satisfy $\boldsymbol{\mu} = 4.5\mathbf{e}$ and the demand dispersion is bounded from above by the covariance matrix

$$\boldsymbol{\Sigma} = \begin{bmatrix} 0.1 & 0 & -0.05 & 0 \\ 0 & 0.1 & 0 & -0.05 \\ -0.05 & 0 & 0.1 & 0 \\ 0 & -0.05 & 0 & 0.1 \end{bmatrix}.$$

An evaluation of the worst-case values-at-risk for all customer subsets reveals that the set of feasible route sets is exactly the same as in the distributionally robust CVRP instance from the proof of Theorem 2.20. Thus, we can use the same argument as in that proof to conclude that there is no deterministic CVRP instance that has the same set of feasible route sets. ∎

Like the first-order generic ambiguity set from the previous section, the worst-case value-at-risk $\sup_{\mathbb{P}\in\mathcal{P}} \mathbb{P}\text{-VaR}_{1-\epsilon}\big[\sum_{i\in S}\tilde{q}_i\big]$ over the ambiguity set (2.21) can be computed in polynomial time.

Theorem 2.26 *The worst-case value-at-risk* $\sup_{\mathbb{P}\in\mathcal{P}} \mathbb{P}\text{-VaR}\big[\sum_{i\in S}\tilde{q}_i\big]$ *over the covariance ambiguity set* (2.21) *is equal to the optimal objective value of the optimization problem*

$$\begin{aligned} \text{maximize} \quad & \mathbf{1}_S{}^\top \boldsymbol{\mu} + \mathbf{1}_S{}^\top \boldsymbol{q} \\ \text{subject to} \quad & \boldsymbol{q}^\top \boldsymbol{\Sigma}^{-1} \boldsymbol{q} \leqslant \frac{1-\epsilon}{\epsilon} \\ & \boldsymbol{q} \in \big[\boldsymbol{q}^\ell,\, \boldsymbol{q}^u\big], \end{aligned} \tag{2.22}$$

where $\boldsymbol{q}^\ell = \max\big\{-\frac{1-\epsilon}{\epsilon}(\overline{\boldsymbol{q}} - \boldsymbol{\mu}),\, \underline{\boldsymbol{q}} - \boldsymbol{\mu}\big\}$ *and* $\boldsymbol{q}^u = \min\big\{\frac{1-\epsilon}{\epsilon}(\boldsymbol{\mu} - \underline{\boldsymbol{q}}),\, \overline{\boldsymbol{q}} - \boldsymbol{\mu}\big\}$.

Please see the appendix of this chapter for the proof of Theorem 2.26.

Problem (2.22) is a convex quadratically constrained quadratic program that maximizes an affine function over the intersection of an ellipsoid and a hyperrectangle. The problem can be solved with a 'practical' complexity of $\mathcal{O}(n^3)$, see [BV04, §11].

We now provide a sequence of distributions that attain the worst-case value-at-risk in the limit.

Proposition 2.27 *A sequence of distributions* $\mathbb{P}^t \in \mathcal{P}$, $t = 1, 2, \ldots$, *that attain the worst-case value-at-risk* $\sup_{\mathbb{P}\in\mathcal{P}} \mathbb{P}\text{-VaR}_{1-\epsilon}\big[\sum_{i\in S}\tilde{q}_i\big]$ *in Theorem 2.26 asymptotically as* $t \longrightarrow \infty$ *can be defined as* $\mathbb{P}^t = (\xi_1 - 1/t)\cdot\delta_{\boldsymbol{q}_1} + (\xi_2 + 1/t)\cdot\delta_{\boldsymbol{q}_2}$, *where* $\boldsymbol{q}_1 = \frac{\boldsymbol{\zeta}_1}{\xi_1}$ *and* $\boldsymbol{q}_2 = \frac{\boldsymbol{\zeta}_2}{\xi_2} + \frac{1}{t(\xi_2+1/t)}\big(\frac{\boldsymbol{\zeta}_1}{\xi_1} - \frac{\boldsymbol{\zeta}_2}{\xi_2}\big)$, *and* $(\xi_i, \boldsymbol{\zeta}_i)$ *is an optimal solution to the convex optimization problem*

$$\begin{array}{ll}\text{minimize} & \xi_1 \\ \text{subject to} & \xi_1 + \xi_2 = 1, \qquad \boldsymbol{\zeta}_1 + \boldsymbol{\zeta}_2 = \boldsymbol{\mu} \\ & \underline{\boldsymbol{q}}\xi_i \leqslant \boldsymbol{\zeta}_i \leqslant \overline{\boldsymbol{q}}\xi_i, \quad \mathbf{1}_S^\top \boldsymbol{\zeta}_2 \geqslant \xi_2 \tau \\ & \dfrac{1}{\xi_1}\left(\boldsymbol{\zeta}_1 - \xi_1\boldsymbol{\mu}\right)\left(\boldsymbol{\zeta}_1 - \xi_1\boldsymbol{\mu}\right)^\top + \dfrac{1}{\xi_2}\left(\boldsymbol{\zeta}_2 - \xi_2\boldsymbol{\mu}\right)\left(\boldsymbol{\zeta}_2 - \xi_2\boldsymbol{\mu}\right)^\top \preceq \boldsymbol{\Sigma} \\ & \xi_i \in \mathbb{R}_+, \ \boldsymbol{\zeta}_i \in \mathbb{R}^n, \ i = 1, 2. \end{array}$$

Proof of Proposition 2.27. The proof follows along similar lines as the proof of Proposition 2.9. ∎

Rather than solving problem (2.22) directly, we exploit strong convex duality, which applies since problem (2.22) affords a Slater point, to conclude that the dual second-order cone program

$$\begin{array}{ll}\text{minimize} & \mathbf{1}_S^\top \boldsymbol{\mu} + \sqrt{\dfrac{1-\epsilon}{\epsilon}} \left\| \boldsymbol{\Sigma}^{\frac{1}{2}} (\mathbf{e} - \boldsymbol{\lambda}) \right\|_2 + \boldsymbol{q}^{\mathrm{u}\top} \boldsymbol{\lambda} \\ \text{subject to} & \boldsymbol{\lambda} \in \mathbb{R}^n_+ \end{array}$$

attains the same optimal objective value as problem (2.22). Due to its benign structure, the dual problem can be solved quickly using the Fast Iterative Shrinkage Thresholding Algorithm [BT09] with adaptive restarts [OC15] if we move the nonnegativity constraints to the objective function through indicator functions and apply a Moreau proximal smoothing [BT12] to the conic quadratic term in the objective function.

An important special case of Theorem 2.26 arises when the upper covariance bound in the ambiguity set (2.21) satisfies $\boldsymbol{\Sigma} = \operatorname{diag}(\sigma_1^2, \ldots, \sigma_n^2)$. This could be due to *a priori* structural knowledge about the customer demands, or by bounding a non-diagonal matrix $\boldsymbol{\Sigma}$ from above (with respect to the positive semidefinite cone) to obtain a conservative (outer) approximation of (2.21).

Corollary 2.28 *If the ambiguity set* (2.21) *satisfies* $\boldsymbol{\Sigma} = \operatorname{diag}(\sigma_1^2, \ldots, \sigma_n^2)$, *then the worst-case value-at-risk* $\sup_{\mathbb{P} \in \mathcal{P}} \mathbb{P}\text{-VaR}\left[\sum_{i \in S} \tilde{q}_i\right]$ *is equal to the optimal objective value of the optimization* *problem*

$$\begin{aligned} \text{maximize} \quad & \mathbf{1}_S^\top \boldsymbol{\mu} + \sum_{i \in S(\theta)} q_i^{\mathrm{u}} + \sqrt{\left[\frac{1-\epsilon}{\epsilon} - \sum_{i \in S(\theta)} \left(\frac{q_i^{\mathrm{u}}}{\sigma_i}\right)^2\right] \left[\sum_{i \in S \setminus S(\theta)} \sigma_i^2\right]} \\ \text{subject to} \quad & \theta \in \mathbb{R}_+, \end{aligned} \tag{2.23}$$

where $S(\theta) = \{i \in S \,:\, \sigma_i^2 > \theta \cdot q_i^u\}$ *and* $\boldsymbol{q}^{\mathrm{u}} = \min\left\{\frac{1-\epsilon}{\epsilon}(\boldsymbol{\mu} - \underline{\boldsymbol{q}}), \overline{\boldsymbol{q}} - \boldsymbol{\mu}\right\}$, *and where the feasible region is restricted to those values of* θ *for which the expression inside the square root is non-negative, that is, for which* $\sum_{i \in S(\theta)} \left(\frac{q_i^u}{\sigma_i}\right)^2 \leqslant \frac{1-\epsilon}{\epsilon}$.

Proof of Corollary 2.28. The statement follows from Theorem 2.26 as well as an adaptation of Lemma 2 in [PP15] that replaces the box constraints $\boldsymbol{q} \in [-\mathbf{e}, +\mathbf{e}]$ from that paper with $\boldsymbol{q} \in [\boldsymbol{q}^\ell, \boldsymbol{q}^{\mathrm{u}}]$ and the ellipsoidal constraint $\boldsymbol{q}^\top \boldsymbol{q} \leqslant \kappa_2$ with $\boldsymbol{q}^\top \boldsymbol{\Sigma}^{-1} \boldsymbol{q} \leqslant \frac{1-\epsilon}{\epsilon}$. ∎

Corollary 2.28 allows us to compute the worst-case value-at-risk $\sup_{\mathbb{P} \in \mathcal{P}} \mathbb{P}\text{-VaR}\big[\sum_{i \in S} \tilde{q}_i\big]$ over the covariance ambiguity set (2.21) with a diagonal upper bound $\boldsymbol{\Sigma}$ in time $\mathcal{O}(|S|)$, given that the ratios $q_i^{\mathrm{u}}/\sigma_i^2$ have been sorted upfront. Indeed, we can determine the set $S(\theta) \subseteq S$ that maximizes (2.23) through a linear search that adds a single customer to the candidate set $S(\theta)$ in each iteration.

2.6 Numerical Results

In Section 2.6.1, we investigate how the parameter values of the marginal ambiguity sets from Section 2.5.1 impact the solution of the associated deterministic CVRP instance. We compare the performance of our tailored RCI cut evaluation schemes for the generic ambiguity sets from Section 2.5.2 with a state-of-the-art commercial solver in Section 2.6.2). And, finally, we compare the runtimes of the resulting branch-and-cut algorithms for the distributionally robust chance constrained CVRP with a corresponding implementation for the deterministic CVRP in Section 2.6.3.

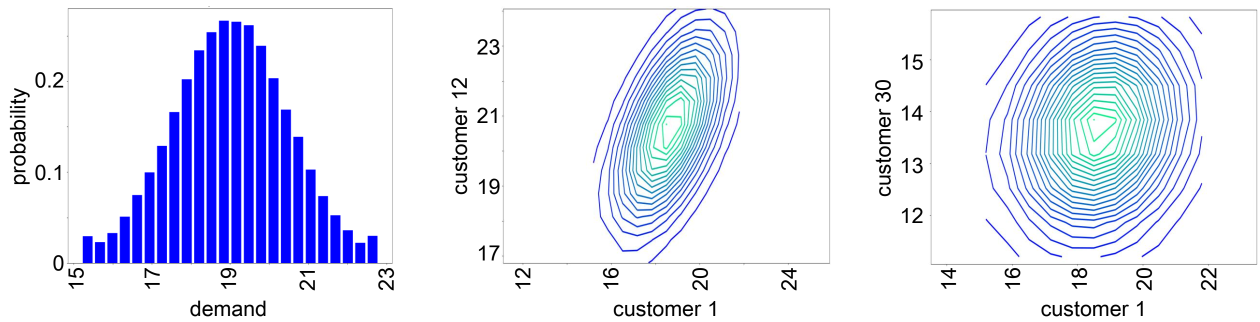

Figure 2.6: Demand distributions for the instance A-n32-k5. The left graph visualizes the histogram for customer 1, whereas the middle (right) graph illustrates the joint demand distribution of customers 1 and 12 (1 and 30), which are located nearby (far away).

With the exception of Section 2.6.2 below, all numerical results are based on the CVRP benchmark problems compiled by [D0́6]. The instances are named 'X-nY-kZ', where X denotes the literature source of the instance, Y is the number of nodes in the instance (including the depot) and Z is the number of vehicles. We only consider those problems for which two-dimensional coordinates for the nodes are available. Following the literature convention, we set the transportation costs c_{ij} to the Euclidean distance between i and j, rounded to the nearest integer.

Since the CVRP benchmark problems contain deterministic customer demands, we generate distributions for our stochastic demands according to the following procedure. The unscaled demand of customer $i \in V_C$ is set to $\tilde{\chi}_i = \frac{1}{2}\tilde{\xi}_i + \frac{1}{2|\mathcal{N}_i|}\sum_{j \in \mathcal{N}_i} \tilde{\xi}_j$, where $\tilde{\boldsymbol{\xi}} \sim \mathcal{N}(\mathbf{0}, \boldsymbol{I})$ is an n-dimensional normally distributed random vector and $\mathcal{N}_i \subseteq V_C$ is the set of the $\lfloor 0.1n \rfloor$ customers closest to i in terms of Euclidean distance. We subsequently apply an affine transformation which ensures that the expected demand of customer i is μ_i, which we identify with customer i's nominal demand from the deterministic CVRP instance, and that 99% of customer i's demand falls into the interval $[\underline{\boldsymbol{q}}, \overline{\boldsymbol{q}}]$, where the bounds $(\underline{\boldsymbol{q}}, \overline{\boldsymbol{q}})$ are set to $(\underline{\boldsymbol{q}}, \overline{\boldsymbol{q}}) = (0.8\boldsymbol{\mu}, 1.2\boldsymbol{\mu})$, unless specified otherwise. Finally, we clamp customer i's scaled demand distribution to the interval $[\underline{\boldsymbol{q}}, \overline{\boldsymbol{q}}]$. Our construction ensures that the customer demands exhibit a dependence structure that is informed by geographical proximity, see Figure 2.6. Since the unused vehicle capacities tend to be small already in the deterministic CVRP instances, we follow the approach in [GWF13b] and increase the vehicle capacities Q in each benchmark instance by 20%. This ensures that all distributionally robust CVRP instances remain feasible. We set the risk threshold to $\epsilon = 0.2$.

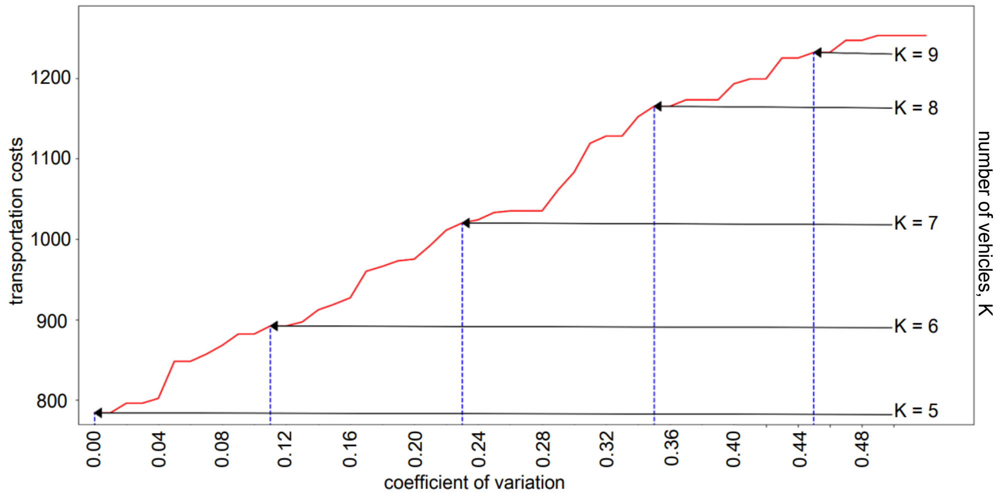

Figure 2.7: Minimum number of vehicles and optimal transportation costs for the instance A-n32-k5 with a marginalized variance ambiguity set and different variation coefficients ρ.

We solve the deterministic and distributionally robust CVRP instances with a 'vanilla' branch-and-cut algorithm that only separates RCI cuts according to the Tabu Search procedure proposed by [ABB+98]. Our branch-and-cut algorithm is implemented in C++ and uses the branch-and-bound capability of CPLEX 12.8.[2] We solve all problems in single-core mode on an Intel Xeon 2.66GHz processor with 8GB memory and a runtime limit of 12 hours.

2.6.1 Marginalized Ambiguity Sets

We first solve a distributionally robust version of the benchmark instance A-n32-k5 with a marginalized variance ambiguity set of the form (2.11). To this end, we identify the expected customer demands $\boldsymbol{\mu}$ with the nominal customer demands from the benchmark instance and set $(\underline{\boldsymbol{q}}, \overline{\boldsymbol{q}}) = (0.5\boldsymbol{\mu}, 2\boldsymbol{\mu})$. Moreover, we select $\sigma_i = (\rho\mu_i)^2$, $i \in V_C$, where ρ represents the coefficient of variation, which is assumed to be common for all customer demands. Contrary to the other experiments, we use the same vehicle capacities as in the benchmark instances.

Figure 2.7 illustrates the minimum number of vehicles required to serve all customers' demands, as well as the resulting transportation costs, as a function of the coefficient of variation ρ. Moreover, Figure 2.8 shows the optimal route sets corresponding to three different values of ρ.

[2] CPLEX website: `https://www.ibm.com/analytics/cplex-optimizer`.

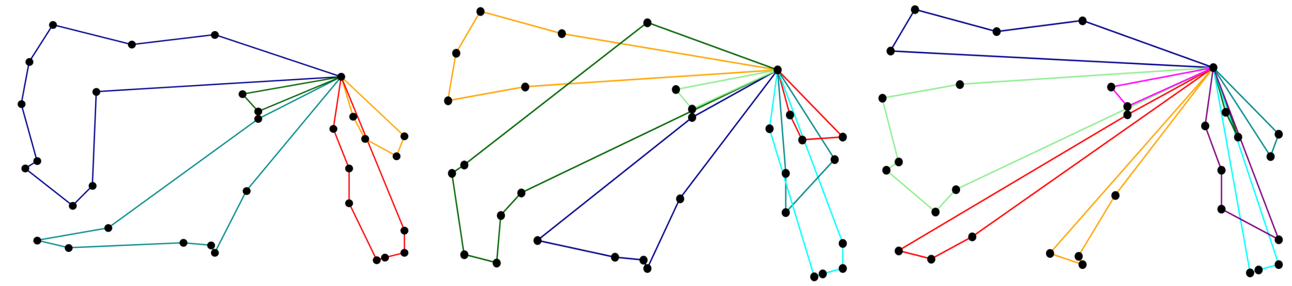

Figure 2.8: Optimal route sets for the instance A-n32-k5 with a marginalized variance ambiguity set and variation coefficients $\rho = 0$ (left; 5 vehicles), $\rho = 0.23$ (middle; 7 vehicles) and $\rho = 0.45$ (right; 9 vehicles).

We observe that a higher coefficient of variation ρ in the ambiguity set (2.11) hedges against larger sets of demand distributions in the distributionally robust CVRP instance, which in turn leads to higher nominal customer demands in the corresponding deterministic CVRP instance. As a result, both the number of vehicles and the transportation costs tend to increase with larger values of ρ.

2.6.2 Generic Ambiguity Sets: RCI Cut Evaluation

We first compare our tailored evaluation of the worst-case value-at-risk $\sup_{\mathbb{P} \in \mathcal{P}} \mathbb{P}\text{-VaR}_{1-\epsilon}\big[\sum_{i \in S} \tilde{q}_i\big]$ for first-order generic moment ambiguity sets (2.17) and covariance ambiguity sets (2.21) with their solution as linear and quadratically constrained quadratic programs via CPLEX, respectively. To this end, we generate random problem instances in which $n \in \{10, 15, \ldots, 200\}$ customers have nominal demands μ_i that are uniformly distributed on the set $\{1, \ldots, 10\}$ as well as random locations that are uniformly distributed on the square $[0, 10]^2$. We generate the demand distributions as described in the beginning of this section.

For the first-order ambiguity set (2.17), we partition the customers into four quadrants of equal size, and we select mean absolute deviations bounds for each quadrant as well as for the cumulative demands based on a sample from the joint demand distribution. Similarly, for the covariance ambiguity set (2.21), we select the covariance bound $\boldsymbol{\Sigma}$ based on a sample from the joint demand distribution. We also consider the special case of a diagonal covariance bound (see

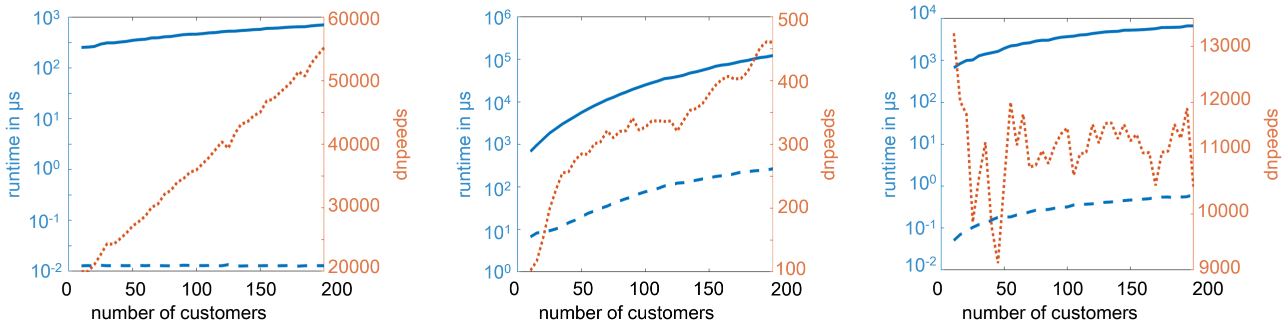

Figure 2.9: Runtimes for RCI cut evaluation. Shown are the average runtimes that CPLEX (solid lines) and our evaluation schemes (dashed lines) for first-order ambiguity sets (left graph), generic covariance ambiguity sets (middle graph) and covariance ambiguity sets with diagonal $\boldsymbol{\Sigma}$ (right graph) require to evaluate the right-hand side of a single RCI cut. The dotted lines represent the implied speedups.

Corollary 2.28) where we set all non-diagonal elements of the previously described covariance bound $\boldsymbol{\Sigma}$ to zero.

Figure 2.9 compares the runtimes of our tailored evaluation schemes with those of CPLEX for evaluating the right-hand side of a single RCI cut, that is, an individual worst-case value-at-risk $\sup_{\mathbb{P}\in\mathcal{P}} \mathbb{P}\text{-VaR}_{1-\epsilon}\big[\sum_{i\in S}\tilde{q}_i\big]$, on 1,000 randomly generated problem instances for each instance size n. While the achieved speedups are most significant for first-order ambiguity sets, they remain substantial for covariance ambiguity sets, especially if the covariance bound $\boldsymbol{\Sigma}$ is diagonal. The results are in line with our theoretical complexity estimates from Section 2.5.2, and they confirm our intuition that it is essential to study special classes of ambiguity sets $\mathcal{P}$ that give rise to easily computable demand estimators $d_{\mathcal{P}}$.

2.6.3 Generic Ambiguity Sets: Branch-and-Cut Scheme

We finally use our RCI cut evaluation schemes for the first-order and the two covariance ambiguity sets from the previous subsection to solve the CVRP benchmark instances of [D0́6]. We compare the runtimes and optimality gaps of the resulting branch-and-cut procedures with those of a deterministic branch-and-cut algorithm applied to the deterministic CVRP with worst-case demands $\boldsymbol{q} = \overline{\boldsymbol{q}}$. The results are summarized in Figure 3.2 as well as in Appendix A.

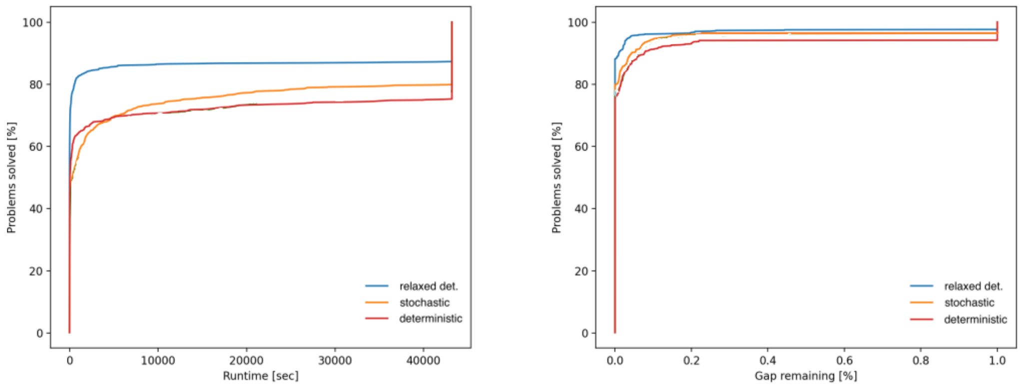

Figure 2.10: Runtimes and optimality gaps for our branch-and-cut schemes. Shown are the runtimes (left graph) and optimality gaps after 12 hours (right graph) for our deterministic branch-and-cut scheme with nominal demands $\boldsymbol{q} = \overline{\boldsymbol{q}}$ (blue, circles) as well as our distributionally robust branch-and-cut schemes over first order ambiguity sets (green, squares), second order ambiguity sets (red, triangles) and second order ambiguity sets with diagonal covariance bounds (cyan, stars).

The results show that our branch-and-cut schemes for the first-order as well as the diagonal covariance ambiguity set perform very similar to the branch-and-cut scheme for the deterministic CVRP, both in terms of the runtimes for successfully solved instances as well as the optimality gaps after 12 hours of runtime. In particular, all three algorithms can solve about 75% of the benchmark instances within the time limit, and the optimality gap is below 10% for roughly 90% of the instances. As expected from the previous subsection, our branch-and-cut scheme for covariance ambiguity sets with a non-diagonal bound $\boldsymbol{\Sigma}$ is slower; it solves about 65% of the benchmark instances within 12 hours, and the optimality gap is below 10% for about 80% of the instances.

To assess the conservatism of the obtained solutions, we consider 55 instances where all of the branch-and-cut schemes determined optimal solutions within the time limit and where the optimal solution of the deterministic CVRP with expected demands $\boldsymbol{q} = \boldsymbol{\mu}$ (henceforth the 'nominal solution') has strictly lower transportation costs than the optimal solution of the deterministic CVRP with component-wise worst-case demands $\boldsymbol{q} = \overline{\boldsymbol{q}}$ (henceforth the 'worst-case solution'). We then compute how much of the objective gap between the nominal solution and the robust solution is covered by each of the distributionally robust solutions. For our first-order ambiguity set as well as the covariance ambiguity set with a diagonal bound, every distributionally robust solution improves upon the worst-case solution, and the solutions close 75.5% of the objective gap on average. For our covariance ambiguity set with a non-diagonal bound, the distributionally robust solutions improve upon the worst-case solutions in 53 out of the 55 instances and close 52.1% of the objective gap on average. The results indicate that the distributionally robust CVRP can help to reduce the conservatism of naïve worst-case solutions.

2.7 Conclusion

Motivated by some of the shortcomings of the classical chance constrained CVRP, which assumes that the uncertain customer demands are governed by a precisely known distribution, we investigated the distributionally robust CVRP, in which this distribution is only partially characterized. In particular, we studied the computational tractability of the distributionally robust CVRP.

The solvability of the distributionally robust CVRP is largely determined by the choice of the ambiguity set. First and foremost, the ambiguity set should lead to a subadditive demand estimator so that standard branch-and-cut schemes can be used to solve the problem. This turns out to be the case for a large class of moment ambiguity sets. Secondly, the demand estimator should be easily computable. To this end, we have identified several classes of first-order and second-order moment ambiguity sets whose demand estimators can be computed by tailored algorithms that outperform an off-the-shelf commercial optimization package by orders of magnitude.

We must point out that despite the benefits of the model presented in this chapter, it has its shortcomings. The model only applies to moment ambiguity sets. This limits its applicability to other ambiguity sets in literature which may have better statistical properties, degree of conservativeness for the optimal solution as well as the amount of data required for a sufficiently accurate calibration of the ambiguity set. This is a fruitful avenue for future research. Moreover, even though our solution algorithms show significantly improved performance over the current literature, there still remains scope to improve the scalability as well as the run time performance for these solution algorithms. Finally, this chapter focuses exclusively on CVRP, which is an important class of VRP. There remain gaps for the proposed framework to be extended to other VRP variants.

We also note that some of our results may have applications outside the domain of vehicle routing. For example, Theorem 2.10 can be readily generalized to show that linear worst-case chance constraints over marginalized moment ambiguity sets reduce to deterministic inequality constraints. It therefore appears instructive to further explore the consequences of highly structured ambiguity sets in distributionally robust optimization in general.

2.8 Appendix

The proof of Theorem 2.8 relies on the following auxiliary result.

Lemma 2.29 (Strong Duality) *Let* $\mathcal{Q} = [\underline{\boldsymbol{q}}, \overline{\boldsymbol{q}}]$, $f : \mathbb{R}^n \mapsto \mathbb{R}$ *be an arbitrary function and* $\boldsymbol{\varphi} : \mathbb{R}^n \mapsto \mathbb{R}^p$ *be continuous. Assume that* $\boldsymbol{\mu} \in \operatorname{int} \mathcal{Q}$ *and that* $\boldsymbol{\varphi}(\boldsymbol{\mu}) < \boldsymbol{\sigma}$*. Then, strong duality holds between the primal moment problem*

$$
\begin{array}{ll}
\text{minimize} & \displaystyle\int_{\mathcal{Q}} f(\boldsymbol{q})\,\mathbb{P}(\mathrm{d}\boldsymbol{q}) \\
\text{subject to} & \displaystyle\int_{\mathcal{Q}} \mathbb{P}(\mathrm{d}\boldsymbol{q}) = 1 \\
& \displaystyle\int_{\mathcal{Q}} \boldsymbol{q}\,\mathbb{P}(\mathrm{d}\boldsymbol{q}) = \boldsymbol{\mu} \\
& \displaystyle\int_{\mathcal{Q}} \boldsymbol{\varphi}(\boldsymbol{q})\,\mathbb{P}(\mathrm{d}\boldsymbol{q}) \leqslant \boldsymbol{\sigma} \\
& \mathbb{P} \in \mathcal{M}_+(\mathcal{Q})
\end{array}
$$

and its semi-infinite dual problem

$$
\begin{array}{lll}
\text{maximize} & \alpha + \boldsymbol{\mu}^\top \boldsymbol{\beta} - \boldsymbol{\sigma}^\top \boldsymbol{\gamma} & \\
\text{subject to} & \alpha + \boldsymbol{q}^\top \boldsymbol{\beta} - \boldsymbol{\varphi}(\boldsymbol{q})^\top \boldsymbol{\gamma} \leqslant f(\boldsymbol{q}) & \forall \boldsymbol{q} \in \mathcal{Q} \\
& \alpha \in \mathbb{R}, \quad \boldsymbol{\beta} \in \mathbb{R}^n, \quad \boldsymbol{\gamma} \in \mathbb{R}^p_+. &
\end{array}
$$

Proof of Lemma 2.29. The result follows from Proposition 3.4 in [Sha01] if we can show that the point $(1, \boldsymbol{\mu}, \boldsymbol{\sigma})$ resides in the interior of the convex cone

$$\mathcal{V} = \left\{ (a, \boldsymbol{b}, \boldsymbol{c}) \in \mathbb{R} \times \mathbb{R}^n \times \mathbb{R}^p \, : \, \exists \mu \in \mathcal{M}_+(\mathcal{Q}) \text{ such that } \begin{array}{l} \int \mu(\mathrm{d}\boldsymbol{\xi}) = a, \\ \int \boldsymbol{q} \, \mu(\mathrm{d}\boldsymbol{\xi}) = \boldsymbol{b}, \\ \int \boldsymbol{\varphi}(\boldsymbol{q}) \, \mu(\mathrm{d}\boldsymbol{\xi}) \leqslant \boldsymbol{c} \end{array} \right\}.$$

In the following, we denote by $\mathbb{B}_\rho(\boldsymbol{x})$ the closed Euclidean ball of radius $\rho > 0$ that is centered at $\boldsymbol{x}$. We prove the statement by showing that any point $(s, \boldsymbol{m}, \boldsymbol{s}) \in \mathbb{B}_\kappa(1) \times \mathbb{B}_\kappa(\boldsymbol{\mu}) \times \mathbb{B}_\kappa(\boldsymbol{\sigma})$, where $\kappa > 0$ is sufficiently small, is contained in $\mathcal{V}$. Indeed, assume that κ is small enough so that $\boldsymbol{m}/s \in \mathcal{Q}$ and $\boldsymbol{\varphi}(\boldsymbol{m}/s) \leqslant \boldsymbol{s}/s$. This is possible since $\boldsymbol{\mu} \in \operatorname{int} \mathcal{Q}$, $\boldsymbol{\varphi}(\boldsymbol{\mu}) < \boldsymbol{\sigma}$ and $\boldsymbol{\varphi}$ is continuous. We then have that the scaled Dirac measure $s \cdot \delta_{\boldsymbol{m}/s}$ satisfies $s \cdot \delta_{\boldsymbol{m}/s} \in \mathcal{M}_+(\mathcal{Q})$, $\int s \cdot \delta_{\boldsymbol{m}/s} = s$, $\int \boldsymbol{q} \, s \cdot \delta_{\boldsymbol{m}/s} = \boldsymbol{m}$ as well as $\int \boldsymbol{\varphi}(\boldsymbol{q}) \, s \cdot \delta_{\boldsymbol{m}/s} = s \cdot \boldsymbol{\varphi}(\boldsymbol{m}/s) \leqslant \boldsymbol{s}$. We thus conclude that $(s, \boldsymbol{m}, \boldsymbol{s}) \in \mathcal{V}$ as desired. ∎

Proof of Theorem 2.8. We claim that the epigraph of the worst-case value-at-risk,

$$M \;=\; \left\{ (\boldsymbol{\lambda}, \tau) \in \mathbb{R}^n \times \mathbb{R} \, : \, \sup_{\mathbb{P} \in \mathcal{P}} \; \mathbb{P}\text{-VaR}_{1-\epsilon}\big[\boldsymbol{\lambda}^\top \tilde{\boldsymbol{q}}\big] \leqslant \tau \right\}, \tag{2.24}$$

is convex for moment ambiguity sets of the form (2.4). We then have

$$\sup_{\mathbb{P} \in \mathcal{P}} \; \mathbb{P}\text{-VaR}_{1-\epsilon}\Big[\sum_{i \in S} \tilde{q}_i\Big] \;=\; n \cdot \sup_{\mathbb{P} \in \mathcal{P}} \; \mathbb{P}\text{-VaR}_{1-\epsilon}\Big[\frac{1}{n} \sum_{i \in S} \tilde{q}_i\Big] \;\leqslant\; \sum_{i \in S} \sup_{\mathbb{P} \in \mathcal{P}} \; \mathbb{P}\text{-VaR}_{1-\epsilon}\big[\tilde{q}_i\big],$$

where the identity follows from the positive homogeneity of the value-at-risk (which carries over to the worst-case value-at-risk), and the inequality follows from the stated convexity of the epigraph of the worst-case value-at-risk [Roc70, Theorem 4.2].

We now show that the epigraph (2.24) is indeed convex for moment ambiguity sets. To this end, we note that $\sup_{\mathbb{P} \in \mathcal{P}} \mathbb{P}\text{-VaR}_{1-\epsilon}\big[\boldsymbol{\lambda}^\top \tilde{\boldsymbol{q}}\big] \leqslant \tau$ if and only if the optimal value of the moment problem

$$\begin{aligned} \text{minimize} \quad & \int_{\mathcal{Q}} \mathbb{I}_{[\boldsymbol{\lambda}^\top \boldsymbol{q} \leqslant \tau]} \, \mathbb{P}(\mathrm{d}\boldsymbol{q}) \\ \text{subject to} \quad & \int_{\mathcal{Q}} \mathbb{P}(\mathrm{d}\boldsymbol{q}) = 1 \\ & \int_{\mathcal{Q}} \boldsymbol{q} \, \mathbb{P}(\mathrm{d}\boldsymbol{q}) = \boldsymbol{\mu} \\ & \int_{\mathcal{Q}} \boldsymbol{\varphi}(\boldsymbol{q}) \, \mathbb{P}(\mathrm{d}\boldsymbol{q}) \leqslant \boldsymbol{\sigma} \\ & \mathbb{P} \in \mathcal{M}_+(\mathcal{Q}) \end{aligned}$$

is greater than or equal to $1 - \epsilon$. By Lemma 2.29, this is the case if and only if the optimal objective value of the semi-infinite dual problem

$$\begin{aligned} \text{maximize} \quad & \alpha + \boldsymbol{\mu}^\top \boldsymbol{\beta} - \boldsymbol{\sigma}^\top \boldsymbol{\gamma} \\ \text{subject to} \quad & \alpha + \boldsymbol{q}^\top \boldsymbol{\beta} - \boldsymbol{\varphi}(\boldsymbol{q})^\top \boldsymbol{\gamma} \leqslant \mathbb{I}_{[\boldsymbol{\lambda}^\top \boldsymbol{q} \leqslant \tau]} \qquad \forall \boldsymbol{q} \in \mathcal{Q} \\ & \alpha \in \mathbb{R}, \;\; \boldsymbol{\beta} \in \mathbb{R}^n, \;\; \boldsymbol{\gamma} \in \mathbb{R}^p_+ \end{aligned}$$

is greater than or equal to $1 - \epsilon$. By splitting up the semi-infinite constraint, we obtain

$$\begin{aligned} \text{maximize} \quad & \alpha + \boldsymbol{\mu}^\top \boldsymbol{\beta} - \boldsymbol{\sigma}^\top \boldsymbol{\gamma} \\ \text{subject to} \quad & \alpha + \boldsymbol{q}^\top \boldsymbol{\beta} - \boldsymbol{\varphi}(\boldsymbol{q})^\top \boldsymbol{\gamma} \leqslant 1 \qquad \forall \boldsymbol{q} \in \mathcal{Q} \\ & \alpha + \boldsymbol{q}^\top \boldsymbol{\beta} - \boldsymbol{\varphi}(\boldsymbol{q})^\top \boldsymbol{\gamma} \leqslant 0 \qquad \forall \boldsymbol{q} \in \mathcal{Q} \, : \, \boldsymbol{\lambda}^\top \boldsymbol{q} > \tau \\ & \alpha \in \mathbb{R}, \;\; \boldsymbol{\beta} \in \mathbb{R}^n, \;\; \boldsymbol{\gamma} \in \mathbb{R}^p_+. \end{aligned} \tag{2.25}$$

We first assume that $\tau \neq [\boldsymbol{\lambda}]_+^\top \overline{\boldsymbol{q}} - [-\boldsymbol{\lambda}]_+^\top \underline{\boldsymbol{q}}$. In that case, we have $\{\boldsymbol{q} \in \mathcal{Q} \, : \, \boldsymbol{\lambda}^\top \boldsymbol{q} > \tau\} \neq \emptyset$ if and only if $\{\boldsymbol{q} \in \mathcal{Q} \, : \, \boldsymbol{\lambda}^\top \boldsymbol{q} \geqslant \tau\} \neq \emptyset$, and we can replace the strict inequality in the parameterization of the second constraint with a weak one due to the convexity (and, *a fortiori*, continuity) of $\boldsymbol{\varphi}$.

The first constraint in (2.25) is satisfied if and only if

$$\left[\begin{array}{ll} \text{maximize} & \alpha + \boldsymbol{q}^\top \boldsymbol{\beta} - \boldsymbol{\varphi}(\boldsymbol{q})^\top \boldsymbol{\gamma} \\ \text{subject to} & \boldsymbol{q} \in \mathcal{Q} \end{array} \right] \leqslant 1 \quad \Longleftrightarrow \quad \left[\begin{array}{ll} \text{minimize} & -\boldsymbol{q}^\top \boldsymbol{\beta} + \boldsymbol{\varphi}(\boldsymbol{q})^\top \boldsymbol{\gamma} \\ \text{subject to} & \boldsymbol{q} \in [\underline{\boldsymbol{q}}, \overline{\boldsymbol{q}}] \end{array} \right] \geqslant \alpha - 1.$$

Strong convex duality, which holds since the support $\mathcal{Q}$ has a nonempty interior, implies that this is the case if and only if the optimal value of the dual problem,

$$\begin{array}{ll} \text{maximize} & \underline{\boldsymbol{q}}^\top \underline{\boldsymbol{\nu}}_1 - \overline{\boldsymbol{q}}^\top \overline{\boldsymbol{\nu}}_1 - \sum_{i=1}^{p} \gamma_i \varphi_i^\star(\boldsymbol{\phi}_i/\gamma_i) \\ \text{subject to} & \sum_{i=1}^{p} \boldsymbol{\phi}_{1i} = \boldsymbol{\beta} + \underline{\boldsymbol{\nu}}_1 - \overline{\boldsymbol{\nu}}_1 \\ & \underline{\boldsymbol{\nu}}_1, \overline{\boldsymbol{\nu}}_1 \in \mathbb{R}^n_+, \quad \boldsymbol{\phi}_{1i} \in \mathbb{R}^n, \ i = 1, \ldots, p, \end{array}$$

is greater than or equal to $\alpha - 1$. Here, $\varphi_i^\star$ is the conjugate function of φ_i.

The second constraint in (2.25) is satisfied if and only if

$$\left[\begin{array}{ll} \text{maximize} & \alpha + \boldsymbol{q}^\top \boldsymbol{\beta} - \boldsymbol{\varphi}(\boldsymbol{q})^\top \boldsymbol{\gamma} \\ \text{subject to} & \boldsymbol{q} \in \mathcal{Q} \\ & \boldsymbol{\lambda}^\top \boldsymbol{q} \geqslant \tau \end{array} \right] \leqslant 0 \iff \left[\begin{array}{ll} \text{minimize} & -\boldsymbol{q}^\top \boldsymbol{\beta} + \boldsymbol{\varphi}(\boldsymbol{q})^\top \boldsymbol{\gamma} \\ \text{subject to} & \boldsymbol{q} \in [\underline{\boldsymbol{q}}, \overline{\boldsymbol{q}}] \\ & \boldsymbol{\lambda}^\top \boldsymbol{q} \geqslant \tau \end{array} \right] \geqslant \alpha. \tag{2.26}$$

In the following, we distinguish three mutually exclusive and collectively exhaustive cases: *(i)* there is a Slater point $\boldsymbol{q} \in \operatorname{int} \mathcal{Q}$ satisfying $\boldsymbol{\lambda}^\top \boldsymbol{q} > \tau$; *(ii)* there is no $\boldsymbol{q} \in \mathcal{Q}$ that satisfies $\boldsymbol{\lambda}^\top \boldsymbol{q} \geqslant \tau$; and *(iii)* there are $\boldsymbol{q} \in \mathcal{Q}$ that satisfy $\boldsymbol{\lambda}^\top \boldsymbol{q} \geqslant \tau$, but none of them satisfies $\boldsymbol{q} \in \operatorname{int} \mathcal{Q}$ and $\boldsymbol{\lambda}^\top \boldsymbol{q} > \tau$. In the first case, strong convex duality holds, and (2.26) is satisfied if and only if the optimal value of the dual problem,

$$\begin{array}{ll} \text{maximize} & \underline{\boldsymbol{q}}^\top \underline{\boldsymbol{\nu}}_0 - \overline{\boldsymbol{q}}^\top \overline{\boldsymbol{\nu}}_0 + \tau\eta - \sum_{i=1}^{p} \gamma_i \varphi_i^\star(\boldsymbol{\phi}_{0i}/\gamma_i) \\ \text{subject to} & \sum_{i=1}^{p} \boldsymbol{\phi}_{0i} = \boldsymbol{\beta} + \underline{\boldsymbol{\nu}}_0 - \overline{\boldsymbol{\nu}}_0 + \eta\boldsymbol{\lambda} \\ & \underline{\boldsymbol{\nu}}_0, \overline{\boldsymbol{\nu}}_0 \in \mathbb{R}^n_+, \quad \eta \in \mathbb{R}_+, \quad \boldsymbol{\phi}_{0i} \in \mathbb{R}^n, \ i = 1, \ldots, p, \end{array} \tag{2.27}$$

is greater than or equal to α. In the second case, fix $\eta \in \mathbb{R}_+$ and set $\underline{\boldsymbol{\nu}}_0 = [-\boldsymbol{\beta} - \eta\boldsymbol{\lambda}]_+$, $\overline{\boldsymbol{\nu}}_0 = [\boldsymbol{\beta} + \eta\boldsymbol{\lambda}]_+$ and $\boldsymbol{\phi}_{0i} = \boldsymbol{0}$, $i = 1, \ldots, p$. This choice is feasible in (2.27) and attains the objective value

$$\underline{\boldsymbol{q}}^\top [-\boldsymbol{\beta} - \eta\boldsymbol{\lambda}]_+ - \overline{\boldsymbol{q}}^\top [\boldsymbol{\beta} + \eta\boldsymbol{\lambda}]_+ + \tau\eta - c \;=\; \eta\Big(\underline{\boldsymbol{q}}^\top [-\boldsymbol{\beta}/\eta - \boldsymbol{\lambda}]_+ - \overline{\boldsymbol{q}}^\top [\boldsymbol{\beta}/\eta + \boldsymbol{\lambda}]_+ + \tau\Big) - c \;\longrightarrow\; +\infty$$

as $\eta \longrightarrow +\infty$ since $\underline{\boldsymbol{q}}^\top [-\boldsymbol{\beta}/\eta - \boldsymbol{\lambda}]_+ - \overline{\boldsymbol{q}}^\top [\boldsymbol{\beta}/\eta + \boldsymbol{\lambda}]_+ \longrightarrow -\widehat{\boldsymbol{q}}^\top \boldsymbol{\lambda}$ for $\widehat{\boldsymbol{q}} \in \mathcal{Q}$ defined via $\hat{q}_i = \underline{q}_i$

if $\lambda_i < 0$ and $\hat{q}_i = \overline{q}_i$ otherwise, $i = 1, \ldots, n$, and $\boldsymbol{\lambda}^\top \boldsymbol{q} < \tau$ for all $\boldsymbol{q} \in \mathcal{Q}$. In this argument, the term $c = \sum_{i=1}^p \gamma_i \varphi_i^\star(\boldsymbol{\phi}_{0i}/\gamma_i) = \boldsymbol{\gamma}^\top \boldsymbol{\varphi}^\star(\mathbf{0})$ is constant. As for the third case, denote by (2.26_ϵ) and (2.27_ϵ) the variants of problems (2.26) and (2.27) where we replace the parameters $(\underline{\boldsymbol{q}}, \overline{\boldsymbol{q}})$ with $(\underline{\boldsymbol{q}} - \epsilon \mathbf{e}, \overline{\boldsymbol{q}} + \epsilon \mathbf{e})$, respectively. Ignoring the trivial case where $\boldsymbol{\lambda} = \mathbf{0}$ and $\tau = 0$, we observe that strong duality holds between (2.26_ϵ) and (2.27_ϵ) for every $\epsilon > 0$. Moreover, one readily verifies that the mapping $\epsilon \mapsto (2.26_\epsilon)$ is right continuous at $\epsilon = 0$, that the problems $(2.26) \equiv (2.26_0)$ and $(2.27) \equiv (2.27_0)$ are both feasible, and that the optimal value of (2.26) is greater than or equal to the optimal value of (2.27) by weak duality. Since the optimal value of $(2.27_{\epsilon'})$ is greater than or equal to the optimal value of (2.27_ϵ) for all $0 \leqslant \epsilon' \leqslant \epsilon$, we thus conclude that the optimal values of the problems (2.26) and (2.27) also coincide.

The previous two paragraphs imply that for all $\tau \in \mathbb{R}$, $\tau \neq [\boldsymbol{\lambda}]_+^\top \overline{\boldsymbol{q}} - [-\boldsymbol{\lambda}]_+^\top \underline{\boldsymbol{q}}$, we have that $\sup_{\mathbb{P} \in \mathcal{P}} \mathbb{P}\text{-VaR}_{1-\epsilon}\big[\boldsymbol{\lambda}^\top \tilde{\boldsymbol{q}}\big] \leqslant \tau$ if and only if

$$\begin{array}{c} \exists \alpha \in \mathbb{R}, \;\; \boldsymbol{\beta} \in \mathbb{R}^n, \;\; \boldsymbol{\gamma} \in \mathbb{R}_+^p, \;\; \underline{\boldsymbol{\nu}}_1, \overline{\boldsymbol{\nu}}_1, \underline{\boldsymbol{\nu}}_0, \overline{\boldsymbol{\nu}}_0 \in \mathbb{R}_+^n, \\ \eta \in \mathbb{R}_+, \;\; \boldsymbol{\phi}_{1i}, \boldsymbol{\phi}_{0i} \in \mathbb{R}^n, \; i = 1, \ldots, p \; : \end{array} \quad \left\{ \begin{array}{l} \alpha + \boldsymbol{\mu}^\top \boldsymbol{\beta} - \boldsymbol{\sigma}^\top \boldsymbol{\gamma} \geqslant 1 - \epsilon \\ \underline{\boldsymbol{q}}^\top \underline{\boldsymbol{\nu}}_1 - \overline{\boldsymbol{q}}^\top \overline{\boldsymbol{\nu}}_1 - \displaystyle\sum_{i=1}^p \gamma_i \varphi_i^\star(\boldsymbol{\phi}_{1i}/\gamma_i) \geqslant \alpha - 1 \\ \underline{\boldsymbol{q}}^\top \underline{\boldsymbol{\nu}}_0 - \overline{\boldsymbol{q}}^\top \overline{\boldsymbol{\nu}}_0 + \tau\eta - \displaystyle\sum_{i=1}^p \gamma_i \varphi_i^\star(\boldsymbol{\phi}_{0i}/\gamma_i) \geqslant \alpha \\ \displaystyle\sum_{i=1}^p \boldsymbol{\phi}_{1i} = \boldsymbol{\beta} + \underline{\boldsymbol{\nu}}_1 - \overline{\boldsymbol{\nu}}_1, \;\; \displaystyle\sum_{i=1}^p \boldsymbol{\phi}_{0i} = \boldsymbol{\beta} + \underline{\boldsymbol{\nu}}_0 - \overline{\boldsymbol{\nu}}_0 + \eta \boldsymbol{\lambda}. \end{array} \right.$$

We claim that any feasible solution to this system of equations satisfies $\eta > 0$. Assume to the contrary that there was a feasible solution with $\eta = 0$. In that case, the constraint system would be independent of τ, and we would have $\sup_{\mathbb{P} \in \mathcal{P}} \mathbb{P}\text{-VaR}_{1-\epsilon}\big[\boldsymbol{\lambda}^\top \tilde{\boldsymbol{q}}\big] \leqslant \tau$ either for all $\tau \in \mathbb{R}$ or for no $\tau \in \mathbb{R}$. However, this cannot be the case since $\tilde{\boldsymbol{q}} \in \mathcal{Q}$ $\mathbb{P}$-a.s. for all $\mathbb{P} \in \mathcal{P}$ and the support $\mathcal{Q}$ is bounded. We thus conclude that $\eta > 0$, which allows us to replace all decision variables by their division through η and replace η with $1/\eta$. We have thus established that for

$\tau \neq [\boldsymbol{\lambda}]_+^\top \overline{\boldsymbol{q}} - [-\boldsymbol{\lambda}]_+^\top \underline{\boldsymbol{q}}$, we have $\sup_{\mathbb{P}\in\mathcal{P}} \mathbb{P}\text{-VaR}_{1-\epsilon}\big[\boldsymbol{\lambda}^\top \tilde{\boldsymbol{q}}\big] \leqslant \tau$ if and only if

$$\begin{array}{c} \exists \alpha \in \mathbb{R},\ \ \boldsymbol{\beta} \in \mathbb{R}^n,\ \ \boldsymbol{\gamma} \in \mathbb{R}^p_+,\ \ \underline{\boldsymbol{\nu}}_1, \overline{\boldsymbol{\nu}}_1, \underline{\boldsymbol{\nu}}_0, \overline{\boldsymbol{\nu}}_0 \in \mathbb{R}^n_+, \\ \eta \in \mathbb{R}_+,\ \ \boldsymbol{\phi}_{1i}, \boldsymbol{\phi}_{0i} \in \mathbb{R}^n,\ i = 1, \ldots, p\ : \end{array} \quad \begin{cases} \alpha + \boldsymbol{\mu}^\top \boldsymbol{\beta} - \boldsymbol{\sigma}^\top \boldsymbol{\gamma} \geqslant (1-\epsilon)\eta \\ \underline{\boldsymbol{q}}^\top \underline{\boldsymbol{\nu}}_1 - \overline{\boldsymbol{q}}^\top \overline{\boldsymbol{\nu}}_1 - \sum_{i=1}^p \gamma_i \varphi_i^\star(\boldsymbol{\phi}_{1i}/\gamma_i) \geqslant \alpha - \eta \\ \underline{\boldsymbol{q}}^\top \underline{\boldsymbol{\nu}}_0 - \overline{\boldsymbol{q}}^\top \overline{\boldsymbol{\nu}}_0 + \tau - \sum_{i=1}^p \gamma_i \varphi_i^\star(\boldsymbol{\phi}_{0i}/\gamma_i) \geqslant \alpha \\ \sum_{i=1}^p \boldsymbol{\phi}_{1i} = \boldsymbol{\beta} + \underline{\boldsymbol{\nu}}_1 - \overline{\boldsymbol{\nu}}_1,\ \ \sum_{i=1}^p \boldsymbol{\phi}_{0i} = \boldsymbol{\beta} + \underline{\boldsymbol{\nu}}_0 - \overline{\boldsymbol{\nu}}_0 + \boldsymbol{\lambda}. \end{cases} \tag{2.28}$$

Assume now that $\tau = [\boldsymbol{\lambda}]_+^\top \overline{\boldsymbol{q}} - [-\boldsymbol{\lambda}]_+^\top \underline{\boldsymbol{q}}$. In that case, the application of our continuity argument to equation (2.25) could imply that $\sup_{\mathbb{P}\in\mathcal{P}} \mathbb{P}\text{-VaR}_{1-\epsilon}\big[\boldsymbol{\lambda}^\top \tilde{\boldsymbol{q}}\big] \leqslant \tau$ but the equation system (2.28) is not satisfiable. To prove that this is not possible, we show that the set-valued mapping $\tau \mapsto S(\tau)$, where $S(\tau)$ is the set of all $(\alpha, \boldsymbol{\beta}, \boldsymbol{\gamma}, \underline{\boldsymbol{\nu}}_i, \overline{\boldsymbol{\nu}}_i, \eta, \boldsymbol{\phi}_{ij})$ satisfying (2.28), is outer semicontinuous [RW97, Definition 5.4]. This is the case if and only if the graph of S—that is, the set of all $\boldsymbol{\lambda} \in \mathbb{R}^n$, $\tau \in \mathbb{R}$ and $\alpha \in \mathbb{R}$, $\boldsymbol{\beta} \in \mathbb{R}^n$, $\boldsymbol{\gamma} \in \mathbb{R}^p_+$, $\underline{\boldsymbol{\nu}}_1, \overline{\boldsymbol{\nu}}_1, \underline{\boldsymbol{\nu}}_0, \overline{\boldsymbol{\nu}}_0 \in \mathbb{R}^n_+$, $\eta \in \mathbb{R}_+$ as well as $\boldsymbol{\phi}_{1i}, \boldsymbol{\phi}_{0i} \in \mathbb{R}^n$, $i = 1, \ldots, p$, satisfying (2.28)—is closed [RW97, Theorem 5.7]. Indeed, the conjugate functions $\varphi_i^\star$ are convex by construction, and their convexity is preserved by the perspective functions [BV04, §3.2.6]. The result now follows since convex functions are continuous [RW97, Theorem 2.35] and the lower level sets of continuous functions are closed [RW97, Theorem 1.6]. We thus conclude that for *all* $\tau \in \mathbb{R}$, we have $\sup_{\mathbb{P}\in\mathcal{P}} \mathbb{P}\text{-VaR}_{1-\epsilon}\big[\boldsymbol{\lambda}^\top \tilde{\boldsymbol{q}}\big] \leqslant \tau$ if and only if (2.28) is satisfiable.

By construction, the set of all $\boldsymbol{\lambda} \in \mathbb{R}^n$, $\tau \in \mathbb{R}$ and $\alpha \in \mathbb{R}$, $\boldsymbol{\beta} \in \mathbb{R}^n$, $\boldsymbol{\gamma} \in \mathbb{R}^p_+$, $\underline{\boldsymbol{\nu}}_1, \overline{\boldsymbol{\nu}}_1, \underline{\boldsymbol{\nu}}_0, \overline{\boldsymbol{\nu}}_0 \in \mathbb{R}^n_+$, $\eta \in \mathbb{R}_+$ as well as $\boldsymbol{\phi}_{1i}, \boldsymbol{\phi}_{0i} \in \mathbb{R}^n$, $i = 1, \ldots, p$, satisfying the equation system (2.28) is convex. The set M is a projection of this set onto $\boldsymbol{\lambda}$ and τ and is thus convex as well. ∎

Proof of Proposition 2.18. The rectangularity of the ambiguity set $\mathcal{P}$ allows us to conclude that

$$\sup_{\mathbb{P}\in\mathcal{P}} \mathbb{P}\text{-VaR}_{1-\epsilon}\big[\tilde{q}_i\big] = \sup_{\mathbb{P}\in\mathcal{P}_i} \mathbb{P}\text{-VaR}_{1-\epsilon}\big[\tilde{q}_i\big]$$

with

$$\mathcal{P}_i = \left\{ \mathbb{P} \in \mathcal{P}_0(\mathbb{R}) \, : \, \left[\begin{array}{l} \mathbb{P}\left[\tilde{q}_i \in [\underline{q}_i, \, \overline{q}_i]\right] = 1, \;\; \mathbb{E}_{\mathbb{P}}\left[\tilde{q}_i\right] = \mu_i, \\ \mathbb{E}_{\mathbb{P}}\left[[\tilde{q}_i - \mu_i]_+^2\right] \leqslant \sigma_i^+, \;\; \mathbb{E}_{\mathbb{P}}\left[[\mu_i - \tilde{q}_i]_+^2\right] \leqslant \sigma_i^- \;\;\; \forall i \in V_C \end{array} \right] \right\}.$$

For a fixed scalar $\tau \in \mathbb{R}$, we then have $\sup_{\mathbb{P} \in \mathcal{P}_i} \mathbb{P}\text{-VaR}_{1-\epsilon}\left[\tilde{q}_i\right] \leqslant \tau$ if and only if the optimal objective value of the moment problem

$$\begin{array}{ll} \text{minimize} & \displaystyle\int_{[\underline{q}_i, \overline{q}_i]} \mathbb{I}_{[q_i \leqslant \tau]} \mathbb{P}(\mathrm{d}q_i) \\ \text{subject to} & \displaystyle\int_{[\underline{q}_i, \overline{q}_i]} \mathbb{P}(\mathrm{d}q_i) = 1 \\ & \displaystyle\int_{[\underline{q}_i, \overline{q}_i]} q_i \, \mathbb{P}(\mathrm{d}q_i) = \mu_i \\ & \displaystyle\int_{[\underline{q}_i, \overline{q}_i]} ([q_i - \mu_i]_+)^2 \, \mathbb{P}(\mathrm{d}q_i) \leqslant \sigma_i^+ \\ & \displaystyle\int_{[\underline{q}_i, \overline{q}_i]} ([\mu_i - q_i]_+)^2 \, \mathbb{P}(\mathrm{d}q_i) \leqslant \sigma_i^- \\ & \mathbb{P} \in \mathcal{M}_+(\mathbb{R}) \end{array}$$

is greater than or equal to $1 - \epsilon$. A similar reasoning as in the proof of Theorem 2.8 shows that this is the case if and only if the optimal objective value of the problem

$$\begin{array}{ll} \text{maximize} & \alpha + \mu_i \beta - \sigma_i^+ \gamma^+ - \sigma_i^- \gamma^- \\ \text{subject to} & \alpha - \mu_i(\chi_1^q - \pi_1^q) + \dfrac{1}{4\gamma^+}(\pi_1^q + \pi_1^0)^2 + \dfrac{1}{4\gamma^-}(\chi_1^q + \chi_1^0)^2 - \underline{q}_i \underline{\phi}_1 + \overline{q}_i \overline{\phi}_1 \leqslant 1 \\ & \alpha - \mu_i(\chi_0^q - \pi_0^q) + \dfrac{1}{4\gamma^+}(\pi_0^q + \pi_0^0)^2 + \dfrac{1}{4\gamma^-}(\chi_0^q + \chi_0^0)^2 - \underline{q}_i \underline{\phi}_0 + \overline{q}_i \overline{\phi}_0 - \tau\omega \leqslant 0 \\ & \pi_1^q - \chi_1^q + \overline{\phi}_1 - \underline{\phi}_1 = \beta, \;\; \pi_0^q - \chi_0^q + \overline{\phi}_0 - \underline{\phi}_0 - \omega = \beta \\ & \alpha, \, \beta \in \mathbb{R}, \, \gamma^+, \gamma^- \in \mathbb{R}_+, \, \chi_j^q, \chi_j^0, \pi_j^q, \pi_j^0, \underline{\phi}_j, \overline{\phi}_j \in \mathbb{R}_+, \, j = 0, 1, \, \omega \in \mathbb{R}_+. \end{array} \tag{2.29}$$

is greater than or equal to $1 - \epsilon$.

We now consider the problem $\sup_{\mathbb{P}\in\mathcal{P}_i} \mathbb{P}\text{-VaR}_{1-\epsilon}[\tilde{q}_i]$, which can be formulated as

$$\begin{aligned}
&\text{minimize} && \tau \\
&\text{subject to} && \sup_{\mathbb{P}\in\mathcal{P}} \mathbb{P}\text{-VaR}_{1-\epsilon}[\tilde{q}_i] \leqslant \tau \\
& && \tau \in \mathbb{R}.
\end{aligned}$$

Our previous arguments imply that this problem is equivalent to

$$\begin{aligned}
&\text{minimize} && \tau \\
&\text{subject to} && \alpha + \mu_i\beta - \sigma_i^+\gamma^+ - \sigma_i^-\gamma^- \geqslant 1-\epsilon \\
& && \alpha - \mu_i(\chi_1^q - \pi_1^q) + \frac{1}{4\gamma^+}(\pi_1^q + \pi_1^0)^2 + \frac{1}{4\gamma^-}(\chi_1^q + \chi_1^0)^2 - \underline{q}_i\underline{\phi}_1 + \overline{q}_i\overline{\phi}_1 \leqslant 1 \\
& && \alpha - \mu_i(\chi_0^q - \pi_0^q) + \frac{1}{4\gamma^+}(\pi_0^q + \pi_0^0)^2 + \frac{1}{4\gamma^-}(\chi_0^q + \chi_0^0)^2 - \underline{q}_i\underline{\phi}_0 + \overline{q}_i\overline{\phi}_0 - \tau\omega \leqslant 0 \\
& && \pi_1^q - \chi_1^q + \overline{\phi}_1 - \underline{\phi}_1 = \beta, \;\; \pi_0^q - \chi_0^q + \overline{\phi}_0 - \underline{\phi}_0 - \omega = \beta \\
& && \alpha,\, \beta \in \mathbb{R},\, \gamma^+,\, \gamma^- \in \mathbb{R}_+,\, \chi_j^q, \chi_j^0, \pi_j^q, \pi_j^0, \underline{\phi}_j, \overline{\phi}_j \in \mathbb{R}_+,\, j = 0,1,\, \omega \in \mathbb{R}_+,\, \tau \in \mathbb{R}.
\end{aligned} \tag{2.30}$$

Similar manipulations as in the proof of Theorem 2.26 allow us to conclude that this problem has the same objective value as

$$\begin{aligned}
&\text{minimize} && (\overline{q}_i - \mu_i)\overline{\phi}_0 + \left(\frac{1-\epsilon}{\epsilon}\right)(\mu_i - \underline{q}_i)\underline{\phi}_1 + \frac{1}{4\gamma^+}\left(\pi_0^q\right)^2 + \left(\frac{1-\epsilon}{\epsilon}\right)\frac{1}{4\gamma^-}\left(\chi_1^q\right)^2 + \mu_i + \frac{\sigma_i^+}{\epsilon}\gamma^+ + \frac{\sigma_i^-}{\epsilon}\gamma^- \\
&\text{subject to} && \pi_0^q + \chi_1^q + \overline{\phi}_0 + \underline{\phi}_1 = 1 \\
& && \gamma^+,\, \gamma^- \in \mathbb{R}_+,\, \chi_1^q, \pi_0^q, \underline{\phi}_1, \overline{\phi}_0 \in \mathbb{R}_+.
\end{aligned}$$

The unconstrained first-order optimality condition with respect to γ^+ gives $\gamma^+ = \pm\frac{1}{2}\sqrt{\frac{\epsilon}{\sigma_i^+}}\pi_0^q$. Since the second derivative $\frac{1}{2}\frac{(\pi_0^q)^2}{(\gamma^+)^3}$ is non-negative for $\gamma^+ \geqslant 0$, we thus conclude that $\gamma^+ = \frac{1}{2}\sqrt{\frac{\epsilon}{\sigma_i^+}}\pi_0^q$ is optimal in the above problem. A similar reasoning shows that $\gamma^- = \frac{1}{2}\sqrt{\frac{1-\epsilon}{\sigma_i^-}}\chi_1^q$ is optimal as well. We thus obtain the equivalent optimization problem

$$\begin{aligned} \text{minimize} \quad & \mu_i + (\overline{q}_i - \mu_i)\overline{\phi}_0 + \left(\frac{1-\epsilon}{\epsilon}\right)(\mu_i - \underline{q}_i)\underline{\phi}_1 + \sqrt{\frac{\sigma_i^+}{\epsilon}}\pi_0^q + \frac{\sqrt{(1-\epsilon)\sigma_i^-}}{\epsilon}\chi_1^q \\ \text{subject to} \quad & \pi_0^q + \chi_1^q + \overline{\phi}_0 + \underline{\phi}_1 = 1 \\ & \chi_1^q, \pi_0^q, \underline{\phi}_1, \overline{\phi}_0 \in \mathbb{R}_+. \end{aligned}$$

Since all objective coefficients are strictly positive, there is an optimal solution that sets one of the four decision variables with minimum objective coefficient to 1 and all other variables to 0. The statement then follows from a case distinction. ∎

Proof of Theorem 2.21. For any fixed scalar $\tau \in \mathbb{R}$, we have $\sup_{\mathbb{P}\in\mathcal{P}} \mathbb{P}\text{-VaR}_{1-\epsilon}\big[\mathbf{1}_S{}^\top \tilde{\boldsymbol{q}}\big] \leqslant \tau$ if and only if the optimal objective value of the moment problem

$$\begin{aligned} \text{minimize} \quad & \int_{\mathcal{Q}} \mathbb{I}_{[\mathbf{1}_S{}^\top \boldsymbol{q} \leqslant \tau]}\, \mathbb{P}(\mathrm{d}\boldsymbol{q}) \\ \text{subject to} \quad & \int_{\mathcal{Q}} \mathbb{P}(\mathrm{d}\boldsymbol{q}) = 1 \\ & \int_{\mathcal{Q}} \boldsymbol{q}\, \mathbb{P}(\mathrm{d}\boldsymbol{q}) = \boldsymbol{\mu} \\ & \int_{\mathcal{Q}} \mathbf{1}_{S_i}^\top |\boldsymbol{q} - \boldsymbol{\mu}|\, \mathbb{P}(\mathrm{d}\boldsymbol{q}) \leqslant \nu_i \qquad \forall i = 1, \ldots, p \\ & \mathbb{P} \in \mathcal{M}_+(\mathcal{Q}) \end{aligned}$$

is greater than or equal to $1-\epsilon$. A similar reasoning as in the proof of Theorem 2.8 shows that this is the case if and only if the optimal objective value of the problem

$$\begin{array}{ll} \text{maximize} & \alpha + \boldsymbol{\mu}^\top \boldsymbol{\beta} - \boldsymbol{\nu}^\top \boldsymbol{\gamma} \\ \text{subject to} & \alpha + \boldsymbol{\mu}^\top (\boldsymbol{\pi}_1^+ - \boldsymbol{\pi}_1^-) + \overline{\boldsymbol{q}}^\top \overline{\boldsymbol{\phi}}_1 - \underline{\boldsymbol{q}}^\top \underline{\boldsymbol{\phi}}_1 \leqslant 1 \\ & \alpha + \boldsymbol{\mu}^\top (\boldsymbol{\pi}_0^+ - \boldsymbol{\pi}_0^-) + \overline{\boldsymbol{q}}^\top \overline{\boldsymbol{\phi}}_0 - \underline{\boldsymbol{q}}^\top \underline{\boldsymbol{\phi}}_0 - \tau\omega \leqslant 0 \\ & \boldsymbol{\pi}_1^+ - \boldsymbol{\pi}_1^- + \overline{\boldsymbol{\phi}}_1 - \underline{\boldsymbol{\phi}}_1 = \boldsymbol{\beta} \\ & \boldsymbol{\pi}_0^+ - \boldsymbol{\pi}_0^- + \overline{\boldsymbol{\phi}}_0 - \underline{\boldsymbol{\phi}}_0 - \mathbf{1}_S \omega = \boldsymbol{\beta} \\ & \boldsymbol{\pi}_1^+ + \boldsymbol{\pi}_1^- \leqslant \sum_{i=1}^p \gamma_i \mathbf{1}_{S_i}, \;\; \boldsymbol{\pi}_0^+ + \boldsymbol{\pi}_0^- \leqslant \sum_{i=1}^p \gamma_i \mathbf{1}_{S_i} \\ & \boldsymbol{\pi}_i^+, \boldsymbol{\pi}_i^-, \overline{\boldsymbol{\phi}}_i, \underline{\boldsymbol{\phi}}_i \in \mathbb{R}_+^n, \; i = 0, 1, \;\; \omega \in \mathbb{R}_+ \\ & \alpha \in \mathbb{R}, \;\; \boldsymbol{\beta} \in \mathbb{R}^n, \;\; \boldsymbol{\gamma} \in \mathbb{R}_+^p. \end{array}$$

is greater than or equal to $1 - \epsilon$.

We now consider the problem $\sup_{\mathbb{P} \in \mathcal{P}} \mathbb{P}\text{-VaR}_{1-\epsilon}\big[\mathbf{1}_S{}^\top \tilde{\boldsymbol{q}}\big]$, which can be formulated as

$$\begin{array}{ll} \text{minimize} & \tau \\ \text{subject to} & \sup_{\mathbb{P} \in \mathcal{P}} \mathbb{P}\text{-VaR}_{1-\epsilon}\big[\mathbf{1}_S{}^\top \tilde{\boldsymbol{q}}\big] \leqslant \tau \\ & \tau \in \mathbb{R}. \end{array}$$

Our previous arguments imply that this problem is equivalent to

$$\begin{array}{ll} \text{minimize} & \tau \\ \text{subject to} & \alpha + \boldsymbol{\mu}^\top \boldsymbol{\beta} - \boldsymbol{\nu}^\top \boldsymbol{\gamma} \geqslant 1 - \epsilon \\ & \alpha + \boldsymbol{\mu}^\top (\boldsymbol{\pi}_1^+ - \boldsymbol{\pi}_1^-) + \overline{\boldsymbol{q}}^\top \overline{\boldsymbol{\phi}}_1 - \underline{\boldsymbol{q}}^\top \underline{\boldsymbol{\phi}}_1 \leqslant 1 \\ & \alpha + \boldsymbol{\mu}^\top (\boldsymbol{\pi}_0^+ - \boldsymbol{\pi}_0^-) + \overline{\boldsymbol{q}}^\top \overline{\boldsymbol{\phi}}_0 - \underline{\boldsymbol{q}}^\top \underline{\boldsymbol{\phi}}_0 - \tau\omega \leqslant 0 \\ & \boldsymbol{\pi}_1^+ - \boldsymbol{\pi}_1^- + \overline{\boldsymbol{\phi}}_1 - \underline{\boldsymbol{\phi}}_1 = \boldsymbol{\beta} \\ & \boldsymbol{\pi}_0^+ - \boldsymbol{\pi}_0^- + \overline{\boldsymbol{\phi}}_0 - \underline{\boldsymbol{\phi}}_0 - \mathbf{1}_S \omega = \boldsymbol{\beta} \\ & \boldsymbol{\pi}_1^+ + \boldsymbol{\pi}_1^- \leqslant \sum_{i=1}^p \gamma_i \mathbf{1}_{S_i}, \;\; \boldsymbol{\pi}_0^+ + \boldsymbol{\pi}_0^- \leqslant \sum_{i=1}^p \gamma_i \mathbf{1}_{S_i} \\ & \boldsymbol{\pi}_i^+, \boldsymbol{\pi}_i^-, \overline{\boldsymbol{\phi}}_i, \underline{\boldsymbol{\phi}}_i \in \mathbb{R}_+^n, \; i = 0, 1, \;\; \omega \in \mathbb{R}_+ \\ & \alpha \in \mathbb{R}, \;\; \boldsymbol{\beta} \in \mathbb{R}^n, \;\; \boldsymbol{\gamma} \in \mathbb{R}_+^p, \;\; \tau \in \mathbb{R}. \end{array} \tag{2.31}$$

Note that in the absence of the first constraint, it would be optimal to choose α as small as possible. We can thus remove the first constraint and replace α with $(1-\epsilon) - \boldsymbol{\mu}^\top\big(\boldsymbol{\pi}_1^+ - \boldsymbol{\pi}_1^- + \overline{\boldsymbol{\phi}}_1 - \underline{\boldsymbol{\phi}}_1\big) + \boldsymbol{\nu}^\top\boldsymbol{\gamma}$ in the second constraint, resulting in

$$\big(\overline{\boldsymbol{q}} - \boldsymbol{\mu}\big)^\top \overline{\boldsymbol{\phi}}_1 - \big(\underline{\boldsymbol{q}} - \boldsymbol{\mu}\big)^\top \underline{\boldsymbol{\phi}}_1 + \boldsymbol{\nu}^\top\boldsymbol{\gamma} \leqslant \epsilon,$$

as well as with $(1-\epsilon) - \boldsymbol{\mu}^\top\big(\boldsymbol{\pi}_0^+ - \boldsymbol{\pi}_0^- + \overline{\boldsymbol{\phi}}_0 - \underline{\boldsymbol{\phi}}_0 - \mathbf{1}_S\omega\big) + \boldsymbol{\nu}^\top\boldsymbol{\gamma}$ in the third constraint, resulting in

$$\big(\overline{\boldsymbol{q}} - \boldsymbol{\mu}\big)^\top \overline{\boldsymbol{\phi}}_0 - \big(\underline{\boldsymbol{q}} - \boldsymbol{\mu}\big)^\top \underline{\boldsymbol{\phi}}_0 + \boldsymbol{\nu}^\top\boldsymbol{\gamma} + \boldsymbol{\mu}^\top\mathbf{1}_S\omega - \tau\omega \leqslant -(1-\epsilon).$$

Moreover, since $\boldsymbol{\beta}$ is unrestricted in sign, we can remove it from the problem by replacing the fourth and fifth constraint in the above problem with the single constraint

$$\boldsymbol{\pi}_1^+ - \boldsymbol{\pi}_1^- + \overline{\boldsymbol{\phi}}_1 - \underline{\boldsymbol{\phi}}_1 = \boldsymbol{\pi}_0^+ - \boldsymbol{\pi}_0^- + \overline{\boldsymbol{\phi}}_0 - \underline{\boldsymbol{\phi}}_0 - \mathbf{1}_S\omega.$$

The optimization problem (2.31) is thus equivalent to

$$\begin{array}{ll}
\text{minimize} & \tau \\
\text{subject to} & \big(\overline{\boldsymbol{q}} - \boldsymbol{\mu}\big)^\top \overline{\boldsymbol{\phi}}_1 - \big(\underline{\boldsymbol{q}} - \boldsymbol{\mu}\big)^\top \underline{\boldsymbol{\phi}}_1 + \boldsymbol{\nu}^\top\boldsymbol{\gamma} \leqslant \epsilon \\
& \big(\overline{\boldsymbol{q}} - \boldsymbol{\mu}\big)^\top \overline{\boldsymbol{\phi}}_0 - \big(\underline{\boldsymbol{q}} - \boldsymbol{\mu}\big)^\top \underline{\boldsymbol{\phi}}_0 + \boldsymbol{\nu}^\top\boldsymbol{\gamma} + \boldsymbol{\mu}^\top\mathbf{1}_S\omega - \tau\omega \leqslant -(1-\epsilon) \\
& \boldsymbol{\pi}_1^+ - \boldsymbol{\pi}_1^- + \overline{\boldsymbol{\phi}}_1 - \underline{\boldsymbol{\phi}}_1 = \boldsymbol{\pi}_0^+ - \boldsymbol{\pi}_0^- + \overline{\boldsymbol{\phi}}_0 - \underline{\boldsymbol{\phi}}_0 - \mathbf{1}_S\omega \\
& \boldsymbol{\pi}_1^+ + \boldsymbol{\pi}_1^- \leqslant \sum_{i=1}^p \gamma_i \mathbf{1}_{S_i}, \quad \boldsymbol{\pi}_0^+ + \boldsymbol{\pi}_0^- \leqslant \sum_{i=1}^p \gamma_i \mathbf{1}_{S_i} \\
& \boldsymbol{\pi}_i^+, \boldsymbol{\pi}_i^-, \overline{\boldsymbol{\phi}}_i, \underline{\boldsymbol{\phi}}_i \in \mathbb{R}_+^n,\ i = 0,1, \quad \omega \in \mathbb{R}_+, \quad \boldsymbol{\gamma} \in \mathbb{R}_+^p, \quad \tau \in \mathbb{R}.
\end{array}$$

We claim that any feasible solution $(\boldsymbol{\pi}_i^+, \boldsymbol{\pi}_i^-, \overline{\boldsymbol{\phi}}_i, \underline{\boldsymbol{\phi}}_i, \omega, \boldsymbol{\gamma}, \tau)$ to this problem must satisfy $\omega > 0$. Indeed, if there was a feasible solution with $\omega = 0$, then the problem would be unbounded, which is impossible because $\sup_{\mathbb{P}\in\mathcal{P}} \mathbb{P}\text{-VaR}_{1-\epsilon}\big[\mathbf{1}_S{}^\top\widetilde{\boldsymbol{q}}\big] \geqslant \sum_{i\in S} \underline{q}_i > -\infty$. We can thus conduct the substitutions $\boldsymbol{\pi}_i^+ \leftarrow \boldsymbol{\pi}_i^+/\omega$, $\boldsymbol{\pi}_i^- \leftarrow \boldsymbol{\pi}_i^-/\omega$, $\overline{\boldsymbol{\phi}}_i \leftarrow \overline{\boldsymbol{\phi}}_i/\omega$, $\underline{\boldsymbol{\phi}}_i \leftarrow \underline{\boldsymbol{\phi}}_i/\omega$, $i = 0,1$, $\boldsymbol{\gamma} \leftarrow \boldsymbol{\gamma}/\omega$ and

$\omega \leftarrow 1/\omega$ to obtain the equivalent problem

$$
\begin{array}{ll}
\text{minimize} & \tau \\
\text{subject to} & \left(\overline{\boldsymbol{q}} - \boldsymbol{\mu}\right)^\top \overline{\boldsymbol{\phi}}_1 - \left(\underline{\boldsymbol{q}} - \boldsymbol{\mu}\right)^\top \underline{\boldsymbol{\phi}}_1 + \boldsymbol{\nu}^\top \boldsymbol{\gamma} \leqslant \epsilon\omega \\
& \left(\overline{\boldsymbol{q}} - \boldsymbol{\mu}\right)^\top \overline{\boldsymbol{\phi}}_0 - \left(\underline{\boldsymbol{q}} - \boldsymbol{\mu}\right)^\top \underline{\boldsymbol{\phi}}_0 + \boldsymbol{\nu}^\top \boldsymbol{\gamma} + \boldsymbol{\mu}^\top \mathbf{1}_S - \tau \leqslant -(1-\epsilon)\omega \\
& \boldsymbol{\pi}_1^+ - \boldsymbol{\pi}_1^- + \overline{\boldsymbol{\phi}}_1 - \underline{\boldsymbol{\phi}}_1 = \boldsymbol{\pi}_0^+ - \boldsymbol{\pi}_0^- + \overline{\boldsymbol{\phi}}_0 - \underline{\boldsymbol{\phi}}_0 - \mathbf{1}_S \\
& \boldsymbol{\pi}_1^+ + \boldsymbol{\pi}_1^- \leqslant \sum_{i=1}^p \gamma_i \mathbf{1}_{S_i}, \quad \boldsymbol{\pi}_0^+ + \boldsymbol{\pi}_0^- \leqslant \sum_{i=1}^p \gamma_i \mathbf{1}_{S_i} \\
& \boldsymbol{\pi}_i^+, \boldsymbol{\pi}_i^-, \overline{\boldsymbol{\phi}}_i, \underline{\boldsymbol{\phi}}_i \in \mathbb{R}_+^n, \; i = 0, 1, \quad \omega \in \mathbb{R}_+, \quad \boldsymbol{\gamma} \in \mathbb{R}_+^p, \quad \tau \in \mathbb{R}.
\end{array}
$$

Note that the second constraint in this problem must be binding at optimality. We can thus remove this constraint as well as the epigraphical variable τ to obtain the equivalent problem

$$
\begin{array}{ll}
\text{minimize} & \left(\overline{\boldsymbol{q}} - \boldsymbol{\mu}\right)^\top \overline{\boldsymbol{\phi}}_0 - \left(\underline{\boldsymbol{q}} - \boldsymbol{\mu}\right)^\top \underline{\boldsymbol{\phi}}_0 + \boldsymbol{\mu}^\top \mathbf{1}_S + \boldsymbol{\nu}^\top \boldsymbol{\gamma} + (1-\epsilon)\omega \\
\text{subject to} & \left(\overline{\boldsymbol{q}} - \boldsymbol{\mu}\right)^\top \overline{\boldsymbol{\phi}}_1 - \left(\underline{\boldsymbol{q}} - \boldsymbol{\mu}\right)^\top \underline{\boldsymbol{\phi}}_1 + \boldsymbol{\nu}^\top \boldsymbol{\gamma} \leqslant \epsilon\omega \\
& \boldsymbol{\pi}_1^+ - \boldsymbol{\pi}_1^- + \overline{\boldsymbol{\phi}}_1 - \underline{\boldsymbol{\phi}}_1 = \boldsymbol{\pi}_0^+ - \boldsymbol{\pi}_0^- + \overline{\boldsymbol{\phi}}_0 - \underline{\boldsymbol{\phi}}_0 - \mathbf{1}_S \\
& \boldsymbol{\pi}_1^+ + \boldsymbol{\pi}_1^- \leqslant \sum_{i=1}^p \gamma_i \mathbf{1}_{S_i}, \quad \boldsymbol{\pi}_0^+ + \boldsymbol{\pi}_0^- \leqslant \sum_{i=1}^p \gamma_i \mathbf{1}_{S_i} \\
& \boldsymbol{\pi}_i^+, \boldsymbol{\pi}_i^-, \overline{\boldsymbol{\phi}}_i, \underline{\boldsymbol{\phi}}_i \in \mathbb{R}_+^n, \; i = 0, 1, \quad \omega \in \mathbb{R}_+, \quad \boldsymbol{\gamma} \in \mathbb{R}_+^p.
\end{array}
$$

In this problem, the left-hand side of the first constraint is nonnegative by construction. We thus conclude that the constraint is binding at optimality, which allows us to remove the constraint as well as the variable ω to obtain the equivalent problem

$$
\begin{array}{ll}
\text{minimize} & \left(\overline{\boldsymbol{q}} - \boldsymbol{\mu}\right)^\top \left(\overline{\boldsymbol{\phi}}_0 + \frac{1-\epsilon}{\epsilon} \cdot \overline{\boldsymbol{\phi}}_1\right) - \left(\underline{\boldsymbol{q}} - \boldsymbol{\mu}\right)^\top \left(\underline{\boldsymbol{\phi}}_0 + \frac{1-\epsilon}{\epsilon} \cdot \underline{\boldsymbol{\phi}}_1\right) + \frac{1}{\epsilon} \boldsymbol{\nu}^\top \boldsymbol{\gamma} + \boldsymbol{\mu}^\top \mathbf{1}_S \\
\text{subject to} & \left(\boldsymbol{\pi}_0^+ + \boldsymbol{\pi}_1^-\right) - \left(\boldsymbol{\pi}_0^- + \boldsymbol{\pi}_1^+\right) + \left(\overline{\boldsymbol{\phi}}_0 + \underline{\boldsymbol{\phi}}_1\right) - \left(\underline{\boldsymbol{\phi}}_0 + \overline{\boldsymbol{\phi}}_1\right) = \mathbf{1}_S \\
& \boldsymbol{\pi}_1^+ + \boldsymbol{\pi}_1^- \leqslant \sum_{i=1}^p \gamma_i \mathbf{1}_{S_i}, \quad \boldsymbol{\pi}_0^+ + \boldsymbol{\pi}_0^- \leqslant \sum_{i=1}^p \gamma_i \mathbf{1}_{S_i} \\
& \boldsymbol{\pi}_i^+, \boldsymbol{\pi}_i^-, \overline{\boldsymbol{\phi}}_i, \underline{\boldsymbol{\phi}}_i \in \mathbb{R}_+^n, \; i = 0, 1, \quad \boldsymbol{\gamma} \in \mathbb{R}_+^p.
\end{array}
$$

The objective function and the second set of constraints imply that larger values of $\boldsymbol{\pi}_i^+$, $\boldsymbol{\pi}_i^-$, $\overline{\boldsymbol{\phi}}_i$ and $\underline{\boldsymbol{\phi}}_i$, $i = 0, 1$, are all detrimental to the objective function. We can thus assume that

$\boldsymbol{\pi}_0^- = \boldsymbol{\pi}_1^+ = \underline{\boldsymbol{\phi}}_0 = \overline{\boldsymbol{\phi}}_1 = \mathbf{0}$ at optimality. This leads to the simplified formulation

$$\begin{array}{ll} \text{minimize} & (\overline{\boldsymbol{q}} - \boldsymbol{\mu})^\top \overline{\boldsymbol{\phi}}_0 - \frac{1-\epsilon}{\epsilon}(\underline{\boldsymbol{q}} - \boldsymbol{\mu})^\top \underline{\boldsymbol{\phi}}_1 + \frac{1}{\epsilon}\boldsymbol{\nu}^\top\boldsymbol{\gamma} + \boldsymbol{\mu}^\top \mathbf{1}_S \\ \text{subject to} & (\boldsymbol{\pi}_0^+ + \boldsymbol{\pi}_1^-) + (\overline{\boldsymbol{\phi}}_0 + \underline{\boldsymbol{\phi}}_1) = \mathbf{1}_S \\ & \boldsymbol{\pi}_1^- \leqslant \sum_{i=1}^p \gamma_i \mathbf{1}_{S_i}, \quad \boldsymbol{\pi}_0^+ \leqslant \sum_{i=1}^p \gamma_i \mathbf{1}_{S_i} \\ & \boldsymbol{\pi}_0^+, \boldsymbol{\pi}_1^-, \overline{\boldsymbol{\phi}}_0, \underline{\boldsymbol{\phi}}_1 \in \mathbb{R}_+^n, \quad \boldsymbol{\gamma} \in \mathbb{R}_+^p. \end{array}$$

Since the constraints are symmetric in $\boldsymbol{\pi}_0^+$ and $\boldsymbol{\pi}_1^-$, we can replace both variable vectors with a single vector $\boldsymbol{\pi} \in \mathbb{R}_+^n$:

$$\begin{array}{ll} \text{minimize} & (\overline{\boldsymbol{q}} - \boldsymbol{\mu})^\top \overline{\boldsymbol{\phi}}_0 - \frac{1-\epsilon}{\epsilon}(\underline{\boldsymbol{q}} - \boldsymbol{\mu})^\top \underline{\boldsymbol{\phi}}_1 + \frac{1}{\epsilon}\boldsymbol{\nu}^\top\boldsymbol{\gamma} + \boldsymbol{\mu}^\top \mathbf{1}_S \\ \text{subject to} & 2\boldsymbol{\pi} + (\overline{\boldsymbol{\phi}}_0 + \underline{\boldsymbol{\phi}}_1) = \mathbf{1}_S \\ & \boldsymbol{\pi} \leqslant \sum_{i=1}^p \gamma_i \mathbf{1}_{S_i} \\ & \boldsymbol{\pi}, \overline{\boldsymbol{\phi}}_0, \underline{\boldsymbol{\phi}}_1 \in \mathbb{R}_+^n, \quad \boldsymbol{\gamma} \in \mathbb{R}_+^p. \end{array}$$

For a fixed value of $\boldsymbol{\gamma}$, the variable vector $\boldsymbol{\pi}$ satisfies $\boldsymbol{\pi} = \min\{\mathbf{1}_S/2 - (\overline{\boldsymbol{\phi}}_0 + \underline{\boldsymbol{\phi}}_1)/2,\ \sum_{i=1}^p \gamma_i \mathbf{1}_{S_i}\}$ at optimality. We can thus remove $\boldsymbol{\pi}$ from the problem and obtain the equivalent reformulation

$$\begin{array}{ll} \text{minimize} & (\overline{\boldsymbol{q}} - \boldsymbol{\mu})^\top \overline{\boldsymbol{\phi}}_0 - \frac{1-\epsilon}{\epsilon}(\underline{\boldsymbol{q}} - \boldsymbol{\mu})^\top \underline{\boldsymbol{\phi}}_1 + \frac{1}{\epsilon}\boldsymbol{\nu}^\top\boldsymbol{\gamma} + \boldsymbol{\mu}^\top \mathbf{1}_S \\ \text{subject to} & \overline{\boldsymbol{\phi}}_0 + \underline{\boldsymbol{\phi}}_1 = \max\left\{\overline{\boldsymbol{\phi}}_0 + \underline{\boldsymbol{\phi}}_1,\ \mathbf{1}_S - 2\sum_{i=1}^p \gamma_i \mathbf{1}_{S_i}\right\} \\ & \overline{\boldsymbol{\phi}}_0, \underline{\boldsymbol{\phi}}_1 \in \mathbb{R}_+^n, \quad \boldsymbol{\gamma} \in \mathbb{R}_+^p. \end{array}$$

The constraint in this problem is equivalent to $\overline{\boldsymbol{\phi}}_0 + \underline{\boldsymbol{\phi}}_1 \geqslant \mathbf{1}_S - 2\sum_{i=1}^p \gamma_i \mathbf{1}_{S_i}$. Since both $\overline{\boldsymbol{\phi}}_0$ and $\underline{\boldsymbol{\phi}}_1$ are penalized in the objective function, we thus conclude that $\overline{\boldsymbol{\phi}}_0 + \underline{\boldsymbol{\phi}}_1 = \left[\mathbf{1}_S - 2\sum_{i=1}^p \gamma_i \mathbf{1}_{S_i}\right]_+$ at optimality. The statement then follows since we can assume that $\overline{\boldsymbol{\phi}}_0{}^\top \underline{\boldsymbol{\phi}}_1 = 0$ at optimality.
■

Proof of Theorem 2.26. For a fixed scalar $\tau \in \mathbb{R}$, we have $\sup_{\mathbb{P} \in \mathcal{P}} \mathbb{P}\text{-VaR}_{1-\epsilon}\left[\mathbf{1}_S{}^\top \tilde{\boldsymbol{q}}\right] \leqslant \tau$ if and only if the optimal objective value of the moment problem

$$\begin{array}{ll}\text{minimize} & \displaystyle\int_{\mathcal{Q}} \mathbb{I}_{[\mathbf{1}_S{}^\top \boldsymbol{q} \leqslant \tau]}\, \mathbb{P}(\mathrm{d}\boldsymbol{q}) \\ \text{subject to} & \displaystyle\int_{\mathcal{Q}} \mathbb{P}(\mathrm{d}\boldsymbol{q}) = 1 \\ & \displaystyle\int_{\mathcal{Q}} \boldsymbol{q}\, \mathbb{P}(\mathrm{d}\boldsymbol{q}) = \boldsymbol{\mu} \\ & \displaystyle\int_{\mathcal{Q}} (\boldsymbol{q}-\boldsymbol{\mu})(\boldsymbol{q}-\boldsymbol{\mu})^\top\, \mathbb{P}(\mathrm{d}\boldsymbol{q}) \preceq \boldsymbol{\Sigma} \\ & \mathbb{P} \in \mathcal{M}_+(\mathbb{R}^n)\end{array}$$

is greater than or equal to $1-\epsilon$. A similar reasoning as in the proof of Theorem 2.8 shows that this is the case if and only if the optimal objective value of the problem

$$\begin{array}{ll}\text{maximize} & \alpha + \boldsymbol{\mu}^\top\boldsymbol{\beta} - \langle \boldsymbol{\Sigma}, \boldsymbol{\Gamma}\rangle \\ \text{subject to} & \alpha + \dfrac{1}{4}(\boldsymbol{\beta} + \underline{\boldsymbol{\phi}}_1 - \overline{\boldsymbol{\phi}}_1)^\top \boldsymbol{\Gamma}^{-1}(\boldsymbol{\beta} + \underline{\boldsymbol{\phi}}_1 - \overline{\boldsymbol{\phi}}_1) \\ & \quad + (\overline{\boldsymbol{q}} - \boldsymbol{\mu})^\top \overline{\boldsymbol{\phi}}_1 - (\underline{\boldsymbol{q}} - \boldsymbol{\mu})^\top \underline{\boldsymbol{\phi}}_1 + \boldsymbol{\mu}^\top\boldsymbol{\beta} \leqslant 1 \\ & \alpha + \dfrac{1}{4}(\boldsymbol{\beta} + \underline{\boldsymbol{\phi}}_0 - \overline{\boldsymbol{\phi}}_0 + \mathbf{1}_S\omega)^\top \boldsymbol{\Gamma}^{-1}(\boldsymbol{\beta} + \underline{\boldsymbol{\phi}}_0 - \overline{\boldsymbol{\phi}}_0 + \mathbf{1}_S\omega) \\ & \quad + (\overline{\boldsymbol{q}} - \boldsymbol{\mu})^\top \overline{\boldsymbol{\phi}}_0 - (\underline{\boldsymbol{q}} - \boldsymbol{\mu})^\top \underline{\boldsymbol{\phi}}_0 + \boldsymbol{\mu}^\top(\boldsymbol{\beta} + \mathbf{1}_S\omega) - \tau\omega \leqslant 0 \\ & \underline{\boldsymbol{\phi}}_i, \overline{\boldsymbol{\phi}}_i \in \mathbb{R}^n_+,\ i = 0,1,\ \ \omega \in \mathbb{R}_+,\ \ \alpha \in \mathbb{R},\ \ \boldsymbol{\beta} \in \mathbb{R}^n,\ \ \boldsymbol{\Gamma} \in \mathbb{S}^{n\times n}_+.\end{array}$$

is greater than or equal to $1-\epsilon$.

We now consider the problem $\sup_{\mathbb{P}\in\mathcal{P}} \mathbb{P}\text{-VaR}_{1-\epsilon}\big[\mathbf{1}_S{}^\top \tilde{\boldsymbol{q}}\big]$, which can be formulated as

$$\begin{array}{ll}\text{minimize} & \tau \\ \text{subject to} & \alpha + \boldsymbol{\mu}^\top\boldsymbol{\beta} - \langle \boldsymbol{\Sigma}, \boldsymbol{\Gamma}\rangle \geqslant 1-\epsilon \\ & \alpha + \dfrac{1}{4}(\boldsymbol{\beta} + \underline{\boldsymbol{\phi}}_1 - \overline{\boldsymbol{\phi}}_1)^\top \boldsymbol{\Gamma}^{-1}(\boldsymbol{\beta} + \underline{\boldsymbol{\phi}}_1 - \overline{\boldsymbol{\phi}}_1) \\ & \quad + (\overline{\boldsymbol{q}} - \boldsymbol{\mu})^\top \overline{\boldsymbol{\phi}}_1 - (\underline{\boldsymbol{q}} - \boldsymbol{\mu})^\top \underline{\boldsymbol{\phi}}_1 + \boldsymbol{\mu}^\top\boldsymbol{\beta} \leqslant 1 \\ & \alpha + \dfrac{1}{4}(\boldsymbol{\beta} + \underline{\boldsymbol{\phi}}_0 - \overline{\boldsymbol{\phi}}_0 + \mathbf{1}_S\omega)^\top \boldsymbol{\Gamma}^{-1}(\boldsymbol{\beta} + \underline{\boldsymbol{\phi}}_0 - \overline{\boldsymbol{\phi}}_0 + \mathbf{1}_S\omega) \\ & \quad + (\overline{\boldsymbol{q}} - \boldsymbol{\mu})^\top \overline{\boldsymbol{\phi}}_0 - (\underline{\boldsymbol{q}} - \boldsymbol{\mu})^\top \underline{\boldsymbol{\phi}}_0 + \boldsymbol{\mu}^\top(\boldsymbol{\beta} + \mathbf{1}_S\omega) - \tau\omega \leqslant 0 \\ & \underline{\boldsymbol{\phi}}_i, \overline{\boldsymbol{\phi}}_i \in \mathbb{R}^n_+,\ i = 0,1,\ \ \omega \in \mathbb{R}_+,\ \ \alpha \in \mathbb{R},\ \ \boldsymbol{\beta} \in \mathbb{R}^n,\ \ \boldsymbol{\Gamma} \in \mathbb{S}^{n\times n}_+,\ \ \tau \in \mathbb{R}.\end{array}$$

As in the proof of Theorem 2.21, we can substitute out α and remove the first constraint, conclude that ω is strictly positive and replace all remaining decision variables (except for τ) with their divisions by ω and remove the variables τ and ω to obtain the equivalent problem

$$\begin{aligned}
\text{minimize} \quad & \frac{1}{\epsilon}\langle \boldsymbol{\Sigma}, \boldsymbol{\Gamma}\rangle + \frac{1}{4}(\boldsymbol{\beta} + \underline{\boldsymbol{\phi}}_0 - \overline{\boldsymbol{\phi}}_0 + \mathbf{1}_S)^\top \boldsymbol{\Gamma}^{-1}(\boldsymbol{\beta} + \underline{\boldsymbol{\phi}}_0 - \overline{\boldsymbol{\phi}}_0 + \mathbf{1}_S) \\
& + \frac{1}{4}\cdot\frac{1-\epsilon}{\epsilon}(\boldsymbol{\beta} + \underline{\boldsymbol{\phi}}_1 - \overline{\boldsymbol{\phi}}_1)^\top \boldsymbol{\Gamma}^{-1}(\boldsymbol{\beta} + \underline{\boldsymbol{\phi}}_1 - \overline{\boldsymbol{\phi}}_1) \\
& + (\overline{\boldsymbol{q}} - \boldsymbol{\mu})^\top \left[\overline{\boldsymbol{\phi}}_0 + \frac{1-\epsilon}{\epsilon}\cdot\overline{\boldsymbol{\phi}}_1\right] - (\underline{\boldsymbol{q}} - \boldsymbol{\mu})^\top \left[\underline{\boldsymbol{\phi}}_0 + \frac{1-\epsilon}{\epsilon}\cdot\underline{\boldsymbol{\phi}}_1\right] + \boldsymbol{\mu}^\top \mathbf{1}_S \\
\text{subject to} \quad & \underline{\boldsymbol{\phi}}_i, \overline{\boldsymbol{\phi}}_i \in \mathbb{R}^n_+,\ i = 0, 1, \ \ \boldsymbol{\beta} \in \mathbb{R}^n, \ \ \boldsymbol{\Gamma} \in \mathbb{S}^{n\times n}_+.
\end{aligned}$$

We can now replace $\boldsymbol{\beta}$ with its optimal value $\boldsymbol{\beta} = \epsilon(\overline{\boldsymbol{\phi}}_0 - \underline{\boldsymbol{\phi}}_0 - \mathbf{1}_S) + (1-\epsilon)(\overline{\boldsymbol{\phi}}_1 - \underline{\boldsymbol{\phi}}_1)$ from the first-order unconstrained optimality condition to obtain the equivalent reformulation

$$\begin{aligned}
\text{minimize} \quad & \frac{1}{\epsilon}\langle \boldsymbol{\Sigma}, \boldsymbol{\Gamma}\rangle + \frac{1}{4}(1-\epsilon)(\overline{\boldsymbol{\phi}}_1 - \underline{\boldsymbol{\phi}}_1 + \underline{\boldsymbol{\phi}}_0 - \overline{\boldsymbol{\phi}}_0 + \mathbf{1}_S)^\top \boldsymbol{\Gamma}^{-1}(\overline{\boldsymbol{\phi}}_1 - \underline{\boldsymbol{\phi}}_1 + \underline{\boldsymbol{\phi}}_0 - \overline{\boldsymbol{\phi}}_0 + \mathbf{1}_S) \\
& + (\overline{\boldsymbol{q}} - \boldsymbol{\mu})^\top \left[\overline{\boldsymbol{\phi}}_0 + \frac{1-\epsilon}{\epsilon}\cdot\overline{\boldsymbol{\phi}}_1\right] - (\underline{\boldsymbol{q}} - \boldsymbol{\mu})^\top \left[\underline{\boldsymbol{\phi}}_0 + \frac{1-\epsilon}{\epsilon}\cdot\underline{\boldsymbol{\phi}}_1\right] + \boldsymbol{\mu}^\top \mathbf{1}_S \\
\text{subject to} \quad & \underline{\boldsymbol{\phi}}_i, \overline{\boldsymbol{\phi}}_i \in \mathbb{R}^n_+,\ i = 0, 1, \ \ \boldsymbol{\Gamma} \in \mathbb{S}^{n\times n}_+.
\end{aligned}$$

Since $\underline{\boldsymbol{\phi}}_i$ and $\overline{\boldsymbol{\phi}}_i$, $i = 0, 1$, are all penalized in the second row of the objective function, we can assume that $\overline{\boldsymbol{\phi}}_1{}^\top \underline{\boldsymbol{\phi}}_0 = 0$ and $\underline{\boldsymbol{\phi}}_1{}^\top \overline{\boldsymbol{\phi}}_0 = 0$ at optimality. This leads to the simplified formulation

$$\begin{aligned}
\text{minimize} \quad & \frac{1}{\epsilon}\langle \boldsymbol{\Sigma}, \boldsymbol{\Gamma}\rangle + \frac{1}{4}(1-\epsilon)(\boldsymbol{\phi}^+ - \boldsymbol{\phi}^- + \mathbf{1}_S)^\top \boldsymbol{\Gamma}^{-1}(\boldsymbol{\phi}^+ - \boldsymbol{\phi}^- + \mathbf{1}_S) \\
& + \boldsymbol{q}^{+\top}\boldsymbol{\phi}^+ + \boldsymbol{q}^{-\top}\boldsymbol{\phi}^- + \boldsymbol{\mu}^\top \mathbf{1}_S \\
\text{subject to} \quad & \boldsymbol{\phi}^+, \boldsymbol{\phi}^- \in \mathbb{R}^n_+, \ \ \boldsymbol{\Gamma} \in \mathbb{S}^{n\times n}_+,
\end{aligned}$$

where $\boldsymbol{q}^+ = \min\left\{\frac{1-\epsilon}{\epsilon}(\overline{\boldsymbol{q}} - \boldsymbol{\mu}),\ -(\underline{\boldsymbol{q}} - \boldsymbol{\mu})\right\}$ and $\boldsymbol{q}^- = \min\left\{-\frac{1-\epsilon}{\epsilon}(\underline{\boldsymbol{q}} - \boldsymbol{\mu}),\ \overline{\boldsymbol{q}} - \boldsymbol{\mu}\right\}$. We apply an epigraph reformulation to obtain the equivalent problem

$$\begin{aligned}
\text{minimize} \quad & \frac{1}{\epsilon}\langle \boldsymbol{\Sigma}, \boldsymbol{\Gamma}\rangle + \frac{1}{4}(1-\epsilon)\kappa + \boldsymbol{q}^{+\top}\boldsymbol{\phi}^+ + \boldsymbol{q}^{-\top}\boldsymbol{\phi}^- + \boldsymbol{\mu}^\top \mathbf{1}_S \\
\text{subject to} \quad & \kappa \geqslant (\boldsymbol{\phi}^+ - \boldsymbol{\phi}^- + \mathbf{1}_S)^\top \boldsymbol{\Gamma}^{-1}(\boldsymbol{\phi}^+ - \boldsymbol{\phi}^- + \mathbf{1}_S) \\
& \boldsymbol{\phi}^+, \boldsymbol{\phi}^- \in \mathbb{R}^n_+, \ \ \boldsymbol{\Gamma} \in \mathbb{S}^{n\times n}_+, \kappa \in \mathbb{R},
\end{aligned} \tag{2.32}$$

and an application of Schur's complement allows us to reformulate the constraint in (2.32) as

$$\begin{pmatrix} \kappa & (\boldsymbol{\phi}^+ - \boldsymbol{\phi}^- + \mathbf{1}_S)^\top \\ (\boldsymbol{\phi}^+ - \boldsymbol{\phi}^- + \mathbf{1}_S) & \boldsymbol{\Gamma} \end{pmatrix} \succeq \mathbf{0}.$$

Strong conic duality, which holds since the primal problem (2.32) is strictly feasible, implies that (2.32) attains the same optimal objective value as its associated dual problem, which—after some minor simplifications—can be expressed as

$$\begin{aligned} \text{maximize} \quad & {\mathbf{1}_S}^\top \boldsymbol{\mu} - 2 \cdot {\mathbf{1}_S}^\top \boldsymbol{\varphi} \\ \text{subject to} \quad & \theta \leqslant \frac{1}{4}(1-\epsilon) \\ & \boldsymbol{\varphi} \in \left[-\boldsymbol{q}^-/2,\ \boldsymbol{q}^+/2\right] \\ & \boldsymbol{\Lambda} \preceq \frac{1}{\epsilon}\boldsymbol{\Sigma} \\ & \begin{pmatrix} \theta & \boldsymbol{\varphi}^\top \\ \boldsymbol{\varphi} & \boldsymbol{\Lambda} \end{pmatrix} \in \mathbb{S}_+^{(n+1)\times(n+1)} \\ & \theta \in \mathbb{R}, \quad \boldsymbol{\varphi} \in \mathbb{R}^n, \quad \boldsymbol{\Lambda} \in \mathbb{S}^{n\times n}. \end{aligned}$$

Applying Schur's complement to the last constraint in this problem shows that the last two constraints are satisfied if and only if $\frac{1}{\theta}\boldsymbol{\varphi}\boldsymbol{\varphi}^\top \preceq \boldsymbol{\Lambda} \preceq \frac{1}{\epsilon}\boldsymbol{\Sigma}$ for some $\boldsymbol{\Lambda} \in \mathbb{S}^{n\times n}$, that is, if and only if $\frac{1}{\theta}\boldsymbol{\varphi}\boldsymbol{\varphi}^\top \preceq \frac{1}{\epsilon}\boldsymbol{\Sigma}$. Since the first constraint imposes the only upper bound on θ, we can replace θ with the right-hand side of that constraint, $\theta = \frac{1}{4}(1-\epsilon)$, to obtain the equivalent reformulation

$$\begin{aligned} \text{maximize} \quad & {\mathbf{1}_S}^\top \boldsymbol{\mu} - 2 \cdot {\mathbf{1}_S}^\top \boldsymbol{\varphi} \\ \text{subject to} \quad & \boldsymbol{\varphi} \in \left[-\boldsymbol{q}^-/2,\ \boldsymbol{q}^+/2\right] \\ & \boldsymbol{\varphi}\boldsymbol{\varphi}^\top \preceq \frac{1-\epsilon}{4\epsilon} \cdot \boldsymbol{\Sigma} \\ & \boldsymbol{\varphi} \in \mathbb{R}^n. \end{aligned}$$

Finally, two further applications of Schur's complement yield

$$\frac{1-\epsilon}{4\epsilon} \cdot \boldsymbol{\Sigma} - \boldsymbol{\varphi}\boldsymbol{\varphi}^\top \succeq \mathbf{0} \iff \begin{pmatrix} 1 & \boldsymbol{\varphi}^\top \\ \boldsymbol{\varphi} & \frac{1-\epsilon}{4\epsilon} \cdot \boldsymbol{\Sigma} \end{pmatrix} \succeq \mathbf{0} \iff 1 - \frac{4\epsilon}{1-\epsilon} \cdot \boldsymbol{\varphi}^\top \boldsymbol{\Sigma}^{-1} \boldsymbol{\varphi} \geqslant 0,$$

which simplifies the problem to

$$\begin{aligned} \text{maximize} \quad & \mathbf{1}_S{}^\top \boldsymbol{\mu} - 2 \cdot \mathbf{1}_S{}^\top \boldsymbol{\varphi} \\ \text{subject to} \quad & \boldsymbol{\varphi} \in \left[-\boldsymbol{q}^-/2,\, \boldsymbol{q}^+/2\right] \\ & \boldsymbol{\varphi}^\top \boldsymbol{\Sigma}^{-1} \boldsymbol{\varphi} \leqslant \frac{1-\epsilon}{4\epsilon} \\ & \boldsymbol{\varphi} \in \mathbb{R}^n. \end{aligned}$$

The statement now follows from the variable transformation $\boldsymbol{q} \leftarrow -2\boldsymbol{\varphi}$. ∎

Chapter 3

A Unifying Framework for the Capacitated Vehicle Routing Problem under Risk and Ambiguity

3.1 Introduction

In the previous chapter, we studied the distributionally robust chance constrained CVRP. We showed that the chance constraints enforced over an ambiguity set is equivalent to the worst-case value-at-risk over the ambiguity set. Moreover, focusing on the class of moment ambiguity sets, we devised solution schemes via the branch-and-cut algorithm that allow for its solution without undue overhead over the deterministic case. Motivated by this insight, this chapter aims to extend the theoretical result from the previous chapter by considering other commonly used risk measures and ambiguity sets.

We consider a generic model for the single-stage CVRP under demand uncertainty. While a number of interesting variants of the CVRP, such as the CVRP with compartments (that is of practical importance to e-groceries), can be treated in our framework; it excludes variants such as the distance constrained CVRP. The focus of this chapter is on treating a wide variety of stochastic, robust and distributionally robust formulations of the CVRP within the same framework. We aim to solve these problems numerically via the 2VF formulation described in the previous chapter due to its many advantages that we highlight later in this chapter. The main advantage is that the 2VF formulation can be solved using the branch-and-cut algorithm offered by many open source solvers, and hence it is easily accessible to a wider range of practitioners. To this end, we identify sufficient conditions that our generic CVRP model must satisfy in order to be solvable using the branch-and-cut algorithm.

In the previous chapter, we considered a specific demand estimator in the 2VF formulation to enable solution of the chance constrained CVRP over a wide range of moment ambiguity sets via the 2VF formulation. In this chapter, we consider a combination of various risk measures or disutility functions with complete or partial characterizations of the probability distribution governing the demands. We provide specific demand estimators to use in the 2VF formulation depending on the properties satisfied by the risk measures over the ambiguity sets considered. This allows the 2VF formulation to be adapted to a solve a number of CVRP variants. In this chapter, we consider popular risk measures such as mean semi-deviation [SDR14], conditional value-at-risk [RU02] and entropic risk measures [FK11] over ambiguity sets such as the Kullback-Leibler divergence ambiguity set [BL15], type-∞ Wasserstein ambiguity set with ∞-norm as ground norm [BSS20], and total variation ambiguity set [BL15]. Additionally, we also consider risk measures that have been proposed in recent vehicle routing literature such as requirements violation index [JQS16], essential riskiness index [ZBST18] and service fulfilment risk index [ZZLS21]. We derive algorithms to efficiently evaluate the demand estimator for the different risk measures considered over the various ambiguity sets.

We identified that our proposed solution scheme for distributionally robust chance constrained CVRP cannot be utilized for ambiguity sets like the Wasserstein ambiguity set or the ϕ-divergence ambiguity set in the previous chapter. We try to address this issue in this chapter. We derive more general demand estimators using results from [DFL18] that enable us to solve the distributioanlly robust chance constrained CVRP over many other ambiguity sets.

More succinctly, the contributions of this chapter may be summarized as follows:

- We derive the sufficient conditions for a CVRP to be amenable to a solution via the 2VF formulation which in turn can be solved using the branch-and-cut algorithm.

- We propose demand estimators that can be used in the 2VF formulation given the properties of the CVRP under consideration. More specifically, we study CVRP under a variety of risk measures and ambiguity sets.

- We consider a general ambiguity set and show that it can be reduced to many popular ambiguity sets such as moment ambiguity set, ∞-type Wasserstein ambiguity set with ∞-norm as ground norm, Kullback-Leibler divergence ambiguity set among others. We derive efficient evaluation schemes for the demand estimators for CVRP variants under this general ambiguity set. Moreover, we extend our findings from the previous chapter to allow the solution of distributionally robust chance constrained CVRP over ambiguity sets other than the moment ambiguity set.

The rest of this chapter is organized as follows. Section 3.2 gives a review of the literature relevant to this chapter. Section 3.3 introduces our problem setting and discusses our assumptions. Section 3.4 presents the sufficient conditions that a CVRP variant must satisfy in order to be amenable to a solution via branch-and-cut. It also provides the demand estimators that can be used in the 2VF formulation given the properties of the risk measure and uncertainty characterization considered for the CVRP. Section 3.5 studies a general ambiguity set in conjunction with many commonly used risk measures. It provides schemes to efficiently evaluate the demand estimator under each of these risk measures. We offer our concluding remarks in Section 3.7.

3.2 Literature Review

In the previous chapter, we reviewed stochastic programming and robust optimization approaches to handling CVRP under demand uncertainty. We also motivated the need for a distributionally robust approach to the solution of this problem, and made a first attempt at studying the distributionally robust chance constrained CVRP. In this chapter, we focus further on the 'risk averse' optimization approach. This approach to handling uncertainty involves modeling the uncertainty via risk measures either as constraints or the objective function of an optimization problem. Risk measures could quantify either the extent of violation or the probability of violation of constraints under uncertainty or both. The risk-averse approach has been treated in literature under stochastic programming [Noy18, MR11], robust optimization [Bro06, NPS09] as well as distributionally robust optimization [EK18, PdHM16, JG18] methods. For an overview of the recent developments in risk averse optimization, we refer the reader to [Rus13, RS09].

Risk-averse optimization has found successes in many application areas, especially in finance and energy. We review the applications of some popular risk measures here. The mean semi-deviation of order u has been used in optimal portfolio design [PP14], reinforcement learning [TCGM17] and chance constrained single newsvendor problem [KP18]. The many applications of conditional value-at-risk include portfolio optimization [KPU02], portfolio hedging [CHS10] and credit risk optimization [AMRU01] in finance, inventory management [ZCW08], supply chain management [WWC$^+$10], energy storage [HSS16], and radiation treatment planning [CMP14]. For further applications of the conditional value-at-risk outside of finance, we refer the reader to [FGS20]. The expected disutility risk measure has been used in literature for structural health monitoring-based decision making [CZG16], decision making under z-information [AMH15] and case-based decision making [GSW02]. The expectiles have applications in credit risk [FMP18], risk management [BB17] and asset allocation [Man07]. The entropic risk measure has been used in dynamic hedging in finance [TS11], energy systems [Gon15] and travelling salesman problem [BBIB19]. Another risk measure of interest is the value-at-risk that has been successfully applied to financial risk management [BS01], engineering [Kum03, LGG08], energy management [vAHMZ11] and supply chain management [GMM00]. We have shown its association with chance constraints in the previous chapter, and also provided a literature review of chance constrained CVRP. An important contribution in this area is that of [DFL18]. They introduce a demand estimator that we extend to treat the value-at-risk under ambiguity sets not limited to the moment ambiguity set. We study each of these risk measures in this chapter.

For the applications of risk measures to vehicle routing problem, the reader is referred to [ZZLS21, JQS16, ZBST18, AJ16, HADJ21, ZLSH21]. These papers deal with the vehicle routing problem under uncertain travel times, and seek to minimize the risk of not arriving at the customer nodes within the stipulated time window. These papers consider the distributionally robust case over different ambiguity sets. While [JQS16, ZBST18, ZLSH21] consider moment ambiguity sets, [ZZLS21] consider a Wasserstein distance-based ambiguity set.

The success of the distributionally robust optimization approach has been highlighted in the previous chapter. The ambiguity sets considered in the above papers and elsewhere in literature have their own merits and drawbacks. Moreover, the choice of an ambiguity set is driven by context. In this chapter, we consider the scenario-wise first-order ambiguity set introduced by [LQZ20, CSX19], and show that it reduces to many commonly used ambiguity sets. Using this ambiguity set along with a number of risk measures allows us to treat a large number of variants of CVRP within a single framework.

To the best of our knowledge, this chapter is the first attempt at extensively studying CVRP under risk and ambiguity.

3.3 Problem Formulation

Consider a complete, directed and weighted graph $G = (V, A, c)$ with nodes $V = \{0, \ldots, n\}$, arcs $A = \{(i, j) \in V \times V \ : \ i \neq j\}$ and transportation costs $c : A \mapsto \mathbb{R}_+$. Here, 0 is the depot node and $V_C = \{1, \ldots, n\}$ represents the set of customer nodes. The vehicle routing problem we wish to study asks for a cost optimal route plan for a set $K = \{1, 2, \ldots, m\}$ of vehicles starting and ending at the depot node 0 such that a given set of constraints is met. Firstly, we require a route plan to form an m-partition of the customer set V_C, that is, the route plan $\mathbf{R}$ has to belong to the set

$$\mathfrak{P}(V_C, m) = \Big\{ \mathbf{R} = \{\boldsymbol{R}_1, \ldots, \boldsymbol{R}_m\} \, : \boldsymbol{R}_k = (R_{k,1}, \ldots, R_{k,n_k}) \text{ with } n_k \geqslant 1 \text{ and } R_{k,i} \in V_C \;\; \forall k, i, \\ R_{k,i} \neq R_{l,j} \;\; \forall (k,i) \neq (l,j), \; \bigcup_{k \in K} \boldsymbol{R}_k = V_C \Big\}.$$

Each route plan $\mathbf{R}$ is a set of m routes $\boldsymbol{R}_k$, which are themselves nonempty ordered lists of customers that the vehicles visit sequentially. Here and in the following, we apply set operations to lists whenever their interpretation is clear. In particular, intersections and unions of ordered lists are interpreted as the application of the respective operators on the sets formed from the involved lists.

In addition to the aforementioned partition requirement, we assume that each route $\boldsymbol{R}_k$ of the route plan $\mathbf{R}$ has to satisfy some (technological, economic, ecological, quality-related or other) *intra-route* constraints [ITV14, §1.3.3], which we describe by the set

$$\mathcal{C} \subseteq \{\boldsymbol{R} = (R_1, \ldots, R_\nu) \, : \, \nu \geqslant 1 \text{ and } R_i \in V_C \;\; \forall i = 1, \ldots, \nu\}.$$

To be feasible, a route plan has to reside in the set $\mathfrak{P}(V_C, m) \cap \mathcal{C}_m$, where $\mathcal{C}_m = \{\mathbf{R} = \{\boldsymbol{R}_1, \ldots, \boldsymbol{R}_m\} \; : \; \boldsymbol{R}_k \in \mathcal{C} \quad \forall k\}$. Note that we do not consider *inter-route* (or global) constraints [ITV14, §1.3.5] that tie the feasibility of a route to the characteristics of other routes (as is the case, *e.g.*, in the presence of globally constrained resources or fairness considerations).

With the above notation, we are interested in solving the problem

$$\begin{aligned} \text{minimize} \quad & \sum_{k \in K} \sum_{l=0}^{n_k} c(R_{k,l}, R_{k,l+1}) \\ \text{subject to} \quad & \mathbf{R} \in \mathfrak{P}(V_C, m) \cap \mathcal{C}_m. \end{aligned} \tag{VRP($\mathcal{C}$)}$$

Here we use the convention that $R_{k,0} = R_{k,n_k+1} = 0$, which ensures that each vehicle starts and ends at the depot. To avoid trivially infeasible problem instances, we assume throughout the chapter that for all customers $i \in V_C$, there is $\boldsymbol{R} \in \mathcal{C}$ such that $i \in \boldsymbol{R}$. In other words, every customer's demand can principally be served by a single vehicle in every problem instance.

For the results in this chapter, we will typically impose the following two assumptions:

(D) $\mathcal{C}$ is *downward closed*, that is, if $\boldsymbol{R} \in \mathcal{C}$ for $\boldsymbol{R} = (R_1, \ldots, R_\nu)$, then $\boldsymbol{S} \in \mathcal{C}$ for all $\boldsymbol{S} = (R_{i_1}, \ldots, R_{i_\sigma})$ with $1 \leqslant \sigma \leqslant \nu$ and $1 \leqslant i_1 < i_2 < \ldots < i_\sigma \leqslant \nu$.

(P) $\mathcal{C}$ is *permutation invariant*, that is, if $\boldsymbol{R} \in \mathcal{C}$ then $\boldsymbol{S} \in \mathcal{C}$ for all permutations $\boldsymbol{S}$ of $\boldsymbol{R}$.

Condition **(D)** implies that we cannot model problems that disallow routes in which vehicles serve "too few" customers, since a subset of the customers of a feasible route can always be served as well (modulo the requirement imposed by $\mathfrak{P}(V_C, m)$ that the omitted customers need to be served by the other vehicles). Condition **(P)** implies that the order of customers within a route does not matter for its feasibility (but it will normally still matter in terms of its optimality). Here and in the following, we say that a set S is contained in a set of lists $\mathcal{S}$ if and only if every permutation of S, expressed as a list, is contained in $\mathcal{S}$. Thus, condition **(P)** is equivalent to requiring that $\boldsymbol{S} \in \mathcal{C}$ only if $S \in \mathcal{C}$ for the set S formed from the elements of $\boldsymbol{S}$.

Example 3.1 (Instances of VRP($\mathcal{C}$)**)** VRP($\mathcal{C}$) *recovers the* classical CVRP *if we set*

$$\mathcal{C} = \left\{ \boldsymbol{R} = (R_1, \ldots, R_\nu) \ : \ \sum_{i \in \boldsymbol{R}} q_i \leqslant Q \right\}, \tag{3.1}$$

where q_i is the demand of customer i and Q is the capacity of each vehicle. The set $\mathcal{C}$ satisfies **(P)** *by definition, and it satisfies* **(D)** *whenever the customer demands $\boldsymbol{q}$ are nonnegative. More generally, we obtain a variant of the* VRP with compartments *if we set*

$$\mathcal{C} = \left\{ \boldsymbol{R} = (R_1, \ldots, R_\nu) \ : \ \sum_{i \in \boldsymbol{R}} q_{ip} \leqslant Q_p \ \ \forall p = 1, \ldots, P \right\}, \tag{3.2}$$

where q_{ip} now denotes the demand of customer i for space in compartment p and Q_p is the capacity of compartment p in each vehicle. Again, both **(D)** *and* **(P)** *are satisfied as long as $\boldsymbol{q}$ is nonnegative.*

We recover the chance constrained CVRP *if we set*

$$\mathcal{C} = \left\{ \boldsymbol{R} = (R_1, \ldots, R_\nu) \,:\, \mathbb{P}\left[\sum_{i \in \boldsymbol{R}} \widetilde{q}_i \leqslant Q \right] \geqslant 1 - \epsilon \right\},$$

where we assume that the customer demands $\widetilde{q}_i$ *are random variables that are governed by the probability distribution* $\mathbb{P}$*, and where* ϵ *is a risk threshold selected by the decision maker. Both the chance constrained CVRP and its extension to multiple compartments satisfy the assumptions* **(D)** *and* **(P)** *as long as the customer demands satisfy* $\widetilde{\boldsymbol{q}} \geqslant \boldsymbol{0}$ $\mathbb{P}$*-almost surely.*

While Example 3.1 shows that the CVRP and some of its variants satisfy the assumptions **(D)** and **(P)**, it is worth pointing out that many other VRP variants do *not* fall under our framework. The distance constrained CVRP, for example, imposes the constraints $\sum_{l=0}^{\nu} t(R_l, R_{l+1}) \leqslant T$ for some distance function t, and these constraints violate **(P)** since different permutations of the customers along a route lead to different route lengths in general. For the same reason, the CVRP with time windows, which requires each customer $i \in V_C$ to be visited at some time $t_i \in [\underline{t}_i, \overline{t}_i]$, violates **(P)**, and it additionally violates **(D)** if we do not permit idle times. As we will see in Section 3.5, however, the assumptions **(D)** and **(P)** are satisfied for a broad range of stochastic, robust and distributionally robust formulations of the CVRP, which form the focus of this chapter.

To solve VRP($\mathcal{C}$) numerically, we consider its reformulation as the well-known two-index vehicle flow model [LN83, LLE04]

$$\begin{array}{lll}
\text{minimize} & \displaystyle\sum_{(i,j) \in A} c(i,j)\, x_{ij} & \\
\text{subject to} & \displaystyle\sum_{\substack{j \in V: \\ (i,j) \in A}} x_{ij} = \sum_{\substack{j \in V: \\ (j,i) \in A}} x_{ji} = \delta_i & \forall i \in V \\
& \displaystyle\sum_{i \in V \setminus S} \sum_{j \in S} x_{ij} \geqslant d(S) & \forall \emptyset \neq S \subseteq V_C \\
& x_{ij} \in \{0,1\} & \forall (i,j) \in A,
\end{array} \qquad (\text{2VF}(d))$$

where $\delta_i = 1$ for $i \in V_C$ and $\delta_0 = m$. We call the function $d : 2^{V_C} \mapsto \mathbb{R}_+$ the *demand estimator*, and the set of constraints involving d are called the *capacity constraints*. By writing the set S

in regular (non-bold) font, we emphasize that S is unordered (as opposed to the ordered list $\boldsymbol{R}_k$, for example). We assume that $d(S) = 0 \Leftrightarrow S = \emptyset$. Note that the value of $d(\emptyset)$ can be chosen freely as it does not affect the formulation. Moreover, the choice $d(S) > 0$ for $S \neq \emptyset$ ensures that route plans containing short cycles are excluded from the feasible region of 2VF(d). Finally, note that for a set S to constitute a feasible route, we must have $d(S) = 1$; the capacity constraints will exclude S as a feasible route at higher values of the demand estimator.

Solving VRP($\mathcal{C}$) via 2VF(d) enjoys several potential advantages. Firstly, mature (and open source) solvers are available to solve 2VF(d), see, *e.g.*, [LLE04] and [STV14]. These algorithms introduce the capacity constraints iteratively as part of a branch-and-cut algorithm. Thus, if we can show that VRP($\mathcal{C}$) is equivalent to 2VF(d) for some demand estimator d, then we can solve VRP($\mathcal{C}$) as long as we can evaluate d efficiently. Secondly, 2VF(d) offers a unified solution framework for different problem variants where only the demand estimator d needs to be adapted. In other words, minor variations of the same branch-and-cut algorithm can be employed to solve different variants of the problem. This is an important consideration for adoption in practice, where it is unreasonable to expect that fundamentally different algorithms will be developed and maintained to solve different variants of the same problem. Finally, 2VF(d) constitutes an important building block also for modern branch-and-cut-and-price algorithms, and we hope that the findings of this chapter are applicable to that algorithm class as well.

We want to investigate when VRP($\mathcal{C}$) is equivalent to 2VF(d), which is amenable to a solution via standard branch-and-cut algorithms. To this end, we first formalize our notion of equivalence.

Definition 3.2 ***Equivalence.*** VRP($\mathcal{C}$) *and* 2VF(d) *are said to be* equivalent *whenever they satisfy:*

(a) Every feasible route plan $\mathbf{R}$ *in* VRP($\mathcal{C}$) *induces a feasible solution* $\boldsymbol{x}$ *in* 2VF(d) *via*

$$x_{ij} = 1 \iff \exists k \in K,\ \exists l \in \{0, \ldots, n_k\} \,:\, (i, j) = (R_{k,l}, R_{k,l+1}). \tag{3.3}$$

(b) Every feasible solution $\boldsymbol{x}$ *in* 2VF(d) *induces a feasible route plan* $\mathbf{R}$ *in* VRP($\mathcal{C}$) *via* (3.3).

Note that if VRP($\mathcal{C}$) and 2VF(d) are equivalent, then any feasible route plan $\mathbf{R}$ in VRP($\mathcal{C}$) induces a *unique* feasible solution $\boldsymbol{x}$ in 2VF(d) via (3.3) and vice versa. In the remainder of the chapter, we refer to these unique solutions as $\boldsymbol{x}(\mathbf{R})$ and $\mathbf{R}(\boldsymbol{x})$, respectively. Note also that the objective functions in VRP($\mathcal{C}$) and 2VF(d) coincide, which justifies our notion of equivalence.

3.4 Theoretical Contributions

3.4.1 Equivalence of VRP($\mathcal{C}$) and 2VF(d)

We first show that the assumptions **(D)** and **(P)** are sufficient for VRP($\mathcal{C}$) and 2VF(d) to be equivalent under a range of demand estimators d, which we characterize explicitly. We then demonstrate that the assumptions **(D)** and**(P)** are tight in the sense that there are VRP($\mathcal{C}$) instances violating either assumption for which no demand estimator d results in an equivalent 2VF(d) instance.

A seemingly natural choice for the demand estimator d in 2VF(d) is

$$\overline{d}^m(S) = \inf\left\{ J \in \mathbb{N} \,:\, S \subseteq \bigcup_{k=1,\ldots,J} \boldsymbol{R}_k \;\text{ for } \{\boldsymbol{R}_1, \ldots, \boldsymbol{R}_J, \ldots, \boldsymbol{R}_m\} \in \mathfrak{P}(V_C, m) \cap \mathcal{C}_m \right\}$$

for $\emptyset \neq S \subseteq V_C$, as well as $\overline{d}^m(\emptyset) = 0$. This demand estimator records the minimum number of vehicles required to serve the customers in S in any feasible route plan $\mathbf{R} \in \mathfrak{P}(V_C, m) \cap \mathcal{C}_m$. Note that $\overline{d}^m(S) = \infty$ is possible if the problem instance is infeasible, which motivates our use of the infimum operator. The capacity constraints under the demand estimator $\overline{d}^m$ are commonly referred to as *generalized capacity constraints.* Since $\overline{d}^m$ is difficult to compute even for simple sets $\mathcal{C}$, however, it is not typically used in practice. Instead, research has focused on relaxations (*i.e.*, lower bounds) of this demand estimator that are easier to calculate while still tight enough to establish an equivalence between VRP($\mathcal{C}$) and 2VF(d). One such demand estimator is

$$\overline{d}^1(S) = \min \left\{ I \in \mathbb{N} \, : \, S \subseteq \bigcup_{k=1,\ldots,I} \boldsymbol{R}_k \ \text{ for some } \boldsymbol{R}_1, \ldots, \boldsymbol{R}_I \in \mathcal{C} \right\}$$

for $\emptyset \neq S \subseteq V_C$, as well as $\overline{d}^1(\emptyset) = 0$. This demand estimator determines the minimum number of vehicles required to serve the customers in $S \subseteq V_C$, but—in contrast to $\overline{d}^m$—it ignores the customers in $V_C \backslash S$. Note that $\overline{d}^1(S)$ is always finite by our earlier assumption that $i \in \boldsymbol{R}$ for some $\boldsymbol{R} \in \mathcal{C}$, $i \in V_C$, and thus the use of the minimum operator is justified. The capacity constraints under the demand estimator $\overline{d}^1$ are commonly referred to as *weak capacity constraints*. Although $\overline{d}^1$ tends to be easier to calculate than $\overline{d}^m$, its computation is still NP-hard for most commonly employed sets $\mathcal{C}$, and thus it is not normally used to identify violated capacity constraints in a branch-and-cut scheme. On the other end of the spectrum, we have the naive demand estimator

$$\underline{d}(S) = \begin{cases} 0 & \text{if } S = \emptyset, \\ 1 & \text{if } \emptyset \neq S \in \mathcal{C}, \\ 2 & \text{otherwise.} \end{cases}$$

Remember that $S \in \mathcal{C}$ if and only if $\boldsymbol{S} \in \mathcal{C}$ for every sequence $\boldsymbol{S}$ that can be formed from the elements of S, and under **(P)** we have $\boldsymbol{S} \in \mathcal{C}$ if and only if $S \in \mathcal{C}$. While the demand estimator $\underline{d}$ is typically easy to compute, the resulting capacity constraints are weak and thus slow down the branch-and-cut scheme significantly. In the remainder of this section, we will see that the above three demand estimators characterize the range of demand estimators under which VRP($\mathcal{C}$) and 2VF(d) are equivalent; in the next section, we will discuss two demand estimators within this range that are preferable to $\overline{d}^m$, $\overline{d}^1$ and $\underline{d}$ due to their favourable tightness-tractability trade-off.

Under the assumptions **(D)** and **(P)**, the three demand estimators form a natural order.

Proposition 3.3 *Assume that* **(D)** *and* **(P)** *are satisfied. Then for any $S \subseteq V_C$, we have*

$$\underline{d}(S) \leqslant \overline{d}^1(S) \leqslant \overline{d}^m(S).$$

Here **(D)** *and* **(P)** *are necessary and sufficient for* $\underline{d} \leqslant \overline{d}^1$*, whereas* $\overline{d}^1 \leqslant \overline{d}^m$ *holds by construction.*

Proof of Proposition 3.3. To show that $\underline{d}(S) \leqslant \overline{d}^1(S)$, we consider the following three cases for $S \subseteq V_C$:

Case (i): Consider $S = \varnothing$. Then $\underline{d}(S) = 0$ and $\overline{d}^1(S) = 0$ by construction.

Case (ii): Consider $S \neq \varnothing$ and $S \in \mathcal{C}$. Then $\underline{d}(S) = 1$. Since at least one set is required to cover a nonempty S, we have $\overline{d}^1(S) \geqslant 1$.

Case (iii): Finally, consider $\varnothing \neq S \notin \mathcal{C}$. Then $\underline{d}(S) = 2$. Assume that $\overline{d}^1(S) < \underline{d}(S)$. Since $S \neq \varnothing$, this must imply that $\overline{d}^1(S) = 1$. The definition of $\overline{d}^1(S)$ then implies that $S \subseteq \boldsymbol{R}_1$ for some $\boldsymbol{R}_1 \in \mathcal{C}$. Since **(D)** holds, we have that **S** constructed from $\boldsymbol{R}_1$, where we remove elements that are not in S, is also in $\mathcal{C}$. Finally, since **(P)** holds, we have $S \in \mathcal{C}$. This, however, contradicts the assumption that $S \notin \mathcal{C}$. Therefore, we must have that $\underline{d}(S) \leqslant \overline{d}^1(S)$.

Next, to show that $\overline{d}^1(S) \leqslant \overline{d}^m(S)$, assume that $\overline{d}^m(S) = t$. From the definition of $\overline{d}^m(S)$, we know that $S \subseteq \bigcup_{i=1,\ldots,t} \boldsymbol{R}_i$ where $\{\boldsymbol{R}_1, \ldots, \boldsymbol{R}_m\} \in \mathcal{C}_m \cap \mathfrak{P}(V_C, m)$. By definition of $\mathcal{C}_m$, we have that $\boldsymbol{R}_i \in \mathcal{C}$ for $i = 1, \ldots, m$. Hence, we have $S \subseteq \bigcup_{i=1,\ldots,t} \boldsymbol{R}_i$ where $\boldsymbol{R}_1, \ldots, \boldsymbol{R}_m \in \mathcal{C}$. Therefore, $\overline{d}^1(S) \leqslant t$.

To show that **(D)** and **(P)** are necessary and sufficient for $\underline{d} \leqslant \overline{d}^1$, we show that any VRP($\mathcal{C}$) instance that violates **(D)** or **(P)** also violates $\underline{d} \leqslant \overline{d}^1$. Assume first that the VRP($\mathcal{C}$) instance violates **(D)**. Then there is $\boldsymbol{R}_1 \in \mathcal{C}$ such that $\boldsymbol{S}_1 \notin \mathcal{C}$ for some subsequence $\boldsymbol{S}_1$ obtained from deleting one or more elements of $\boldsymbol{R}_1$. This implies that $S \notin \mathcal{C}$ for the set S formed from the elements of $\boldsymbol{S}_1$, and thus $\underline{d}(S) = 2 > \overline{d}^1(S)$. Assume now that the VRP($\mathcal{C}$) instance violates **(P)**. Then there is $\boldsymbol{R}_1 \in \mathcal{C}$ such that $S \notin \mathcal{C}$ for the set S formed from the elements of $\boldsymbol{R}_1$, again implying that $\underline{d}(S) = 2 > \overline{d}^1(S)$. ∎

It is easy to construct instances where the three demand estimators in Proposition 3.3 produce the same values for all $S \subseteq V_C$. The following example is inspired by [CH93] and shows that the inequalities in Proposition 3.3 can also all be strict.

Example 3.4 *Consider the* VRP($\mathcal{C}$) *instance with* $n = 5$ *customers,* $m = 5$ *vehicles and* $\mathcal{C} = \{\{(1)\}, \ldots, \{(5)\}, \{(1,5)\}\}$*. For* $S = \{1, 2, 3, 5\}$*, we have* $\underline{d}(S) = 2$ *since* $S \notin \mathcal{C}$*,* $\overline{d}^1(S) = 3$ *since* $S \subseteq \{(2)\} \cup \{(3)\} \cup \{(1,5)\}$*, and* $\overline{d}^m(S) = 4$ *since no route plan can serve customers* 1 *and* 5 *in the same route and at the same time utilize all* 5 *vehicles.*

The natural ordering from Proposition 3.3 typically ceases to hold when the assumptions **(D)** and **(P)** are violated. We now show that under the assumptions **(D)** and **(P)**, VRP($\mathcal{C}$) and 2VF(d) are equivalent *essentially* if and only if the demand estimator d satisfies $\underline{d} \leqslant d \leqslant \overline{d}^m$. We qualify this equivalence with 'essentially' as there are pathological cases in which demand estimators $d \ngeqslant \underline{d}$ also result in equivalent formulations, as we will discuss further below in Proposition 3.6.

Theorem 3.5 VRP($\mathcal{C}$) *is equivalent to* 2VF(d) *for any* d *satisfying* $\underline{d} \leqslant d \leqslant \overline{d}^m$*.*

Proof of Theorem 3.5. We note that the theorem is proved if we show the following:

(i) Any feasible route plan $\mathbf{R} \in \mathcal{C}_m \cap \mathfrak{P}(V_C, m)$ induces a solution $\boldsymbol{x}(\mathbf{R})$ feasible in 2VF(d) for every $d \leqslant \overline{d}^m$.

(ii) Any solution $\boldsymbol{x}$ feasible in 2VF(d) induces a feasible route plan $\mathbf{R}(\boldsymbol{x}) \in \mathcal{C}_m \cap \mathfrak{P}(V_C, m)$ for every $d \geqslant \underline{d}$.

We begin by showing *(i)*. Fix any $\mathbf{R} \in \mathcal{C}_m \cap \mathfrak{P}(V_C, m)$ and any $d \leqslant \overline{d}^m$. We need to show that $\boldsymbol{x}(\mathbf{R})$ as defined in (3.3) is feasible in 2VF(d). From the definition of $\boldsymbol{x}(\mathbf{R})$ in (3.3), $\boldsymbol{x}(\mathbf{R})$ satisfies the binarity and degree constraints of 2VF(d). Moreover, for any $\emptyset \neq S \subseteq V_C$, we have

$$
\begin{aligned}
d(S) \leqslant \overline{d}^m(S) &= \inf\left\{J \in \mathbb{N} : S \subseteq \bigcup_{k=1,\ldots,J} \boldsymbol{R}'_k \text{ for some } \{\boldsymbol{R}'_1,\ldots,\boldsymbol{R}'_J,\ldots,\boldsymbol{R}'_m\} \in \mathcal{C}_m \cap \mathfrak{P}(V_C,m)\right\} \\
&\leqslant \inf\left\{J \in \mathbb{N} : S \subseteq \bigcup_{k=1,\ldots,J} \boldsymbol{R}_{j_k} \text{ for } j_1,\ldots,j_J \in \{1,\ldots,m\}\right\} \\
&= |k \in K \,:\, \boldsymbol{R}_k \cap S \neq \varnothing| \leqslant \sum_{i\in V\setminus S}\sum_{j\in S} x_{ij}(\mathbf{R}).
\end{aligned}
$$

The second inequality above holds since $\mathbf{R} \in \mathcal{C}_m \cap \mathfrak{P}(V_C,m)$. Then the minimum number of routes required to cover S for $\{\boldsymbol{R}_1,\ldots,\boldsymbol{R}_m\} \in \mathcal{C}_m \cap \mathfrak{P}(V_C,m)$ cannot be less than the minimum number of routes required to cover S for *any* feasible route plan $\mathbf{R}' \in \mathcal{C}_m \cap \mathfrak{P}(V_C,m)$. The last equality follows since the minimum number of routes belonging to $\mathbf{R}$ required to cover S is equal to the number of routes $\boldsymbol{R}_k$, $k = 1,\ldots,m$, that have a nonempty intersection with S. In view of the last inequality, let $j_k \in \boldsymbol{R}_k \cap S$ be the first customer on the route $\boldsymbol{R}_k$ that is contained in S, where $k \in K$ satisfies $\boldsymbol{R}_k \cap S \neq \varnothing$. By definition of j_k, we have $\sum_{i\in V\setminus S} x_{ij_k}(\mathbf{R}) = 1$. The inequality now follows from the fact that there are $|k \in K : \boldsymbol{R}_k \cap S \neq \varnothing|$ different customer nodes j_k with this property.[1] Thus, we have shown that $\boldsymbol{x}(\mathbf{R})$ satisfies the RCI constraints in 2VF(d).

Next we prove *(ii)*. Let $\boldsymbol{x}$ be a feasible solution in 2VF(d) where $d \geqslant \underline{d}$. We construct a route plan $\mathbf{R}(\boldsymbol{x})$, in the following abbreviated as $\mathbf{R}$, satisfying (3.3) as follows. Since $\sum_{j\in V_C} x_{0j} = m$, there is $j_1,\ldots,j_m \in V_C$, $j_1 < \ldots < j_m$, such that $x_{0,j_1} = \ldots = x_{0,j_m} = 1$. For each route $\boldsymbol{R}_k$, $k \in K$, we set $R_{k,1} \leftarrow j_k$ and $n_k \leftarrow 1$. Since $\sum_{j\in V} x_{R_{k,n_k},j} = 1$, we either have $x_{R_{k,n_k},j} = 1$ for some $j \in V_C$ or $x_{R_{k,n_k},0} = 1$. In the former case, we extend route $\boldsymbol{R}_k$ by the customer $R_{k,n_k+1} \leftarrow j$, we set $n_k \leftarrow n_k + 1$ and we continue the procedure with customer j. In the latter case, we have completed the route $\boldsymbol{R}_k$. By construction, the route plan $\mathbf{R}$ satisfies (3.3).

We first show that $\mathbf{R} \in \mathfrak{P}(V_C,m)$. Note that $n_k \geqslant 1$ due to the existence of the customers $j_1,\ldots,j_m$. The degree constraints in 2VF(d) ensure that $R_{k,i} \neq R_{l,j}$ for all $(k,i) \neq (l,j)$. It remains to be shown that $\bigcup_k \boldsymbol{R}_k = V_C$. Imagine, to the contrary, that there is a customer

[1] Note that the same vehicle may enter and leave the set S multiple times, hence we cannot strengthen the inequality to an equality in general.

$j \in V_C$ such that $j \notin \bigcup_k \boldsymbol{R}_k$. By construction of the above algorithm, j must lie on a short cycle $S \subset V_C$ that is not connected to the depot node 0. Since $S \neq \emptyset$, its associated RCI constraint would require that $\sum_{i \in V \setminus S} \sum_{j \in S} x_{ij} \geqslant d(S) \geqslant \underline{d}(S) \geqslant 1$. However, $\sum_{i \in V \setminus S} \sum_{j \in S} x_{ij} = 0$ because S is a short cycle not connected to the depot node 0. Thus, the RCI constraint associated with S is violated.

We now show that $\{\boldsymbol{R}_1, \ldots, \boldsymbol{R}_m\} \in \mathcal{C}_m$. We have $\sum_{i \in V \setminus \boldsymbol{R}_k} \sum_{j \in \boldsymbol{R}_k} x_{ij} = 1 \geqslant d(R_k) \geqslant \underline{d}(R_k)$, where R_k is the set formed from the customers in $\boldsymbol{R}_k$. Here, the equality follows from the construction of the routes $\boldsymbol{R}_k$ and the two inequalities hold due to the feasibility of $\boldsymbol{x}$ in 2VF(d) and the fact that $d \geqslant \underline{d}$, respectively. Since $\boldsymbol{R}_k \neq \emptyset$, we thus conclude that $\underline{d}(R_k) = 1$, that is, $\boldsymbol{R}_k \in \mathcal{C}$, for all $k \in K$. By definition, we have $\{\boldsymbol{R}_1, \ldots, \boldsymbol{R}_m\} \in \mathcal{C}_m$. Consequently, we have $\mathbf{R} \in \mathcal{C}_m \cap \mathfrak{P}(V_C, m)$ as desired. ∎

Note that while the assumptions **(D)** and **(P)** are not required for the statement of Theorem 3.5, they are typically required for the function interval $[\underline{d}, \overline{d}^m]$ to be nonempty (*cf.* Proposition 3.3).

Proposition 3.6 *Fix any* VRP($\mathcal{C}$) *instance satisfying* **(D)** *and* **(P)**.

(i) If $\mathfrak{P}(V_C, m) \subseteq \mathcal{C}_m$ *and* $d \leqslant \overline{d}^m$, *then* VRP($\mathcal{C}$) *is equivalent to* 2VF(d) *even if* $d \ngeqslant \underline{d}$.

(ii) If $\mathfrak{P}(V_C, m) \nsubseteq \mathcal{C}_m$ *and* $d \leqslant \overline{d}^m$, *then there are* $d \ngeqslant \underline{d}$ *such that* VRP($\mathcal{C}$) *and* 2VF(d) *are equivalent, but there are also* $d \ngeqslant \underline{d}$ *such that* VRP($\mathcal{C}$) *and* 2VF(d) *are not equivalent.*

(iii) VRP($\mathcal{C}$) *fails to be equivalent to* 2VF(d) *for every* $d \nleqslant \overline{d}^m$.

Proof of Proposition 3.6. In view of assertion *(i)*, fix any VRP($\mathcal{C}$) instance and demand estimator d as described in the statement. The first part of the proof of Theorem 3.5 implies that any route plan $\mathbf{R}$ feasible in VRP($\mathcal{C}$) induces a solution $\boldsymbol{x}(\mathbf{R})$ that is feasible in 2VF(d). Thus, we only need to show that any solution $\boldsymbol{x}$ feasible in 2VF(d) also induces a route plan $\mathbf{R}(\boldsymbol{x})$ that is feasible in VRP($\mathcal{C}$). Indeed, the route plan $\mathbf{R}(\boldsymbol{x})$ considered in the second part of the proof of Theorem 3.5 satisfies $n_k \geqslant 1$ and $R_{k,i}(\boldsymbol{x}) \neq R_{l,j}(\boldsymbol{x})$ for all $(k, i) \neq (l, j)$ by construction.

Moreover, we have $\bigcup_k \boldsymbol{R}_k(\boldsymbol{x}) = V_C$ since $d(S) > 0$ for all nonempty $S \subseteq V_C$ disallows any short cycles in $\boldsymbol{x}$. We thus conclude that $\mathbf{R}(\boldsymbol{x}) \in \mathfrak{P}(V_C, m)$. Since $\mathfrak{P}(V_C, m) \subseteq \mathcal{C}_m$, it follows that $\mathbf{R}(\boldsymbol{x}) \in \mathcal{C}_m$ as well.

As for assertion *(ii)*, we first show that for any VRP($\mathcal{C}$) instance with $\mathfrak{P}(V_C, m) \nsubseteq \mathcal{C}_m$ the demand estimator d defined through $d(S) = 0$ if $S = \emptyset$ and $d(S) = 1$ otherwise satisfies $d \ngeq \underline{d}$ and implies that VRP($\mathcal{C}$) and 2VF(d) are *not* equivalent. To see that $d \ngeq \underline{d}$, we note that $\underline{d}(V_C) > 1$ since otherwise $V_C \in \mathcal{C}$, which would in turn imply by **(D)** that $\mathfrak{P}(V_C, 1) \subseteq \mathcal{C}$ in contradiction to our assumption for $m = 1$. To see that VRP($\mathcal{C}$) and 2VF(d) are not equivalent, fix any $\mathbf{R} \in \mathfrak{P}(V_C, m) \backslash \mathcal{C}_m$. We show that the solution $\boldsymbol{x}(\mathbf{R})$ defined through (3.3) is feasible in 2VF(d), which implies that VRP($\mathcal{C}$) and 2VF(d) are not equivalent. Indeed, $\boldsymbol{x}(\mathbf{R})$ satisfies the binarity and degree constraints in 2VF(d) by construction, and it satisfies all RCI constraints since $\sum_{i \in V \setminus S} \sum_{j \in S} x_{ij}(\mathbf{R}) \geqslant 1 = d(S)$ for all nonempty $S \subseteq V_C$.

We now show that for any VRP($\mathcal{C}$) instance with $\mathfrak{P}(V_C, m) \nsubseteq \mathcal{C}_m$ the demand estimator d defined through $d(S) = 1$ if $S = V_C$ and $d(S) = \underline{d}(S)$ otherwise satisfies $d \ngeq \underline{d}$ and makes VRP($\mathcal{C}$) and 2VF(d) equivalent. To see that $d \ngeq \underline{d}$, we note that $d(V_C) = 1 < \underline{d}(V_C) = 2$ since $V_C \notin \mathcal{C}$. In fact, if every permutation of V_C, expressed as a list, was in $\mathcal{C}$, then by **(D)** we would have that $\mathfrak{P}(V_C, 1) \subseteq \mathcal{C}$, in contradiction to our assumptions. To see that VRP($\mathcal{C}$) and 2VF(d) are equivalent under d, we again only need to show that any solution $\boldsymbol{x}$ feasible in 2VF(d) induces a route plan $\mathbf{R}(\boldsymbol{x})$ that is feasible in VRP($\mathcal{C}$). The route plan $\mathbf{R}(\boldsymbol{x})$ constructed in the second part of the proof of Theorem 3.5 satisfies $n_k \geqslant 1$, $R_{k,i}(\boldsymbol{x}) \neq R_{l,j}(\boldsymbol{x})$ for all $(k, i) \neq (l, j)$ and $\bigcup_k \boldsymbol{R}_k(\boldsymbol{x}) = V_C$. Thus, we have $\mathbf{R} \in \mathfrak{P}(V_C, m)$. To see that $\mathbf{R}(\boldsymbol{x}) \in \mathcal{C}_m$, we note that $\boldsymbol{R}_k(\boldsymbol{x}) \in \mathcal{C}$ for all $k \in K$ as the RCI constraints $\sum_{i \in V \setminus \boldsymbol{R}_k(\boldsymbol{x})} \sum_{j \in \boldsymbol{R}_k(\boldsymbol{x})} x_{ij} = 1 \geqslant d(\boldsymbol{R}_k(\boldsymbol{x})) = \underline{d}(\boldsymbol{R}_k(\boldsymbol{x}))$ are satisfied. By definition of $\mathcal{C}_m$, we have $\mathbf{R}(\boldsymbol{x}) \in \mathcal{C}_m$, that is, VRP($\mathcal{C}$) and 2VF($d$) are indeed equivalent.

In view of assertion *(iii)*, fix any VRP($\mathcal{C}$) instance and demand estimator d as described in the statement. We prove the assertion by constructing a route plan $\mathbf{R}'$ feasible in VRP($\mathcal{C}$) such that the associated solution $\boldsymbol{x}(\mathbf{R}')$ is not feasible in 2VF(d). To this end, fix $S \subseteq V_C$ such that $d(S) > \overline{d}^m(S)$, and let $\mathbf{R} = \{\boldsymbol{R}_1, \ldots, \boldsymbol{R}_m\}$ be such that $S \subseteq \bigcup_{k=1,\ldots,\overline{d}^m(S)} \boldsymbol{R}_k$. Such a route plan exists since $d(S) > \overline{d}^m(S)$ implies that $\overline{d}^m(S) \neq \infty$. We now construct the desired route plan $\mathbf{R}' = \{\boldsymbol{R}'_1, \ldots, \boldsymbol{R}'_m\}$ from $\mathbf{R}$ as follows. We set $\boldsymbol{R}'_k = \boldsymbol{R}_k$ for any route k satisfying $\boldsymbol{R}_k \cap S = \emptyset$. For the other routes $\boldsymbol{R}_k$, we obtain $\boldsymbol{R}'_k$ by reordering the customers in $\boldsymbol{R}_k$ such that those in $\boldsymbol{R}_k \cap S$ appear first (in any order). The assumption **(P)** implies that $\mathbf{R}' \in \mathcal{C}_m \cap \mathfrak{P}(V_C, m)$ as well. For the solution $\boldsymbol{x}(\mathbf{R}')$ constructed from (3.3), however, we observe that

$$\begin{aligned}\sum_{i \in V \setminus S} \sum_{j \in S} x_{ij}(\mathbf{R}') &= \sum_{i \in V \setminus S} \sum_{\substack{k \in K: \\ S \cap \boldsymbol{R}'_k \neq \emptyset}} \sum_{j \in S \cap \boldsymbol{R}'_k} x_{ij}(\mathbf{R}') = \sum_{\substack{k \in K: \\ S \cap \boldsymbol{R}'_k \neq \emptyset}} \sum_{i \in V \setminus S} \sum_{j \in S \cap \boldsymbol{R}'_k} x_{ij}(\mathbf{R}') \\ &= \sum_{\substack{k \in K: \\ S \cap \boldsymbol{R}'_k \neq \emptyset}} 1 = |k \in K \,:\, S \cap \boldsymbol{R}'_k \neq \emptyset| = \overline{d}^m(S),\end{aligned}$$

where the third equality follows from the reordering of the customers in $\mathbf{R}'$. Since $d(S) > \overline{d}^m(S)$, the solution $\boldsymbol{x}(\mathbf{R}')$ is infeasible in $2\mathrm{VF}(d)$ even though $\mathbf{R}'$ is feasible in $\mathrm{VRP}(\mathcal{C})$. ∎

From Theorem 3.5 and Proposition 3.6 we conclude that under the assumptions **(D)**, **(P)** and $d \geqslant \underline{d}$, the requirement $d \leqslant \overline{d}^m$ is necessary and sufficient for the equivalence of $\mathrm{VRP}(\mathcal{C})$ and $2\mathrm{VF}(d)$. In contrast, under the assumptions **(D)**, **(P)** and $d \leqslant \overline{d}^m$, the requirement $d \geqslant \underline{d}$ is sufficient but not necessary for the equivalence of the two formulations.

We close this section by showing that there are $\mathrm{VRP}(\mathcal{C})$ instances violating either **(D)** or **(P)** for which no demand estimator d results in an equivalent $2\mathrm{VF}(d)$ instance. This establishes that the assumptions **(D)** and **(P)** are not only sufficient, but also (in the aforementioned sense) tight.

Theorem 3.7 *There are* $\mathrm{VRP}(\mathcal{C})$ *instances violating either of the assumptions* **(D)** *or* **(P)** *that have no equivalent* $2\mathrm{VF}(d)$ *instances.*

We split the proof of Theorem 3.7 into the following 2 lemmas.

Lemma 3.8 *There exist* $\mathrm{VRP}(\mathcal{C})$ *instances violating* **(D)** *but satisfying* **(P)** *such that* $\mathrm{VRP}(\mathcal{C})$ *and* $2\mathrm{VF}(d)$ *are not equivalent for any demand estimators* d*.*

Proof of Lemma 3.8. Consider the VRP($\mathcal{C}$) instance with $n = 4$ customers, $m = 2$ vehicles, $\mathcal{C}$ consisting of all lists of $\mathfrak{P}(V_C, 1)$ that comprise 1, 3 or 4 elements and $\mathcal{C}_2 = [\mathcal{C}]^2$. This instance satisfies the assumption **(P)**, but it violates **(D)** since $(1, 2) \notin \mathcal{C}$ even though $(1, 2, 3) \in \mathcal{C}$. The feasible route plans of VRP($\mathcal{C}$) are all partitions in $\mathfrak{P}(V_C, 2)$ where one vehicle serves 1 customer and the other vehicle serves the remaining 3 customers.

We claim that there is no demand estimator d such that 2VF(d) has the same set of feasible solutions. Indeed, note that any admissible d must satisfy $d(S) \leqslant 2$ for all $S \subseteq V_C$ in order to result in a feasible 2VF(d) instance. Moreover, to allow for the feasible solutions $\boldsymbol{x}(\{(1, 2, 3), (4)\})$ and $\boldsymbol{x}(\{(1), (2, 3, 4)\})$, any admissible d must satisfy $d(S) \leqslant 1$ for all nonempty subsets of $\{1, 2, 3\}$ and $\{2, 3, 4\}$. This implies, however, that any admissible demand estimator must result in a 2VF(d) instance that also allows for the infeasible solution $\boldsymbol{x}(\{(1, 2), (3, 4)\})$. ∎

Lemma 3.9 *There exist* VRP($\mathcal{C}$) *instances violating* **(P)** *but satisfying* **(D)** *such that* VRP($\mathcal{C}$) *and* 2VF(d) *are not equivalent for any demand estimators d.*

Proof of Lemma 3.9. Consider the VRP($\mathcal{C}$) instance with $n = 2$ customers, $m = 1$ vehicle and $\mathcal{C} = \{(1), (2), (1, 2)\}$. This instance satisfies **(D)**, but it violates **(P)** since $(2, 1) \notin \mathcal{C}$ even though $(1, 2) \in \mathcal{C}$. The only feasible route plan for VRP($\mathcal{C}$) is $\{(1, 2)\}$.

We claim that there is no demand estimator d such that 2VF(d) has the same set of feasible solutions. Indeed, for the solution $\boldsymbol{x}(\{(1, 2)\})$ to be feasible in 2VF(d), any admissible demand estimator d must satisfy $d(\{1\})$, $d(\{2\})$, $d(\{1, 2\}) \leqslant 1$. However, any such demand estimator d would then also allow the infeasible route plan $\boldsymbol{x}(\{(2, 1)\})$. ∎

Proof of Theorem 3.7. The proof follows immediately from Lemmas 3.8–3.9. ∎

On the flipside, however, there are VRP($\mathcal{C}$) instances violating both **(D)** and **(P)** for which there still exist demand estimators d under which VRP($\mathcal{C}$) and 2VF(d) are equivalent.

In summary, we have shown that under **(D)** and **(P)**, we have $\underline{d} \leqslant \overline{d}^1 \leqslant \overline{d}^m$ (*cf.* Proposition 3.3), and any demand estimator $d \in [\underline{d}, \overline{d}^m]$ makes VRP($\mathcal{C}$) and 2VF(d) equivalent (*cf.* Theorem 3.5). In contrast, if a VRP($\mathcal{C}$) instance violates either **(D)** or **(P)**, then there may not be any demand estimator d that leads to an equivalent 2VF(d) formulation (*cf.* Theorem 3.7). In the remainder of this chapter, we will focus on VRP($\mathcal{C}$) instances that satisfy both assumptions **(D)** and **(P)**.

3.4.2 Demand Estimators for 2VF(d)

In this section, we represent the intra-route constraints as

$$\mathcal{C} = \Big\{ \boldsymbol{R} = (R_1, \ldots, R_\nu) \,:\, \nu \geqslant 1 \text{ and } R_i \in V_C \ \ \forall i, \ \ \varphi\left(\mathbf{1}_{\boldsymbol{R}}\right) \leqslant B \Big\}, \tag{3.4}$$

where $\varphi : [0,1]^n \mapsto \mathbb{R}$. To recover the classical CVRP, for example, we can choose $\varphi(\boldsymbol{y}) = \sum_{i \in V_C} q_i y_i$ and $B = Q$. Note that any class of intra-route constraints from Section 3.3 that satisfies **(P)** admits a representation of the form (3.4), for example by selecting $B = 0$ and $\varphi(\boldsymbol{y}) = 0$ if $\boldsymbol{y} = \mathbf{1}_{\boldsymbol{R}}$ for some $\boldsymbol{R} \in \mathcal{C}$, $\varphi(\boldsymbol{y}) = 1$ otherwise. However, we will be particularly interested in sets $\mathcal{C}$ and functions φ that satisfy certain properties. First and foremost, the assumptions **(D)** and **(P)** should be satisfied in order to ensure that the VRP($\mathcal{C}$) instance has an equivalent 2VF(d) instance.

Proposition 3.10 *A* VRP($\mathcal{C}$) *instance with intra-route constraints expressible in the form of* (3.4) *satisfies* **(P)** *by construction, and it satisfies* **(D)** *whenever φ is monotone.*

Proof of Proposition 3.10. For any permutation $\boldsymbol{S}$ of $\boldsymbol{R} \in \mathcal{C}$, we have $\mathbf{1}_{\boldsymbol{S}} = \mathbf{1}_{\boldsymbol{R}}$ and thus $\varphi(\mathbf{1}_{\boldsymbol{S}}) = \varphi(\mathbf{1}_{\boldsymbol{R}}) \leqslant B$, implying that $\boldsymbol{S} \in \mathcal{C}$. Therefore, assumption **(P)** is satisfied. To prove that $\mathcal{C}$ satisfies **(D)** whenever φ is monotone, consider any $\boldsymbol{R} = (R_1, \ldots, R_\nu) \in \mathcal{C}$ and $\boldsymbol{S} = (R_{i_1}, \ldots, R_{i_\sigma})$ such that $1 \leqslant \sigma \leqslant \nu$ and $1 \leqslant i_1 < i_2 < \ldots < i_\sigma \leqslant \nu$. We then have $\mathbf{1}_{\boldsymbol{S}} \leqslant \mathbf{1}_{\boldsymbol{R}}$, and the monotonicity of φ implies that $\varphi\left(\mathbf{1}_{\boldsymbol{S}}\right) \leqslant \varphi\left(\mathbf{1}_{\boldsymbol{R}}\right) \leqslant B$. Thus, $\boldsymbol{S} \in \mathcal{C}$, and assumption **(D)** holds. ∎

Recall that φ is monotone if $\varphi(\boldsymbol{x}) \leqslant \varphi(\boldsymbol{y})$ for all $\boldsymbol{x}, \boldsymbol{y} \in [0,1]^n$ satisfying $\boldsymbol{x} \leqslant \boldsymbol{y}$.

We now consider two demand estimators that turn out to be of special interest due to their tractability as well as their versatility. The *summation demand estimator* d^{S} is defined as

$$d^{\mathrm{S}}(S) = \max\left\{1, \lceil \varphi\left(\mathbf{1}_S\right)/B \rceil\right\} \qquad \forall \emptyset \neq S \subseteq V_C,$$

as well as $d^{\mathrm{S}}(\emptyset) = 0$. For the classical CVRP with $\varphi(\boldsymbol{y}) = \sum_{i \in V_C} q_i y_i$ and $B = Q$, the use of the summation demand estimator d^{S} in 2VF(d) reduces to the well-known *rounded capacity inequalities*. In the previous chapter, we have used d^{S} with $\varphi(\boldsymbol{y}) = \text{WC-VaR}(\widetilde{\boldsymbol{q}}^\top \boldsymbol{y})$, the worst-case value-at-risk of the customer demands, to solve a 2VF(d) formulation of the chance constrained CVRP. The *packing demand estimator* d^{P} is defined as

$$d^{\mathrm{P}}(S) = \min\left\{I \in \mathbb{N} : \exists \boldsymbol{Y} \in [0,1]^{n \times I} \text{ such that } \boldsymbol{Y}\mathbf{e} = \mathbf{1}_S,\ \ \varphi(\boldsymbol{y}_k) \leqslant B\ \ \forall k = 1, \ldots, I\right\}$$

for all $\emptyset \neq S \subseteq V_C$, as well as $d^{\mathrm{P}}(\emptyset) = 0$. Here, $\boldsymbol{y}_k \in \mathbb{R}^n$ is the k-th column of the matrix $\boldsymbol{Y}$, $k = 1, \ldots, I$. To our best knowledge, the packing demand estimator d^{P} has not been studied previously. It can be interpreted as the optimal value of a fractional bin packing problem; this interpretation is formalized in the following proposition.

Proposition 3.11 *If φ is monotone and we restrict ourselves to binary assignment matrices $\boldsymbol{Y} \in \{0,1\}^{n \times I}$ in d^{P}, then d^{P} coincides with the demand estimator $\overline{d}^1$ defined in Section 3.4.1.*

Proof of Proposition 3.11. By definition, we have $d^{\mathrm{P}}(\emptyset) = \overline{d}^1(\emptyset) = 0$. For any $\emptyset \neq S \subseteq$

V_C, we have

$$
\begin{aligned}
\overline{d}^1(S) &= \min\left\{ I \in \mathbb{N} \,:\, S \subseteq \textstyle\bigcup_{k=1,\dots,I} \boldsymbol{R}_k \ \text{ for some } \boldsymbol{R}_1, \dots, \boldsymbol{R}_I \in \mathcal{C} \right\} \\
&= \min\left\{ I \in \mathbb{N} \,:\, S \subseteq \textstyle\bigcup_{k=1,\dots,I} \boldsymbol{R}_k \ \text{ such that } \varphi\left(\mathbf{1}_{\boldsymbol{R}_k}\right) \leqslant B \text{ for all } k \in \{1, \dots, I\} \right\} \\
&= \min\left\{ I \in \mathbb{N} \,:\, \exists \boldsymbol{X} \in \{0,1\}^{n \times I} \ \text{ such that } \boldsymbol{X}\mathbf{e} \geqslant \mathbf{1}_S, \ \ \varphi(\boldsymbol{x}_k) \leqslant B \ \ \forall k \in \{1, \dots, I\} \right\} \\
&= \min\left\{ I \in \mathbb{N} \,:\, \exists \boldsymbol{X} \in \{0,1\}^{n \times I} \ \text{ such that } \boldsymbol{X}\mathbf{e} = \mathbf{1}_S, \ \ \varphi(\boldsymbol{x}_k) \leqslant B \ \ \forall k \in \{1, \dots, I\} \right\} \\
&= d^{\mathrm{P}}(S)
\end{aligned}
$$

The second identity follows from the definition of $\mathcal{C}$ as defined in (3.4). The union in the second identity can be enforced by the constraint $\boldsymbol{X}\mathbf{e} \geqslant \mathbf{1}_S$ where $\boldsymbol{x}_k \in \{0,1\}^n$ for $k \in \{1, \dots, I\}$ so that a customer can be assigned to more than one vehicle. Choose any $\boldsymbol{X}$ that is feasible in the third identity. Since φ is monotone, for each $i \in S$, we can arbitrarily choose one of the k's for which $x_{ik} = 1$ and set $x_{ik'} = 0$ for all $k' \neq k$. The monotonicity of φ guarantees that this new solution $\boldsymbol{x}_k$, $k \in \{1, \dots, I\}$ is also feasible, which leads to the fourth identity. ∎

The evaluation of the packing demand estimator d^{P} requires the solution of an assignment problem, which can become computationally prohibitive if d^{P} has to be evaluated frequently. It turns out, however, that d^{P} admits a closed-form solution when φ is convex.

Proposition 3.12 *If φ is convex, then the packing demand estimator d^{P} evaluates to*

$$
d^{\mathrm{P}}(S) = \min\left\{ I \in \mathbb{N} \,:\, \varphi(\mathbf{1}_S / I) \leqslant B \right\} \qquad \forall \varnothing \neq S \subseteq V_C.
$$

Proof of Proposition 3.12. We denote the two expressions for the packing estimator d^{P} as

$$
d_1(S) = \min\left\{ I \in \mathbb{N} \,:\, \exists \boldsymbol{X} \in [0,1]^{n \times I} \ \text{ such that } \boldsymbol{X}\mathbf{e} = \mathbf{1}_S, \ \ \varphi(\boldsymbol{x}_k) \leqslant B \ \ \forall k = 1, \dots, I \right\}
$$

and

$$d_2(S) = \min\{I \in \mathbb{N} \, : \, \varphi(\mathbf{1}_S/I) \leqslant B\},$$

where $\varnothing \neq S \subseteq V_C$. We want to show that $d_1(S) = d_2(S)$ for all $\varnothing \neq S \subseteq V_C$. One readily verifies that $d_1(S) \leqslant d_2(S)$ since for any $I \in \mathbb{N}$ feasible in the minimization problem that defines $d_2(S)$, $(I', \boldsymbol{X}') = (I, \mathbf{1}_S \, \mathbf{e}^\top / I)$ is feasible in the minimization problem that defines $d_1(S)$ and achieves the same objective value I. To see that $d_1(S) \geqslant d_2(S)$, fix any solution $(I, \boldsymbol{X})$ that is feasible in the minimization problem that defines $d_1(S)$. In the following, we prove that $\varphi(\mathbf{1}_S/I) \leqslant B$, which shows that I is also feasible in the minimization problem that defines $d_2(S)$.

Let Π be the group of all permutations $\pi : \{1, \ldots, I\} \mapsto \{1, \ldots, I\}$ of the set $\{1, \ldots, I\}$, and define $\pi(\boldsymbol{X}) = (\boldsymbol{x}_{\pi(1)}, \ldots, \boldsymbol{x}_{\pi(I)})$ for $\pi \in \Pi$. By construction, $\pi(\boldsymbol{X})$ is feasible in $d_1(S)$ for any $\pi \in \Pi$. Moreover, since the feasible region of $d_1(S)$ is convex by assumption, the convex combination

$$\boldsymbol{X}' \;=\; \frac{1}{|\Pi|} \sum_{\pi \in \Pi} \pi(\boldsymbol{X})$$

is also feasible in $d_1(S)$. However, the k-th column of $\boldsymbol{X}'$ satisfies

$$\boldsymbol{x}'_k \;=\; \frac{1}{I!} \cdot \sum_{\pi \in \Pi} \boldsymbol{x}_{\pi(k)} \;=\; \frac{1}{I!} \cdot \sum_{l=1}^{I} \sum_{\substack{\pi \in \Pi: \\ \pi(k) = l}} \boldsymbol{x}_{\pi(k)} \;=\; \frac{1}{I!} \cdot \sum_{l=1}^{I} (I-1)! \cdot \boldsymbol{x}_l \;=\; \frac{\mathbf{1}_S}{I},$$

where the first and penultimate equalities follow from the fact that a set with ℓ elements admits $\ell!$ permutations, and the last identify holds since $\boldsymbol{X}\mathbf{e} = \mathbf{1}_S$ as $\boldsymbol{X}$ is feasible in $d_2(S)$. ∎

One can construct counterexamples which show that the statement of Proposition 5 ceases to hold when φ is not convex. In summary, the summation demand estimator d^{S} requires a single evaluation of φ. Assuming that φ is monotone and convex, the packing demand estimator d^{P} requires $\mathcal{O}(\log m)$ evaluations of φ since the monotonicity of φ allows us to determine the minimizer $I^\star$ in Proposition 3.12 via a binary search. Thus, both demand estimators can be computed efficiently whenever φ allows for an efficient evaluation. As we will see in the next section, this is the case for a broad range of CVRP variants under stochastic, robust and distributionally robust descriptions of the uncertainty governing the customer demands.

We now study the applicability of the two demand estimators d^{S} and d^{P}.

Theorem 3.13 *Assume that φ is monotone.*

(i) If φ is subadditive, *we have $\underline{d} \leqslant d^{\mathrm{S}} \leqslant d^{\mathrm{P}} \leqslant \overline{d}^m$. If φ is also positive homogeneous then $d^{\mathrm{S}} = d^{\mathrm{P}}$; otherwise, $d^{\mathrm{S}} = d^{\mathrm{P}}$ does not hold in general.*

(ii) If φ is additive, *we have $\underline{d} \leqslant d^{\mathrm{S}} = d^{\mathrm{P}} \leqslant \overline{d}^m$. Furthermore,* $\mathrm{VRP}(\mathcal{C})$ *can be reformulated as a deterministic CVRP instance, and every deterministic CVRP instance can be reformulated as a* $\mathrm{VRP}(\mathcal{C})$ *instance with additive φ.*

(iii) If φ is convex *but* not subadditive, *then $\underline{d} \leqslant d^{\mathrm{P}} \leqslant \overline{d}^m$, whereas $d^{\mathrm{S}} \leqslant \overline{d}^m$ does not hold in general.*

Proof of Theorem 3.13. We first show that $\underline{d} \leqslant d^{\mathrm{P}} \leqslant \overline{d}^m$, irrespective of whether φ is sub- or superadditive. The fact that $d^{\mathrm{P}} \leqslant \overline{d}^m$ follows from Proposition 3.11, which implies that $d^{\mathrm{P}} \leqslant \overline{d}^1$, and Proposition 3.3, which shows that $\overline{d}^1 \leqslant \overline{d}^m$. To see that $d^{\mathrm{P}} \geqslant \underline{d}$, we note that $d^P(S) \geqslant 1 = \underline{d}(S)$ for all $S \neq \emptyset$ by construction, while $d^P(S) \geqslant 2 = \underline{d}(S)$ for all $\emptyset \neq S \notin \mathcal{C}$ since $\varphi(\mathbf{1}_S) > B$.

As for statement *(i)*, we note that $d^{\mathrm{S}} \geqslant \underline{d}$ by construction. To see that $d^{\mathrm{S}} \leqslant d^{\mathrm{P}}$ when φ is subadditive, we observe that for any $\emptyset \neq S \subseteq V_C$ and any $I \in \mathbb{N}$, we have

$$
\begin{aligned}
I \geqslant d^{\mathrm{P}}(S) \quad &\Longleftrightarrow \quad \exists \boldsymbol{X} \in [0,1]^{n \times I} \text{ such that } \boldsymbol{X}\mathbf{e} = \mathbf{1}_S, \quad \varphi(\boldsymbol{x}_k) \leqslant B \ \ \forall k = 1, \ldots, I \\
&\Longrightarrow \quad \varphi(\boldsymbol{x}_1) + \ldots + \varphi(\boldsymbol{x}_I) \leqslant I \cdot B \\
&\Longrightarrow \quad \varphi(\mathbf{1}_S) \leqslant I \cdot B \\
&\Longleftrightarrow \quad I \geqslant d^{\mathrm{S}}(S).
\end{aligned}
$$

Here, the first line holds by construction of d^{P}. The third line follows from the subadditivity of φ and the fact that $\boldsymbol{X}\mathbf{e} = \mathbf{1}_S$, and the last line holds by construction of d^{S} and since $I \in \mathbb{N}$.

If φ is subadditive and positive homogeneous, then for any $\emptyset \neq S \subseteq V_C$ and any $I \in \mathbb{N}$, Proposition 3.12 implies that $I \geqslant d^{\mathrm{P}}(S)$ if and only if $\varphi(\mathbf{1}_S/I) \leqslant B$, that is, $\varphi(\mathbf{1}_S) \leqslant I \cdot B$. By construction of d^{S} and since $I \in \mathbb{N}$, we thus have $I \geqslant d^{\mathrm{P}}(S)$ if and only if $I \geqslant d^{\mathrm{S}}(S)$.

To see that $d^{\mathrm{P}} = d^{\mathrm{S}}$ does not hold in general when φ is subadditive but not positive homogeneous, consider a VRP($\mathcal{C}$) instance with $n = 3$ customers, $m = 3$ vehicles and a set $\mathcal{C}$ of the form (3.4) with $\varphi(x_1, x_2, x_3) = \sqrt{x_1 + x_2 + x_3}$ as well as $B = 1$. Note that φ is subadditive but not positive homogeneous. One readily verifies that $d^{\mathrm{P}}(V_C) = 3$ but $d^{\mathrm{S}}(V_C) = 2$.

In view of statement *(ii)*, we first show that $d^{\mathrm{S}} = d^{\mathrm{P}}$ whenever φ is additive. We know from statement *(i)* that $d^{\mathrm{S}} \leqslant d^{\mathrm{P}}$ in this setting, so we only need to show that $d^{\mathrm{S}} \geqslant d^{\mathrm{P}}$ as well. Imagine, to the contrary, that $d^{\mathrm{S}}(S) = I' < d^{\mathrm{P}}(S)$ for some $\emptyset \neq S \subseteq V_C$. In that case, we have $\varphi(\mathbf{1}_S)/B \leqslant I'$. The additivity of φ implies that $I' \cdot \varphi(\mathbf{1}_S/I') = \varphi(\mathbf{1}_S) \leqslant I' \cdot B$, however, and the solution $I = I'$ and $\boldsymbol{X}$ given by $\boldsymbol{x}_k = \mathbf{1}_S/I'$ for all $k = 1, \ldots, I'$ is feasible in the minimization problem that defines d^{P}. We thus have $d^{\mathrm{P}}(S) \leqslant I'$, which contradicts the assumption that $d^{\mathrm{S}}(S) < d^{\mathrm{P}}(S)$, and we therefore have $d^{\mathrm{S}} = d^{\mathrm{P}}$ as desired.

When φ is additive, we have $\varphi(\mathbf{1}_S) = \sum_{i \in S} \varphi(\mathbf{e}_i)$. Thus, any VRP($\mathcal{C}$) instance with additive φ can be reformulated as a deterministic CVRP instance with customer demands $q_i = \varphi(\mathbf{e}_i)$ and vehicle capacity $Q = B$. Likewise, one readily verifies that any deterministic CVRP instance can be formulated as an instance of VRP($\mathcal{C}$) with $\varphi(\boldsymbol{x}) = \boldsymbol{q}^\top \boldsymbol{x}$ and $B = Q$.

As for statement *(iii)*, we only need to show that $d^{\mathrm{S}} \leqslant \overline{d}^m$ does not hold in general when φ is not subadditive. Indeed, consider a VRP($\mathcal{C}$) instance with $n = 3$ customers, $m = 3$ vehicles and the set $\mathcal{C}$ of the form (3.4) with $\varphi(x_1, x_2, x_3) = \exp(x_1 + x_2 + x_3) - 1$ as well as $B = 2$. Note that φ is not subadditive. One readily verifies that $d^{\mathrm{S}}(V_C) = 10$ but $\overline{d}^m(V_C) = 3$. ∎

Recall that φ is subadditive whenever $\varphi(\boldsymbol{x} + \boldsymbol{y}) \leqslant \varphi(\boldsymbol{x}) + \varphi(\boldsymbol{y})$ for all $\boldsymbol{x}, \boldsymbol{y} \in [0,1]^n$ satisfying $\boldsymbol{x} + \boldsymbol{y} \in [0,1]^n$, and that φ is additive if the inequality holds as equality. Likewise, φ is positive homogeneous if $\varphi(\lambda \boldsymbol{x}) = \lambda \varphi(\boldsymbol{x})$ for all $\lambda > 0$ and all $\boldsymbol{x} \in [0,1]^n$ satisfying $\lambda \boldsymbol{x} \in [0,1]^n$. A subadditive and positive homogeneous function is also called sublinear.

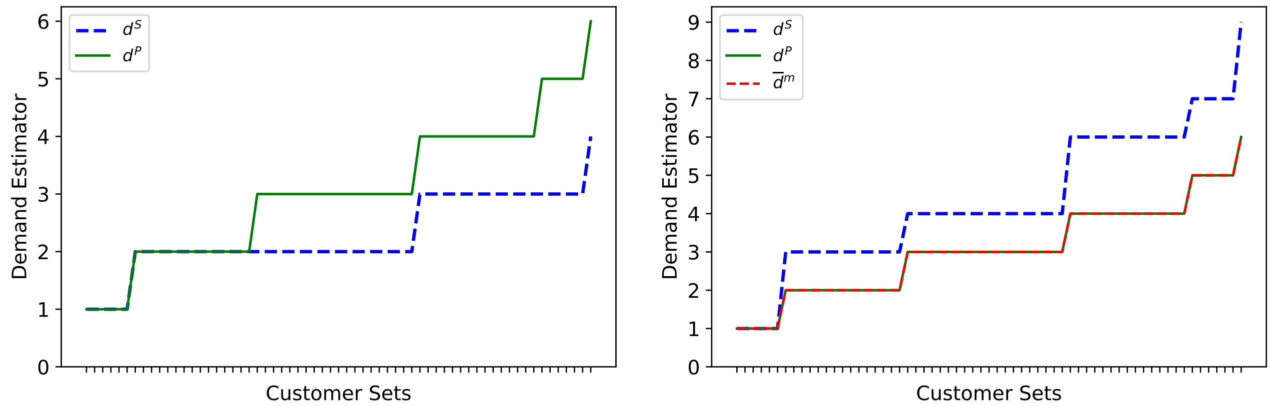

Figure 3.1: Demand estimators for a stochastic CVRP instance with 6 customers and joint probability distribution for customer demands as $\mathbb{P}[\widetilde{\boldsymbol{q}} = 5\mathbf{e}] = 0.05$, $\mathbb{P}[\widetilde{\boldsymbol{q}} = 16\mathbf{e}] = 0.9$ and $\mathbb{P}[\widetilde{\boldsymbol{q}} = 30\mathbf{e}] = 0.05$ for (a) expected ramp disutility $\mathbb{E}_{\mathbb{P}}[\max\{\sum_{i \in S} \widetilde{q}_i, 30\}]$ (on the left) with $B = 30$, and (b) entropic risk measure $10 \log \mathbb{E}_{\mathbb{P}}[\exp^{0.1(\sum_{i \in S} \widetilde{q}_i)}]$ (on the right) with $B = 17.2$.

Theorem 3.13 shows that for a subadditive and positive homogeneous function φ, the summation and packing demand estimators coincide, and we should use the summation demand estimator due to its favorable complexity. We will see in the next section that examples of subadditive and positive homogeneous φ include all coherent risk measures (such as the mean semi-deviation of order u, the conditional value-at-risk and expectile risk measures) as well as the underperformance risk index under a stochastic as well as a distributionally robust description of the uncertainty. If, on the other hand, φ is subadditive but not positive homogeneous, then the packing demand estimator can result in tighter capacity constraints. An example of a subadditive function φ that fails to be positive homogeneous is the ramp disutility function (discussed in the next section) under a stochastic as well as a distributionally robust description of the uncertainty. Figure 3.1 (left) illustrates how the packing demand estimator can yield tighter capacity constraints than the summation demand estimator for this risk measure. An example of an additive function φ is the expected loss risk measure over a stochastic description of the uncertainty. Examples of convex functions φ that fail to be subadditive include, as the next section shows, the expected disutility, entropic risk measures, the essential riskiness index, the service fulfillment risk index and the requirements violation index. Figure 3.1 (right) illustrates that in this case, we have to use the packing demand estimator as the summation demand estimator may fall outside the interval $[\underline{d}, \overline{d}^m]$ and thus cut off feasible route plans. Since all of the aforementioned risk measures are convex, the packing demand estimator can be computed efficiently for all of them.

3.5 Efficient Reformulation for Demand Estimators

From now on, we focus on the intra-route constraints of the distributionally robust CVRP, where the uncertain customer demands $\widetilde{\boldsymbol{q}}$ can be governed by any distribution $\mathbb{P}$ from the ambiguity set $\mathcal{P}$, and the feasibility of a route depends on its worst-case risk over all distributions $\mathbb{P} \in \mathcal{P}$:

$$\mathcal{C} = \left\{ \boldsymbol{R} = (R_1, \ldots, R_\nu) \,:\, \nu \geqslant 1 \text{ and } R_i \in V_C \;\; \forall i, \;\; \sup_{\mathbb{P} \in \mathcal{P}} \rho_{\mathbb{P}} \left[\sum_{i \in \boldsymbol{R}} \widetilde{q}_i \right] \leqslant Q \right\} \tag{3.5}$$

We call the collection $\rho = \{\rho_{\mathbb{P}}\}_{\mathbb{P} \in \mathcal{P}}$ of risk measures an *ambiguous risk measure*. Each individual risk measure $\rho_{\mathbb{P}}$ maps scalar random variables to real numbers with the interpretation that larger numbers correspond to greater risks, and the ambiguous risk measure ρ allows us to quantify the worst-case risk over all distributions $\mathbb{P} \in \mathcal{P}$. The upper bound Q represents either the homogeneous capacity of all vehicles (if the risk measure maps to quantities that have the same unit as the customer demands, such as the worst-case expectation or the worst-case (conditional) value-at-risk) or more generally a bound on the acceptable risk (*e.g.*, if the risk measure corresponds to the expected disutility). The intra-route constraints (3.5) emerge as a special case of the intra-route constraints (3.4) studied in Section 3.4.2 when we set $\varphi(\boldsymbol{y}) = \sup_{\mathbb{P} \in \mathcal{P}} \rho_{\mathbb{P}} \left[\boldsymbol{y}^\top \widetilde{\boldsymbol{q}} \right]$ for $\boldsymbol{y} \in [0,1]^n$ and $B = Q$. Note that the intra-route constraints (3.5) of the distributionally robust CVRP generalize those of the stochastic CVRP, which correspond to instances of (3.5) with singleton ambiguity sets, as well as those of the robust CVRP, which emerge if the ambiguity set $\mathcal{P}$ contains all Dirac distributions supported on a subset of $\mathbb{R}^n_+$ (which is commonly called the *uncertainty set*).

We assume that $\widetilde{\boldsymbol{q}} \geqslant \boldsymbol{0}$ $\mathbb{P}$-almost surely for all $\mathbb{P} \in \mathcal{P}$, and we require the worst-case risk measure φ to be monotone, that is, $\varphi(\boldsymbol{x}) \leqslant \varphi(\boldsymbol{y})$ whenever $\boldsymbol{x} \leqslant \boldsymbol{y}$. Taken together, both conditions imply via Proposition 3.10 that the corresponding instance of VRP($\mathcal{C}$) satisfies the assumptions

(D) and **(P)**. Additionally, we will be interested in cases where the worst-case risk measure is subadditive and/or convex so that we can apply the demand estimators d^{S} and d^{P} from Section 3.4.2 to solve the corresponding instance of 2VF(d). Finally, we will be interested in worst-case risk measures that can be evaluated quickly so that the resulting 2VF(d) instances can be solved efficiently.

Throughout this section, we consider the scenario-wise first-order ambiguity set

$$\mathcal{P} \;=\; \left\{ \mathbb{P} \in \mathcal{P}_0(\mathbb{R}^n_+ \times \mathcal{W}) : \exists \boldsymbol{s} \in \mathcal{S} \text{ such that } \begin{bmatrix} \mathbb{P}\left[\underline{\boldsymbol{q}}^w \leqslant \widetilde{\boldsymbol{q}} \leqslant \overline{\boldsymbol{q}}^w \,|\, \tilde{w} = w\right] = 1 \\ \mathbb{E}_{\mathbb{P}}\left[\widetilde{\boldsymbol{q}} \,|\, \tilde{w} = w\right] = \boldsymbol{\mu}^w \\ \mathbb{E}_{\mathbb{P}}\left[|\widetilde{\boldsymbol{q}} - \boldsymbol{\mu}^w| \,|\, \tilde{w} = w\right] \leqslant \boldsymbol{\nu}^w \\ \mathbb{P}\left[\tilde{w} = w\right] = s_w \end{bmatrix} \forall w \in \mathcal{W} \right\} \tag{3.6}$$

proposed by [CSX19] and [LQZ20]. Here, $\tilde{w}$ is a random scenario supported on the set $\mathcal{W} = \{1, \ldots, W\}$, $[\underline{\boldsymbol{q}}^w, \overline{\boldsymbol{q}}^w]$ is the support of the uncertain demands $\widetilde{\boldsymbol{q}}$ in scenario $w \in \mathcal{W}$, $\boldsymbol{\mu}^w \in (\underline{\boldsymbol{q}}^w, \overline{\boldsymbol{q}}^w)$ and $\boldsymbol{\nu}^w > \mathbf{0}$ represent the expectation and the mean absolute deviation of the demand vector under scenario w, respectively, $\boldsymbol{s}$ denotes the scenario probabilities that are only known to be contained in the convex subset $\mathcal{S}$ of the probability simplex in $\mathbb{R}^W$, and $\mathcal{P}_0(\mathbb{R}^n_+ \times \mathcal{W})$ is the set of all probability distributions supported on $\mathbb{R}^n_+ \times \mathcal{W}$. We allow for the mean and mean absolute deviation conditions to be absent in (3.6), in which case some of the risk measures considered below simplify. All of our results also extend to ambiguity sets in which the mean absolute deviation is replaced by the expectation of a piecewise affine convex function (*cf.* [LQZ20]), which allows us to stipulate, among others, approximate upper bounds on the marginal variances or the Huber losses of the customer demands [WKS14].

As we show in the following, the ambiguity set (3.6) is very versatile and allows us to model a range of well-known ambiguity sets from the literature.

Example 3.14 (Ambiguity Set $\mathcal{P}$) *The ambiguity set* (3.6) *recovers a* stochastic CVRP

$$\mathcal{P} \;=\; \left\{ \mathbb{P} \in \mathcal{P}_0(\mathbb{R}^n_+) \;:\; \mathbb{P}\left[\boldsymbol{q} = \widehat{\boldsymbol{q}}^w\right] = \hat{s}_w \;\; \forall w \in \mathcal{W} \right\},$$

if we set $\underline{\boldsymbol{q}}^w = \overline{\boldsymbol{q}}^w = \widehat{\boldsymbol{q}}^w$, $w \in \mathcal{W}$, $\mathcal{S} = \{\widehat{\boldsymbol{s}}\}$ *and disregard the expectation and mean absolute deviation constraints. Likewise, we obtain a distributionally robust CVRP over the* marginalized moment ambiguity set *[GW20]*

$$\mathcal{P} \;=\; \left\{\mathbb{P} \in \mathcal{P}_0(\mathbb{R}^n_+) \;:\; \mathbb{P}\left[\underline{\boldsymbol{q}} \leqslant \widetilde{\boldsymbol{q}} \leqslant \overline{\boldsymbol{q}}\right] = 1,\;\; \mathbb{E}_{\mathbb{P}}\left[\widetilde{\boldsymbol{q}}\right] = \boldsymbol{\mu},\;\; \mathbb{E}_{\mathbb{P}}\left[|\widetilde{\boldsymbol{q}} - \boldsymbol{\mu}|\right] \leqslant \boldsymbol{\nu}\right\}$$

if we set $W = 1$ *and* $\mathcal{S} = \{1\}$. *We recover a distributionally robust CVRP over the* type-∞ Wasserstein ambiguity set *[BSS20]*

$$\mathcal{P} \;=\; \left\{\mathbb{P} \in \mathcal{P}_0(\mathbb{R}^n_+) \;:\; \mathsf{d}^{\mathrm{W}}_{\infty}\left(\mathbb{P},\; \frac{1}{W}\sum_{w \in \mathcal{W}} \delta_{\widehat{\boldsymbol{q}}^w}\right) \leqslant \theta\right\},$$

where $\frac{1}{W}\sum_{w \in \mathcal{W}} \delta_{\widehat{\boldsymbol{q}}^w}$ *is the empirical distribution over the historical demands* $\widehat{\boldsymbol{q}}^1, \ldots, \widehat{\boldsymbol{q}}^W$ *and*

$$\mathsf{d}^{\mathrm{W}}_{\infty}(\mathbb{P}, \mathbb{Q}) \;=\; \inf\left\{\Pi\text{-ess sup}\,\left\|\widetilde{\boldsymbol{\xi}} - \widetilde{\boldsymbol{\xi}}'\right\|_{\infty} \;:\; \left[\begin{array}{c}\Pi \text{ is a joint distribution over } \widetilde{\boldsymbol{\xi}} \text{ and } \widetilde{\boldsymbol{\xi}}' \\ \text{with marginals } \mathbb{P} \text{ and } \mathbb{Q}\end{array}\right]\right\}$$

is the type-∞ Wasserstein distance with the ∞-norm as ground metric, by setting $\underline{\boldsymbol{q}} = [\widehat{\boldsymbol{q}}^w - \theta \cdot \mathbf{e}]_+$ *and* $\overline{\boldsymbol{q}} = \widehat{\boldsymbol{q}}^w + \theta \cdot \mathbf{e}$ *for all* $w \in \mathcal{W}$, $\mathcal{S} = \left\{\frac{1}{W} \cdot \mathbf{e}\right\}$ *and disregarding the expectation and mean absolute deviation constraints, see Proposition 3 of [BSS20]. A distributionally robust CVRP over the* Kullback-Leibler (KL) divergence ambiguity set *[BL15, §3.1]*

$$\mathcal{P} \;=\; \left\{\mathbb{P} \in \mathcal{P}_0(\mathbb{R}^n_+) \;:\; \operatorname{supp}(\mathbb{P}) = \left\{\widehat{\boldsymbol{q}}^1, \ldots, \widehat{\boldsymbol{q}}^W\right\},\;\; \mathsf{d}^{\mathrm{KL}}\left(\mathbb{P},\; \frac{1}{W}\sum_{w \in \mathcal{W}} \delta_{\widehat{\boldsymbol{q}}^w}\right) \leqslant \theta\right\},$$

where $\operatorname{supp}(\mathbb{P})$ *denotes the support of the distribution* $\mathbb{P}$ *and*

$$\mathsf{d}^{\mathrm{KL}}\left(\sum_{w \in \mathcal{W}} p_w \cdot \delta_{\widehat{\boldsymbol{q}}^w},\; \sum_{w \in \mathcal{W}} q_w \cdot \delta_{\widehat{\boldsymbol{q}}^w}\right) \;=\; \sum_{w \in \mathcal{W}} p_w \log\left(\frac{p_w}{q_w}\right)$$

is the KL divergence between two discrete distributions over the common support $\left\{\widehat{\boldsymbol{q}}^1, \ldots, \widehat{\boldsymbol{q}}^W\right\}$, *is recovered if we fix* $\underline{\boldsymbol{q}}^w = \overline{\boldsymbol{q}}^w = \widehat{\boldsymbol{q}}^w$ *for all* $w \in \mathcal{W}$, $\mathcal{S} = \left\{\boldsymbol{s} \in \mathbb{R}^W_+ \;:\; \sum_{w \in \mathcal{W}} s_w \log(s_w W) \leqslant \theta,\; \mathbf{e}^\top \boldsymbol{s} = 1\right\}$ *and disregard the expectation and mean absolute deviation constraints. We recover a distribu-*

tionally robust CVRP over the total variation ambiguity set *[BL15, §3.1]*

$$\mathcal{P} \;=\; \left\{ \mathbb{P} \in \mathcal{P}_0(\mathbb{R}^n_+) \;:\; \operatorname{supp}(\mathbb{P}) = \left\{ \widehat{\boldsymbol{q}}^1, \ldots, \widehat{\boldsymbol{q}}^W \right\},\;\; \mathsf{d}^{\mathrm{TV}} \left(\mathbb{P},\, \frac{1}{W} \sum_{w \in \mathcal{W}} \delta_{\widehat{\boldsymbol{q}}^w} \right) \leqslant \theta \right\},$$

where $\operatorname{supp}(\mathbb{P})$ *denotes the support of the distribution* $\mathbb{P}$ *and*

$$\mathsf{d}^{\mathrm{TV}} \left(\sum_{w \in \mathcal{W}} p_w \cdot \delta_{\widehat{\boldsymbol{q}}^w},\, \sum_{w \in \mathcal{W}} q_w \cdot \delta_{\widehat{\boldsymbol{q}}^w} \right) \;=\; \sum_{w \in \mathcal{W}} q_w \cdot \left| \frac{p_w}{q_w} - 1 \right|$$

is the total variation between two discrete distributions over the common support $\left\{ \widehat{\boldsymbol{q}}^1, \ldots, \widehat{\boldsymbol{q}}^W \right\}$, *finally, if we fix* $\underline{\boldsymbol{q}}^w = \overline{\boldsymbol{q}}^w = \widehat{\boldsymbol{q}}^w$ *for all* $w \in \mathcal{W}$, $\mathcal{S} = \left\{ \boldsymbol{s} \in \mathbb{R}^W_+ \;:\; \left\| \boldsymbol{s} - \frac{1}{W} \cdot \mathbf{e} \right\|_1 \leqslant \theta,\; \mathbf{e}^\top \boldsymbol{s} = 1 \right\}$ *and disregard the expectation and mean absolute deviation constraints.*

Example 3.14 highlight the diversity of the ambiguity sets that can be modeled under the consideration of fixed scenario probabilities in ambiguity set defined in (3.6). In the rest of this chapter, we focus on the ambiguity set $\mathcal{P}$ of the form (3.6) with $\mathcal{S} = \{\widehat{\boldsymbol{s}}\}$. We next discuss how VRP($\mathcal{C}$) with the intra-route constraints (3.5) can be solved via its reformulation 2VF(d) under this ambiguity set.

[LQZ20] optimize the worst-case expectation in two-stage distributionally robust optimization problems where the uncertain parameters affect the constraint right-hand sides of the second-stage problem. They show that for ambiguity sets of the form (3.6) with known scenario probabilities $\widehat{\boldsymbol{s}}$, the worst-case expectation is attained by a discrete distribution that does not depend on the first-stage decisions, and thus the two-stage distributionally robust optimization problem reduces to a two-stage stochastic program. Our setting differs from theirs in the following aspects: *(i)* we consider the random quantity $\boldsymbol{x}^\top \widetilde{\boldsymbol{q}}$ that is parametric in the weights $\boldsymbol{x}$, rather than the optimal value of a second-stage problem that is parametric in the first-stage decisions; *(ii)* we consider a broad range of risk measures, whereas [LQZ20] focus on the expected value, the expected disutility and the optimized certainty equivalent; and *(iii)* the random vector $\widetilde{\boldsymbol{q}}$ multiplies the parameters $\boldsymbol{x}$ in our context, whereas it is isolated on the constraint right-hand sides in their setting. Nevertheless, we can adapt the arguments of [LQZ20] to show that the worst-case risk $\varphi(\boldsymbol{x})$ is attained by a finite demand distribution that is independent of ρ and $\boldsymbol{x}$.

Theorem 3.15 ([LQZ20]) *Fix an ambiguity set $\mathcal{P}$ of the form* (3.6) *where $\mathcal{S} = \{\widehat{\boldsymbol{s}}\}$, and assume that $\varphi(\cdot)$ can be represented as a worst-case expectation $\sup_{\mathbb{P}\in\mathcal{P}} \mathbb{E}_{\mathbb{P}}\left[f(\cdot^\top \widetilde{\boldsymbol{q}})\right]$ of a convex function $f : \mathbb{R} \to \mathbb{R}$. Then for all $\boldsymbol{x} \in [0,1]^n$, Algorithm 2 in Appendix B identifies a common $W(2n+1)$-point worst-case distribution $\mathbb{P}^\star = \sum_{w\in\mathcal{W}} \sum_{i=1}^{2n+1} \hat{s}_w p^\star_{wi} \cdot \delta_{\boldsymbol{q}^\star_{wi}} \in \mathcal{P}$ that is independent of f and $\boldsymbol{x}$.*

Proof of Theorem 3.15. Fix any $\boldsymbol{x} \in [0,1]^n$. Since f is convex and $\boldsymbol{x} \geqslant \mathbf{0}$, it follows from Theorem 2.2.6(a) of [SLCB05] that the mapping $\boldsymbol{q} \mapsto f(\boldsymbol{x}^\top \boldsymbol{q})$ is supermodular. Following from the rectangularity of $\mathcal{P}$, we can write

$$\begin{aligned}
\sup_{\mathbb{P}\in\mathcal{P}} \mathbb{E}_{\mathbb{P}}[f(\boldsymbol{x}^\top \widetilde{\boldsymbol{q}})] &= \max_{\boldsymbol{s}\in\mathcal{S}} \sup_{\mathbb{P}_w\in\mathcal{P}^w : w\in\mathcal{W}} \sum_{w\in\mathcal{W}} s_w \mathbb{E}_{\mathbb{P}_w}[f(\boldsymbol{x}^\top \widetilde{\boldsymbol{q}})] \\
&= \sup_{\mathbb{P}_w\in\mathcal{P}^w : w\in\mathcal{W}} \sum_{w\in\mathcal{W}} \hat{s}_w \mathbb{E}_{\mathbb{P}_w}[f(\boldsymbol{x}^\top \widetilde{\boldsymbol{q}})] = \sum_{w\in\mathcal{W}} \hat{s}_w \sup_{\mathbb{P}_w\in\mathcal{P}^w} \mathbb{E}_{\mathbb{P}_w}[f(\boldsymbol{x}^\top \widetilde{\boldsymbol{q}})]
\end{aligned}$$

where $\mathcal{P}^w$ is as defined in (3.7). The second identity holds because $\mathcal{S}$ is a singleton.

We can then apply Proposition 3 of [LQZ20] to evaluate $\sup_{\mathbb{P}_w\in\mathcal{P}^w} \mathbb{E}_{\mathbb{P}_w}\left[f\left(\boldsymbol{x}^\top \widetilde{\boldsymbol{q}}\right)\right]$ for each $w \in \mathcal{W}$. Note that this proposition assumes that the function inside the worst-case expectation constitutes the second-stage cost of a two-stage distributionally robust optimization problem; since the proof of that result only makes use of the supermodularity of the second-stage cost function, however, the proposition extends to our setting. Hence, we have $\sup_{\mathbb{P}_w\in\mathcal{P}^w} \mathbb{E}_{\mathbb{P}_w}\left[f\left(\boldsymbol{x}^\top \widetilde{\boldsymbol{q}}\right)\right] = \sum_{j=1}^{2n+1} p^\star_{wj} f\left(\sum_{i\in V_C} x_i q^\star_{wji}\right)$ where $p^\star_{wj}, \boldsymbol{q}^\star_{wj}$ for $j = 1, \ldots, 2n+1$ and $w \in \mathcal{W}$ are obtained from Algorithm 2. This implies that

$$\sup_{\mathbb{P}\in\mathcal{P}} \mathbb{E}_{\mathbb{P}}[f(\boldsymbol{x}^\top \widetilde{\boldsymbol{q}})] = \sum_{w\in\mathcal{W}} \hat{s}_w \sup_{\mathbb{P}_w\in\mathcal{P}^w} \mathbb{E}_{\mathbb{P}_w}[f(\boldsymbol{x}^\top \widetilde{\boldsymbol{q}})] = \sum_{w\in\mathcal{W}} \hat{s}_w \sum_{j=1}^{2n+1} p^\star_{wj} f\left(\sum_{i\in V_C} x_i q^\star_{wji}\right).$$

From here it follows that a worst-case distribution is the $W(2n+1)$-point distribution $\mathbb{P}^\star = \sum_{w\in\mathcal{W}} \hat{s}_w \sum_{j=1}^{2n+1} p^\star_{wj} \cdot \delta_{\boldsymbol{q}^\star_{wj}} \in \mathcal{P}$. ∎

The intuition underlying Theorem 3.15 is as follows. If we condition on the event $\tilde{w} = w$, then the resulting ambiguity set $\mathcal{P}^w$ becomes rectangular in the customers $i \in V_C$ in the sense that

$$\begin{aligned} \mathcal{P}^w &= \left\{ \mathbb{P} \in \mathcal{P}_0(\mathbb{R}^n_+) \,:\, \exists \mathbb{Q} \in \mathcal{P} \text{ such that } \mathbb{P}[\cdot] = \mathbb{Q}[\cdot \mid \tilde{w} = w] \right\} \\ &= \bigtimes_{i \in V_C} \left\{ \mathbb{P} \in \mathcal{P}_0(\mathbb{R}) : \mathbb{P}\left[\underline{q}_i^w \leqslant \widetilde{q}_i \leqslant \overline{q}_i^w \right] = 1,\;\; \mathbb{E}_{\mathbb{P}}[\widetilde{q}_i] = \mu_i^w,\;\; \mathbb{E}_{\mathbb{P}}[|\widetilde{q}_i - \mu_i^w|] \leqslant \nu_i^w \right\}. \end{aligned} \tag{3.7}$$

One can then verify that for a convex function f, $\sup_{\mathbb{P} \in \mathcal{P}^w} \mathbb{E}_{\mathbb{P}}\left[f(\boldsymbol{x}^\top \widetilde{\boldsymbol{q}}) \right]$ is attained by a distribution $\mathbb{P}^\star$ that only places positive probability on demand realizations $\boldsymbol{q} \in \bigtimes_{i \in V_C} \left\{ \underline{q}_i^w,\, \mu_i^w,\, \overline{q}_i^w \right\}$, and that these probabilities do not depend on f or $\boldsymbol{x}$. This, however, only allows us to conclude that there is a worst-case distribution with an exponentially large number 3^n of realizations. Next, fix any worst-case distribution $\mathbb{P}^\star$ supported on the demands $\boldsymbol{q} \in \bigtimes_{i \in V_C} \left\{ \underline{q}_i^w,\, \mu_i^w,\, \overline{q}_i^w \right\}$, and assume that $\mathbb{P}^\star[\boldsymbol{q}]$, $\mathbb{P}^\star[\boldsymbol{q}'] > 0$ for an unordered pair of demands $\boldsymbol{q}$ and $\boldsymbol{q}'$, that is, $\boldsymbol{q}$ and $\boldsymbol{q}'$ satisfying neither $\boldsymbol{q} \leqslant \boldsymbol{q}'$ nor $\boldsymbol{q} \geqslant \boldsymbol{q}'$. In that case, we can move equal amounts of probability mass from the demand realizations $\boldsymbol{q}$ and $\boldsymbol{q}'$ to their join $\max\{\boldsymbol{q}, \boldsymbol{q}'\}$ and meet $\min\{\boldsymbol{q}, \boldsymbol{q}'\}$ without affecting the marginal distributions of $\mathbb{P}^\star$ and thus guaranteeing, by the rectangularity of $\mathcal{P}^w$, that the new distribution is also in $\mathcal{P}^w$. On the other hand, one can show that the new distribution has a weakly larger expected value since $f(\boldsymbol{x}^\top \max\{\boldsymbol{q}, \boldsymbol{q}'\}) + f(\boldsymbol{x}^\top \min\{\boldsymbol{q}, \boldsymbol{q}'\}) \geqslant f(\boldsymbol{x}^\top \boldsymbol{q}) + f(\boldsymbol{x}^\top \boldsymbol{q}')$. We can repeat this procedure iteratively until $\mathbb{P}^\star$ no longer places positive probability on any unordered pairs, in which case all probability is concentrated on at most $2n + 1$ demand realizations. Of course, this iterative mass transportation procedure is impractical as it may require exponentially many iterations depending on the initial distribution. Instead, Algorithm 2 in Appendix B computes a worst-case probability distribution over $\mathcal{P}^w$ in $\mathcal{O}(n)$ iterations. Applying the same principle to each ambiguity set $\mathcal{P}^w$, $w \in \mathcal{W}$, we obtain in $\mathcal{O}(Wn)$ iterations a $W(2n+1)$-point distribution $\mathbb{P}^\star$ that maximizes the expectation of $f(\boldsymbol{x}^\top \widetilde{\boldsymbol{q}})$ over all $\mathbb{P} \in \mathcal{P}$.

Theorem 3.15 implies that for suitable ambiguous risk measures ρ, the distributionally robust CVRP over the ambiguity set (3.6) with known scenario probabilities $\mathcal{S} = \{\widehat{\boldsymbol{s}}\}$ reduces to a stochastic CVRP over a probability distribution that does not depend on ρ or $\boldsymbol{x}$. Note, however, that the risk itself depends on the choice of ρ and $\boldsymbol{x}$, and hence the feasible region of the distributionally robust CVRP varies for different risk measures ρ.

In the remainder of this section, we review a number of popular risk measures, we show how their worst-case risk can be computed efficiently, and we discuss which of the demand estimators d^{S} and d^{P} can be employed in their associated reformulations 2VF(d).

Theorem 3.16 (Expected Disutility-Based Risk Measures) *Fix an ambiguity set $\mathcal{P}$ of the form* (3.6) *with $\mathcal{S} = \{\widehat{\boldsymbol{s}}\}$.*

1. Expected Disutility. *The worst-case expected disutility $\rho_{\mathrm{ED}} = \sup_{\mathbb{P}\in\mathcal{P}} \mathbb{P}\text{-ED}$ with*

$$\mathbb{P}\text{-ED}(\boldsymbol{x}^\top \widetilde{\boldsymbol{q}}) = \mathbb{E}_{\mathbb{P}}\left[U\left(\boldsymbol{x}^\top \widetilde{\boldsymbol{q}}\right)\right],$$

where the disutility function U is monotonically non-decreasing and convex with $U(0) \geqslant 0$, affords a $W(2n+1)$-point worst-case distribution that can be computed with Algorithm 2 and that is independent of U and $\boldsymbol{x}$. Moreover, ρ_{ED} is monotone, convex and not *subadditive.*

2. Essential Riskiness Index [ZBST18]. *The essential riskiness index ρ_{ERI} with*

$$\rho_{\mathrm{ERI}}(\boldsymbol{x}^\top \widetilde{\boldsymbol{q}}) = \min\left\{\alpha \geqslant 0 \;:\; \sup_{\mathbb{P}\in\mathcal{P}} \mathbb{E}_{\mathbb{P}}\left[\max\left\{\boldsymbol{x}^\top \widetilde{\boldsymbol{q}} - \overline{\rho},\; -\alpha\right\}\right] \leqslant 0\right\},$$

where $\boldsymbol{x}^\top \widetilde{\boldsymbol{q}} - \overline{\rho}$ represents the excess demand over the acceptable demand threshold $\overline{\rho}$, can be computed in time $\mathcal{O}(nW \log nW)$, with an initial computation of time $\mathcal{O}(n^2 W)$ for each 2VF(d) *instance. Moreover, ρ_{ERI} is monotone, convex and* not *subadditive.*

3. Expectiles. *The worst-case expectile risk measure ρ_{E} with*

$$\rho_{\mathrm{E}}\big(\boldsymbol{x}^\top \widetilde{\boldsymbol{q}}\big) \;=\; \arg\min_{u\in\mathbb{R}} \left\{\sup_{\mathbb{P}\in\mathcal{P}} \alpha \mathbb{E}_{\mathbb{P}}\left[\left(\left[\boldsymbol{x}^\top \widetilde{\boldsymbol{q}} - u\right]_+\right)^2\right] + (1-\alpha) \sup_{\mathbb{P}\in\mathcal{P}} \mathbb{E}_{\mathbb{P}}\left[\left(\left[\boldsymbol{x}^\top \widetilde{\boldsymbol{q}} - u\right]_-\right)^2\right]\right\},$$

where $[\cdot]_+ = \max\{\cdot, 0\}$, $[\cdot]_- = \max\{-\cdot, 0\}$ and $\alpha \in [1/2, 1)$, can be computed in time $\mathcal{O}(nW \log nW)$, with an initial computation of time $\mathcal{O}(n^2 W)$ for each 2VF(d) *instance.*

Moreover, ρ_{E} is monotone, convex and subadditive.

4. Entropic Risk. *The worst-case entropic risk $\rho_{\mathrm{ent}} = \sup_{\mathbb{P}\in\mathcal{P}} \mathbb{P}\text{-ent}$ with*

$$\mathbb{P}\text{-ent}\big(\boldsymbol{x}^\top\widetilde{\boldsymbol{q}}\big) \;=\; \frac{1}{\theta}\log\mathbb{E}_{\mathbb{P}}\left[\exp^{\theta\cdot\boldsymbol{x}^\top\widetilde{\boldsymbol{q}}}\right],$$

where $\theta > 0$, affords a $W(2n+1)$-point worst-case distribution that can be computed with Algorithm 2 and that is independent of ρ and $\boldsymbol{x}$. Moreover, ρ_{ent} is monotone, convex and not *subadditive.*

5. Requirements Violation Index [JQS16] *The requirements violation index ρ_{RV} with*

$$\rho_{\mathrm{RV}}(\boldsymbol{x}^\top\widetilde{\boldsymbol{q}}) = \inf\left\{\alpha \geqslant 0 \;:\; C_\alpha(\boldsymbol{x}^\top\widetilde{\boldsymbol{q}}) \leqslant \overline{\rho}\right\},$$

where C_α is the worst-case certainty equivalent under an exponential disutility,

$$C_\alpha(\boldsymbol{x}^\top\widetilde{\boldsymbol{q}}) = \begin{cases} \sup\limits_{\mathbb{P}\in\mathcal{P}} \;\alpha\log\mathbb{E}_{\mathbb{P}}\left[\exp\left(\dfrac{\boldsymbol{x}^\top\widetilde{\boldsymbol{q}}}{\alpha}\right)\right] & \text{if } \alpha > 0 \\ \lim\limits_{\gamma\to 0} C_\gamma(\boldsymbol{x}^\top\widetilde{\boldsymbol{q}}) & \text{if } \alpha = 0, \end{cases}$$

and $\overline{\rho}$ is the acceptable demand threshold, can be computed using bisection search, with an initial computation of time $\mathcal{O}(n^2W)$ for each $2\mathrm{VF}(d)$ instance. Moreover, ρ_{RV} is monotone, convex and not *subadditive.*

Proof of Theorem 3.16. The proof follows from Lemmas 3.29- 3.33 in the appendix of this chapter. ∎

For the requirement violation index, it is not easy to upper bound α, therefore we cannot give a priori estimate of the complexity of computing ρ_{RV}.

Since the worst-case expectiles are subadditive as well as positive homogeneous [BB15, Theorem 4.9(b)], Theorem 3.13 *(i)* implies that both demand estimators d^{S} and d^{P} can be applied and yield the same results. We thus prefer d^{S} for its ease of computation. In contrast, the other risk measures of Theorem 3.16 fail to be subadditive, and Theorem 3.13 *(iii)* implies that we have to use the demand estimator d^{P}. Fortunately, since all of these risk measures are convex, d^{P} can be computed efficiently thanks to Proposition 3.12.

Two commonly used risk measures are variants of the worst-case expected disutility. The worst-case *expected demand* $\sup_{\mathbb{P}\in\mathcal{P}} \mathbb{E}_{\mathbb{P}}[\cdot]$ emerges as a special case of the worst-case expected disutility if we set $U(x) = x$. Following from the worst-case distribution $\mathbb{P}^\star$ identified via Theorem 3.15, we notice that $\sup_{\mathbb{P}\in\mathcal{P}} \mathbb{E}_{\mathbb{P}}[\cdot]$ is additive. Hence, Theorem 3.13 *(ii)* implies that the corresponding worst-case distributionally robust CVRP instance reduces to a deterministic CVRP. The worst-case *expected ramp disutility* $\sup_{\mathbb{P}\in\mathcal{P}} \mathbb{E}_{\mathbb{P}}[\max\{\cdot, \tau\}]$, where $\tau \in \mathbb{R}_+$, is monotone and subadditive but not positive homogeneous. According to Theorem 3.13 *(i)*, we thus prefer the packing demand estimator d^{P} as it can offer tighter bounds than d^{S}.

Theorem 3.17 (CVaR-Based Risk Measures) *Fix an ambiguity set $\mathcal{P}$ of the form* (3.6) *with $\mathcal{S} = \{\widehat{\boldsymbol{s}}\}$.*

1. Conditional Value-at-Risk. *The worst-case conditional value-at-risk at level $1-\epsilon$, $\rho_{\mathrm{CVaR}} = \sup_{\mathbb{P}\in\mathcal{P}} \mathbb{P}\text{-CVaR}_{1-\epsilon}$ with*

$$\mathbb{P}\text{-CVaR}_{1-\epsilon}(\boldsymbol{x}^\top \widetilde{\boldsymbol{q}}) = \inf_{u\in\mathbb{R}} \; u + \frac{1}{1-\epsilon}\mathbb{E}_{\mathbb{P}}\left[\boldsymbol{x}^\top \widetilde{\boldsymbol{q}} - u\right]_+ ,$$

where $\epsilon \in [0, 1)$, can be computed in time $\mathcal{O}(nW \log(nW))$, with an initial computation of time $\mathcal{O}(n^2 W)$ per $2\mathrm{VF}(d)$ *instance. Moreover, ρ_{CVaR} is monotone, convex and subadditive.*

2. Service Fulfillment Risk Index [ZZLS21]. *The service fulfillment risk index ρ_{SRI} with*

$$\rho_{\mathrm{SRI}}\left(\boldsymbol{x}^\top \widetilde{\boldsymbol{q}}\right) = \inf\left\{\alpha \geqslant 0 \;:\; \rho_{\text{-CVaR}_\gamma}\left(\max\left\{\boldsymbol{x}^\top \widetilde{\boldsymbol{q}} - \overline{\rho}, \, -\alpha\right\}\right) \leqslant 0\right\}$$

where $\boldsymbol{x}^\top \widetilde{\boldsymbol{q}} - \overline{\rho}$ represents the excess demand over the acceptable demand threshold $\overline{\rho}$, can be computed to δ-accuracy in time $\mathcal{O}\left(nW \log\left(\left(\overline{\rho} - \sum_{w\in\mathcal{W}} \hat{s}_w \sum_{j=1}^{2n+1} p^\star_{wj} \sum_{i\in V_C} x_i q^\star_{wji}\right)/\delta\gamma\right)\right)$, with an initial computation of time $\mathcal{O}(n^2 W)$ per $2\mathrm{VF}(d)$ *instance. Moreover, ρ_{SRI} is monotone, convex but not subadditive.*

Proof of Theorem 3.17. The proof follows from Lemmas 3.34- 3.35 in the appendix of this chapter. ∎

Since the worst-case conditional value-at-risk is subadditive and positive homogeneous [RU02, Corollary 12], Theorem 3.13 *(i)* implies that we can use either d^{P} or d^{S}, and both demand estimators yield the same results. We thus prefer d^{S} because it is easier to evaluate than d^{P}. In contrast, the service fulfilment risk index is not subadditive, and Theorem 3.13 *(iii)* implies that we have to use d^{P}. Fortunately, d^{P} can be evaluated efficiently since the service fulfilment risk index is convex.

Theorem 3.18 (Other Risk Measures) *Fix an ambiguity set $\mathcal{P}$ of the form (3.6) with $\mathcal{S} = \{\widehat{\boldsymbol{s}}\}$.*

1. Mean Semi-Deviation. *The worst-case mean semi-deviation $\rho_{\mathrm{MSD}} = \sup_{\mathbb{P}\in\mathcal{P}} \mathbb{P}\text{-MSD}$ of order u with*

$$\mathbb{P}\text{-MSD}(\boldsymbol{x}^\top \widetilde{\boldsymbol{q}}) \;=\; \mathbb{E}_{\mathbb{P}}\left[\boldsymbol{x}^\top \widetilde{\boldsymbol{q}}\right] + \alpha\left(\mathbb{E}_{\mathbb{P}}\left[\boldsymbol{x}^\top \widetilde{\boldsymbol{q}} - \mathbb{E}_{\mathbb{P}}\left[\boldsymbol{x}^\top \widetilde{\boldsymbol{q}}\right]\right]_+^u\right)^{\frac{1}{u}}, \quad \text{where } u \geqslant 1 \text{ and } \alpha \in [0,1],$$

   affords a $W(2n+1)$-point worst-case distribution that can be computed with Algorithm 2 and that is independent of α, u and $\boldsymbol{x}$. Moreover, ρ_{MSD} is monotone, convex and subadditive.

2. Underperformance Risk Index [HLQS15]. *The underperformance risk index ρ_{URI} with*

$$\rho_{\mathrm{URI}}(\boldsymbol{x}^\top \widetilde{\boldsymbol{q}}) = \inf\left\{\frac{1}{\alpha} \;:\; \sup_{\mathbb{P}\in\mathcal{P}} \psi_{\mathbb{P}}\left(\alpha\left(\boldsymbol{x}^\top \widetilde{\boldsymbol{q}} - \overline{\rho}\right)\right) \leqslant 0, \;\; \alpha > 0\right\},$$

   where $\psi_{\mathbb{P}}$ is a monotone, translation invariant, convex risk measure satisfying $\psi_{\mathbb{P}}(0) = 0$, that can be expressed as the expectation of a convex function and $\overline{\rho}$ is the acceptable demand threshold, can be evaluated using bisection search, with an initial computation of time $\mathcal{O}(n^2 W)$ per $2\mathrm{VF}(d)$ instance. Moreover, ρ_{URI} is monotone, convex and subadditive.

Proof of Theorem 3.18. The proof follows from Lemmas 3.36- 3.37 in the appendix of this chapter. ∎

It is not straightforward to upper bound α given the general form of the underperformance risk index, therefore we cannot give an a priori estimate of the complexity of computing ρ_{URI}.

Since both risk measures in Theorem 3.18 are subadditive and positive homogeneous (*cf.* [SDR14, Example 6.20] and [HLQS15, Definition 3]), Theorem 3.13 *(i)* implies that d^{S} and d^{P} are both applicable and yield the same results. We thus prefer the summation demand estimator d^{S} for its ease of computation.

We next discuss how the above results simplify when the expectation and mean absolute deviation conditions in the ambiguity set (3.6) are absent.

Observation 3.19 *Fix an ambiguity set of the form* (3.6) *with* $\mathcal{S} = \{\widehat{\boldsymbol{s}}\}$*, where the expectation and mean absolute deviation constraints are absent. Consider* $\varphi(\cdot)$ *that can be expressed as a worst-case expectation* $\sup_{\mathbb{P}\in\mathcal{P}} \mathbb{E}_{\mathbb{P}}[f(\cdot^\top \widetilde{\boldsymbol{q}})]$ *of convex monotonically non-decreasing function* $f : \mathbb{R} \mapsto \mathbb{R}$*. Then* $\varphi(\cdot)$ *is maximized over* $\mathcal{P}$ *by the* W*-point distribution* $\mathbb{P}^\star = \sum_{w\in\mathcal{W}} \hat{s}_w \cdot \delta_{\overline{\boldsymbol{q}}^w}$ *that is independent of* f *and* $\boldsymbol{x}$*.*

Proof of Observation 3.19. Fix $\boldsymbol{x} \in [0,1]^n$ and an ambiguity set $\mathcal{P}$ of the form (3.6) with $\mathcal{S} = \{\widehat{\boldsymbol{s}}\}$, and expectation and mean absolute deviation constraints absent. We have

$$\begin{aligned}\sup_{\mathbb{P}\in\mathcal{P}} \mathbb{E}_{\mathbb{P}}\left[f(\boldsymbol{x}^\top \widetilde{\boldsymbol{q}})\right] &= \max_{\boldsymbol{s}\in\mathcal{S}} \sup_{\mathbb{P}_w\in\mathcal{P}^w : w\in\mathcal{W}} \sum_{w\in\mathcal{W}} \hat{s}_w \mathbb{E}_{\mathbb{P}_w}\left[f(\boldsymbol{x}^\top \widetilde{\boldsymbol{q}})\right] \\ &= \sum_{w\in\mathcal{W}} \hat{s}_w \sup_{\mathbb{P}_w\in\mathcal{P}^w} \mathbb{E}_{\mathbb{P}_w}\left[f(\boldsymbol{x}^\top \widetilde{\boldsymbol{q}})\right]\end{aligned}$$

where $\mathcal{P}^w = \left\{\mathbb{P} : \mathbb{P}\left(\underline{\boldsymbol{q}}^w \leqslant \boldsymbol{q} \leqslant \underline{\boldsymbol{q}}^w\right) = 1,\ \mathbb{P} \in \mathcal{P}(\mathcal{Q}^w)\right\}$. From our assumption that $f(\cdot)$ is monotonically non-decreasing, $\mathbb{E}_{\mathbb{P}_w}\left[f(\boldsymbol{x}^\top \widetilde{\boldsymbol{q}})\right]$ is maximized at $\max\{\boldsymbol{q} : \boldsymbol{q} \in \mathcal{Q}^w\} = \overline{\boldsymbol{q}}^w$ for each scenario $w \in \mathcal{W}$. Therefore, we have

$$\sup_{\mathbb{P}\in\mathcal{P}} \mathbb{E}_{\mathbb{P}}\left[f(\boldsymbol{x}^\top \widetilde{\boldsymbol{q}})\right] = \sum_{w\in\mathcal{W}} \hat{s}_w \sup_{\mathbb{P}_w\in\mathcal{P}^w} \mathbb{E}_{\mathbb{P}_w}\left[f(\boldsymbol{x}^\top \widetilde{\boldsymbol{q}})\right] = \sum_{w\in\mathcal{W}} \hat{s}_w \mathbb{E}_{\mathbb{P}_w}\left[f(\boldsymbol{x}^\top \overline{\boldsymbol{q}}^w)\right]$$

where $\mathbb{P}^\star_w = \delta_{\overline{\boldsymbol{q}}^w}$ for each $w \in \mathcal{W}$, and the statement of the observation follows. ∎

Observation 3.19 allows us to consider worst-case risk measures over ∞-type Wasserstein ambiguity sets (*cf.* Example 3.14), which are now readily verified to be maximized by the worst-case distribution $\mathbb{P}^\star = 1/W \cdot \sum_{w\in\mathcal{W}} \delta_{\widehat{\boldsymbol{q}}^w+\theta\mathbf{e}}$ that does not depend on the risk measure ρ or the current solution $\boldsymbol{x}$. Moreover, for an ambiguity set $\mathcal{P}$ as described in Observation 3.19, the worst-case distribution can be identified in time $\mathcal{O}(W)$, as opposed to $\mathcal{O}(n^2W)$ as identified through Theorem 3.15.

Remark 3.20 (Incremental Evaluation of Risk Measures) *In branch-and-cut implementations, the worst-case risk $\varphi(\boldsymbol{x})$ rarely needs to be computed from scratch; instead, it is computed iteratively for vectors $\boldsymbol{x}$ that differ in one or very few components. In this case, incremental evaluations of the worst-case risks in Theorems 3.16–3.18 can reduce the runtime for the cut evaluation by a factor of n.*

In the following section, we consider the value-at-risk and explain why the discussion so far cannot be used for this risk measure. Finally, we suggest a special scheme to handle value-at-risk.

3.5.1 Special Case: Value-at-Risk

In this section, we consider the ambiguous chance constrained CVRP with technology sets

$$\mathcal{C}_{\text{CC}} = \left\{ \boldsymbol{R} = (R_1, \ldots, R_\nu) \;:\; \nu \geqslant 1 \text{ and } R_i \in V_C \;\; \forall i, \;\; \mathbb{P}\left[\sum_{i\in\boldsymbol{R}} \widetilde{q}_i \leqslant B\right] \geqslant 1-\epsilon \;\; \forall \mathbb{P}\in\mathcal{P} \right\}, \quad (3.8)$$

where the ambiguity set $\mathcal{P}$ is of the form (3.6) and $\epsilon \in [0,1]$ is a risk threshold selected by the decision maker. In the following, we assume that $\epsilon < 1/m$.

Observation 3.21 *For any $S \subseteq V_C$, we have*

$$\mathbb{P}\left[\sum_{i \in \boldsymbol{R}} \tilde{q}_i \leqslant B\right] \geqslant 1-\epsilon \;\; \forall \mathbb{P} \in \mathcal{P} \quad \Longleftrightarrow \quad \varphi_{\mathrm{VaR}}(\mathbf{1}_{\boldsymbol{R}}) \leqslant B,$$

where $\varphi_{\mathrm{VaR}}(\boldsymbol{x}) = \sup_{\mathbb{P} \in \mathcal{P}} \mathbb{P}\text{-VaR}_{1-\epsilon}\left[\boldsymbol{x}^\top \tilde{\boldsymbol{q}}\right]$ and $\mathbb{P}\text{-VaR}_{1-\epsilon}$ denotes the $(1-\epsilon)$-value-at-risk.

Proof of Observation 3.21. We need to show that $\mathbb{P}\left[\sum_{i \in \boldsymbol{R}} \tilde{q}_i \leqslant B\right] \geqslant 1-\epsilon \;\; \forall \mathbb{P} \in \mathcal{P} \iff \varphi_{\mathrm{VaR}}(\mathbf{1}_{\boldsymbol{R}}) \leqslant B$ where $\varphi_{\mathrm{VaR}}(\boldsymbol{x}) = \sup_{\mathbb{P} \in \mathcal{P}} \mathbb{P}\text{-VaR}_{1-\epsilon}\left[\boldsymbol{x}^\top \tilde{\boldsymbol{q}}\right]$ and $\mathbb{P}\text{-VaR}_{1-\epsilon}$ denotes the $(1-\epsilon)$-value-at-risk. We notice the following:

$$\begin{aligned}
\inf\{u \in \mathbb{R} : \mathbb{P}\left[\textstyle\sum_{i \in \boldsymbol{R}} \tilde{q}_i \leqslant u\right] \geqslant 1-\epsilon\} \leqslant B \;\; \forall \mathbb{P} \in \mathcal{P} &\iff \mathbb{P}\text{-VaR}_{1-\epsilon}\left[\textstyle\sum_{i \in \boldsymbol{R}} \tilde{q}_i\right] \leqslant B \;\; \forall \mathbb{P} \in \mathcal{P} \\
&\iff \sup_{\mathbb{P} \in \mathcal{P}} \mathbb{P}\text{-VaR}_{1-\epsilon}\left[\textstyle\sum_{i \in \boldsymbol{R}} \tilde{q}_i\right] \leqslant B \\
&\iff \varphi_{\mathrm{VaR}}(\mathbf{1}_{\boldsymbol{R}}) \leqslant B.
\end{aligned}$$

The statement of the observation then follows. ∎

Observation 3.21, whose statement is well known and immediately follows from the properties of the value-at-risk, allows us to use technology sets of the form (3.5) with $\varphi = \varphi_{\mathrm{VaR}}$ to model the ambiguous chance constrained CVRP. In order to solve the corresponding 2VF(d) formulation, φ_{VaR} has to satisfy certain properties as outlined in Section 3.4.2. We examine this next.

Proposition 3.22 *For an ambiguity set of the form* (3.6)*, φ_{VaR} is monotone and positive homogeneous, but it is neither subadditive nor convex.*

Proof of Proposition 3.22. Note that $\mathbb{P}$-VaR is monotone and positive homogeneous for all $\mathbb{P} \in \mathcal{P}$ [FS10, p. 3]. Consequently, for $\boldsymbol{x} \in [0,1]^n$, $\varphi_{\mathrm{VaR}}(\boldsymbol{x}) = \sup_{\mathbb{P} \in \mathcal{P}} \mathbb{P}\mathrm{VaR}_{1-\epsilon}(\boldsymbol{x}^\top \tilde{\boldsymbol{q}})$ is monotone and positive homogeneous by Lemma 3.28. Next, we prove that φ_{VaR} is neither convex nor subadditive. To this end, consider the ambiguity set $\mathcal{P}$ with $\mathcal{S} = \{\widehat{\boldsymbol{s}}\}$, $\underline{\boldsymbol{q}}^w = \overline{\boldsymbol{q}}^w = \widehat{\boldsymbol{q}}^w$ for each $w \in \mathcal{W}$, and the expectation and mean absolute deviation constraints disregarded. For $\boldsymbol{x} \in [0,1]^n$ and this choice of ambiguity set, $\varphi(\boldsymbol{x})$ reduces to $\mathbb{P}\text{-VaR}_{1-\epsilon}(\boldsymbol{x}^\top \widetilde{\boldsymbol{q}})$ for the distribution $\mathbb{P}$ under which the demands attain the values $\widehat{\boldsymbol{q}}$ with probability s_w for each $w \in \mathcal{W}$.

Thus, $\varphi(\boldsymbol{x})$ in this case involves finding the value-at-risk over the discrete scenario probability distribution $\widehat{\boldsymbol{s}}$. We know that the $\mathbb{P}$-VaR for a single distribution is neither convex nor subadditive [FS10, p. 3]. Therefore, $\varphi(\boldsymbol{x})$ is neither convex nor subadditive. ∎

Following from the discussion surrounding Theorem 3.13, we conclude that we cannot use the demand estimator d^{S} in conjunction with φ_{VaR}, and the demand estimator d^{P} is difficult to evaluate.

Example 3.23 *Consider an ambiguous chance constrained CVRP instance with $n = 2$ customers and $m = 2$ vehicles. Fix an ambiguity set of the form (3.6) with $W = 3$, $\boldsymbol{s} = 0.3\mathbf{e}$, expectation and mean absolute deviation constraints disregarded, and $\overline{\boldsymbol{q}}^w = \underline{\boldsymbol{q}}^w = \widehat{\boldsymbol{q}}^w$ for each $w \in \mathcal{W}$. Further, let $\widehat{\boldsymbol{q}}^1 = (1,3)^\top$, $\widehat{\boldsymbol{q}}^2 = (8,3)^\top$ and $\widehat{\boldsymbol{q}}^3 = (1,11)^\top$. Setting $\epsilon = 0.3$ and $B = 3$, we have $\mathcal{C}_{\mathrm{CC}} = \{(1),(2)\}$, which implies that $\overline{d}^m(V_C) = 2$. On the other hand, the technology sets (3.5) with $\varphi = \varphi_{\mathrm{VaR}}$ yield $d^S(V_C) = \max\{1, \lceil 11/3 \rceil\} = 4 > \overline{d}^m(V_C)$, and Theorem 3.5 implies that this demand estimator cannot be used. To evaluate d^P under these technology sets, we need to solve a non-convex optimization problem. However, note that $\boldsymbol{Y}$ with $\boldsymbol{y}_1 = (1,0)^\top$ and $\boldsymbol{y}_2 = (0,1)^\top$ is a feasible solution for d^P, which implies that $d^P(V_C) \leqslant 2 = \overline{d}^m(V_C)$.*

In our previous chapter, we use the demand estimator d^{S} to solve the ambiguous chance constrained CVRP over moment ambiguity sets. This is possible since for their class of moment ambiguity sets, φ_{VaR} is monotone, positive homogeneous, convex and subadditive. In contrast, our scenario-wise ambiguity sets (3.6) require a different approach, which we develop in the remaining of this section.

To this end, following [DFL18], we define $\varphi_{\text{mVaR}} : [0,1]^n \to \mathbb{R}$ as

$$\varphi_{\text{mVaR}}(\boldsymbol{x}) = B \cdot \max_{k \in K} \; a(\boldsymbol{x}, k)$$

where $a(\boldsymbol{x}, 1) = 1$ and $a(\boldsymbol{x}, k) = \min\{k, \lceil \sup_{\mathbb{P} \in \mathcal{P}} \mathbb{P}\text{-VaR}_{1-(k-1)\epsilon}(\boldsymbol{x}^\top \widetilde{\boldsymbol{q}})/B \rceil\}$ otherwise, as well as

$$\mathcal{C}_{\text{mVaR}} = \{\boldsymbol{R} = (R_1, \ldots, R_\nu) \; : \; \nu \geqslant 1 \text{ and } R_i \in V_C \;\; \forall i, \;\; \varphi_{\text{mVaR}}(\boldsymbol{x}) \leqslant B\}\,.$$

Proposition 3.24 *We have* $\mathcal{C}_{\text{mVaR}} = \mathcal{C}_{\text{CC}}$.

Proof of Proposition 3.24. To prove the statement of the proposition, we need to show that $\boldsymbol{R} \in \mathcal{C}_{\text{CC}} \iff \boldsymbol{R} \in \mathcal{C}_{\text{mVaR}}$. We observe that $\boldsymbol{R} \in \mathcal{C}_{\text{mVaR}} \iff \varphi_{\text{mVaR}}(\mathbf{1}_{\boldsymbol{R}}) = B$. While "$\Longleftarrow$" is trivial, the "$\Longrightarrow$" holds because $a(\boldsymbol{x}, 1) = 1$ ensures that $\varphi_{\text{mVaR}}(\mathbf{1}_{\boldsymbol{R}}) \neq 0$. We notice the following:

$$\begin{aligned}
\boldsymbol{R} \in \mathcal{C}_{\text{CC}} \quad & \iff \sup\nolimits_{\mathbb{P} \in \mathcal{P}} \mathbb{P}\text{-VaR}_{1-\epsilon}(\mathbf{1}_{\boldsymbol{R}}^\top \widetilde{\boldsymbol{q}}) \leqslant B \\
& \iff \lceil \sup\nolimits_{\mathbb{P} \in \mathcal{P}} \mathbb{P}\text{-VaR}_{1-\epsilon}(\mathbf{1}_{\boldsymbol{R}}^\top \widetilde{\boldsymbol{q}})/B \rceil \leqslant 1 \\
& \iff \lceil \sup\nolimits_{\mathbb{P} \in \mathcal{P}} \mathbb{P}\text{-VaR}_{1-(k-1)\epsilon}(\mathbf{1}_{\boldsymbol{R}}^\top \widetilde{\boldsymbol{q}})/B \rceil \leqslant 1 \text{ for } k = 2 \\
& \iff \lceil \sup\nolimits_{\mathbb{P} \in \mathcal{P}} \mathbb{P}\text{-VaR}_{1-(k-1)\epsilon}(\mathbf{1}_{\boldsymbol{R}}^\top \widetilde{\boldsymbol{q}})/B \rceil \leqslant 1 \;\; \forall k \in K : k \geqslant 2 \\
& \iff \min\{k, \lceil \sup\nolimits_{\mathbb{P} \in \mathcal{P}} \mathbb{P}\text{-VaR}_{1-(k-1)\epsilon}(\mathbf{1}_{\boldsymbol{R}}^\top \widetilde{\boldsymbol{q}})/B \rceil\} \leqslant 1 \;\; \forall k \in K : k \geqslant 2 \\
& \iff \max\nolimits_{k=2,\ldots,m} a(\mathbf{1}_{\boldsymbol{R}}, k) \leqslant 1 \iff \max\nolimits_{k \in K} a(\mathbf{1}_{\boldsymbol{R}}, k) = 1 \\
& \iff \varphi_{\text{mVaR}}(\mathbf{1}_{\boldsymbol{R}}) = B \iff \boldsymbol{R} \in \mathcal{C}_{\text{mVaR}}
\end{aligned}$$

The fourth equivalence holds because $\sup_{\mathbb{P} \in \mathcal{P}} \mathbb{P}\text{-VaR}_{1-(k-1)\epsilon}(\mathbf{1}_{\boldsymbol{R}}^\top \widetilde{\boldsymbol{q}})$ is non-increasing in k. The seventh equivalence follows from the fact that $a(\mathbf{1}_{\boldsymbol{R}}, 1) = 1$ by definition. The final equivalence follows from our observation at the beginning of this proof. ∎

While [DFL18] show that φ_{mVaR} is a valid lower bound for the minimum vehicle requirements in their edge-based formulation. They relax the edge-based formulation in order to use the branch-cut-price algorithm. They show that a route that is feasible in the chance constrained problem is feasible in their relaxed formulation. We make this tighter in Proposition 3.24 by showing that the set of feasible routes under chance constraints ($\mathcal{C}_{\text{CC}}$) is exactly the same as the set of feasible routes under φ_{mVaR}. Moreover, in contrast to φ_{VaR}, φ_{mVaR} has desirable features in view of our demand estimators.

Proposition 3.25 *The function φ_{mVaR} is monotone and subadditive, but it is neither convex nor positive homogeneous.*

Proof of Proposition 3.25. The monotonicity and subadditivity of φ_{mVaR} follow from Lemmas 3.41 and 3.42, respectively that we prove in the appendix of this chapter. It is straightforward to see that φ_{mVaR} does not satisfy positive homogeneity. This is because for any $\lambda \in \mathbb{R}_+$, we have $\varphi_{\text{mVaR}}(\lambda \boldsymbol{x})/B \in \mathbb{Z}_+$ whereas $\lambda \varphi_{\text{mVaR}}(\boldsymbol{x})/B \in \mathbb{R}_+$ where $\boldsymbol{x} \in [0,1]^n$.

In order to prove the non-convexity of φ_{mVaR}, consider an ambiguous chance constrained CVRP instance with $n = 3$ customers, $m = 3$ vehicles, $\epsilon = 0.1$ and $B = 20.6$. Consider an ambiguity set of the form (3.6) with $W = 1$, $\underline{\boldsymbol{q}}^1 = (1,5,1)^\top$, $\overline{\boldsymbol{q}}^1 = (30,20,30)^2$, $\boldsymbol{\mu}^1 = (16,10,16)^\top$ and $\boldsymbol{\nu}^1 = (2,0.5,2)^\top$. Fixing $\boldsymbol{y}_1 = (1,0,1)^\top$, $\boldsymbol{y}_2 = (0,1,0)^\top$ and $\lambda = 0.67$, we have $\varphi_{\text{mVaR}}(\boldsymbol{y}_1) = 2B, \varphi_{\text{mVaR}}(\boldsymbol{y}_2) = 1B, \varphi_{\text{mVaR}}(\lambda \boldsymbol{y}_1 + (1-\lambda)\boldsymbol{y}_2) = 2B$. Clearly, $\varphi_{\text{mVaR}}(\lambda \boldsymbol{y}_1 + (1-\lambda)\boldsymbol{y}_2) > \lambda \varphi_{\text{mVaR}}(\boldsymbol{y}_1) + (1-\lambda)\varphi_{\text{mVaR}}(\boldsymbol{y}_2) = (5/3)B$. ∎

The monotonicity of φ_{mVaR} guarantees via Proposition 3.10 that the technology sets (3.5) with $\varphi = \varphi_{\text{mVaR}}$ satisfy **(D)** and **(P)**. Since φ_{mVaR} is subadditive but not positive homogeneous, Theorem 3.13 implies that $d^{\text{S}} \leqslant d^{\text{P}}$ and that $d^{\text{S}} = d^{\text{P}}$ does not hold in general. However, d^{P} is hard to evaluate due to the non-convexity of φ_{mVaR}, and we thus prefer to use d^{S}.

Example 3.26 *Consider the ambiguous chance constrained CVRP of Example 3.23. We have $a(\mathbf{1}_{V_C}, 1) = 1$ by definition and $a(\mathbf{1}_{V_C}, 2) = \min\{2,4\} = 2$, implying that $\varphi_{\text{mVaR}}(\mathbf{1}_{V_C}) = 2B = 6$ and thus $d^S(\mathbf{1}_{V_C}) = 2 = \overline{d}^m$.*

In the remainder of this section, we derive an efficient reformulation to evaluate φ_{mVaR}.

Theorem 3.27 *For an ambiguity set of the form* (3.6) *with* $\mathcal{S} = \{\widehat{\boldsymbol{s}}\}$, $\varphi_{\mathrm{mVaR}}(\boldsymbol{x})$ *can be evaluated in time* $\mathcal{O}(nWm\log m\log(1/\delta - 1)\log((\overline{u} - \underline{u})/\delta))$. *Here*

$$\overline{u} = \max_{w\in\mathcal{W}} \sum_{i\in V_C} x_i \left(\mu_i^w + \min\left\{\overline{q}_i^w - \mu_i^w,\ \left(\frac{1-\delta}{\delta}\right)(\mu_i^w - \underline{q}_i^w),\ \frac{\nu_i^w}{2\delta}\right\}\right)$$

and

$$\underline{u} = \min_{w\in\mathcal{W}} \sum_{i\in V_C} x_i \left(\mu_i^w + \min\left\{\overline{q}_i^w - \mu_i^w,\ \frac{\nu_i^w}{2}\right\}\right).$$

Proof of Theorem 3.27. Fix an ambiguity set of the form (3.6) with $\mathcal{S} = \{\widehat{\boldsymbol{s}}\}$ and $\boldsymbol{x} \in [0,1]^n$. By definition we have $\varphi_{\mathrm{mVaR}}(\boldsymbol{x}) = B\max_{k\in K} a(\boldsymbol{x}, k)$ where $a(\boldsymbol{x}, k) = \min\{k, Z_k\}$, and $Z_k = \sup_{\mathbb{P}\in\mathcal{P}} \mathbb{P}\text{-VaR}_{1-(k-1)\epsilon}(\boldsymbol{x}^\top\widetilde{\boldsymbol{q}})$. We first find Z_k for a fixed $k \in K$. For $\boldsymbol{x} \in [0,1]^n$, we have

$$\begin{aligned}
\sup_{\mathbb{P}\in\mathcal{P}} \mathbb{P}\text{-VaR}_{1-(k-1)\epsilon}(\boldsymbol{x}^\top\widetilde{\boldsymbol{q}}) &= \inf_{u\in\mathbb{R}} \left\{u \ :\ \inf_{\mathbb{P}\in\mathcal{P}} \mathbb{P}(\boldsymbol{x}^\top\widetilde{\boldsymbol{q}} \leqslant u) \geqslant 1-(k-1)\epsilon\right\} \\
&= \inf_{u\in\mathbb{R}} \left\{u \ :\ \min_{\boldsymbol{s}\in\mathcal{S}} \inf_{\mathbb{P}_w\in\mathcal{P}^w : w\in\mathcal{W}} \sum_{w\in\mathcal{W}} s_w \mathbb{P}_w(\boldsymbol{x}^\top\widetilde{\boldsymbol{q}} \leqslant u) \geqslant 1-(k-1)\epsilon\right\} \\
&= \inf_{u\in\mathbb{R}} \left\{u \ :\ \min_{\boldsymbol{s}\in\mathcal{S}} \sum_{w\in\mathcal{W}} s_w \inf_{\mathbb{P}_w\in\mathcal{P}^w} \mathbb{P}_w(\boldsymbol{x}^\top\widetilde{\boldsymbol{q}} \leqslant u) \geqslant 1-(k-1)\epsilon\right\} \\
&= \inf_{u\in\mathbb{R}} \left\{u \ :\ \sum_{w\in\mathcal{W}} \hat{s}_w \inf_{\mathbb{P}_w\in\mathcal{P}^w} \mathbb{P}_w(\boldsymbol{x}^\top\widetilde{\boldsymbol{q}} \leqslant u) \geqslant 1-(k-1)\epsilon\right\}
\end{aligned}$$

The second identity follows from the rectangularity of $\mathcal{P}$ and the law of total probability. The fourth identity holds because $\mathcal{S} = \{\widehat{\boldsymbol{s}}\}$ by assumption. For a fixed $u \in \mathbb{R}$, the satisfaction of the inequality

$$\sum_{w\in\mathcal{W}} \hat{s}_w \inf_{\mathbb{P}_w\in\mathcal{P}^w} \mathbb{P}_w(\boldsymbol{x}^\top\widetilde{\boldsymbol{q}} \leqslant u) \geqslant 1-(k-1)\epsilon$$

can be verified easily if we can compute the expressions

$$\inf_{\mathbb{P}_w\in\mathcal{P}^w} \mathbb{P}_w(\boldsymbol{x}^\top\widetilde{\boldsymbol{q}} \leqslant u), \quad w \in \mathcal{W}.$$

Note that for any $w \in \mathcal{W}$, Proposition 2.13 in the previous chapter implies that

$$\begin{aligned}\inf_{\mathbb{P}_w \in \mathcal{P}^w} \mathbb{P}_w(\boldsymbol{x}^\top \widetilde{\boldsymbol{q}} \leqslant u) &= \sup_{\theta_w \in [0,1]} \left\{ 1 - \theta_w \ : \ \sup_{\mathbb{P}_w \in \mathcal{P}^w} \mathbb{P}_w\text{-VaR}_{1-\theta_w}(\boldsymbol{x}^\top \widetilde{\boldsymbol{q}}) \leqslant u \right\} \\ &= \sup_{\theta_w \in [0,1]} \left\{ 1 - \theta_w \ : \ \sum_{i \in V_C} x_i \left(\mu_i^w + \min\left\{ \overline{q}_i^w - \mu_i^w,\ \left(\frac{1-\theta_w}{\theta_w}\right)(\mu_i^w - \underline{q}_i^w),\ \frac{\nu_i^w}{2\theta_w} \right\} \right) \leqslant u \right\},\end{aligned}$$

and the last supremum can be evaluated via a bisection over $\theta_w \in [0,1]$. Combining this bisection with a bisection over $u \in \mathbb{R}$ yields the desired result. We now find lower and upper bounds for u. Notice that the function $\sum_{i \in V_C} x_i \left(\mu_i^w + \min\left\{ \overline{q}_i^w - \mu_i^w,\ \left(\frac{1-\theta_w}{\theta_w}\right)(\mu_i^w - \underline{q}_i^w),\ \frac{\nu_i^w}{2\theta_w} \right\} \right)$ is non-increasing in θ_w. As a result, this function attains the maximum value when $\theta_w = \delta$ for each $w \in \mathcal{W}$ where $\delta \to 0$, and it attains the minimum value when $\theta_w = 1$ for each $w \in \mathcal{W}$. Accordingly, a lower bound for u is given by $\underline{u} = \min_{w \in \mathcal{W}} \sum_{i \in V_C} x_i \left(\mu_i^w + \min\left\{ \overline{q}_i^w - \mu_i^w,\ \frac{\nu_i^w}{2} \right\} \right)$ and an upper bound for u is given by $\overline{u} = \max_{w \in \mathcal{W}} \sum_{i \in V_C} x_i \left(\mu_i^w + \min\left\{ \overline{q}_i^w - \mu_i^w,\ \left(\frac{1-\delta}{\delta}\right)(\mu_i^w - \underline{q}_i^w),\ \frac{\nu_i^w}{2\delta} \right\} \right)$. The bisection search for the optimal u for a fixed k thus takes time $\mathcal{O}(\log(1/\delta - 1)\log((\overline{u} - \underline{u})/\delta))$.

We have $Z_k = \lceil u/B \rceil$ for $k \in K$. Let $k^\star := \min \arg\max a(\boldsymbol{x}, k)$ where $a(\boldsymbol{x}, k) = \min\{k, Z_k\}$. We claim that for all $k \in K$: *(i)* if $k > Z_k$, then $k > k^\star$, and *(ii)* if $k \leqslant Z_k$, then $k \leqslant k^\star$. If we can prove our claim, we can conduct a binary search over K to find $k^\star$. Based on our earlier discussion, $a(\boldsymbol{x}, k)$ at each iteration of the binary search can be evaluated in time $\mathcal{O}(\log(1/\delta - 1)\log((\overline{u} - \underline{u})/\delta))$, and thus the overall algorithm terminates in time $\mathcal{O}(nWm\log m \log(1/\delta - 1)\log((\overline{u} - \underline{u})/\delta))$. Finally, we prove our claim below.

In view of *(i)*, assume to the contrary that there is $k' > Z_{k'}$ such that $1 \leqslant k' \leqslant k^\star$. We then have $Z_{k'} < k' \leqslant k^\star \leqslant Z_{k^\star}$, where $k^\star \leqslant Z_{k^\star}$ due to Lemma 3.38, which shows that $\max_{k \in K} a(\boldsymbol{x}, k) = k^\star$. However, this contradicts the fact that $Z_{k^\star} \leqslant Z_{k'}$ since $k' \leqslant k^\star$ by assumption and Z_k is a monotonically non-increasing function in k. As for *(ii)*, assume to the contrary that there is $k' \leqslant Z_{k'}$ such that $k' > k^\star$. We then have $k^\star < k' \leqslant Z_{k'} \leqslant Z_{k^\star}$, where the last inequality holds because Z_k is a monotonically non-increasing function in k. This implies that $a(\boldsymbol{x}, k') = k' > a(\boldsymbol{x}, k^\star)$, which contradicts the fact that $k^\star \in \arg\max a(\boldsymbol{x}, k)$. ∎

Thus, Theorem 3.27 allows us to evaluate d^{S} for φ_{mVaR} for use in our 2VF(d) formulation to solve the ambiguous chance constrained CVRP.

3.6 Numerical Experiments

Our numerical experiments use the standard CVRP benchmark instances compiled by [D0́6]. Each instance label 'X-nY-kZ' indicates the literature source X of the instance, the number Y of nodes (including the depot) as well as the number Z of vehicles. Since our ambiguity set construction below is based on geographic information, we disregard instances that do not provide Euclidean coordinates for the nodes. Following the literature convention, we identify the transportation costs c_{ij} with the 2-norm distance between i and j, rounded to the nearest integer number.

The customer demands in the CVRP benchmark problems are deterministic. To construct stochastic demands whose distribution is characterized by an ambiguity set of the form (3.6), we subdivide each instance into 4 quadrants (northwest, northeast, southwest and southeast) according to the nodal coordinates. We then create $W = 4$ scenarios with equal probabilities $\hat{\boldsymbol{s}} = \mathbf{e}/4$, each of which is associated with one of the quadrants. In each scenario we set the expected demands of the customers in the associated quadrant to 110%, of the customers in the horizontally or vertically adjacent quadrants to 100%, and of the customers in the diagonally opposite quadrant to 90% of the nominal demands from the deterministic instance. The lower and upper demand bounds undercut and exceed these expected demands in each scenario by 10% of the nominal demands. The mean absolute deviations of the customer demands are set to those of a Normal distribution that is centered at the mean demands and that places 90% of its probability mass onto the demand interval. Since the CVRP benchmark instances tend to have little slack in the vehicle capacities, we follow [GWF13a] and [GW20] and increase the vehicle capacities Q by 20% to ensure that the distributionally robust instances are feasible.

We implemented a 'vanilla' CVRP solution scheme that augments the branch-and-cut capacity of CPLEX Studio 20.1.0 with an RCI cut separation procedure that follows the tabu search algorithm outlined by [ABB+98]. Our method is implemented in C++, and the source code

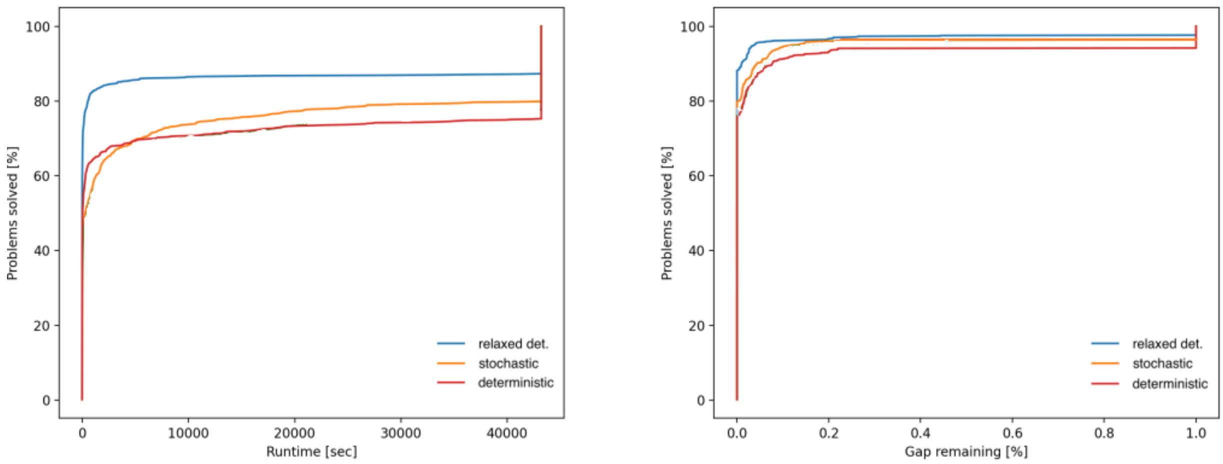

Figure 3.2: Runtimes and optimality gaps for our branch-and-cut schemes. Shown are the runtimes (left graph) and optimality gaps after 12 hours (right graph) for the deterministic branch-and-cut scheme as well as the distributionally robust branch-and-cut schemes with known scenario probabilities.

is available on the authors' webpages[2] (see Footnote 2). All problems are solved in single-core mode on an Intel Xeon 2.66GHz processor with 8GB main memory and a runtime limit of 12 hours.

3.6.1 Runtime Comparison

In our first experiment, we compare the runtimes and optimality gaps of our branch-and-cut algorithm for the deterministic CVRP with those of our algorithm for the distributionally robust CVRP under the 90%-CVaR risk measure. To this end, we consider two variants of the deterministic CVRP: one ('deterministic') where the original vehicle capacities are employed, and another one ('relaxed deterministic') where the vehicle capacities are increased by 20% as in the uncertainty-affected CVRP. We also consider our ambiguity set (3.6) in the 'stochastic' case, the scenario probabilities are known to be $\hat{\boldsymbol{s}} = \mathrm{e}/4$. The results are summarized in Figure 3.2 and presented in further detail in Table C.1 in Appendix C.

[2]The source code is available at: `http://wp.doc.ic.ac.uk/wwiesema/sourcecodes/`.

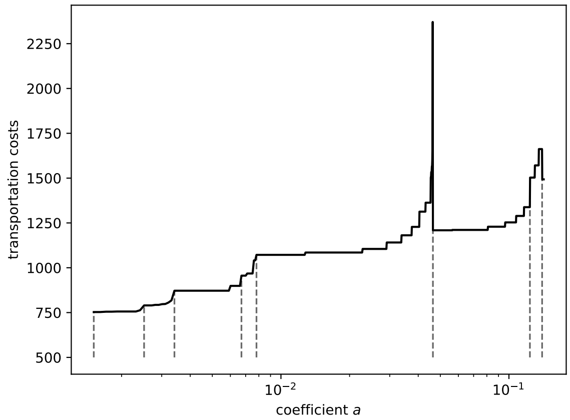

Figure 3.3: Minimum number of vehicles and optimal transportation costs for A-n32-k5 with an exponential class of disutility functions parameterized by a. The vertical lines indicate the parameter ranges covered by 5, 6, . . . , 11 vehicles (from left to right).

The results show that, as expected, increasing the vehicles' capacity by 20% in the deterministic CVRP substantially simplifies the problem instances. If the price to paid by accounting for uncertainty was to be small, we would expect the runtimes and optimality gaps for the stochastic and ambiguous instances to be contained in the interval spanned by the deterministic and relaxed deterministic instances. In fact, although the stochastic instance enjoy a capacity increase of 20% (akin to the relaxed deterministic instances), the incorporation of demand variability and distributional ambiguity as well as risk and ambiguity aversion reduce the factually available vehicle capacity. On the other hand, our construction of the stochastic instance guarantees that the uncertain customer demands never exceed 20% of their nominal values from the deterministic instances. The results show that, broadly, the runtimes and optimality gaps for the stochastic instance are upper and lower bounded by those of the deterministic and the relaxed deterministic instances, which indicates that the computational price to be paid is mainly determined by the slack in the vehicle capacities and less so by the incorporation of risk and ambiguity. We thus conclude that the same branch-and-cut algorithm can solve all three problem classes in runtimes and optimality gaps that are of the same order of magnitude.

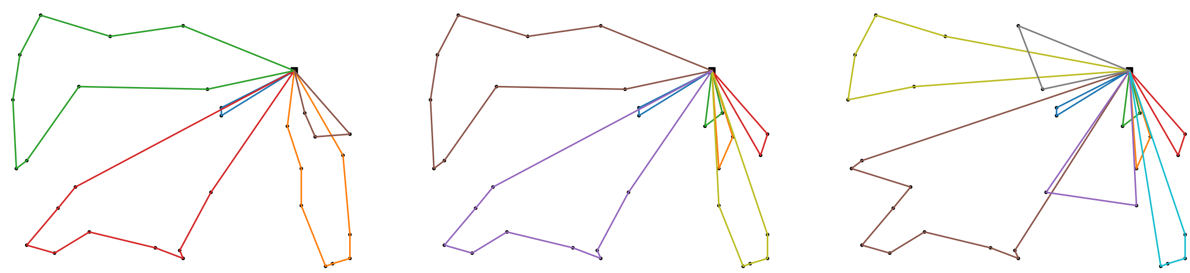

Figure 3.4: Optimal route plans for A-n32-k5 with exponential disutilities $a = 0$ (left; 5 vehicles), $a = 3.41\text{E-}3$ (middle; 7 vehicles) and $a = 7.81\text{E-}3$ (right; 9 vehicles).

3.6.2 The Impact of Risk Aversion

In our second experiment, we focus on the benchmark instance A-n32-k5 and solve the distributionally robust CVRP associated with the family of exponential disutility functions $U_a(q) = (\exp(aq) - 1)/a$, $a > 0$, and $U_0(q) = q$. The scalar parameter $a \in \mathbb{R}_+$ controls the risk aversion of the decision maker: $a = 0$ reflects a neutral stance towards demand variability, whereas larger values correspond to an increasing risk aversion. For every value of a, we set the budget B in (3.5) to $B = U_a(1.2Q)$, where Q is the nominal vehicle capacity from the deterministic CVRP instance and the factor 1.2 corresponds to the 20% capacity increase described earlier. This choice ensures that the feasibility of route plans for deterministic demands is unaffected by the choice of the risk aversion a and coincides with that of the deterministic instance (apart from the 20% capacity increase). Figure 3.3 visualizes how the minimum number of vehicles required to serve the customer demands, as well as the resulting transportation costs, vary as a function of the risk aversion a. Moreover, Figure 3.4 illustrates the optimal route plans for three different choices of a. We observe that higher degrees of risk aversion require larger numbers of vehicles to serve the customer demands, which in turn tends to increase the transportation costs (apart from two dips where the necessity to increase the number of vehicles results in smaller overall costs).

3.7 Conclusion

In this chapter, we have extensively studied the CVRP under risk and ambiguity. We have characterized the CVRP variants that can be treated under the 2VF formulation allowing solution via the branch-and-cut algorithm. We proposed custom demand estimators suitable to a wide choice of risk measures and ambiguity sets for the distributionally robust CVRP. The work in this chapter allows a variety of CVRP variants to be handled by a single solution framework with only minimal adaptations.

We also derived schemes to efficiently evaluate demand estimators for a wide range of risk measures under a scenario-wise first-order ambiguity set for fixed scenario probabilities. In the future, algorithms could be developed to consider the case of uncertain scenario probabilities wherein $\mathcal{S}$ is a convex subset of the probability simplex in $\mathbb{R}^W$ in the definition of (3.6). This will allow our framework to be extended to an even wider range of CVRP variants.

In the previous chapter, we have shown that the distributionally robust CVRP under value-at-risk and moment ambiguity sets can be solved without much undue difficulty compared to the deterministic CVRP. It is, thus, of interest to numerically compare the performance of the distributionally robust CVRP under different consideration of risk measures and ambiguity sets.

3.8 Appendix

We first prove a lemma that we have used repeatedly to prove a number of results in this chapter. This lemma proves that the below mentioned properties of a risk measure carry on to the worst-case risk. The rest of the appendix details lemmas that are required for the proofs of results in the main text.

Lemma 3.28 *Fix $\boldsymbol{x}, \boldsymbol{y} \in [0,1]^n$. If $\rho_{\mathbb{P}}(\boldsymbol{x}^\top \widetilde{\boldsymbol{q}})$ satisfies (X) for all $\mathbb{P} \in \mathcal{P}$, then $\varphi(\boldsymbol{x}) = \sup_{\mathbb{P}\in\mathcal{P}} \rho_{\mathbb{P}}(\boldsymbol{x}^\top \widetilde{\boldsymbol{q}})$ satisfies (X), where (X) could be any property (i) to (iv) in List 1.*

List 1. *[Properties of Risk Measures] For any random variable* $\widetilde{\boldsymbol{q}}$ *and* $\boldsymbol{x}, \boldsymbol{y} \in [0,1]^n$, $\rho_{\mathbb{P}}$ *satisfies:*

(i) monotonicity: If $\boldsymbol{x}^\top \widetilde{\boldsymbol{q}} \leqslant \boldsymbol{y}^\top \widetilde{\boldsymbol{q}}$ $\mathbb{P}$*-a.s., then* $\rho_{\mathbb{P}}(\boldsymbol{x}^\top \widetilde{\boldsymbol{q}}) \leqslant \rho_{\mathbb{P}}(\boldsymbol{y}^\top \widetilde{\boldsymbol{q}})$.

(ii) positive homogeneity: For $\lambda \geqslant 0$, $\rho_{\mathbb{P}}(\lambda \boldsymbol{x}^\top \widetilde{\boldsymbol{q}}) = \lambda \rho_{\mathbb{P}}(\boldsymbol{x}^\top \widetilde{\boldsymbol{q}})$.

(iii) subadditivity: $\rho_{\mathbb{P}}(\boldsymbol{x}^\top \widetilde{\boldsymbol{q}} + \boldsymbol{y}^\top \widetilde{\boldsymbol{q}}) \leqslant \rho_{\mathbb{P}}(\boldsymbol{x}^\top \widetilde{\boldsymbol{q}}) + \rho_{\mathbb{P}}(\boldsymbol{y}^\top \widetilde{\boldsymbol{q}})$.

(iv) convexity: For $\lambda \in [0,1]$, $\rho_{\mathbb{P}}(\lambda \boldsymbol{x}^\top \widetilde{\boldsymbol{q}} + (1-\lambda)\boldsymbol{y}^\top \widetilde{\boldsymbol{q}}) \leqslant \lambda \rho_{\mathbb{P}}(\boldsymbol{x}^\top \widetilde{\boldsymbol{q}}) + (1-\lambda)\rho_{\mathbb{P}}(\boldsymbol{y}^\top \widetilde{\boldsymbol{q}})$.

Proof of Lemma 3.28. Fix $\boldsymbol{x}, \boldsymbol{y} \in [0,1]^n$. We begin by showing *(i)*. Assume that $\boldsymbol{x}^\top \widetilde{\boldsymbol{q}} \leqslant \boldsymbol{y}^\top \widetilde{\boldsymbol{q}}$ $\mathbb{P}$-a.s. for all $\mathbb{P} \in \mathcal{P}$. Following from monotonicity of $\rho_{\mathbb{P}}$ for all $\mathbb{P} \in \mathcal{P}$, we notice that

$$\begin{aligned}
&\rho_{\mathbb{P}}(\boldsymbol{x}^\top \widetilde{\boldsymbol{q}}) \leqslant \rho_{\mathbb{P}}(\boldsymbol{y}^\top \widetilde{\boldsymbol{q}}) \;\; \forall \mathbb{P} \in \mathcal{P} \implies \rho_{\mathbb{P}}(\boldsymbol{x}^\top \widetilde{\boldsymbol{q}}) \leqslant \sup_{\mathbb{P} \in \mathcal{P}} \rho_{\mathbb{P}}(\boldsymbol{y}^\top \widetilde{\boldsymbol{q}}) \;\; \forall \mathbb{P} \in \mathcal{P} \\
&\iff \sup_{\mathbb{P} \in \mathcal{P}} \rho_{\mathbb{P}}(\boldsymbol{x}^\top \widetilde{\boldsymbol{q}}) \leqslant \sup_{\mathbb{P} \in \mathcal{P}} \rho_{\mathbb{P}}(\boldsymbol{y}^\top \widetilde{\boldsymbol{q}}) \iff \varphi(\boldsymbol{x}) \leqslant \varphi(\boldsymbol{y})
\end{aligned}$$

Thus, for $\boldsymbol{x} \leqslant \boldsymbol{y}$, $\varphi(\boldsymbol{x}) \leqslant \varphi(\boldsymbol{y})$.

We next show *(ii)*. Consider any $\lambda \geqslant 0$. We observe the following:

$$\varphi(\lambda \boldsymbol{x}) \;=\; \sup_{\mathbb{P} \in \mathcal{P}} \rho_{\mathbb{P}}(\lambda \boldsymbol{x}^\top \widetilde{\boldsymbol{q}}) \;=\; \sup_{\mathbb{P} \in \mathcal{P}} \lambda \rho_{\mathbb{P}}(\boldsymbol{x}^\top \widetilde{\boldsymbol{q}}) \;=\; \lambda \sup_{\mathbb{P} \in \mathcal{P}} \rho_{\mathbb{P}}(\boldsymbol{x}^\top \widetilde{\boldsymbol{q}}) \;=\; \lambda \varphi(\boldsymbol{x})$$

The second identity above follows from positive homogeneity of $\rho_{\mathbb{P}}$ for all $\mathbb{P} \in \mathcal{P}$.

Next, we show *(iii)*. We notice the following:

$$\begin{aligned}
& \rho_{\mathbb{P}}((\boldsymbol{x}+\boldsymbol{y})^\top \widetilde{\boldsymbol{q}}) \leqslant \rho_{\mathbb{P}}(\boldsymbol{x}^\top \widetilde{\boldsymbol{q}}) + \rho_{\mathbb{P}}(\boldsymbol{y}^\top \widetilde{\boldsymbol{q}}) && \forall \mathbb{P} \in \mathcal{P} \\
\implies\; & \rho_{\mathbb{P}}((\boldsymbol{x}+\boldsymbol{y})^\top \widetilde{\boldsymbol{q}}) \leqslant \sup_{\mathbb{P} \in \mathcal{P}} (\rho_{\mathbb{P}}(\boldsymbol{x}^\top \widetilde{\boldsymbol{q}} + \rho_{\mathbb{P}}(\boldsymbol{y}^\top \widetilde{\boldsymbol{q}})) && \forall \mathbb{P} \in \mathcal{P} \\
\implies\; & \rho_{\mathbb{P}}((\boldsymbol{x}+\boldsymbol{y})^\top \widetilde{\boldsymbol{q}}) \leqslant \sup_{\mathbb{P} \in \mathcal{P}} \rho_{\mathbb{P}}(\boldsymbol{x}^\top \widetilde{\boldsymbol{q}}) + \sup_{\mathbb{P} \in \mathcal{P}} \rho_{\mathbb{P}}(\boldsymbol{y}^\top \widetilde{\boldsymbol{q}}) && \forall \mathbb{P} \in \mathcal{P} \\
\iff\; & \sup_{\mathbb{P} \in \mathcal{P}} \rho_{\mathbb{P}}((\boldsymbol{x}+\boldsymbol{y})^\top \widetilde{\boldsymbol{q}}) \leqslant \sup_{\mathbb{P} \in \mathcal{P}} \rho_{\mathbb{P}}(\boldsymbol{x}^\top \widetilde{\boldsymbol{q}}) + \sup_{\mathbb{P} \in \mathcal{P}} \rho_{\mathbb{P}}(\boldsymbol{y}^\top \widetilde{\boldsymbol{q}}) \\
\iff\; & \varphi(\boldsymbol{x}+\boldsymbol{y}) \leqslant \varphi(\boldsymbol{x}) + \varphi(\boldsymbol{y})
\end{aligned}$$

The second implication follows from the subadditivity of sup.

To show *(iv)*, consider any $\lambda \in [0,1]$. Following from the assumption of convexity of $\rho_{\mathbb{P}}$ for all $\mathbb{P} \in \mathcal{P}$, we have

$$
\begin{aligned}
& \rho_{\mathbb{P}}(\lambda \boldsymbol{x}^\top \widetilde{\boldsymbol{q}} + (1-\lambda)\boldsymbol{y}^\top \widetilde{\boldsymbol{q}}) \leqslant \lambda \rho_{\mathbb{P}}(\boldsymbol{x}^\top \widetilde{\boldsymbol{q}}) + (1-\lambda)\rho_{\mathbb{P}}(\boldsymbol{y}^\top \widetilde{\boldsymbol{q}}) && \forall \mathbb{P} \in \mathcal{P} \\
\Longrightarrow \quad & \rho_{\mathbb{P}}(\lambda \boldsymbol{x}^\top \widetilde{\boldsymbol{q}} + (1-\lambda)\boldsymbol{y}^\top \widetilde{\boldsymbol{q}}) \leqslant \sup\nolimits_{\mathbb{P} \in \mathcal{P}}(\lambda \rho_{\mathbb{P}}(\boldsymbol{x}^\top \widetilde{\boldsymbol{q}}) + (1-\lambda)\rho_{\mathbb{P}}(\boldsymbol{y}^\top \widetilde{\boldsymbol{q}})) && \forall \mathbb{P} \in \mathcal{P} \\
\Longrightarrow \quad & \rho_{\mathbb{P}}(\lambda \boldsymbol{x}^\top \widetilde{\boldsymbol{q}} + (1-\lambda)\boldsymbol{y}^\top \widetilde{\boldsymbol{q}}) \leqslant \lambda \sup\nolimits_{\mathbb{P} \in \mathcal{P}} \rho_{\mathbb{P}}(\boldsymbol{x}^\top \widetilde{\boldsymbol{q}}) + (1-\lambda) \sup\nolimits_{\mathbb{P} \in \mathcal{P}} \rho_{\mathbb{P}}(\boldsymbol{y}^\top \widetilde{\boldsymbol{q}}) && \forall \mathbb{P} \in \mathcal{P} \\
\Longleftrightarrow \quad & \sup\nolimits_{\mathbb{P} \in \mathcal{P}} \rho_{\mathbb{P}}(\lambda \boldsymbol{x}^\top \widetilde{\boldsymbol{q}} + (1-\lambda)\boldsymbol{y}^\top \widetilde{\boldsymbol{q}}) \leqslant \lambda \sup\nolimits_{\mathbb{P} \in \mathcal{P}} \rho_{\mathbb{P}}(\boldsymbol{x}^\top \widetilde{\boldsymbol{q}}) + (1-\lambda) \sup\nolimits_{\mathbb{P} \in \mathcal{P}} \rho_{\mathbb{P}}(\boldsymbol{y}^\top \widetilde{\boldsymbol{q}}) \\
\Longleftrightarrow \quad & \varphi(\lambda \boldsymbol{x} + (1-\lambda)\boldsymbol{y}) \leqslant \lambda \varphi(\boldsymbol{x}) + (1-\lambda)\varphi(\boldsymbol{y})
\end{aligned}
$$

The second implication follows from the subadditivity of sup. ∎

Lemma 3.29 (Expected Disutility) *The worst-case expected disutility $\rho_{\mathrm{ED}} = \sup_{\mathbb{P} \in \mathcal{P}} \mathbb{P}\text{-ED}$ with*

$$\mathbb{P}\text{-ED}(\boldsymbol{x}^\top \widetilde{\boldsymbol{q}}) = \mathbb{E}_{\mathbb{P}}\left[U\left(\boldsymbol{x}^\top \widetilde{\boldsymbol{q}}\right)\right],$$

where the disutility function U is monotone and convex with $U(0) \geqslant 0$, is monotone, convex and not *subadditive. Moreover for an ambiguity set of the form* (3.6) *with $\mathcal{S} = \{\widehat{\boldsymbol{s}}\}$, ρ_{ED} affords a $W(2n+1)$-point worst-case distribution that can be computed with Algorithm 2 and that is independent of U and $\boldsymbol{x}$.*

Proof of Lemma 3.29. Note that $\mathbb{E}_{\mathbb{P}}[U(\cdot)]$ is monotone and convex for all $\mathbb{P} \in \mathcal{P}$ since $U(\cdot)$ is monotone and convex by assumption. Following from Lemma 3.28, ρ_{ED} is monotone and convex since $\mathbb{P}$-ED is monotone and convex. We next show that ρ_{ED} is not subadditive. To this end, consider $\mathcal{P}$ of the form (3.6) with $W = 2$, $\boldsymbol{s} = (0.3, 0.7)^\top$, and $\widehat{\boldsymbol{q}}^w = \overline{\boldsymbol{q}}^w = \underline{\boldsymbol{q}}^w$, and assume for simplicity that the expectation and mean absolute deviation constraints are absent (the example can easily be adapted to the presence of these constraints). Consider a CVRP instance with $n = 2$, $\widehat{\boldsymbol{q}}^1 = (5,7)^\top$, $\widehat{\boldsymbol{q}}^2 = (6,3)^\top$, $U(X) = X^2$, $\boldsymbol{x}_1 = (1,0)^\top$ and $\boldsymbol{x}_2 = (0,1)^\top$. We have $\rho_{\mathrm{ED}}(\boldsymbol{x}_1^\top \widetilde{\boldsymbol{q}}) = 32.7$, $\rho_{\mathrm{ED}}(\boldsymbol{x}_2^\top \widetilde{\boldsymbol{q}}) = 21$ and $\rho_{\mathrm{ED}}((\boldsymbol{x}_1 + \boldsymbol{x}_2)^\top \widetilde{\boldsymbol{q}}) = 99.9$. Clearly, $\rho_{\mathrm{ED}}(\boldsymbol{x}_1^\top \widetilde{\boldsymbol{q}}) + \rho_{\mathrm{ED}}(\boldsymbol{x}_2^\top \widetilde{\boldsymbol{q}}) = 53.7 < \rho_{\mathrm{ED}}((\boldsymbol{x}_1 + \boldsymbol{x}_2)^\top \widetilde{\boldsymbol{q}})$. Therefore, ρ_{ED} is not subadditive.

Notice that $\varphi(\boldsymbol{x}) = \rho_{\mathrm{ED}}(\boldsymbol{x}^\top \widetilde{\boldsymbol{q}})$ satisfies the assumptions of Theorem 3.15. It follows that $\mathbb{P}^\star = \sum_{w\in\mathcal{W}} \sum_{j=1}^{2n+1} \hat{s}_w p^\star_{wj} \cdot \delta_{\boldsymbol{q}^\star_{wj}} \in \mathcal{P}$ where $p^\star_{wj}, \boldsymbol{q}^\star_{wj}$ for $j = 1, \ldots, 2n+1$ and $w \in \mathcal{W}$ are obtained from Algorithm 2 in Appendix B is a worst-case distribution, and $\mathbb{P}^\star$ is independent of $U(\cdot)$ and $\boldsymbol{x}$. Therefore, we have $\rho_{\mathrm{ED}}(\boldsymbol{x}^\top \widetilde{\boldsymbol{q}}) = \sum_{w\in\mathcal{W}} \hat{s}_w \sum_{j=1}^{2n+1} p^\star_{wj} U\left(\sum_{i\in V_C} x_i q^\star_{wji}\right)$. ∎

Lemma 3.30 (Essential Riskiness Index) *The essential riskiness index ρ_{ERI} with*

$$\rho_{\mathrm{ERI}}(\boldsymbol{x}^\top \widetilde{\boldsymbol{q}}) = \min\left\{\alpha \geqslant 0 \ : \ \sup_{\mathbb{P}\in\mathcal{P}} \mathbb{E}_{\mathbb{P}}\left[\max\left\{\boldsymbol{x}^\top \widetilde{\boldsymbol{q}} - \overline{\rho},\ -\alpha\right\}\right] \leqslant 0\right\},$$

where $\boldsymbol{x}^\top \widetilde{\boldsymbol{q}} - \overline{\rho}$ represents the excess demand over the acceptable demand threshold $\overline{\rho}$, is monotone, convex and not *subadditive. Moreover, for an ambiguity set $\mathcal{P}$ of the form* (3.6) *with $\mathcal{S} = \{\widehat{\boldsymbol{s}}\}$, $\rho_{\mathrm{ERI}}(\boldsymbol{x}^\top \widetilde{\boldsymbol{q}})$ can be computed in time $\mathcal{O}(nW \log nW)$, with an initial computation of time $\mathcal{O}(n^2 W)$ for each* 2VF(d) *instance.*

Proof of Lemma 3.30. Notice that the mapping $X \mapsto \max\{X, -\alpha\}$ is convex for a fixed $\alpha \geqslant 0$. Consider an ambiguity set $\mathcal{P}$ of the form (3.6) with $\mathcal{S} = \{\widehat{\boldsymbol{s}}\}$. Fixing $\alpha \geqslant 0$, $\varphi(\boldsymbol{x}) = \rho_{\mathrm{ERI}}(\boldsymbol{x}^\top \widetilde{\boldsymbol{q}})$ satisfies the assumptions of Theorem 3.15. Using Theorem 3.15, we have $\mathbb{P}^\star = \sum_{w\in\mathcal{W}} \sum_{i=1}^{2n+1} \hat{s}_w p^\star_{wj} \cdot \delta_{\boldsymbol{q}^\star_{wj}} \in \mathcal{P}$ is a worst-case distribution where $p^\star_{wj}, \boldsymbol{q}^\star_{wj}$ for $j = 1, \ldots, 2n+1$ and $w \in \mathcal{W}$ are obtained from Algorithm 2 in Appendix B, and $\mathbb{P}^\star$ is independent of $\overline{\rho}$, α and $\boldsymbol{x}$. Therefore, $\sup_{\mathbb{P}\in\mathcal{P}} \mathbb{E}_{\mathbb{P}}[\max\{\boldsymbol{x}^\top \widetilde{\boldsymbol{q}} - \overline{\rho}, -\alpha\}] = \sum_{w\in\mathcal{W}} \hat{s}_w \sum_{j=1}^{2n+1} p^\star_{wj} \max\{\boldsymbol{x}^\top \boldsymbol{q}^\star_{wj} - \overline{\rho}, -\alpha\}$. Hence, we have

$$\rho_{\mathrm{ERI}}(\boldsymbol{x}^\top \widetilde{\boldsymbol{q}}) = \min\left\{\alpha \geqslant 0 \,\middle|\, \sum_{w\in\mathcal{W}} \hat{s}_w \sum_{j=1}^{2n+1} p^\star_{wj} \max\left\{\boldsymbol{x}^\top \boldsymbol{q}^\star_{wj} - \overline{\rho}, -\alpha\right\} \leqslant 0\right\}.$$

The expression $\sum_{w\in\mathcal{W}} \hat{s}_w \sum_{j=1}^{2n+1} p^\star_{wj} \max\{\boldsymbol{x}^\top \boldsymbol{q}^\star_{wj} - \overline{\rho}, -\alpha\}$ is monotonically non-increasing and piecewise affine in α with breakpoints $\{\overline{\rho} - \boldsymbol{x}^\top \boldsymbol{q}^\star_{wj} \ : \ w \in \mathcal{W}, j = 1, \ldots, 2n+1\}$. We can thus sort these breakpoints in time $\mathcal{O}(nW \log nW)$ and conduct a binary search over them to determine the root of the equation $\sum_{w\in\mathcal{W}} \hat{s}_w \sum_{j=1}^{2n+1} p^\star_{wj} \max\{\boldsymbol{x}^\top \boldsymbol{q}^\star_{wj} - \overline{\rho}, -\alpha\} = 0$. The binary search requires $\mathcal{O}(\log nW)$ iterations, and the evaluation of the summation in each iteration requires time $\mathcal{O}(nW)$. Since the worst-case distribution $\mathbb{P}^\star$ is independent of α and $\boldsymbol{x}$, it can be determined once per 2VF(d) instance.

By Proposition 3 of [ZBST18], $\rho_{\text{ERI}}(\cdot)$ is convex. Next, we prove the monotonicity of ρ_{ERI}. Consider $\boldsymbol{x}, \boldsymbol{y} \in [0,1]^n$ and assume that $\boldsymbol{x}^\top \widetilde{\boldsymbol{q}} \leqslant \boldsymbol{y}^\top \widetilde{\boldsymbol{q}}$ $\mathbb{P}$-a.s. for all $\mathbb{P} \in \mathcal{P}$. This implies that $\boldsymbol{x}^\top \widetilde{\boldsymbol{q}} \leqslant \boldsymbol{y}^\top \widetilde{\boldsymbol{q}}$ $\mathbb{P}^\star$-a.s. Let $\alpha_y^\star := \rho_{ERI}(\boldsymbol{y}^\top \widetilde{\boldsymbol{q}})$. By our assumption, we have $\mathbb{E}_{\mathbb{P}^\star}[\max\{\boldsymbol{x}^\top \widetilde{\boldsymbol{q}} - \overline{\rho}, -\alpha_y^\star\}] \leqslant \mathbb{E}_{\mathbb{P}^\star}[\max\{\boldsymbol{y}^\top \widetilde{\boldsymbol{q}} - \overline{\rho}, -\alpha_y^\star\}] \leqslant 0$. This implies that $\alpha_y^\star$ is a feasible solution for $\rho_{\text{ERI}}(\boldsymbol{x}^\top \widetilde{\boldsymbol{q}})$. Therefore, we must have $\rho_{\text{ERI}}(\boldsymbol{x}^\top \widetilde{\boldsymbol{q}}) \leqslant \alpha_y^\star = \rho_{\text{ERI}}(\boldsymbol{y}^\top \widetilde{\boldsymbol{q}})$, which proves the monotonicity of ρ_{ERI}. Next we show that ρ_{ERI} is not subadditive. To this end, consider a CVRP instance with $n = 2$ customers and an ambiguity set $\mathcal{P}$ of the form (3.6) with $W = 2$, $\mathcal{S} = \{\hat{s}\}$ and $\overline{\boldsymbol{q}} = \underline{\boldsymbol{q}} = \widehat{\boldsymbol{q}}$ where $\widehat{\boldsymbol{s}} = (0.2, 0.8)^\top$, $\widehat{\boldsymbol{q}}^1 = (5, 10)^\top$ and $\widehat{\boldsymbol{q}}^2 = (10, 5)^\top$. Consider $\boldsymbol{x} = (1, 0)^\top$ and $\boldsymbol{y} = (0, 1)^\top$ and $\overline{\rho} = 12$. We have $\rho_{\text{ERI}}((\boldsymbol{x} + \boldsymbol{y})^\top \widetilde{\boldsymbol{q}}) = \infty$, $\rho_{\text{ERI}}(\boldsymbol{x}^\top \widetilde{\boldsymbol{q}}) = \rho_{\text{ERI}}(\boldsymbol{y}^\top \widetilde{\boldsymbol{q}}) = 0$. Clearly, ρ_{ERI} does not satisfy subadditivity. ∎

Lemma 3.31 (Expectiles) *The worst-case expectile risk measure ρ_{E} with*

$$\rho_{\text{E}}\big(\boldsymbol{x}^\top \widetilde{\boldsymbol{q}}\big) \;=\; \operatorname*{arg\,min}_{u \in \mathbb{R}} \left\{ \sup_{\mathbb{P} \in \mathcal{P}} \; \alpha \mathbb{E}_{\mathbb{P}} \left[\left(\left[\boldsymbol{x}^\top \widetilde{\boldsymbol{q}} - u \right]_+ \right)^2 \right] + (1 - \alpha) \sup_{\mathbb{P} \in \mathcal{P}} \; \mathbb{E}_{\mathbb{P}} \left[\left(\left[\boldsymbol{x}^\top \widetilde{\boldsymbol{q}} - u \right]_- \right)^2 \right] \right\},$$

where $[\cdot]_+ = \max\{\cdot, 0\}$, $[\cdot]_- = \max\{-\cdot, 0\}$ and $\alpha \in [1/2, 1)$, is monotone, convex and subadditive. Moreover, for an ambiguity set of the form (3.6) with $\mathcal{S} = \{\widehat{\boldsymbol{s}}\}$, ρ_{E} can be computed in time $\mathcal{O}(nW \log nW)$, with an initial computation of time $\mathcal{O}(n^2 W)$ for each 2VF(d) instance.

Proof of Lemma 3.31. Fix an ambiguity set $\mathcal{P}$ of the form (3.6) with $\mathcal{S} = \{\widehat{\boldsymbol{s}}\}$, and $\boldsymbol{x} \in [0,1]^n$ and $\alpha \in [1/2, 1)$. Fix $u \in \mathbb{R}$. Notice that $[y - u]_- = [u - y]_+$ for $y \in \mathbb{R}$. The functions $[y - u]_+$, $[y - u]_-$ and y^2 are convex in y. Moreover, y^2 is an increasing function in y which implies that $([y - u]_+)^2$ and $([y - u]_-)^2$ are convex in y. Thus, $\sup_{\mathbb{P} \in \mathcal{P}} \mathbb{E}_{\mathbb{P}} \left[\left(\left[\boldsymbol{x}^\top \widetilde{\boldsymbol{q}} - u \right]_+ \right)^2 \right]$ and $\sup_{\mathbb{P} \in \mathcal{P}} \; \mathbb{E}_{\mathbb{P}} \left[\left(\left[\boldsymbol{x}^\top \widetilde{\boldsymbol{q}} - u \right]_- \right)^2 \right]$ satisfy the assumptions of Theorem 3.15, which implies that the worst-case distribution is the $W(2n+1)$-point distribution $\mathbb{P}^\star = \sum_{w \in \mathcal{W}} \sum_{j=1}^{2n+1} \hat{s}_w p_{wj}^\star \cdot \delta_{\boldsymbol{q}_{wj}^\star} \in \mathcal{P}$ that is independent of u and $\boldsymbol{x}$, and $p_{wj}^\star, \boldsymbol{q}_{wj}^\star$ for $w \in \mathcal{W}$ and $j = 1, \ldots, 2n+1$ are obtained from

Algorithm 2 in Appendix B. Accordingly, we have

$$\begin{aligned}
&\sup_{\mathbb{P}\in\mathcal{P}} \mathbb{E}_{\mathbb{P}}\left[\alpha\left(\left[\boldsymbol{x}^\top\widetilde{\boldsymbol{q}}-u\right]_+\right)^2\right] + \sup_{\mathbb{P}\in\mathcal{P}} \mathbb{E}_{\mathbb{P}}\left[(1-\alpha)\left(\left[\boldsymbol{x}^\top\widetilde{\boldsymbol{q}}-u\right]_-\right)^2\right] \\
&= \sum_{w\in\mathcal{W}} \hat{s}_w \sum_{j=1}^{2n+1} p^\star_{wj}\left[\alpha\left(\left[\sum_{i\in V_C} x_i q^\star_{wji}-u\right]_+\right)^2 + (1-\alpha)\left(\left[\sum_{i\in V_C} x_i q^\star_{wji}-u\right]_-\right)^2\right]
\end{aligned}$$

The above expression is convex in u with breakpoints $\{\sum_{i\in V_C} x_i q^\star_{wji} \,:\, w\in\mathcal{W},\, j=1,\ldots,2n+1\}$. We can thus sort these breakpoints in time $\mathcal{O}(nW\log nW)$ and conduct a trisection search over them to determine the value of u that minimizes this expression. The trisection search requires $\mathcal{O}(\log nW)$ iterations, and the evaluation of the expression in each iteration requires time $\mathcal{O}(nW)$ since the value of $\sum_{i\in V_C} x_i q^\star_{wji}$ can be precomputed and stored for a 2VF(d) instance. Since the worst-case distribution $\mathbb{P}^\star$ is independent of u and $\boldsymbol{x}$, it can be determined once per 2VF(d) instance.

From the above discussion, we notice that

$$\rho_E\big(\boldsymbol{x}^\top\widetilde{\boldsymbol{q}}\big) \;=\; \arg\min_{u\in\mathbb{R}}\left\{\mathbb{E}_{\mathbb{P}^\star}\left[\alpha\left(\left[\boldsymbol{x}^\top\widetilde{\boldsymbol{q}}-u\right]_+\right)^2\right] + \mathbb{E}_{\mathbb{P}^\star}\left[(1-\alpha)\left(\left[\boldsymbol{x}^\top\widetilde{\boldsymbol{q}}-u\right]_-\right)^2\right]\right\}$$

where $\mathbb{P}^\star$ is the worst-case distribution identified via Theorem 3.15. Following from Proposition 6 of [BKMG14], ρ_{E} is coherent for $\alpha\in[1/2,1)$ which implies that it is monotone, convex and subadditive for $\alpha\in[1/2,1)$. ∎

Lemma 3.32 (Entropic Risk) *The worst-case entropic risk measure,* $\rho_{\mathrm{ent}} = \sup_{\mathbb{P}\in\mathcal{P}}$ $\mathbb{P}$-ent *with*

$$\mathbb{P}\text{-ent}\big(\boldsymbol{x}^\top\widetilde{\boldsymbol{q}}\big) \;=\; \frac{1}{\theta}\log\mathbb{E}_{\mathbb{P}}\left[\exp^{\theta\cdot\boldsymbol{x}^\top\widetilde{\boldsymbol{q}}}\right],$$

where $\theta>0$, *is monotone, convex and* not *subadditive. Moreover, for an ambiguity set* $\mathcal{P}$ *of the form* (3.6) *with* $\mathcal{S}=\{\widehat{\boldsymbol{s}}\}$, ρ_{ent} *affords a* $W(2n+1)$*-point worst-case distribution that can be computed with Algorithm 2 and that is independent of* θ *and* $\boldsymbol{x}$.

Proof of Lemma 3.32. By Definition 2.3 of [FK11], $\mathbb{P}$-ent is monotone and convex. Following from Lemma 3.28, $\varphi(\boldsymbol{x}) = \rho_{ent}(\boldsymbol{x}^\top \widetilde{\boldsymbol{q}})$ is monotone and convex. To show that ρ_{ent} is not subadditive, consider the ambiguity set described in the proof of Lemma 3.29. Let $n = 2$, $\theta = 1$, $\boldsymbol{x}_1 = (1, 0)^\top$ and $\boldsymbol{x}_2 = (0, 1)^\top$. Then $\rho_{\text{ent}}(\boldsymbol{x}_1^\top \widetilde{\boldsymbol{q}}) = 5.79$, $\rho_{\text{ent}}(\boldsymbol{x}_2^\top \widetilde{\boldsymbol{q}}) = 5.84$ and $\rho_{\text{ent}}((\boldsymbol{x}_1+\boldsymbol{x}_2)^\top \widetilde{\boldsymbol{q}}) = 17.81$. Clearly, $\rho_{\text{ent}}((\boldsymbol{x}_1+\boldsymbol{x}_2)^\top \widetilde{\boldsymbol{q}}) > 11.63 = \rho_{\text{ent}}(\boldsymbol{x}_1^\top \widetilde{\boldsymbol{q}}) + \rho_{\text{ent}}(\boldsymbol{x}_2^\top \widetilde{\boldsymbol{q}})$, implying that ρ_{ent} is not subadditive.

For fixed $\boldsymbol{x} \in [0, 1]^n$, we have

$$\begin{aligned} \sup_{\mathbb{P}\in\mathcal{P}} \left[\frac{1}{\theta} \log \mathbb{E}_{\mathbb{P}} \left[\exp^{\theta \cdot \boldsymbol{x}^\top \widetilde{\boldsymbol{q}}}\right]\right] &= \frac{1}{\theta} \sup_{\mathbb{P}\in\mathcal{P}} \left[\log \mathbb{E}_{\mathbb{P}} \left[\exp^{\theta \cdot \boldsymbol{x}^\top \widetilde{\boldsymbol{q}}}\right]\right] \\ &= \frac{1}{\theta} \left[\log \sup_{\mathbb{P}\in\mathcal{P}} \mathbb{E}_{\mathbb{P}} \left[\exp^{\theta \cdot \boldsymbol{x}^\top \widetilde{\boldsymbol{q}}}\right]\right] \end{aligned}$$

The second identity holds because $x \mapsto \log(x)$ is an increasing function. Notice that the embedded worst-case expectation satisfies the assumptions of Theorem 3.15, which implies that the worst-case distribution is the $W(2n+1)$-point distribution $\mathbb{P}^\star = \sum_{w\in\mathcal{W}} \sum_{j=1}^{2n+1} \hat{s}_w p^\star_{wj} \cdot \delta_{\boldsymbol{q}^\star_{wj}} \in \mathcal{P}$ that is independent of θ and $\boldsymbol{x}$, and $p^\star_{wj}, \boldsymbol{q}^\star_{wj}$ for $w \in \mathcal{W}$ and $j = 1, \ldots, 2n + 1$ are obtained from Algorithm 2 in Appendix B. Hence, we have

$$\sup_{\mathbb{P}\in\mathcal{P}} \mathbb{E}_{\mathbb{P}} \left[\exp^{\theta \cdot \boldsymbol{x}^\top \widetilde{\boldsymbol{q}}}\right] = \sum_{w\in\mathcal{W}} \hat{s}_w \sum_{j=1}^{2n+1} p^\star_{wj} \left[\exp^{\theta \cdot \sum_{i\in V_C} x_i q^\star_{wji}}\right],$$

which implies that

$$\sup_{\mathbb{P}\in\mathcal{P}} \frac{1}{\theta} \log \mathbb{E}_{\mathbb{P}} \left[\exp^{\theta \cdot \boldsymbol{x}^\top \widetilde{\boldsymbol{q}}}\right] = \frac{1}{\theta} \log \left[\sum_{w\in\mathcal{W}} \hat{s}_w \sum_{j=1}^{2n+1} p^\star_{wj} \left[\exp^{\theta \cdot \sum_{i\in V_C} x_i q^\star_{wji}}\right]\right]. \quad \blacksquare$$

Lemma 3.33 (Requirements Violation Index) *The requirements violation index ρ_{RV} with*

$$\rho_{\text{RV}}(\boldsymbol{x}^\top \widetilde{\boldsymbol{q}}) = \inf \left\{\alpha \geqslant 0 \,:\, C_\alpha(\boldsymbol{x}^\top \widetilde{\boldsymbol{q}}) \leqslant \overline{\rho}\right\},$$

where C_α is the worst-case certainty equivalent under an exponential disutility and $\overline{\rho}$ is the acceptable demand threshold, is monotone, convex but not *subadditive. Moreover, for an ambi-*

guity set $\mathcal{P}$ of the form (3.6) with $\mathcal{S} = \{\widehat{\boldsymbol{s}}\}$, $\rho_{\mathrm{RV}}(\boldsymbol{x}^\top \widetilde{\boldsymbol{q}})$ can be evaluated using bisection search, with an initial computation of time $\mathcal{O}(n^2 W)$ for each 2VF(d) instance.

Proof of Lemma 3.33. Fix an ambiguity set $\mathcal{P}$ of the form (3.6) with $\mathcal{S} = \{\widehat{\boldsymbol{s}}\}$ and $\boldsymbol{x} \in [0,1]^n$. Replacing the worst-case certainty equivalent with its definition and using Lemma 3.32 with $\theta = 1/\alpha$, we have

$$C_\alpha(\boldsymbol{x}^\top \widetilde{\boldsymbol{q}}) \;=\; \sup_{\mathbb{P}\in\mathcal{P}} \alpha \log \mathbb{E}_{\mathbb{P}}\left(\exp\left(\frac{\boldsymbol{x}^\top \widetilde{\boldsymbol{q}}}{\alpha}\right)\right) = \alpha \log\left(\sum_{w\in\mathcal{W}} \hat{s}_w \sum_{j=1}^{2n+1} p^\star_{wj} \exp\left(\sum_{i\in V_C} x_i q^\star_{wji}/\alpha\right)\right),$$

where $p^\star_{wj}, \boldsymbol{q}^\star_{wj}$ for $j = 1,\ldots,2n+1$ and $w \in \mathcal{W}$ are obtained from Algorithm 2 in Appendix B.

By Lemma 1 of [JQS16], $\lim_{\alpha\to\infty} C_\alpha(\boldsymbol{x}^\top \widetilde{\boldsymbol{q}}) = \sup_{\mathbb{P}\in\mathcal{P}} \mathbb{E}_{\mathbb{P}}[\boldsymbol{x}^\top \widetilde{\boldsymbol{q}}]$. By the abandonment property of ρ_{RV} [JQS16, Proposition 1], if $\sup_{\mathbb{P}\in\mathcal{P}} \mathbb{E}_{\mathbb{P}}[\boldsymbol{x}^\top \widetilde{\boldsymbol{q}}] > \overline{\rho}$, then $\rho_{\mathrm{RV}}(\boldsymbol{x}^\top \widetilde{\boldsymbol{q}}) = \infty$. Note that the function C_α is monotonically decreasing in α [JQS16, Lemma 1]. If $\sup_{\mathbb{P}\in\mathcal{P}} \mathbb{E}_{\mathbb{P}}[\boldsymbol{x}^\top \widetilde{\boldsymbol{q}}] \leqslant \overline{\rho}$, it implies that there exists a finite value for $\rho_{\mathrm{RV}}(\boldsymbol{x}^\top \widetilde{\boldsymbol{q}})$ and we proceed as follows. For $\alpha = 1$, we check if $C_\alpha(\boldsymbol{x}^\top \widetilde{\boldsymbol{q}}) \leqslant \overline{\rho}$. If it is, we do a bisection search over [0, 1] to find an ϵ-minimizer. Otherwise, starting from $\alpha = 1$ we search for an α_u by multiplying α by 2 at every search iteration, such that $C_{\alpha_u}(\boldsymbol{x}^\top \widetilde{\boldsymbol{q}}) \leqslant \overline{\rho}$ holds. We then do a bisection search over $[\alpha_u/2, \alpha_u]$ to find $\rho_{\mathrm{RV}}(\boldsymbol{x}^\top \widetilde{\boldsymbol{q}})$.

The convexity of ρ_{RV} follows from Proposition 1 of [JQS16]. We now prove that ρ_{RV} is monotone. Consider $\boldsymbol{x}, \boldsymbol{y} \in [0,1]^n$ and assume that $\boldsymbol{x}^\top \widetilde{\boldsymbol{q}} \leqslant \boldsymbol{y}^\top \widetilde{\boldsymbol{q}}$ $\mathbb{P}$-a.s. for all $\mathbb{P} \in \mathcal{P}$. This implies that $\boldsymbol{x}^\top \widetilde{\boldsymbol{q}} \leqslant \boldsymbol{y}^\top \widetilde{\boldsymbol{q}}$ $\mathbb{P}^\star$-a.s. Let $\alpha^\star_y := \rho_{\mathrm{RV}}(\boldsymbol{y}^\top \widetilde{\boldsymbol{q}})$. By our assumption, we have

$$\alpha^\star_y \log\left(\sum_{w\in\mathcal{W}} \hat{s}_w \sum_{j=1}^{2n+1} p^\star_{wj} \exp\left(\sum_{i\in V_C} x_i q^\star_{wji}/\alpha^\star_y\right)\right) \leqslant \alpha^\star_y \log\left(\sum_{w\in\mathcal{W}} \hat{s}_w \sum_{j=1}^{2n+1} p^\star_{wj} \exp\left(\sum_{i\in V_C} y_i q^\star_{wji}/\alpha^\star_y\right)\right) \leqslant \overline{\rho}.$$

Since $\mathbb{P}^\star$ is independent of $\boldsymbol{x}, \boldsymbol{y}$, this implies that $\alpha^\star_y$ is a feasible solution for $\rho_{\mathrm{RV}}(\boldsymbol{x}^\top \widetilde{\boldsymbol{q}})$. Therefore, we must have $\rho_{\mathrm{RV}}(\boldsymbol{x}^\top \widetilde{\boldsymbol{q}}) \leqslant \alpha^\star_y = \rho_{\mathrm{RV}}(\boldsymbol{y}^\top \widetilde{\boldsymbol{q}})$, which proves the monotonicity of ρ_{RV}. Finally, we show that ρ_{RV} is not subadditive. To this end, consider the same CVRP instance and $\mathcal{P}$ as in the proof of Lemma 3.30. Consider $\boldsymbol{x} = (1,0)^\top$, $\boldsymbol{y} = (0,1)^\top$ and $\overline{\rho} = 12$. We have $\rho_{\mathrm{RV}}(\boldsymbol{x}^\top \widetilde{\boldsymbol{q}}) = 0$, $\rho_{\mathrm{RV}}(\boldsymbol{y}^\top \widetilde{\boldsymbol{q}}) = 0$ and $\rho_{\mathrm{RV}}((\boldsymbol{x}+\boldsymbol{y})^\top \widetilde{\boldsymbol{q}}) = \infty$. Clearly, ρ_{RV} does not satisfy subadditivity. ∎

Lemma 3.34 (CVaR) *The worst-case conditional value-at-risk,* $\rho_{\text{CVaR}} = \sup_{\mathbb{P}\in\mathcal{P}} \mathbb{P}\text{-CVaR}_{1-\epsilon}$ *with*

$$\mathbb{P}\text{-CVaR}_{1-\epsilon}(\boldsymbol{x}^\top\widetilde{\boldsymbol{q}}) = \inf_{u\in\mathbb{R}} u + \frac{1}{1-\epsilon}\mathbb{E}_{\mathbb{P}}[\boldsymbol{x}^\top\widetilde{\boldsymbol{q}} - u]_+$$

where $\epsilon \in [0,1)$ *is monotone, convex and subadditive. Moreover, for an ambiguity set* $\mathcal{P}$ *of the form* (3.6) *with* $\mathcal{S} = \{\widehat{\boldsymbol{s}}\}$ *and for* $\boldsymbol{x} \in [0,1]^n$*,* $\rho_{\text{CVaR}}(\boldsymbol{x}^\top\widetilde{\boldsymbol{q}})$ *can be evaluated in time* $\mathcal{O}(nW\log(nW))$*, with an initial computation time of* $\mathcal{O}(n^2W)$ *that needs to be executed once per* 2VF(d) *instance.*

Proof of Lemma 3.34. By Corollary 12 of [RU02], $\mathbb{P}$-CVaR is coherent, which implies that it is monotone, convex and subadditive. Following from Lemma 3.28, ρ_{CVaR} is monotone, convex and subadditive. For $\boldsymbol{x} \in [0,1]^n$, we have

$$\varphi(\boldsymbol{x}) = \sup_{\mathbb{P}\in\mathcal{P}} \mathbb{P}\text{-CVaR}_{1-\epsilon}(\boldsymbol{x}^\top\widetilde{\boldsymbol{q}}) = \sup_{\mathbb{P}\in\mathcal{P}}\inf_{u\in\mathbb{R}} u + \frac{1}{1-\epsilon}\mathbb{E}_{\mathbb{P}}[\boldsymbol{x}^\top\widetilde{\boldsymbol{q}} - u]_+ = \inf_{u\in\mathbb{R}} u + \frac{1}{1-\epsilon}\sup_{\mathbb{P}\in\mathcal{P}}\mathbb{E}_{\mathbb{P}}[\boldsymbol{x}^\top\widetilde{\boldsymbol{q}} - u]_+.$$

The final identity here follows from Proposition 3.1 of [SK02]. For a fixed $u \in \mathbb{R}$, the function $[\boldsymbol{x}^\top\boldsymbol{q} - u]_+$ is convex. Thus, $\sup_{\mathbb{P}\in\mathcal{P}}\mathbb{E}_{\mathbb{P}}[\boldsymbol{x}^\top\widetilde{\boldsymbol{q}} - u]_+$ satisfies the assumptions of Theorem 3.15. Hence, the worst-case distribution is the $W(2n+1)$-point distribution $\mathbb{P}^\star = \sum_{w\in\mathcal{W}}\sum_{j=1}^{2n+1}\hat{s}_w p^\star_{wj}\cdot\delta_{\boldsymbol{q}^\star_{wj}} \in \mathcal{P}$ that is independent of $\mathbb{P}$-CVaR and $\boldsymbol{x}$, and $p^\star_{wj}, \boldsymbol{q}^\star_{wj}$ for $w \in \mathcal{W}$ and $j = 1,\ldots,2n+1$ are obtained from Algorithm 2 in Appendix B. It follows that

$$\sup_{\mathbb{P}\in\mathcal{P}}\mathbb{E}_{\mathbb{P}}[\boldsymbol{x}^\top\widetilde{\boldsymbol{q}} - u]_+ = \sum_{w\in\mathcal{W}}\hat{s}_w\sum_{j=1}^{2n+1}p^\star_{wj}\left[\sum_{i\in V_C}x_i q^\star_{wji} - u\right]_+$$

where $p^\star_{wj}, q^\star_{wji}$ for $j = 1,\ldots,2n+1$ and $w \in \mathcal{W}$ is obtained from Algorithm 2. Thus,

$$\rho_{\text{CVaR}}(\boldsymbol{x}^\top\widetilde{\boldsymbol{q}}) \quad = \inf_{u\in\mathbb{R}} u + \sum_{w\in\mathcal{W}}\hat{s}_w\sum_{j=1}^{2n+1}p^\star_{wj}[x_i q^\star_{wji} - u]_+.$$

Note that the objective function is convex and has kinks at $q^\star_{wji}$ where $j = 1,\ldots,2n+1$ and $w \in \mathcal{W}$. Hence, we can obtain the optimal $u^\star$ by performing a trisection search over these breakpoints that are sorted in time $\mathcal{O}(nW\log(nW))$. The trisection search requires $\mathcal{O}(nW)$ iterations, and Each iteration requires time $\mathcal{O}(nW)$ to evaluate the expression assuming that

Algorithm 1: Trisection Algorithm for finding $u^\star$ for CVaR

Input: Let $\phi_{(2n+1)\cdot(w-1)+j} = x_i q^\star_{wji}$ such that $\phi_1 \leqslant \phi_2 \leqslant \ldots \leqslant \phi_L$ where $L = (2n+1) \times W$, $j = 1, \ldots, 2n+1$, $w \in \mathcal{W}$.

Initialize $a = 1$, $b = (2n+1) \times W$;

while $|a - b| \geqslant 1$ **do**

  $c = a + \lceil (b-a)/3 \rceil; d = a + \lceil 2(b-a)/3 \rceil$;

  $f(\phi_c) = \phi_c + \sum_{w\in\mathcal{W}} \hat{s}_w \sum_{j=1}^{2n+1} [\sum_{i\in V_C} x_i q^\star_{wji} - \phi_c]_+$, $f(\phi_d) = \phi_d + \sum_{w\in\mathcal{W}} \hat{s}_w \sum_{j=1}^{2n+1} [\sum_{i\in V_C} x_i q^\star_{wji} - \phi_d]_+$;

  if $f(\phi_c) < f(\phi_d)$ **then** $b \leftarrow d$;

  else if $f(\phi_c) > f(\phi_d)$ **then** $a \leftarrow c$;

  else $a \leftarrow c$, $b \leftarrow d$;

end

return $f(\phi_a)$;

we are storing value of $\boldsymbol{x}^\top \widetilde{\boldsymbol{q}}$. The overall algorithm to find $u^\star$ is outlined in Algorithm 1. ∎

Lemma 3.35 (Service Fulfilment Risk Index) *The service fulfillment risk index* ρ_{SRI} *with*

$$\rho_{\text{SRI}}\left(\boldsymbol{x}^\top \widetilde{\boldsymbol{q}}\right) = \inf\left\{\alpha \geqslant 0 \,\middle|\, \rho_{\text{CVaR}_\gamma}\left(\max\{\boldsymbol{x}^\top \widetilde{\boldsymbol{q}} - \overline{\rho}, -\alpha\}\right) \leqslant 0\right\}$$

where $\gamma \in [0,1]$ *and* $\boldsymbol{x}^\top \widetilde{\boldsymbol{q}} - \overline{\rho}$ *represents the excess demand over the acceptable demand threshold* $\overline{\rho}$*, is monotone, convex but not subadditive. Moreover, for an ambiguity set* $\mathcal{P}$ *of the form* (3.6) *with* $\mathcal{S} = \{\widehat{\boldsymbol{s}}\}$ *and for* $\boldsymbol{x} \in [0,1]^n$*,* $\rho_{\text{SRI}}(\boldsymbol{x}^\top \widetilde{\boldsymbol{q}})$ *can be computed to* δ*-accuracy in time* $\mathcal{O}\left(nW \log\left(M/\delta\gamma\right)\right)$ *where* $M = \overline{\rho} - \sum_{w\in\mathcal{W}} \hat{s}_w \sum_{j=1}^{2n+1} p^\star_{wj} \sum_{i\in V_C} x_i q^\star_{wji}$*, with an initial computation time of* $\mathcal{O}(n^2 W)$ *that needs to be executed once per* 2VF(d) *instance.*

Proof of Lemma 3.35. Following from Theorem 1 of [ZZLS21], ρ_{SRI} can be equivalently expressed as

$$\rho_{\text{SRI}}\left(\boldsymbol{x}^\top \widetilde{\boldsymbol{q}}\right) = \inf\left\{\alpha \geqslant 0 \;:\; \sup_{\mathbb{P}\in\mathcal{P}} \mathbb{E}_{\mathbb{P}}\left[\max\left\{\boldsymbol{x}^\top \widetilde{\boldsymbol{q}} - \overline{\rho} + \alpha, 0\right\}\right] \leqslant (1-\gamma)\alpha\right\}.$$

Fix an ambiguity set $\mathcal{P}$ of the form (3.6) with $\mathcal{S} = \{\widehat{\boldsymbol{s}}\}$, and $\boldsymbol{x} \in [0,1]^n$. Since the function $\max\{\boldsymbol{x}^\top \widetilde{\boldsymbol{q}} - \overline{\rho} + \alpha, 0\}$ is convex for a fixed $\alpha \geqslant 0$, $\sup_{\mathbb{P}\in\mathcal{P}} \mathbb{E}_{\mathbb{P}}[\max\{\boldsymbol{x}^\top \widetilde{\boldsymbol{q}} - \overline{\rho} + \alpha, 0\}]$ satisfies the assumptions of Theorem 3.15. Hence, the worst-case distribution is the $W(2n+1)$-point distribution $\mathbb{P}^\star = \sum_{w\in\mathcal{W}}\sum_{j=1}^{2n+1}\hat{s}_w p^\star_{wj}\cdot\delta_{\boldsymbol{q}^\star_{wj}} \in \mathcal{P}$ that is independent of $\overline{\rho}$ and $\boldsymbol{x}$, and $p^\star_{wj}, \boldsymbol{q}^\star_{wj}$ for $w \in \mathcal{W}$ and $j = 1,\ldots,2n+1$ are obtained from Algorithm 2 in Appendix B. Accordingly, we have

$$\sup_{\mathbb{P}\in\mathcal{P}} \mathbb{E}_{\mathbb{P}}[\max\{\boldsymbol{x}^\top\widetilde{\boldsymbol{q}} - \overline{\rho} + \alpha, 0\}] = \sum_{w\in\mathcal{W}} \hat{s}_w \sum_{j=1}^{2n+1} p^\star_{wj} \left[\max\left\{\sum_{i\in V_C} x_i q^\star_{wji} - \overline{\rho} + \alpha, 0\right\}\right].$$

Therefore,

$$\begin{aligned}\rho_{\text{SRI}}\left(\boldsymbol{x}^\top\widetilde{\boldsymbol{q}}\right) &= \min\left\{\alpha \geqslant 0 \;:\; \sum_{w\in\mathcal{W}} \hat{s}_w \sum_{j=1}^{2n+1} p^\star_{wj} \left[\max\left\{\sum_{i\in V_C} x_i q^\star_{wji} - \overline{\rho} + \alpha, 0\right\}\right] \leqslant (1-\gamma)\alpha\right\} \\ &= \min\left\{\alpha \geqslant 0 \;:\; \sum_{w\in\mathcal{W}} \hat{s}_w \sum_{j=1}^{2n+1} p^\star_{wj} \left[\max\left\{\sum_{i\in V_C} x_i q^\star_{wji} - \overline{\rho} + \alpha, 0\right\}\right] - (1-\gamma)\alpha \leqslant 0\right\}.\end{aligned}$$

The function in the constraint is convex in α. We can use bisection search to find the minimum α for which the constraint is satisfied. To this end, we first find an upper bound α_u for the search region for α. Note that for the case $\sum_{i\in V_C} x_i q^\star_{wji} - \overline{\rho} + \alpha \leqslant 0$, the constraint in the problem for finding $\rho_{\text{SRI}}\left(\boldsymbol{x}^\top\widetilde{\boldsymbol{q}}\right)$ holds trivially. Consider the case $\sum_{i\in V_C} x_i q^\star_{wji} - \overline{\rho} + \alpha > 0$. This implies that α must satisfy the constraint in the definition of $\rho_{\text{SRI}}\left(\boldsymbol{x}^\top\widetilde{\boldsymbol{q}}\right)$:

$$\begin{aligned} & \textstyle\sum_{w\in\mathcal{W}} \hat{s}_w \sum_{j=1}^{2n+1} p^\star_{wj} \left[\sum_{i\in V_C} x_i q^\star_{wji} - \overline{\rho} + \alpha\right] - (1-\gamma)\alpha \leqslant 0 \\ \iff & \textstyle\sum_{w\in\mathcal{W}} \hat{s}_w \sum_{j=1}^{2n+1} p^\star_{wj} \sum_{i\in V_C} x_i q^\star_{wji} - \overline{\rho} + \alpha - (1-\gamma)\alpha \leqslant 0 \\ \iff & \textstyle\sum_{w\in\mathcal{W}} \hat{s}_w \sum_{j=1}^{2n+1} p^\star_{wj} \sum_{i\in V_C} x_i q^\star_{wji} - \overline{\rho} + \gamma\alpha \leqslant 0 \\ \iff & \alpha \leqslant \tfrac{1}{\gamma}\left(\overline{\rho} - \textstyle\sum_{w\in\mathcal{W}} \hat{s}_w \sum_{j=1}^{2n+1} p^\star_{wj} \sum_{i\in V_C} x_i q^\star_{wji}\right)\end{aligned}$$

Thus, $\alpha_u = \frac{1}{\gamma}\left(\overline{\rho} - \sum_{w\in\mathcal{W}} \hat{s}_w \sum_{j=1}^{2n+1} p^\star_{wj} \sum_{i\in V_C} x_i q^\star_{wji}\right)$, and the bisection search to find $\alpha^\star$ requires $\mathcal{O}\left(\log\left(\overline{\rho} - \sum_{w\in\mathcal{W}} \hat{s}_w \sum_{j=1}^{2n+1} p^\star_{wj} \sum_{i\in V_C} x_i q^\star_{wji}/\delta\gamma\right)\right)$ iterations to obtain a δ-minimizer, and each iteration takes time $\mathcal{O}(nW)$ to evaluate the value of the LHS of the constraint.

By Proposition 1 of [ZZLS21], ρ_{SRI} is convex. Next, we prove the monotonicity of ρ_{SRI}. Consider $\boldsymbol{x}, \boldsymbol{y} \in [0,1]^n$ and assume that $\boldsymbol{x}^\top\widetilde{\boldsymbol{q}} \leqslant \boldsymbol{y}^\top\widetilde{\boldsymbol{q}}$ $\mathbb{P}$-a.s. for all $\mathbb{P} \in \mathcal{P}$. This implies that $\boldsymbol{x}^\top\widetilde{\boldsymbol{q}} \leqslant \boldsymbol{y}^\top\widetilde{\boldsymbol{q}}$

$\mathbb{P}^\star$-a.s. Let $\alpha_y^\star := \rho_{\mathrm{SRI}}(\boldsymbol{y}^\top\widetilde{\boldsymbol{q}})$. By our assumption, we have

$$\mathbb{E}_{\mathbb{P}^\star}[\max\{\boldsymbol{x}^\top\widetilde{\boldsymbol{q}} - \overline{\rho} + \alpha_y^\star, 0\}] \leqslant \mathbb{E}_{\mathbb{P}^\star}[\max\{\boldsymbol{y}^\top\widetilde{\boldsymbol{q}} - \overline{\rho} + \alpha_y^\star, 0\}] \leqslant (1-\gamma)\alpha_y^\star.$$

Since $\mathbb{P}^\star$ is independent of $\alpha_y^\star$, this implies that $\alpha_y^\star$ is a feasible solution for $\rho_{\mathrm{SRI}}(\boldsymbol{x}^\top\widetilde{\boldsymbol{q}})$. Therefore, we must have $\rho_{\mathrm{SRI}}(\boldsymbol{x}^\top\widetilde{\boldsymbol{q}}) \leqslant \alpha_y^\star = \rho_{\mathrm{SRI}}(\boldsymbol{y}^\top\widetilde{\boldsymbol{q}})$, which proves the monotonicity of ρ_{SRI}. Next we show that ρ_{SRI} is not subadditive. Consider the same CVRP instance and ambiguity set as described in the proof of Lemma 3.30. Consider $\boldsymbol{x} = (1,0)^\top$, $\boldsymbol{y} = (0,1)^\top$, $\gamma = 1$ and $\overline{\rho} = 12$. We have $\rho_{\mathrm{SRI}}((\boldsymbol{x}+\boldsymbol{y})^\top\widetilde{\boldsymbol{q}}) = \infty$, $\rho_{\mathrm{SRI}}(\boldsymbol{x}^\top\widetilde{\boldsymbol{q}}) = \rho_{\mathrm{SRI}}(\boldsymbol{y}^\top\widetilde{\boldsymbol{q}}) = 0$. Clearly, ρ_{SRI} does not satisfy subadditivity. ∎

Lemma 3.36 (Mean Semi-Deviation) *The worst-case mean semi-deviation of order u, $\rho_{\mathrm{MSD}} = \sup_{\mathbb{P}\in\mathcal{P}} \mathbb{P}\text{-MSD}$ with*

$$\mathbb{P}\text{-MSD}\big(\boldsymbol{x}^\top\widetilde{\boldsymbol{q}}\big) \;=\; \mathbb{E}_{\mathbb{P}}\big[\boldsymbol{x}^\top\widetilde{\boldsymbol{q}}\big] + \alpha\left(\mathbb{E}_{\mathbb{P}}\big[\boldsymbol{x}^\top\widetilde{\boldsymbol{q}} - \mathbb{E}_{\mathbb{P}}\big[\boldsymbol{x}^\top\widetilde{\boldsymbol{q}}\big]\big]_+^u\right)^{\frac{1}{u}} \quad \text{for } u \geqslant 1 \text{ and } \alpha \in [0,1],$$

is monotone, convex and subadditive. Moreover, for an ambiguity set $\mathcal{P}$ of the form (3.6) *with $\mathcal{S} = \{\widehat{\boldsymbol{s}}\}$ and for $\boldsymbol{x} \in [0,1]^n$, ρ_{MSD} affords a $W(2n+1)$-point worst-case distribution that can be computed with Algorithm 2, and that is independent of α, u and $\boldsymbol{x}$.*

Proof of Lemma 3.36. The mean semi-deviation of order u is coherent [SDR14, Example 6.20], which implies that it is monotone, convex and subadditive. Following from Lemma 3.28,

$\sup_{\mathbb{P}\in\mathcal{P}} \mathbb{P}$-MSD is monotone, convex and subadditive. For fixed $\boldsymbol{x} \in [0,1]^n$, we can write

$$\begin{aligned}
&\sup_{\mathbb{P}\in\mathcal{P}} \left[\mathbb{E}_{\mathbb{P}} \left[\boldsymbol{x}^\top \widetilde{\boldsymbol{q}} \right] + \alpha \left(\mathbb{E}_{\mathbb{P}} \left[\boldsymbol{x}^\top \widetilde{\boldsymbol{q}} - \mathbb{E}_{\mathbb{P}} \left[\boldsymbol{x}^\top \widetilde{\boldsymbol{q}} \right] \right]_+^u \right)^{1/u} \right] \\
&= \max_{\boldsymbol{s}\in\mathcal{S}} \sup_{\mathbb{P}_w\in\mathcal{P}^w: w\in\mathcal{W}} \left[\sum_{w\in\mathcal{W}} s_w \mathbb{E}_{\mathbb{P}_w} \left[\boldsymbol{x}^\top \widetilde{\boldsymbol{q}} \right] + \alpha \left(\sum_{w\in\mathcal{W}} s_w \mathbb{E}_{\mathbb{P}_w} \left[\boldsymbol{x}^\top \widetilde{\boldsymbol{q}} - \sum_{w\in\mathcal{W}} s_w \mathbb{E}_{\mathbb{P}_w} \left[\boldsymbol{x}^\top \widetilde{\boldsymbol{q}} \right] \right]_+^u \right)^{1/u} \right] \\
&= \sup_{\mathbb{P}_w\in\mathcal{P}^w: w\in\mathcal{W}} \left[\sum_{w\in\mathcal{W}} \hat{s}_w \mathbb{E}_{\mathbb{P}_w} \left[\boldsymbol{x}^\top \widetilde{\boldsymbol{q}} \right] + \alpha \left(\sum_{w\in\mathcal{W}} \hat{s}_w \mathbb{E}_{\mathbb{P}_w} \left[\boldsymbol{x}^\top \widetilde{\boldsymbol{q}} - \sum_{w\in\mathcal{W}} \hat{s}_w \mathbb{E}_{\mathbb{P}_w} \left[\boldsymbol{x}^\top \widetilde{\boldsymbol{q}} \right] \right]_+^u \right)^{1/u} \right] \\
&= \sup_{\mathbb{P}_w\in\mathcal{P}^w: w\in\mathcal{W}} \left[\sum_{w\in\mathcal{W}} \hat{s}_w \boldsymbol{x}^\top \boldsymbol{\mu}^w + \alpha \left(\sum_{w\in\mathcal{W}} \hat{s}_w \mathbb{E}_{\mathbb{P}_w} \left[\boldsymbol{x}^\top \widetilde{\boldsymbol{q}} - \sum_{w\in\mathcal{W}} \hat{s}_w \boldsymbol{x}^\top \boldsymbol{\mu}^w \right]_+^u \right)^{1/u} \right] \\
&= \sum_{w\in\mathcal{W}} \hat{s}_w \boldsymbol{x}^\top \boldsymbol{\mu}^w + \alpha \sup_{\mathbb{P}_w\in\mathcal{P}^w: w\in\mathcal{W}} \left(\sum_{w\in\mathcal{W}} \hat{s}_w \mathbb{E}_{\mathbb{P}_w} \left[\boldsymbol{x}^\top \widetilde{\boldsymbol{q}} - \sum_{w\in\mathcal{W}} \hat{s}_w \boldsymbol{x}^\top \boldsymbol{\mu}^w \right]_+^u \right)^{1/u} \\
&= \sum_{w\in\mathcal{W}} \hat{s}_w \boldsymbol{x}^\top \boldsymbol{\mu}^w + \alpha \left(\sup_{\mathbb{P}_w\in\mathcal{P}^w: w\in\mathcal{W}} \sum_{w\in\mathcal{W}} \hat{s}_w \mathbb{E}_{\mathbb{P}_w} \left[\boldsymbol{x}^\top \widetilde{\boldsymbol{q}} - \sum_{w\in\mathcal{W}} \hat{s}_w \boldsymbol{x}^\top \boldsymbol{\mu}^w \right]_+^u \right)^{1/u} \\
&= \sum_{w\in\mathcal{W}} \hat{s}_w \boldsymbol{x}^\top \boldsymbol{\mu}^w + \alpha \left(\sum_{w\in\mathcal{W}} \hat{s}_w \sup_{\mathbb{P}_w\in\mathcal{P}^w} \mathbb{E}_{\mathbb{P}_w} \left[\boldsymbol{x}^\top \widetilde{\boldsymbol{q}} - \sum_{w\in\mathcal{W}} \hat{s}_w \boldsymbol{x}^\top \boldsymbol{\mu}^w \right]_+^u \right)^{1/u}
\end{aligned}$$

The second identity follows from the rectangularity of $\mathcal{P}$ where $\mathcal{P}^w$ is as defined in (3.7). The third identity holds because $\mathcal{S}$ is a singleton. The fourth identity holds from the definition of $\mathbb{E}_{\mathbb{P}_w}$. Since $u \geqslant 1$, $1/u \in (0,1]$. Note that the function $x \mapsto x^{\frac{1}{u}}$ is monotonically increasing for $x \in \mathbb{R}_+$. The sixth identity then follows. The final identity holds because $\widehat{\boldsymbol{s}}$ is independent of $\mathcal{P}^w$.

Notice that the function $\left[\boldsymbol{x}^\top \widetilde{\boldsymbol{q}} - \sum_{w\in\mathcal{W}} \hat{s}_w \boldsymbol{x}^\top \boldsymbol{\mu}^w\right]_+^u$ is convex, hence $\sup_{\mathbb{P}\in\mathcal{P}} \mathbb{E}_{\mathbb{P}} \left[\boldsymbol{x}^\top \widetilde{\boldsymbol{q}} - \sum_{w\in\mathcal{W}} \hat{s}_w \boldsymbol{x}^\top \boldsymbol{\mu}^w\right]_+^u$ satisfies the assumptions of Theorem 3.15. Thus the worst-case distribution is the $W(2n+1)$-point distribution $\mathbb{P}^\star = \sum_{w\in\mathcal{W}} \sum_{j=1}^{2n+1} \hat{s}_w p_{wj}^\star \delta_{\boldsymbol{q}_{wj}^\star} \in \mathcal{P}$ that is independent of α, u and $\boldsymbol{x}$, and $p_{wj}^\star, \boldsymbol{q}_{wj}^\star$ for $w \in \mathcal{W}$ and $j = 1, \ldots, 2n+1$ are obtained from Algorithm 2 in Appendix B. Therefore, we have

$$\sup_{\mathbb{P}_w\in\mathcal{P}^w} \mathbb{E}_{\mathbb{P}_w} \left[\boldsymbol{x}^\top \widetilde{\boldsymbol{q}} - \sum_{w\in\mathcal{W}} \hat{s}_w \boldsymbol{x}^\top \boldsymbol{\mu}^w \right]_+^u = \sum_{j=1}^{2n+1} p_{wj}^\star \left[\sum_{i\in V_C} x_i q_{wji}^\star - \sum_{w\in\mathcal{W}} \hat{s}_w \boldsymbol{x}^\top \boldsymbol{\mu}^w \right]_+^u$$

which implies that

$$\rho_{\text{MSD}}(\boldsymbol{x}^\top \widetilde{\boldsymbol{q}}) = \sum_{w \in \mathcal{W}} \hat{s}_w \boldsymbol{x}^\top \boldsymbol{\mu}^w + \alpha \left(\sum_{w \in \mathcal{W}} \hat{s}_w \sum_{j=1}^{2n+1} p^\star_{wj} \left[\sum_{i \in V_C} x_i q^\star_{wji} - \sum_{w \in \mathcal{W}} \hat{s}_w \boldsymbol{x}^\top \boldsymbol{\mu}^w \right]_+^u \right)^{\frac{1}{u}}. \quad \blacksquare$$

Lemma 3.37 (Underperformance Risk Index) *The underperformance fulfillment risk index ρ_{URI} with*

$$\rho_{\text{URI}}(\boldsymbol{x}^\top \widetilde{\boldsymbol{q}}) = \inf \left\{ \frac{1}{\alpha} \ : \ \sup_{\mathbb{P} \in \mathcal{P}} \psi_{\mathbb{P}}(\alpha(\boldsymbol{x}^\top \widetilde{\boldsymbol{q}} - \overline{\rho})) \leqslant 0, \ \alpha > 0 \right\}$$

where $\psi_{\mathbb{P}}$ is a monotone, translation invariant, convex risk measure that can be expressed as the expectation of a convex function and $\boldsymbol{x}^\top \widetilde{\boldsymbol{q}} - \overline{\rho}$ is the excess demand over an acceptable threshold $\overline{\rho}$, can be evaluated using bisection search, with an initial computation of time $\mathcal{O}(n^2 W)$ that needs to be executed once per 2VF(d) *instance. Moreover, the underperformance risk index is monotone, convex and subadditive.*

Proof of Lemma 3.37. By Definition 3 of [HLQS15], ρ_{URI} is monotone, convex and positive homogeneous. Convexity and positive homogeneity of ρ_{URI} imply that ρ_{URI} is subadditive. Fix an ambiguity set $\mathcal{P}$ of the form (3.6) with $\mathcal{S} = \{\widehat{\boldsymbol{s}}\}$, and $\boldsymbol{x} \in [0,1]^n$. Following from our assumption that $\psi_{\mathbb{P}}$ can be expressed as the expectation of a convex function, we have $\sup_{\mathbb{P} \in \mathcal{P}} \psi_{\mathbb{P}}(\alpha \boldsymbol{x}^\top \widetilde{\boldsymbol{q}}) = \sup_{\mathbb{P} \in \mathcal{P}} \mathbb{E}_{\mathbb{P}} f(\alpha(\boldsymbol{x}^\top \widetilde{\boldsymbol{q}} - \overline{\rho}))$ where f is convex. Since the assumptions of Theorem 3.15 are satisfied, the worst case distribution is the $W(2n+1)$-point probability distribution $\mathbb{P}^\star = \sum_{w \in \mathcal{W}} \hat{s}_w \sum_{j=1}^{2n+1} p^\star_{wj} \delta_{\boldsymbol{q}^\star_{wj}}$ where $p^\star_{wj}, \boldsymbol{q}^\star_{wj}$ for $w \in \mathcal{W}$ and $j = 1, \ldots, 2n+1$ are obtained from Algorithm 2 in Appendix B. Thus, we have $\sup_{\mathbb{P} \in \mathcal{P}} \psi_{\mathbb{P}}(\alpha(\boldsymbol{x}^\top \widetilde{\boldsymbol{q}} - \overline{\rho})) = \sup_{\mathbb{P} \in \mathcal{P}} \mathbb{E}_{\mathbb{P}} f(\alpha(\boldsymbol{x}^\top \widetilde{\boldsymbol{q}} - \overline{\rho})) = \sum_{w \in \mathcal{W}} \hat{s}_w \sum_{j=1}^{2n+1} p^\star_{wj} f(\alpha(\sum_{i \in V_C} x_i q^\star_{wji} - \overline{\rho}))$. Thus, we have

$$\begin{aligned} \rho_{\text{URI}}(\boldsymbol{x}^\top \widetilde{\boldsymbol{q}}) &= \inf \left\{ \tfrac{1}{\alpha} \ : \ \sup_{\mathbb{P} \in \mathcal{P}} \psi_{\mathbb{P}} \left(\alpha(\boldsymbol{x}^\top \widetilde{\boldsymbol{q}} - \overline{\rho}) \right) \leqslant 0, \ \alpha > 0 \right\} \\ &= \inf \left\{ \tfrac{1}{\alpha} \ : \ \textstyle\sum_{w \in \mathcal{W}} \hat{s}_w \sum_{j=1}^{2n+1} p^\star_{wj} f \left(\alpha(\sum_{i \in V_C} x_i q^\star_{wji} - \overline{\rho}) \right) \leqslant 0, \ \alpha > 0 \right\} \end{aligned}$$

The function f in the constraint is convex in α. Thus we can use bisection search to find the smallest α to ϵ-accuracy. The bisection search requires $\mathcal{O}(\log(\overline{\alpha}(f)/\epsilon))$ iterations where $\overline{\alpha}$

denotes the upper bound on the search region for α, and each iteration requires $\mathcal{O}(M)$ time to evaluate the value of the LHS of the constraint. We now find $\overline{\alpha}$. To this end, note that for a fixed $\alpha > 0$ by the monotone property of $\psi_{\mathbb{P}}$ we have

$$\psi_{\delta_{\underline{\boldsymbol{q}}^w}}\left(\alpha(\boldsymbol{x}^\top \underline{\boldsymbol{q}}^w - \overline{\rho})\right) \leqslant \sup_{\mathbb{P}_w \in \mathcal{P}^w} \psi_{\mathbb{P}_w}\left(\alpha(\boldsymbol{x}^\top \widetilde{\boldsymbol{q}} - \overline{\rho})\right) \leqslant \psi_{\delta_{\overline{\boldsymbol{q}}^w}}\left(\alpha(\boldsymbol{x}^\top \overline{\boldsymbol{q}}^w - \overline{\rho})\right).$$

From the definition of ρ_{URI}, it follows that $\rho_{\text{URI}}(\boldsymbol{x}^\top \widetilde{\boldsymbol{q}}) \leqslant \inf\left\{\frac{1}{\alpha} : \sum_{w \in \mathcal{W}} \hat{s}_w f(\alpha(\boldsymbol{x}^\top \overline{\boldsymbol{q}}^w - \overline{\rho})) \leqslant 0\right\}$. Thus, we must have $\overline{\alpha} = \sup\left\{\alpha > 0 : \sum_{w \in \mathcal{W}} \hat{s}_w f(\alpha(\boldsymbol{x}^\top \overline{\boldsymbol{q}}^w - \overline{\rho})) \leqslant 0\right\}$ which can be evaluated using bisection search once per 2VF(d) instance. ∎

Lemma 3.38 *Let* $k^\star = \min \arg\max\{a(\boldsymbol{x}, k) : k \in K\}$. *Then* $a(\boldsymbol{x}, k^\star) = k^\star$.

Proof of Lemma 3.38. Let $k^\star = \min \arg\max\{a(\boldsymbol{x}, k) : k \in K\}$. If $k^\star = 1$, we have $a(\boldsymbol{x}, k^\star) = 1$ by definition. Next, consider the case $k^\star \geqslant 2$. Let $Z_k = \lceil \sup_{\mathbb{P} \in \mathcal{P}} \mathbb{P}\text{-VaR}_{1-(k-1)\epsilon}\left(\boldsymbol{x}^\top \widetilde{\boldsymbol{q}}\right)/B \rceil$. Then $a(\boldsymbol{x}, k) = \min\{k, Z_k\}$. We need to show that $k^\star \leqslant Z_{k^\star}$.

Assume to the contrary that $Z_{k^\star} < k^\star$ which implies that $a(\boldsymbol{x}, k^\star) = Z_{k^\star}$. Then $Z_{k^\star} \leqslant (k^\star - 1)$ because $Z_{k^\star} \in \mathbb{Z}_+$. Further, note that $Z_{k^\star} \leqslant Z_{k^\star - 1}$ because $\sup_{\mathbb{P} \in \mathcal{P}} \mathbb{P}\text{-VaR}_{1-(k^\star-1)\epsilon}\left(\boldsymbol{x}^\top \widetilde{\boldsymbol{q}}\right) \leqslant \sup_{\mathbb{P} \in \mathcal{P}} \mathbb{P}\text{-VaR}_{1-(k^\star-1-1)\epsilon}\left(\boldsymbol{x}^\top \widetilde{\boldsymbol{q}}\right)$. Thus, we have the following two relationships: $Z_{k^\star} \leqslant (k^\star - 1) < k^\star$ and $Z_{k^\star} \leqslant Z_{k^\star - 1}$. The following two cases arise:

Case(i): $(k^\star - 1) \leqslant Z_{k^\star - 1}$. We have either $Z_{k^\star} \leqslant (k^\star - 1) \leqslant Z_{k^\star - 1} \leqslant k^\star$ or $Z_{k^\star} \leqslant (k^\star - 1) < k^\star \leqslant Z_{k^\star - 1}$. Clearly, $a(\boldsymbol{x}, k^\star - 1) = (k^\star - 1) \geqslant a(\boldsymbol{x}, k^\star) = Z_{k^\star}$. This implies that $k^\star - 1 \in \arg\max\{a(\boldsymbol{x}, k) : k \in K\}$. This violates the optimality of $k^\star = \min \arg\max\{a(\boldsymbol{x}, k) : k \in K\}$ because $k^\star - 1 < k^\star$.

Case(ii): $(k^\star - 1) > Z_{k^\star - 1}$. Following from $Z_{k^\star} \leqslant (k^\star - 1) < k^\star$ and $Z_{k^\star} \leqslant Z_{k^\star - 1}$, we have $Z_{k^\star} \leqslant Z_{k^\star - 1} < (k^\star - 1) < k^\star$. We have $a(\boldsymbol{x}, k^\star - 1) = Z_{k^\star - 1} \geqslant a(\boldsymbol{x}, k^\star) = Z_{k^\star}$ which implies that $k^\star - 1 \in \arg\max\{a(\boldsymbol{x}, k) : k \in K\}$. This violates the optimality of $k^\star = \min \arg\max\{a(\boldsymbol{x}, k) : k \in K\}$ because $k^\star - 1 < k^\star$. ∎

Lemma 3.39 *Let* $k^\star = \min\arg\max\{a(\boldsymbol{x}, k) : k \in K\}$. *Then* $a(\boldsymbol{x}, k^\star + 1) \leqslant k^\star$, *that is,* $\sup_{\mathbb{P}\in\mathcal{P}} \mathbb{P}\text{-VaR}_{1-k^\star\epsilon}\left(\boldsymbol{x}^\top\widetilde{\boldsymbol{q}}\right) \leqslant k^\star B$.

Proof of Lemma 3.39. From the definition of $k^\star$ we have $a(\boldsymbol{x}, k^\star + 1) \leqslant \max\{a(\boldsymbol{x}, k) : k \in K\} = a(\boldsymbol{x}, k^\star)$. From Lemma 3.38, we have $a(\boldsymbol{x}, k^\star) = k^\star$. This means that

$$\min\left\{(k^\star + 1), \left\lceil \sup_{\mathbb{P}\in\mathcal{P}} \mathbb{P}\text{-VaR}_{1-k^\star\epsilon}\left(\boldsymbol{x}^\top\widetilde{\boldsymbol{q}}\right)/B\right\rceil\right\} \leqslant k^\star.$$

But $k^\star + 1 > k^\star$. Hence, we have $\sup_{\mathbb{P}\in\mathcal{P}} \mathbb{P}\text{-VaR}_{1-k^\star\epsilon}\left(\boldsymbol{x}^\top\widetilde{\boldsymbol{q}}\right) \leqslant k^\star B$. ∎

Lemma 3.40 *For any two random variables* $\tilde{X}_1$ *and* $\tilde{X}_2$*, we have* $\sup_{\mathbb{P}\in\mathcal{P}} \mathbb{P}\text{-VaR}_{1-\epsilon_1-\epsilon_2}(\tilde{X}_1 + \tilde{X}_2) \leqslant \sup_{\mathbb{P}\in\mathcal{P}} \mathbb{P}\text{-VaR}_{1-\epsilon_1}(\tilde{X}_1) + \sup_{\mathbb{P}\in\mathcal{P}} \mathbb{P}\text{-VaR}_{1-\epsilon_2}(\tilde{X}_2)$.

Proof of Lemma 3.40. Notice that $\sup_{\mathbb{P}\in\mathcal{P}} \mathbb{P}\text{-VaR}_{1-\epsilon_1-\epsilon_2}(\tilde{X}_1+\tilde{X}_2) \leqslant \sup_{\mathbb{P}\in\mathcal{P}} \mathbb{P}\text{-VaR}_{1-\epsilon_1}(\tilde{X}_1)+ \sup_{\mathbb{P}\in\mathcal{P}} \mathbb{P}\text{-VaR}_{1-\epsilon_2}(\tilde{X}_2)$ holds if and only if $\mathbb{P}(\tilde{X}_1 + \tilde{X}_2 \leqslant \varphi_1 + \varphi_2) \geqslant 1 - \epsilon_1 - \epsilon_2$ holds for all $\mathbb{P} \in \mathcal{P}$ where $\varphi_1 = \sup_{\mathbb{P}\in\mathcal{P}} \mathbb{P}\text{-VaR}_{1-\epsilon_1}(\tilde{X}_1)$ and $\varphi_2 = \sup_{\mathbb{P}\in\mathcal{P}} \mathbb{P}\text{-VaR}_{1-\epsilon_2}(\tilde{X}_2)$.

Fix $\mathbb{P} \in \mathcal{P}$. We observe the following:

$$\begin{aligned}
\mathbb{P}(\tilde{X}_1 + \tilde{X}_2 \leqslant \varphi_1 + \varphi_2) &\geqslant \mathbb{P}(\tilde{X}_1 \leqslant \varphi_1 \cap \tilde{X}_2 \leqslant \varphi_2) \\
&= 1 - \mathbb{P}(\tilde{X}_1 > \varphi_1 \cup \tilde{X}_2 > \varphi_2) \\
&\geqslant 1 - [\mathbb{P}(\tilde{X}_1 > \varphi_1) + \mathbb{P}(\tilde{X}_2 > \varphi_2)] \\
&= 1 - [1 - \mathbb{P}(\tilde{X}_1 \leqslant \varphi_1) + 1 - \mathbb{P}(\tilde{X}_2 \leqslant \varphi_2)] \\
&= 1 - \epsilon_1 - \epsilon_2.
\end{aligned}$$

The second inequality follows from Bonferroni inequality. Since this holds for any arbitrary $\mathbb{P} \in \mathcal{P}$, it holds for all $\mathbb{P} \in \mathcal{P}$ thus proving the statement of the lemma. ∎

Lemma 3.41 *For an ambiguity set of the form* (3.6), φ_{mVaR} *satisfies monotonicity.*

Proof of Lemma 3.41. Consider $\boldsymbol{x}, \boldsymbol{y} \in [0,1]^n$ satisfying $\boldsymbol{x} \leqslant \boldsymbol{y}$. Fix some $k \in K$. Since $\mathbb{P}$-VaR is monotone [FS10, p. 3], and $\widetilde{\boldsymbol{q}} \geqslant \mathbf{0}$ $\mathbb{P}$-a.s., we have $\lceil \sup_{\mathbb{P}\in\mathcal{P}} \mathbb{P}\text{-VaR}_{1-(k-1)\epsilon}(\boldsymbol{x}^\top \widetilde{\boldsymbol{q}})/B \rceil \leqslant \lceil \sup_{\mathbb{P}\in\mathcal{P}} \mathbb{P}\text{-VaR}_{1-(k-1)\epsilon}(\boldsymbol{y}^\top \widetilde{\boldsymbol{q}})/B \rceil$ following from Lemma 3.28. It follows that

$$\min\left\{k, \left\lceil \sup_{\mathbb{P}\in\mathcal{P}} \mathbb{P}\text{-VaR}_{1-(k-1)\epsilon}(\boldsymbol{x}^\top \widetilde{\boldsymbol{q}})/B \right\rceil\right\} \leqslant \min\left\{k, \left\lceil \sup_{\mathbb{P}\in\mathcal{P}} \mathbb{P}\text{-VaR}_{1-(k-1)\epsilon}(\boldsymbol{y}^\top \widetilde{\boldsymbol{q}})/B \right\rceil\right\}.$$

Since this holds for any $k \in K$, it follows that

$$\min\left\{k, \left\lceil \sup_{\mathbb{P}\in\mathcal{P}} \mathbb{P}\text{-VaR}_{1-(k-1)\epsilon}(\boldsymbol{x}^\top \widetilde{\boldsymbol{q}})/B \right\rceil\right\} \leqslant \max_{k\in K} \min\left\{k, \left\lceil \sup_{\mathbb{P}\in\mathcal{P}} \mathbb{P}\text{-VaR}_{1-(k'-1)\epsilon}(\boldsymbol{y}^\top \widetilde{\boldsymbol{q}})/B \right\rceil\right\} \quad \forall k \in K.$$

Therefore, we must have

$$\max_{k\in K} \min\left\{k, \left\lceil \sup_{\mathbb{P}\in\mathcal{P}} \mathbb{P}\text{-VaR}_{1-(k-1)\epsilon}(\boldsymbol{x}^\top \widetilde{\boldsymbol{q}})/B \right\rceil\right\} \leqslant \max_{k\in K} \min\left\{k, \left\lceil \sup_{\mathbb{P}\in\mathcal{P}} \mathbb{P}\text{-VaR}_{1-(k-1)\epsilon}(\boldsymbol{y}^\top \widetilde{\boldsymbol{q}})/B \right\rceil\right\}. \quad \blacksquare$$

Lemma 3.42 *For an ambiguity set of the form* (3.6), φ_{mVaR} *satisfies subadditivity.*

Proof of Lemma 3.42. To prove subadditivity of φ_{mVaR}, we need to show that for all $\boldsymbol{x}_1, \boldsymbol{x}_2 \in [0,1]^n$ satisfying $\boldsymbol{x}_1 + \boldsymbol{x}_2 \leqslant \mathbf{e}$, we have

$$\varphi_{\text{mVaR}}(\boldsymbol{x}_1+\boldsymbol{x}_2) = B \max_{k\in K} a(\boldsymbol{x}_1+\boldsymbol{x}_2, k) \leqslant B \max_{k\in K} a(\boldsymbol{x}_1, k) + B \max_{k\in K} a(\boldsymbol{x}_2, k) = \varphi_{\text{mVaR}}(\boldsymbol{x}_1) + \varphi_{\text{mVaR}}(\boldsymbol{x}_2). \tag{3.9}$$

From Lemma 3.38, we have $\max\{a(\boldsymbol{x}_1, k) : k \in K\} = k_1^\star$ and $\max\{a(\boldsymbol{x}_2, k) : k \in K\} = k_2^\star$ for some $k_1^\star, k_2^\star \in K$. Then $\varphi_{\text{mVaR}}(\boldsymbol{x}_1) = k_1^\star B$ and $\varphi_{\text{mVaR}}(\boldsymbol{x}_2) = k_2^\star B$.

Assume to the contrary that φ_{mVaR} violates subadditivity. Then there exist $\boldsymbol{x}_1, \boldsymbol{x}_2 \in [0,1]^n$

such that

$$
\begin{aligned}
& \varphi_{\mathrm{mVaR}}(\boldsymbol{x}_1 + \boldsymbol{x}_2) > \varphi_{\mathrm{mVaR}}(\boldsymbol{x}_1) + \varphi_{\mathrm{mVaR}}(\boldsymbol{x}_2) \\
\iff \quad & B \max_{k \in K} a(\boldsymbol{x}_1 + \boldsymbol{x}_2, k) > (k_1^\star + k_2^\star) B \\
\iff \quad & \max_{k \in K} a(\boldsymbol{x}_1 + \boldsymbol{x}_2, k) > k_1^\star + k_2^\star \\
\iff \quad & \exists k \in K \ : \ a(\boldsymbol{x}_1 + \boldsymbol{x}_2, k) > k_1^\star + k_2^\star \\
\iff \quad & \exists k \in \{k_1^\star + k_2^\star + 1, \dots, m\} \ : \ a(\boldsymbol{x}_1 + \boldsymbol{x}_2, k) > k_1^\star + k_2^\star \\
\iff \quad & a(\boldsymbol{x}_1 + \boldsymbol{x}_2, k') > k_1^\star + k_2^\star \ \text{ for some } k_1^\star + k_2^\star + 1 \leqslant k' \leqslant m \\
\iff \quad & \min \left\{ k', \left\lceil \sup_{\mathbb{P} \in \mathcal{P}} \mathbb{P}\text{-VaR}_{1-(k'-1)\epsilon} \left((\boldsymbol{x}_1 + \boldsymbol{x}_2)^\top \widetilde{\boldsymbol{q}} \right) / B \right\rceil \right\} > k_1^\star + k_2^\star \ \text{ for some } k_1^\star + k_2^\star + 1 \leqslant k' \leqslant m \\
\iff \quad & \left\lceil \sup_{\mathbb{P} \in \mathcal{P}} \mathbb{P}\text{-VaR}_{1-(k'-1)\epsilon} \left((\boldsymbol{x}_1 + \boldsymbol{x}_2)^\top \widetilde{\boldsymbol{q}} \right) / B \right\rceil > k_1^\star + k_2^\star \ \text{ for some } k_1^\star + k_2^\star + 1 \leqslant k' \leqslant m \\
\iff \quad & \sup_{\mathbb{P} \in \mathcal{P}} \mathbb{P}\text{-VaR}_{1-(k'-1)\epsilon} \left((\boldsymbol{x}_1 + \boldsymbol{x}_2)^\top \widetilde{\boldsymbol{q}} \right) / B > k_1^\star + k_2^\star \ \text{ for some } k_1^\star + k_2^\star + 1 \leqslant k' \leqslant m \\
\iff \quad & \sup_{\mathbb{P} \in \mathcal{P}} \mathbb{P}\text{-VaR}_{1-(k'-1)\epsilon} \left((\boldsymbol{x}_1 + \boldsymbol{x}_2)^\top \widetilde{\boldsymbol{q}} \right) > (k_1^\star + k_2^\star) B \ \text{ for some } k_1^\star + k_2^\star + 1 \leqslant k' \leqslant m
\end{aligned}
\tag{3.10}
$$

Let $\epsilon_1 = k_1^\star \epsilon$ and $\epsilon_2 = k_2^\star \epsilon$. Since we assumed that $\epsilon < 1/m$, for $k_1, k_2 \in K$ it follows that $\epsilon_1, \epsilon_2 \in (0, 1)$. We have

$$
\begin{aligned}
\sup_{\mathbb{P} \in \mathcal{P}} \mathbb{P}\text{-VaR}_{1-(k'-1)\epsilon} \left((\boldsymbol{x}_1 + \boldsymbol{x}_2)^\top \widetilde{\boldsymbol{q}} \right) & \leqslant \sup_{\mathbb{P} \in \mathcal{P}} \mathbb{P}\text{-VaR}_{1-(k_1^\star + k_2^\star)\epsilon} \left((\boldsymbol{x}_1 + \boldsymbol{x}_2)^\top \widetilde{\boldsymbol{q}} \right) \\
& = \sup_{\mathbb{P} \in \mathcal{P}} \mathbb{P}\text{-VaR}_{1-\epsilon_1-\epsilon_2} \left((\boldsymbol{x}_1 + \boldsymbol{x}_2)^\top \widetilde{\boldsymbol{q}} \right) \\
& \leqslant \sup_{\mathbb{P} \in \mathcal{P}} \mathbb{P}\text{-VaR}_{1-\epsilon_1} \left(\boldsymbol{x}_1^\top \widetilde{\boldsymbol{q}} \right) + \sup_{\mathbb{P} \in \mathcal{P}} \mathbb{P}\text{-VaR}_{1-\epsilon_2} \left(\boldsymbol{x}_2^\top \widetilde{\boldsymbol{q}} \right) \\
& \leqslant (k_1^\star + k_2^\star) B
\end{aligned}
$$

The first inequality above holds because $k' \geqslant k_1^\star + k_2^\star + 1$. The second inequality above follows from Lemma 3.40, while the third inequality follows from Lemma 3.39. Clearly, this violates (3.10) above, and we have that φ_{mVaR} is subadditive. This concludes the proof. ∎

Chapter 4

Optimal Elective Scheduling during the SARS-CoV-2 Pandemic

4.1 Introduction

In the previous two chapters of this thesis, single-stage decision making problems under uncertainty were studied. The chapters focused on the vehicle routing problem under uncertainty in particular. In these chapters, the proposed models relax the assumptions in literature, and develop solution algorithms that scale better than has been proposed in literature so far. This chapter studies the multi-stage decision-making problem under uncertainty using the dynamic programming paradigm. As described in Chapter 1, this approach suffers from the curse of dimensionality. This chapter aims to develop a model that can produce approximate solutions of good quality to large-scale dynamic programming problems.

The first wave of COVID-19 posed challenges to healthcare systems around the world, and created opportunities for applying our proposed framework. The following paragraphs describe in detail the research problems that arose in the light of COVID-19, and how this chapter contributes towards solving those problems.

Across health systems globally, hospitals struggled to meet the demand surges caused by the SARS-CoV-2 (hereafter COVID) pandemic. Despite the expansion of hospital capacity (*e.g.,* through field hospitals; [MSC+20] and [CDL+21]) and the implementation of lockdown measures to smooth over time the pressures on care provision, policy makers were faced with an unprecedented challenge in managing scarce hospital capacity and treating non-COVID patients whilst maintaining the ability to respond to any potential future increases in demand for COVID care.

In this context, care prioritization policies become vital to mitigate the morbidity and mortality associated with surges of demand overflowing the existing capacity. prioritization policies are common in health systems where the available resources are insufficient to cope with significant seasonal demand peaks [RMA+19]. While those pressures are normally short-lived and do not require a drastic change in care prioritization or investments in extra capacity, the pressures of the COVID pandemic are more severe due to its prolonged duration, the uncertainty in the number of COVID patients that require care, the timing of the demand surges, the intensity of resource usage required to address the needs of COVID patients and the fact that the pandemic impacts the entire population. In response, several countries deployed a wide range of prioritization policies to delay access to care for some patients who are perceived as requiring less urgent treatment [NHS20d, NIC20]. The National Health Service (NHS) in England, for example, provided national level guidance on the cancellation of non-urgent elective (*i.e.*, planned) procedures as well as a prioritization to intensive care of COVID patients below the age of 65 and with a high capacity to benefit [GFP20]. The ethical guidelines published by the German Interdisciplinary Association for Intensive Care and Emergency Medicine discuss the prioritization to intensive care of COVID patients who do not suffer from severe respiratory illness [DIV20]. The Italian College of Anesthesia, Analgesia, Resuscitation and Intensive Care advised the prioritization to intensive care of COVID patients above 70 years of age that do not have more than one admission per year for a range of diseases [RBG+20]. We refer the reader to [JBA20] for a review of the prioritization guidelines applied in different countries during 2020.

The aforementioned blanket policies tend to prioritize COVID patients in detriment to patients with other diseases without systematically accounting for the trade-offs between the provision of COVID and non-COVID care. For example, non-prioritized patients that see their planned care postponed or cancelled might have a higher capacity to benefit from treatment than those prioritized; also, these patients' diseases might progress considerably while they wait for care, and they may subsequently require emergency or more complex treatment, thus creating further pressures on hospital capacity. As a result, blanket policies are likely to impact morbidity and mortality as well as increase the financial burden on health systems. Against this backdrop, the Nuffield Council on Bioethics, the UK's main health and healthcare ethics authority, urged policy makers to develop optimal tools and national guidance to best allocate scarce hospital capacity to minimize the detrimental impact the pandemic has on population health [The20].

In this chapter, we develop an optimization-based prioritization scheme that schedules patients into general & acute (G&A) as well as critical care (CC) so as to minimize overall years of life lost (YLL),[1] hospital costs or a combination of both objectives. We consider a national-level scale (rather than an individual hospital) in order to inform strategic public health policy-making, which is particularly relevant in the case of a pandemic affecting an entire country. Our optimization scheme is dynamic and considers weekly patient cohorts subdivided into different patient groups (defined by disease, age group and admission method: elective and emergency) over a 52-weeks' time horizon. We model each patient as a dynamic program (DP) whose states encode the patient's health status (proxied by the categorization elective/emergency, recovered or deceased) and treatment condition (waiting for treatment, in G&A or in CC), whose actions describe the treatment options (admit or move to G&A or to CC, deny care or discharge from hospital), whose transition probabilities characterize the stochastic evolution of the patient's health and whose rewards amount to the years of life gained, the hospital costs saved, or a combination thereof. Our model simultaneously optimizes the treatment of all patients while accounting for capacity constraints on the supply side, including the availability of G&A as well as CC beds and staff (senior doctors, junior doctors and nurses). By clustering the patients into groups (defined through the same arrival time, disease type, age group and admission type) that can each be described through the same DP, we obtain a weakly coupled counting DP that records for each patient group how many patients are in a particular state,

[1] YLL quantifies the years of life lost due to premature deaths, accounting for the age at which deaths occur.

and how many times which action is applied to those patients. We show that this weakly coupled counting DP is amenable to a fluid approximation that gives rise to a tractable linear program (LP). Moreover, the solutions to this LP allow us to recover near-optimal solutions to the weakly coupled counting DP with high probability. We demonstrate the power of our modeling framework in a case study of the NHS in England, where we cluster approximately 10 million patients (the entire population in need of care) into 3,120 patient groups whose admission we manage over the course of one year in weekly granularity.

The contributions of this chapter may be summarized as follows.

(i) We develop the concept of weakly coupled counting DPs, which constitute large-scale DPs that are amenable to a tractable fluid relaxation. The fluid relaxation can be solved as an LP, and it allows recovering high-quality solutions to the weakly coupled counting DP.

(ii) We apply our findings to a case study of the NHS in England, where we show how weakly coupled counting DPs allow to prioritize access to elective and emergency care.

While the concept of weakly coupled counting DPs was developed with the outlined healthcare application in mind, we emphasize its applicability in other applications as well, such as B2C marketing where current and prospective customers should be assigned to marketing campaigns based on their purchase likelihood. Here, customers can be modelled as DPs whose states encode the current product portfolio as well as preferences learnt from previous campaigns, and whose actions describe the inclusion to (or exclusion from) a particular campaign.

The remainder of the chapter is organized as follows. We present the literature review in Section 4.2. We introduce weakly coupled counting DPs, which will serve as our model of the health system, in Section 4.3.1. Section 4.3.2 shows that weakly coupled counting DPs are amenable to a fluid approximation that allows us to obtain high-quality solutions in polynomial time. Section 4.4 discusses our case study of the NHS in England, and reports on numerical results for this case study. Section 4.5 concludes with a discussion of possible extensions to our model.

4.2 Literature Review

The methodology and application of this chapter builds upon a rich body of medical and methodological literature, which we review in the remainder of this section.

Under normal operation, elective care is typically scheduled via prioritization schemes [MCP03, DRR+20]. Recent months have seen a rapidly growing body of literature that discusses the scheduling of elective care surgeries in light of the COVID pandemic. In contrast to our work, which studies hospital care in a broader sense, the majority of that literature focuses on prioritization of COVID care (*e.g.*, [PWL+20]) or surgeries (mostly for cancer), with most papers evaluating the impact of the pandemic on elective surgeries [FIS+20, NCH20, SJB+20, YKD+20], proposing guidelines based on best practices in individual hospitals [AFS20, ESL+20, TTK+20] or reviewing the guidelines of national authorities [Bur20]. These guidelines are developed by domain experts and tend to be qualitative in nature [MF20, SHG+20]. In contrast, [BPS+20], [BLM+20], [DGN+20], [GCF+20] and [VSR+20] employ machine learning techniques (such as support vector machines, tree ensembles and neural networks) to estimate the mortality risk of COVID patients, which can subsequently be used as a proxy of need for patient prioritization. While these contributions are important, they highlight prioritization schemes within a specific disease or sub-group of patients or care settings within a single hospital, and they are static and thus consider neither the dynamic nature of surges in demand nor the complexity of the dynamic needs of patients. In contrast, we propose a national prioritization scheme across all disease groups that accounts for future demand surges and capacity fluctuations as well as the evolution of the patients' needs over the course of the pandemic, which to the best of our best knowledge has not been proposed so far.

As an alternative to static prioritization schemes, the operations research literature has studied the dynamic management of G&A and CC capacity via admissions and discharge policies. For example, [BK11] and [MQZ+15] propose capacity management policies for G&A beds using queueing theory and robust optimization, [CFBE12], [KCO+15] and [OAZ20] develop capacity management policies for CC beds via queueing theory, DPs and simulation, and [HAVO11] and [SHDH+19] study hospital-wide capacity management policies using DPs. These approaches aim to optimize the often conflicting goals of short-term and long-term patient welfare as well as hospital costs, subject to constraints on the available resources. In contrast to our work, these papers focus on individual hospitals, which allows them to model hospital operations and within-hospital patients' care pathways at a finer granularity: admissions and discharge decisions are often taken at an hourly granularity, and some models account for longer-term implications of decisions such as readmissions.

From a methodological viewpoint, our work contributes to the rich body of research on dynamic programming. Dating back to the early work of [Bel52], DPs have become one of the major paradigms to model, analyze and solve dynamic decision problems affected by uncertainty [Ber95, Put14]. Classical DPs suffer from the *curse of dimensionality* since their state and action spaces tend to grow exponentially with the problem dimension. As a result, several methodologies have been developed by different research communities to circumvent the unfavorable scalability of classical DPs through (combinations of) decomposition and approximation techniques.

Factored Markov decision processes assume that the states of a DP can be described by assignments of values to state variables that evolve and contribute to the system's rewards largely independently, and they employ dynamic Bayesian networks to compactly represent the stochastic state evolution. The resulting optimization problems, while still exponential in size, can often be approximated well through sparse value function approximations that give rise to polynomial-time solution schemes [BDG95, GKP01, GKP$^+$03]. Translated into our context, however, the state of a factored Markov decision process would have to record the health and treatment state of millions of patients, which appears to be beyond the current state of the art in that domain (which seems to scale to tens or hundreds of state variables). Moreover, factored Markov decision processes do not offer a decomposition in terms of the actions, which is crucial in our context where the policy maker has to decide upon the treatment of each patient.

The literature on multi-armed and restless bandit problems studies large-scale DPs where independent components are coupled through a small number of linking constraints [GGW11]. Since bandit problems typically assume that only one or a few arms are pulled in every round, which amounts to a single or a few patients' treatment conditions being revised at any time point, however, their fundamental modeling assumptions appear to be at odds with our intentions.

Approximate dynamic programs offer a very general methodology to control large-scale DPs by approximating the value function through a linear combination of basis functions [BT96, Pow07]. While this allows to drastically reduce the number of decision variables, the number of constraints remains exponential and thus necessitates the use of additional approximation schemes such as constraint sampling [DFVR04]. More importantly, approximate dynamic programs do not exploit any specific problem structure, which is an essential feature in our problem where the different patients evolve largely independently.

More recently, approximate dynamic programs have been adapted by [Haw03] and [AM08] to weakly coupled DPs, which explicitly account for the decomposability of the overall system into largely independently evolving constituent DPs that are coupled by a small number of resource constraints. [AM08] analyze the tightness of two approximation schemes, namely a Lagrangian relaxation that dualizes the resource constraints and an LP that imposes an additively separable value function, and they propose solution schemes based on stochastic subgradient descent and column generation. In our context, the resulting problems would be very large in scale as they would contain millions of constituent DPs, and it is unlikely that approximation guarantees similar to ours could be obtained as the constituent DPs are assumed to be pairwise different and thus cannot be aggregated to a smaller number of counting DPs.

To the best of our knowledge, the work of [BM16] is the closest to the methodology proposed in this chapter. The authors develop a fluid approximation for large-scale DPs that decompose into largely independently evolving constituent DPs. Similar to our approximation, the authors show that their approximation is a relaxation that offers an upper bound on the optimal objective value of the original problem. Their formulation, however, scales linearly in the number of constituent DPs, which in unsuitable for our problem that comprises several million patient DPs. Moreover, since their approach can model rich dependencies between the constituent DPs (as opposed to the linear resource constraints that we employ), their action space cannot describe individual actions for each DP without incurring an exponential growth in problem size.

Finally, it remains unclear whether the fluid approximation of [BM16] can offer performance guarantees comparable to the ones developed in this chapter.

Notation. For a finite set $\mathcal{X} = \{1, \dots, X\}$, we denote by $\Delta(\mathcal{X})$ the set of all probability distributions supported on $\mathcal{X}$, that is, all functions $p : \mathcal{X} \to \mathbb{R}_+$ satisfying $\sum_{x \in \mathcal{X}} p(x) = 1$. For a logical expression $\mathcal{E}$, we let $\mathbf{1}[\mathcal{E}] = 1$ if $\mathcal{E}$ is true and $\mathbf{1}[\mathcal{E}] = 0$ otherwise.

4.3 Theoretical Contributions

In this section, we introduce the concept of weakly coupled counting dynamic programs and provide a fluid approximation to allow tractable solution of the otherwise intractable problem of large-scale weakly coupled dynamic programs.

4.3.1 Weakly Coupled Counting Dynamic Programs

Section 4.3.1.1 shows how multiple DPs, each of which competes for the same set of resources, can be aggregated to a weakly coupled DP. Subsequently, Section 4.3.1.2 introduces the concept of a counting DP, which records how many DPs of a similar structure are in a particular state at any point in time. We will later use DPs to model individual patients and counting DPs to aggregate patients to patient groups with similar characteristics (arrival time, age group and disease type), respectively. Finally, we introduce weakly coupled counting DPs, which will allow us to combine multiple patient groups to represent our model of the entire health system.

4.3.1.1 Weakly Coupled Dynamic Programs

We model individual patients, which form the basis of our healthcare model, as DPs. The states of the DP record the patient's health (elective/emergency, recovered or deceased) and treatment state (waiting for treatment, in G&A or in CC). The action of the DP describe the treatment options (admit or move to G&A or to CC, deny care or discharge from hospital). Finally, the

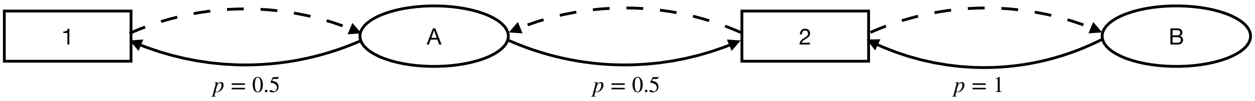

Figure 4.1: DP with two states and two actions. The rectangular (oval) nodes represent the states (actions). Each dashed line represents the choice of an action in a period t, whereas the solid lines represent the state transitions from period t to period $t+1$.

transition probabilities of the DP characterize the stochastic evolution of the patient's health, and the rewards amount to the years of life gained, the costs saved, or a combination thereof.

Definition 4.1 (DP) *For a finite time horizon $\mathcal{T} = \{1, \ldots, T\}$, a* DP *is specified by the tuple $(\mathcal{S}, \mathcal{A}, q, p, r)$, where $\mathcal{S} = \{1, \ldots, S\}$ denotes the finite state space, $\mathcal{A} = \{1, \ldots, A\}$ is the finite action space with $\mathcal{A}_t(s) \subseteq \mathcal{A}$ the admissible actions in state $s \in \mathcal{S}$ at time $t \in \mathcal{T}$, $q \in \Delta(\mathcal{S})$ are the initial state probabilities, $p = \{p_t\}_t$ with $p_t : \mathcal{S} \times \mathcal{A} \to \Delta(\mathcal{S})$, $t \in \mathcal{T}$, are the Markovian transition probabilities, and $r = \{r_t\}_t$ with $r_t : \mathcal{S} \times \mathcal{A} \to \mathbb{R}$, $t \in \mathcal{T}$, are the expected rewards.*

In a DP, a *policy* $\pi = \{\pi_t\}_t$ with $\pi_t : \mathcal{S} \to \mathcal{A}$ specifies for each time period $t \in \mathcal{T}$ and each state $s \in \mathcal{S}$ what action $\pi_t(s) \in \mathcal{A}$ is taken. A feasible policy π must satisfy $\pi_t(s) \in \mathcal{A}_t(s)$ for all $t \in \mathcal{T}$ and $s \in \mathcal{S}$. Under the policy π, a DP evolves as follows. The initial state $\tilde{s}_1$ is random and satisfies $\mathbb{P}[\tilde{s}_1 = s] = q(s)$ for $s \in \mathcal{S}$. For $t \in \mathcal{T} \backslash \{T\}$, the transitions are governed by

$$\mathbb{P}\left[\tilde{s}_{t+1} = s'\right] \;=\; \sum_{s \in \mathcal{S}} p_t(s' \mid s, \pi_t(s)) \cdot \mathbb{P}\left[\tilde{s}_t = s\right] \qquad \forall s' \in \mathcal{S}.$$

The expected total reward of a policy π is $\mathbb{E}\left[\sum_{t \in \mathcal{T}} r_t(\tilde{s}_t, \pi_t(\tilde{s}_t))\right]$.

Example 4.2 (DP) *Figure 4.1 illustrates a DP with the states* 1 *and* 2 *and the actions A (admissible in both states) and B (admissible in state* 2 *only). Under action A, the system transitions to either state with probability 1/2, whereas the system remains in state 2 if action B is taken. The expected rewards are $r_t(1, \mathrm{A}) = 0$ and $r_t(2, \mathrm{A}) = r_t(2, \mathrm{B}) = 1$. As a result, the unique optimal policy π takes action A in state 1 and action B in state 2, respectively. If the initial state probability is $\boldsymbol{q} = [0, 1]^\top$, the expected total reward of the policy is 1.*

Our healthcare model combines all individual patient DPs to a single DP that records the state of each patient while also restricting the admissible policies to those that satisfy certain resource constraints (*e.g.*, the availability of G&A and CC beds, nurses and doctors).

Definition 4.3 (Weakly Coupled DP) *For a finite set of DPs* $(\mathcal{S}_i, \mathcal{A}_i, q_i, p_i, r_i)$, $i \in \mathcal{I} = \{1, \ldots, I\}$, *over the same time horizon* $\mathcal{T} = \{1, \ldots, T\}$, *the* weakly coupled DP $(\{\mathcal{S}_i, \mathcal{A}_i, q_i, p_i, r_i\}_i)$ *is the DP* $(\mathcal{S}, \mathcal{A}, q, p, r)$ *with state space* $\mathcal{S} = \times_{i\in\mathcal{I}} \mathcal{S}_i$, *action space* $\mathcal{A} = \times_{i\in\mathcal{I}} \mathcal{A}_i$ *with* $\mathcal{A}_t(s) = \times_{i\in\mathcal{I}} \mathcal{A}_{it}(s_i)$, $s \in \mathcal{S}$, *and*

$$\mathcal{A}_t^{\mathrm{C}}(s) \;=\; \left\{ a \in \mathcal{A}_t(s) \;:\; \sum_{i\in\mathcal{I}} c_{tli}(s_i, a_i) \leqslant b_{tl} \;\;\forall l \in \mathcal{L} \right\},$$

initial state probabilities $q(s) = \prod_{i\in\mathcal{I}} q_i(s_i)$ *for* $s \in \mathcal{S}$, *transition probabilities* $p_t(s' \mid s, a) = \prod_{i\in\mathcal{I}} p_{it}(s'_i \mid s_i, a_i)$ *for* $s, s' \in \mathcal{S}$ *and* $a \in \mathcal{A}$ *and expected rewards* $r_t(s, a) = \sum_{i\in\mathcal{I}} r_{it}(s_i, a_i)$.

Weakly coupled DPs have been studied, among others, by [Haw03] and [AM08]. In a weakly coupled DP, the admissible actions $a \in \mathcal{A}_t^{\mathrm{C}}(s)$ in state $s \in \mathcal{S}$ must satisfy the constraints $a_i \in \mathcal{A}_{it}(s_i)$ of the individual DPs $i \in \mathcal{I}$ as well as the coupling resource constraints $a \in \mathcal{A}_t^{\mathrm{C}}(s)$. In particular, the feasibility of an action $a_i \in \mathcal{A}_i$ for the i-th constituent DP is not just determined by the state $s_i \in \mathcal{S}_i$, but it depends (through the resource constraints) on the states $s_{i'} \in \mathcal{S}_{i'}$, $i' \in \mathcal{I} \backslash \{i\}$, of the other constituent DPs as well. The constraints in $\mathcal{A}_t^{\mathrm{C}}$ allow us to model the resource consumption of individual patients (such as a G&A or CC bed, as well as fractions of doctor and nurse times – each of which can be modeled as a distinct resource $l \in \mathcal{L}$). Note also that the aggregation of multiple DPs to a weakly coupled DP is lossless in the sense that the state $s \in \mathcal{S}$ of a weakly coupled DP records the state $s_i \in \mathcal{S}_i$ of each constituent DP $i \in \mathcal{I}$.

In a weakly coupled DP, a *policy* $\pi = \{\pi_t\}_t$ with $\pi_t : \mathcal{S} \to \mathcal{A}$ specifies for each time period $t \in \mathcal{T}$, each DP $i \in \mathcal{I}$ and each state $s \in \mathcal{S}$ what action $[\pi_t(s)]_i \in \mathcal{A}_i$ is selected. A feasible policy π must satisfy $\pi_t(s) \in \mathcal{A}_t^{\mathrm{C}}(s)$ for all $t \in \mathcal{T}$ and $s \in \mathcal{S}$. We emphasize that the policy can choose the action $[\pi_t(s)]_i \in \mathcal{A}_i$ for the i-th DP in view of the states of all other constituent DPs, rather than just the state s_i; this is important in view of satisfying the coupling constraints. Under π, a weakly coupled DP evolves as follows. The initial state $\tilde{s}_1$ is random and satisfies

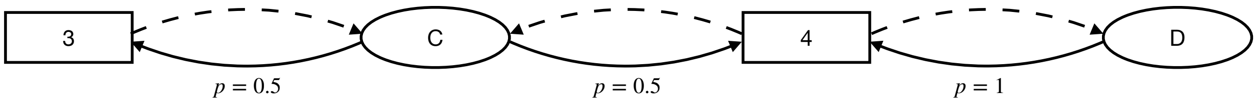

Figure 4.2: DP with two states 3 and 4 as well as two actions C (admissible in both states) and D (admissible in state 4 only). The expected rewards are $r_t(3, \mathrm{C}) = 0$ and $r_t(4, \mathrm{C}) = r_t(4, \mathrm{D}) = 1$.

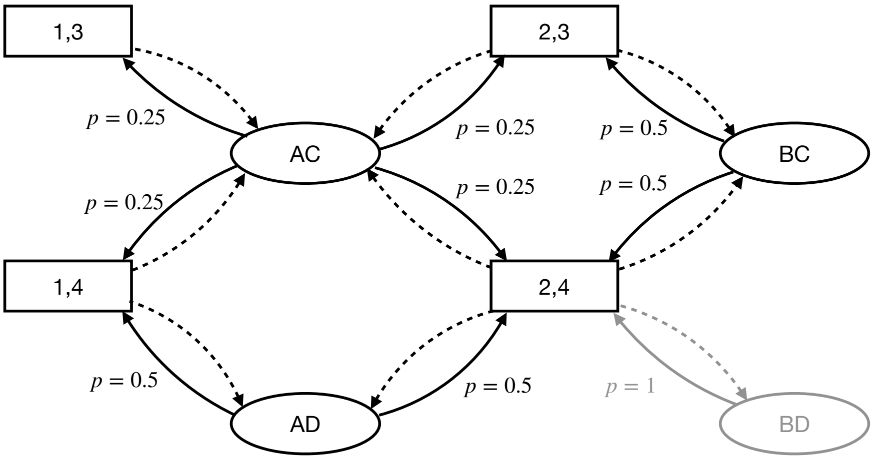

Figure 4.3: A weakly coupled DP is itself a DP. The values in the rectangular nodes record the states of the first and second DP, while the letters in the oval nodes denote the actions applied to each DP. The action BD violates the resource constraint.

$\mathbb{P}[\tilde{s}_1 = s] = \prod_{i\in\mathcal{I}} q_i(s_i) = q(s)$ for $s \in \mathcal{S}$. For $t \in \mathcal{T}\backslash\{T\}$, the transitions are governed by

$$\mathbb{P}\left[\tilde{s}_{t+1} = s'\right] = \sum_{s\in\mathcal{S}} \left[\prod_{i\in\mathcal{I}} p_{it}(s'_i \mid s_i, [\pi_t(s)]_i)\right] \cdot \mathbb{P}\left[\tilde{s}_t = s\right] = \sum_{s\in\mathcal{S}} p_t(s' \mid s, \pi_t(s)) \cdot \mathbb{P}\left[\tilde{s}_t = s\right] \qquad \forall s' \in \mathcal{S}.$$

The expected total reward of a policy π is $\mathbb{E}\left[\sum_{t\in\mathcal{T}} r_t(\tilde{s}_t, \pi_t(\tilde{s}_t))\right]$.

Example 4.4 (Weakly Coupled DP) *Figure 4.3 combines the DP from Example 4.2 with the DP from Figure 4.2 to a weakly coupled DP that is subjected to the resource constraint* $\mathbf{1}[s_1 = 2 \wedge a_1 = \mathrm{B}] + \mathbf{1}[s_2 = 4 \wedge a_2 = \mathrm{D}] \leqslant 1$*, that is, at most one of the actions B and D can be selected in any period. As a result, any optimal policy* π *selects one of the actions B or D (but not both) whenever they are admissible.*

4.3.1.2 Weakly Coupled Counting Dynamic Programs

Since it offers a lossless aggregation of its constituent DPs, the state and action spaces of a weakly coupled DP exhibit an undesirable scaling behavior:

$$|\mathcal{S}| \;=\; \prod_{i\in\mathcal{I}} |\mathcal{S}_i| \quad \text{and} \quad |\mathcal{A}| \;=\; \prod_{i\in\mathcal{I}} |\mathcal{A}_i|$$

The health system that we intend to model contains approximately 10 million patient DPs with 15 possible states and 6 possible actions each, thus resulting in a weakly coupled DP with approximately $15^{10,000,000}$ states and $6^{10,000,000}$ actions. Clearly, such a weakly coupled DP has to undergo a drastic dimensionality reduction before it is practical from a computational perspective.

To reduce the computational complexity of weakly coupled DPs, we first show how multiple DPs with the same state and action spaces and the same time horizon can be aggregated to a counting DP that records how many DPs are in which state at what point in time. Counting DPs will allow us to aggregate patients of the same patient group, which is characterized by the arrival time $t \in \mathcal{T}$ in our health system as well as the age group and disease type.

Definition 4.5 (Counting DP) *For a finite time horizon* $\mathcal{T} = \{1, \dots, T\}$ *and* n *independent and identically distributed (i.i.d.) copies of a DP* $(\mathcal{S}, \mathcal{A}, q, p, r)$*, a* counting DP $(\mathfrak{S}, \mathfrak{A}, \mathfrak{q}, \mathfrak{p}, \mathfrak{r}; n)$ *is a DP with state space* $\mathfrak{S} = \{\sigma : \mathcal{S} \to \mathbb{N}_0\}$*, action space* $\mathfrak{A} = \{\alpha : \mathcal{S} \times \mathcal{A} \to \mathbb{N}_0\}$*, admissible actions*

$$\mathfrak{A}_t(\sigma) \;=\; \left\{ \alpha \in \mathfrak{A} \,:\, \sum_{a\in\mathcal{A}} \alpha(s,a) = \sigma(s) \;\; \forall s \in \mathcal{S}, \;\; \alpha(s,a) = 0 \;\; \forall s \in \mathcal{S}, \; \forall a \in \mathcal{A} \setminus \mathcal{A}_t(s) \right\},$$

initial state probabilities

$$\mathfrak{q}(\sigma) \;=\; \frac{n!}{\prod_{s\in\mathcal{S}} \sigma(s)!} \cdot \prod_{s\in\mathcal{S}} q(s)^{\sigma(s)} \qquad \forall \sigma \in \mathfrak{S} \,:\, \sum_{s\in\mathcal{S}} \sigma(s) = n$$

and $\mathfrak{q}(\sigma) = 0$ *otherwise, transition probabilities* $\mathfrak{p} = \{\mathfrak{p}_t\}_t$ *with*

$$\mathfrak{p}_t(\sigma' \,|\, \sigma, \alpha) \;=\; \sum_{\theta \in \Gamma(\sigma,\alpha,\sigma')} \prod_{s \in \mathcal{S}} \prod_{a \in \mathcal{A}} \left[\frac{\alpha(s,a)!}{\prod_{s' \in \mathcal{S}} \theta(s,a,s')!} \cdot \prod_{s' \in \mathcal{S}} p_t(s' \,|\, s,a)^{\theta(s,a,s')} \right]$$

with admissible transportation plans from state $\sigma \in \mathfrak{S}$ *to state* $\sigma' \in \mathfrak{S}$ *under action* $\alpha \in \mathfrak{A}$

$$\Gamma(\sigma,\alpha,\sigma') \;=\; \Bigg\{ \theta : \mathcal{S} \times \mathcal{A} \times \mathcal{S} \to \mathbb{N}_0 \;:\; \sum_{s' \in \mathcal{S}} \theta(s,a,s') = \alpha(s,a) \qquad \forall s \in \mathcal{S},\, \forall a \in \mathcal{A}, \\ \sum_{s \in \mathcal{S}} \sum_{a \in \mathcal{A}} \theta(s,a,s') = \sigma'(s') \quad \forall s' \in \mathcal{S} \Bigg\}$$

and expected rewards $\mathfrak{r} = \{\mathfrak{r}_t\}_t$ *with* $\mathfrak{r}_t(\sigma,\alpha) = \sum_{s \in \mathcal{S}} \sum_{a \in \mathcal{A}} r_t(s,a) \cdot \alpha(s,a)$.

By construction, a counting DP can only reach states $\sigma \in \mathfrak{S}$ satisfying $\sum_{s \in \mathcal{S}} \sigma(s) = n$. Any admissible action $\alpha \in \mathfrak{A}_t(\sigma)$ thus satisfies $\sum_{s \in \mathcal{S}} \sum_{a \in \mathcal{A}} \alpha(s,a) = n$. Note that the state σ can be recovered from any admissible action α through the fact that $\sum_{a \in \mathcal{A}} \alpha(s,a) = \sigma(s)$ for all $s \in \mathcal{S}$. Thus, the transition probabilities, admissible transportation plans and expected rewards only depend on α and not on σ; to keep the notation consistent, however, we continue to include σ.

In a counting DP, a *policy* $\pi = \{\pi_t\}_t$ with $\pi_t : \mathfrak{S} \to \mathfrak{A}$ specifies for each time period $t \in \mathcal{T}$ and each counting state $\sigma \in \mathfrak{S}$ what action $\pi_t(\sigma) \in \mathfrak{A}$ is selected. A feasible policy must satisfy $\pi_t(\sigma) \in \mathfrak{A}_t(\sigma)$ for all $t \in \mathcal{T}$ and $\sigma \in \mathfrak{S}$. Under π, a counting DP evolves exactly like an ordinary DP. The initial state $\tilde{\sigma}_1$ is random and satisfies $\mathbb{P}[\tilde{\sigma}_1 = \sigma] = \mathfrak{q}(\sigma)$ for $\sigma \in \mathfrak{S}$. For $t \in \mathcal{T} \backslash \{T\}$, the transitions are governed by

$$\mathbb{P}\left[\tilde{\sigma}_{t+1} = \sigma'\right] \;=\; \sum_{\sigma \in \mathfrak{S}} \mathfrak{p}_t(\sigma' \,|\, \sigma, \pi_t(\sigma)) \cdot \mathbb{P}\left[\tilde{\sigma}_t = \sigma\right] \qquad \forall \sigma' \in \mathfrak{S}.$$

The expected total reward of a policy π is $\mathbb{E}\left[\sum_{t \in \mathcal{T}} \mathfrak{r}_t(\tilde{\sigma}_t, \pi_t(\tilde{\sigma}_t))\right]$.

To better understand Definition 4.5, consider n i.i.d. copies of a DP $(\mathcal{S}, \mathcal{A}, q, p, r)$ whose states and actions at time $t \in \mathcal{T}$ are recorded by the random variables $\tilde{s}_{ti}$ and $\tilde{a}_{ti}$, $i \in \mathcal{I} = \{1, \ldots, n\}$, respectively. By construction, the random quantity $|\{i \in \mathcal{I} \,:\, \tilde{s}_{1i} = s\}|$ of DPs in state $s \in \mathcal{S}$ at time period 1 follows a multinomial distribution with parameters $(n; q)$, and its probability mass function coincides with $\mathfrak{q}$ in Definition 4.5. In other words, the initial state $\tilde{\sigma}_1$ of the counting DP records how many of the n DPs are in each state $s \in \mathcal{S}$ at time $t = 1$. Similarly, for any fixed states $\sigma, \sigma' \in \mathfrak{S}$, action $\alpha \in \mathfrak{A}$, transportation plan $\theta \in \Gamma(\sigma, \alpha, \sigma')$ and state-action pair $(s, a) \in \mathcal{S} \times \mathcal{A}$, the inner expression in the definition of the transition probabilities $\mathfrak{p}_t$ evaluates to

$$\begin{aligned} &\frac{\alpha(s,a)!}{\prod_{s' \in \mathcal{S}} \theta(s,a,s')!} \cdot \prod_{s' \in \mathcal{S}} p_t(s' \mid s,a)^{\theta(s,a,s')} \\ = \ &\mathbb{P}\Big[|\{i \in \mathcal{I} \, : \, (\tilde{s}_{ti}, \tilde{a}_{ti}, \tilde{s}_{t+1,i}) = (s,a,s')\}| = \theta(s,a,s') \ \ \forall s' \in \mathcal{S} \ \Big| \\ &\qquad\qquad\qquad |\{i \in \mathcal{I} \, : \, (\tilde{s}_{ti}, \tilde{a}_{ti}) = (s,a)\}| = \alpha(s,a) \Big], \end{aligned}$$

since, given $|\{i \in \mathcal{I} \, : \, (\tilde{s}_{ti}, \tilde{a}_{ti}) = (s,a)\}|$, the quantity $|\{i \in \mathcal{I} \, : \, (\tilde{s}_{ti}, \tilde{a}_{ti}, \tilde{s}_{t+1,i}) = (s,a,s')\}|$ follows a multinomial distribution with parameters $(\alpha(s,a); p_t(\cdot \mid s,a))$. Multiplying these expressions over all $(s,a) \in \mathcal{S} \times \mathcal{A}$ (since the DPs evolve independently) and summing over all transportation plans $\theta \in \Gamma(\sigma, \alpha, \sigma')$ (by the additivity of probabilities of pairwise disjoint events) shows that the transition probability $\mathfrak{p}_t(\sigma'|\sigma,\alpha)$ records the probability of the event $|\{i \in \mathcal{I} \, : \, \tilde{s}_{t+1,i} = s\}| = \sigma'(s)$, simultaneously for all $s \in \mathcal{S}$, conditional on the event $|\{i \in \mathcal{I} \, : \, (\tilde{s}_{ti}, \tilde{a}_{ti}) = (s,a)\}| = \alpha(s,a)$, simultaneously for all $(s,a) \in \mathcal{S} \times \mathcal{A}$. Thus, for a given policy π the counting DP records for each time period $t \in \mathcal{T}$ how many of the n DPs are in each of the states $s \in \mathcal{S}$ under π.

Perhaps surprisingly, despite its aggregation, a feasible policy to a counting DP gives rise to feasible policies for the constituent DPs that do not incur any loss in the expected total reward.

Proposition 4.6 *For a DP $(\mathcal{S}, \mathcal{A}, q, p, r)$ and $n \in \mathbb{N}$, consider the corresponding counting DP $(\mathfrak{S}, \mathfrak{A}, \mathfrak{q}, \mathfrak{p}, \mathfrak{r}; n)$ as well as the weakly coupled DP $(\{\mathcal{S}_i, \mathcal{A}_i, q_i, p_i, r_i\}_i)$ with $(\mathcal{S}_i, \mathcal{A}_i, q_i, p_i, r_i) = (\mathcal{S}, \mathcal{A}, q, p, r)$, $i \in \mathcal{I} = \{1, \ldots, n\}$, and no resource constraints. Fix any feasible policy π to the counting DP. Then any policy π' to the weakly coupled DP satisfying*

$$\begin{aligned} |\{i \in \mathcal{I} \, : \, s_i = s' \ \wedge \ \pi'_{ti}(s_i) = a'\}| = [\pi_t(\sigma)](s', a') \qquad &\forall t \in \mathcal{T}, \ \forall \sigma \in \mathfrak{S}, \ \forall (s', a') \in \mathcal{S} \times \mathcal{A}, \\ &\forall s \in \mathcal{S}^n \, : \, [|\{i \in \mathcal{I} \, : \, s_i = s''\}| = \sigma(s'') \ \ \forall s'' \in \mathcal{S}] \end{aligned}$$

is feasible, and π and π' attain the same expected total reward.

Proof of Proposition 4.6. Denote by $\tilde{\sigma} = \{\tilde{\sigma}_t\}_t$ the random state evolution of the counting DP under policy π and by $\tilde{s}' = \{\tilde{s}'_t\}_t$ the random state evolution of the weakly coupled DP under any fixed policy π' satisfying the conditions in the statement of the proposition, respectively. We also define the counting state evolution of the weakly coupled DP as $\tilde{\sigma}' = \{\tilde{\sigma}'_t\}_t$ with

$$\tilde{\sigma}'_t(s) \;=\; |\{i \in \mathcal{I} \,:\, \tilde{s}'_{ti} = s\}| \qquad \forall t \in \mathcal{T},\ \forall s \in \mathcal{S}.$$

We prove the statement in two steps. We first argue that the counting state evolutions $\tilde{\sigma}_t$ and $\tilde{\sigma}'_t$ of the counting DP and the weakly coupled DP share the same distributions for all $t \in \mathcal{T}$. We subsequently use this insight to show that the expected total rewards of π and π' in their respective DPs coincide. Since the weakly coupled DP has no resource constraints, the policy π' is feasible by construction, and the statement of the proposition thus follows.

As for the first step, we note that the conditions in the statement of the proposition ensure that whenever the counting states $\tilde{\sigma}_t$ and $\tilde{\sigma}'_t$ of the counting DP and the weakly coupled DP are both equal to $\sigma_t \in \mathfrak{S}$, then the policies π_t and π'_t apply each action $a \in \mathcal{A}$ to DPs in state $s \in \mathcal{S}$ precisely $[\pi_t(\sigma_t)](s, a)$ many times. Moreover, Definition 4.5 implies that the transition probabilities $\mathfrak{p}$ of the counting DP record the aggregate transitions of n i.i.d. DPs with individual transition probabilities p under policy π, whereas the weakly coupled DP by construction records the individual transitions of these DPs under policy π'. We thus conclude that the transition probabilities of the counting states $\tilde{\sigma}_t$ and $\tilde{\sigma}'_t$ are identical under π and π'. Moreover, the construction of the initial state distribution $\mathfrak{q}$ in Definition 4.5 and the definition of $\tilde{s}'_{1i}$, $i \in \mathcal{I}$, as i.i.d. random variables governed by the distribution q imply that $\tilde{\sigma}_1$ and $\tilde{\sigma}'_1$ share the same distribution. A simple induction therefore shows that $\tilde{\sigma}_t$ and $\tilde{\sigma}'_t$ share the same distributions across all time periods $t \in \mathcal{T}$.

In view of the second step, we observe that the expected total reward of the weakly coupled

DP under policy π' evaluates to

$$\begin{aligned}
\mathbb{E}\left[\sum_{t\in\mathcal{T}}\sum_{i=1}^{n} r_t(\tilde{s}'_{ti}, \pi'_{ti}(\tilde{s}'_{ti}))\right] &= \mathbb{E}\left[\sum_{t\in\mathcal{T}}\sum_{i=1}^{n}\sum_{s\in\mathcal{S}}\sum_{a\in\mathcal{A}} r_t(s,a)\cdot \mathbf{1}\left[\tilde{s}'_{ti} = s \ \wedge \ \pi'_{ti}(\tilde{s}'_{ti}) = a\right]\right] \\
&= \mathbb{E}\left[\sum_{t\in\mathcal{T}}\sum_{s\in\mathcal{S}}\sum_{a\in\mathcal{A}} r_t(s,a)\cdot |\{i\in\mathcal{I} \ : \ \tilde{s}'_{ti} = s \ \wedge \ \pi'_{ti}(\tilde{s}'_{ti}) = a\}|\right] \\
&= \mathbb{E}\left[\sum_{t\in\mathcal{T}}\sum_{s\in\mathcal{S}}\sum_{a\in\mathcal{A}} r_t(s,a)\cdot [\pi_t(\tilde{\sigma}'_t)](s,a)\right] \\
&= \mathbb{E}\left[\sum_{t\in\mathcal{T}}\sum_{s\in\mathcal{S}}\sum_{a\in\mathcal{A}} r_t(s,a)\cdot [\pi_t(\tilde{\sigma}_t)](s,a)\right],
\end{aligned}$$

where the first and second identity hold by construction, the third identity uses the properties of π' from the statement of the proposition, and the last identity exploits the fact that $\tilde{\sigma}_t$ and $\tilde{\sigma}'_t$ share the same distribution. The statement now follows from the fact that the last expression evaluates the expected total reward of the counting DP under the policy π. ∎

The equation in the statement of Proposition 4.6 ensures that for all states $s \in \mathcal{S}^n$ of the weakly coupled DP that correspond to a given state $\sigma \in \mathfrak{S}$ of the counting DP, the number of times we apply an action $a' \in \mathcal{A}$ to a DP in state $s' \in \mathcal{S}$ also coincide under π and π'.

Proposition 4.6 states that any policy π to a counting DP can be converted into individual policies π'_i to the constituent DPs that generate the same expected total reward. To this end, we simply need to distribute the action multiplicities $[\pi_t(\sigma)](s,a)$ for each state of the counting DP among the $\sigma(s)$ many DPs that are in state s at time t. It is noteworthy that any such distribution scheme is admissible, and they all result in the same expected total reward.

Aggregating individual patient DPs to a counting DP is *not* a lossless transformation: While a counting DP faithfully records the stochastic evolution of *the population* of individual DPs, it no longer records which state *a particular DP* is in. In other words, while the state of the i-th DP remains identifiable when the individual DPs are aggregated to a weakly coupled DP, its state is no longer identifiable by the state σ of the corresponding counting DP. In the context of our healthcare model, this implies that we have to assign the same (state/action-dependent)

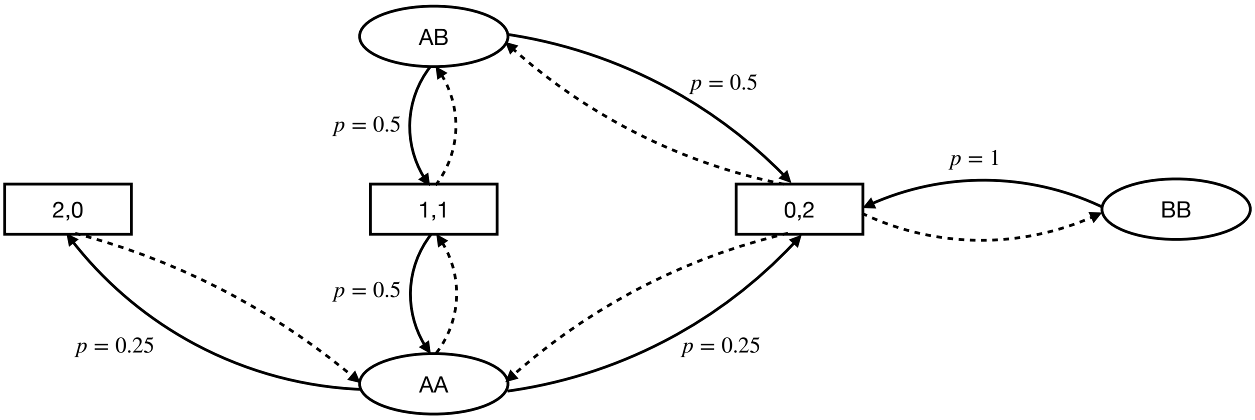

Figure 4.4: Counting DP for the DP from Example 4.2.

transition probabilities and rewards to all patients in the same patient group. This loss of flexibility is acceptable for our purpose, which is to inform a nation-wide prioritization policy (as opposed to an admissions schedule for an individual hospital), and it results in a tremendous gain in computational tractability: for $5,000$ patients of the same patient group with 15 states and 6 actions, for example, the $15^{5,000}$ states and $6^{5,000}$ actions of the associated weakly coupled DP reduce to less than $5,000^{15}$ states and $5,000^{15\cdot 6}$ actions for the associated counting DP.

Example 4.7 (Counting DP) *Figure 4.4 presents a counting DP for* $n = 2$ *copies of the DP from Example 4.2. The states of the counting DP are characterized by two values that record the numbers of the constituent DPs in state* 1 *and* 2*, respectively, and the actions of the counting DP are characterized by the numbers of times that action A or action B is chosen. State* $(1, 1)$ *represents that both the constituent DPs are in state 1, state* $1, 2$ *represents that one DP is in state* 1 *while the other DP is in states* 2*, and so on. Notice that counting DPs do not record which DP is in which state, but rather the number of DPs in each state. Action* (A, A) *represents that action* A *is applied to both DPs, action* (A, B) *represents that action* A *is applied to one DP while action* B *is applied to the other DP. Once again, the actions in counting DPs only record the number of DPs to which each action is applied.*

We now combine the concepts of weakly coupled DPs (*cf.* Definition 4.3) and counting DPs (*cf.* Definition 4.5) to weakly coupled counting DPs, which aggregate the various patient groups in our health system and restrict the admissible policies in view of the resource constraints.

Definition 4.8 (Weakly Coupled Counting DP) *For a finite set of counting DPs, denoted as* $(\mathfrak{S}_j, \mathfrak{A}_j, \mathfrak{q}_j, \mathfrak{p}_j, \mathfrak{r}_j; n_j)$*,* $j \in \mathcal{J} = \{1, \ldots, J\}$*, over the same time horizon* $\mathcal{T} = \{1, \ldots, T\}$*, the* weakly coupled counting DP $(\{\mathfrak{S}_j, \mathfrak{A}_j, \mathfrak{q}_j, \mathfrak{p}_j, \mathfrak{r}_j\}_j; \{n_j\}_j)$ *is the DP* $(\mathfrak{S}, \mathfrak{A}, \mathfrak{q}, \mathfrak{p}, \mathfrak{r})$ *with state space* $\mathfrak{S} = \times_{j\in\mathcal{J}} \mathfrak{S}_j$*, action space* $\mathfrak{A} = \times_{j\in\mathcal{J}} \mathfrak{A}_j$ *with* $\mathfrak{A}_t(\sigma) = \times_{j\in\mathcal{J}} \mathfrak{A}_{jt}(\sigma_j)$*,* $\sigma \in \mathfrak{S}$*, and*

$$\mathfrak{A}_t^{\mathrm{C}}(\sigma) \;=\; \left\{ \alpha \in \mathfrak{A}_t(\sigma) \,:\, \sum_{j\in\mathcal{J}} \sum_{s\in\mathcal{S}_j} \sum_{a\in\mathcal{A}_j} c_{tlj}(s,a) \cdot \alpha_j(s,a) \leqslant b_{tl} \quad \forall l \in \mathcal{L} \right\},$$

initial state probabilities $\mathfrak{q}(\sigma) = \prod_{j\in\mathcal{J}} q_j(\sigma_j)$ *for* $\sigma \in \mathfrak{S}$*, transition probabilities* $\mathfrak{p}_t(\sigma' \,|\, \sigma, \alpha) = \prod_{j\in\mathcal{J}} \mathfrak{p}_{jt}(\sigma'_j \,|\, \sigma_j, \alpha_j)$ *for* $\sigma, \sigma' \in \mathfrak{S}$ *and* $\alpha \in \mathfrak{A}$ *and expected rewards* $\mathfrak{r}_t(\sigma, \alpha) = \sum_{j\in\mathcal{J}} \mathfrak{r}_{jt}(\sigma_j, \alpha_j)$*.*

In a weakly coupled counting DP, a *policy* $\pi = \{\pi_t\}_t$ with $\pi_t : \mathfrak{S} \to \mathfrak{A}$ specifies for each time period $t \in \mathcal{T}$, each counting DP $j \in \mathcal{J}$ and each state $\sigma \in \mathfrak{S}$ what action $[\pi_t(\sigma)]_j \in \mathfrak{A}_j$ is selected. A feasible policy π must satisfy $\pi_t(\sigma) \in \mathfrak{A}_t^{\mathrm{C}}(\sigma)$ for all $t \in \mathcal{T}$ and $\sigma \in \mathfrak{S}$. Under π, a weakly coupled counting DP evolves as follows. The initial state $\tilde{\sigma}_1$ is random and satisfies $\mathbb{P}[\tilde{\sigma}_1 = \sigma] = \prod_{j\in\mathcal{J}} \mathfrak{q}_j(\sigma_j) = \mathfrak{q}(\sigma)$ for $\sigma \in \mathfrak{S}$. For $t \in \mathcal{T} \backslash \{T\}$, the transitions are governed by

$$\begin{aligned} \mathbb{P}\left[\tilde{\sigma}_{t+1} = \sigma'\right] \;&=\; \sum_{\sigma\in\mathfrak{S}} \left[\prod_{j\in\mathcal{J}} \mathfrak{p}_{jt}(\sigma'_j \,|\, \sigma_j, [\pi_t(\sigma)]_j) \right] \cdot \mathbb{P}\left[\tilde{\sigma}_t = \sigma\right] \\ &=\; \sum_{\sigma\in\mathfrak{S}} \mathfrak{p}_t(\sigma' \,|\, \sigma, \pi_t(\sigma)) \cdot \mathbb{P}\left[\tilde{\sigma}_t = \sigma\right] \qquad\qquad \forall \sigma' \in \mathfrak{S}. \end{aligned}$$

The expected total reward of a policy π is $\mathbb{E}\left[\sum_{t\in\mathcal{T}} \mathfrak{r}_t(\tilde{\sigma}_t, \pi_t(\tilde{\sigma}_t))\right]$.

A straightforward adaptation of Proposition 4.6 allows us to convert any feasible policy to the weakly coupled counting DP into policies for the constituent DPs that generate the same expected total reward. We skip the statement and proof since neither requires any new ideas.

For later reference, we define the *policy set* of a weakly coupled counting DP as $\Pi = \times_{t\in\mathcal{T}} \Pi_t$ with $\Pi_t = \{[\pi_t : \mathfrak{S} \to \mathfrak{A}] \,:\, \pi_t(\sigma) \in \mathfrak{A}_t(\sigma) \quad \forall \sigma \in \mathfrak{S}\}$ and the *set of feasible policies* as $\Pi^{\mathrm{C}} = \times_{t\in\mathcal{T}} \Pi_t^{\mathrm{C}}$ with $\Pi_t^{\mathrm{C}} = \{\pi_t \in \Pi_t \,:\, \pi_t(\sigma) \in \mathfrak{A}_t^{\mathrm{C}}(\sigma) \;\; \forall \sigma \in \mathfrak{S}\}$, respectively. We denote the *set of state trajectories* as $\Sigma = \times_{t\in\mathcal{T}} \mathfrak{S}$; the random state evolution $\tilde{\sigma} = \{\tilde{\sigma}\}_t$ then takes values in Σ.

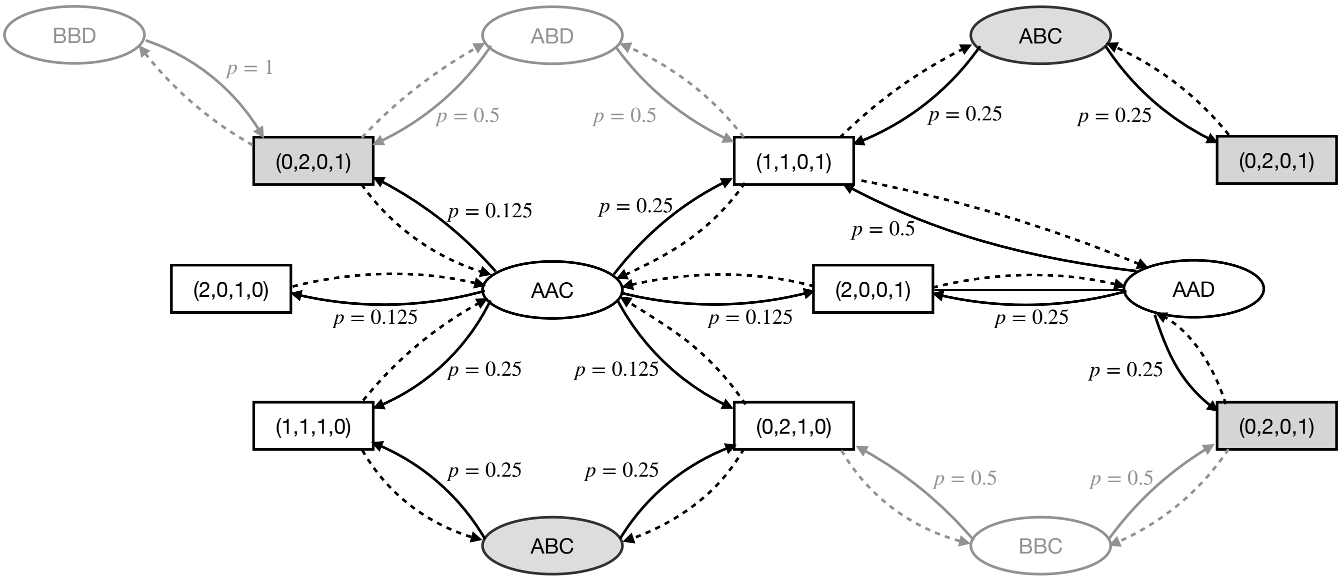

Figure 4.5: Weakly coupled counting DP from Example 4.9. The values in the rectangular nodes record how many DPs are in state $1, \ldots, 4$ (from left to right), while the letters in the oval nodes represent the actions applied to each counting DP (A and B to the first one; C and D to the second one). Grey shaded nodes are duplicated for ease of illustration. The actions ABD, BBC and BBD violate the resource constraint.

Example 4.9 (Weakly Coupled Counting DP) *Figure 4.5 combines $n_1 = 2$ copies of the DP from Figure 4.1 with $n_2 = 1$ copy of the DP from Figure 4.2 to a weakly coupled counting DP that is subjected to the resource constraint $\alpha_1(2, \mathrm{B}) + \alpha_2(4, D) \leqslant 1$, that is, at most one of the actions B or D can be selected in any period. As a result, any optimal policy π selects either B (once) or D, but never both B and D, whenever they are admissible.*

4.3.2 Fluid Approximation

Our healthcare model will comprise approximately 10 million patients spread among 3,120 patient groups with 15 states and 6 actions each. Assuming, for the sake of the argument, an even spread of around 3,200 patients per patient group, the resulting weakly coupled counting DP would contain about $(3,200^{1}5)^{3,120}$ states and $(3,200^{15 \cdot 6})^{3,120}$ actions, which remains intractable. However, (weakly coupled) counting DPs lend themselves to a continuous approximation which is particularly suitable when the involved numbers of DPs are large, as is the case in our application.

To facilitate an efficient solution of the weakly coupled counting DP that represents our healthcare model, Section 4.3.2.1 introduces the concept of weakly coupled k-counting DPs, which split each constituent DP into k independently evolving parts. Taking the limit as $k \longrightarrow \infty$, we arrive at the concept of a fluid limit, which treats all patients of our healthcare model as 'fluid' that flows between the different states (controlled by the policy maker's actions). Section 4.3.2.2 shows that the resulting fluid DP can be solved efficiently by an LP that scales gracefully in the dimensions of the original weakly coupled counting DP. Sections 4.3.2.3 and 4.3.2.4, finally, shows that the LP from Section 4.3.2.2 allows us to recover high-quality solutions to the weakly coupled counting DP with high probability.

4.3.2.1 Weakly Coupled k-Counting Dynamic Programs and the Fluid Limit

We first consider a counting DP where each constituent DP is split into k parts that evolve independently of each other and that jointly account for the DP.

Definition 4.10 (k-Counting DP) *For a finite time horizon $\mathcal{T} = \{1, \ldots, T\}$ and n i.i.d. copies of a DP $(\mathcal{S}, \mathcal{A}, q, p, r)$ formed of k i.i.d. parts each, a k-*counting DP $(\mathfrak{S}, \mathfrak{A}, \mathfrak{q}, \mathfrak{p}, \mathfrak{r}; n, k)$ *is a DP with state space $\mathfrak{S} = \{\sigma : \mathcal{S} \to \mathbb{N}_0/k\}$, action space $\mathfrak{A} = \{\alpha : \mathcal{S} \times \mathcal{A} \to \mathbb{N}_0/k\}$ and admissible actions*

$$\mathfrak{A}_t(\sigma) \;=\; \left\{\alpha \in \mathfrak{A} \,:\, \sum_{a \in \mathcal{A}} \alpha(s,a) = \sigma(s) \;\; \forall s \in \mathcal{S}, \;\; \alpha(s,a) = 0 \;\; \forall s \in \mathcal{S}, \; \forall a \in \mathcal{A} \backslash \mathcal{A}_t(s)\right\},$$

initial state probabilities

$$\mathfrak{q}(\sigma) \;=\; \frac{[nk]!}{\prod_{s \in \mathcal{S}} [k\sigma(s)]!} \cdot \prod_{s \in \mathcal{S}} q(s)^{k\sigma(s)} \qquad \forall \sigma \in \mathfrak{S} \,:\, \sum_{s \in \mathcal{S}} \sigma(s) = n$$

and $\mathfrak{q}(\sigma) = 0$ otherwise, transition probabilities $\mathfrak{p} = \{\mathfrak{p}_t\}_t$ with

$$\mathfrak{p}_t(\sigma' \,|\, \sigma, \alpha) \;=\; \sum_{\theta \in \Gamma(\sigma,\alpha,\sigma')} \prod_{s \in \mathcal{S}} \prod_{a \in \mathcal{A}} \left[\frac{[k\alpha(s,a)]!}{\prod_{s' \in \mathcal{S}} [k\theta(s,a,s')]!} \cdot \prod_{s' \in \mathcal{S}} p_t(s' \,|\, s,a)^{k\theta(s,a,s')} \right]$$

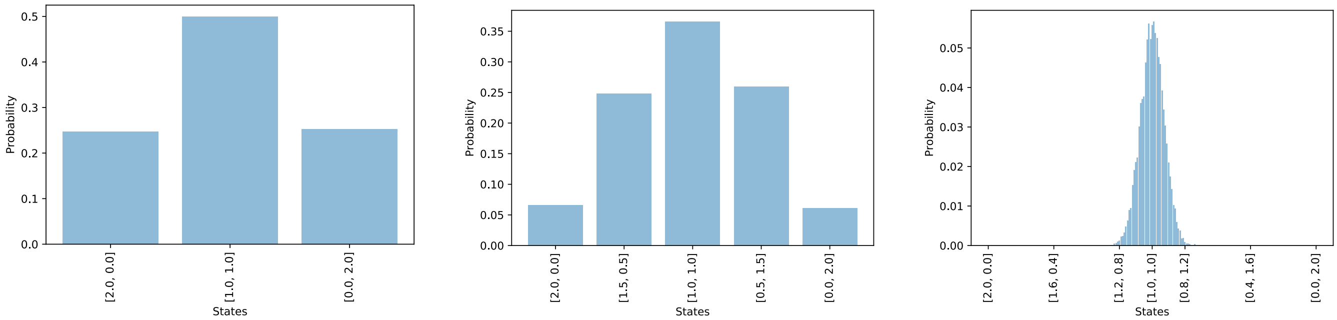

Figure 4.6: Next state distribution for a k-counting DP with $k = 1$ (left), $k = 2$ (middle) and $k = 100$ (right).

with admissible transportation plans from state $\sigma \in \mathfrak{S}$ to state $\sigma' \in \mathfrak{S}$ under action $\alpha \in \mathfrak{A}$

$$\Gamma(\sigma, \alpha, \sigma') = \Bigg\{ \theta : \mathcal{S} \times \mathcal{A} \times \mathcal{S} \to \mathbb{N}_0/k \, : \, \sum_{s' \in \mathcal{S}} \theta(s, a, s') = \alpha(s, a) \qquad \forall s \in \mathcal{S}, \, \forall a \in \mathcal{A}, \\ \sum_{s \in \mathcal{S}} \sum_{a \in \mathcal{A}} \theta(s, a, s') = \sigma'(s') \quad \forall s' \in \mathcal{S} \Bigg\}$$

and expected rewards $\mathfrak{r} = \{\mathfrak{r}_t\}_t$ with $\mathfrak{r}_t(\sigma, \alpha) = \sum_{s \in \mathcal{S}} \sum_{a \in \mathcal{A}} r_t(s, a) \cdot \alpha(s, a)$.

Definition 4.10 uses the notational shorthand $\mathbb{N}_0/k = \{0, 1/k, 2/k, \ldots\}$. Note that each of the nk parts in a k-counting DP only accounts for a fraction $1/k$ of a DP, whereas each of the n parts in a counting DP accounts for an entire DP. Other than that, Definition 4.10 coincides with Definition 4.5.

A *policy* $\pi = \{\pi_t\}_t$ with $\pi_t : \mathfrak{S} \to \mathfrak{A}$ in a k-counting DP is defined analogously to a policy in an ordinary counting DP. In particular, π is feasible if $\pi_t(\sigma) \in \mathfrak{A}_t(\sigma)$ for all $t \in \mathcal{T}$ and $\sigma \in \mathfrak{S}$. Under π, the initial state $\tilde{\sigma}_1$ of the k-counting DP is random and satisfies $\mathbb{P}[\tilde{\sigma}_1 = \sigma] = \mathfrak{q}(\sigma)$ for $\sigma \in \mathfrak{S}$, and for $t \in \mathcal{T} \setminus \{T\}$ the transitions satisfy

$$\mathbb{P}\left[\tilde{\sigma}_{t+1} = \sigma'\right] = \sum_{\sigma \in \mathfrak{S}} \mathfrak{p}_t(\sigma' \,|\, \sigma, \pi_t(\sigma)) \cdot \mathbb{P}\left[\tilde{\sigma}_t = \sigma\right] \qquad \forall \sigma' \in \mathfrak{S}.$$

The expected total reward of a policy π is $\mathbb{E}\left[\sum_{t \in \mathcal{T}} \mathfrak{r}_t(\tilde{\sigma}_t, \pi_t(\tilde{\sigma}_t))\right]$.

Example 4.11 (k-Counting DP) *For the counting DP from Example 4.7, Figure 4.6 illustrates the distribution of the next state $\tilde{\sigma}_{t+1}$ if the current state satisfies $\tilde{\sigma}_t = (2, 0)$ pointwise* *and we implement the action α characterized by $\alpha_t(s, \mathrm{A}) = \sigma_t(s)$ and $\alpha_t(s, \mathrm{B}) = 0$, $s \in \mathcal{S}$, for various values of k. The figure shows that the next state distribution converges to a Dirac distribution that places all probability mass on the state $\sigma_{t+1} = (1, 1)$.*

Definition 4.12 (Weakly Coupled k-Counting DP) *For a finite set of k-counting DPs $(\mathfrak{S}_j, \mathfrak{A}_j, \mathfrak{q}_j, \mathfrak{p}_j, \mathfrak{r}_j; n_j, k)$, $j \in \mathcal{J} = \{1, \ldots, J\}$, over the same time horizon $\mathcal{T} = \{1, \ldots, T\}$, the* weakly coupled k-counting DP $(\{\mathfrak{S}_j, \mathfrak{A}_j, \mathfrak{q}_j, \mathfrak{p}_j, \mathfrak{r}_j\}_j; \{n_j\}_j, k)$ *is the DP $(\mathfrak{S}, \mathfrak{A}, \mathfrak{q}, \mathfrak{p}, \mathfrak{r})$ with state space $\mathfrak{S} = \times_{j\in\mathcal{J}} \mathfrak{S}_j$, action space $\mathfrak{A} = \times_{j\in\mathcal{J}} \mathfrak{A}_j$ with $\mathfrak{A}_t(\sigma) = \times_{j\in\mathcal{J}} \mathfrak{A}_{jt}(\sigma_j)$, $\sigma \in \mathfrak{S}$, and*

$$\mathfrak{A}_t^{\mathrm{C}}(\sigma) \;=\; \left\{ \alpha \in \mathfrak{A}_t(\sigma) \;:\; \sum_{j\in\mathcal{J}} \sum_{s\in\mathcal{S}_j} \sum_{a\in\mathcal{A}_j} c_{tlj}(s,a) \cdot \alpha_j(s,a) \leqslant b_{tl} \quad \forall l \in \mathcal{L} \right\},$$

initial state probabilities $\mathfrak{q}(\sigma) = \prod_{j\in\mathcal{J}} q_j(\sigma_j)$ for $\sigma \in \mathfrak{S}$, transition probabilities $\mathfrak{p}_t(\sigma' \,|\, \sigma, \alpha) = \prod_{j\in\mathcal{J}} \mathfrak{p}_{jt}(\sigma'_j \,|\, \sigma_j, \alpha_j)$ for $\sigma, \sigma' \in \mathfrak{S}$ and $\alpha \in \mathfrak{A}$ and expected rewards $\mathfrak{r}_t(\sigma, \alpha) = \sum_{j\in\mathcal{J}} \mathfrak{r}_{jt}(\sigma_j, \alpha_j)$.

In a weakly coupled k-counting DP, a *policy* $\pi = \{\pi_t\}_t$ with $\pi_t : \mathfrak{S} \to \mathfrak{A}$ specifies for each time period $t \in \mathcal{T}$, each k-counting DP $j \in \mathcal{J}$ and each state $\sigma \in \mathfrak{S}$ what action $[\pi_t(\sigma)]_j \in \mathfrak{A}_j$ is selected. A feasible policy π must satisfy $\pi_t(\sigma) \in \mathfrak{A}_t^{\mathrm{C}}(\sigma)$ for all $\sigma \in \mathfrak{S}$ and $t \in \mathcal{T}$. Under π, the initial state $\tilde{\sigma}_1$ of the weakly coupled k-counting DP is random and satisfies $\mathbb{P}[\tilde{\sigma}_1 = \sigma] = \prod_{j\in\mathcal{J}} \mathfrak{q}_j(\sigma_j) = \mathfrak{q}(\sigma)$ for $\sigma \in \mathfrak{S}$. For $t \in \mathcal{T}\backslash\{T\}$, the transitions are governed by

$$\begin{aligned} \mathbb{P}\left[\tilde{\sigma}_{t+1} = \sigma'\right] \;&=\; \sum_{\sigma\in\mathfrak{S}} \left[\prod_{j\in\mathcal{J}} \mathfrak{p}_{jt}(\sigma'_j \,|\, \sigma_j, [\pi_t(\sigma)]_j) \right] \cdot \mathbb{P}\left[\tilde{\sigma}_t = \sigma\right] \\ &=\; \sum_{\sigma\in\mathfrak{S}} \mathfrak{p}_t(\sigma' \,|\, \sigma, \pi_t(\sigma)) \cdot \mathbb{P}\left[\tilde{\sigma}_t = \sigma\right] \qquad\qquad \forall \sigma' \in \mathfrak{S}. \end{aligned}$$

The expected total reward of a policy π is $\mathbb{E}\left[\sum_{t\in\mathcal{T}} \mathfrak{r}_t(\tilde{\sigma}_t, \pi_t(\tilde{\sigma}_t))\right]$.

Fix a sequence of weakly coupled k-counting DPs $(\{\mathfrak{S}_j^k, \mathfrak{A}_j^k, \mathfrak{q}_j^k, \mathfrak{p}_j^k, \mathfrak{r}_j^k\}_j; \{n_j^k\}_j, k)$, $k \in \mathbb{N}$, where each constituent k-counting DP $(\mathfrak{S}_j^k, \mathfrak{A}_j^k, \mathfrak{q}_j^k, \mathfrak{p}_j^k, \mathfrak{r}_j^k; n_j^k, k)$, $j \in \mathcal{J}$, is based on the same DP $(\mathcal{S}_j, \mathcal{A}_j, q_j, p_j, r_j)$ for all $k \in \mathbb{N}$ and where $n_j^k = n_j^l$ for all $k, l \in \mathbb{N}$. Let $\tilde{s}_{t,(j,i,\ell)}^k$ be the random state of the ℓ-th part of the i-th DP in the j-th counting DP of the k-th weakly coupled k-counting DP at time t. Consistency requires that the random state evolution $\tilde{\sigma}^k = \{\tilde{\sigma}_t^k\}_t$ of the

k-th weakly coupled k-counting DP satisfies $\tilde{\sigma}^k_{tj}(s) = \sum_{i=1}^{n_j} \frac{1}{k} \sum_{\ell=1}^{k} \mathbf{1}[\tilde{s}^k_{t,(j,i,\ell)} = s]$ pointwise for all $k \in \mathbb{N}$, $t \in \mathcal{T}$, $j \in \mathcal{J}$ and $s \in \mathcal{S}_j$. The random initial state $\tilde{\sigma}^k_1$ of the k-th weakly coupled k-counting DP then satisfies

$$\tilde{\sigma}^k_{1j}(s) \;=\; \sum_{i=1}^{n_j} \frac{1}{k} \sum_{\ell=1}^{k} \mathbf{1}[\tilde{s}^k_{1,(j,i,\ell)} = s] \;\underset{k\longrightarrow\infty}{\longrightarrow}\; \sum_{i=1}^{n_j} \mathbb{E}\big[\mathbf{1}[\tilde{s}^1_{1,(j,1,1)} = s]\big] \;=\; \sum_{i\in\mathcal{I}(j)} \mathbb{P}\big[\tilde{s}^1_{1,(j,1,1)} = s\big] \;=\; n_j{\cdot}q_j(s)$$

for all $j \in \mathcal{J}$ and $s \in \mathcal{S}_j$, and the convergence takes place almost surely due to the strong law of large numbers. Similarly, assume that the state of the k-th weakly coupled k-counting DP at time $t \in \mathcal{T}$ is $\tilde{\sigma}^k_t = \sigma^k_t$, that the action $\alpha^k_t \in \mathfrak{A}^k_t(\sigma^k_t)$ is taken, and that the associated states of the DP parts are $\tilde{s}^k_{t,(j,i,\ell)} = s^k_{t,(j,i,\ell)}$. Consistency then requires that $\sigma^k_{tj}(s) = \sum_{a\in\mathcal{A}_j} \alpha^k_{tj}(s,a)$ for all $k \in \mathbb{N}$, $j \in \mathcal{J}$ and $s \in \mathcal{S}_j$. Assuming that σ^k_t and α^k_t converge to σ_t and α_t as $k \longrightarrow \infty$, we observe that

$$\tilde{\sigma}^k_{t+1,j}(s') \;=\; \sum_{i=1}^{n_j} \frac{1}{k} \sum_{\ell=1}^{k} \mathbf{1}[\tilde{s}^k_{t+1,(j,i,\ell)} = s'] \;\underset{k\longrightarrow\infty}{\longrightarrow}\; \sum_{s\in\mathcal{S}_j} \sum_{a\in\mathcal{A}_j} p_{jt}(s' \,|\, s,a) \cdot \alpha_{tj}(s,a)$$

for all $j \in \mathcal{J}$ and $s' \in \mathcal{S}_j$, and the convergence again takes place almost surely. Indeed, the strong law of large numbers implies that $\frac{1}{k} \sum_{\ell=1}^{k} \mathbf{1}[\tilde{s}^k_{t+1,(j,i,\ell)} = s']$ converges to its expected value, that is, the probability of $\tilde{s}^k_{t+1,(j,i,\ell)}$ being s'. The probability of $\tilde{s}^k_{t+1,(j,i,\ell)}$ being s' if $s^k_{t,(j,i,\ell)} = s$ and action $a \in \mathcal{A}_j$ is taken, on the other hand, is $p_{jt}(s' \,|\, s,a)$. As k approaches ∞, α^k_{tj} converges to α_{tj}, and thus the number of DP parts in state s that action a is applied to converges to $\alpha_{tj}(s,a) \cdot k$.

The above observation motivates the *fluid limit* that we obtain when $k \longrightarrow \infty$. In what follows, we denote by $\delta(\cdot)$ the Dirac delta function satisfying $\delta(x) = 0$ for all $x \neq 0$ and $\int \delta(x)\,\mathrm{d}x = 1$.

Definition 4.13 (Fluid DP) *For a weakly coupled counting DP* $(\{\mathfrak{S}_j, \mathfrak{A}_j, \mathfrak{q}_j, \mathfrak{p}_j, \mathfrak{r}_j\}_j; \{n_j\}_j)$, *the* fluid DP $(\{\overline{\mathfrak{S}}_j, \overline{\mathfrak{A}}_j, \overline{\mathfrak{q}}_j, \overline{\mathfrak{p}}_j, \overline{\mathfrak{r}}_j\}_j; \{n_j\}_j)$ *is a DP with continuous state space* $\overline{\mathfrak{S}} = \times_{j\in\mathcal{J}} \overline{\mathfrak{S}}_j$ *with* $\overline{\mathfrak{S}}_j = \{\sigma_j : \mathcal{S}_j \to \mathbb{R}_+\}$, *continuous action space* $\overline{\mathfrak{A}} = \times_{j\in\mathcal{J}} \overline{\mathfrak{A}}_j$ *with* $\overline{\mathfrak{A}}_j = \{\alpha_j : \mathcal{S}_j \times \mathcal{A}_j \to \mathbb{R}_+\}$,

$\overline{\mathfrak{A}}_t(\sigma) = \times_{j\in\mathcal{J}} \overline{\mathfrak{A}}_{jt}(\sigma_j)$ with

$$\overline{\mathfrak{A}}_{jt}(\sigma_j) \;=\; \left\{ \alpha_j \in \overline{\mathfrak{A}}_j \;:\; \sum_{a\in\mathcal{A}_j} \alpha_j(s,a) = \sigma_j(s) \;\; \forall s \in \mathcal{S}_j, \;\; \alpha_j(s,a) = 0 \;\; \forall s \in \mathcal{S}_j, \; \forall a \in \mathcal{A}_j \backslash \mathcal{A}_{jt}(s) \right\}$$

and

$$\overline{\mathfrak{A}}_t^{\mathrm{C}}(\sigma) \;=\; \left\{ \alpha \in \overline{\mathfrak{A}}_t(\sigma) \;:\; \sum_{j\in\mathcal{J}} \sum_{s\in\mathcal{S}_j} \sum_{a\in\mathcal{A}_j} c_{tlj}(s,a)\cdot\alpha_j(s,a) \leqslant b_{tl} \;\; \forall l \in \mathcal{L} \right\},$$

initial state probabilities

$$\overline{\mathfrak{q}}(\sigma) \;=\; \prod_{j\in\mathcal{J}} \prod_{s\in\mathcal{S}_j} \delta\left(\sigma_j(s) - n_j \cdot q_j(s)\right) \qquad \forall \sigma \in \overline{\mathfrak{S}}, \tag{4.1}$$

transition probabilities $\overline{\mathfrak{p}} = \{\overline{\mathfrak{p}}_t\}_t$ with

$$\overline{\mathfrak{p}}_t(\sigma' \,|\, \sigma, \alpha) \;=\; \prod_{j\in\mathcal{J}} \prod_{s'\in\mathcal{S}_j} \delta\left(\sigma_j(s') - \sum_{s\in\mathcal{S}_j} \sum_{a\in\mathcal{A}_j} p_t(s'|s,a)\cdot\alpha(s,a) \right) \quad \forall \sigma, \sigma' \in \overline{\mathfrak{S}}, \; \forall \alpha \in \overline{\mathfrak{A}}, \; \forall t \in \mathcal{T} \tag{4.2}$$

and expected rewards $\overline{\mathfrak{r}} = \{\overline{\mathfrak{r}}_t\}_t$ with $\overline{\mathfrak{r}}_t(\sigma,\alpha) = \sum_{j\in\mathcal{J}} \mathfrak{r}_{jt}(\sigma_j,\alpha_j)$.

A policy $\pi = \{\pi_t\}_t$ for the fluid DP with $\pi_t : \overline{\mathfrak{S}} \to \overline{\mathfrak{A}}$ specifies for each time period $t \in \mathcal{T}$, each counting DP $j \in \mathcal{J}$ and each state $\sigma \in \overline{\mathfrak{S}}$ what action $[\pi_t(\sigma)]_j \in \overline{\mathfrak{A}}_j$ is selected. A feasible policy π must satisfy $\pi_t(\sigma) \in \overline{\mathfrak{A}}_t^{\mathrm{C}}(\sigma)$ for all $t \in \mathcal{T}$ and $\sigma \in \overline{\mathfrak{S}}$. Under π, the initial state $\tilde{\sigma}_1$ of the fluid DP satisfies $\tilde{\sigma}_{1j}(s) = n_j \cdot q_j(s)$ almost surely for all $j \in \mathcal{J}$ and $s \in \mathcal{S}_j$. For $t \in \mathcal{T}\backslash\{T\}$, under the assumption that $\tilde{\sigma}_t = \sigma_t$ almost surely, the transitions satisfy

$$\tilde{\sigma}_{t+1,j}(s') \;=\; \sum_{s\in\mathcal{S}_j} \sum_{a\in\mathcal{A}_j} p_t(s'|s,a)\cdot[\pi_t(\sigma_t)]_j(s,a) \qquad \forall j \in \mathcal{J}, \; \forall s' \in \mathcal{S}_j \text{ almost surely.}$$

The expected total reward of a policy π is $\mathbb{E}\left[\sum_{t\in\mathcal{T}} \mathfrak{r}_t(\tilde{\sigma}_t, \pi_t(\tilde{\sigma}_t))\right]$.

The state and action spaces of a weakly coupled k-counting DP are of the size $\mathcal{O}\left(\prod_{j\in\mathcal{J}} (k\cdot n_j)^{|\mathcal{S}_j|}\right)$ and $\mathcal{O}\left(\prod_{j\in\mathcal{J}} (k\cdot n_j)^{|\mathcal{S}_j|\cdot|\mathcal{A}_j|}\right)$, respectively, and they thus scale exponentially in the number of involved counting DPs as well as the numbers of states and actions of the underlying DPs. In contrast, the state of the associated fluid DP can almost surely be described by a real vector of length $\sum_{j\in\mathcal{J}} |\mathcal{S}_j|$, and an action in the fluid DP is described by a real vector of length $\sum_{j\in\mathcal{J}} |\mathcal{S}_j| \cdot |\mathcal{A}_j|$. The next section will exploit this reduction in complexity to formulate the fluid DP as a linear program that scales gracefully in the parameters of the corresponding weakly coupled counting DP.

For later reference, we define the *policy set* of a fluid DP as $\overline{\Pi} = \bigtimes_{t\in\mathcal{T}} \overline{\Pi}_t$ with $\overline{\Pi}_t = \{[\pi_t : \overline{\mathfrak{S}} \to \overline{\mathfrak{A}}] \,:\, \pi_t(\sigma) \in \overline{\mathfrak{A}}_t(\sigma) \quad \forall \sigma \in \overline{\mathfrak{S}}\}$ and the *set of feasible policies* as $\overline{\Pi}^{\mathrm{C}} = \bigtimes_{t\in\mathcal{T}} \overline{\Pi}_t^{\mathrm{C}}$ with $\overline{\Pi}_t^{\mathrm{C}} = \{\pi_t \in \overline{\Pi}_t \,:\, \pi_t(\sigma) \in \overline{\mathfrak{A}}_t^{\mathrm{C}}(\sigma) \quad \forall \sigma \in \overline{\mathfrak{S}}\}$, respectively. We denote the *set of state trajectories* as $\overline{\Sigma} = \bigtimes_{t\in\mathcal{T}} \overline{\mathfrak{S}}$; the random state evolution $\tilde{\sigma} = \{\tilde{\sigma}\}_t$ then takes values in $\overline{\Sigma}$.

At this point, we make a summary of the major assumptions of our model. The transition probabilities are Markovian, and hence memoryless. For the weakly coupled DP of Definition 4.3, we assume that there are $J \ll I$ groups such that each DP $i \in \mathcal{I}$ belongs to exactly one of the groups $j \in \mathcal{J} = \{1, \ldots, J\}$, and any two DPs of the same group share the same state and action spaces, initial state and transition probabilities as well as expected rewards.

4.3.2.2 Linear Programming Formulation for the Fluid Limit

We now demonstrate that an optimal policy for a fluid DP can be obtained through a linear program with $\mathcal{O}\left(|\mathcal{T}| \cdot \sum_{j\in\mathcal{J}} |\mathcal{S}_j||\mathcal{A}_j|\right)$ decision variables and $\mathcal{O}\left(|\mathcal{T}| \cdot \max\left\{\sum_{j\in\mathcal{J}} |\mathcal{S}_j|,\ |\mathcal{L}|\right\}\right)$ constraints. Our healthcare model comprises $|\mathcal{T}| = 52$ time periods (one year in weekly granularity), $|\mathcal{J}| = 3,120$ counting DPs (52 arrival times, 3 age groups and 20 disease groups), as well as $|\mathcal{S}_j| = 15$ states and $|\mathcal{A}_j| = 6$ actions per patient DP. The resulting LP, while nontrivial in size, can be solved quickly and reliably on standard hardware with off-the-shelf software.

For a weakly coupled counting DP $(\{\mathfrak{S}_j, \mathfrak{A}_j, \mathfrak{q}_j, \mathfrak{p}_j, \mathfrak{r}_j\}_j; \{n_j\}_j)$, consider the *fluid LP* defined as

$$\begin{array}{lll}
\underset{\sigma,\,\pi}{\text{maximize}} & \displaystyle\sum_{t\in\mathcal{T}}\sum_{j\in\mathcal{J}}\sum_{s\in\mathcal{S}_j}\sum_{a\in\mathcal{A}_j} r_{jt}(s,a)\cdot\pi_{tj}(s,a) & \\
\text{subject to} & \sigma_{1j}(s) = n_j\cdot q_j(s) & \forall j\in\mathcal{J},\ \forall s\in\mathcal{S}_j \\
& \sigma_{t+1,j}(s') = \displaystyle\sum_{s\in\mathcal{S}_j}\sum_{a\in\mathcal{A}_j} p_{jt}(s'\,|\,s,a)\cdot\pi_{tj}(s,a) & \forall j\in\mathcal{J},\ \forall s'\in\mathcal{S}_j,\ \forall t\in\mathcal{T}\backslash\{T\} \\
& \displaystyle\sum_{j\in\mathcal{J}}\sum_{s\in\mathcal{S}_j}\sum_{a\in\mathcal{A}_j} c_{tlj}(s,a)\cdot\pi_{tj}(s,a)\leqslant b_{tl} & \forall l\in\mathcal{L},\ \forall t\in\mathcal{T} \\
& \displaystyle\sum_{a\in\mathcal{A}_j}\pi_{tj}(s,a) = \sigma_{tj}(s) & \forall j\in\mathcal{J},\ \forall s\in\mathcal{S}_j,\ \forall t\in\mathcal{T} \\
& \pi_{tj}(s,a) = 0 & \forall j\in\mathcal{J},\ \forall s\in\mathcal{S}_j,\ \forall a\in\mathcal{A}_j\backslash\mathcal{A}_{jt}(s),\ \forall t\in\mathcal{T} \\
& \sigma_{tj}(s),\ \pi_{tj}(s,a)\geqslant 0 & \forall j\in\mathcal{J},\ \forall (s,a)\in\mathcal{S}_j\times\mathcal{A}_j,\ \forall t\in\mathcal{T}.
\end{array} \tag{4.3}$$

Note that in contrast to the policy set of a fluid DP, which is infinite-dimensional, the feasible region of the fluid LP (4.3) is finite-dimensional since it assigns a sequence of actions $\{\pi_t\}_t$ to a *single* state trajectory $\sigma \in \overline{\Sigma}$. This turns out to be sufficient since for a fixed policy, the fluid DP evolves according to a single state trajectory almost surely.

We first verify that the fluid LP (4.3) determines an optimal policy for the fluid DP, together with its associated (almost sure) state evolution.

Proposition 4.14 *Fix a weakly coupled counting DP* $(\{\mathfrak{S}_j, \mathfrak{A}_j, \mathfrak{q}_j, \mathfrak{p}_j, \mathfrak{r}_j\}_j; \{n_j\}_j)$.

(i) *If the fluid DP admits a feasible policy* $\overline{\pi}^0 \in \overline{\Pi}^{\mathrm{C}}$, *then a feasible solution* $(\sigma^{\mathrm{LP}}, \pi^{\mathrm{LP}})$ *to the fluid LP* (4.3) *with objective value* θ^{LP} *gives rise to a feasible policy* $\overline{\pi} \in \overline{\Pi}^{\mathrm{C}}$ *to the fluid DP via*

$$\overline{\pi}_t(\sigma) = \begin{cases} \pi_t^{\mathrm{LP}} & \text{if } \sigma = \sigma_t^{\mathrm{LP}}, \\ \overline{\pi}_t^0(\sigma) & \text{otherwise} \end{cases} \qquad \forall t\in\mathcal{T},\ \forall \sigma\in\overline{\mathfrak{S}},$$

together with its state evolution $\tilde{\sigma} = \{\tilde{\sigma}_t\}_t$ *satisfying* $\tilde{\sigma} = \sigma^{\mathrm{LP}}$ *almost surely. Moreover, the expected total reward of* $\overline{\pi}$ *is* θ^{LP}.

(ii) *A feasible policy* $\overline{\pi} \in \overline{\Pi}^{\mathrm{C}}$ *to the fluid DP with associated state evolution* $\tilde{\sigma} = \{\tilde{\sigma}_t\}_t$ *and an expected total reward of* θ^{DP} *gives rise to a feasible solution* $(\sigma^{\mathrm{LP}}, \pi^{\mathrm{LP}})$ *to the fluid*

LP (4.3) *with objective value* θ^{DP} *via*

$$\sigma^{\mathrm{LP}}_{tj}(s') \;=\; \begin{cases} n_j \cdot q_j(s') & \text{if } t = 1, \\ \displaystyle\sum_{s \in \mathcal{S}_j} \sum_{a \in \mathcal{A}_j} p_{j,t-1}(s' \mid s, a) \cdot \pi^{\mathrm{LP}}_{t-1,j}(s,a) & \text{otherwise} \end{cases}$$

for all $t \in \mathcal{T}$, $j \in \mathcal{J}$ *and* $s' \in \mathcal{S}_j$, *as well as* $\pi^{\mathrm{LP}}_t = \overline{\pi}_t(\sigma^{\mathrm{LP}}_t)$ *for all* $t \in \mathcal{T}$.

Proof of Proposition 4.14. In view of statement *(i)*, we first verify that $\overline{\pi} \in \overline{\Pi}^{\mathrm{C}}$, that is, $\overline{\pi}$ is a feasible policy for the fluid DP. To this end, we need to confirm that $\overline{\pi}_t(\sigma) \in \overline{\mathfrak{A}}^{\mathrm{C}}_t(\sigma)$ for all $t \in \mathcal{T}$ and all $\sigma \in \overline{\mathfrak{S}}$. Due to the feasibility of $\overline{\pi}^0$, this is the case for all $t \in \mathcal{T}$ and all $\sigma \in \overline{\mathfrak{S}} \backslash \{\sigma^{\mathrm{LP}}_t\}$. To verify that $\overline{\pi}_t(\sigma^{\mathrm{LP}}_t) \in \overline{\mathfrak{A}}^{\mathrm{C}}_t(\sigma^{\mathrm{LP}}_t)$ for all $t \in \mathcal{T}$ as well, we observe that $[\overline{\pi}_t(\sigma^{\mathrm{LP}}_t)]_j \in \overline{\mathfrak{A}}_j$, $j \in \mathcal{J}$, by construction, while $\sum_{j \in \mathcal{J}} \sum_{s \in \mathcal{S}_j} \sum_{a \in \mathcal{A}_j} c_{tlj}(s,a) \cdot [\overline{\pi}_t(\sigma^{\mathrm{LP}}_t)])_j(s,a) \leqslant b_{tl}$, $\sum_{a \in \mathcal{A}_j} [\overline{\pi}_t(\sigma^{\mathrm{LP}}_t)]_j(s,a) = \sigma^{\mathrm{LP}}_{tj}(s)$ and $[\overline{\pi}_t(\sigma^{\mathrm{LP}}_t)]_j(s,a) = 0$ hold for all $j \in \mathcal{J}$, $s \in \mathcal{S}_j$, $a \in \mathcal{A}_j \backslash \mathcal{A}_{jt}(s)$, $l \in \mathcal{L}$ and $t \in \mathcal{T}$ due to the third, fourth and fifth constraint in the fluid LP (4.3), respectively.

We next show via induction over $t \in \mathcal{T}$ that the random state evolution $\tilde{\sigma} = \{\tilde{\sigma}_t\}_t$ of the fluid DP under the policy $\overline{\pi}$ satisfies $\tilde{\sigma} = \sigma^{\mathrm{LP}}$ almost surely. For $\tilde{\sigma}_1$, this immediately follows from the initial state probabilities in the definition of the fluid DP as well as the first constraint of the fluid LP. Assume now that $\tilde{\sigma}_t = \sigma^{\mathrm{LP}}_t$ almost surely for some $t \in \mathcal{T} \backslash \{T\}$. We then have $\overline{\pi}_t(\tilde{\sigma}_t) = \pi^{\mathrm{LP}}_t$ almost surely, and the transition probabilities in the definition of the fluid DP as well as the second constraint of the fluid LP imply that $\tilde{\sigma}_{t+1} = \sigma^{\mathrm{LP}}_{t+1}$ almost surely as well. Since $\tilde{\sigma} = \sigma^{\mathrm{LP}}$ almost surely and $\overline{\pi}_t(\sigma^{\mathrm{LP}}_t) = \pi^{\mathrm{LP}}_t$ for all $t \in \mathcal{T}$, the expected total reward of the policy $\overline{\pi}$ is indeed θ^{LP} as claimed. This proves the first statement.

Consider now statement *(ii)*. A similar induction argument as in the previous paragraph shows that the random state evolution $\tilde{\sigma} = \{\tilde{\sigma}_t\}_t$ of the fluid DP satisfies $\tilde{\sigma} = \sigma^{\mathrm{LP}}$ and the policy $\overline{\pi}$ of the fluid DP satisfies $\overline{\pi}_t(\tilde{\sigma}_t) = \pi^{\mathrm{LP}}_t$ for all $t \in \mathcal{T}$ almost surely. The feasibility of $(\sigma^{\mathrm{LP}}, \pi^{\mathrm{LP}})$ in the fluid LP (4.3) then follows from the initial state and transition probabilities in the definition of the fluid DP as well as the fact that $\overline{\pi}$ is a feasible policy for the fluid DP. Moreover, since $\pi^{\mathrm{LP}}_t = \overline{\pi}_t(\tilde{\sigma}_t)$ almost surely for all $t \in \mathcal{T}$, the objective value of $(\sigma^{\mathrm{LP}}, \pi^{\mathrm{LP}})$ in (4.3) is indeed θ^{DP} as claimed. ∎

Proposition 4.14 immediately implies that optimal solutions to the fluid LP (4.3) give rise to optimal policies to the fluid DP and vice versa. The existence of a feasible policy $\overline{\pi}^0$ in part *(i)* is necessary since we require a fluid DP policy to be feasible pointwise in every state, rather than almost surely.

We now show that the fluid LP (4.3) constitutes a relaxation of the weakly coupled counting DP from Definition 4.8. While the result is intuitive, given that the associated fluid DP can be interpreted as a continuous relaxation of the weakly coupled counting DP, its proof is nontrivial since the fluid DP visits 'fractional' states that are not present in the weakly coupled counting DP.

Theorem 4.15 *The optimal value of the fluid LP* (4.3) *is greater than or equal to the optimal expected total reward of its associated weakly coupled counting DP* $(\{\mathfrak{S}_j, \mathfrak{A}_j, \mathfrak{q}_j, \mathfrak{p}_j, \mathfrak{r}_j\}_j; \{n_j\}_j)$.

Proof of Theorem 4.15. Denote by $F(\tau, \sigma_\tau)$ the truncated fluid LP that starts in period $\tau \in \mathcal{T}$ with the state $\sigma_\tau \in \overline{\mathfrak{S}}$:

$$
\begin{array}{lll}
\underset{\sigma,\,\pi}{\text{maximize}} & \displaystyle\sum_{t=\tau}^{T} f(t, \pi_t) & \\
\text{subject to} & \sigma_{t+1,j}(s') = \displaystyle\sum_{s \in \mathcal{S}_j} \sum_{a \in \mathcal{A}_j} p_{jt}(s' \mid s, a) \cdot \pi_{tj}(s, a) & \forall j \in \mathcal{J},\ \forall s' \in \mathcal{S}_j,\ \forall t = \tau, \ldots, T-1 \\
& \pi_t \in \overline{\Pi}_t^{1\mathrm{C}}(\sigma_t) & \forall t = \tau, \ldots, T \\
& \sigma_{tj}(s) \geqslant 0 & \forall j \in \mathcal{J},\ \forall s \in \mathcal{S}_j,\ \forall t = \tau, \ldots, T
\end{array}
$$

Here, the objective function satisfies

$$
f(t, \pi_t) \;=\; \sum_{j \in \mathcal{J}} \sum_{s \in \mathcal{S}_j} \sum_{a \in \mathcal{A}_j} r_{jt}(s, a) \cdot \pi_{tj}(s, a),
$$

and the constraints satisfy

$$\pi_t \in \overline{\Pi}_t^{1C}(\sigma_t) \quad \Longleftrightarrow \quad \begin{cases} \sum_{j \in \mathcal{J}} \sum_{s \in \mathcal{S}_j} \sum_{a \in \mathcal{A}_j} c_{tlj}(s,a) \cdot \pi_{tj}(s,a) \leqslant b_{tl} & \forall l \in \mathcal{L} \\ \sum_{a \in \mathcal{A}_j} \pi_{tj}(s,a) = \sigma_{tj}(s) & \forall j \in \mathcal{J},\ \forall s \in \mathcal{S}_j \\ \pi_{tj}(s,a) = 0 & \forall j \in \mathcal{J},\ \forall s \in \mathcal{S}_j,\ \forall a \in \mathcal{A}_j \backslash \mathcal{A}_{jt}(s) \\ \pi_{tj}(s,a) \geqslant 0 & \forall j \in \mathcal{J},\ \forall (s,a) \in \mathcal{S}_j \times \mathcal{A}_j. \end{cases}$$

Setting $F(T+1, \sigma_{T+1}) = 0$ for all $\sigma_{T+1} \in \overline{\mathfrak{S}}$, one readily verifies that the truncated fluid LP satisfies

$$F(t, \sigma_t) \;=\; \max_{\pi_t \in \overline{\Pi}_t^{1C}(\sigma_t)} \left\{ f(t, \pi_t) + F\left(t+1,\ \sum_{s \in \mathcal{S}_j} \sum_{a \in \mathcal{A}_j} p_{jt}(s' \,|\, s, a) \cdot \pi_{tj}(s,a) \right) \right\}.$$

We show via induction that $F(t, \cdot)$ is concave for all $t \in \mathcal{T} \cup \{T+1\}$. This is trivially the case for $t = T+1$. Assume now that $F(t+1, \cdot)$ is concave and represent $F(t, \cdot)$ as

$$F(t, \sigma_t) \;=\; \max_{\pi_t \in \overline{\mathfrak{A}}} \left\{ f(t, \pi_t) + F\left(t+1,\ \sum_{s \in \mathcal{S}_j} \sum_{a \in \mathcal{A}_j} p_{jt}(s' \,|\, s, a) \cdot \pi_{tj}(s,a) \right) - \mathbb{I}(\sigma_t, \pi_t) \right\},$$

where $\mathbb{I}(\sigma_t, \pi_t) = 0$ if $\pi_t \in \overline{\Pi}_t^{1C}(\sigma_t)$ and $\mathbb{I}(\sigma_t, \pi_t) = \infty$ otherwise. Since $\mathbb{I}(\sigma_t, \pi_t)$ is convex, $F(t, \cdot)$ is concave as it represents a sup-projection of a concave function [RW97, Proposition 2.22]. We thus conclude that $F(t, \cdot)$ is concave for all $t \in \mathcal{T} \cup \{T+1\}$.

Denote now by $G(t, \sigma_t)$ the optimal value of the weakly coupled counting DP, which satisfies

$$G(t, \sigma_t) \;=\; \max_{\pi_t \in \Pi_t^{1C}(\sigma_t)} \left\{ f(t, \pi_t) + \mathbb{E}\left[G(t+1, \tilde{\sigma}_{t+1}) \,|\, \tilde{\sigma}_{t+1} \sim \mathfrak{p}(\cdot \,|\, \sigma_t, \pi_t) \right] \right\}$$

for $t \in \mathcal{T}$ and $\sigma_t \in \mathfrak{S}$ with $\Pi_t^{1C}(\sigma_t) = \overline{\Pi}_t^{1C}(\sigma_t) \cap \mathfrak{A}$ as well as $G(T+1, \sigma_t) = 0$ for all $\sigma_t \in \mathfrak{S}$. We show via induction that $F(t, \sigma_t) \geqslant G(t, \sigma_t)$ for all $t \in \mathcal{T} \cup \{T+1\}$ and all $\sigma_t \in \mathfrak{S}$. The statement trivially holds for $t = T+1$. Assume now that $F(t+1, \sigma_{t+1}) \geqslant G(t+1, \sigma_{t+1})$ for some $t \in \mathcal{T}$ and all $\sigma_{t+1} \in \mathfrak{S}$. We then have

$$\begin{aligned}
F(t, \sigma_t) &= \max_{\pi_t \in \overline{\Pi}_t^{1\mathrm{C}}(\sigma_t)} \left\{ f(t, \pi_t) + F\left(t+1,\ \sum_{s \in \mathcal{S}_j} \sum_{a \in \mathcal{A}_j} p_{jt}(s' \,|\, s, a) \cdot \pi_{tj}(s, a) \right) \right\} \\
&\geqslant \max_{\pi_t \in \Pi_t^{1\mathrm{C}}(\sigma_t)} \left\{ f(t, \pi_t) + F\left(t+1,\ \sum_{s \in \mathcal{S}_j} \sum_{a \in \mathcal{A}_j} p_{jt}(s' \,|\, s, a) \cdot \pi_{tj}(s, a) \right) \right\} \\
&= \max_{\pi_t \in \Pi_t^{1\mathrm{C}}(\sigma_t)} \left\{ f(t, \pi_t) + F\left(t+1,\ \mathbb{E}\left[\tilde{\sigma}_{t+1} \,|\, \tilde{\sigma}_{t+1} \sim \mathfrak{p}(\cdot \,|\, \sigma_t, \pi_t)\right]\right) \right\} \\
&\geqslant \max_{\pi_t \in \Pi_t^{1\mathrm{C}}(\sigma_t)} \left\{ f(t, \pi_t) + \mathbb{E}\left[F\left(t+1,\ \tilde{\sigma}_{t+1}\right) \,|\, \tilde{\sigma}_{t+1} \sim \mathfrak{p}(\cdot \,|\, \sigma_t, \pi_t)\right] \right\} \\
&\geqslant \max_{\pi_t \in \Pi_t^{1\mathrm{C}}(\sigma_t)} \left\{ f(t, \pi_t) + \mathbb{E}\left[G\left(t+1,\ \tilde{\sigma}_{t+1}\right) \,|\, \tilde{\sigma}_{t+1} \sim \mathfrak{p}(\cdot \,|\, \sigma_t, \pi_t)\right] \right\} \\
&= G(t, \sigma_t)
\end{aligned}$$

for all $\sigma_t \in \mathfrak{S}$, where the first and last identities hold by definition of F and G, respectively. The first inequality follows from $\Pi_t^{1\mathrm{C}}(\sigma_t) = \overline{\Pi}_t^{1\mathrm{C}}(\sigma_t) \cap \mathfrak{A} \subseteq \overline{\Pi}_t^{1\mathrm{C}}(\sigma_t)$, the second equality holds since the expected number of DPs in the j-th counting DP that are in state s' at time $t+1$ is the sum of all DPs in that counting DP that are in any state s at time t and whose associated action a transitions them into state s', the individual probability of which is given by $p_{jt}(s' \,|\, s, a)$. The second inequality is due to Jensen's inequality, which is applicable since F has been shown to be concave, and the last inequality follows from the induction hypothesis.

Denote now by θ^{LP} the optimal objective value of the fluid LP (4.3) and by θ^{DP} the expected total reward of the weakly coupled counting DP under an optimal policy, respectively. We have

$$\begin{aligned}
\theta^{\mathrm{LP}} \;=\; F(1,\, \sigma_1) \;&=\; F\left(1,\, \mathbb{E}\left[\tilde{\sigma}_1 \,|\, \tilde{\sigma}_1 \sim \mathfrak{q}\right]\right) \\
&\geqslant\; \mathbb{E}\left[F\left(1,\, \tilde{\sigma}_1\right) \,|\, \tilde{\sigma}_1 \sim \mathfrak{q}\right] \;\geqslant\; \mathbb{E}\left[G\left(1,\, \tilde{\sigma}_1\right) \,|\, \tilde{\sigma}_1 \sim \mathfrak{q}\right] \;=\; \theta^{\mathrm{DP}},
\end{aligned}$$

where $\sigma_{1j} = n_j \cdot q_j$, $j \in \mathcal{J}$, and the two inequalities follow from Jensen's inequality and our induction argument from the previous paragraph, respectively. The claim of the theorem thus follows. ∎

Proposition 4.14 and Theorem 4.15 immediately imply that the fluid DP is a relaxation of the associated weakly coupled counting DP in the following sense.

Corollary 4.16 *The optimal expected total reward of a fluid DP is greater than or equal to the optimal expected total reward of its associated weakly coupled counting DP.*

An optimal solution $(\sigma^{\mathrm{LP}}, \pi^{\mathrm{LP}})$ to the fluid LP (4.3) does not only give rise to an optimal policy for the fluid DP, but it also allows us to construct near-optimal policies for the weakly coupled counting DP. In this section, we study two such constructions: one that is based on a deterministic rounding scheme (Section 4.3.2.3) and one that is based on a randomization approach (Section 4.3.2.4).

4.3.2.3 Approximation Guarantees: Deterministic Rounded Policies

Fix a weakly coupled counting DP $(\{\mathfrak{S}_j, \mathfrak{A}_j, \mathfrak{q}_j, \mathfrak{p}_j, \mathfrak{r}_j\}_j; \{n_j\}_j)$ as well as an optimal solution $(\sigma^{\mathrm{LP}}, \pi^{\mathrm{LP}}) \in \overline{\Sigma} \times \overline{\mathfrak{A}}^T$ to its associated fluid LP (4.3). We consider the policy

$$\pi^{\star} \;=\; \mathrm{Pr}\left[\mathrm{L}(\sigma^{\mathrm{LP}}, \pi^{\mathrm{LP}})\right],$$

where the lifting operator L maps $(\sigma^{\mathrm{LP}}, \pi^{\mathrm{LP}})$ to a policy $\overline{\pi} = \mathrm{L}(\sigma^{\mathrm{LP}}, \pi^{\mathrm{LP}})$ for the fluid DP via

$$[\overline{\pi}_t(\sigma)]_j(s,a) \;=\; \frac{\pi^{\mathrm{LP}}_{tj}(s,a)}{\sigma^{\mathrm{LP}}_{tj}(s)} \cdot \sigma_{tj}(s) \qquad \forall t \in \mathcal{T},\ \forall \sigma \in \overline{\mathfrak{S}},\ \forall j \in \mathcal{J},\ \forall (s,a) \in \mathcal{S}_j \times \mathcal{A}_j,$$

where we adopt the convention that $0/0 = 0$, and the projection operator Pr maps $\overline{\pi}$ to a policy $\pi^{\star}$ for the weakly coupled counting DP according to

$$[\mathrm{Pr}(\overline{\pi})]_t(\sigma) \in \operatorname*{arg\,min}_{\alpha \in \mathfrak{A}_t(\sigma)} \|\overline{\pi}_t(\sigma) - \alpha\|_1 \qquad \forall t \in \mathcal{T},\ \forall \sigma \in \mathfrak{S},$$

where $\|\overline{\pi}_t(\sigma) - \alpha\|_1 = \sum_{j \in \mathcal{J}} \sum_{s \in \mathcal{S}_j} \sum_{a \in \mathcal{A}_j} |[\overline{\pi}_t(\sigma)]_j(s,a) - \alpha_j(s,a)|$. We will see below that the minimum in the above equation is indeed attained. Intuitively speaking, the lifted policy $\overline{\pi}$

employs the actions in each counting state σ with the same frequency as π^{LP} does in the almost sure trajectory σ^{LP} from the fluid LP in the same time period, and the projected policy $\pi^\star$ rounds this policy to the nearest discrete policy that obeys the constraints of $\overline{\Pi}$. We note that neither $(\sigma^{\mathrm{LP}}, \pi^{\mathrm{LP}})$ nor $\pi^\star$ is unique in general. In the remainder, all statements apply to *any* policy $\pi^\star$ emerging from the above construction.

Recall from Proposition 4.14 *(i)* that feasible solutions to the fluid LP (4.3) give rise to feasible policies to the fluid DP, provided that $\overline{\Pi}^{\mathrm{C}}$ is non-empty. Since we did not assume non-emptiness of $\overline{\Pi}^{\mathrm{C}}$ here, the lifted policy $\overline{\pi}$ may violate the resource constraints of the fluid DP.

Observation 4.17 *The lifted policy $\overline{\pi}$ satisfies $\overline{\pi} \in \overline{\Pi}$, but it may not be contained in $\overline{\Pi}^{\mathrm{C}}$.*

Proof of Observation 4.17. To see that $\overline{\pi} \in \overline{\Pi}$, we need to show that $\overline{\pi}_t \in \overline{\Pi}_t$ for all $t \in \mathcal{T}$, that is, $\overline{\pi}_t(\sigma) \in \overline{\mathfrak{A}}_t(\sigma)$ for all $t \in \mathcal{T}$ and $\sigma \in \overline{\mathfrak{S}}$, which in turn amounts to showing that $[\overline{\pi}_t(\sigma)]_j \in \overline{\mathfrak{A}}_j$, $\sum_{a \in \mathcal{A}_j} [\overline{\pi}_t(\sigma)]_j(s,a) = \sigma_j(s)$ and $[\overline{\pi}_t(\sigma)]_j(s,a) = 0$ for all $t \in \mathcal{T}$, $\sigma \in \overline{\mathfrak{S}}$, $j \in \mathcal{J}$, $s \in \mathcal{S}_j$ and all $a \in \mathcal{A}_j \backslash \mathcal{A}_{jt}(s)$. Out of these constraints, $[\overline{\pi}_t(\sigma)]_j \in \overline{\mathfrak{A}}_j$ holds by construction, while

$$\sum_{a \in \mathcal{A}_j} [\overline{\pi}_t(\sigma)]_j(s,a) \;=\; \sum_{a \in \mathcal{A}_j} \frac{\pi^{\mathrm{LP}}_{tj}(s,a)}{\sigma^{\mathrm{LP}}_{tj}(s)} \cdot \sigma_j(s) \;=\; \sigma_j(s)$$

holds due to the fourth constraint in the fluid LP (4.3), and $[\overline{\pi}_t(\sigma)]_j(s,a) = 0$ is ensured by the fifth constraint of the fluid LP. We thus have $\overline{\pi} \in \overline{\Pi}$ as claimed.

We complete the proof by constructing a weakly coupled counting DP for which the fluid DP policy $\overline{\pi}$ constructed from any optimal solution $(\sigma^{\mathrm{LP}}, \pi^{\mathrm{LP}})$ to the fluid LP (4.3) satisfies $\overline{\pi} \notin \overline{\Pi}^{\mathrm{C}}$. To this end, set $\mathcal{T} = \mathcal{J} = \{1\}$, $\mathcal{S}_1 = \{1, 2\}$, $\mathcal{A}_1 = \{1\}$, $n_1 = 2$ and $q(1) = q(2) = 1/2$, while the resource constraint requires that $[\pi(\sigma)]_1(1,1) \leqslant 1$. One readily verifies that $(\sigma^{\mathrm{LP}}, \pi^{\mathrm{LP}})$ defined by $\sigma^{\mathrm{LP}}_1(1) = \sigma^{\mathrm{LP}}_1(2) = 1$ and $\pi^{\mathrm{LP}}_1(1,1) = \pi^{\mathrm{LP}}_1(2,1) = 1$ is the unique feasible solution to the fluid LP (4.3). The corresponding fluid DP policy $\overline{\pi}$, however, necessarily violates the resource constraint in the state $\sigma_1 \in \overline{\mathfrak{S}}$ defined via $\sigma_1(1) = 2$ and $\sigma_1(2) = 0$. (Recall that a feasible policy to the fluid DP must be feasible in *every* state of the fluid DP, not just the almost sure state.) ∎

The proof of Observation 4.17 implies that the projected policy $\pi^\star$ may violate the resource constraints of the weakly coupled counting DP as well. We next show, however, that $\pi^\star$ is contained in the policy set Π of the weakly coupled counting DP, and that it is close to the lifted policy $\overline{\pi}$.

Proposition 4.18 *We have $\pi^\star \in \Pi$ as well as $\|\pi_t^\star(\sigma) - \overline{\pi}_t(\sigma)\|_\infty < 1$ for all $t \in \mathcal{T}$ and $\sigma \in \mathfrak{S}$.*

Proof of Proposition 4.18. First note that $\overline{\pi} \in \overline{\Pi}$ according to Observation 4.17, which implies that $\overline{\mathfrak{A}}_t(\sigma) \neq \emptyset$ for all $t \in \mathcal{T}$ and $\sigma \in \mathfrak{S}$. From the construction of $\mathfrak{A}_t(\sigma)$ and $\overline{\mathfrak{A}}_t(\sigma)$ in the Definitions 4.8 and 4.13, respectively, one then readily verifies that $\mathfrak{A}_t(\sigma) \neq \emptyset$ for all $t \in \mathcal{T}$ and $\sigma \in \mathfrak{S}$ as well. We thus conclude that a policy $\pi^\star = \Pr(\overline{\pi})$ indeed exists and satisfies $\pi^\star \in \Pi$.

To see that $\|\pi_t^\star(\sigma) - \overline{\pi}_t(\sigma)\|_\infty < 1$ for all $t \in \mathcal{T}$ and all $\sigma \in \mathfrak{S}$, recall that

$$\pi_t^\star(\sigma) \in \underset{\alpha \in \mathfrak{A}_t(\sigma)}{\arg\min} \; \|\overline{\pi}_t(\sigma) - \alpha\|_1$$

by definition, where $\|\overline{\pi}_t(\sigma) - \alpha\|_1 = \sum_{j \in \mathcal{J}} \sum_{s \in \mathcal{S}_j} \sum_{a \in \mathcal{A}_j} |[\overline{\pi}_t(\sigma)]_j(s,a) - \alpha_j(s,a)|$. Since both the objective function and the constraints of this optimization problem are separable in $j \in \mathcal{J}$ and $s \in \mathcal{S}_j$, the component $[\Pr(\overline{\pi})_t(\sigma)]_j\,(s,\cdot)$ is any solution of the following minimization problem:

$$\begin{array}{lll}
\underset{\alpha}{\text{minimize}} & \|[\overline{\pi}_t(\sigma)]_j(s,\cdot) - \alpha\|_1 & \\
\text{subject to} & \displaystyle\sum_{a \in \mathcal{A}_j} \alpha(a) = \sum_{a \in \mathcal{A}_j} [\overline{\pi}_t(\sigma)]_j(s,a) & \\
& \alpha(a) = 0 & \forall a \in \mathcal{A}_j \backslash \mathcal{A}_{jt}(s) \\
& \alpha : \mathcal{A}_j \to \mathbb{N}_0 &
\end{array}$$

We show that any solution $\alpha^\star$ to this optimization problem satisfies $\|\overline{\pi}_t(\sigma)]_j(s,\cdot) - \alpha^\star\|_\infty < 1$. Assume to the contrary that there is $a \in \mathcal{A}_j$ such that $\alpha^\star(a) \geqslant [\overline{\pi}_t(\sigma)]_j(s,a) + 1$; the proof for $\alpha^\star(a) \leqslant [\overline{\pi}_t(\sigma)]_j(s,a) - 1$ is symmetric. Since $\sum_{a \in \mathcal{A}_j} \alpha^\star(a) = \sum_{a \in \mathcal{A}_j} [\overline{\pi}_t(\sigma)]_j(s,a)$, this implies that there is another action $a' \in \mathcal{A}_{jt}(s)$ such that $\alpha^\star(a') < [\overline{\pi}_t(\sigma)]_j(s,a')$. Consider now the alternative solution α' defined via $\alpha'(a) = \alpha^\star(a) - 1$, $\alpha'(a') = \alpha^\star(a') + 1$ and $\alpha'(\cdot) = \alpha^\star(\cdot)$ elsewhere. One readily verifies that α' is also feasible, and basic algebraic manipulations show that

$$\begin{aligned}
&\left\|\alpha' - [\overline{\pi}_t(\sigma)]_j(s,\cdot)\right\|_1 \; - \; \left\|\alpha^\star - [\overline{\pi}_t(\sigma)]_j(s,\cdot)\right\|_1 \\
&= \; |\alpha'(a) - [\overline{\pi}_t(\sigma)]_j(s,a)| \; - \; |\alpha^\star(a) - [\overline{\pi}_t(\sigma)]_j(s,a)| \\
&\qquad\qquad + \; |\alpha'(a') - [\overline{\pi}_t(\sigma)]_j(s,a')| \; - \; |\alpha^\star(a') - [\overline{\pi}_t(\sigma)]_j(s,a')| \\
&= \; \big(\alpha^\star(a) - 1 - [\overline{\pi}_t(\sigma)]_j(s,a)\big) \; - \; \big(\alpha^\star(a) - [\overline{\pi}_t(\sigma)]_j(s,a)\big) \\
&\qquad\qquad + \; \big|\alpha^\star(a') + 1 - [\overline{\pi}_t(\sigma)]_j(s,a')\big)\big| \; - \; \big([\overline{\pi}_t(\sigma)]_j(s,a') - \alpha^\star(a')\big) \\
&= \; -1 \; + \; \big|\alpha^\star(a') + 1 - [\overline{\pi}_t(\sigma)]_j(s,a')\big| \; - \; \big([\overline{\pi}_t(\sigma)]_j(s,a') - \alpha^\star(a')\big) \\
&= \; -2\min\big\{[\overline{\pi}_t(\sigma)]_j(s,a') - \alpha^\star(a'),\; 1\big\} \; < \; 0,
\end{aligned}$$

where the last equality holds since the expression in the penultimate line evaluates to

$$-1 \; + \; \big([\overline{\pi}_t(\sigma)]_j(s,a') - \alpha^\star(a') - 1\big) \; - \; \big([\overline{\pi}_t(\sigma)]_j(s,a') - \alpha^\star(a')\big) \; = \; -2$$

if $\alpha^\star(a') + 1 - [\overline{\pi}_t(\sigma)]_j(s,a') \leqslant 0$ and to

$$-1 \; + \; \big(\alpha^\star(a') + 1 - [\overline{\pi}_t(\sigma)]_j(s,a')\big) \; - \; \big([\overline{\pi}_t(\sigma)]_j(s,a') - \alpha^\star(a')\big) \; = \; -2\big([\overline{\pi}_t(\sigma)]_j(s,a') - \alpha^\star(a')\big)$$

if $\alpha^\star(a') + 1 - [\overline{\pi}_t(\sigma)]_j(s,a') > 0$. This contradicts the assumed optimality of $\alpha^\star$, and we thus have $\|\overline{\pi}_t(\sigma)]_j(s,\cdot) - \alpha^\star\|_\infty < 1$ for all $j \in \mathcal{J}$, $s \in \mathcal{S}_j$. Since our arguments do not depend on the choice of $t \in \mathcal{T}$, $\sigma \in \mathfrak{S}$, we conclude that $\|\pi_t^\star(\sigma) \; - \; \overline{\pi}_t(\sigma)\|_\infty < 1$ for all $t \in \mathcal{T}$, $\sigma \in \mathfrak{S}$ as claimed. ∎

Despite potentially violating the resource constraints of Π^{C}, we now show that under suitable assumptions, the projected policy $\pi^\star$ is close to Π^{C} with high probability. The proximity of $\pi^\star$

to Π^{C} will crucially depend on the two quantities

$$\frac{\overline{p}_j^t - 1}{\overline{p}_j - 1}, \quad \text{where} \quad \overline{p}_j \;=\; \max \left\{ \sum_{s \in \mathcal{S}_j} \sum_{a \in \mathcal{A}_j} p_{jt}(s'|s,a) \;:\; t \in \mathcal{T},\; s' \in \mathcal{S}_j \right\}, \; j \in \mathcal{J},$$

as well as

$$\epsilon \;=\; \max \left\{ \sqrt{\frac{\log n_j}{2 n_j}} \;:\; j \in \mathcal{J} \right\}.$$

Note that $\overline{p}_j \in [0,\, |\mathcal{S}_j| \cdot |\mathcal{A}_j|]$ by construction, and thus

$$\frac{\overline{p}_j^t - 1}{\overline{p}_j - 1} \;\in\; \left[1,\, \frac{[|\mathcal{S}_j| \cdot |\mathcal{A}_j|]^t - 1}{|\mathcal{S}_j| \cdot |\mathcal{A}_j| - 1}\right] \;\approx\; \left[1,\, [|\mathcal{S}_j| \cdot |\mathcal{A}_j|]^{t-1}\right].$$

We emphasize that $(\overline{p}_j^t - 1) \,/\, (\overline{p}_j - 1)$ does not grow with the numbers n_j of DPs in each counting DP. The quantity ϵ, on the other hand, vanishes quickly when $n_j \to \infty$ for all $j \in \mathcal{J}$.

We are now ready to analyze the performance of $\pi^\star$ in the weakly coupled counting DP.

Theorem 4.19 (Rounded Policy; Expected Total Reward) *Denote by $\theta^\star$ and θ^{DP} the expected total reward of the rounded policy $\pi^\star$ and an optimal policy for the weakly coupled counting DP $(\{\mathfrak{S}_j, \mathfrak{A}_j, \mathfrak{q}_j, \mathfrak{p}_j, \mathfrak{r}_j\}_j; \{n_j\}_j)$, respectively. We then have*

$$\theta^\star \;\geqslant\; \theta^{\mathrm{DP}} \;-\; \sum_{t \in \mathcal{T}} \sum_{j \in \mathcal{J}} \sum_{s \in \mathcal{S}_j} \sum_{a \in \mathcal{A}_j} r_{jt}(s,a) \cdot \frac{\overline{p}_j^t - 1}{\overline{p}_j - 1}$$

as well as, with probability at least $1 - 2|\mathcal{T}| \cdot \sum_{j \in \mathcal{J}} |\mathcal{S}_j| / n_j$ for all $t \in \mathcal{T}$ and $l \in \mathcal{L}$ simultaneously,

$$\sum_{j \in \mathcal{J}} \sum_{s \in \mathcal{S}_j} \sum_{a \in \mathcal{A}_j} c_{tlj}(s,a) \cdot [\pi_t^\star(\tilde{\sigma}_t^\star)]_j(s,a) \leqslant b_{tl} + \sum_{j \in \mathcal{J}} (1 + \epsilon n_j) \sum_{s \in \mathcal{S}_j} \sum_{a \in \mathcal{A}_j} c_{tlj}(s,a) \cdot \frac{\overline{p}_j^t - 1}{\overline{p}_j - 1},$$

where $\tilde{\sigma}^\star = \{\tilde{\sigma}_t^\star\}_t$ is the random state evolution of the weakly coupled counting DP under $\pi^\star$.

Proof of Theorem 4.19. In view of the bound on the expected total reward, we observe that

$$\begin{aligned}
\theta^\star &= \sum_{t\in\mathcal{T}}\sum_{j\in\mathcal{J}}\sum_{s\in\mathcal{S}_j}\sum_{a\in\mathcal{A}_j} r_{jt}(s,a)\cdot\mathbb{E}\left[[\pi_t^\star(\tilde{\sigma}_t^\star)]_j(s,a)\right] \\
&\geqslant \sum_{t\in\mathcal{T}}\sum_{j\in\mathcal{J}}\sum_{s\in\mathcal{S}_j}\sum_{a\in\mathcal{A}_j} r_{jt}(s,a)\cdot\left(\pi_{tj}^{\mathrm{LP}}(s,a)-\frac{\overline{p}_j^t-1}{\overline{p}_j-1}\right) \\
&= \sum_{t\in\mathcal{T}}\sum_{j\in\mathcal{J}}\sum_{s\in\mathcal{S}_j}\sum_{a\in\mathcal{A}_j} r_{jt}(s,a)\cdot\pi_{tj}^{\mathrm{LP}}(s,a) \;-\; \sum_{t\in\mathcal{T}}\sum_{j\in\mathcal{J}}\sum_{s\in\mathcal{S}_j}\sum_{a\in\mathcal{A}_j} r_{jt}(s,a)\cdot\frac{\overline{p}_j^t-1}{\overline{p}_j-1} \\
&= \theta^{\mathrm{LP}} \;-\; \sum_{t\in\mathcal{T}}\sum_{j\in\mathcal{J}}\sum_{s\in\mathcal{S}_j}\sum_{a\in\mathcal{A}_j} r_{jt}(s,a)\cdot\frac{\overline{p}_j^t-1}{\overline{p}_j-1} \\
&\geqslant \theta^{\mathrm{DP}} \;-\; \sum_{t\in\mathcal{T}}\sum_{j\in\mathcal{J}}\sum_{s\in\mathcal{S}_j}\sum_{a\in\mathcal{A}_j} r_{jt}(s,a)\cdot\frac{\overline{p}_j^t-1}{\overline{p}_j-1},
\end{aligned}$$

where the first identity holds by definition of $\theta^\star$, the first inequality follows from Lemma 4.24 in the appendix of this chapter, the third identity holds by definition of θ^{LP}, and the second inequality is due to Theorem 4.15.

As for the resource violation, we have with probability at least $1-2|\mathcal{T}|\cdot\sum_{j\in\mathcal{J}}|\mathcal{S}_j|/n_j$ that

$$\begin{aligned}
&\sum_{j\in\mathcal{J}}\sum_{s\in\mathcal{S}_j}\sum_{a\in\mathcal{A}_j} c_{tlj}(s,a)\cdot[\pi_t^\star(\tilde{\sigma}_t^\star)]_j(s,a) \\
\leqslant\; &\sum_{j\in\mathcal{J}}\sum_{s\in\mathcal{S}_j}\sum_{a\in\mathcal{A}_j} c_{tlj}(s,a)\cdot\left(\pi_{tj}^{\mathrm{LP}}(s,a)+(1+\epsilon n_j)\cdot\frac{\overline{p}_j^t-1}{\overline{p}_j-1}\right) \\
=\; &\sum_{j\in\mathcal{J}}\sum_{s\in\mathcal{S}_j}\sum_{a\in\mathcal{A}_j} c_{tlj}(s,a)\cdot\pi_{tj}^{\mathrm{LP}}(s,a)+\sum_{j\in\mathcal{J}}\sum_{s\in\mathcal{S}_j}\sum_{a\in\mathcal{A}_j}(1+\epsilon n_j)\cdot\frac{\overline{p}_j^t-1}{\overline{p}_j-1}\cdot c_{tlj}(s,a) \\
\leqslant\; & b_{tl}+\sum_{j\in\mathcal{J}}(1+\epsilon n_j)\cdot\sum_{s\in\mathcal{S}_j}\sum_{a\in\mathcal{A}_j} c_{tlj}(s,a)\cdot\frac{\overline{p}_j^t-1}{\overline{p}_j-1},
\end{aligned}$$

where the first inequality is due to Lemma 4.25 in the appendix of this chapter, and the second inequality holds since π^{LP} is a feasible solution to the fluid LP (4.3) and hence satisfies the third constraint of the LP. ∎

Theorem 4.20 (Rounded Policy; Worst-Case Total Reward) *Denote by $\tilde{\theta}^\star$ the random total reward of the rounded policy $\pi^\star$ and by θ^{DP} the expected total reward of an optimal policy* *for the weakly coupled counting DP* $(\{\mathfrak{S}_j, \mathfrak{A}_j, \mathfrak{q}_j, \mathfrak{p}_j, \mathfrak{r}_j\}_j; \{n_j\}_j)$*, respectively. We then have*

$$\tilde{\theta}^\star \ \geqslant\ \theta^{\mathrm{DP}} \ - \sum_{t\in\mathcal{T}} \sum_{j\in\mathcal{J}} \sum_{s\in\mathcal{S}_j} \sum_{a\in\mathcal{A}_j} r_{jt}(s,a) \cdot (1+\epsilon n_j) \cdot \frac{\overline{p}_j^t - 1}{\overline{p}_j - 1}$$

as well as, for all $t \in \mathcal{T}$ *and* $l \in \mathcal{L}$ *simultaneously,*

$$\sum_{j\in\mathcal{J}} \sum_{s\in\mathcal{S}_j} \sum_{a\in\mathcal{A}_j} c_{tlj}(s,a) \cdot [\pi_t^\star(\tilde{\sigma}_t^\star)]_j(s,a) \leqslant b_{tl} + \sum_{j\in\mathcal{J}} (1+\epsilon n_j) \sum_{s\in\mathcal{S}_j} \sum_{a\in\mathcal{A}_j} c_{tlj}(s,a) \cdot \frac{\overline{p}_j^t - 1}{\overline{p}_j - 1},$$

both with probability at least $1 - 2|\mathcal{T}| \cdot \sum_{j\in\mathcal{J}} |\mathcal{S}_j|/n_j$*, where* $\tilde{\sigma}^\star = \{\tilde{\sigma}_t^\star\}_t$ *is the random state evolution of the weakly coupled counting DP under* $\pi^\star$*.*

Proof of Theorem 4.20. The bound on the resource violation is the same as in Theorem 4.19, and we refer to its proof for the justification of the bound. In view of the bound on the total reward, we observe that with probability at least $1 - 2|\mathcal{T}| \cdot \sum_{j\in\mathcal{J}} |\mathcal{S}_j|/n_j$, we have

$$\begin{aligned}
\tilde{\theta}^\star &= \sum_{t\in\mathcal{T}} \sum_{j\in\mathcal{J}} \sum_{s\in\mathcal{S}_j} \sum_{a\in\mathcal{A}_j} r_{jt}(s,a) \cdot [\pi_t^\star(\tilde{\sigma}_t^\star)]_j(s,a) \\
&\geqslant \sum_{t\in\mathcal{T}} \sum_{j\in\mathcal{J}} \sum_{s\in\mathcal{S}_j} \sum_{a\in\mathcal{A}_j} r_{jt}(s,a) \cdot \left(\pi_{tj}^{\mathrm{LP}}(s,a) - (1+\epsilon n_j) \cdot \frac{\overline{p}_j^t - 1}{\overline{p}_j - 1} \right) \\
&= \sum_{t\in\mathcal{T}} \sum_{j\in\mathcal{J}} \sum_{s\in\mathcal{S}_j} \sum_{a\in\mathcal{A}_j} r_{jt}(s,a) \cdot \pi_{tj}^{\mathrm{LP}}(s,a) \ - \sum_{t\in\mathcal{T}} \sum_{j\in\mathcal{J}} \sum_{s\in\mathcal{S}_j} \sum_{a\in\mathcal{A}_j} r_{jt}(s,a) \cdot (1+\epsilon n_j) \cdot \frac{\overline{p}_j^t - 1}{\overline{p}_j - 1} \\
&= \theta^{\mathrm{LP}} \ - \sum_{t\in\mathcal{T}} \sum_{j\in\mathcal{J}} \sum_{s\in\mathcal{S}_j} \sum_{a\in\mathcal{A}_j} r_{jt}(s,a) \cdot (1+\epsilon n_j) \cdot \frac{\overline{p}_j^t - 1}{\overline{p}_j - 1} \\
&\geqslant \theta^{\mathrm{DP}} \ - \sum_{t\in\mathcal{T}} \sum_{j\in\mathcal{J}} \sum_{s\in\mathcal{S}_j} \sum_{a\in\mathcal{A}_j} r_{jt}(s,a) \cdot (1+\epsilon n_j) \cdot \frac{\overline{p}_j^t - 1}{\overline{p}_j - 1},
\end{aligned}$$

where the first identity holds pointwise by definition of $\tilde{\theta}^\star$, the first inequality is due to Lemma 4.25 in the appendix of this chapter, the third identity holds by definition of θ^{LP}, and the second inequality is due to Theorem 4.15. ∎

To interpret the above performance guarantees in light of our healthcare model, we consider an asymptotic setting where $n_j \to \infty$ for all $j \in \mathcal{J}$, and where the available resources $b_{tl} \propto \sum_{j\in\mathcal{J}} n_j$

scale in the number of patients to be treated. One can verify that in this case, the expected total reward $\theta^{\mathrm{DP}} \propto \sum_{j \in \mathcal{J}} n_j$ of the weakly coupled counting DP under the optimal policy scales with the number of patients as well. In contrast, we assume that the number $|\mathcal{T}|$ of time periods, the number $|\mathcal{J}|$ of patient groups as well as the number of states $|\mathcal{S}_j|$ and actions $|\mathcal{A}_j|$ per patient group remain constant. In that setting, Theorem 4.19 shows that the expected total reward $\theta^\star$ of the rounded policy $\pi^\star$ equals the optimal expected total reward θ^{DP} minus a constant term, since the expression subtracted on the right-hand side of the objective bound does not grow with n_j, $j \in \mathcal{J}$. In contrast, Theorems 4.19 and 4.20 show that the worst-case total reward as well as the resource consumptions deviate from the optimal expected total reward θ^{DP} and the resource availabilities b_{tl}, respectively, by constants multiplied with ϵn_j, where $\epsilon n_j \propto \sqrt{n_j \log n_j}$. While these expressions are no longer constants, they are sublinear and thus imply that the worst-case suboptimality as well as the resource violations, on a percentage basis, vanish as well when the number of patients grows. The results also reveal the price to be paid when moving from a guarantee in expectation (*cf.* Theorem 4.19) to a guarantee in terms of the worst case (*cf.* Theorem 4.20): The suboptimality increases from an additive constant to a sublinear expression.

A question of practical concern is how the policy $\pi^\star$ to the weakly coupled counting DP can be computed from a solution $(\sigma^{\mathrm{LP}}, \pi^{\mathrm{LP}})$ to the fluid LP (4.3). This appears difficult as the lifted policy $\mathrm{L}(\sigma^{\mathrm{LP}}, \pi^{\mathrm{LP}})$ lives in an infinite-dimensional space and the projection operator Pr seems to require the solution of a combinatorial optimization problem. Fortunately, given $(\sigma^{\mathrm{LP}}, \pi^{\mathrm{LP}})$, the policy $\pi^\star$ affords a simple characterization in closed form.

Proposition 4.21 *For all $t \in \mathcal{T}$, $\sigma \in \mathfrak{S}$, $j \in \mathcal{J}$ and $(s,a) \in \mathcal{S}_j \times \mathcal{A}_j$, the policy $\pi^\star$ satisfies*

$$[\pi^\star_t(\sigma)]_j\,(s,a) \;=\; \lfloor [\overline{\pi}_t(\sigma)]_j(s,a) \rfloor + \mathbf{1}[(s,a) \in \mathcal{I}_{tj}(\sigma)],$$

where $\mathcal{I}_{tj}(\sigma) \subseteq \mathcal{S}_j \times \mathcal{A}_j$ contains the pairs $(s,a) \in \mathcal{S}_j \times \mathcal{A}_j$ corresponding to the $\|\mathrm{frac}([\overline{\pi}_t(\sigma)]_j(s,\cdot))\|_1$ largest components of $\mathrm{frac}([\overline{\pi}_t(\sigma)]_j(s,\cdot))$.

Proof of Proposition 4.21. Fix any $t \in \mathcal{T}$, $\sigma \in \mathfrak{S}$, $j \in \mathcal{J}$ and $s \in \mathcal{S}_j$. By construction,

$[\pi^\star_t(\sigma)]_j\,(s,\cdot)$ is any solution to the problem

$$\begin{aligned}
\underset{\alpha}{\text{minimize}} \quad & \|[\overline{\pi}_t(\sigma)]_j(s,\cdot) - \alpha\|_1 \\
\text{subject to} \quad & \sum_{a\in\mathcal{A}_j} \alpha(a) = \sum_{a\in\mathcal{A}_j} [\overline{\pi}_t(\sigma)]_j(s,a) \\
& \alpha(a) = 0 \qquad\qquad \forall a \in \mathcal{A}_j \backslash \mathcal{A}_{jt}(s) \\
& \alpha : \mathcal{A}_j \to \mathbb{N}_0.
\end{aligned}$$

By Proposition 4.18, we have $\|\pi^\star_t(\sigma) - \overline{\pi}_t(\sigma)\|_\infty < 1$, which implies that

$$\lfloor[\overline{\pi}_t(\sigma)]_j(s,a)\rfloor \;\leqslant\; [\pi^\star_t(\sigma)]_j\,(s,a) \;\leqslant\; \lfloor[\overline{\pi}_t(\sigma)]_j(s,a)\rfloor + 1 \qquad \forall a \in \mathcal{A}_j.$$

The substitutions $\beta \leftarrow \text{frac}([\overline{\pi}_t(\sigma)]_j(s,\cdot))$ and $\alpha \leftarrow \alpha - \lfloor[\overline{\pi}_t(\sigma)]_j(s,\cdot)\rfloor$ thus imply that $[\pi^\star_t(\sigma)]_j\,(s,\cdot) - \lfloor[\overline{\pi}_t(\sigma)]_j(s,\cdot)\rfloor$ is any solution to the problem

$$\begin{aligned}
\underset{\alpha}{\text{minimize}} \quad & \|\beta - \alpha\|_1 \\
\text{subject to} \quad & \sum_{a\in\mathcal{A}_j} \alpha(a) = \sum_{a\in\mathcal{A}_j} \beta(\alpha) \\
& \alpha(a) = 0 \qquad\qquad \forall a \in \mathcal{A}_j \backslash \mathcal{A}_{jt}(s) \\
& \alpha : \mathcal{A}_j \to \{0,1\}.
\end{aligned}$$

Define the set $\mathcal{A}_j(s,\alpha) = \{a \in \mathcal{A}_j \,:\, \alpha(a) = 1\}$ and observe that $|\mathcal{A}_j(s,\alpha)| = \sum_{a\in\mathcal{A}_j} \alpha(a) = \sum_{a\in\mathcal{A}_j} \beta(a) = \|\beta\|_1$. Moreover, the objective function in the above problem evaluates to

$$\begin{aligned}
\|\beta - \alpha\|_1 \;&=\; \sum_{a\in\mathcal{A}_j(s,\alpha)} (1 - \beta(a)) \;+\; \sum_{a\notin\mathcal{A}_j(s,\alpha)} \beta(a) \\
&=\; |\mathcal{A}_j(s,\alpha)| \;-\; 2 \sum_{a\in\mathcal{A}_j(s,\alpha)} \beta(a) \;+\; \sum_{a\in\mathcal{A}_j} \beta(a) \;=\; 2\,\|\beta\|_1 \;-\; 2 \sum_{a\in\mathcal{A}_j(s,\alpha)} \beta(a).
\end{aligned}$$

Since $|\mathcal{A}_j(s,\alpha)| = \|\beta\|_1$ does not depend on the choice of α (as long as α is feasible), the optimal choice of $\mathcal{A}_j(s,\alpha)$ consists of the $\|\beta\|_1$ largest entries of β. Moreover, any optimal policy $\pi^\star$ must satisfy $[\pi^\star_t(\sigma)]_j\,(s,a) = \lfloor[\overline{\pi}_t(\sigma)]_j(s,a)\rfloor + \mathbf{1}[a \in \mathcal{A}_j(s,\alpha)]$, $a \in \mathcal{A}_j$. The statement then follows from the fact that $\mathcal{I}_{tj}(\sigma) = \{(s,a) \in \mathcal{S}_j \times \mathcal{A}_j \,:\, a \in \mathcal{A}_j(s,\alpha)\}$. ∎

Proposition 4.21 denotes by $\text{frac}(x) = x - \lfloor x \rfloor$ the fractional part of a number $x \in \mathbb{R}$, which we apply to functions component-wise. Note that $\|\text{frac}([\overline{\pi}_t(\sigma)]_j(s,\cdot))\|_1 \in \mathbb{N}_0$ since $\sum_{a \in \mathcal{A}_j} [\overline{\pi}_t(\sigma)]_j(s,a) = \sigma_j(s) \in \mathbb{N}_0$ for all $\sigma \in \mathfrak{S}$ and all $s \in \mathcal{S}_j$. We emphasize that the set $\mathcal{I}_{tj}(\sigma)$ is not necessarily unique.

4.3.2.4 Approximation Guarantees: Randomized Policies

We now utilize an optimal solution $(\sigma^{\text{LP}}, \pi^{\text{LP}})$ to the fluid LP (4.3) to construct a *randomized* policy for our health system. Our analysis will crucially rely on the actions applied to each constituent DP being independent. We therefore cannot operate on the weakly coupled counting DP, which abstracts away from the dependence structure between the constituent DPs. Instead, we transform the weakly coupled counting DP $(\{\mathfrak{S}_j, \mathfrak{A}_j, \mathfrak{q}_j, \mathfrak{p}_j, \mathfrak{r}_j\}_j; \{n_j\}_j)$ representing our healthcare model to a weakly coupled DP $(\{\mathcal{S}_i, \mathcal{A}_i, q_i, p_i, r_i\}_i)$ as follows. We use the same time horizon $\mathcal{T}$, we set $\mathcal{I} = \bigcup_{j \in \mathcal{J}} \{(j,i) \,:\, i = 1, \ldots, n_j\}$, $\mathcal{S}_{(j,i)} = \mathcal{S}_j$, $\mathcal{A}_{(j,i)} = \mathcal{A}_j$, $\mathcal{A}_{t,(j,i)}(s) = \mathcal{A}_{tj}(s)$, $s \in \mathcal{S}_j$, $q_{(j,i)} = q_j$ and $p_{t,(j,i)} = p_{tj}$ for all $t \in \mathcal{T}$ and $(j,i) \in \mathcal{I}$. The weakly coupled DP thus records the state and action of the i-th DP in the j-th counting DP, $(j,i) \in \mathcal{I}$, in the (j,i)-th DP explicitly, whereas the weakly coupled counting DP aggregates the DPs $(j,1), \ldots, (j,n_j)$ to the j-th counting DP, $j \in \mathcal{J}$.

Recall that a deterministic policy $\pi = \{\pi_t\}_t$, $\pi_t : \mathcal{S} \to \mathcal{A}$, for the weakly coupled DP assigns an action $a \in \mathcal{A}$ to each possible state $s \in \mathcal{S}$ for each time period $t \in \mathcal{T}$. We now consider randomized policies $\pi = \{\pi_t\}_t$, $\pi_t : \mathcal{S} \to \Delta(\mathcal{A})$, for the weakly coupled DP that assign probability distributions over all actions $a \in \mathcal{A}$ to each possible state $s \in \mathcal{S}$ for each time period $t \in \mathcal{T}$.

Fix a weakly coupled counting DP $(\{\mathfrak{S}_j, \mathfrak{A}_j, \mathfrak{q}_j, \mathfrak{p}_j, \mathfrak{r}_j\}_j; \{n_j\}_j)$ as well as an optimal solution $(\sigma^{\text{LP}}, \pi^{\text{LP}})$ to its associated fluid LP (4.3). We consider the following randomized policy $\pi^\star = \{\pi^\star_t\}_t$:

$$[\pi^\star_t(s)](a) \;=\; \prod_{j \in \mathcal{J}} \prod_{i=1}^{n_j} \frac{\pi^{\text{LP}}_{tj}(s_{(j,i)}, a_{(j,i)})}{\sigma^{\text{LP}}_{tj}(s_{(j,i)})} \qquad \forall t \in \mathcal{T},\ \forall (s,a) \in \mathcal{S} \times \mathcal{A}$$

Again, we adopt the convention that $0/0 = 0$. Intuitively speaking, the randomized policy $\pi^\star$

considers each constituent DP $(j,i) \in \mathcal{I}$ independently, and it employs each action $a_{(j,i)} \in \mathcal{A}_{(j,i)}$ with a probability that equals the fraction of times this action has been selected in the fluid LP (4.3) under the almost sure trajectory in the same time period.

We now study the performance of $\pi^\star$ in the weakly coupled DP. Our results use the random states $\tilde{s}_{t,(j,i)}$ of the (j,i)-th DP and the random actions $\tilde{a}_{t,(j,i)}$ applied to this DP in time period t.

Theorem 4.22 (Randomized Policy; Expected Total Reward) *Denote by $\theta^\star$ and θ^{DP} the expected total reward of the randomized policy $\pi^\star$ and an optimal policy for the weakly coupled counting DP $(\{\mathfrak{S}_j, \mathfrak{A}_j, \mathfrak{q}_j, \mathfrak{p}_j, \mathfrak{r}_j\}_j; \{n_j\}_j)$, respectively. We then have*

$$\theta^\star \;\geqslant\; \theta^{\mathrm{DP}}$$

as well as, with probability at least $1 - 2|\mathcal{T}| \cdot \sum_{j \in \mathcal{J}} |\mathcal{S}_j| \cdot |\mathcal{A}_j| \,/\, n_j$,

$$\sum_{j \in \mathcal{J}} \sum_{i=1}^{n_j} c_{tlj}(\tilde{s}_{t,(j,i)}, \tilde{a}_{t,(j,i)}) \leqslant b_{tl} + \epsilon \cdot \sum_{j \in \mathcal{J}} n_j \sum_{s \in \mathcal{S}_j} \sum_{a \in \mathcal{A}_j} c_{tlj}(s,a) \qquad \forall t \in \mathcal{T},\ \forall l \in \mathcal{L}.$$

Proof of Theorem 4.22. In view of the bound on the expected total reward, we have

$$\begin{aligned}
\theta^\star \;&=\; \mathbb{E}\left[\sum_{t \in \mathcal{T}} \sum_{j \in \mathcal{J}} \sum_{i=1}^{n_j} r_{jt}(\tilde{s}_{t,(j,i)}, \tilde{a}_{t,(j,i)})\right] \\
&=\; \mathbb{E}\left[\sum_{t \in \mathcal{T}} \sum_{j \in \mathcal{J}} \sum_{i=1}^{n_j} \sum_{s \in \mathcal{S}_j} \sum_{a \in \mathcal{A}_j} r_{jt}(s,a) \cdot \mathbf{1}\left[\tilde{s}_{t,(j,i)} = s \;\wedge\; \tilde{a}_{t,(j,i)} = a\right]\right] \\
&=\; \sum_{t \in \mathcal{T}} \sum_{j \in \mathcal{J}} \sum_{s \in \mathcal{S}_j} \sum_{a \in \mathcal{A}_j} r_{jt}(s,a) \cdot \mathbb{E}\left[\tilde{\alpha}^\star_{tj}(s,a)\right] \\
&=\; \sum_{t \in \mathcal{T}} \sum_{j \in \mathcal{J}} \sum_{s \in \mathcal{S}_j} \sum_{a \in \mathcal{A}_j} r_{jt}(s,a) \cdot \pi^{\mathrm{LP}}_{tj}(s,a) \\
&=\; \theta^{\mathrm{LP}} \;\geqslant\; \theta^{\mathrm{DP}},
\end{aligned}$$

where the first identity holds by definition of $\theta^\star$, the third identity follows from the definition of $\alpha^\star_{tj}(s,a)$ in Lemma 4.27, the fourth identity is due to Lemma 4.27, the last identity holds by definition of θ^{LP}, and the inequality follows from Theorem 4.15.

As for the resource violation, with probability at least $1 - 2|\mathcal{T}| \cdot \sum_{j\in\mathcal{J}} |\mathcal{S}_j| \cdot |\mathcal{A}_j| \,/\, n_j$ we have

$$\begin{aligned}
\sum_{j\in\mathcal{J}} \sum_{i=1}^{n_j} c_{tlj}(\tilde{s}_{t,(j,i)}, \tilde{a}_{t,(j,i)}) \; &= \; \sum_{j\in\mathcal{J}} \sum_{i=1}^{n_j} \sum_{s\in\mathcal{S}_j} \sum_{a\in\mathcal{A}_j} c_{tlj}(s,a) \cdot \mathbf{1}\left[\tilde{s}_{t,(j,i)} = s \;\wedge\; \tilde{a}_{t,(j,i)} = a\right] \\
&= \; \sum_{j\in\mathcal{J}} \sum_{s\in\mathcal{S}_j} \sum_{a\in\mathcal{A}_j} c_{tlj}(s,a) \cdot \tilde{\alpha}^{\star}_{tj}(s,a) \\
&\leqslant \; \sum_{j\in\mathcal{J}} \sum_{s\in\mathcal{S}_j} \sum_{a\in\mathcal{A}_j} c_{tlj}(s,a) \cdot \left(\pi^{\mathrm{LP}}_{tj}(s,a) + \epsilon n_j\right) \\
&\leqslant \; b_{tl} + \epsilon \sum_{j\in\mathcal{J}} n_j \cdot \sum_{s\in\mathcal{S}_j} \sum_{a\in\mathcal{A}_j} c_{tlj}(s,a)
\end{aligned}$$

for all $l \in \mathcal{L}$ and $t \in \mathcal{T}$, where the second identity follows from the definition of $\tilde{\alpha}^{\star}_{tj}(s,a)$ in Lemma 4.27, the first inequality is due to the statement of Lemma 4.27, and the second inequality is implied by the third constraint of the fluid LP (4.3). ∎

Theorem 4.23 (Randomized Policy; Worst-Case Total Reward) *Denote by $\tilde{\theta}^{\star}$ the random total reward of the randomized policy $\pi^{\star}$ and by θ^{DP} the expected total reward of an optimal policy for the weakly coupled counting DP $(\{\mathfrak{S}_j, \mathfrak{A}_j, \mathfrak{q}_j, \mathfrak{p}_j, \mathfrak{r}_j\}_j; \{n_j\}_j)$, respectively. We then have*

$$\tilde{\theta}^{\star} \;\geqslant\; \theta^{\mathrm{DP}} \;-\; \epsilon \cdot \sum_{t\in\mathcal{T}} \sum_{j\in\mathcal{J}} n_j \sum_{s\in\mathcal{S}_j} \sum_{a\in\mathcal{A}_j} r_{jt}(s,a)$$

as well as

$$\sum_{j\in\mathcal{J}} \sum_{i=1}^{n_j} c_{tlj}(\tilde{s}_{t,(j,i)}, \tilde{a}_{t,(j,i)}) \leqslant b_{tl} + \epsilon \cdot \sum_{j\in\mathcal{J}} n_j \sum_{s\in\mathcal{S}_j} \sum_{a\in\mathcal{A}_j} c_{tlj}(s,a) \qquad \forall t \in \mathcal{T},\, \forall l \in \mathcal{L},$$

both with probability at least $1 - 2|\mathcal{T}| \cdot \sum_{j\in\mathcal{J}} |\mathcal{S}_j| \cdot |\mathcal{A}_j| \,/\, n_j$.

Proof of Theorem 4.23. The bound on the resource violation is the same as in Theorem 4.22, and we refer to its proof for the justification of the bound. In view of the bound on the expected total reward, we observe that with probability at least $1 - 2|\mathcal{T}| \cdot \sum_{j \in \mathcal{J}} |\mathcal{S}_j| \cdot |\mathcal{A}_j| \,/\, n_j$, we have

$$\begin{aligned}
\tilde{\theta}^\star &= \sum_{t \in \mathcal{T}} \sum_{j \in \mathcal{J}} \sum_{i=1}^{n_j} r_{jt}(\tilde{s}_{t,(j,i)}, \tilde{a}_{t,(j,i)}) \\
&= \sum_{t \in \mathcal{T}} \sum_{j \in \mathcal{J}} \sum_{s \in \mathcal{S}_j} \sum_{a \in \mathcal{A}_j} r_{jt}(s,a) \cdot \tilde{\alpha}^\star_{tj}(s,a) \\
&\geqslant \sum_{t \in \mathcal{T}} \sum_{j \in \mathcal{J}} \sum_{s \in \mathcal{S}_j} \sum_{a \in \mathcal{A}_j} r_{jt}(s,a) \cdot \left(\pi^{\mathrm{LP}}_{tj}(s,a) - \epsilon n_j\right) \\
&= \sum_{t \in \mathcal{T}} \sum_{j \in \mathcal{J}} \sum_{s \in \mathcal{S}_j} \sum_{a \in \mathcal{A}_j} r_{jt}(s,a) \cdot \pi^{\mathrm{LP}}_{tj}(s,a) \; - \; \sum_{t \in \mathcal{T}} \sum_{j \in \mathcal{J}} \sum_{s \in \mathcal{S}_j} \sum_{a \in \mathcal{A}_j} r_{jt}(s,a) \cdot \epsilon n_j \\
&= \theta^{\mathrm{LP}} \; - \; \epsilon \cdot \sum_{t \in \mathcal{T}} \sum_{j \in \mathcal{J}} n_j \sum_{s \in \mathcal{S}_j} \sum_{a \in \mathcal{A}_j} r_{jt}(s,a) \\
&\geqslant \theta^{\mathrm{DP}} \; - \; \epsilon \cdot \sum_{t \in \mathcal{T}} \sum_{j \in \mathcal{J}} n_j \sum_{s \in \mathcal{S}_j} \sum_{a \in \mathcal{A}_j} r_{jt}(s,a),
\end{aligned}$$

where the first identity is due to the definition of $\tilde{\theta}^\star$, the second identity follows from the definition of $\tilde{\alpha}^\star_{tj}(s,a)$ in Lemma 4.27, the first inequality is due to the statement of Lemma 4.27, the last identity follows from the definition of θ^{LP}, and the second inequality is due to Theorem 4.15. ∎

The bounds of Theorems 4.22 and 4.23 are stronger than those of Theorems 4.19 and 4.20 in the sense that the expected total reward bound does not contain any additive constants and the worst-case total reward and the resource violation bounds contain smaller additive expressions (which nevertheless exhibit the same asymptotic behavior). On the flip side, the rounded policy from the previous section offers more implementational leeway since it can be converted into many different policies for the constituent DPs that all generate the same expected total reward (*cf.* Proposition 4.6), whereas the randomized policy requires an i.i.d. application of the actions across the constituent DPs.

4.3.2.5 Synthetic Experiments

To obtain further insights into our randomized policy from Section 4.3.2.4, we compare our policy with some standard weakly coupled DP policies from the literature on a stylized problem. To this end, consider a multi-armed bandit problem with a finite time horizon $T \in \{5, 25, 50\}$ where $N \in \{1{,}000, 100{,}000, 1{,}000{,}000\}$ bandits are spread equally across $J = 10$ different groups. Across all groups $j \in \mathcal{J}$, each bandit has the same number of states $|\mathcal{S}_j| \in \{2, 3, 4, 5\}$ and actions $|\mathcal{A}_j| = 2$ ('pull arm' and 'do nothing'). For each group j, we sample the initial state probabilities q_j as well as the (non-stationary) transition probabilities p_{jt} under the 'pull arm' action uniformly at random, whereas each bandit deterministically resides in its current state under the 'do nothing' action. Likewise, the rewards r_{jt} are state-dependent and drawn uniformly at random from the interval $[0, 1]$ under the 'pull arm' action, whereas they are zero under the 'do nothing' action. We have a single resource constraint which requires that in each time period at most $b \in \{1\% \cdot N, 5\% \cdot N, 10\% \cdot N, 25\% \cdot N\}$ arms can be pulled. The goal is to find a policy that decides which arms to pull in each time period so as to maximize the expected total reward. Note that our bandit problem is characterized by a large number of bandits, each equipped with a small number of states and actions, that are spread across a relatively small number of groups and subjected to a fairly tight resource constraint. These properties are reminiscent of the healthcare case study introduced in Section 4.4.

We compare our randomized policy from Section 4.3.2.4 against the Lagrangian relaxation proposed by [Haw03] and later studied by [AM08] as well as the LP-based relaxation proposed by [AM08]. In the LP-based relaxation, we follow the constraint sampling approach of [DFVR04] and randomly sample 10,000 constraints. In all three approaches, we exploit the group structure inherent in the bandit problem, which implies that the associated LP formulations scale in the number of groups (as opposed to the number of bandits) and can thus be solved within seconds with standard solvers. Without further modification, all three policies can violate the resource constraint. We thus update each policy by replacing the 'pull arm' action with the 'do nothing' action in bandits in order of ascending regret, as predicted by the value function approximation of each method, until the resource constraint is satisfied. We report the performance of all three approaches as relative improvements over a naive uniform sampling strategy that randomly selects b arms to be pulled in each time stage.

We compare the performance of the three policies, and reports the average relative infeasibility of each policy prior to applying the 'do nothing' actions. The results are presented in Table D.1 and Table D.2 in Appendix D, respectively. All results are reported as averages over 100 randomly constructed test instances. Note that by construction, the policies derived from the Lagrangian and the LP-based relaxations take the same action for any two bandits of the same group that reside in the same state. For bandits with few states that are operated under tight resource constraints, this increases the likelihood of pulling either too few or too many arms. Indeed, the two tables indicate that the policy derived from the Lagrangian relaxation tends to pull too few arms and thus sacrifices optimality, whereas the LP-based policy pulls too many arms, implying that many 'pull arm' actions need to be subsequently replaced with 'do nothing' actions. Further investigations revealed that this behavior is caused by the fact that an unrealistically large number of constraints would have to be sampled for the LP-based relaxation to provide reasonably accurate approximations of the true reward to-go functions. In contrast, our randomized policy can take different actions for bandits of the same group even if they reside in the same state. Because of this, the infeasible variant of our randomized policy tends to result in small violations of the resource constraint that decrease quickly when either the number of bandits or the slack in the resource constraint increases. Since little adaptation is required to make our randomized policy resource feasible, it comes at no surprise that it performs best overall.

4.4 Numerical Results

In this section, we describe our case study of the NHS in England. In particular, we discuss the overall setup of our case study (Section 4.4.1), the employed data sources (Section 4.4.2) as well as the DPs that model the patients of our healthcare model (Section 4.4.3).

4.4.1 Experimental Setup

We apply our framework to the NHS in England during the COVID pandemic. We aim to optimally schedule elective procedures over a 56-week planning horizon (52 reported weeks plus an additional 4 weeks to avoid end-of-time-horizon effects), starting from March 2, 2020, with the objective of minimizing YLL. We consider a total of 10.45 million non-COVID patients that are subdivided into *(i)* electives (3.9 millions) and emergencies (6.55 millions), *(ii)* 20 disease groups and *(iii)* 3 age groups (under 25 years, 25–64 years, over 64 years). We also consider 349,279 COVID patients, all of whom are emergencies. Note that even though we use minimization of YLL as our objective, other metrics could also be used such as minimizing mortality, Quality-Adjusted Life Years (QALYs), costs, or a combination thereof. However, quantifying and gathering data for QALYs may not be straightforward.

Our model has a weekly granularity. At the beginning of each week, a new inflow of patients in need of elective and emergency care (hereafter denoted as elective and emergency patients, respectively) enters the system. Strictly speaking, our model distinguishes between different medical procedures, and thus one and the same patient in need of several procedures is included as multiple different patients in our model. For ease of exposition, however, we continue to talk about patients in the following. Patients are then admitted to hospital, and they evolve over the duration of the week. Emergencies are always admitted to hospital upon arrival (if capacity permits). Elective patients who are not immediately admitted to hospital wait in a queue. While in the queue, an elective patient's condition might worsen and hence require emergency admission. Based on the severity of their conditions and resource availability, patients are first admitted to G&A or to CC and can transition between G&A and CC in the following weeks of hospitalization until they are eventually discharged from hospital (recovered or deceased). Transitions between G&A and CC are decided upon at the beginning of each week, and they are based on transition probabilities that are specific to the different patient groups and admission types (elective or emergency).

4.4.2 Data Sources

We combine a large set of modeling and administrative data to create a comprehensive open-source dataset for the NHS in England that includes elective and emergency patient inflows, transition probabilities, availability and requirement of resources and cost of care. To this end, we leverage several data sources. Non-COVID patient inflows are forecasted with local linear trend models with trigonometric seasonality time series methods using individual level patient records across all hospitals in England from the Hospital Episode Statistics (HES), see [NHS20e]. HES contain patient level data with diagnoses, individual characteristics, care received, date of admission and time and mode of discharge from hospital.

Weekly inflows of COVID patients are generated by a susceptible-exposed-infected-recovered dynamic transmission model of SARS-CoV-2. Epidemic projections are made using the integrated epidemic/economic model Daedalus [HCF+20], in which the population consists of four age groups: pre-schoolers, school-age children, working-age adults and retired. The working-age population is further divided into 63 economic sectors plus non-working adults. Each of these groups is further divided into eight subgroups with respect to the disease status: the susceptible, the exposed, the asymptomatic infectious, the infected with mild symptoms, the infected with influenza-like symptoms, the hospitalized, the recovered and the dead. The model fits four parameters to English hospital occupancy data [NHS20b] from March 20, 2020 to June 30, 2020: epidemic onset, basic reproductive number, lockdown onset, and reduction in transmission during lockdown due to pandemic mitigation strategies. In our numerical studies, we consider an epidemiological scenario defined by a lockdown enforced on January 1, 2021 and the maximum value of the reproductive number $R_{\max} = 1.2$ attained during the post-lockdown period.

The evolution of hospitalized non-COVID and COVID patients is modeled with Kaplan-Meier estimators using, respectively, HES data and individual clinical data from patients who received care at the Imperial College Healthcare NHS Trust [PDM+20]. Staff resources are calculated from the 2020 NHS Electronic Staff Records dataset, and G&A and CC bed availabilities are obtained from the February 2020 KH03-Quarterly Bed Availability and Occupancy Dataset and from the February 2020 Critical Care Monthly Situation Reports datasets [NHS20a, NHS20c]. Staff-to-bed ratios are calculated using the Royal College of Physicians guidance [RCP20, Roy20]. Our model always considers properly staffed beds (accounting for the applicable staff-to-bed ratios); indeed, staff has emerged as a key resource bottleneck during the pandemic. Years of life lost (YLL) are calculated using standard life tables data provided by the Office for National Statistics [Off19]. For the purpose of calculating YLL, the population of England was divided into 3 age groups: 0-24, 25-64, and 65+ years, and the YLL per death factor is obtained by averaging the age specific life expectancy across all ages within each age group. Finally, the YLL per death factor is multiplied by the number of deaths (obtained from the optimization model) per age group to obtain the total YLL. Patients are individually costed using the National Cost Collection dataset from 2015 to 2019 [NHS20f] matched to HES data at Health Resource Group level (HRGs equivalent to Diagnosis Related Groups international coding system).

Table 4.1 and Figure 4.7 summarize the main input data for our case study. Table 4.1 reports the availability of beds and staff in G&A and CC across the NHS in England, together with the corresponding staff-to-bed ratios. Figure 4.7 shows the weekly inflows of elective and emergency patients from March 2020 to February 2021, categorized by disease type according to the International Classification of Diseases (ICD) standard. The figure only displays the five largest patient groups individually, whereas the smaller remaining groups are collective referred to as "Others". We observe a seasonal trend in patient inflows as well as dips in January, March/April, May/June and September that are associated with winter/weather, school and long bank holiday effects.

All data are made available open-source;[2] for additional information on the data sources as well as the data treatment methodology, we refer the interested reader to [DGG$^+$21b].

[2]Source code and data available at: `https://github.com/ImperialCollegeLondon/dp2lp`

Table 4.1: Availability of resources and staff-to-bed ratios.

	Capacity				Staff-to-bed Ratio		
	Beds	Senior Doctors	Junior Doctors	Nurses	Senior Doctors	Junior Doctors	Nurses
G&A	102,186	10,764	8,539	43,214	15	15	5
CC	4,122	1,013	963	18,856	15	8	1

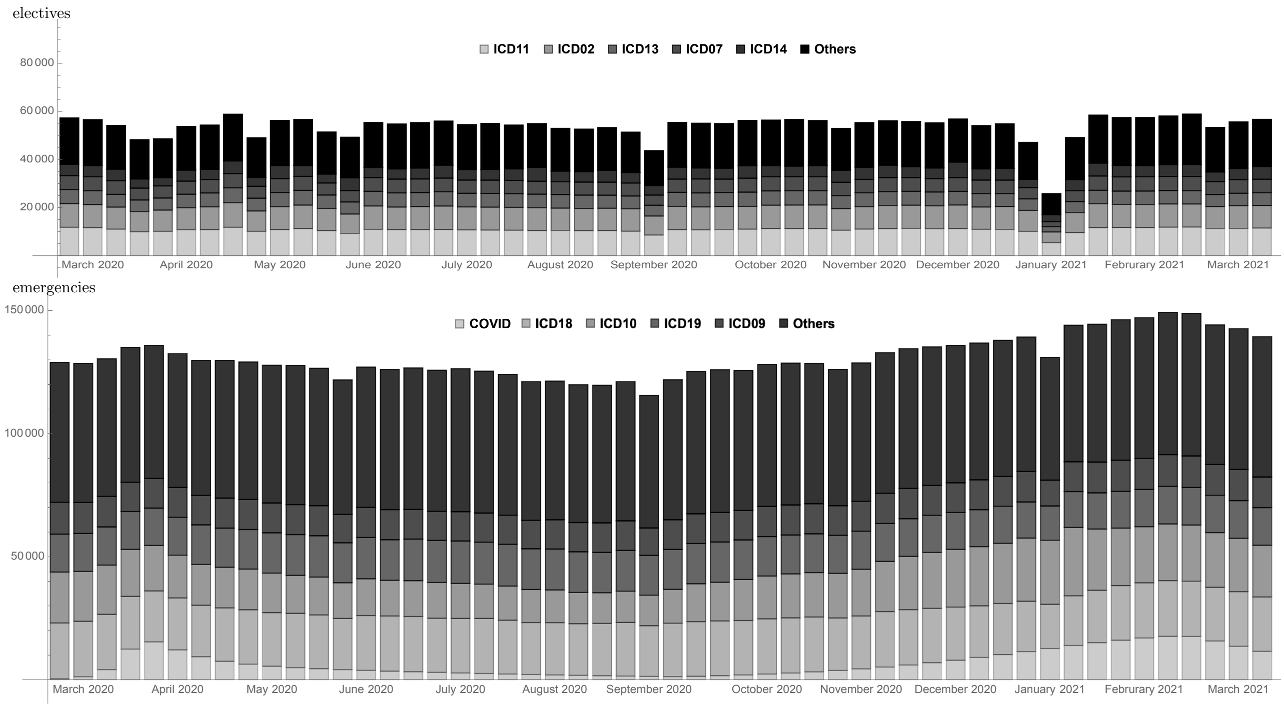

Figure 4.7: Weekly inflows of elective (top) and emergency (bottom) patients categorized by disease group (ICD02: neoplasms; ICD07: diseases of the eye and adnexa; ICD09: diseases of the circulatory system; ICD10: diseases of the respiratory system; ICD11: diseases of the digestive system; ICD13: diseases of the musculoskeletal system and connective tissue; ICD14: diseases of the genitourinary system; ICD18: symptoms, signs and abnormal clinical and laboratory findings, not elsewhere classified; ICD19: injury, poisoning and certain other consequences of external causes).

4.4.3 Dynamic Programming Model of an Individual Patient

Recall that the patients in our healthcare model are partitioned into 3,120 groups, each of which is characterized by an arrival time in the system (52 weeks), one out of 20 disease types and one out of 3 age groups. We associate a DP with each of these patient groups. All DPs share the same state and action sets, but the DPs of different patient groups differ in their admissible actions per time period and state, their transition probabilities as well their expected rewards.

Figure 4.8 offers a schematic representation of a patient DP. Apart from the patients that enter our healthcare model in the first week, each patient is *Dormant* until the beginning of week

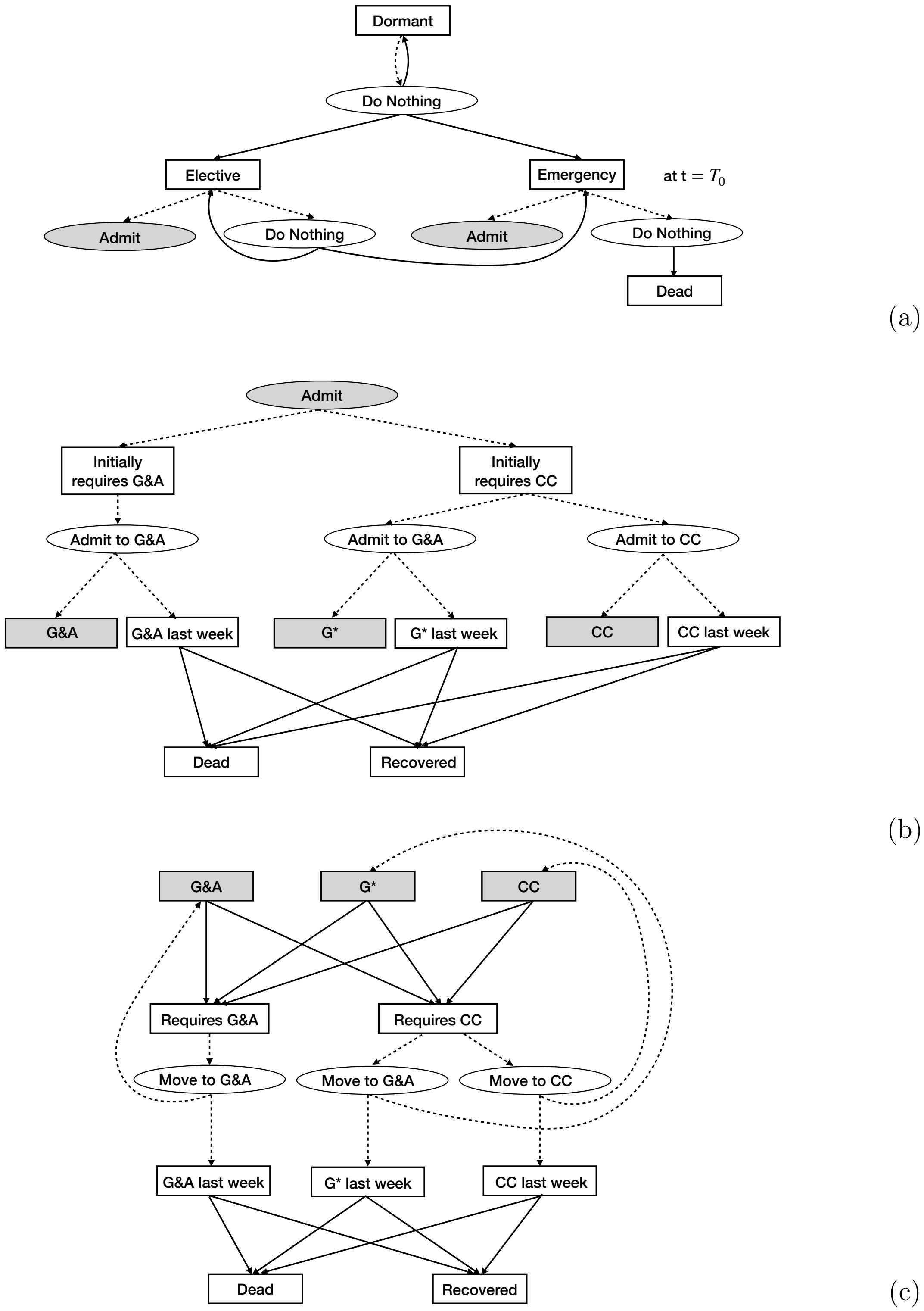

Figure 4.8: Schematic representation of a patient DP, from admission to hospital (a) to discharge (c). Rectangular (oval) nodes correspond to states (actions), and grey shaded nodes are exploded in the subsequent subfigure. Dotted lines correspond to immediate actions and instantaneous transitions, and full lines represent weekly transitions.

$t = T_0$, at which point she enters the system either as to be admitted for a planned procedure (*Elective*) or as emergency (*Emergency*). Emergency patients are admitted to hospital immediately if capacity permits; we assume that emergency patients who are denied admission die, which is represented by the *Dead* state. Elective patients that are not immediately admitted to hospital, on the other hand, remain waiting and run a risk of requiring emergency care in subsequent weeks.

Upon admission to hospital as elective or emergency, a patient requires either G&A (*Initially requires G&A* state) or CC (*Initially requires CC* state). A patient in need of G&A is admitted to G&A (*G&A* state), whereas a patient requiring CC can be assigned to either CC (*CC* state) or, in case of capacity shortages, to G&A. In the latter case, the transition into a designated *G** state implies that the patient subsequently evolves according to a different set of transition probabilities that account for an increased mortality risk associated with the denial of CC.

In the following weeks, depending on her response to the treatment, the patient can either require the same care regime or be moved to another one (*cf.* the *Requires G&A* and *Requires CC* states). Depending on resource availability, the patient then transitions between the three states *G&A*, *CC* or *G** until she eventually reaches the corresponding *Last Week* state, after which she is discharged from hospital (*Recovered* or *Dead*). We assume that a patient in a *Last Week* state only consumes half of the hospital resources, which mimics a half-week stay at the hospital. The inclusion of designated *Last Week* states allows us to account for the empirical fact that for some disease types, a large fraction of the patients require hospitalization for a few days only.

We next present the numerical results of our NHS England case study and compare our optimized schedule (hereafter OS) against a COVID prioritization policy (hereafter CP) that resembles the one implemented in England during the pandemic (Section 4.4.5). All experiments were run on a 2.7GHz quad-core Intel i7 processor with 16GB RAM using IBM ILOG CPLEX Optimization Studio 20.1. The runtimes of the fluid LP (4.3) ranged between 1.5 and 2 minutes.

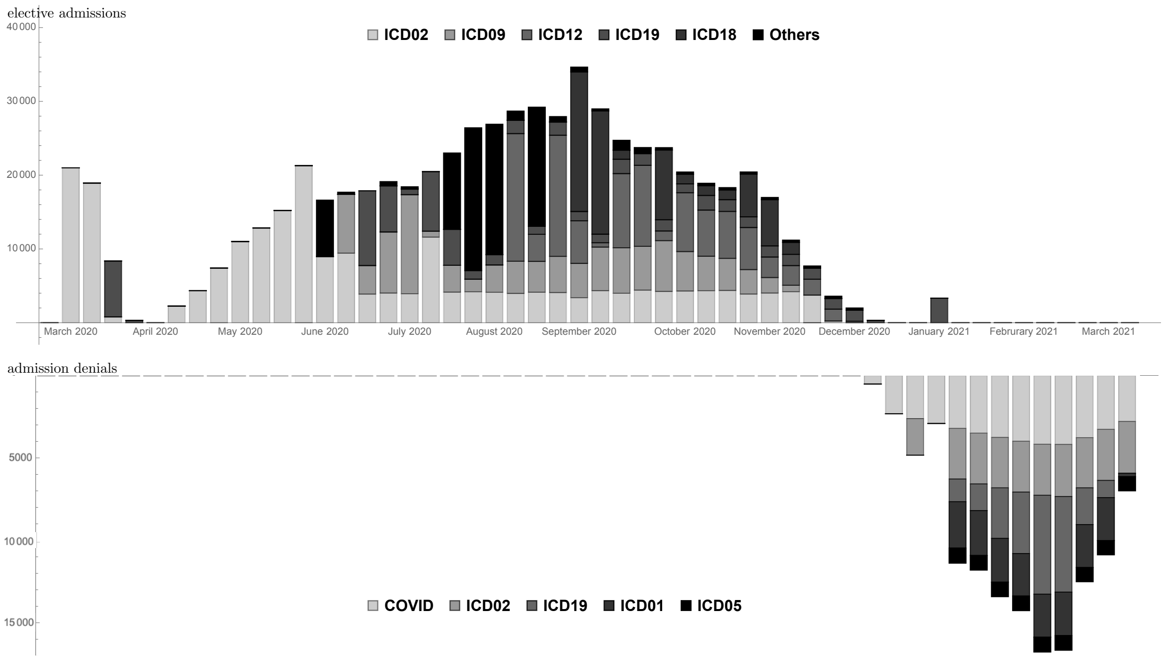

Figure 4.9: Weekly elective admissions (top) and admission denials (bottom) under the OS, categorized by disease group (ICD01: certain infectious and parasitic diseases; ICD02: neoplasms; ICD05: mental and behavioural disorders; ICD09: diseases of the circulatory system; ICD12: diseases of the skin and subcutaneous tissue; ICD18: symptoms, signs and abnormal clinical and laboratory findings, not elsewhere classified; ICD19: injury, poisoning and certain other consequences of external causes).

4.4.4 Optimized Schedule

Figure 4.9 shows the weekly elective admissions and emergency denials of the OS. Over the 52-week planning horizon, the OS admits to hospital 6,939,573 emergency patients (not shown), while 654,308 elective patients are admitted to hospital from week 1 to week 43 (upper part of Figure 4.9). Among the admitted elective patients, the most numerous groups are cancer patients (230,928), patients affected by diseases of the circulatory system (107,048) and diseases of the skin and subcutaneous tissue (101,790). In the last weeks of the planning horizon, due to the high inflow of COVID patients during the second wave of the pandemic, the available resources are insufficient to cope with the surge in demand. As a result, admission to hospital is denied to 125,346 emergency patients during weeks 38-52 (lower part of Figure 4.9). All of these patients are above 65 years of age, and most of them are COVID (40,962), cancer (30,069) and injury & poisoning (24,870) patients. The OS denies admission to hospital to these elderly patients as they have the lowest chances of benefiting from care.

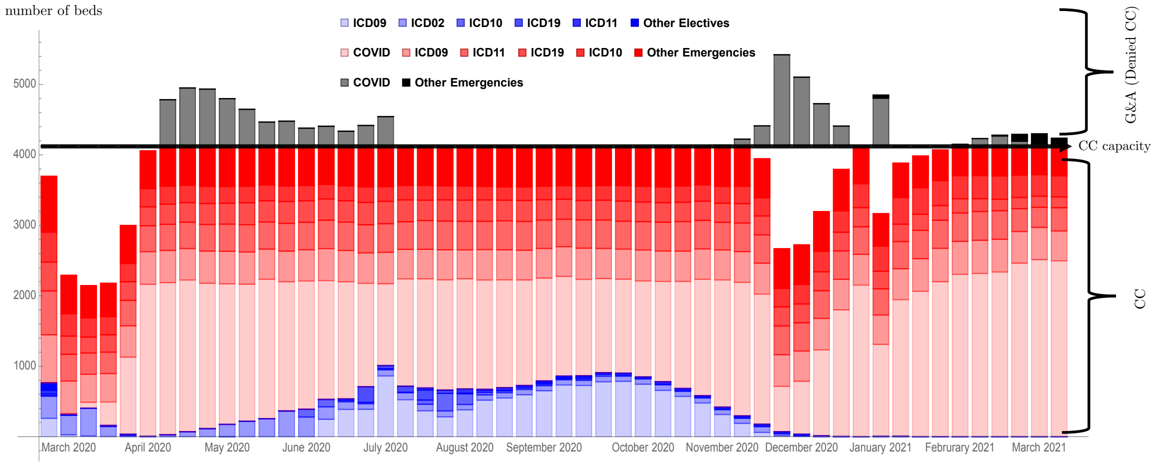

Figure 4.10: Weekly bed occupancy in CC by disease group (ICD02: neoplasms; ICD09: diseases of the circulatory system; ICD10: diseases of the respiratory system; ICD11: diseases of the digestive system; ICD19: injury, poisoning and certain other consequences of external causes). Patients who are denied CC, and have hence been moved to the $G^{\star}$ state, are shown above the CC capacity line.

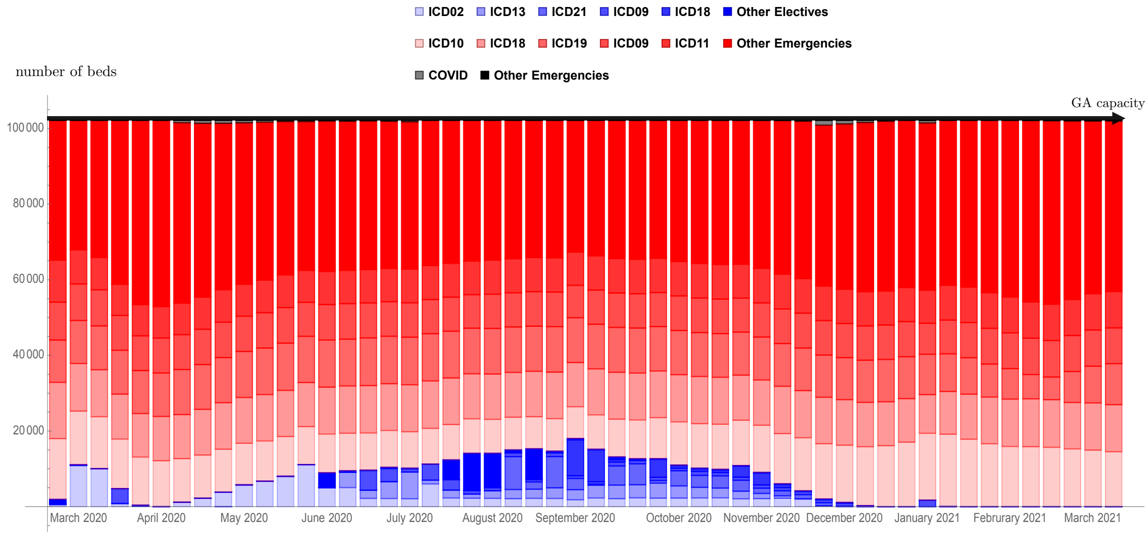

Figure 4.11: Weekly bed occupancy in G&A by disease group (ICD02: neoplasms; ICD09: diseases of the circulatory system; ICD10: diseases of the respiratory system; ICD11: diseases of the digestive system; ICD13: diseases of the musculoskeletal system and connective tissue; ICD18: symptoms, signs and abnormal clinical and laboratory findings, not elsewhere classified; ICD19: injury, poisoning and certain other consequences of external causes; ICD21: factors influencing health status and contact with health services).

Figures 4.10 and 4.11 show the bed occupancy in CC and G&A, respectively. A large share of CC beds is occupied by COVID patients (40.2% average occupancy over the planning horizon), while 9.4% of the available CC beds are assigned (on average) to elective patients. During both

		Mar	Apr	May	Jun	Jul	Aug	Sep	Oct	Nov	Dec	Jan	Feb	Mar
LP	G&A	100%	100%	100%	100%	100%	100%	100%	100%	100%	100%	100%	100%	100%
	CC	63%	93%	100%	100%	100%	100%	100%	100%	100%	76%	91%	99%	100%
DR	G&A	100%	101%	100%	100%	100%	100%	100%	100%	100%	100%	99%	101%	100%
	CC	63%	94%	99%	100%	100%	100%	100%	98%	99%	78%	93%	101%	101%
R	G&A	100%	100%	100%	100%	100%	100%	100%	100%	100%	100%	99%	100%	100%
	CC	66%	95%	107%	108%	101%	104%	97%	96%	100%	76%	90%	100%	101%

Table 4.2: Average monthly G&A and CC bed occupancy for the fluid LP (*LP*), the deterministic rounded policy (*DR*) and the randomized policy (*R*). All numbers are rounded to the closest integer. The first 10 months (last 3 months) fall into the year 2020 (2021).

the first and the second wave of the pandemic, capacity is insufficient, and CC is denied to some patients. The affected patients are almost exclusively COVID patients above 65 years of age, who are transferred to $G^\star$ due to their longer hospital stays as well as their lower capacity to benefit from treatment. G&A resources are fully utilized over the entire planning horizon, and the share of elective patients in G&A is on average 6.6%. The largest group of emergency patients in G&A are patients affected by diseases of the respiratory system, while cancer patients are the largest elective patient group. Overall, the OS results in 8,233,216 YLL over the 52 weeks planning horizon, with COVID patients contributing to 64% of the YLL.

We now investigate the performance of the deterministic rounded and the randomized policy from Sections 4.3.2.3 and 4.3.2.4. Recall that both of these approximation schemes generate policies $\pi \in \Pi$ for the weakly coupled counting DP whose objective values are close to the objective value of the fluid LP (which itself overestimates the optimal value of the weakly coupled counting DP) and whose resource violations are small, with high probability. For our case study, the deterministic rounded policy results in a YLL increase of 0.02% (from 8,233,216 to 8,235,198) as well as a 0.04% higher G&A and a 0.31% higher CC occupancy (across the entire time horizon). Likewise, the randomized policy results in a YLL *de*crease of 0.01% (from 8,233,216 to 8,232,570) as well as a 0.05% higher G&A and a 1.56% higher CC occupancy. Table 4.2 compares the monthly bed occupancy of the fluid LP (4.3) with the bed occupancy of our two approximation schemes in further detail. We conclude that both policies offer approximations of high quality.

Figure 4.12 visualizes the trade-off between the competing objectives of minimizing YLL and costs. To this end, we define the rewards of the individual DPs as convex combinations of the

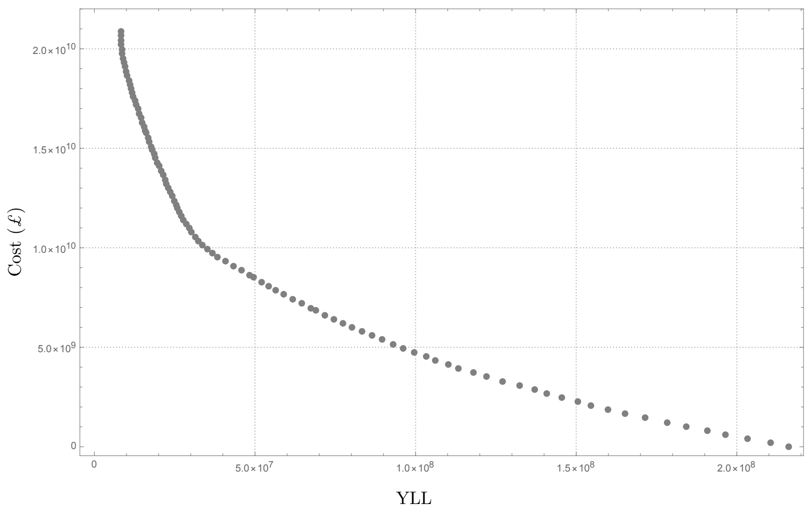

Figure 4.12: Pareto analysis: YLL vs. total cost of care.

patient's contributions to the overall YLL and cost of care. When the OS solely minimizes YLL, the total healthcare costs amount to £20,659 million. If we were to (hypothetically) not treat any patients, on the other hand, the YLL would increase from 8,233,216 to 216,255,399. As expected, significant reductions of YLL (or total cost of care) can be achieved when optimizing convex combinations of both objectives, rather than one of them in isolation. Recall that our model focuses on the variable costs of treatments, which are directly proportional to the number of hospital admissions. Thus, treating no patients results in zero costs in Figure 4.12 since we disregard the fixed costs associated with the running and maintenance of the hospitals, staff, prevention activities and primary care.

4.4.5 Comparison with COVID Prioritization Policies

The results from the previous section suggest that denying hospital or CC admission to COVID patients might be beneficial in case of capacity shortages. This contrasts with current practice, where many countries prioritize COVID patients to the detriment of other patients. In the following, we thus compare our OS against a CP policy that always admits COVID patients and that strongly penalizes CC denial to COVID patients in the objective. Other than that, the CP policy coincides with the OS; in particular, within the aforementioned restrictions, the CP policy optimally schedules care across all patients groups.

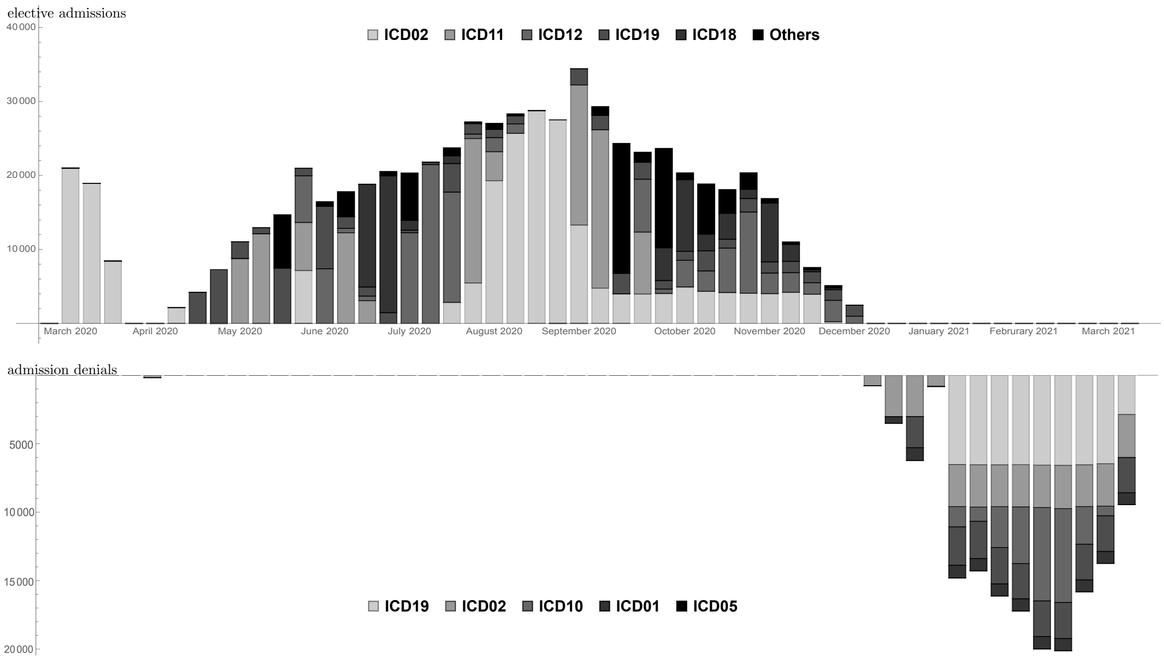

Figure 4.13: Weekly elective admissions (top) and admission denials (bottom) under the CP policy, categorized by disease group (ICD01: certain infectious and parasitic diseases; ICD02: neoplasms; ICD05: mental and behavioural disorders; ICD10: diseases of the respiratory system; ICD11: diseases of the digestive system; ICD12: diseases of the skin and subcutaneous tissue; ICD18: symptoms, signs and abnormal clinical and laboratory findings, not elsewhere classified; ICD19: injury, poisoning and certain other consequences of external causes).

Figure 4.13 shows that, while the total number of elective admissions is similar to the OS (655,415), emergency admission denials are significantly higher under the CP policy (153,092, +22.1% compared to the OS). Specifically, while all COVID patients are admitted to hospital, emergency admission is denied to patients above 65 years of age affected by injury & poisoning (55,130), cancer (35,663) and diseases of the respiratory system (26,784). The higher numbers of emergency admission denials are due to the longer treatment of COVID patients, relative to patients affected by other diseases. Under the CP policy, an average 71.6% of the CC beds are occupied by COVID patients (+75.6% compared to the OS), and the CC occupancy reaches 100% during the second wave of the pandemic (weeks 42-52). The share of electives in CC and G&A is reduced to 4.4% (-53.2% compared to the OS) and 6.5% (-1.5% compared to the OS), respectively.

Overall, the prioritization of COVID patients in admission to hospital and CC leads to an 8.7% increase in the total YLL under the CP policy compared to the OS. Figure 4.14 shows a breakdown of this total 719,868 YLL across the different disease groups. Significant losses in years

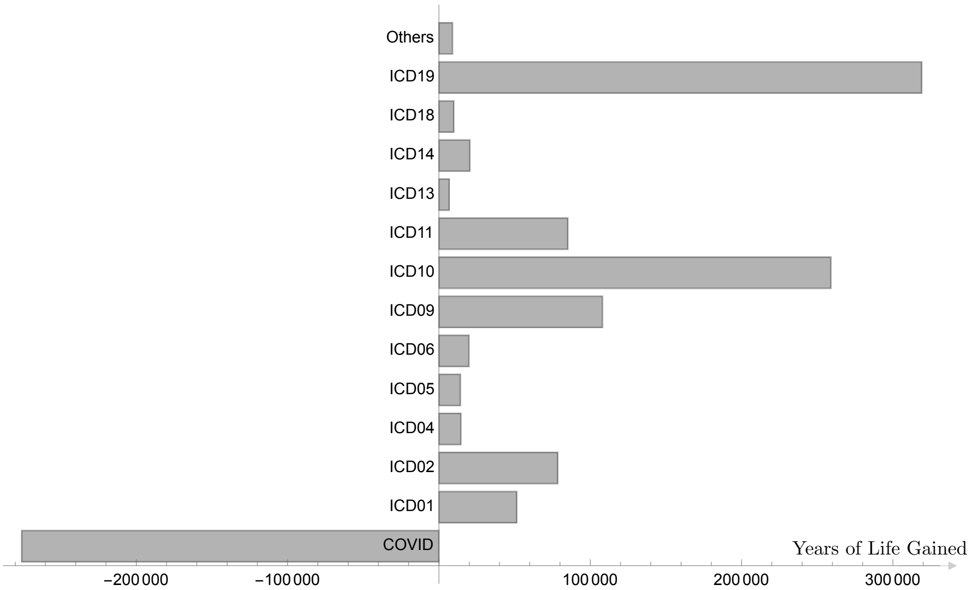

Figure 4.14: Years of Life Gained (*i.e.*, YLL avoided) by the OS relative to the CP policy, categorized by disease group (ICD01: certain infectious and parasitic diseases; ICD02: neoplasms; ICD04: endocrine, nutritional and metabolic diseases; ICD05: mental and behavioural disorders; ICD06: diseases of the nervous system; ICD09: diseases of the circulatory system; ICD10: diseases of the respiratory system; ICD11: diseases of the digestive system; ICD13: diseases of the musculoskeletal system and connective tissue; ICD14: diseases of the genitourinary system; ICD18: symptoms, signs and abnormal clinical and laboratory findings, not elsewhere classified; ICD19: injury, poisoning and certain other consequences of external causes).

of life are seen for patients affected by injury & poisoning (318,955), diseases of the respiratory system (259,012), diseases of the circulatory system (108,085), diseases of the digestive system (85,134) and cancer (78,464), to the benefit of elderly COVID patients (275,691).

We emphasize that the CP policy constitutes an overly optimistic representation of the current practice in England, where not only COVID patients are prioritized but also the other patient groups are scheduled suboptimally based on static prioritization schemes. Thus, we expect our results to underestimate the benefits of the OS over the current practice. We refer the interested reader to the associated paper [DGG+21b] for a comparison of the OS against a set of government admission policies across a range of scenarios.

4.5 Conclusion

4.5.1 Managerial Insights

The COVID prioritization policies described in Section 4.4.5 represents an optimistic view of the actual policy that was implemented by NHS England during the initial waves of COVID-19. The discussion in Section 4.4.5 clearly shows the benefits of using an optimized policy for scheduling patients versus using blanket prioritization policies that were implemented in practice.

We recognize that the optimal policies suggested in the previous section, even though beneficial to the public in the long run, may be hard to implement owing to its requirement to turn away some of the frailest patients. However, the optimized policies developed in this chapter should be used as a guiding framework to ensure that the resources are allocated in a way that patients who stand to benefit the most from treatment can get it in time. This also implies lower costs for NHS England over the longer term since it costs more to treat patients who are sicker because they did not receive appropriate treatment on time. Moreover, more efforts need to be made to educate the public on the benefits of using the approach suggested in this chapter, to sway public opinion in favor of implementing policies driven by optimization models in the future.

4.5.2 Additional Considerations

Our approach of modeling the health system via a weakly coupled counting DP and subsequently determining a near-optimal solution via the fluid LP (4.3) is very versatile. In this section, we highlight some extensions of our method that can help to obtain better informed, fairer and more resilient decisions as well as further insights into the characteristics of the optimal solution.

Relaxation of Model Assumptions. Our healthcare model makes a number of strong assumptions that can be relaxed. Firstly, with the exception of the patients that have been denied CC (and that have thus transferred to the state $G^\star$), the transitions in our model—such as the weekly probability of an elective patient turning into an emergency or the weekly probability of a hospitalized patient recovering or dying—are Markovian and hence memoryless. In reality, disease progression may exhibit a more complicated dependence on waiting time, and this time dependency differs across the different patient groups. We can readily model non-Markovian transitions by adding memory to the states of the patient DPs (*e.g.*, how many weeks has a patient been waiting for her surgery, and how many weeks has a patient spent in hospital). An interesting problem that arises in this context is how to best approximate non-Markovian transitions via a small number of additional states. Secondly, our model assumes that the timing and the magnitude of the patient inflows as well as the availability of staff is independent of the hospital occupancy rates. Since COVID is highly infectious, however, both non-COVID patients and hospital staff get exposed to the virus and—in absence of protective behavior—may spread it to the community. It would therefore be instructive to study the impact of hospital occupancy rates, which are immediate consequences of the admissions decisions in our model, on hospital acquired infections, changes in care seeking behavior as well as workload-dependent staff absenteeism [GSS13]. Thirdly, our model assumes that capacity can be re-assigned between COVID and non-COVID cases on short notice. Since COVID patients require isolation and dedicated staff to reduce the risk of infections, this is not the case in practice, and our model may therefore overestimate the available capacity. We believe that this issue is attenuated by the fact that we are modeling the health system of an entire nation, as opposed to an individual hospital. Finally, our model disregards geographical differences in patient numbers, hospital resources and treatment efficiency. While this appears to be an acceptable approximation in our case study, a more elaborate model could subdivide the country into different regions and impose that patients can only be treated in hospitals that are sufficiently close.

Alternative Objectives, Constraints and Decisions. While YLL and costs are natural objectives to minimize, one could also consider the incorporation of inequity aversion in the population distribution of healthcare utilization and/or health outcomes. . This would enable the policy maker to sacrifice some efficiency in favor of providing people of different age, gender, ethnicity and medical history equal chances of survival. Further refinements of our model could include additional policy restrictions, such as prioritizing CC access for patients that are already hospitalized or ensuring that patients of every disease and age group are admitted to hospital within a certain maximum time interval. While some of these restrictions can be readily included as linear constraints, others may require the imposition of logical constraints and thus result in mixed-integer linear programs. Finally, additional tactical and strategic decisions, such as the construction of temporary field hospitals, the enlistment of retired staff and medical students, changes to the employed staff-to-bed ratios as well as alterations in the design of the hospitals (*e.g.*, the erection of isolation wards for COVID patients), can be readily incorporated into our model through the inclusion of additional continuous or discrete decision variables.

Regularization against Data Uncertainty. Our healthcare model can be safeguarded against the impact of uncertainty in the patient inflows, transition probabilities and resource availabilities. To this end, we can replace the weakly coupled counting DP with a robust counterpart that determines the optimal policy in view of the worst rewards and transition probabilities from within a pre-specified uncertainty set, which can itself be selected so as to offer rigorous statistical guarantees. Robust policies have attracted significant interest in the context of Markov decision processes [Iye05, NG05, WKR13], and similar concepts can be readily applied to our weakly coupled counting DP. Assuming that the uncertainty set is polyhedral, the resulting robust version of our fluid LP (4.3) is amenable to the 'robust optimization trick' [BTEN09, BBC11a] and thus reduces to a linear program of moderately larger size than the nominal fluid LP (4.3).

Sensitivity Analysis. An important advantage of our LP-based approach is that the optimal solution to our healthcare model is amenable to sensitivity analysis. The shadow prices of the patient inflow constraints, for example, allow us to evaluate the impact of additional elective and emergency patients of a particular age group and disease type at different times during the pandemic. The shadow prices of the resource constraints inform about the value of different resources over time, and they allow to investigate the impact of changes to the required staff-to-bed ratios. The sensitivity of the optimal objective value with respect to the transition probabilities, finally, allows us to quantify the impact of improvements to certain treatments (*e.g.*, the administration of medicines to shorten the hospitalization of COVID patients) on the overall health outcome.

4.6 Appendix

The proofs of Theorems 4.19 and 4.20 rely on the following auxiliary results. In the following statements, we fix the weakly coupled counting DP $(\{\mathfrak{S}_j, \mathfrak{A}_j, \mathfrak{q}_j, \mathfrak{p}_j, \mathfrak{r}_j\}_j; \{n_j\}_j)$, a rounded policy $\pi^\star$ satisfying the conditions of Section 4.3.2.3 and its associated random state evolution $\tilde{\sigma}^\star = \{\tilde{\sigma}^\star_t\}_t$, as well as the quantities $\theta^\star$ and θ^{DP} from the statements of Theorems 4.19 and 4.20.

Lemma 4.24 *The following inequalities hold for all $t \in \mathcal{T}$, $j \in \mathcal{J}$ and $(s, a) \in \mathcal{S}_j \times \mathcal{A}_j$:*

$$\begin{aligned} \left|\mathbb{E}\left[\tilde{\sigma}^\star_{tj}(s)\right] - \sigma^{\text{LP}}_{tj}(s)\right| \;&\leqslant\; \frac{\overline{p}_j^t - 1}{\overline{p}_j - 1} - 1, \\ \left|\mathbb{E}\left[[\pi^\star_t(\tilde{\sigma}^\star_t)]_j(s,a)\right] - \pi^{\text{LP}}_{tj}(s,a)\right| \;&\leqslant\; \frac{\overline{p}_j^t - 1}{\overline{p}_j - 1}. \end{aligned}$$

Proof of Lemma 4.24. We prove the statement via induction over $t \in \mathcal{T}$. For $t = 1$, Definition 4.8 of a weakly coupled counting DP states that

$$\mathbb{E}\left[\tilde{\sigma}^\star_{1j}(s)\right] \;=\; n_j \cdot q_j(s) \;=\; \sigma^{LP}_{1j}(s) \qquad \forall j \in \mathcal{J},\ \forall s \in \mathcal{S}_j, \tag{4.4}$$

and Proposition 4.18 implies that

$$|\mathbb{E}\left[[\pi^\star_1(\tilde{\sigma}^\star_1)]_j(s,a)\right] - \mathbb{E}\left[[\overline{\pi}_1(\tilde{\sigma}^\star_1)]_j(s,a)\right]| \;\leqslant\; 1 \qquad \forall j \in \mathcal{J},\ \forall (s,a) \in \mathcal{S}_j \times \mathcal{A}_j.$$

Moreover, we have

$$\mathbb{E}\left[[\overline{\pi}_1(\tilde{\sigma}^\star_1)]_j(s,a)\right] \;=\; \frac{\pi^{\text{LP}}_{1j}(s,a)}{\sigma^{\text{LP}}_{1j}(s)} \cdot \mathbb{E}\left[\tilde{\sigma}^\star_{1j}(s)\right] \;=\; \pi^{\text{LP}}_{1j}(s) \qquad \forall j \in \mathcal{J},\ \forall s \in \mathcal{S}_j,$$

where the first identity follows from the definition of $\overline{\pi}$, while the second identity is due to (4.4). This proves the statement for $t = 1$.

Assume now that the statement holds for some $t \in \mathcal{T} \backslash \{T\}$. We then have

$$\mathbb{E}\left[\tilde{\sigma}^\star_{t+1,j}(s') \,|\, \pi^\star_t(\tilde{\sigma}^\star_t)\right] \;=\; \sum_{s \in \mathcal{S}_j} \sum_{a \in \mathcal{A}_j} p_{jt}(s'|s,a) \cdot [\pi^\star_t(\tilde{\sigma}^\star_t)]_j(s,a) \qquad \forall j \in \mathcal{J},\ \forall s' \in \mathcal{S}_j.$$

Taking expectation on both sides, we see that for all $j \in \mathcal{J}$ and all $s' \in \mathcal{S}_j$, we have that

$$\begin{aligned}
\mathbb{E}\left[\tilde{\sigma}^\star_{t+1,j}(s')\right] &= \sum_{s\in\mathcal{S}_j}\sum_{a\in\mathcal{A}_j} p_{jt}(s'|s,a)\cdot\mathbb{E}\left[[\pi^\star_t(\tilde{\sigma}^\star_t)]_j(s,a)\right] \\
&= \sum_{s\in\mathcal{S}_j}\sum_{a\in\mathcal{A}_j} p_{jt}(s'|s,a)\cdot\left(\pi^{\mathrm{LP}}_{tj}(s,a)+\mathbb{E}\left[[\pi^\star_t(\tilde{\sigma}^\star_t)]_j(s,a)\right]-\pi^{\mathrm{LP}}_{tj}(s,a)\right) \\
&= \sigma^{\mathrm{LP}}_{t+1,j}(s')+\sum_{s\in\mathcal{S}_j}\sum_{a\in\mathcal{A}_j} p_{jt}(s'|s,a)\left(\mathbb{E}\left[[\pi^\star_t(\tilde{\sigma}^\star_t)]_j(s,a)\right]-\pi^{\mathrm{LP}}_{tj}(s,a)\right),
\end{aligned}$$

where the last identity follows from the second constraint of the fluid LP (4.3), which implies that $\sigma^{\mathrm{LP}}_{t+1,j}(s') = \sum_{s\in\mathcal{S}_j}\sum_{a\in\mathcal{A}_j} p_{jt}(s'|s,a)\cdot\pi^{\mathrm{LP}}_{tj}(s,a)$ for all $t \in \mathcal{T}\backslash\{T\}$, $j \in \mathcal{J}$ and $s' \in \mathcal{S}_j$. Subtracting $\sigma^{\mathrm{LP}}_{t+1,j}(s')$ on both sides and taking absolute values, we see that

$$\begin{aligned}
\left|\mathbb{E}\left[\tilde{\sigma}^\star_{t+1,j}(s')\right]-\sigma^{\mathrm{LP}}_{t+1,j}(s')\right| &= \sum_{s\in\mathcal{S}_j}\sum_{a\in\mathcal{A}_j} p_{jt}(s'|s,a)\left|\mathbb{E}\left[[\pi^\star_t(\tilde{\sigma}^\star_t)]_j(s,a)\right]-\pi^{\mathrm{LP}}_{tj}(s,a)\right| \\
&\leqslant \sum_{s\in\mathcal{S}_j}\sum_{a\in\mathcal{A}_j} p_{jt}(s'|s,a)\cdot\frac{\overline{p}_j^t-1}{\overline{p}_j-1} \\
&\leqslant \overline{p}_j\cdot\frac{\overline{p}_j^t-1}{\overline{p}_j-1} = \frac{\overline{p}_j^{t+1}-1}{\overline{p}_j-1}-1,
\end{aligned}$$

where the two inequalities follow from the induction hypothesis and the definition of $\overline{p}_j$, respectively. Similarly, the definition of $\overline{\pi}$ implies that

$$\begin{aligned}
\left|\mathbb{E}\left[[\overline{\pi}_{t+1}(\tilde{\sigma}^\star_{t+1})]_j(s,a)\right]-\pi^{\mathrm{LP}}_{t+1,j}(s,a)\right| &= \left|\frac{\pi^{\mathrm{LP}}_{t+1,j}(s,a)}{\sigma^{\mathrm{LP}}_{t+1,j}(s)}\cdot\mathbb{E}\left[\tilde{\sigma}^\star_{t+1,j}(s)\right]-\pi^{\mathrm{LP}}_{t+1,j}(s,a)\right| \\
&= \frac{\pi^{\mathrm{LP}}_{t+1,j}(s,a)}{\sigma^{\mathrm{LP}}_{t+1,j}(s)}\cdot\left|\mathbb{E}\left[\tilde{\sigma}^\star_{t+1,j}(s)\right]-\sigma^{\mathrm{LP}}_{t+1,j}(s)\right| \\
&\leqslant \left|\mathbb{E}\left[\tilde{\sigma}^\star_{t+1,j}(s)\right]-\sigma^{\mathrm{LP}}_{t+1,j}(s)\right| \\
&\leqslant \frac{\overline{p}_j^{t+1}-1}{\overline{p}_j-1}-1,
\end{aligned} \tag{4.5}$$

where the first identity holds by definition of $\overline{\pi}_{t+1}$, the first inequality follows from the fact that $\pi^{\mathrm{LP}}_{t+1,j}(s,a) \leqslant \sigma^{\mathrm{LP}}_{t+1,j}(s)$, which is implied by the fourth constraint of the fluid LP (4.3), and the second inequality is due to the induction hypothesis. Proposition 4.18 implies that

$$\left|\mathbb{E}\left[[\pi^\star_{t+1}(\tilde{\sigma}^\star_{t+1})]_j(s,a)\right]-\mathbb{E}\left[[\overline{\pi}_{t+1}(\tilde{\sigma}^\star_{t+1})]_j(s,a)\right]\right| \leqslant 1 \qquad \forall j\in\mathcal{J},\ \forall (s,a)\in\mathcal{S}_j\times\mathcal{A}_j,$$

which in turn implies through the triangle inequality that

$$\left|\mathbb{E}\left[[\pi^\star_{t+1}(\tilde{\sigma}^\star_{t+1})]_j(s,a)\right] - \pi^{\mathrm{LP}}_{t+1,j}(s,a)\right| \;\leqslant\; 1 + \left|\mathbb{E}\left[[\overline{\pi}_{t+1}(\tilde{\sigma}^\star_{t+1})]_j(s,a)\right] - \pi^{\mathrm{LP}}_{t+1,j}(s,a)\right|$$

for all $j \in \mathcal{J}$ and all $(s,a) \in \mathcal{S}_j \times \mathcal{A}_j$, and equation (4.5) implies that the right-hand side expression is less than or equal to $(\overline{p}_j^{t+1} - 1)/(\overline{p}_j - 1)$ as desired. This completes the proof. ■

Lemma 4.25 *With probability at least* $1 - 2|\mathcal{T}| \cdot \sum_{j \in \mathcal{J}} |\mathcal{S}_j|/n_j$*, we have*

$$\left|[\pi^\star_t(\tilde{\sigma}^\star_t)]_j(s,a) - \pi^{\mathrm{LP}}_{tj}(s,a)\right| \;\leqslant\; (1 + \epsilon n_j) \cdot \frac{\overline{p}_j^t - 1}{\overline{p}_j - 1} \qquad \forall t \in \mathcal{T},\ \forall j \in \mathcal{J},\ \forall (s,a) \in \mathcal{S}_j \times \mathcal{A}_j.$$

Proof of Lemma 4.25. We prove the statement via induction over $t \in \mathcal{T}$. For $t = 1$, Proposition 4.18 implies that

$$|[\pi^\star_1(\tilde{\sigma}^\star_1)]_j(s,a) - [\overline{\pi}_1(\tilde{\sigma}^\star_1)]_j(s,a)| \;\leqslant\; 1 \quad \forall j \in \mathcal{J},\ \forall (s,a) \in \mathcal{S}_j \times \mathcal{A}_j$$

pointwise. Moreover, we have

$$[\overline{\pi}_1(\tilde{\sigma}^\star_1)]_j(s,a) \;=\; \frac{\pi^{\mathrm{LP}}_{1j}(s,a)}{\sigma^{\mathrm{LP}}_{1j}(s)} \cdot \tilde{\sigma}^\star_{1j}(s) \;=\; \pi^{\mathrm{LP}}_{1j}(s,a) + \pi^{\mathrm{LP}}_{1j}(s,a) \cdot \frac{\tilde{\sigma}^\star_{1j}(s) - \sigma^{\mathrm{LP}}_{1j}(s)}{\sigma^{\mathrm{LP}}_{1j}(s)}$$

for all $j \in \mathcal{J}$ and $(s,a) \in \mathcal{S}_j \times \mathcal{A}_j$ pointwise, where the first identity follows from the definition of $\overline{\pi}$. This in turn implies that

$$\left|[\overline{\pi}_1(\tilde{\sigma}^\star_1)]_j(s,a) - \pi^{\mathrm{LP}}_{1j}(s,a)\right| \;=\; \left|\pi^{\mathrm{LP}}_{1j}(s,a) \cdot \frac{\tilde{\sigma}^\star_{1j}(s) - \sigma^{\mathrm{LP}}_{1j}(s)}{\sigma^{\mathrm{LP}}_{1j}(s)}\right| \;\leqslant\; \left|\tilde{\sigma}^\star_{1j}(s) - \sigma^{\mathrm{LP}}_{1j}(s)\right|$$

for all $j \in \mathcal{J}$ and $(s,a) \in \mathcal{S}_j \times \mathcal{A}_j$ pointwise, where the inequality follows from the fact that $\pi^{\mathrm{LP}}_{1j}(s,a) \,/\, \sigma^{\mathrm{LP}}_{1j}(s) \leqslant 1$ due to the fourth constraint in the fluid LP (4.3) (also for $\sigma^{\mathrm{LP}}_{1j}(s) = 0$, in which case our earlier convention implies that the fraction vanishes). The statement for $t = 1$ now follows from the triangle inequality if we can show that $\left|\tilde{\sigma}^\star_{1j}(s) - \sigma^{\mathrm{LP}}_{1j}(s)\right| \leqslant 1 + \epsilon n_j$ simultaneously for all $j \in \mathcal{J}$ and $s \in \mathcal{S}_j$ with probability at least $1 - 2|\mathcal{T}| \cdot \sum_{j \in \mathcal{J}} |\mathcal{S}_j|/n_j$. To see this, we note that

$$\mathbb{P}\left[\left|\tilde{\sigma}^\star_{1j}(s) - n_j \cdot q_j(s)\right| \leqslant \epsilon n_j\right] \geqslant 1 - \frac{2}{n_j} \qquad \forall j \in \mathcal{J},\ \forall s \in \mathcal{S}_j$$

according to Hoeffding's inequality, and $\sigma^{\mathrm{LP}}_{1j}(s) = n_j \cdot q_j(s)$ according to the first constraint in the fluid LP (4.3). The result then follows from the union bound.

Assume now that the statement holds for $t \in \mathcal{T}\backslash\{T\}$. The same argument as before shows that

$$\left|[\pi^\star_{t+1}(\tilde{\sigma}^\star_{t+1})]_j(s,a) - [\overline{\pi}_{t+1}(\tilde{\sigma}^\star_{t+1})]_j(s,a)\right| \leqslant 1 \tag{4.6}$$

as well as

$$\left|[\overline{\pi}_{t+1}(\tilde{\sigma}^\star_{t+1})]_j(s,a) - \pi^{\mathrm{LP}}_{t+1,j}(s,a)\right| \leqslant \left|\tilde{\sigma}^\star_{t+1,j}(s) - \sigma^{\mathrm{LP}}_{t+1,j}(s)\right|$$

for all $j \in \mathcal{J}$ and $(s,a) \in \mathcal{S}_j \times \mathcal{A}_j$ pointwise. The result again follows from the triangle inequality if we can show that

$$\left|\tilde{\sigma}^\star_{t+1,j}(s) - \sigma^{\mathrm{LP}}_{t+1,j}(s)\right| \leqslant (1 + \epsilon n_j) \cdot \frac{\overline{p}_j^{\,t+1} - 1}{\overline{p}_j - 1} - 1 \tag{4.7}$$

simultaneously for all $j \in \mathcal{J}$ and $s \in \mathcal{S}_j$ with probability at least $1 - 2|\mathcal{T}| \cdot \sum_{j\in\mathcal{J}} |\mathcal{S}_j|/n_j$. The remainder of the proof is thus dedicated to proving the bound (4.7).

Note first that

$$\mathbb{E}\left[\tilde{\sigma}^\star_{t+1,j}(s') \,|\, \pi^\star_t(\tilde{\sigma}^\star_t)\right] = \sum_{s\in\mathcal{S}_j}\sum_{a\in\mathcal{A}_j} p_{jt}(s'|s,a) \cdot [\pi^\star_t(\tilde{\sigma}^\star_t)]_j(s,a) \qquad \forall j \in \mathcal{J},\ \forall s' \in \mathcal{S}_j.$$

Hoeffding's inequality, which applies since the random variables $\tilde{\sigma}^\star_{t+1,j}(s')$ are conditionally independent given $\pi^\star_t(\tilde{\sigma}^\star_t)$, then implies that

$$\mathbb{P}\left[\left|\tilde{\sigma}^\star_{t+1,j}(s') - \sum_{s\in\mathcal{S}_j}\sum_{a\in\mathcal{A}_j} p_{jt}(s|s,a) \cdot \pi^0_{tj}(s,a)\right| \leqslant \epsilon n_j \;\middle|\; \pi^\star_t(\tilde{\sigma}^\star_t) = \pi^0_t\right] \geqslant 1 - 2\mathrm{e}^{-2\epsilon^2 n_j} \geqslant 1 - \frac{2}{n_j}$$

for all $j \in \mathcal{J}$ and $s' \in \mathcal{S}_j$, and an application of the union bound shows that

$$\mathbb{P}\left[\left|\tilde{\sigma}^\star_{t+1,j}(s') - \sum_{s\in\mathcal{S}_j}\sum_{a\in\mathcal{A}_j} p_{jt}(s'|s,a)\cdot\pi^0_{tj}(s,a)\right| \leqslant \epsilon n_j \;\; \forall j\in\mathcal{J},\; \forall s'\in\mathcal{S}_j \;\middle|\; \pi^\star_t(\tilde{\sigma}^\star_t) \;=\; \pi^0_t\right] \;\geqslant\; 1-\sum_{j\in\mathcal{J}}\frac{2|\mathcal{S}_j|}{n_j}. \tag{4.8}$$

Note next that for any $\pi^0_t \in \mathfrak{A}$, we have

$$\begin{aligned}
&\sum_{s\in\mathcal{S}_j}\sum_{a\in\mathcal{A}_j} p_{jt}(s'|s,a)\cdot\pi^0_{tj}(s,a)\\
&= \sum_{s\in\mathcal{S}_j}\sum_{a\in\mathcal{A}_j} p_{jt}(s'|s,a)\cdot\left(\pi^0_{tj}(s,a)-\pi^{\mathrm{LP}}_{tj}(s,a)\right) \;+\; \sum_{s\in\mathcal{S}_j}\sum_{a\in\mathcal{A}_j} p_{jt}(s'|s,a)\cdot\pi^{\mathrm{LP}}_{tj}(s,a)\\
&= \sum_{s\in\mathcal{S}_j}\sum_{a\in\mathcal{A}_j} p_{jt}(s'|s,a)\cdot\left(\pi^0_{tj}(s,a)-\pi^{\mathrm{LP}}_{tj}(s,a)\right) \;+\; \sigma^{\mathrm{LP}}_{t+1,j}(s')
\end{aligned} \tag{4.9}$$

for all $s' \in \mathcal{S}_j$, where the last identity follows from the second constraint of the fluid LP (4.3). Consider next the set

$$\Gamma \;=\; \left\{\pi_t\in\mathfrak{A} \,:\, \left|\pi_{tj}(s,a)-\pi^{\mathrm{LP}}_{tj}(s,a)\right| \;\leqslant\; (1+\epsilon n_j)\cdot\frac{\overline{p}_j^{\,t}-1}{\overline{p}_j-1} \;\; \forall j\in\mathcal{J},\; \forall (s,a)\in\mathcal{S}_j\times\mathcal{A}_j\right\}$$

of partial policies π_t that are sufficiently close to π^{LP}_t. For any $\pi^0_t \in \Gamma$, we have

$$\mathbb{P}\left[\left|\tilde{\sigma}^\star_{t+1,j}(s')-\sigma^{\mathrm{LP}}_{t+1,j}(s')\right| \;\leqslant\; (1+\epsilon n_j)\cdot\frac{\overline{p}_j^{\,t+1}-1}{\overline{p}_j-1}-1 \;\; \forall j\in\mathcal{J},\; \forall s'\in\mathcal{S}_j \;\middle|\; \pi^\star_t(\tilde{\sigma}^\star_t)=\pi^0_t\right] \;\geqslant\; 1-\sum_{j\in\mathcal{J}}\frac{2|\mathcal{S}_j|}{n_j} \tag{4.10}$$

since

$$\begin{aligned}
&\left|\tilde{\sigma}^\star_{t+1,j}(s')-\sigma^{\mathrm{LP}}_{t+1,j}(s')\right|\\
&\leqslant \left|\tilde{\sigma}^\star_{t+1,j}(s') - \sum_{s\in\mathcal{S}_j}\sum_{a\in\mathcal{A}_j} p_{jt}(s'|s,a)\cdot\pi^0_{tj}(s,a)\right| \;+\; \left|\sum_{s\in\mathcal{S}_j}\sum_{a\in\mathcal{A}_j} p_{jt}(s'|s,a)\cdot\pi^0_{tj}(s,a)-\sigma^{\mathrm{LP}}_{t+1,j}(s')\right|\\
&\leqslant \epsilon n_j \;+\; \sum_{s\in\mathcal{S}_j}\sum_{a\in\mathcal{A}_j} p_{jt}(s'|s,a)\cdot(1+\epsilon n_j)\cdot\frac{\overline{p}_j^{\,t}-1}{\overline{p}_j-1}\\
&\leqslant \epsilon n_j \;+\; (1+\epsilon n_j)\cdot\frac{\overline{p}_j^{\,t+1}-\overline{p}_j}{\overline{p}_j-1} \;\;=\;\; (1+\epsilon n_j)\cdot\frac{\overline{p}_j^{\,t+1}-1}{\overline{p}_j-1}-1,
\end{aligned}$$

where the first inequality holds pointwise due to the triangle inequality, the second inequality holds conditionally with probability at least $1 - 2\sum_{j\in\mathcal{J}} |\mathcal{S}_j|/n_j$ due to (4.8), (4.9) and the fact that $\pi_t^0 \in \Gamma$, and the third inequality holds by definition of $\overline{p}_j$.

Going over to unconditional probabilities, we finally obtain

$$\begin{aligned}
&\mathbb{P}\left[\left|\tilde{\sigma}^{\star}_{t+1,j}(s') - \sigma^{\mathrm{LP}}_{t+1,j}(s')\right| \leqslant (1+\epsilon n_j)\cdot\frac{\overline{p}_j^{t+1}-1}{\overline{p}_j-1} - 1 \;\; \forall j \in \mathcal{J},\; \forall s' \in \mathcal{S}_j\right] \\
=\;& \sum_{\pi_t^0} \mathbb{P}\left[\left|\tilde{\sigma}^{\star}_{t+1,j}(s') - \sigma^{\mathrm{LP}}_{t+1,j}(s')\right| \leqslant (1+\epsilon n_j)\cdot\frac{\overline{p}_j^{t+1}-1}{\overline{p}_j-1} - 1 \;\; \forall j \in \mathcal{J},\; \forall s' \in \mathcal{S}_j \;\middle|\; \pi_t^{\star}(\tilde{\sigma}_t^{\star}) = \pi_t^0\right] \\
&\qquad \cdot \mathbb{P}\left[\pi_t^{\star}(\tilde{\sigma}_t^{\star}) = \pi_t^0\right] \\
\geqslant\;& \sum_{\pi_t^0\in\Gamma} \mathbb{P}\left[\left|\tilde{\sigma}^{\star}_{t+1,j}(s') - \sigma^{\mathrm{LP}}_{t+1,j}(s')\right| \leqslant (1+\epsilon n_j)\cdot\frac{\overline{p}_j^{t+1}-1}{\overline{p}_j-1} - 1 \;\; \forall j \in \mathcal{J},\; \forall s' \in \mathcal{S}_j \;\middle|\; \pi_t^{\star}(\tilde{\sigma}_t^{\star}) = \pi_t^0\right] \\
&\qquad \cdot \mathbb{P}\left[\pi_t^{\star}(\tilde{\sigma}_t^{\star}) = \pi_t^0\right] \\
\geqslant\;& \sum_{\pi_t^0\in\Gamma} \left(1 - \sum_{j\in\mathcal{J}} \frac{2|\mathcal{S}_j|}{n_j}\right) \cdot \mathbb{P}\left[\pi_t^{\star}(\tilde{\sigma}_t^{\star}) = \pi_t^0\right] \\
\geqslant\;& \left(1 - \sum_{j\in\mathcal{J}} \frac{2|\mathcal{S}_j|}{n_j}\right) \cdot \left(1 - t\cdot\sum_{j\in\mathcal{J}} \frac{2|\mathcal{S}_j|}{n_j}\right) \;\;\geqslant\;\; 1 - (t+1)\cdot\sum_{j\in\mathcal{J}} \frac{2|\mathcal{S}_j|}{n_j},
\end{aligned}$$

where the identity is due to the law of total probability, the first inequality holds because we restrict ourselves to $\pi_t^0 \in \Gamma$, the second inequality follows from (4.10), the third inequality is due to the definition of Γ as well as the induction hypothesis, and the last inequality holds since $(1-x)(1-tx) = 1-(t+1)x+tx^2 \geqslant 1-(t+1)x$ for all $x \in \mathbb{R}$. This shows the bound (4.7) and thereby completes the proof. ∎

Next, we provide the auxiliary results required for the proofs of Theorems 4.22 and 4.23.

Lemma 4.26 *The following equations hold for all $t \in \mathcal{T}$, $(j,i) \in \mathcal{J} \times \{1,\ldots,n_j\}$ and $(s,a) \in \mathcal{S}_j \times \mathcal{A}_j$:*

$$\mathbb{P}\left[\tilde{s}_{t,(j,i)} = s \;\wedge\; \tilde{a}_{t,(j,i)} = a\right] \;=\; \frac{\pi^{\mathrm{LP}}_{tj}(s,a)}{n_j}.$$

Proof of Lemma 4.26. According to our definition of the randomized policy $\pi^{\star}$, we have

$$\mathbb{P}\left[\tilde{a}_{t,(j,i)} = a \,\middle|\, \tilde{s}_{t,(j,i)} = s\right] \;=\; \frac{\pi^{\mathrm{LP}}_{tj}(s,a)}{\sigma^{\mathrm{LP}}_{tj}(s)} \qquad \forall (s,a) \in \mathcal{S}_j \times \mathcal{A}_j$$

for each $t \in \mathcal{T}$ and $(j,i) \in \mathcal{J} \times \{1,\ldots,n_j\}$, which in turn implies that

$$\mathbb{P}\left[\tilde{s}_{t,(j,i)} = s \;\wedge\; \tilde{a}_{t,(j,i)} = a\right] \;=\; \mathbb{P}\left[\tilde{a}_{t,(j,i)} = a \,|\, \tilde{s}_{t,(j,i)} = s\right] \cdot \mathbb{P}\left[\tilde{s}_{t,(j,i)} = s\right] = \frac{\pi^{\mathrm{LP}}_{tj}(s,a)}{\sigma^{\mathrm{LP}}_{tj}(s)} \cdot \mathbb{P}\left[\tilde{s}_{t,(j,i)} = s\right]. \tag{4.11}$$

In the remainder of the proof, we show via induction on $t \in \mathcal{T}$ that $\mathbb{P}\left[\tilde{s}_{t,(j,i)} = s\right] = \sigma^{\mathrm{LP}}_{tj}(s) / n_j$ for all $t \in \mathcal{T}$, $(j,i) \in \mathcal{J} \times \{1,\ldots,n_j\}$ and $s \in \mathcal{S}_j$, which concludes the proof.

For $t = 1$, the definition of the weakly coupled DP implies that $\mathbb{P}\left[\tilde{s}_{t,(j,i)} = s\right] = q_j(s)$, and the first constraint of the fluid LP (4.3) ensures that $\sigma^{\mathrm{LP}}_{1j}(s) = n_j \cdot q_j(s)$. Assume now that $\mathbb{P}\left[\tilde{s}_{t,(j,i)} = s\right] = \sigma^{\mathrm{LP}}_{tj}(s) / n_j$ for some $t \in \mathcal{T} \backslash \{T\}$. We then have

$$\begin{aligned}
\mathbb{P}\left[\tilde{s}_{t+1,(j,i)} = s'\right] \;&=\; \sum_{s \in \mathcal{S}_j} \sum_{a \in \mathcal{A}_j} p_{jt}(s'|s,a) \cdot \mathbb{P}\left[\tilde{s}_{t,(j,i)} = s \;\wedge\; \tilde{a}_{t,(j,i)} = a\right] \\
&=\; \sum_{s \in \mathcal{S}_j} \sum_{a \in \mathcal{A}_j} p_{jt}(s'|s,a) \cdot \frac{\pi^{\mathrm{LP}}_{tj}(s,a)}{\sigma^{\mathrm{LP}}_{tj}(s)} \cdot \mathbb{P}\left[\tilde{s}_{t,(j,i)} = s\right] \\
&=\; \sum_{s \in \mathcal{S}_j} \sum_{a \in \mathcal{A}_j} p_{jt}(s'|s,a) \cdot \frac{\pi^{\mathrm{LP}}_{tj}(s,a)}{n_j} \;=\; \frac{\sigma^{\mathrm{LP}}_{t+1,j}(s')}{n_j},
\end{aligned}$$

where the first identity follows from the definition of the weakly coupled DP, the second identity is due to (4.11), the third identity follows from the induction hypothesis, and the last identity is due to the second constraint of the fluid LP (4.3). ∎

Lemma 4.27 *Let $\tilde{\alpha}^{\star}_{tj}(s,a) = \sum_{i=1}^{n_j} \mathbf{1}\left[\tilde{s}_{t,(j,i)} = s \;\wedge\; \tilde{a}_{t,(j,i)} = a\right]$ record the number of DPs in the j-th counting DP that are in state s and to which action a is applied at time t. Then*

$$\mathbb{E}\left[\tilde{\alpha}^{\star}_{tj}(s,a)\right] \;=\; \pi^{\mathrm{LP}}_{tj}(s,a) \qquad \forall t \in \mathcal{T},\ \forall j \in \mathcal{J},\ \forall (s,a) \in \mathcal{S}_j \times \mathcal{A}_j.$$

Furthermore, with probability at least $1 - 2|\mathcal{T}| \cdot \sum_{j \in \mathcal{J}} |\mathcal{S}_j| \cdot |\mathcal{A}_j| / n_j$, we have

$$\left|\tilde{\alpha}^{\star}_{tj}(s,a) - \pi^{\mathrm{LP}}_{tj}(s,a)\right| \;\leqslant\; \epsilon n_j \qquad \forall t \in \mathcal{T},\ \forall j \in \mathcal{J},\ \forall (s,a) \in \mathcal{S}_j \times \mathcal{A}_j.$$

Proof of Lemma 4.27. In view of the first statement, we note that

$$\mathbb{E}\left[\tilde{\alpha}^{\star}_{tj}(s,a)\right] \;=\; \sum_{i=1}^{n_j} \mathbb{P}\left[\tilde{s}_{t,(j,i)} = s \;\wedge\; \tilde{a}_{t,(j,i)} = a\right] \;=\; \sum_{i=1}^{n_j} \frac{\pi^{\mathrm{LP}}_{tj}(s,a)}{n_j} \;=\; \pi^{\mathrm{LP}}_{tj}(s,a),$$

where the first and second identity follow from the definition of $\tilde{\alpha}^{\star}_{tj}(s,a)$ and Lemma 4.26, respectively.

As for the second statement, note that $\tilde{\alpha}^{\star}_{tj}(s,a)$ is a sum of i.i.d. random variables. Hoeffding's inequality then implies that

$$\mathbb{P}\left[\left|\tilde{\alpha}^{\star}_{tj}(s,a) - \pi^{\mathrm{LP}}_{tj}(s,a)\right| \leqslant \epsilon n_j\right] \;\geqslant\; 1 - 2\mathrm{e}^{2\epsilon^2 n_j} \;\geqslant\; 1 - \frac{2}{n_j}$$

for all $t \in \mathcal{T}$, $j \in \mathcal{J}$ and $(s,a) \in \mathcal{S}_j \times \mathcal{A}_j$, and the statement thus follows from the union bound.
∎

Chapter 5

Conclusion

5.1 Summary of the Thesis

Large organizations face numerous problems that involve decision making based on uncertain or incomplete information. These could either be single-stage or multi-stage decision making problems. This thesis has aimed to study problems in both areas, and propose models and develop solutions that improve upon the literature.

This thesis focused on two key problem areas: one is the problem of vehicle routing in logistics operations, and the other is that of optimizing the scheduling of elective patients in order to improve healthcare operations. In Chapters 2 and 3, we studied the problem of vehicle routing under demand uncertainty, while Chapter 4 studied the problem of optimal prioritization of elective patients during a pandemic.

In the wide domain of vehicle routing, we restricted our attention to the problem of the single-stage capacitated vehicle routing problem (CVRP) under distributional ambiguity of the customer demands. In Chapter 2, we studied the chance-constrained vehicle routing problem under this setting. The chance-constrained CVRP is a notoriously hard problem to solve. However, we showed that under a wide consideration of moment ambiguity sets, the distributionally robust chance constrained CVRP enjoys a similar computational complexity as the classical, deterministic CVRP. This is the first study that attempted the application of the distributionally robust optimization paradigm to the CVRP, and has opened up possibilities of addressing uncertainty using existing algorithms, without undue overhead over deterministic models. The distributionally robust optimization approach allowed for relaxing the assumptions of independence of customer demands and the knowledge of the governing probability distribution, which although restrictive were common in the vehicle routing literature.

Chapter 3 extended on the findings of Chapter 2 by considering various risk measures in conjunction with different characterizations of the ambiguity sets that allows us to solve different variants of the CVRP. The consideration of a very general ambiguous set allows us to bridge the paradigms of stochastic optimization, robust optimization and distributionally robust optimization. To our best knowledge, this chapter is the first attempt at proposing a framework for the stochastic and distributionally robust CVRP that combines multiple ambiguity sets with different risk measures and disutility functions. Moreover, our proposed method based on the branch-and-cut algorithm allows the solution of a wide class of problems with only minimal adaptation. Even more generally, we developed a framework that identifies the necessary conditions that a problem must satisfy to be amenable to our treatment. This allows extensions of our method to variants of the VRP other than the CVRP.

Chapter 4 studied the problem of multi-stage decision making using the dynamic programming approach. More specifically, it looked at large-scale weakly coupled dynamic programs. These problems are intractable and are solved using approximation solution schemes. This chapter introduced the concept of k-counting dynamic programs that allow to approximately solve intractable large weakly coupled dynamic program by a tractable fluid linear program. The fluid LP scales gracefully with the problem data. Moreover, the fluid relaxation allows us to recover high quality solutions to the weakly coupled counting DP.

The method developed in Chapter 4 is applied to the problem of optimal prioritization of elective patients in NHS England during the COVID-19 pandemic that caused an unprecedented surge in the number of emergency patients seeking care over a prolonged period of time. To the best of our knowledge, this case study is the largest and most detailed application of weakly coupled dynamic programs to date. The case study provided compelling evidence that prioritizing COVID patients over patients from other disease groups led to worsened outcomes in terms of mortality as well as costs in treating patients who did not receive timely care. Our decision making tool can hopefully be utilized during future demand surges for hospital care to achieve better healthcare outcomes than was witnessed during COVID-19, through improved allocation of limited hospital resources to patients.

5.2 Future Work

Chapter 2 develops a method that solves the distributional robust chance-constrained CVRP wherein the customer demands belong to the class of moment ambiguity sets. We show that the developed method cannot be extended to other ambiguity sets. Chapter 3 alleviates this shortcoming by considering a more general ambiguity set for the distributional robust CVRP under a variety of risk measures and disutility functions. The consideration of a general ambiguity set allows us to encompass the KL-divergence ambiguity set, type-∞ Wasserstein ambiguity set, and the total variation ambiguity sets. Even more general cases of the ambiguity sets have been considered in the paper [GHW21] that was produced from this chapter. This leaves a gap for the study and comparison of alternative model-based ambiguity sets for the uncertainty-affected CVRP that offer realistic descriptions of the uncertain customer demands while avoiding the curse of dimensionality that plagues direct characterizations of high-dimensional probability distributions.

Secondly, even though Chapter 3 considers a very general formulation of the VRP, the developed framework can only be applied to the CVRP and some of its variants such as CVRP with compartments. This leaves avenue for future research to develop similar frameworks for other variants of the VRP that allow solution of a wide class of problems with minimal adaptations to a general solution method.

Finally, it remains of interest to further improve the computational scalability of our approach described in Chapter 2 and Chapter 3 using algorithms like branch-cut-and-price which have proven to be attractive in solving the deterministic CVRP.

Chapter 4 studies a large weakly-coupled dynamic program and develops a fluid relaxation that allows solution via a linear program that is tractable and scales economically in the size of the problem. However, the model requires the problem parameters to be known exactly. As has been motivated in the thesis, this is rarely the case. This creates a gap for the study of the robust version of our model which considers the problem parameters as uncertain. Moreover, the transition probabilities of the dynamic program are considered to be Markovian and hence memoryless. In the future, non-Markovian transitions could be modeled by adding memory to the states of the dynamic programs.

The model developed in Chapter 4 is applied to the problem of elective patients scheduling in NHS England during COVID-19. However, the model makes many simplifying assumptions, such as allocation of hospital beds between COVID and non-COVID patients without separation, and homogeneity of patients within a disease group. This leaves space for further improvement of the model specific to this healthcare application. Moreover, the model developed in this chapter can also be extended to solve large-scale problems in other application areas such as B2C marketing, assortment optimization and inventory control problems.

Bibliography

[ABB+98] P. Augerat, J. M. Belenguer, E. Benavent, A. Corberán, and D. Naddef. Separating capacity constraints in the CVRP using tabu search. *European Journal of Operational Research*, 106(2–3):546–557, 1998.

[AFS20] M. Argenziano, K. Fischkoff, and C. R. Smith. Surgery scheduling in a crisis. *New England Journal of Medicine*, 382(23):e87, 2020.

[AJ16] Y. Adulyasak and P. Jaillet. Models and algorithms for stochastic and robust vehicle routing with deadlines. *Transportation Science*, 50(2):608–626, 2016.

[AM08] D. Adelman and A. J. Mersereau. Relaxations of weakly coupled stochastic dynamic programs. *Operations Research*, 56(3):712–727, 2008.

[AMH15] R.R. Aliev, D.A.T. Mraiziq, and O.H. Huseynov. Expected utility based decision making under z-information and its application. *Computational Intelligence and Neuroscience*, 2015.

[AMRU01] F. Andersson, H. Mausser, D. Rosen, and S. Uryasev. Credit risk optimization with conditional value-at-risk criterion. *Mathematical Optimization Series B*, 89:273–291, 2001.

[BB12] C. Bandi and D. Bertsimas. Tractable stochastic analysis in high dimensions via robust optimization. *Mathematical Programming*, 134(1):23–70, 2012.

[BB15] F. Bellini and V. Bignozzi. On elicitable risk measures. *Quantitative Finance*, 15(5):725–733, 2015.

[BB17] F. Bellini and E. Di Bernardino. Risk management with expectiles. *The European Journal of Finance*, 23(6):487–506, 2017.

[BBC11a] D. Bertsimas, D. B. Brown, and C. Caramanis. Theory and applications of robust optimization. *SIAM Review*, 53(3):464–501, 2011.

[BBC11b] D. Bertsimas, D.B. Brown, and C. Caramanis. Theory and applications of robust optimization. *SIAM Review*, 53(3):464–501, 2011.

[BBIB19] M.E. Bruni, L. Brosco, G. Ielpa, and P. Beraldi. The risk-averse profitable touring problem. In *ICORES2019 - Proceedings of the 8th International Conference on Operations Research and Enterprise Systems*, pages 459–466, 2019.

[BDG95] C. Boutilier, R. Dearden, and M. Goldszmidt. Exploiting structure in policy construction. In *Proceedings of the International Joint Conference on Artificial Intelligence*, volume 14, pages 1104–1113, 1995.

[Bel52] R. Bellman. On the theory of dynamic programming. *Proceedings of the National Academy of Sciences of the United States of America*, 38(8):716–719, 1952.

[Ber95] Dimitri P Bertsekas. *Dynamic programming and optimal control*, volume 1. Athena Scientific, 1995.

[BGK18] D. Bertsimas, V. Gupta, and N. Kallus. Data-driven robust optimization. *Mathematical Programming*, 167(2):235–292, 2018.

[BK11] R. Bekker and P. M. Koeleman. Scheduling admissions and reducing variability in bed demand. *Health Care Management Science*, 14(3):237–249, 2011.

[BKMG14] F. Bellini, B. Klaar, A. Muller, and E.R. Giannin. Generalized quantiles as risk measures. *Insurance: Mathematics and Economics*, 54:41–48, 2014.

[BL11] J.R. Birge and F. Louveaux. *Introduction to stochastic programming.* Springer, 2011.

[BL15] G. Bayraksan and D.K. Love. Phi-divergence constrained ambiguous stochastic programs for data-driven optimization. *INFORMS Tutorials in Operations Research*, 2015.

[BLM+20] D. Bertsimas, G. Lukin, L. Mingardi, et al. COVID-19 mortality risk assessment: An international multi-center study. *PLOS ONE*, 15(12):1–13, 2020.

[BM16] D. Bertsimas and V. V. Mišić. Decomposable Markov decision processes: A fluid optimization approach. *Operations Research*, 64(6):1537–1555, 2016.

[BPS+20] D. Bertsimas, J. Pauphilet, J. Stevens, et al. Predicting inpatient flow at a major hospital using interpretable analytics. *medRxiv*, 2020.05.12.20098848v2, 2020.

[Bro06] D.B. Brown. *Risk and Robust Optimization.* PhD thesis, Massachuetts Institute of Technology, 2006.

[BS01] S. Basak and A. Shapiro. Value-at-risk-based risk management: Optimal policies and asset prices. *The Review of Financial Studies*, 14(2):371–405, 2001.

[BS04] D. Bertsimas and M. Sim. The price of robustness. *Operations Research*, 52(1):35–53, 2004.

[BSL96] D. Bertsimas and D. Simchi-Levi. A new generation of vehicle routing research: Robust algorithms, addressing uncertainty. *Operations Research*, 44(2):286–304, 1996.

[BSS20] D. Bertsimas, S. Shtern, and B. Sturt. A data-driven approach to multistage stochastic linear optimization. Available on Optimization Online, 2020.

[BT96] D. P. Bertsekas and J. N. Tsitsiklis. *Neuro-Dynamic Programming*. Athena Scientific, 1996.

[BT09] A. Beck and M. Teboulle. A fast iterative shrinkage-thresholding algorithm for linear inverse problems. *SIAM Journal on Imaging Sciences*, 2(1):183–202, 2009.

[BT12] A. Beck and M. Teboulle. Smoothing and first order methods: A unified framework. *SIAM Journal on Optimization*, 22(2):557–580, 2012.

[BTdHdW$^+$13] A. Ben-Tal, D. den Hertog, A. de Waegenaere, B. Melenberg, and G. Rennen. Robust solutions of optimization problems affected by uncertain probabilities. *Operations Research*, 59(2):341–357, 2013.

[BTEN09] Aharon Ben-Tal, Laurent El Ghaoui, and Arkadi Nemirovski. *Robust Optimization*. Princeton University Press, 2009.

[BTN01] A. Ben-Tal and A. Nemirovski. *Lectures on modern convex optimization: analysis, algorithms, and engineering applications*. SIAM, 2001.

[Bur20] T. K. Burki. Cancer guidelines during the COVID-19 pandemic. *The Lancet Oncology*, 21(5):629–630, 2020.

[BV04] S. Boyd and L. Vandenberghe. *Convex Optimization*. Cambridge University Press, 2004.

[CB02] G. Casella and R. L. Berger. *Statistical Inference*. Duxbury Thomson Learning, 2nd edition, 2002.

[CBM18] J. G. Carlsson, M. Behroozi, and K. Mihic. Wasserstein distance and the distributionally robust TSP. *Operations Research*, 66(6):1603–1624, 2018.

[CC59] A. Charnes and W.W. Cooper. Chance-constrained programming. *Management Science*, 6(1):73–79, 1959.

[CD13] J. G. Carlsson and E. Delage. Robust partitioning for stochastic multivehicle routing. *Operations Research*, 61(3):546–557, 2013.

[CDL+21] P. Christen, J. D'Aeth, A. Lochen, et al. The J-IDEA pandemic planner: A framework for implementing hospital provision interventions during the COVID-19 pandemic. *Medical Care, Published Ahead-of-Print*, 2021.

[CFBE12] Carri W Chan, Vivek F Farias, Nicholas Bambos, and Gabriel J Escobar. Optimizing intensive care unit discharge decisions with patient readmissions. *Operations Research*, 60(6):1323–1341, 2012.

[CH93] G. Cornuejols and F. Harche. Polyhedral study of the capacitated vehicle routing problem. *Mathematical Programming*, 60:21–52, 1993.

[Che07] M. R. Chernick. *Bootstrap Methods: A Guide for Practitioners and Researchers.* Wiley-Blackwell, 2nd edition, 2007.

[CHS10] Z. Cao, R.D.F. Harris, and J. Shen. Hedging and value at risk: A semi-parametric approach. *The Journal of Futures Markets*, 30(8):780–794, 2010.

[CLSV06] J. F. Cordeau, G. Laporte, M. W. P. Savelsbergh, and D. Vigo. Vehicle routing. In C. Barnhart and G. Laporte, editors, *Handbooks in Operations Research and Management Science: Transportation*, volume 14, chapter 6, pages 367–428. North Holland, 2006.

[CMP14] T.C.Y. Chan, H. Mahmoudzadeh, and T.G. Purdie. A robust-cvar optimization approach with application to breast cancer therapy. *European Journal of Operational Research*, 238:876–885, 2014.

[CSX19] Z. Chen, M. Sim, and H. Xu. Distributionally robust optimization with infinitely constrained ambiguity sets. *Operations Research*, 67(5):1328–1344, 2019.

[CZG16] C. Cappello, D. Zonta, and B. Glišić. Expected utility theory for monitoring-based decision-making. *Proceedings of the IEEE*, 104(8):1647–1661, 2016.

[D0́6] B. D. Díaz. The VRP web. `http://www.bernabe.dorronsoro.es/vrp/`, 2006. Online; accessed August 2018.

[DDG+02] J. Dhaene, M. Denuit, M. J. Goovaerts, R. Kaas, and D. Vyncke. The concept of comonotonicity in actuarial science and finance: Theory. *Insurance: Mathematics and Economics*, 31(1):3–33, 2002.

[DFL18] T. Dinh, R. Fukasawa, and J. Luedtke. Exact algorithms for the chance-constrained vehicle routing problem. *Mathematical Programming B*, 172(1–2):105–138, 2018.

[DFVR04] D. P. De Farias and B. Van Roy. On constraint sampling in the linear programming approach to approximate dynamic programming. *Mathematics of Operations Research*, 29(3):462–478, 2004.

[DGG+21a] J. C. D'Aeth, S. Ghosal, F. Grimm, et al. Optimal hospital care scheduling during the SARS-CoV-2 pandemic. 2021. Available on Optimization Online.

[DGG+21b] J. C. D'Aeth, S. Ghosal, F. Grimm, et al. Optimal national prioritization policies for hospital care during the SARS-CoV-2 pandemic. *Nature Computational Science*, 1:521–531, 2021.

[DGN+20] C. Davis, M. Gao, M. Nichols, et al. Predicting hospital utilization and inpatient mortality of patients tested for COVID-19. *medRxiv*, 2020.12.04.20244137, 2020.

[DIV20] DIVI. Entscheidungen über die Zuteilung von Ressourcen in der Notfall und der Intensivmedizin im Kontext der COVID-19-Pandemie. `https://www.divi.de/joomlatools-files/docman-files/publikationen/covid-19-dokumente/200325-covid-19-ethik-empfehlung-v1.pdf`, 2020. Accessed on 6 February 2021.

[DLL93] M. Dror, G. Laporte, and F. V. Louveaux. Vehicle routing with stochastic demands and restricted failures. *Methods and Models of Operations Research*, 37:273–283, 1993.

[DR59] G. B. Dantzig and J. H. Ramser. The truck dispatching problem. *Management Science*, 6(1):80–91, 1959.

[DRR+20] J. Déry, A. Ruiz, F. Routhier, et al. A systematic review of patient prioritization tools in non-emergency healthcare services. *Systematic Reviews*, 9(227):1–14, 2020.

[DS06] M. Dyer and L. Stougie. Computational complexity of stochastic programming problems. *Mathematical Programming*, 106(3):423–432, 2006.

[DT86] M. Dror and P. Trudeau. Stochastic vehicle routing with modified savings algorithm. *European Journal of Operational Research*, 23(2):228–235, 1986.

[DY10] E. Delage and Y. Ye. Distributionally robust optimization under moment uncertainty with application to data-driven problems. *Operations Research*, 58(3):595–612, 2010.

[Edw20] Edward Rothberg. Should your company be using mathematical optimization? ask yourself these four questions to find out. `https://www.forbes.com/sites/forbestechcouncil/2020/07/07/should-your-company-be-using-mathematical-optimization-ask-yourself-these-four-q` `?sh=5261031167ec`, 2020. Accessed on 16 January 2022.

[EK18] P.M. Esfahani and D. Kuhn. Data-driven distributionally robust optimization using the wasserstein metric: performance guarantees and tractable reformulations. *Mathematical Programming A*, 171:115–166, 2018.

[EOO03] L. El Ghaoui, M. Oks, and F. Oustry. Worst-case value-at-risk and robust portfolio optimization: A conic programming approach. *Operations Research*, 51(4):543–556, 2003.

[ESL+20] D. G. Eichberg, A. H. Shah, E. M. Luther, et al. Letter: Academic neurosurgery department response to COVID-19 pandemic: the University of Miami/Jackson Memorial Hospital model. *Neurosurgery*, 87(1):E63–E65, 2020.

[FBJ18] A. Flajolet, S. Blandin, and P. Jaillet. Robust adaptive routing under uncertainty. *Operations Research*, 66(1):210–229, 2018.

[FGS20] C. Fillippi, G. Guastaroba, and M.G. Speranza. Conditional value-at-risk beyond finance: a survey. *International Transactions in Operational Research*, 27(3):273–291, 2020.

[FIS+20] K. Fujita, T. Ito, Z. Saito, et al. Impact of COVID-19 pandemic on lung cancer treatment scheduling. *Thoracic Cancer*, 11(10):2983–2986, 2020.

[FK11] H. Föllmer and T. Knispel. Entropic risk measures: Coherence vs convexity, model ambiguity and robust large deviations. *Stochastics and Dynamics*, 11:1–19, 2011.

[FLL+06] R. Fukasawa, H. Longo, J. Lysgaard, M. Poggi de Aragão, M. Reis, E. Uchoa, and R. F. Werneck. Robust branch-and-cut-and-price for the capacitated vehicle routing problem. *Mathematical Programming*, 106(3):491–511, 2006.

[FMP18] M. Fischer, T. Moser, and M. Pfeuffer. A discussion on recent risk measures with application to credit risk: Calculating risk contributions and identifying risk concentrations. *Risks*, 6(142), 2018.

[FS10] H. Föllmer and A. Schied. Convex and coherent risk measures. In R. Cont, editor, *Encyclopedia of Quantitative Finance*. John Wiley and Sons, 2010.

[GCF+20] Y. Gao, G. Cai, W. Fang, et al. Machine learning based early warning system enables accurate mortality risk prediction for COVID-19. *Nature Communications*, 11(1):1–10, 2020.

[GFP20] T. Gardner, C. Fraser, and S. Peytrignet. Elective care in England: Assessing the impact of COVID-19 and where next. Technical report, The Health Foundation, 2020.

[GGW11] J. Gittins, K. Glazebrook, and R. Weber. *Multi-armed bandit allocation indices*. John Wiley & Sons, 2011.

[GHW21] S. Ghosal, C.P. Ho, and W.Wiesemann. A unifying framework for the capacitated vehicle routing problem under risk and ambiguity. Available on Optimization Online, 2021.

[GI03] D. Goldfarb and G. Iyengar. Robust portfolio selection problems. *Mathematics of Operations Research*, 28(1):1–38, 2003.

[GKP01] C. Guestrin, D. Koller, and R. Parr. Multiagent planning with factored MDPs. In *Advances in Neural Information Processing Systems*, volume 1, pages 1523–1530, 2001.

[GKP+03] C. Guestrin, D. Koller, R. Parr, et al. Efficient solution algorithms for factored MDPs. *Journal of Artificial Intelligence Research*, 19:399–468, 2003.

[GLS96] M. Gendreau, G. Laporte, and R. Séguin. Stochastic vehicle routing. *European Journal of Operational Research*, 88(1):3–12, 1996.

[GMM00] A. Gupta, C.D. Maranas, and C.M. McDonald. Mid-term supply chain planning under demand uncertainty: customer demand satisfaction and inventory management. *Computers and Chemical Engineering*, 24(12):2613–2621, 2000.

[Gon15] J. Gonzalez. *Modelling and Controlling Risk in Energy Systems*. PhD thesis, University of Manchester, Manchester, U.K., 2015.

[GRW08] B. L. Golden, S. Raghavan, and E. A. Wasil, editors. *The Vehicle Routing Problem: Latest Advances and New Challenges*. Springer, New York, NY, USA, 2008.

[GSS13] Linda V. Green, Sergei Savin, and Nicos Savva. "Nursevendor problem": Personnel staffing in the presence of endogenous absenteeism. *Management Science*, 59(10):2237–2256, 2013.

[GSW02] I. Gilboa, D. Schmeidler, and P.P. Wakker. Utility in case-based decision theory. *Journal of Economic Theory*, 102(2):483–502, 2002.

[GW20] S. Ghosal and W. Wiesemann. The distributionally robust chance constrained vehicle routing problem. *Operations Research*, 68(3):716–732, 2020.

[GWF13a] C. E. Gounaris, W. Wiesemann, and C. A. Floudas. The robust capacitated vehicle routing problem under demand uncertainty. *Operations Research*, 61(3):677–693, 2013.

[GWF13b] C.E. Gounaris, W. Wiesemann, and C.A. Floudas. The robust capacitated vehicle routing problem under demand uncertainty. *Operations Research*, 61(3):677–693, 2013.

[GY79] B.L. Golden and J.R. Yee. A framework for probabilistic vehicle routing. *AIIE Transactions*, 11(2):109–112, 1979.

[HADJ21] M. Hoogeboom, Y. Adulyasak, W. Dullaert, and P. Jaillet. The robust vehicle routing problem with time window assignments. *Transportation Science*, 55(2):395–413, 2021.

[HAVO11] J. E. Helm, S. AhmadBeygi, and M. P. Van Oyen. Design and analysis of hospital admission control for operational effectiveness. *Production and Operations Management*, 20(3):359–374, 2011.

[Haw03] J. T. Hawkins. *A Langrangian Decomposition Dpproach to Weakly Coupled Dynamic Optimization Problems and its Applications*. PhD thesis, Massachusetts Institute of Technology, 2003.

[HCF+20] D. Haw, P. Christen, G. Forchini, et al. DAEDALUS: An economic-epidemiological model to optimize economic activity while containing the SARS-CoV-2 pandemic. Technical report, Imperial College London, 2020.

[HH13] Z. Hu and L. J. Hong. Kullback-Leibler divergence constrained distributionally robust optimization. Available on Optimization Online, 2013.

[HKW16] G. A. Hanasusanto, D. Kuhn, and W. Wiesemann. A comment on “Computational complexity of stochastic programming problems”. *Mathematical Programming*, 159(1):557–569, 2016.

[HLQS15] N.G. Hall, D.Z. Long, J. Qi, and M. Sim. Managing underperformance risk in project portfolio selection. *Operations Research*, 63(3):660–675, 2015.

[HRKW15] G. A. Hanasusanto, V. Roitch, D. Kuhn, and W. Wiesemann. A distributionally robust perspective on uncertainty quantification and chance constrained programming. *Mathematical Programming*, 151(1):35–62, 2015.

[HRKW17] G. Hanasusanto, V. Roitch, D. Kuhn, and W. Wiesemann. Ambiguous joint chance constraints under mean and dispersion information. *Operations Research*, 65(3):751–767, 2017.

[HSS16] R. Hemmati, H. Saboori, and S. Saboori. Stochastic risk-averse coordinated scheduling of grid integrated energy storage units in transmission constrained wind-thermal systems within a conditional value-at-risk framework. *Energy*, 113:762–775, 2016.

[ITV14] S. Irnich, P. Toth, and D. Vigo. The family of vehicle routing problems. In P. Toth and D. Vigo, editors, *Vehicle Routing: Problems, Methods, and Applications*, pages 1–33. MOS-SIAM, 2nd edition, 2014.

[Iye05] G. N. Iyengar. Robust dynamic programming. *Mathematics of Operations Research*, 30(2):257–280, 2005.

[JBA20] S. Joebges and N. Biller-Andorno. Ethics guidelines on COVID-19 triage—an emerging international consensus. *Critical Care*, 24(1):201, 2020.

[JG18] R. Jiang and Y. Guan. Risk-averse two-stage stochastic program with distributional ambiguity. *Operations Research*, 66(5):1390–1405, 2018.

[JQS16] P. Jaillet, J. Qi, and M. Sim. Routing optimization under uncertainty. *Operations Research*, 64(1):186–200, 2016.

[KCO+15] S. Kim, C. W. Chan, M. Olivares, et al. ICU Admission control: An empirical study of capacity allocation and its implication for patient outcomes. *Management Science*, 61(1):19–38, 2015.

[KJ21] S. Küçükyavuz and R. Jiang. Chance-constrained optimization: A review of mixed-integer conic formulations and applications. Preprint arXiv:2101.08746, 2021.

[KP18] D.S. Kalogerias and W.B. Powell. Recursive optimization of convex risk measures: Mean-semideviation models. Preprint arXiv:1804.00636, 2018.

[KPU02] P. Krokhmal, J. Palmquist, and S. Uryasev. Portfolio optimization with conditional value-at-risk objective and constraints. *Journal of Risk*, 4:43–68, 2002.

[Kum03] M. Kumral. Application of chance-constrained programming based on multi-objective simulated annealing to solve a mineral blending problem. *Engineering Optimization*, 35(6):661–673, 2003.

[Lap09] G. Laporte. Fifty years of vehicle routing. *Transportation Science*, 43(4):408–416, 2009.

[LGG08] P. Li, H. Garcia, and W. Gunter. Chance constrained programming approach to process optimization under uncertainty. *Computer Aided Chemical Engineering*, 32(1):1245–1250, 2008.

[LLE04] J. Lysgaard, A. N. Letchford, and R. W. Eglese. A new branch-and-cut algorithm for the capacitated vehicle routing problem. *Mathematical Programming*, 100(2):423–445, 2004.

[LLM92] G. Laporte, F. Louveaux, and H. Mercure. The vehicle routing problem with stochastic travel times. *Transportation Science*, 26(3):161–170, 1992.

[LN83] G. Laporte and Y. Norbert. A branch and bound algorithm for the capacitated vehicle routing problem. *Operations Research Spektrum*, 5(2):77–85, 1983.

[LND85] G. Laporte, Y. Norbert, and M. Desrochers. Optimal routing under capacity and distance restrictions. *Operations Research*, 33(5):1050–1073, 1985.

[LQZ20] D.Z. Long, J. Qi, and A. Zhang. Supermodularity in two-stage distributionally robust optimization. Available on Optimization Online, 2020.

[LSM14] Q. Li, A. M. C. So, and W.-K. Ma. Distributionally robust chance-constrained transmit beamforming for multiuser MISO downlink. In *2014 IEEE International Conference on Acoustics, Speech and Signal Processing (ICASSP)*, pages 3479–3483, 2014.

[Man07] S. Manganelli. Risk management with expectiles. *Working Paper Series 723, European Central Bank*, 2007.

[MCP03] A. D. MacCormick, W. G. Collecutt, and B. R. Parry. Prioritizing patients for elective surgery: A systematic review. *ANZ Journal of Surgery*, 73(8):633–642, 2003.

[MF20] D. Moris and E. Felekouras. Surgery scheduling in a crisis: Effect on cancer patients. *Journal of BUON*, 25(4):2123–2124, 2020.

[MQZ+15] F. Meng, J. Qi, M. Zhang, J. Ang, S. Chu, and M. Sim. A robust optimization model for managing elective admission in a public hospital. *Operations Research*, 63(6):1452–1467, 2015.

[MR11] N. Miller and A. Ruszczynski. Risk-averse two-stage stochastic linear programming: Modeling and decomposition. *Operations Research*, 59(1):125–132, 2011.

[MSC+20] R. McCabe, N. Schmit, P. Christen, et al. Adapting hospital capacity to meet changing demands during the COVID-19 pandemic. *BMC Medicine*, 18(329):1–12, 2020.

[NCH20] D. Negopdiev, COVIDSurg Collaborative, and E. Hoste. Elective surgery cancellations due to the COVID-19 pandemic: global predictive modelling to inform surgical recovery plans. *British Journal of Surgery*, 107(11):1440–1449, 2020.

[Nem12] A. Nemirovski. On safe tractable approximations of chance constraints. *European Journal of Operational Research*, 219(3):707–718, 2012.

[NG05] A. Nilim and L. El Ghaoui. Robust control of Markov decision processes with uncertain transition matrices. *Operations Research*, 53(5):780–798, 2005.

[NHS20a] NHS. Bed Availability and Occupancy. https://www.england.nhs.uk/statistics/statistical-work-areas/bed-availability-and-occupancy/, 2020. Accessed on 6 February 2021.

[NHS20b] NHS. COVID-19 Hospital Activity. https://www.england.nhs.uk/statistics/statistical-work-areas/covid-19-hospital-activity/, 2020. Accessed on 6 February 2021.

[NHS20c] NHS. Critical Care Bed Capacity and Urgent Operations Cancelled. https://www.england.nhs.uk/statistics/statistical-work-areas/critical-care-capacity/, 2020. Accessed on 6 February 2021.

[NHS20d] NHS. Important and Urgent: Next Steps on NHS Response to COVID-19. https://www.england.nhs.uk/coronavirus/wp-content/uploads/sites/52/2020/03/urgent-next-steps-on-nhs-response-to-covid-19-letter-simon-stevens.pdf, 2020. Accessed on 6 February 2021.

[NHS20e] NHS Digital. Hospital Episode Statistics (HES). https://digital.nhs.uk/data-and-information/data-tools-and-services/data-services/hospital-episode-statistics, 2020. Accessed on 6 February 2021.

[NHS20f] NHS England. NHS England National Cost Collection for the NHS. https://www.england.nhs.uk/national-cost-collection/, 2020. Accessed on 6 February 2021.

[NIC20] NICE. COVID-19 Rapid Guideline: Critical care in adults. `https://www.nice.org.uk/guidance/ng159`, 2020. Accessed on 6 February 2021.

[Noy18] N. Noyan. Risk-averse stochastic modeling and optimization. In *INFORMS Tutorials in Operations Research: Recent Advances in Optimization and Modeling of Contemporary Problems*, chapter 10, pages 221–254. INFORMS, 2018.

[NPS09] K. Natarajan, D.A. Pachamanova, and M. Sim. Constructing risk measures from uncertainty sets. *Operations Research*, 57(5):1129–1141, 2009.

[OAW17] J. Oyola, H. Arntzen, and D.L. Woodruff. The stochastic vehicle routing problem, a literature review, part ii: solution methods. *EURO Journal on Transportation and Logistics*, 6(4):349–388, 2017.

[OAW18] J. Oyola, H. Arntzen, and D.L. Woodruff. The stochastic vehicle routing problem, a literature review, part i: methods. *EURO Journal on Transportation and Logistics*, 7(3):193–221, 2018.

[OAZ20] H. Ouyang, N.T. Argon, and S. Ziya. Allocation of intensive care unit beds in periods of high demand. *Operations Research*, 68(2):591–608, 2020.

[OC15] B. O'Donoghue and E. Candès. Adaptive restart for accelerated gradient schemes. *Foundations of Computational Mathematics*, 15(3):715–732, 2015.

[Off19] Office for National Statistics. Past and projected period and cohort life tables, 2018-based, UK. `https://www.ons.gov.uk/peoplepopulationandcommunity/birthsdeathsandmarriages/lifeexpectancies/bulletins/pastandprojecteddatafromtheperiodandcohortlifetables/1981to2068`, 2019. Accessed on 6 February 2021.

[PBTdM18] K. Postek, A. Ben-Tal, D. den Hertog, and B. Melenberg. Robust optimization with ambiguous stochastic constraints under mean and dispersion information. *Operations Research*, 66(3):814–833, 2018.

[PdHM16] K. Postek, D. den Hertog, and B. Melenberg. Computationally tractable counterparts of distributionally robust constraints on risk measures. *SIAM Review*, 58(4):603–650, 2016.

[PDM+20] P. N. Perez-Guzman, A. Daunt, S. Mukherjee, et al. Clinical characteristics and predictors of outcomes of hospitalized patients with COVID-19 in a multi-ethnic London

NHS Trust: A retrospective cohort study. *Clinical Infectious Diseases: An Official Publication of the Infectious Diseases Society of America*, ciaa1091, 2020.

[Pfl00] G. C. Pflug. Some remarks on the value-at-risk and the conditional value-at-risk. In S. P. Uryasev, editor, *Probabilistic Constrained Optimization*, pages 272–281. Kluwer Academic Publishers, 2000.

[PGH01] T. Pham-Gia and T.L. Hung. The mean and median absolute deviations. *Mathematical and Computer Modelling*, 34(7-8):921–936, 2001.

[PM19] A. Parmentier and F. Meunier. Stochastic shortest paths and risk measures. Preprint arXiv:1908.05659, 2019.

[Pow07] W. B. Powell. *Approximate Dynamic Programming: Solving the Curses of Dimensionality*. John Wiley & Sons, 2007.

[Pow16] W.B. Powell. Perspectives of approximate dynamic programming. *Annals of Operations Research*, 241:319–356, 2016.

[PP14] M.Ç. Pinar and A.B. Paç. Mean semi-deviation from a target and robust portfolio choice under distribution and mean return ambiguity. *Journal of Computational and Applied Mathematics*, 259(B):394–405, 2014.

[PP15] A. A. Pessoa and M. Poss. Robust network design with uncertain outsourcing cost. *INFORMS Journal on Computing*, 27(3):507–524, 2015.

[PPPU17] D. Pecin, A. Pessoa, M. Poggi, and E. Uchoa. Improved branch-cut-and-price for capacitated vehicle routing. *Mathematical Programming Computation*, 9(1):61–100, 2017.

[Put14] M. L. Puterman. *Markov Decision Processes: Discrete Stochastic Dynamic Programming*. John Wiley & Sons, 2014.

[PWL+20] J. Phua, L. Weng, L. Ling, et al. Intensive care management of coronavirus disease 2019 (COVID-19): challenges and recommendations. *The Lancet Respiratory Medicine*, 8(5):506–517, 2020.

[RBG+20] L. Riccioni, G. Bertolini, A. Giannini, et al. Raccomandazioni di etica clinica per l'ammissione a trattamenti intensivi e per la loro sospensione, in condizioni eccezionali di squilibrio tra necessità e risorse disponibili. *Recenti Progressi in Medicina*, 111(4):207–211, 2020.

[RCP20] RCP London. Safe medical staffing. https://www.rcplondon.ac.uk/projects/outputs/safe-medical-staffing, 2020. Accessed on 6 February 2021.

[RMA+19] D. Rizmie, M. Miraldo, R. Atun, et al. The effect of extreme temperature on emergency admissions across vulnerable populations in England: An observational study. *The Lancet*, 394(Special Issue 2):S7, 2019.

[Roc70] R. T. Rockafellar. *Convex Analysis*. Princeton University Press, 1970.

[Roy20] Royal College of Nursing. Staffing levels — Advice guides — Royal College of Nursing. https://www.rcn.org.uk/get-help/rcn-advice/staffing-levels, 2020. Accessed on 6 February 2021.

[RS09] A. Ruszczynski and A. Shapiro. Risk averse optimization. In A. Shapiro, D. Dentcheva, and A. Ruszczynski, editors, *Lectures on Stochastic Programming: Modeling and Theory*, chapter 6, pages 253–332. SIAM, 2009.

[RU02] R. T. Rockafeller and S. Uryasev. Conditional value-at-risk for general loss distributions. *Journal of Banking and Finance*, 26(7):1443–1471, 2002.

[Rus13] A. Ruszczynski. Advances in risk-averse optimization. *INFORMS Tutorials in Operations Research*, pages 168–190, 2013.

[RW97] R. T. Rockafellar and R. J.-B. Wets. *Variational Analysis*. Springer, 1997.

[SDR14] A. Shapiro, D. Dentcheva, and A. Ruszczyński. *Lectures on Stochastic Programming: Modeling and Theory*. MOS-SIAM, 2nd edition, 2014.

[Seg14] J. Segers. On the asymptotic distribution of the mean absolute deviation about the mean. Available on arXiv, 2014.

[SG83] W. R. Stewart and B. L. Golden. Stochastic vehicle routing: A comprehensive approach. *European Journal of Operational Research*, 14(4):371–385, 1983.

[Sha01] A. Shapiro. On duality theory of conic linear problems. In M. A. Goberna and M. A. López, editors, *Semi-Infinite Programming*, pages 135–165. Kluwer Academic Publishers, 2001.

[SHDH+19] P. Shi, J. Helm, J. Deglise-Hawkinson, et al. Timing it right: Balancing inpatient congestion versus readmission risk at discharge. *Available at SSRN 3202975*, 2019.

[SHG+20] A. Soltany, M. Hamouda, A. Ghzawi, et al. A scoping review of the impact of COVID-19 pandemic on surgical practice. *Annals of Medicine and Surgery*, 57:24–36, 2020.

[SJB+20] A. Sud, M. E. Jones, J. Broggio, et al. Collateral damage: the impact on outcomes from cancer surgery of the COVID-19 pandemic. *Annals of Oncology*, 31(8):1065–1074, 2020.

[SK02] A. Shapiro and A. J. Kleywegt. Minmax analysis of stochastic problems. *Optimization Methods and Software*, 17(3):523–542, 2002.

[SLCB05] D. Simchi-Levi, X. Chen, and J. Bramel. *The Logic of Logistics.* Springer New York, 3rd edition, 2005.

[SO08] I. Sungur and F. Ordonez. A robust optimization approach for the capacitated vehicle routing problem with demand uncertainty. *IIE Transactions*, 40(5):509–523, 2008.

[STV14] F. Semet, P. Toth, and D. Vigo. Classical exact algorithms for the capacitated vehicle routing problem. In P. Toth and D. Vigo, editors, *Vehicle Routing: Problems, Methods, and Applications*, pages 37–57. MOS-SIAM, 2nd edition, 2014.

[TCGM17] A. Tamar, Y. Chow, M. Ghavamzadeh, and S. Mannor. Sequential decision making with coherent risk. *IEEE Transactions on Automatic Control*, 62(7):3323–3338, 2017.

[The20] The Nuffield Council on Bioethics. Statement: The need for national guidance on resource allocation decisions in the COVID-19 pandemic. `https://www.nuffieldbioethics.org/news/statement-the-need-for-national-guidance-on-resource-allocation-decisions-in-the-covid-19-pandemic`, 2020. Accessed on 6 February 2021.

[TS11] A. Toussaint and R. Sircar. A framework for dynamic hedging under convex risk measures. In R. Dalang, M. Dozzi, and F. Russo, editors, *Seminar on Stochastic Analysis, Random Fields and Applications VI. Progress in Probability*, volume 63, pages 429–451. Springer, 2011.

[TTK+20] CW. D. Tzeng, M. Teshome, M. HG Katz, et al. Cancer surgery scheduling during and after the COVID-19 first wave: the MD Anderson cancer center experience. *Annals of Surgery*, 272(2):e106–e111, 2020.

[TV14] P. Toth and D. Vigo, editors. *Vehicle Routing: Problems, Methods, and Applications.* MOS-SIAM, 2nd edition, 2014.

[vAHMZ11] W. van Ackooij, R. Henrion, A. Möller, and R. Zorgati. Chance constrained programming and its applications to energy management. In I. Dritsas, editor, *Stochastic*

Optimization - Seeing the Optimal for the Uncertain, chapter 13, pages 291–320. IntechOpen Rijeka, 2011.

[VSR+20] A. Vaid, S. Somani, A. J. Russak, et al. Machine learning to predict mortality and critical events in COVID-19 positive New York City patients: A cohort study. *Journal of Medical Internet Research*, 22(11):1–19, 2020.

[WKR13] W. Wiesemann, D. Kuhn, and B. Rustem. Robust Markov decision processes. *Mathematics of Operations Research*, 38(1):153–183, 2013.

[WKS14] W. Wiesemann, D. Kuhn, and M. Sim. Distributionally robust convex optimization. *Operations Research*, 62(6):1358–1376, 2014.

[WWC+10] J. Wu, S. Wang, X. Chao, C.T. Ng, and T.C.E. Cheng. Impact of risk aversion on optimal decisions in supply contracts. *International Journal of Production Economics*, 128:569–576, 2010.

[WZ05] S.W. Wallace and W.T. Ziemba. *Applications of stochastic programming.* SIAM, 2005.

[XA18] W. Xie and S. Ahmed. On deterministic reformulations of distributionally robust joint chance constrained optimization problems. *SIAM Journal on Optimization*, 28(2):1151–1182, 2018.

[YKD+20] D. H. Yoon, S. Koller, P. M. N. Duldulao, et al. COVID-19 impact on colorectal daily practice—how long will it take to catch up? *Journal of Gastrointestinal Surgery*, 25:260–268, 2020.

[YMB00] W-H. Yang, K. Mathur, and R.H. Ballou. Stochastic vehicle routing problem with restocking. *Transportation Science*, 34(1):99–112, 2000.

[ZBST18] Y. Zhang, R. Baldacci, M. Sim, and J. Tang. Routing optimization with time windows under uncertainty. *Mathematical Programming A*, pages 1–43, 2018.

[ZCW08] Y.J. Zhou, X.H. Chen, and Z.R. Wang. Optimal ordering quantities for multi-products with stochastic demand: Return-cvar model. *International Journal of Production Economics*, 112:782–795, 2008.

[ZG18] C. Zhao and Y. Guan. Data-driven risk-averse stochastic optimization with Wasserstein metric. *Operations Research Letters*, 46(2):262–267, 2018.

[ZJ18] C. Zhao and R. Jiang. Distributionally robust contingency-constrained unit commitment. *IEEE Transactions on Power Systems*, 33(1):94–102, 2018.

[ZKR13] S. Zymler, D. Kuhn, and B. Rustem. Distributionally robust joint chance constraints with second-order moment information. *Mathematical Programming*, 137(1–2):167–198, 2013.

[ZLSH21] D. Zhang, D. Li, H. Sun, and L. Hou. A vehicle routing problem with distribution uncertainty in deadlines. *European Journal of Operational Research*, 292:311–326, 2021.

[ZZLS21] Y. Zhang, Z. Zhang, A. Lim, and M. Sim. Robust data-driven vehicle routing with time windows. *Operations Research*, 69(2):469–485, 2021.

Appendix A

Detailed Numerical Results for Chapter 2

Table C.1 summarizes the best determined solution as well as the runtime of our branch-and-cut scheme for the deterministic CVRP ('Deterministic') as well as the distributionally robust CVRP over a first order ambiguity set ('First Order'), a second order ambiguity set ('Second Order') as well as a second order ambiguity set with diagonal covariance bounds ('Diagonal'). Instances that have been solved to certified optimality (within the runtime limit of 12 hours) are marked with an asterisk: in this case, the 'Opt' column denotes the optimal objective value, and the 't (sec)' column provides the runtime. For all other instances, the 'Opt' column denotes the objective value of the best route set found, and the '[LB]' column presents the lower bound at termination.

We also provide detailed numerical results for each branch-and-cut scheme in turn. To this end, Tables A.2–A.5 provide the percentage gap at the root node (measured relative to the best route set found at termination), the time to process the root node, the number of RCI cuts introduced throughout the execution of our branch-and-cut scheme, the amount of time spent on identifying RCI cuts as well as the number of branch-and-bound nodes created.

	Deterministic		**First Order**		**Second Order**		**Diagonal**	
Problem	Opt	t (sec) [LB]	Opt	t (sec) [LB]	Opt	t (sec) [LB]	Opt	t (sec) [LB]
A-n32-k5	784.0*	0.17	753.0*	0.18	756.0*	0.24	753.0*	0.19
A-n33-k5	661.0*	0.4	639.0*	0.31	652.0*	3.61	639.0*	0.62
A-n33-k6	742.0*	0.68	716.0*	0.91	731.0*	34.02	716.0*	1.28
A-n34-k5	778.0*	0.78	702.0*	0.27	724.0*	34.21	702.0*	0.26
A-n36-k5	799.0*	1.82	762.0*	5.39	770.0*	14.79	762.0*	10.57
A-n37-k5	669.0*	0.2	656.0*	0.62	663.0*	1.5	656.0*	0.28
A-n37-k6	949.0*	35.67	884.0*	6.98	902.0*	95.44	884.0*	12.33
A-n38-k5	730.0*	1.67	684.0*	2.83	704.0*	10.76	684.0*	1.22
A-n39-k5	822.0*	10.09	767.0*	13.11	792.0*	409.91	767.0*	8.49
A-n39-k6	831.0*	2.47	791.0*	3.02	800.0*	56.15	791.0*	2.17
A-n44-k6	937.0*	43.99	903.0*	241.45	917.0*	2088.51	903.0*	160.27
A-n45-k6	944.0*	25.07	873.0*	1.94	903.0*	70.57	873.0*	2.36
A-n45-k7	1146.0*	484.95	1077.0*	4510.15	1119.0	[1095.0]	1077.0*	2614.56
A-n46-k7	917.0*	2.67	887.0*	7.28	892.0*	11.99	887.0*	20.46
A-n48-k7	1073.0*	28.28	1027.0*	6439.49	1036.0*	11257.9	1027.0*	27366.7
A-n53-k7	1010.0*	27.12	968.0*	30.43	980.0*	192.44	968.0*	19.55
A-n54-k7	1167.0*	528.51	1087.0*	4709.69	1138.0	[1090.83]	1087.0*	12903.8
A-n55-k9	1073.0*	18.31	1023.0*	57.89	1047.0*	1396.58	1023.0*	88.19
A-n60-k9	1371.0	[1342.33]	1320.0	[1225.95]	1362.0	[1234.71]	1265.0	[1233.0]
A-n61-k9	1044.0	[1021.4]	958.0*	1829.01	998.0	[969.727]	958.0*	5888.66
A-n62-k8	1288.0*	8480.34	1237.0	[1160.15]	1245.0	[1185.42]	1228.0	[1162.67]
A-n63-k9	1682.0	[1588.17]	1605.0	[1444.61]	1588.0	[1465.27]	1551.0	[1442.24]
A-n63-k10	1326.0	[1293.44]	1231.0	[1212.3]	1254.0	[1219.17]	1233.0	[1203.94]
A-n64-k9	1457.0	[1360.81]	1380.0	[1267.45]	no-feas	—	1421.0	[1271.71]
A-n65-k9	1174.0*	1080.06	1098.0*	994.57	1193.0	[1100.48]	1098.0*	2119.66
A-n69-k9	1159.0	[1143.28]	1094.0	[1091.54]	1143.0	[1085.97]	1094.0*	16385.9
A-n80-k10	no-feas	—	1744.0	[1588.17]	1778.0	[1596.94]	1863.0	[1582.24]
B-n31-k5	672.0*	0.25	651.0*	0.63	652.0*	1.35	651.0*	0.26
B-n34-k5	788.0*	1.32	764.0	[757.8]	769.0*	29.69	768.0	[755.5]
B-n35-k5	955.0*	0.28	867.0*	0.05	888.0*	5.74	867.0*	0.07
B-n38-k6	805.0*	0.3	732.0*	0.29	732.0*	0.62	732.0*	0.25
B-n39-k5	549.0*	0.27	521.0*	0.19	532.0*	0.38	521.0*	0.15
B-n41-k6	829.0*	1.02	791.0*	1.6	797.0*	8.05	791.0*	0.68
B-n43-k6	742.0*	14.58	680.0*	4.69	683.0*	4.49	680.0*	2.88
B-n44-k7	909.0*	1.74	841.0*	1.78	847.0*	21.92	841.0*	2.02
B-n45-k5	751.0*	3.78	677.0*	2.36	702.0*	3.33	677.0*	2.47
B-n45-k6	678.0*	13.82	626.0*	2.36	660.0*	59.67	626.0*	4.19

Table A.1: Optimally solved instances are highlighted with an asterisk, and the adjacent entries report the solution times t. For all other instances, we present the best solution found within 12 hours and the lower bound at termination.

Problem	Deterministic Opt	Deterministic t (sec) [LB]	First Order Opt	First Order t (sec) [LB]	Second Order Opt	Second Order t (sec) [LB]	Diagonal Opt	Diagonal t (sec) [LB]
B-n50-k7	741.0⋆	0.52	679.0⋆	0.1	724.0⋆	2.99	679.0⋆	0.13
B-n50-k8	1312.0⋆	1487.59	1233.0	[1209.0]	1231.0⋆	12567.6	1230.0	[1214.84]
B-n51-k7	1032.0⋆	6.63	929.0⋆	3.63	964.0⋆	17285.8	929.0⋆	1.66
B-n52-k7	747.0⋆	0.44	676.0⋆	0.96	679.0⋆	2.33	676.0⋆	0.45
B-n56-k7	707.0⋆	0.73	623.0⋆	7.43	624.0⋆	60.66	623.0⋆	2.02
B-n57-k9	1598.0⋆	94.52	1541.0⋆	15505.3	1580.0	[1547.24]	1541.0⋆	1788.11
B-n63-k10	1496.0⋆	3488.23	1434.0	[1368.87]	1587.0	[1379.17]	1419.0	[1362.11]
B-n64-k9	861.0⋆	141.12	803.0⋆	6.67	803.0⋆	3.21	803.0⋆	2.87
B-n66-k9	1316.0⋆	6490.27	1212.0⋆	14206.8	1361.0	[1208.0]	1212.0⋆	4563.34
B-n67-k10	1032.0⋆	65.55	980.0⋆	340.58	1014.0⋆	2416.87	980.0⋆	690.97
B-n68-k9	1275.0	[1266.71]	1315.0	[1154.56]	1354.0	[1176.14]	1207.0	[1153.67]
B-n78-k10	1221.0⋆	3359.2	1132.0	[1105.92]	1148.0	[1129.2]	1123.0	[1104.28]
E-n101-k8	820.0	[806.437]	793.0	[784.607]	806.0	[785.587]	799.0	[783.205]
E-n101-k14	1206.0	[1024.4]	1034.0	[991.635]	no-feas	—	1240.0	[989.23]
E-n22-k4	375.0⋆	0.03	373.0⋆	0.02	373.0⋆	0.02	373.0⋆	0.02
E-n23-k3	569.0⋆	0.01	564.0⋆	0.0	569.0⋆	0.04	564.0⋆	0.0
E-n30-k3	534.0⋆	2.25	492.0⋆	0.05	495.0⋆	0.11	492.0⋆	0.04
E-n33-k4	835.0⋆	0.41	814.0⋆	0.45	814.0⋆	2.17	814.0⋆	0.53
E-n51-k5	521.0⋆	0.88	516.0⋆	36.0	516.0⋆	15.45	516.0⋆	34.72
E-n76-k7	682.0⋆	13066.8	661.0⋆	1909.01	667.0	[665.143]	661.0⋆	6614.39
E-n76-k8	737.0	[725.244]	706.0	[700.631]	716.0	[700.12]	706.0	[699.462]
E-n76-k10	851.0	[801.247]	792.0	[765.87]	799.0	[767.762]	790.0	[765.091]
E-n76-k14	no-feas	—	973.0	[912.894]	1004.0	[915.242]	968.0	[911.564]
F-n135-k7	1162.0⋆	106.59	1086.0⋆	13961.3	1209.0	[1094.58]	1086.0⋆	26643.3
F-n45-k4	724.0⋆	0.18	715.0⋆	0.59	720.0⋆	0.76	715.0⋆	0.5
F-n72-k4	237.0⋆	11.59	232.0⋆	0.43	232.0⋆	1.53	232.0⋆	0.33
M-n101-k10	820.0⋆	5.58	804.0⋆	52.45	809.0⋆	102.53	804.0⋆	36.29
M-n121-k7	1041.0	[1017.04]	1065.0	[945.488]	no-feas	—	997.0	[949.634]
M-n151-k12	1120.0	[968.683]	no-feas	—	no-feas	—	1182.0	[935.127]
P-n19-k2	212.0⋆	0.03	195.0⋆	0.0	195.0⋆	0.0	195.0⋆	0.0
P-n20-k2	216.0⋆	0.05	208.0⋆	0.01	209.0⋆	0.02	208.0⋆	0.01
P-n21-k2	211.0⋆	0.03	208.0⋆	0.01	211.0⋆	0.02	208.0⋆	0.01
P-n22-k2	216.0⋆	0.03	213.0⋆	0.03	215.0⋆	0.03	213.0⋆	0.03
P-n22-k8	604.0⋆	0.3	559.0⋆	0.04	593.0⋆	0.55	559.0⋆	0.07
P-n23-k8	529.0⋆	5.62	504.0⋆	0.92	524.0⋆	43.7	504.0⋆	1.25
P-n40-k5	458.0⋆	0.39	449.0⋆	0.26	454.0⋆	4.02	449.0⋆	0.39
P-n45-k5	510.0⋆	2.17	500.0⋆	2.13	501.0⋆	16.21	500.0⋆	2.37
P-n50-k7	554.0⋆	32.13	543.0⋆	24.85	545.0⋆	114.94	543.0⋆	31.51
P-n50-k8	644.0	[620.417]	588.0⋆	130.92	592.0⋆	390.6	588.0⋆	77.8
P-n50-k10	696.0⋆	7635.86	662.0⋆	208.73	670.0⋆	1013.43	662.0⋆	208.7
P-n51-k10	741.0⋆	7841.63	695.0⋆	134.74	714.0⋆	7168.28	695.0⋆	84.04

Table A.1: (Continued from previous page.)

Problem	Deterministic		First Order		Second Order		Diagonal	
	Opt	t (sec) [LB]	Opt	t (sec) [LB]	Opt	t (sec) [LB]	Opt	t (sec) [LB]
P-n55-k10	696.0	[694.0]	665.0⋆	237.22	680.0⋆	23861.2	665.0⋆	171.93
P-n55-k7	568.0⋆	339.01	551.0⋆	50.72	554.0⋆	152.11	551.0⋆	55.96
P-n55-k8	594.0⋆	97.82	575.0⋆	21.8	584.0⋆	386.29	575.0⋆	5.53
P-n55-k15	no-feas	—	886.0⋆	4922.87	933.0	[885.795]	886.0⋆	3433.36
P-n60-k10	744.0⋆	30258.2	712.0⋆	2678.99	716.0⋆	9448.37	712.0⋆	5553.23
P-n60-k15	973.0	[948.558]	926.0⋆	17824.9	949.0	[920.5]	926.0⋆	17177.0
P-n65-k10	799.0	[782.652]	761.0⋆	23003.3	770.0	[761.0]	761.0⋆	25022.8
P-n70-k10	830.0	[803.776]	789.0	[768.618]	801.0	[768.222]	796.0	[768.104]
P-n76-k4	593.0⋆	16.13	588.0⋆	4.89	589.0⋆	103.87	588.0⋆	4.14
P-n76-k5	627.0⋆	570.43	614.0⋆	1457.71	615.0⋆	873.37	614.0⋆	595.71
P-n101-k4	681.0⋆	9.27	673.0⋆	3.34	673.0⋆	8.93	673.0⋆	3.98
att-n48-k4	40002.0⋆	3.25	38637.0⋆	1.73	38966.0⋆	6.58	38637.0⋆	1.21

Table A.1: (Continued from previous page.)

Problem	Root gap	Root time (sec)	# of Cuts	Cuts time (sec)	# of B&B nodes
A-n32-k5	8.80%	0.03	223	0.04	45
A-n33-k5	2.53%	0.15	274	0.12	59
A-n33-k6	1.61%	0.42	307	0.16	59
A-n34-k5	2.83%	0.35	358	0.21	74
A-n36-k5	2.07%	0.32	522	0.79	330
A-n37-k5	0.00%	0.18	103	0.02	0
A-n37-k6	4.97%	0.75	2,758	10.79	2,940
A-n38-k5	12.88%	0.05	697	0.62	255
A-n39-k5	17.86%	0.04	1,604	2.41	774
A-n39-k6	4.75%	0.29	665	1.04	351
A-n44-k6	4.12%	0.75	2,898	12.30	2,689
A-n45-k6	5.15%	0.65	2,017	6.91	1,602
A-n45-k7	4.78%	2.40	6,351	63.29	13,686
A-n46-k7	1.06%	0.60	854	0.93	136
A-n48-k7	3.77%	1.57	2,303	8.25	1,245
A-n53-k7	10.80%	0.12	1,822	8.50	1,485
A-n54-k7	5.01%	3.41	5,213	68.83	12,059
A-n55-k9	2.70%	1.49	1,121	8.24	1,774
A-n60-k9	13.68%	1.74	24,243	2,253.15	296,214
A-n61-k9	5.79%	3.24	50,713	647.81	106,151
A-n62-k8	13.52%	1.53	11,191	483.35	76,017
A-n63-k9	17.42%	4.65	37,127	1,391.02	199,160
A-n63-k10	22.40%	0.08	27,591	1,794.41	227,390
A-n64-k9	15.95%	2.74	45,515	972.17	131,772
A-n65-k9	6.08%	3.07	4,982	178.73	18,669
A-n69-k9	6.34%	4.14	23,146	1,712.53	170,185
A-n80-k10	1,611.78%	4.97	55,387	813.87	59,793
B-n31-k5	4.61%	0.10	276	0.04	43
B-n34-k5	6.21%	0.20	513	0.46	295
B-n35-k5	7.51%	0.13	318	0.03	67
B-n38-k6	0.24%	0.23	186	0.05	14
B-n39-k5	3.28%	0.10	202	0.08	32
B-n41-k6	4.34%	0.41	407	0.29	144
B-n43-k6	20.65%	0.09	2,081	4.38	1,167
B-n44-k7	9.35%	0.73	885	0.22	22
B-n45-k5	0.90%	0.63	912	1.27	473
B-n45-k6	3.05%	0.52	1,586	5.29	1,505

Table A.2: Detailed numerical results for our deterministic branch-and-cut scheme. Shown is the gap at the root node, the time required to process the root node, the number of RCI cuts introduced throughout the search, the time spent on identifying RCI cuts and the size of the overall branch-and-bound tree (in order of appearance).

Problem	Root gap	Root time (sec)	# of Cuts	Cuts time (sec)	# of B&B nodes
B-n50-k7	4.12%	0.09	423	0.14	73
B-n50-k8	11.90%	2.62	10,186	137.43	20,986
B-n51-k7	6.36%	0.33	1,068	2.41	798
B-n52-k7	4.21%	0.15	287	0.09	33
B-n56-k7	3.49%	0.08	387	0.23	43
B-n57-k9	9.89%	0.10	3,446	29.59	3,903
B-n63-k10	11.43%	5.37	23,103	161.14	16,698
B-n64-k9	6.11%	0.32	5,842	27.82	3,169
B-n66-k9	17.28%	5.51	22,026	268.89	30,531
B-n67-k10	5.97%	1.71	2,692	17.61	2,455
B-n68-k9	11.66%	2.82	25,156	1,488.26	255,735
B-n78-k10	16.79%	2.84	16,680	178.24	15,615
E-n101-k8	4.50%	3.60	30,712	1,108.90	109,437
E-n101-k14	20.17%	0.72	58,691	1,389.14	65,811
E-n22-k4	0.80%	0.03	41	0.00	3
E-n23-k3	0.00%	0.01	12	0.00	0
E-n30-k3	9.59%	0.04	663	0.72	1,319
E-n33-k4	1.22%	0.33	221	0.05	10
E-n51-k5	2.00%	0.38	373	0.25	23
E-n76-k7	4.01%	3.05	13,073	609.01	111,864
E-n76-k8	5.61%	5.77	23,396	1,304.07	169,627
E-n76-k10	9.97%	7.59	46,341	899.08	68,335
E-n76-k14	1,004.04%	2.61	73,328	1,157.97	58,012
F-n135-k7	7.20%	4.28	2,875	9.45	559
F-n45-k4	2.07%	0.05	173	0.04	27
F-n72-k4	1.69%	0.77	1,431	2.89	1,533
M-n101-k10	0.77%	4.90	609	0.51	13
M-n121-k7	9.19%	31.06	15,294	1,171.71	94,427
M-n151-k12	17.09%	20.39	38,922	1,129.98	43,820
P-n19-k2	0.00%	0.03	25	0.00	0
P-n20-k2	1.70%	0.03	64	0.01	33
P-n21-k2	0.24%	0.03	30	0.00	2
P-n22-k2	0.00%	0.03	30	0.00	0
P-n22-k8	4.33%	0.02	355	0.14	67
P-n23-k8	10.42%	0.03	1,747	2.48	471
P-n40-k5	1.52%	0.18	203	0.13	28
P-n45-k5	4.31%	0.04	789	0.93	257
P-n50-k7	3.17%	0.66	2,346	11.15	1,841
P-n50-k8	10.07%	0.71	45,881	771.23	140,653
P-n50-k10	6.24%	1.11	15,289	625.22	76,105
P-n51-k10	6.59%	0.92	20,397	376.89	44,558

Table A.2: (Continued from previous page.)

Problem	Root gap	Root time (sec)	# of Cuts	Cuts time (sec)	# of B&B nodes
P-n55-k10	5.74%	1.35	18,663	2,761.96	439,225
P-n55-k7	4.24%	0.53	4,957	67.23	13,381
P-n55-k8	3.99%	0.77	3,306	27.15	4,988
P-n55-k15	986.58%	3.89	85,026	779.67	60,092
P-n60-k10	6.26%	2.89	18,509	1,817.38	220,933
P-n60-k15	11.18%	0.16	29,304	2,736.74	217,385
P-n65-k10	6.44%	3.13	26,086	1,869.01	220,693
P-n70-k10	7.81%	4.15	38,508	1,277.46	100,265
P-n76-k4	1.32%	1.48	1,637	3.30	694
P-n76-k5	3.55%	1.94	5,427	54.18	11,008
P-n101-k4	0.77%	1.87	961	2.65	404
att-n48-k4	2.62%	0.51	547	1.19	951

Table A.2: (Continued from previous page.)

Problem	Root gap	Root time (sec)	# of Cuts	Cuts time (sec)	# of B&B nodes
A-n32-k5	0.64%	0.16	87	0.02	6
A-n33-k5	7.08%	0.04	224	0.12	81
A-n33-k6	2.65%	0.17	334	0.36	205
A-n34-k5	2.14%	0.12	185	0.06	44
A-n36-k5	8.19%	0.07	749	1.90	1,613
A-n37-k5	3.66%	0.13	259	0.21	125
A-n37-k6	9.07%	0.17	1,044	2.76	1,288
A-n38-k5	4.24%	0.22	636	1.03	493
A-n39-k5	6.26%	0.64	1,412	3.19	1,460
A-n39-k6	4.63%	0.19	537	1.30	747
A-n44-k6	5.83%	0.64	4,040	35.06	13,726
A-n45-k6	3.79%	0.48	334	0.71	219
A-n45-k7	14.90%	0.20	13,254	304.42	91,182
A-n46-k7	5.88%	0.13	1,026	3.08	940
A-n48-k7	8.81%	0.72	9,168	350.46	133,682
A-n53-k7	8.32%	0.25	1,284	11.10	2,504
A-n54-k7	7.28%	3.11	6,864	395.41	114,838
A-n55-k9	7.54%	0.44	2,129	24.05	4,667
A-n60-k9	19.03%	0.69	41,073	1,200.80	235,201
A-n61-k9	10.10%	0.67	8,835	207.29	29,502
A-n62-k8	18.19%	0.90	33,033	921.39	140,083
A-n63-k9	21.80%	0.66	45,214	1,189.42	230,934
A-n63-k10	13.15%	0.47	19,973	2,248.64	388,767
A-n64-k9	12.52%	10.18	41,546	944.52	133,645
A-n65-k9	8.01%	0.70	5,914	140.58	28,429
A-n69-k9	7.52%	1.13	14,681	2,457.60	407,054
A-n80-k10	19.59%	0.59	38,716	1,037.21	102,557
B-n31-k5	1.96%	0.11	421	0.18	154
B-n34-k5	3.80%	0.15	22,506	830.25	1,006,939
B-n35-k5	0.17%	0.05	36	0.00	5
B-n38-k6	4.17%	0.03	314	0.09	78
B-n39-k5	2.98%	0.06	203	0.03	68
B-n41-k6	1.69%	0.10	634	0.64	309
B-n43-k6	7.79%	0.09	1,007	1.74	595
B-n44-k7	18.61%	0.08	612	0.62	100
B-n45-k5	2.73%	0.27	526	0.97	365
B-n45-k6	2.39%	0.32	660	0.87	383

Table A.3: Detailed numerical results for our distributionally robust branch-and-cut scheme over first order ambiguity sets. The columns are the same as in Table A.2.

Problem	Root gap	Root time (sec)	# of Cuts	Cuts time (sec)	# of B&B nodes
B-n50-k7	1.18%	0.08	87	0.01	19
B-n50-k8	11.92%	0.81	31,056	1,375.71	393,742
B-n51-k7	1.27%	0.12	695	2.08	667
B-n52-k7	4.73%	0.16	400	0.32	122
B-n56-k7	3.37%	0.41	960	3.14	1,034
B-n57-k9	6.77%	0.33	19,596	1,422.81	242,756
B-n63-k10	17.19%	0.23	36,888	1,991.49	372,514
B-n64-k9	3.13%	0.34	734	3.80	437
B-n66-k9	14.29%	0.74	24,773	515.11	75,099
B-n67-k10	7.92%	0.18	3,435	102.70	14,767
B-n68-k9	22.59%	1.10	37,064	1,503.80	221,916
B-n78-k10	18.37%	1.00	22,453	2,512.12	332,470
E-n101-k8	3.70%	1.10	23,580	1,699.66	120,921
E-n101-k14	8.13%	0.92	34,050	2,525.48	112,334
E-n22-k4	0.00%	0.02	17	0.00	0
E-n23-k3	0.00%	0.00	6	0.00	0
E-n30-k3	0.24%	0.04	39	0.01	2
E-n33-k4	2.18%	0.14	372	0.08	102
E-n51-k5	3.69%	0.42	1,709	9.45	3,565
E-n76-k7	4.39%	0.67	7,776	187.81	28,781
E-n76-k8	5.69%	1.80	14,279	2,435.24	304,396
E-n76-k10	9.18%	0.44	29,876	1,787.28	221,637
E-n76-k14	10.95%	1.42	37,663	2,619.79	195,994
F-n135-k7	9.28%	4.90	11,290	743.93	79,677
F-n45-k4	3.87%	0.05	380	0.10	105
F-n72-k4	0.00%	0.41	69	0.02	0
M-n101-k10	4.73%	2.07	1,319	24.62	2,003
M-n121-k7	21.29%	2.17	25,715	889.68	100,398
M-n151-k12	1,007.57%	17.79	33,566	1,780.50	52,380
P-n19-k2	0.00%	0.00	2	0.00	0
P-n20-k2	0.00%	0.01	8	0.00	0
P-n21-k2	0.00%	0.01	10	0.00	0
P-n22-k2	0.35%	0.03	19	0.00	4
P-n22-k8	0.00%	0.04	34	0.00	0
P-n23-k8	5.65%	0.02	429	0.50	282
P-n40-k5	0.98%	0.15	117	0.07	18
P-n45-k5	3.20%	0.11	493	1.06	397
P-n50-k7	4.71%	0.33	1,427	10.26	3,145
P-n50-k8	4.96%	0.64	2,405	38.69	10,523
P-n50-k10	5.72%	0.44	3,556	64.73	12,038

Table A.3: (Continued from previous page.)

Problem	Root gap	Root time (sec)	# of Cuts	Cuts time (sec)	# of B&B nodes
P-n51-k10	5.07%	0.34	2,574	48.55	8,253
P-n55-k10	5.00%	0.63	3,233	75.73	13,805
P-n55-k7	3.31%	0.41	1,936	17.92	4,612
P-n55-k8	3.22%	0.28	1,372	10.28	1,821
P-n55-k15	5.76%	0.59	11,686	820.36	84,568
P-n60-k10	5.80%	1.25	5,997	478.57	77,248
P-n60-k15	5.89%	0.66	9,642	3,647.42	397,186
P-n65-k10	6.92%	0.36	11,478	2,064.94	290,779
P-n70-k10	8.20%	0.78	19,677	3,024.37	400,755
P-n76-k4	2.64%	0.41	669	2.07	422
P-n76-k5	3.89%	0.62	7,598	108.29	25,154
P-n101-k4	0.78%	0.62	312	1.10	123
att-n48-k4	1.54%	0.36	379	0.54	394

Table A.3: (Continued from previous page.)

Problem	Root gap	Root time (sec)	# of Cuts	Cuts time (sec)	# of B&B nodes
A-n32-k5	0.88%	0.17	100	0.07	3
A-n33-k5	9.27%	0.05	366	2.96	472
A-n33-k6	5.24%	0.22	968	26.66	4,342
A-n34-k5	4.76%	0.23	1,232	25.71	4,234
A-n36-k5	6.30%	0.21	659	11.97	1,472
A-n37-k5	4.90%	0.10	243	1.15	70
A-n37-k6	9.13%	0.25	1,963	67.19	7,016
A-n38-k5	4.81%	0.28	657	8.75	933
A-n39-k5	10.41%	0.31	3,884	167.48	22,474
A-n39-k6	5.32%	0.24	1,725	43.72	3,427
A-n44-k6	7.94%	0.47	6,821	907.55	58,357
A-n45-k6	9.52%	0.11	1,465	55.35	3,617
A-n45-k7	14.54%	0.29	30,388	7,769.22	454,813
A-n46-k7	4.61%	0.41	565	10.32	403
A-n48-k7	11.31%	0.50	9,292	3,841.96	148,705
A-n53-k7	7.41%	0.45	1,530	160.80	5,100
A-n54-k7	15.64%	0.50	32,890	8,621.02	273,935
A-n55-k9	7.56%	1.30	5,775	890.82	30,153
A-n60-k9	24.01%	0.14	31,016	11,954.02	228,278
A-n61-k9	12.84%	0.66	19,059	13,276.38	304,638
A-n62-k8	19.74%	1.05	30,499	6,682.17	196,778
A-n63-k9	21.39%	0.92	36,943	9,421.22	226,004
A-n63-k10	20.45%	0.07	30,239	10,365.47	216,149
A-n64-k9	1,236.57%	0.34	51,599	5,620.44	130,836
A-n65-k9	16.33%	0.91	32,861	11,697.69	316,333
A-n69-k9	11.88%	2.03	26,141	12,435.64	244,488
A-n80-k10	19.83%	1.71	42,743	10,253.69	134,555
B-n31-k5	1.76%	0.13	437	0.88	250
B-n34-k5	8.19%	0.13	1,200	23.28	3,333
B-n35-k5	1.34%	0.09	870	4.16	783
B-n38-k6	4.17%	0.02	317	0.41	80
B-n39-k5	3.99%	0.07	275	0.14	84
B-n41-k6	2.22%	0.19	662	6.36	1,024
B-n43-k6	8.20%	0.06	806	3.12	376
B-n44-k7	19.19%	0.07	1,149	17.78	1,121
B-n45-k5	7.95%	0.09	308	2.74	247
B-n45-k6	2.70%	0.13	1,273	47.87	4,590

Table A.4: Detailed numerical results for our distributionally robust branch-and-cut scheme over second order ambiguity sets. The columns are the same as in Table A.2.

Problem	Root gap	Root time (sec)	# of Cuts	Cuts time (sec)	# of B&B nodes
B-n50-k7	1.75%	0.09	593	2.16	241
B-n50-k8	13.48%	0.13	16,809	3,840.93	116,174
B-n51-k7	3.30%	0.32	14,994	4,899.57	404,450
B-n52-k7	2.36%	0.24	400	1.69	128
B-n56-k7	3.89%	0.42	1,629	51.74	1,720
B-n57-k9	7.31%	0.40	27,203	13,061.37	459,242
B-n63-k10	23.09%	0.60	43,961	10,941.47	272,627
B-n64-k9	3.55%	0.52	266	2.48	24
B-n66-k9	24.98%	0.63	56,503	6,127.27	158,376
B-n67-k10	10.89%	0.18	7,345	1,655.82	31,546
B-n68-k9	22.17%	0.69	37,478	14,580.46	293,702
B-n78-k10	17.13%	2.99	30,486	14,825.17	139,882
E-n101-k8	5.06%	1.54	29,045	14,248.27	121,826
E-n101-k14	1,054.00%	0.91	36,531	19,669.39	73,112
E-n22-k4	0.00%	0.02	18	0.00	0
E-n23-k3	0.00%	0.02	10	0.02	0
E-n30-k3	0.13%	0.08	47	0.03	3
E-n33-k4	2.58%	0.16	534	1.43	235
E-n51-k5	3.91%	0.29	814	12.59	942
E-n76-k7	5.10%	0.57	14,438	15,433.94	284,828
E-n76-k8	8.00%	0.34	16,598	19,485.62	271,932
E-n76-k10	9.48%	1.28	30,125	14,273.25	136,172
E-n76-k14	15.29%	0.44	47,456	15,796.83	118,497
F-n135-k7	16.10%	9.14	28,690	14,498.58	55,654
F-n45-k4	4.54%	0.05	204	0.51	69
F-n72-k4	0.86%	0.39	140	1.11	24
M-n101-k10	4.46%	1.57	958	94.88	478
M-n121-k7	950.33%	3.42	20,421	14,041.34	69,004
M-n151-k12	998.08%	3.98	19,697	26,267.34	40,896
P-n19-k2	0.00%	0.00	2	0.00	0
P-n20-k2	0.00%	0.02	10	0.00	0
P-n21-k2	0.95%	0.01	21	0.01	5
P-n22-k2	1.55%	0.02	31	0.01	9
P-n22-k8	2.56%	0.03	277	0.43	95
P-n23-k8	9.26%	0.02	1,956	33.25	5,106
P-n40-k5	1.55%	0.24	355	3.40	297
P-n45-k5	2.59%	0.04	660	14.21	1,292
P-n50-k7	5.31%	0.45	1,853	93.86	3,666
P-n50-k8	7.70%	0.19	2,732	306.98	9,854
P-n50-k10	7.91%	0.28	3,907	785.45	18,990

Table A.4: (Continued from previous page.)

Problem	Root gap	Root time (sec)	# of Cuts	Cuts time (sec)	# of B&B nodes
P-n51-k10	7.63%	0.36	6,623	4,141.96	132,791
P-n55-k10	7.76%	0.40	12,911	10,772.11	261,138
P-n55-k7	3.92%	0.44	1,937	124.32	4,649
P-n55-k8	5.06%	0.32	2,768	297.57	9,981
P-n55-k15	10.68%	0.40	36,951	18,004.99	232,056
P-n60-k10	7.61%	0.44	5,653	6,506.57	123,579
P-n60-k15	7.73%	1.07	16,838	28,090.32	214,042
P-n65-k10	7.86%	0.67	10,710	24,639.16	294,987
P-n70-k10	9.64%	1.35	20,694	18,413.52	245,107
P-n76-k4	2.80%	0.36	1,549	80.69	2,438
P-n76-k5	3.60%	0.68	4,342	567.82	12,544
P-n101-k4	0.79%	0.80	206	7.50	107
att-n48-k4	1.65%	0.45	476	4.72	560

Table A.4: (Continued from previous page.)

Problem	Root gap	Root time (sec)	# of Cuts	Cuts time (sec)	# of B&B nodes
A-n32-k5	0.59%	0.18	59	0.01	4
A-n33-k5	7.08%	0.05	298	0.29	220
A-n33-k6	3.14%	0.19	403	0.51	391
A-n34-k5	3.15%	0.18	130	0.04	13
A-n36-k5	8.14%	0.06	1,189	3.45	2,421
A-n37-k5	3.09%	0.14	94	0.08	38
A-n37-k6	8.19%	0.16	1,201	4.77	2,657
A-n38-k5	2.34%	0.35	388	0.39	204
A-n39-k5	6.52%	0.33	1,057	2.28	1,218
A-n39-k6	4.96%	0.14	478	0.99	736
A-n44-k6	5.98%	0.55	3,590	27.83	11,279
A-n45-k6	4.19%	0.33	588	0.89	259
A-n45-k7	12.33%	0.40	8,480	253.71	74,868
A-n46-k7	5.88%	0.16	1,968	6.61	1,723
A-n48-k7	11.19%	0.25	13,612	1,005.50	412,658
A-n53-k7	7.15%	0.45	1,070	8.35	2,040
A-n54-k7	11.98%	0.46	10,251	831.14	233,414
A-n55-k9	7.93%	0.35	2,052	40.24	7,419
A-n60-k9	15.69%	0.55	24,807	2,156.01	308,711
A-n61-k9	10.65%	0.34	11,494	651.52	100,321
A-n62-k8	17.26%	0.35	35,582	1,151.97	282,771
A-n63-k9	16.00%	4.32	45,954	1,204.07	196,922
A-n63-k10	12.26%	0.65	21,539	2,570.20	368,590
A-n64-k9	19.04%	0.42	47,264	1,287.94	218,242
A-n65-k9	8.25%	1.61	9,073	229.99	41,152
A-n69-k9	7.80%	0.78	12,260	1,445.01	189,889
A-n80-k10	22.56%	4.63	45,429	1,287.34	147,232
B-n31-k5	1.91%	0.10	227	0.05	68
B-n34-k5	8.79%	0.08	18,094	1,625.71	1,711,050
B-n35-k5	0.00%	0.07	37	0.00	2
B-n38-k6	4.17%	0.04	195	0.09	55
B-n39-k5	2.98%	0.07	139	0.02	31
B-n41-k6	0.54%	0.40	181	0.17	68
B-n43-k6	7.79%	0.08	576	1.10	504
B-n44-k7	18.61%	0.08	644	0.67	154
B-n45-k5	4.13%	0.23	468	1.14	495
B-n45-k6	2.65%	0.34	965	1.49	634

Table A.5: Detailed numerical results for our distributionally robust branch-and-cut scheme over second order ambiguity sets with diagonal covariance bounds. The columns have the same interpretation as in Table A.2.

Problem	Root gap	Root time (sec)	# of Cuts	Cuts time (sec)	# of B&B nodes
B-n50-k7	1.18%	0.08	102	0.02	24
B-n50-k8	11.13%	0.81	25,668	1,574.21	368,764
B-n51-k7	1.27%	0.12	430	0.91	263
B-n52-k7	4.73%	0.13	307	0.09	78
B-n56-k7	3.49%	0.46	465	0.73	260
B-n57-k9	6.55%	0.71	9,297	288.68	39,564
B-n63-k10	16.31%	0.24	32,541	3,134.08	518,803
B-n64-k9	2.88%	0.45	730	0.97	180
B-n66-k9	14.60%	0.63	12,257	330.91	60,197
B-n67-k10	7.92%	0.21	4,569	164.72	24,308
B-n68-k9	15.63%	0.67	39,837	2,391.10	407,652
B-n78-k10	17.12%	1.12	17,842	3,132.44	323,583
E-n101-k8	4.06%	2.07	22,403	2,245.80	168,540
E-n101-k14	23.35%	1.27	33,049	3,777.12	194,335
E-n22-k4	0.00%	0.02	18	0.00	0
E-n23-k3	0.00%	0.00	6	0.00	0
E-n30-k3	1.07%	0.04	44	0.00	2
E-n33-k4	2.21%	0.13	294	0.12	127
E-n51-k5	3.49%	0.46	1,749	9.24	4,370
E-n76-k7	4.53%	0.63	11,179	580.14	78,018
E-n76-k8	5.92%	1.37	11,679	3,486.02	243,887
E-n76-k10	8.92%	0.49	23,723	2,574.44	252,486
E-n76-k14	11.90%	0.58	31,041	3,238.67	199,176
F-n135-k7	9.53%	4.29	16,108	1,917.77	123,567
F-n45-k4	3.87%	0.04	313	0.12	134
F-n72-k4	0.81%	0.31	92	0.02	2
M-n101-k10	5.76%	0.73	1,257	18.00	1,501
M-n121-k7	15.67%	2.86	26,325	993.00	67,071
M-n151-k12	23.35%	20.86	30,041	3,050.43	88,252
P-n19-k2	0.00%	0.00	2	0.00	0
P-n20-k2	0.00%	0.01	8	0.00	0
P-n21-k2	0.00%	0.01	11	0.00	0
P-n22-k2	0.63%	0.03	26	0.00	7
P-n22-k8	0.00%	0.07	36	0.00	0
P-n23-k8	5.65%	0.02	657	0.63	458
P-n40-k5	1.11%	0.14	162	0.15	66
P-n45-k5	3.20%	0.11	471	1.18	582
P-n50-k7	4.10%	0.55	1,380	13.13	4,200
P-n50-k8	4.74%	0.56	2,438	27.12	5,894
P-n50-k10	6.06%	0.28	2,890	68.16	14,987

Table A.5: (Continued from previous page.)

Problem	Root gap	Root time (sec)	# of Cuts	Cuts time (sec)	# of B&B nodes
P-n51-k10	5.47%	0.21	2,745	33.21	6,673
P-n55-k10	5.40%	0.43	3,688	55.22	11,508
P-n55-k7	4.13%	0.24	1,732	21.91	5,742
P-n55-k8	3.31%	0.28	743	3.08	781
P-n55-k15	5.59%	0.37	8,309	955.02	95,393
P-n60-k10	6.48%	0.63	7,364	828.66	136,069
P-n60-k15	6.74%	0.33	9,798	4,132.93	462,037
P-n65-k10	5.80%	0.61	11,542	2,407.29	360,166
P-n70-k10	9.17%	0.44	22,465	3,135.99	345,192
P-n76-k4	2.64%	0.40	618	1.62	341
P-n76-k5	3.21%	0.65	4,857	74.25	23,370
P-n101-k4	0.82%	0.96	368	1.36	180
att-n48-k4	1.83%	0.33	320	0.33	234

Table A.5: (Continued from previous page.)

Appendix B

Worst-Case Distribution for Scenario-Wise First-Order Ambiguity Set with Fixed Scenario Probabilities

For the scenario-wise first-order ambiguity set $\mathcal{P}$ described in (3.6), the worst-case expected value of a supermodular function can be evaluated using Proposition B.1. We describe this proposition here to keep our paper self-contained. Following from the rectangularity of $\mathcal{P}$, for each $w \in \mathcal{W}$ we define

$$\mathcal{P}^w = \left\{ \mathbb{P}_w \in \mathcal{P}_0(\mathbb{R}^n) : \mathbb{P}_w[\underline{\boldsymbol{q}}^w \leqslant \widetilde{\boldsymbol{q}} \leqslant \overline{\boldsymbol{q}}^w] = 1,\, \mathbb{E}_{\mathbb{P}_w}[\widetilde{\boldsymbol{q}}] = \boldsymbol{\mu}^w,\, \mathbb{E}_{\mathbb{P}_w}[|\widetilde{\boldsymbol{q}} - \boldsymbol{\mu}^w|] \leqslant \boldsymbol{\nu}^w \right\}.$$

Proposition B.1 ([LQZ20]) *If $g(\boldsymbol{x}, \boldsymbol{z})$ is supermodular in $\boldsymbol{z}$ for any $\boldsymbol{x}$, we have $\sup_{\mathbb{P} \in \mathcal{P}^w} \mathbb{E}_{\mathbb{P}}[g(\boldsymbol{x}, \widetilde{\boldsymbol{z}})] = \sum_{i \in [2n+1]} p_i^w g(\boldsymbol{x}, \boldsymbol{z}_i^w)$ for any $\boldsymbol{x}$, where $\boldsymbol{p}^w, \boldsymbol{z}^w$ are output by Algorithm 2 when the input is $\mathcal{P}^w$.*

Algorithm 2: Algorithm for finding worst-case distribution

Input: $\boldsymbol{\mu}^w$, $\boldsymbol{\nu}^w$, $\underline{\boldsymbol{q}}^w, \overline{\boldsymbol{q}}^w$ for each $w \in \mathcal{W}$ for ambiguity set $\mathcal{P}^w$ described in (3.6).

for $w \in \mathcal{W}$ **do**

For each $i \in [n]$, initialize $\mathbb{P}^{w\star}(\widetilde{q}_i = \underline{q}_i^w) = \frac{\hat{\nu}_i^w}{2(\mu_i^w - \underline{q}_i^w)}$,
$\mathbb{P}^{w\star}(\widetilde{q}_i = \mu_i^w) = 1 - \frac{\hat{\nu}_i^w(\overline{q}_i^w - \underline{q}_i^w)}{2(\overline{q}_i^w - \mu_i^w)(\mu_i^w - \underline{q}_i^w)}$ and $\mathbb{P}^{w\star}(\widetilde{q}_i = \overline{q}_i^w) = \frac{\hat{\nu}_i^w}{2(\overline{q}_i^w - \mu_i^w)}$ where
$\hat{\nu}_i^w = \min\left\{\nu_i^w, \frac{2(\overline{q}_i^w - \mu_i^w)(\mu_i^w - \underline{q}_i^w)}{\overline{q}_i^w - \underline{q}_i^w}\right\}$

$\boldsymbol{z}_1^w = \underline{\boldsymbol{q}}^w$, $\boldsymbol{m}^1 = (\mathbb{P}^{w\star}(\widetilde{q}_1 = \underline{q}_1^w), \mathbb{P}^{w\star}(\widetilde{q}_2 = \underline{q}_2^w), \ldots, \mathbb{P}^{w\star}(\widetilde{q}_n = \underline{q}_n^w))$,
$p_1^w = \min\{m_1^1, \ldots, m_n^1\}$ and $j = 1$

while $j \leqslant 2n$ **do**

choose r_j as the minimal index in $[n]$ such that $m_{r_j}^j = p_{wj}^\star$

$\boldsymbol{z}_{j+1}^w = \boldsymbol{z}_j^w$, $\boldsymbol{m}^{j+1} = \boldsymbol{m}^j - p_{wj}^\star \mathbf{1}$

update $z_{r_j,j+1}^w = \mu_{r_j}^w$ if its existing value is $\underline{q}_{r_j}^w$ and $z_{r_j,j+1}^w = \overline{q}_{r_j}^w$ if its existing value is $\mu_{r_j}^w$

update $m_{r_j}^{j+1} = \mathbb{P}^{w\star}(\widetilde{q}_{r_j} = z_{r_j,j+1}^w)$

$p_{j+1} = \min\{m_1^{j+1}, \ldots, m_n^{j+1}\}$

update $j = j + 1$

end

return $\boldsymbol{z}_1^w, \boldsymbol{z}_2^w, \ldots, \boldsymbol{z}_{2n+1}^w$ and $p^w = (p_1^w, p_2^w, \ldots, p_{2n+1}^w)$

end

Appendix C

Detailed Numerical Results for Chapter 3

Table C.1 reports the best feasible solution ('Opt'; accompanied by an asterisk if it is confirmed to be optimal) and the best lower bound ('LB'; value in brackets unless solved to optimality) identified by, as well as the runtime ('t'; unless not solved to optimality, in which case the runtime is 12h) incurred by our branch-and-cut scheme for the deterministic CVRP ('Deterministic') and the distributionally robust CVRP with known scenario probabilities ('Stochastic').

	Deterministic		**Stochastic**	
Problem	Opt	t (sec) [LB]	Opt	t (sec) [LB]
A-n32-k5	745.0*	0.1	745.0*	0.32
A-n33-k5	617.0*	0.09	639.0*	5.14
A-n33-k6	703.0*	0.4	707.0*	31.94
A-n34-k5	701.0*	0.1	701.0*	1.26
A-n36-k5	732.0*	0.15	743.0*	13.35
A-n37-k5	651.0*	0.16	653.0*	3.6
A-n37-k6	861.0*	1.8	877.0*	232.77
A-n38-k5	648.0*	0.07	654.0*	1.08
A-n39-k5	735.0*	0.42	758.0*	47.12
A-n39-k6	774.0*	0.6	774.0*	11.65

Table C.1: Runtimes and optimality gaps for the benchmark instances of [D0́6]. Optimally solved instances are highlighted with an asterisk and accompanied by the runtime t. For all other instances, we report the upper and lower bound after 12 hours.

Problem	**Deterministic** Opt	t (sec) [LB]	**Stochastic** Opt	t (sec) [LB]
A-n44-k6	891.0⋆	29.07	892.0⋆	692.84
A-n45-k6	869.0⋆	1.93	872.0⋆	87.95
A-n45-k7	1034.0⋆	5.42	1051.0⋆	514.83
A-n46-k7	851.0⋆	0.52	871.0⋆	43.66
A-n48-k7	967.0⋆	0.91	967.0⋆	10.91
A-n53-k7	954.0⋆	2.22	959.0⋆	159.08
A-n54-k7	1051.0⋆	65.48	1068.0⋆	3821.02
A-n55-k9	985.0⋆	1.2	992.0⋆	21.01
A-n60-k9	1202.0⋆	24.35	1214.0⋆	4693.07
A-n61-k9	939.0⋆	5.48	942.0⋆	257.96
A-n62-k8	1132.0⋆	9.2	1153.0⋆	1283.46
A-n63-k9	1446.0⋆	1975.6	1476	[1444.05]
A-n63-k10	1176.0⋆	34.68	1178.0⋆	234.11
A-n64-k9	1290	[1277.83]	1333	[1267.2]
A-n65-k9	1082.0⋆	56.79	1085.0⋆	1150
A-n69-k9	1076.0⋆	190.54	1082.0⋆	10061.2
A-n80-k10	1612	[1587.4]	1641	[1587.1]
B-n31-k5	645.0⋆	0.08	651.0⋆	0.82
B-n34-k5	703.0⋆	0.18	737.0⋆	0.62
B-n35-k5	866.0⋆	0.04	866.0⋆	0.11
B-n38-k6	726.0⋆	0.09	730.0⋆	18.46
B-n39-k5	517.0⋆	0.14	521.0⋆	0.17
B-n41-k6	786.0⋆	0.08	786.0⋆	4.26
B-n43-k6	655.0⋆	0.87	662.0⋆	717.52
B-n44-k7	819.0⋆	4.5	835.0⋆	1598.4
B-n45-k5	630.0⋆	0.11	666.0⋆	3.61
B-n45-k6	616.0⋆	0.42	626.0⋆	6.2
B-n50-k7	657.0⋆	0.13	661.0⋆	0.83
B-n50-k8	1145.0⋆	2.62	1202	[1158.33]
B-n51-k7	913.0⋆	0.06	917.0⋆	0.32
B-n52-k7	673.0⋆	0.14	673.0⋆	0.53
B-n56-k7	621.0⋆	0.43	622.0⋆	14.44
B-n57-k9	1511.0⋆	9.16	1535.0⋆	5829.33
B-n63-k10	1347.0⋆	137.91	1361.0⋆	8751.78
B-n64-k9	790.0⋆	1.06	796.0⋆	10.3
B-n66-k9	1170.0⋆	573.06	1202.0⋆	32405.8
B-n67-k10	946.0⋆	3.01	974.0⋆	1499.96
B-n68-k9	1114.0⋆	20.66	1117.0⋆	394.49
B-n78-k10	1079.0⋆	28.7	1101	[1089.5]
E-n101-k8	780.0⋆	159.12	787	[783.05]
E-n101-k14	1012	[991.132]	1048	[984.161]
E-n22-k4	370.0⋆	0.01	370.0⋆	0.25
E-n23-k3	564.0⋆	0	564.0⋆	0
E-n30-k3	475.0⋆	0.02	475.0⋆	0.02
E-n33-k4	791.0⋆	0.15	791.0⋆	0.36
E-n51-k5	510.0⋆	4.77	514.0⋆	364.7
E-n76-k7	656.0⋆	97.12	660.0⋆	10538.1
E-n76-k8	699.0⋆	6245.56	703	[694.866]
E-n76-k10	772	[769.85]	784	[759.652]
E-n76-k14	939	[912.383]	960	[900.633]
F-n135-k7	1069.0⋆	348.29	1076.0⋆	4619.5
F-n45-k4	706.0⋆	0.16	710.0⋆	1.11
F-n72-k4	232.0⋆	0.28	232.0⋆	0.43
M-n101-k10	795.0⋆	4.71	798.0⋆	108.72
M-n121-k7	962	[949.444]	981	[949.303]
M-n151-k12	no-feas	[935.76]	no-feas	[932.814]

Table C.1: (Continued from previous page.)

Problem	Deterministic		Stochastic	
	Opt	t (sec) [LB]	Opt	t (sec) [LB]
P-n19-k2	195.0*	0	195.0*	0
P-n20-k2	208.0*	0	208.0*	0.01
P-n21-k2	208.0*	0	208.0*	0.01
P-n22-k2	213.0*	0.01	213.0*	0.02
P-n22-k8	549.0*	0.01	549.0*	0.02
P-n23-k8	486.0*	0.19	491.0*	15.09
P-n40-k5	448.0*	0.23	449.0*	1.52
P-n45-k5	496.0*	0.52	496.0*	15.73
P-n50-k7	531.0*	3.56	539.0*	480.6
P-n50-k8	580.0*	19.7	584.0*	748.81
P-n50-k10	649.0*	25.32	652.0*	1221.82
P-n51-k10	686.0*	19.01	688.0*	1116.65
P-n55-k10	656.0*	43.25	658.0*	1719.87
P-n55-k7	539.0*	0.71	543.0*	120.47
P-n55-k8	571.0*	3.01	572.0*	276.58
P-n55-k15	868.0*	176.34	871.0*	6372.02
P-n60-k10	703.0*	434.76	704.0*	14903.3
P-n60-k15	904.0*	275.71	911.0*	34400.8
P-n65-k10	750.0*	449.65	757	[748.853]
P-n70-k10	773	[769.264]	781	[760.688]
P-n76-k4	588.0*	1.61	588.0*	21.87
P-n76-k5	608.0*	8.49	612.0*	4477.6
P-n101-k4	673.0*	0.99	673.0*	25.56
att-n48-k4	38634.0*	0.59	38637.0*	7.58

Table C.1: (Continued from previous page.)

Appendix D

Detailed Numerical Results for Chapter 4

Table D.1 presents the performance of the randomized policy, Lagrangian relaxation and LP-based relaxation on the multi-armed bandit instances described in 4.3.2.5. Table D.2 reports the average relative infeasibility of each policy prior to applying the 'do nothing' actions for the same instances.

		1,000 bandits				100,000 bandits				1,000,000 bandits			
		1%	5%	10%	25%	1%	5%	10%	25%	1%	5%	10%	25%
2 states	$T = 5$	95.89%	89.29%	87.82%	74.42%	90.52%	87.52%	88.24%	72.87%	90.14%	88.15%	87.36%	72.07%
		-92.73%	-26.54%	45.78%	59.86%	-93.79%	-35.87%	46.24%	58.48%	-90.98%	-26.22%	45.00%	57.62%
		119.32%	79.08%	71.52%	57.52%	91.55%	83.14%	78.90%	61.71%	90.19%	83.62%	77.08%	63.27%
2 states	$T = 25$	89.78%	90.92%	87.42%	74.50%	91.09%	89.39%	85.72%	73.28%	90.37%	89.25%	84.88%	73.20%
		-89.91%	-9.79%	58.00%	62.23%	-90.88%	-15.61%	52.44%	59.36%	-89.38%	-14.67%	51.65%	58.94%
		92.61%	81.77%	72.40%	29.66%	80.83%	56.98%	47.20%	52.43%	82.55%	54.30%	51.37%	58.11%
2 states	$T = 50$	93.84%	92.28%	88.23%	74.43%	90.48%	89.58%	86.02%	73.53%	90.49%	89.34%	86.00%	73.62%
		-86.08%	-1.31%	59.39%	60.37%	-89.48%	-2.96%	54.70%	57.59%	-87.05%	-4.56%	55.38%	57.98%
		100.83%	84.24%	71.08%	19.16%	71.82%	41.31%	36.59%	51.54%	71.43%	40.71%	45.79%	57.47%
3 states	$T = 5$	100.26%	93.91%	89.21%	74.43%	93.89%	90.61%	86.44%	74.26%	94.09%	89.33%	88.63%	74.15%
		-82.70%	22.49%	62.33%	66.83%	-84.06%	8.13%	53.02%	63.91%	-82.61%	11.89%	56.88%	64.83%
		120.47%	82.58%	73.36%	57.80%	94.55%	84.96%	76.22%	60.55%	93.70%	84.63%	77.63%	63.49%
3 states	$T = 25$	93.93%	92.82%	88.88%	75.61%	94.66%	91.95%	87.47%	75.93%	93.31%	91.60%	87.79%	75.86%
		-76.57%	30.11%	65.83%	68.14%	-80.50%	29.17%	60.95%	65.74%	-77.42%	27.67%	60.68%	65.92%
		95.19%	81.32%	69.88%	28.51%	82.97%	60.33%	43.24%	44.99%	84.10%	52.18%	42.89%	54.16%
3 states	$T = 50$	95.66%	92.66%	89.14%	76.48%	93.71%	91.76%	87.99%	75.57%	93.53%	91.59%	88.02%	75.73%
		-68.25%	35.72%	65.80%	67.67%	-71.41%	30.30%	61.58%	64.87%	-72.69%	29.33%	60.66%	64.58%
		100.59%	82.03%	66.46%	20.57%	77.04%	42.03%	31.10%	41.66%	74.48%	36.44%	33.99%	52.65%
4 states	$T = 5$	96.48%	96.80%	88.64%	75.04%	95.75%	94.79%	87.45%	75.40%	96.19%	93.17%	87.48%	75.22%
		-70.90%	42.29%	70.26%	70.64%	-78.18%	34.24%	63.20%	68.30%	-79.17%	36.79%	61.71%	68.54%
		116.25%	85.67%	74.73%	58.53%	95.94%	85.69%	76.68%	60.02%	95.67%	87.36%	76.21%	61.37%
4 states	$T = 25$	99.29%	93.26%	89.30%	76.92%	94.69%	92.92%	88.64%	75.92%	94.84%	92.98%	88.27%	75.88%
		-63.00%	55.66%	72.45%	71.58%	-68.00%	48.23%	66.97%	68.95%	-66.91%	46.45%	67.05%	68.01%
		97.69%	81.02%	70.22%	29.39%	81.98%	63.04%	44.02%	37.61%	86.17%	53.29%	38.63%	50.00%
4 states	$T = 50$	96.29%	93.87%	89.60%	77.29%	95.09%	92.83%	89.13%	76.76%	94.61%	92.86%	88.84%	76.52%
		-46.67%	55.75%	73.16%	71.49%	-57.01%	48.35%	67.21%	68.83%	-54.70%	46.35%	66.73%	68.33%
		100.55%	82.23%	63.10%	20.01%	80.18%	45.23%	30.42%	33.13%	77.44%	35.26%	26.85%	48.38%
5 states	$T = 5$	96.99%	92.88%	87.51%	75.63%	95.88%	92.72%	88.38%	75.71%	96.73%	91.75%	88.46%	76.26%
		-66.29%	58.32%	72.54%	72.76%	-71.36%	44.46%	69.52%	70.20%	-73.61%	48.73%	70.88%	71.19%
		117.79%	81.27%	74.72%	59.70%	95.66%	84.43%	77.97%	59.62%	95.37%	85.25%	76.57%	61.08%
5 states	$T = 25$	97.04%	93.31%	88.82%	77.29%	95.70%	93.45%	89.29%	76.99%	95.58%	93.20%	89.95%	76.73%
		-52.51%	65.65%	77.07%	73.92%	-50.81%	59.60%	72.94%	71.08%	-53.24%	57.51%	73.51%	70.75%
		96.59%	81.41%	69.60%	29.84%	82.77%	64.89%	46.43%	32.19%	86.00%	53.60%	36.99%	46.33%
5 states	$T = 50$	95.98%	93.77%	89.93%	77.73%	96.12%	93.23%	89.34%	77.35%	95.99%	93.40%	89.02%	77.15%
		-33.99%	65.23%	77.91%	73.73%	-39.22%	59.28%	72.49%	70.90%	-41.57%	58.12%	71.41%	70.76%
		98.21%	80.65%	60.27%	20.17%	81.18%	46.68%	31.41%	26.42%	79.39%	37.24%	24.92%	44.23%

Table D.1: Relative improvement of our randomized policy (top entry), the policy derived from the Lagrangian relaxation (middle entry) and the policy derived from the LP-based relaxation (bottom entry) over the naive uniform sampling strategy, reported for different numbers of states and time horizons (rows) as well as numbers of bandits and resource restrictions (columns). Positive percentages correspond to improvements, whereas negative percentages (up to a hypothetical bound of -100%) correspond to inferior performances.

		1,000 bandits				100,000 bandits				1,000,000 bandits			
		1%	5%	10%	25%	1%	5%	10%	25%	1%	5%	10%	25%
2 states	$T = 5$	11.42%	4.61%	2.64%	1.34%	1.18%	0.43%	0.26%	0.14%	0.35%	0.12%	0.08%	0.05%
		5.56%	6.12%	4.80%	3.73%	0.00%	6.52%	7.13%	3.62%	10.63%	6.42%	5.66%	3.87%
		9,852.42%	1,854.85%	857.34%	248.80%	9,846.18%	1,839.72%	837.88%	272.16%	9,854.76%	1,829.53%	848.59%	279.44%
2 states	$T = 25$	11.52%	4.30%	2.39%	1.38%	1.18%	0.40%	0.24%	0.13%	0.40%	0.13%	0.07%	0.04%
		16.15%	19.36%	13.49%	5.11%	13.98%	18.30%	13.76%	4.90%	21.35%	19.29%	13.54%	5.31%
		9,558.84%	1,781.46%	797.11%	136.57%	9,575.05%	1,593.23%	753.09%	261.22%	9,512.71%	1,715.45%	819.84%	274.85%
2 states	$T = 50$	11.58%	4.44%	2.28%	1.32%	1.21%	0.43%	0.23%	0.13%	0.38%	0.13%	0.07%	0.04%
		25.72%	23.79%	15.16%	4.58%	20.02%	24.22%	15.68%	4.45%	29.72%	24.70%	15.63%	4.36%
		9,539.30%	1,764.79%	777.00%	107.38%	9,160.27%	1,485.35%	742.29%	261.17%	9,055.03%	1,686.66%	817.71%	274.59%
3 states	$T = 5$	12.26%	4.95%	3.16%	1.41%	1.19%	0.44%	0.28%	0.17%	0.37%	0.13%	0.09%	0.05%
		4.44%	5.50%	5.78%	3.93%	3.99%	4.88%	4.54%	3.44%	6.22%	5.17%	5.78%	3.72%
		9,812.60%	1,842.34%	852.71%	254.24%	9,843.04%	1,845.09%	836.17%	270.16%	9,848.90%	1,826.05%	848.94%	282.88%
3 states	$T = 25$	11.48%	4.58%	2.87%	1.60%	1.18%	0.45%	0.28%	0.17%	0.37%	0.14%	0.08%	0.05%
		22.04%	18.26%	11.48%	4.66%	16.69%	18.75%	10.98%	4.08%	23.06%	19.04%	11.44%	4.09%
		9,414.54%	1,747.68%	772.19%	128.57%	9,535.88%	1,551.54%	735.07%	260.71%	9,493.85%	1,694.42%	822.85%	279.58%
3 states	$T = 50$	12.11%	4.40%	2.80%	1.65%	1.17%	0.45%	0.29%	0.16%	0.39%	0.14%	0.09%	0.05%
		34.58%	23.20%	12.80%	3.91%	33.98%	22.75%	12.34%	3.76%	33.82%	22.63%	11.95%	3.72%
		9,396.16%	1,731.74%	726.24%	101.95%	9,142.11%	1,433.38%	721.01%	261.05%	8,959.21%	1,668.09%	821.41%	279.61%
4 states	$T = 5$	12.62%	5.24%	3.03%	1.69%	1.30%	0.47%	0.26%	0.18%	0.44%	0.15%	0.09%	0.06%
		4.84%	5.57%	5.50%	3.35%	4.93%	4.06%	3.76%	2.68%	3.22%	3.75%	4.14%	3.06%
		9,819.56%	1,840.30%	846.01%	257.45%	9,856.50%	1,842.75%	833.76%	269.76%	9,854.64%	1,824.87%	850.83%	284.24%
4 states	$T = 25$	11.76%	4.46%	3.27%	1.70%	1.17%	0.45%	0.31%	0.17%	0.37%	0.14%	0.10%	0.06%
		22.48%	16.85%	10.37%	3.75%	20.24%	15.82%	9.11%	3.53%	21.71%	17.03%	9.64%	3.55%
		9,364.50%	1,733.33%	769.89%	129.02%	9,502.87%	1,521.88%	722.30%	258.39%	9,488.01%	1,682.21%	822.72%	281.45%
4 states	$T = 50$	11.68%	4.65%	3.11%	1.82%	1.18%	0.46%	0.30%	0.17%	0.36%	0.15%	0.10%	0.06%
		38.87%	19.62%	10.57%	3.56%	36.84%	19.65%	9.49%	3.19%	37.43%	18.83%	9.87%	3.32%
		9,326.02%	1,705.99%	696.89%	102.62%	9,148.06%	1,401.22%	708.12%	260.60%	8,889.27%	1,657.74%	822.10%	281.78%
5 states	$T = 5$	11.76%	4.86%	3.34%	1.69%	1.26%	0.45%	0.29%	0.20%	0.40%	0.17%	0.10%	0.06%
		5.70%	6.01%	4.95%	3.08%	5.15%	5.43%	4.45%	2.66%	4.59%	4.56%	4.28%	2.64%
		9,815.70%	1,840.57%	851.08%	256.88%	9,837.56%	1,841.28%	839.13%	269.54%	9,841.84%	1,829.21%	848.14%	285.24%
5 states	$T = 25$	11.98%	4.70%	3.17%	1.90%	1.24%	0.47%	0.32%	0.19%	0.39%	0.16%	0.10%	0.06%
		21.48%	15.06%	8.66%	3.40%	25.31%	13.82%	8.24%	3.02%	21.95%	14.04%	8.19%	2.77%
		9,315.27%	1,721.81%	765.65%	131.72%	9,488.40%	1,511.20%	712.30%	257.49%	9,464.97%	1,670.25%	819.48%	282.48%
5 states	$T = 50$	12.17%	4.71%	3.22%	1.82%	1.15%	0.49%	0.31%	0.18%	0.39%	0.15%	0.10%	0.06%
		35.69%	16.60%	9.11%	3.15%	37.86%	17.18%	8.47%	2.64%	37.15%	16.20%	8.46%	2.61%
		9,259.07%	1,687.92%	662.82%	103.20%	9,123.29%	1,380.53%	700.65%	259.12%	8,850.53%	1,646.12%	820.74%	282.95%

Table D.2: Relative infeasibility of our randomized policy (top entry), the policy derived from the Lagrangian relaxation (middle entry) and the policy derived from the LP-based relaxation (bottom entry), prior to the correction with 'do nothing' actions. Each infeasibility is reported as the number of arms pulled in excess of the resource limit, as a percentage of the resource limit, averaged of all time periods (*e.g.*, '100%' would indicate that twice as many arms were being pulled as permitted by the resource constraint).